Functional genomics in the stroke-prone spontaneously hypertensive rat: Genome wide and candidate gene analysis

James Polke BSc

Submitted in fulfilment of the requirements for the degree of doctor of philosophy

University of Glasgow
Faculty of Medicine

March 2008 (c)

Declaration

I declare that this thesis has been written entirely by myself and is a record of research performed by myself with the exception of microarray hybridisations (Martin McBride), rat carotid artery virus infusion surgery (Elizabeth Beattie), wire myography (Angela Spiers), and some of the methods involved in carotid artery immunohistochemistry (Andrew Carswell). Rat embryo microinjections and implantations were performed by scientists at the Central Research Facility, University of Glasgow and at the Institute of Physiology, Academy of Sciences of the Czech Republic, Prague. This work has not been submitted previously for a higher degree. The research was carried out at the BHF Cardiovascular Research Facility under the supervision of Dr Martin McBride and Prof Anna Dominiczak.

James Polke

Acknowledgements

I would first of all like to acknowledge Martin and Anna for their guidance during my PhD, their support has been invaluable and I thank them for the opportunity to develop so many new skills.

I would like to thank Stuart Nicklin, Delyth Graham, Wai Kwong-Lee, William Miller and Andy Baker for their help with experimental design and training in many laboratory techniques. Thanks also to Elizabeth Beattie, Angela Spiers, Andy Carswell, Mark Lynch, Nicola Britton, Wendy Crawford and Carelene Hamilton for their technical help, and to John McClure for advice on statistical analysis.

I'm grateful to all my friends at the BHFGCRC that have helped to make my time in Glasgow so enjoyable.

Finally, thank you to my family for their unwavering support.

Table of Contents

Declaration 2
Acknowledgements 3
Table of Contents 4
List of Figures 9
List of Tables 11
List of Tables 11
List of Abbreviations and Acronyms 12
Summary 16
1 Introduction 19
1.1 Genetics of Human Hypertension 20
1.1.1 Blood Pressure Control 20
1.1.2 Epidemiology of Human Hypertension 23
1.1.3 Monogenic Forms of Hypertension 24
1.1.3.1 Glucocorticoid-Remediable Aldosteronism (GRA) 25
1.1.3.2 Apparent Mineralocorticoid Excess (AME) 25
1.1.3.3 Liddle Syndrome 26
1.1.3.4 Pseudohypoaldosteronism type II 26
1.1.3.5 PPARγ Mutations Causing Insulin Resistance, Diabetes Mellitus and Hypertension 28
1.1.3.6 Variably Penetrant Hypertension, Hypercholesterolaemia and Hypomagnesia 29
1.1.3.7 Hypertension with Brachydactyly 29
1.1.3.8 Mineralocorticoid Receptor Mutation Causing Hypertension Exacerbated in Pregnancy 30
1.1.3.9 Early Onset Coronary Artery Disease and Other Cardiovascular Symptoms, Including Hypertension 30
1.1.3.10 Monogenic Hypertension Genes in Essential Hypertension 31
1.1.4 Identifying Essential Hypertension Genes 32
1.1.4.1 Candidate Gene Analysis in Human Essential Hypertension 33
1.1.4.2 Genome-Wide Linkage Studies 37
1.1.4.3 Genome-Wide Association Studies 41
1.2 Rat Models of Human Hypertension 42
1.2.1 The Stroke-Prone Spontaneously Hypertensive Rat (SHRSP) 43
1.2.2 Identifying Quantitative Trait Loci 46
1.2.3 Recombinant Inbred Strains 47
1.2.3.1 Congenic Strains 48
1.2.3.2 Subcongenics 48
1.2.3.3 Microarray Expression Analysis and Congenics 53
1.2.3.4 Expression Genetics 57
1.2.3.5 QTL Interactions in Complex Disease 58
1.3 Oxidative Stress and Endothelial Dysfunction 59
1.3.1 Oxidative Stress Defence 63
1.3.2 Direct ROS metabolism 63
1.3.3 Glutathione and Glutathione s-Transferases 64
2 Materials and Methods 67
2.1 General Laboratory Practice 68
2.2 General Techniques 69
2.2.1 Nucleic Acid Extraction 69

2.2.2 Measuring Nucleic Acid Concentration 69
2.2.3 Polymerase Chain Reaction 70
2.2.4 Agarose Gel Electrophoresis 71
2.2.5 Determining Protein Concentration 71
2.3 Tissue Culture 72
2.3.1 Cell Passage and Cryostorage 72
2.3.2 Cell Counting 73
2.3.3 Plasmid Transfection of Cultured Cells 73
2.3.4 B-Galactosidase Expression Staining 74
2.4 DNA Sequencing 74
2.4.1 PCR Clean-up 74
2.4.2 Dideoxy Sequencing 75
2.4.3 Sequencing Reaction Purification 75
2.4.4 Capillary Electrophoresis 76
2.4.5 Sequencing Analysis 76
2.5 DNA Cloning 76
2.5.1 Transformation of Competent Bacteria 76
2.5.2 Glycerol Stocks 77
2.5.3 Plasmid DNA Purification 77
2.5.4 Restriction Digestion 78
2.5.5 Agarose Gel DNA Extraction 78
2.5.6 Ligation 79
2.5.7 Selecting Positive Clones 79
2.6 Western Blotting 80
2.6.1 SDS-Polyacrylamide Electrophoresis 80
2.6.2 Protein Blotting 80
2.6.3 Antibody Probing and Washing 81
2.6.4 Enhanced Chemiluminescence and Detection 81
2.6.5 Membrane Stripping and Re-Probing 82
2.6.6 Densitometry 82
2.7 Quantitative Real-Time PCR 83
2.7.1 Preparation of DNA-free cDNA 83
2.7.2 Real-Time PCR 84
2.8 Statistical Analysis 88
3 Microarray Renal Gene Expression Profiling in the 5 Week-Old SHRSP 89
3.1 Introduction 90
3.2 Aims 93
3.3 Methods 94
3.3.1 Renal Microarray mRNA Expression Analysis 94
3.3.1.1 RNA Extraction and Validation 94
3.3.1.2 First and Second Strand cDNA Synthesis 94
3.3.1.3 Double Stranded cDNA Clean-up 95
3.3.1.4 Biotin-labelled cRNA Synthesis, Clean-up and Validation 95
3.3.1.5 cRNA Fragmentation 96
3.3.1.6 Microarray Hybridisation and Data Collection 96
3.3.1.7 Microarray Data Analysis 97
3.3.2 Gstm1 western blotting 97
3.3.3 Kidney Glutathione Measurements 97

3.3.4 Kidney Superoxide Measurements 98
3.3.5 Quantitative RT-PCR 98
3.3.6 DNA Sequencing 99
3.4 Results 100
3.4.1 mRNA and cRNA Validation 100
3.4.2 Renal Microarray mRNA Expression Profiling 101
3.4.2.1 Microarray Data Quality Control 101
3.4.2.2 Rank Products Analysis 102
3.4.2.3 *Gstm1* qRT-PCR and Western Blotting 104
3.4.2.4 Ingenuity Pathway Analysis 104
3.4.3 Kidney GSH Concentrations 108
3.4.4 Kidney Superoxide Measurements 111
3.4.5 qRT-PCR of Other Candidate Genes 111
3.4.6 Promoter and Coding DNA Sequencing 113
3.5 Discussion 115
4 Gstm1 Expression and Promoter Analysis 122
4.1 Introduction 123
4.2 Aims 126
4.3 Methods 127
4.3.1 Renal *Gstm1* Quantitative Real-time PCR 127
4.3.2 *Gstm1* Promoter and Exon Sequencing 127
4.3.3 Renal Anti-Nitrotyrosine Western Blotting 127
4.3.4 Promoter Sequence Alignment 128
4.3.5 Promoter Sequence PCR 128
4.3.6 Promoter Sequence Cloning 128
4.3.7 Promoter Activity Analysis 130
4.3.7.1 Optimising Transfection of NRK52E Cells 130
4.3.7.2 Luciferase Activity Assay 131
4.3.7.3 β-Galactosidase Activity Assay 131
4.3.7.4 pGL3 Basic Subcloning 132
4.3.7.5 Site-Directed Mutagenesis 133
4.3.8 Transfac Professional Promoter Sequence Analysis 134
4.3.8.1 Generating Transcription Factor Matrix Tables 135
4.3.8.2 Transcription Factor Binding Site Analysis 136
4.4 Results 137
4.4.1 Renal *Gstm1* Quantitative Real-Time PCR 137
4.4.2 *Gstm1* Sequencing 137
4.4.3 Renal Anti-Nitrotyrosine Western Blotting 138
4.4.4 Rat and Mouse *Gstm1* Promoter Sequence Alignments 139
4.4.5 Promoter Sequence Cloning 142
4.4.5.1 Optimising NRK52E Transfections 143
4.4.5.2 Comparing SHRSP and WKY Promoter Activities 144
4.4.5.3 Luciferase Activities of Novel Subcloned SP1.6 plasmids 144
4.4.5.4 Luciferase Activities of Novel SP1.6 Site-Directed Mutagenesis Plasmids 145
4.4.6 Transfac Professional Matrix Table 146
4.4.7 Transcription Factor Binding Site Analysis 147
4.5 Discussion 154

5 Adenovirus-Mediated Modulation of *Gstm1* Expression *in-vitro* and *in-vivo* 162
5.1 Introduction 163
5.2 Aims 167
5.3 Methods 168
5.3.1 Generating viruses by homologous recombination in HEK293 cells 168
5.3.1.1 Anti-*Gstm* family shRNA sequence cloning 168
5.3.1.2 Cloning *Gstm1* cDNA and Verifying Gstm1 Expression 169
5.3.1.3 Co-Transfection into HEK293 Cells 169
5.3.2 Arklone P virus extraction 171
5.3.3 Pure virus stock preparation 171
5.3.4 Calculating Virus Titres 172
5.3.5 *In-vitro* Virus Infections 174
5.3.6 Gstm1 Western Blotting 174
5.3.7 GST Activity Assays 174
5.3.8 Taqman RT-PCR of *Gstm* Isoforms 175
5.3.9 Sequencing of RNAi Target Sequences 175
5.3.10 Cytotoxicity Assays 176
5.3.11 Local Delivery of RAd WKY Gstm1 to SHRSP Carotid Arteries 176
5.3.11.1 Surgical Procedure and Viral Delivery 176
5.3.11.2 Carotid Artery Wire Myography 177
5.3.11.3 RNA Extraction from Carotid Arteries and cDNA Sequencing 178
5.3.11.4 Carotid Artery Gstm1 Immunohistochemistry 178
5.4 Results 180
5.4.1 Recombinant Virus Construction and Titring 180
5.4.2 K-NpA Gstm1 Plasmid Transfections in HeLa cells 181
5.4.3 Optimising *In-vitro* Viral Infections 182
5.4.4 Gstm Knockdown by RAd Gstmf shRNA in NRK52E Cells 183
5.4.5 Gstmf Target Site Sequencing in *Gstm1,2,3,5* and *7* 186
5.4.6 Gstm1 Expression from Crude Viral Stocks 187
5.4.7 Comparing WKY and SHRSP Gstm1 Overexpression Viruses 188
5.4.8 miRNA Alignments in the WKY and SHRSP Gstm1 3'UTR 188
5.4.9 Gstm1 expression in RGE Cells and Cytotoxicity Assays 190
5.4.10 Local Delivery of RAd WKY Gstm1 to SHRSP Carotid Arteries 191
5.4.10.1 Optimising Viral Dose and Expression Time 191
5.4.10.2 Gstm1 Expression in Carotid Arteries 192
5.4.10.3 Wire Myography to Assess NO Bioavailability 192
5.5 Discussion 195
6 Production of a *Gstm1* Transgenic Rat 201
6.1 Introduction 202
6.2 Aims 206
6.3 Methods 207
6.3.1 BAC Microinjection Construct Preparation 207
6.3.1.1 BAC Selection and Purification 207
6.3.1.2 BAC Restriction Digestion and Electrophoresis 209
6.3.1.3 Direct BAC Sequencing 210
6.3.2 Linear Microinjection Fragment Preparation 210
6.3.2.1 pEF1 WKY Gstm1 Cloning 210

6.3.2.2 Restriction Digestion of pEF1 WKY Gstm1 to Generate Linear Fragment....211
6.3.2.3 Gstm1 Expression from pEF1 WKY Gstm1....212
6.3.3 Superovulation, Microinjection and Implantation....212
6.3.4 Transgenic Screening....213
6.4 Results....214
6.4.1 BAC Restriction Digestion and Electrophoresis....214
6.4.2 Direct BAC Sequencing....217
6.4.3 Gstm1 Expression from pEF1 WKY Gstm1....217
6.4.4 Transgenic Screening....217
6.5 Discussion....220
7 General Discussion....223
Appendix....234
Publications, Awards and Presentations....257
References....259

List of Figures

Figure 1.1 - The renin angiotensin aldosterone system 22
Figure 1.2 - Traditional and speed congenic breeding 49
Figure 1.3 - Chromosome 2 congenic strains and blood pressures 52
Figure 1.4 - Chromosome 2 subcongenic strains derived from SP.WKYGla2a ... 54
Figure 1.5 - Oxidative stress in cardiovascular disease 61
Figure 1.6 - Catalysis of glutathione conjugation to CDNB by GST enzymes 65
Figure 3.1 - Agilent Bioanalyser 2100 assessment of mRNA quality 100
Figure 3.2 - Agilent Bioanalyser 2100 assessment of cRNA quality..... 101
Figure 3.3 - Differential renal mRNA expression in pairwise comparisons of different strains and timepoints 103
Figure 3.4 - Differential expression of *Gstm1* at 5 and 16 weeks of age confirmed by qRT-PCR..... 106
Figure 3.5 - Reduced renal Gstm1 protein in the 5 week-old SHRSP……106
Figure 3.6 - IPA canonical pathway analysis of renal 5 and 16 week microarray data..... 107
Figure 3.7 - KEGG glutathione metabolism pathway 109
Figure 3.8 - Kidney GSH concentrations in 5 and 16 week-old SHRSP, 2c* and WKYs..... 110
Figure 3.9 – Kidney superoxide levels in 5 week old SHRSP, 2c* and WKY rats 111
Figure 3.10 - Taqman qRT-PCR of genes differentially expressed in microarrays 112
Figure 3.11 – PCR and sequencing candidate gene coding and regulatory regions 113
Figure 3.12 - Renal glutathione metabolism..... 116
Figure 4.1 - Subcloning to generate novel 1.6 kb promoter constructs 132
Figure 4.2 – PCR sewing for site-directed mutagenesis 134
Figure 4.3 - Renal *Gstm1* mRNA expression in the SHRSP, SHR, BN and WKY 137
Figure 4.4 – Anti-nitrotyrosine western blot in 16 week SHRSP, 2c* and WKY kidneys..... 139
Figure 4.5 - zPicture alignment of rat and mouse *Gstm1* promoters..... 140
Figure 4.6 - Individual alignments of rat *Gstm1* promoter polymorphisms with mouse *Gstm1* promoter sequences..... 141

Figure 4.7 - Agarose gel and sequencing images from *Gstm1* promoter cloning 142
Figure 4.8 - Optimisating transfection of NRK52E cells 143
Figure 4.9 - Luciferase activities of 0.9 kb -2.5 kb *Gstm1* promoter sequences.144
Figure 4.10 – Luciferase activities of subcloned 1.6 kb promoter plasmids 145
Figure 4.11 - Luciferase activities of novel site-directed mutagenesis plasmids 146
Figure 5.1 - Exploitation of the endogenous RNA interference pathway in experimental biology 165
Figure 5.2 - Generation of recombinant adenoviruses by recombination in HEK293 cells 168
Figure 5.3 - PCR screen following *Gstm1* cDNA cloning 181
Figure 5.4 - Transfection of K-NpA Gstm1 cDNA plasmids into HeLa cells 182
Figure 5.5 - Optimisation of *in-vitro* virus infections with RAd35 183
Figure 5.6 - Anti-Gstm family shRNA-mediated mRNA knockdown of *Gstm* isoforms 185
Figure 5.7 - Anti-Gstm family shRNA-mediated knockdown of Gstm1 protein ...186
Figure 5.8 - Verification of Gstm1 overexpression viruses 187
Figure 5.9 - Adenovirus-mediated WKY and SHRSP Gstm1 expression in HeLa cells.....189
Figure 5.10 - Cytotoxicity assays in RGE cells treated with TBHP.....190
Figure 5.11 - β-galactosidase expression in RAd35-infected SHRSP carotid arteries.....191
Figure 5.12 - *Gstm1* expression in infused and uninfused carotid arteries.....193
Figure 5.13 - Gstm1 immunohistochemistry in SHRSP carotid arteries 194
Figure 5.14 - NO bioavailability in SHRSP carotid arteries 194
Figure 6.1 - Linear depiction of transcripts encoded by the circular CH230-90M3 BAC 208
Figure 6.2 - pEF1 WKY Gstm1 plasmid 212
Figure 6.3 - Agarose electrophoresis of *HindIII*-digested CH230-90M3 BAC.....215
Figure 6.4 - PFGE of *NotI*-digested CH230-90M3 BAC 216
Figure 6.5 - Electropherogram from direct sequencing of 90M3 217
Figure 6.6 - Gstm1 protein expression from pEF1 WKY Gstm1.....217
Figure 6.7 - PCR Screening for BAC and linear fragment transgenic rats 219

List of Tables

Table 1.1 - Physiological systems involved in the control of blood pressure 21
Table 1.2 - Genome-wide linkage studies for essential hypertension loci in humans 40
Table 1.3 - Rat inbred models used in hypertension genetic research 44
Table 3.1 - Quality control data from Test3 chips. 102
Table 3.2 - Differentially expressed probesets encoded from the 2c* congenic interval 105
Table 3.3 - Differentially expressed glutathione metabolism genes 110
Table 3.4 - Candidate gene coding and regulatory sequence variants 114
Table 4.1 - Transcription factors implicated in regulation of expression of human, mouse and rat GST genes 125
Table 4.2 - *Gstm1* coding and promoter SNPs in the SHRSP, SHR, WKY and BN 138
Table 4.3 - Transfac alignment data of Nrf2, Maf and Bach1 matrices with SNP11+10 149
Table 4.4 - TF matrices that aligned with SNPs in cluster 1-7 and cluster 8-12 . 151
Table 5.1 - Recombinant adenovirus particle, pfu and genome titres 181
Table 6.1 - Transgenic rat strains for the study of cardiovascular diseases 203
Table 6.2 - Microinjected embryos implanted at Glasgow University 218
Table 6.3 - Microinjected embryos implanted at Academy of Sciences of the Czech Republic 218
Table A1 – Primer Sequences 234
Table A2 – Differentially expressed probesets implicating the 2c* congenic interval at 5 weeks of age 238
Table A3 – Differentially expressed probesets implicating the 2c* congenic interval at 16 weeks of age 239
Table A4 – Differentially expressed probesets implicating the 2c* congenic interval between 5 and 16 weeks of age 240
Table A5 – Transfac Match output for all Gstm1 promoter SNPs 243

List of Abbreviations and Acronyms

11βHSD-2	11 β-hydroxysteroid dehydrogenase
18-OH-DOC	18-hydroxy-11deoxycorticosterone
2D-DIGE	2 Dimensional difference in gel electrophoresis
AAV	Adeno-associated virus
ACE	Angiotensin converting enzyme
ADH	Anti-diuretic hormone
AGT	Angiotensinogen
AME	Apparent mineralocorticoid excess
Ang	Angiotensin
Anp	Atrial natiuretic peptide
Aqp2	Aquaporin-2
ARE	Antioxidant response element
AT1R	AngII type 1 receptor
BAC	Bacterial artificial chromosome
BCA	Bicinchoninic acid assay
BDKR	Bradykinin receptor
BGH	Bovine growth hormone
BH_4	Tetrahydrobiopterin
BN	Brown Norway rat
Bnp	Brain natiuretic peptide
BRIGHT	BRitish Genetics of HyperTension
BSA	Bovine serum albumin
BSO	Buthionine sulphoxide
CAD	Coronary artery disease
CDNB.	1-chloro-2,4-dintrobenzene
CEBPB	CCAAT/enhancer binding protein-β
ChIP	Chromatin immunoprecipitation
CNV	Copy number variation
CTMP	Carboxy-terminal modulator protein
Cu/Zn-SOD	Copper/zinc SOD
CYP11B1	11 β-hydroxylase gene
CYP11B2	Aldosterone synthase gene
DCNB	1,2-dichloro-4-nitrobenzene
DMSO	Dimethylsulfoxide
DNA	Deoxyribonucleic acid
DSR	Dahl salt resistant rat
DSS	Dahl salt sensitive rat
DTT	Dithiothreitol
ECACC	European Collection of Cell Culture
ecSOD	Extracellular SOD
Edg1	Endothelial differentiation gene receptor 1
EDRF	Endothelium-derived relaxing factor
EDTA	Ethylenediaminetetraacetic acid
EF1α	Elongation factor 1 α subunit

EMSA	Electrophoretic mobility shift assay
ENCODE	Encyclopaedia of DNA elements
eNOS	Endothelial nitric oxide synthase
eQTL	Expression QTL
FBS	Foetal bovine-serum
FCS	Foetal calf serum
FDR	False-discovery rate
FHH	Fawn hooded hypertensive rat
FHL	Fawn hooded low blood pressure rat
Gcl	Glutamate cysteine ligase
GFP	Green fluorescent protein
GGT1	Gammglutamyltranspeptidase I
GH	Genetically hypertensive rat
GK	Goto-Kakizaki rat
Gnai3	Guanine nucleotide binding protein
GPx	Glutathione peroxidase
GRA	Glucocorticoid-remediable aldosteronism
GSH	Glutathione
GSS	Glutathione synthase
GSSG	Glutathione disulfide
GST	Glutathione s-transferase
Gstm1	Glutathione s-transferase mu type 1
H_2O_2	Hydrogen peroxide
HCG	Human chorionic gonadotrophin
HDL	High-density lipoprotein
Hist2H2aa	Histone 2, H2aa
iCE	Internet Contig Explorer
IGF-1	Insulin-like growth factor-1
IMCD	Inner-medullary collecting duct
iNOS	Inducible NOS
IP	Intraperitoneal
IPA	Ingenuity Pathway Analysis
IPTG	Isopropyl-beta-D-thiogalactopyranoside
ISIAH	Inherited stress-induced arterial hypertensive
LAR	Luciferase assay reagent
LB	Luria broth
LDL	Low-density lipoprotein
LH	Lyon hypertensive rat
LHRH	Leutenising hormone releasing hormone
LL	Lyon low blood pressure rat
LN	Lyon Normotensive rat
L-NAME	N-Nitro-L-Arginine Methyl Ester
LOD	Logarithm of odds
LRP6	LDL receptor-related protein 6
MCS	Multiple cloning site
miRNA	MicroRNA
MNS	Milan normotensive strain
Mn-SOD	Mitochondrial manganese SOD

MOI	Multiplicity of infection
MOPS	3-morpholinopropanesulfonic acid
MR	Mineralocorticoid receptor
NAD(P)H oxidase	Nicotinamide adenine (phosphate) dinucleotide oxidase
NCCT	NaCl cotransporter
NEFA	Non-esterified fatty acid
NEP	Neutral endopeptidase
nNOS	Neuronal NOS
NO	Nitric oxide
NQO1	NADPH:quinone reductase
Nrf2	Nuclear-factor-erythroid 2-related factor 2
NRK52E	Normal rat kidney epithelial cells
O2-·	Superoxide anion
OH·	Hydroxyl radical
ONOO-	Peroxynitrite
PAC	Bacteriophage P1 artificial chromosome
PBS	Phosphate-buffered saline
PCP	Prolylcarboxypeptidase
PCR	Polymerase chain reaction
PDGF	Platelet-derived growth factor
PE	Phenylephrine
PEP	Prolylendopeptidase
pfu	Plaque forming unit
PHR	Prague hypertensive rat
PI 3-kinase	Phosphatidylinositol 3-kinase
Pik3c3	Phosphatidylinositol 3-kinase
PIK3R1	PI3 kinase regulatory subunit 1
PKBα	Protein kinase B alpha
PKCα	Protein kinase C alpha
PMSG	Pregnant mare's serum gonadotrophin
PNR	Prague normotensive rat
PPAR	Peroxisome proliferator-activated receptor
PPARM	PPAR responsive enhancer module
Prcc.	Papillary renal cell carcinoma
PSS	Physiological saline solution
qRT-PCR	Quantitative real-time PCR
QTL	Quantitative trait locus
RA	Retinoic acid
RAAS	Renin angiotensin aldosterone system
RAd	Recombinant adenovirus
RGE	Rat glomerular endothelial
RISC	RNA-induced silencing complex
RLB	Reporter Lysis Buffer
RNA	Ribonucleic acid
ROS	Reactive oxygen species
rRNA	ribosomal RNA
SAP	Shrimp alkaline phosphatase
SBH	DOCA salt sensitive Sabra rat

SBN	DOCA salt resistant Sabra rat
SDS	Sodium dodecyl sulphate
SHR	Spontaneously hypertensive rat
shRNA	Short-hairpin RNA
SHRSP	Stroke-prone spontaneously hypertensive rat
siRNA	Short interfering RNA
SOD	Superoxide dismutase
SPRIPlate	Solid phase reversible immobilisation plate
Sreb1f	Sterol regulatory element binding transcription factor 1
TBE	Tris-Borate EDTA
TBHP	Tert-butyl hydrogen peroxide
TF	Transcription factor
TGF	Tubuloglomerular feedback
Tris	Trishydroxymethylaminomethane
TZDs	Thiazolidinediones
UGT	Uridine diphosphate-glucuronosyl-transferase
UTR	Untranslated region
Vcam1	Vascular cell adhesion molecule 1
Vegf-A	Vascular endothelial growth factor
VSMC	Vascular smooth muscle cell
WKY	Wistar Kyoto rat
WNK	With no lysine (K)
WTCCC	The Wellcome Trust Case Control Consortium
X-gal	5-Bromo-4-chloro-3-indolyl β-D-galactopyranoside
YAC	Yeast artificial chromosome

Summary

Hypertension is an increasing public health burden worldwide, it affects over 25% of the adult population and is a significant risk factor in a number of other cardiovascular diseases such as atherosclerosis, heart disease and stroke. Numerous family and population studies have identified candidate genes associated with essential hypertension in humans, though no major effect loci have been replicated. The experiments performed in this project employed a number of functional genomic techniques to investigate the genetic causes of high blood pressure in the stroke-prone spontaneously hypertensive rat (SHRSP), an inbred model of essential hypertension.

A genome-wide scan previously performed in the Glasgow laboratory by cross-breeding the SHRSP and the Wistar Kyoto (WKY) normotensive control strain identified a quantitative trait locus (QTL) on rat chromosome 2 encoding genes involved in blood pressure regulation. This QTL was confirmed and further refined by congenic breeding: introgressing genomic regions from the WKY onto the background of the SHRSP, generating rats with reduced blood pressure compared to the SHRSP. Renal microarray gene expression profiling in the 16 week old SHRSP, WKY and congenic 2c* strain identified a positional and functional candidate gene, glutathione s-transferase μ type 1 (*Gstm1*) which is involved in defence against oxidative stress and is down-regulated in the SHRSP.

One of the aims of these investigations was to assess differences in gene expression between normotensive and hypertensive rats prior to the onset of hypertension in the SHRSP. Microarray gene expression profiling measured renal expression in 5 week old SHRSP, WKY and 2c* rats, showing reduced expression of *Gstm1* in the SHRSP. This verified *Gstm1* as a robust candidate gene since its differential expression precedes the development of high blood pressure in the SHRSP. Gene expression data was also combined with the previous data from 16 week old rats to examine differences between strains at both timepoints; Ingenuity Pathway Analysis software was employed to assess the differential expression of groups of genes according to their role in well-described biological pathways. Several differentially expressed genes from within and outwith the congenic interval in addition to *Gstm1* were identified that are involved in glutathione (GSH) metabolism, leading to the hypothesis that renal oxidative stress caused by impaired GSH metabolism may contribute hypertension in the SHRSP. Renal GSH levels were measured at 5 and 16 weeks of age, showing lower levels in the SHRSP at both timepoints

compared to the WKY, while in the 2c*, GSH levels were similar to the SHRSP at 5 weeks of age and similar to the WKY at 16 weeks of age. This verified the likely effect of genes from the 2c* congenic interval on differential GSH metabolism, and renal superoxide levels were also shown to be increased in the SHRSP at 5 weeks of age, however quantitative real-time PCR did not verify the microarray results in some cases.

Reduced kidney *Gstm1* expression was also confirmed in the spontaneously hypertensive rat (SHR), while expression in the normotensive Brown Norway (BN) rat was equivalent to the WKY. 13 promoter single-nucleotide polymorphisms (SNPs), a missense mutation and a 3' untranslated region (UTR) SNP were identified in *Gstm1* in SHRSP and SHR that were not carried by the WKY or BN. Rat and mouse *Gstm1* promoter sequences were aligned, identifying a conserved antioxidant response element and regions of homology likely to encode functionally important regulatory elements. Luciferase reporter constructs compared transcriptional activities of SHRSP and WKY *Gstm1* promoters of increasing length, encompassing progressively more SNPs. Following subcloning to isolate the transcriptional effects of two clusters of SNPs in reduced expression in the SHRSP, luciferase activities suggested that an interaction between one or more SNP in each cluster contributed to reduced transcription. Further novel constructs were generated by site-directed mutagenesis to investigate this interaction but no consistent effects on expression were observed, implying complex regulation of *Gstm1* expression. The Transfac database was used to identify several potential transcription factor binding sites affected by the SHRSP mutations, the strongest candidate being peroxisome proliferator-activated receptor gamma (PPARγ), with binding sites affected in both implicated clusters.

Recombinant adenoviruses were employed in experiments to assess the functional effects of modulating *Gstm* expression *in-vitro* and *in-vivo*. Previous experiments had demonstrated effective *Gstm1* knockdown *in-vitro* using a short-interfering RNA sequence designed to reduce expression of several *Gstm* family genes. This sequence was expressed as a short-hairpin RNA (shRNA) by an adenoviral vector. Consistent 32-58% knockdown of *Gstm1*, *2* and *3* was achieved *in-vitro*, though several mismatches in the target shRNA sequence prevented effective knockdown of *Gstm5*. Reduced expression was not measured for *Gstm7*, despite only a single mismatch that was also observed in the *Gstm2* coding sequence, this was accounted for by low endogenous *Gstm7* expression. Total cellular GST activity was not reduced by the anti-Gstm family shRNA adenovirus. Adenoviruses were generated to express SHRSP and WKY *Gstm1* sequences. WKY *Gstm1*-overexpression adenovirus was infused into carotid arteries of *Gstm1* rats and nitric-oxide (NO)-

bioavailability was compared to contralateral uninfused vessels by wire myography 48 hours later. Overexpression of *Gstm1* did not improve NO-bioavailability.

Significant progress was made towards the generation of a transgenic SHRSP rat overexpressing *Gstm1*. A bacterial artificial chromosome (BAC) encoding *Gstm1* was purified and a linear *Gstm1* expression construct was cloned and purified in which *Gstm1* expression was driven by the ubiquitous human elongation factor 1 alpha subunit promoter. Eight rounds of microinjections were performed resulting in the birth of 78 pups, though none were transgenic when screened by PCR.

In summary, a wide range of functional genomic techniques were applied in the analysis of a genetic model hypertension, involving genome-wide and candidate gene approaches. While the role of *Gstm1* in hypertension in the SHRSP is yet to be fully understood, a number of tools have been developed that will aid in further investigations and guide the analysis of other candidates.

1 Introduction

1.1 Genetics of Human Hypertension

1.1.1 Blood Pressure Control

It is essential that the supply of blood from the heart to all organs of the body is well controlled in order to deliver oxygen, nutrients and hormones at the appropriate rate and to ensure removal of metabolic waste products such as carbon dioxide. Many physiological mechanisms exist to ensure that acute and long-term local and global blood flow is maintained at the appropriate level to individual organs in response to tissue needs. The most fundamental of these mechanisms is the control of mean arterial blood pressure, it is also one of the most complex physiological systems, involving the endocrine and nervous systems, the endothelium, kidneys and the maintenance of heart and blood vessel architecture. Grossly, arterial pressure is dictated by the following relationship: BP = Cardiac Output X Vascular Resistance. A number of the homeostatic systems involved in blood pressure control are summarised in table 1.1, these systems form a complex web of interaction and feedback to maintain appropriate blood pressure in response to changes in diet, activity, stress and other environmental factors. The organ principally responsible for long term blood pressure control is the kidney, it regulates blood volume by controlling salt and water levels. Its importance in blood pressure control was elegantly shown by experiments involving renal transplantation between hypertensive and normotensive rats, the blood pressure of hypertensive rats receiving kidneys from normotensive strains fell, while the blood pressure of normotensive rats receiving a hypertensive rat kidneys increased (Bianchi et al. 1974a).

The major mechanism responsible for blood pressure control is the renin angiotensin aldosterone system (RAAS) (figure 1.1); the most studied aspects of the RAAS involve the vasoconstrictory mechanisms of angiotensin converting enzyme (ACE) and angiotensin II (Ang II), though in recent years there has been substantial progress in our understanding of the role played by ACE2 and angiotensin 1-7 peptide (Ang-(1-7)) in vasodilation, cardioprotection and salt and water homeostasis. Angiotensinogen (AGT), produced in the liver, is the inactive 485 amino-acid precursor to angiotensin I (Ang I), it circulates freely in the plasma. The conversion of AGT to Ang I is mediated by renin, which is released from the juxtaglomerular apparatus in response to decreased renal perfusion, or decreased

Physiological System	Relation to Blood Pressure
The renin-angiotensin system, renal body fluid regulation.	The major mechanisms of long-term blood pressure control involve salt and water homeostasis in the kidney.
Arterial Baroreceptor Reflexes	Increased BP stimulates baroreceptors, inhibiting the vasoconstrictor centre and exciting the vagal centre in the brain, causing vasodilation, decreased heart rate and strength of heart contraction. Converse response to reduced BP.
Renin-Angiotensin Vasoconstrictor Mechanism	The short-term effect of angiotensin II is to stimulate vasoconstriction of arterioles, causing an increase in peripheral resistance and an increase in BP.
Stress-Relaxation Mechanism	Increased blood pressure stretches the blood vessel walls, they stretch to accommodate this and consequently reduce blood pressure.
Carotid and Aortic Chemoreceptors	Chemoreceptors detect oxygen lack and carbon dioxide and hydrogen excess, exciting the vasomotor centre to increase heart rate and cause vasoconstriction.
Endothelium-derived vasoactive substances	Alter vascular tone. Examples include nitric oxide (vasodilatory) and endothelin (vasoconstrictive).
Natriuretic Peptides	Released in response to increased BP. Cause cardiac and vascular vasodilation, inhibit renal and vascular effects of angiotensin II, inhibit cardiac
Capillary Fluid Shift	Reduced capillary pressure results in increased osmosis from the tissue fluid to the vasculature, increasing blood volume. Increased capillary pressure has the opposite effect.
Kidney Kinin-kallikrein system	Responds to increased sodium by stimulating salt and water secretion, reducing BP.
Central Nervous System Ischaemic Response	Reduced nutrient flow in the brain vasomotor centre strongly excites it to activate parasympathetic responses, increasing heart rate and constricting blood vessels. Principally an emergency response to very low blood pressure to prevent brain injury.

Table 1.1 - Physiological systems involved in the control of blood pressure

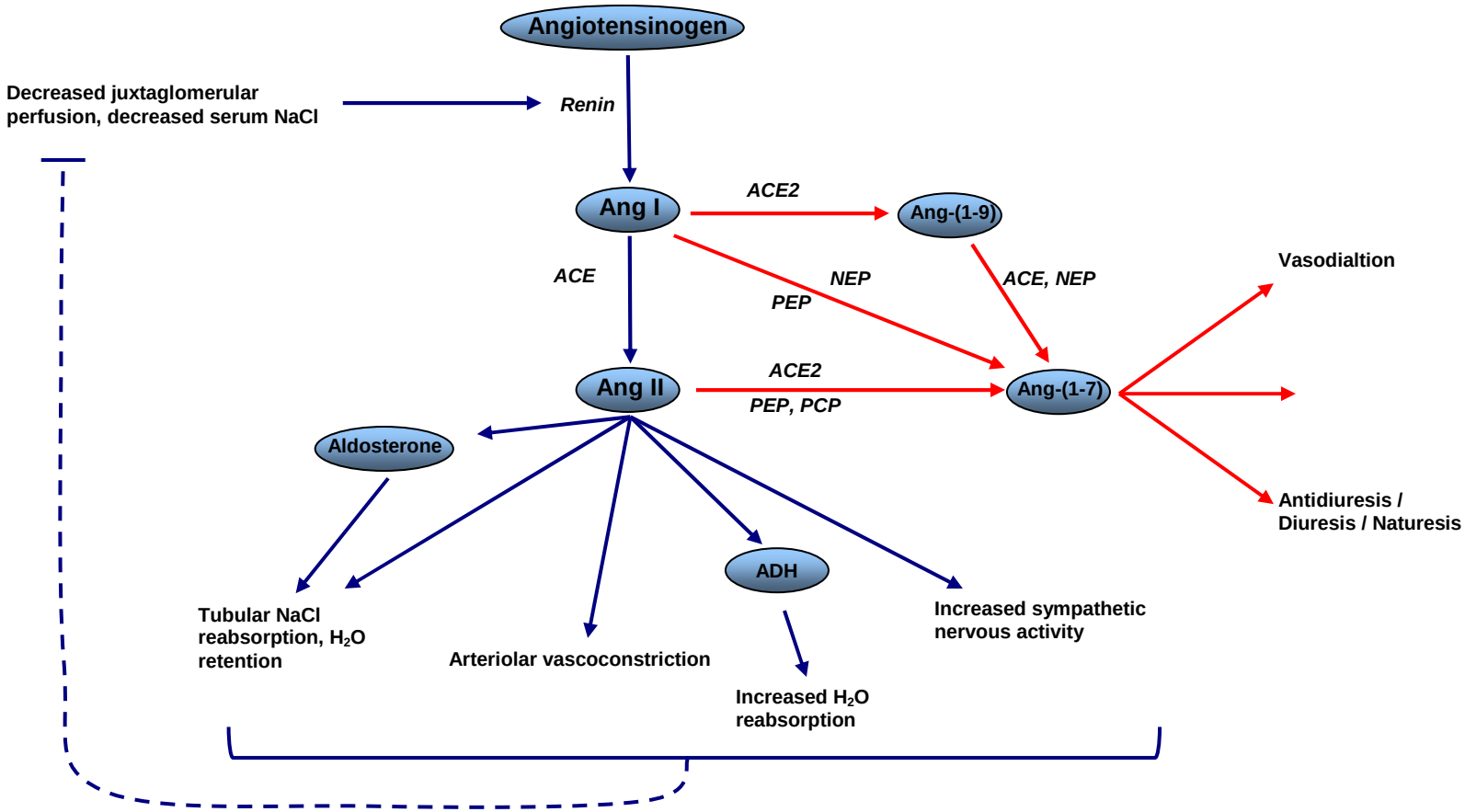

Figure 1.1 - The renin angiotensin aldosterone system

The ACE/Ang II axis (blue arrows) mediates increased blood pressure in response to decreased glomerular bloodflow and plasma salt levels, while the ACE2/Ang-(1-7) axis (red arrows) has a blood-pressure lowering effect. See text for details. ACE: angiotensin converting enzyme, Ang: angiotensin, NEP: neutral endopeptidase 24.11, PEP: prolylendopeptidase PCP: prolylcarboxypeptidase.

serum sodium chloride (NaCl) concentration. Ang I, an inactive 10 amino acid peptide, is converted to Ang II by ACE, a membrane-bound enzyme that resides predominantly in the endothelial surfaces of the lungs. Ang II, an 8 amino acid peptide, is a potent effector of many downstream systems leading to increased blood pressure: it stimulates aldosterone secretion from the adrenal gland, leading to kidney tubular sodium and chloride reabsorption and water retention, it also acts directly on tubular receptors with the same result, it stimulates sympathetic nervous activity, causing increased heart rate and blood vessel constriction, it also stimulates arteriolar constriction directly. Finally, Ang II also stimulates the pituitary gland to secrete anti-diurectic hormone (ADH), resulting in increased water reabsorption in the kidney collecting ducts. A negative feedback loop exists whereby increased juxtaglomerular perfusion caused by the above effects reduces renin release. Ang I and Ang II are also substrates for the generation of Ang-(1-7), directly or via Ang-(1-9), in number of reactions catalysed by ACE2, ACE, neutral endopeptidase 24.11 (NEP), prolylendopeptidase (PEP) and prolylcarboxypeptidase (PCP) (figure 1.1). Ang-(1-7) is a 7 amino acid peptide that was once considered an inactive metabolite of Ang II until it was demonstrated to mediate the release of vasopressin from *in-vitro* pituitary explants (Schiavone et al. 1988). The discovery of ACE2 (Tipnis et al. 2000;Donoghue et al. 2000) was the catalyst for further elucidation of the role of Ang-(1-7), and the ACE2/Ang-(1-7) system is now recognised as a major counter-regulatory mechanism of the ACE/Ang II system. Our understanding of the actions of Ang-(1-7) is far from complete but has been show to have endothelium-dependent vasodilatory effects in several tissue beds, a response recently shown to be mediated by nitric oxide (NO) (Sampaio et al. 2007). Ang-(1-7) also plays a role in cardioprotection, reducing cardiac Ang II levels in rats (Mendes et al. 2005), and mediating blood-pressure independent prevention of cardiac fibrosis and hypertrophy in experimental models (Tallant et al. 2005;Grobe et al. 2006). The renal effects of ACE2 and Ang-(1-7) are not well understood at present, with conflicting reports suggesting that Ang-(1-7) can mediate the retention or secretion of salt and water depending on the experimental system or segment of nephron examined (DelliPizzi et al. 1994;Santos et al. 1996;Vallon et al. 1997).

1.1.2 Epidemiology of Human Hypertension

Blood pressure is a quantitative phenotype that shows continuous variation from high to low values throughout populations. It is clinically accepted that optimal adult blood

pressure is <120/80 mmHg (systolic/diastolic), whilst the normal range is typically <139/89 mmHg. High blood pressure, or hypertension, is defined as systolic pressure over 140 mmHg and/or diastolic pressure over 90 mmHg (Guidelines Subcommittee WHO-ISH 1999;Mancia et al. 2007). Hypertension is a health concern because is a major risk factor for a number of cardiovascular diseases including stroke, atherosclerosis, type II diabetes, coronary heart disease and renal disease. It affects 26% of adults worldwide, its prevalence is predicted to increase to 29% by 2025 (Kearney et al. 2005).

In approximately 5% of hypertensives, increased blood pressure is secondary to a factor such as constriction of a blood vessel, an imbalance of hormones or monogenic disease, the remaining 95% have idiopathic or essential hypertension. Factors that contribute to essential hypertension are known to include environmental and genetic causes. Environmental factors include high dietary sodium intake, excess alcohol consumption, smoking, stress, and increased body weight. Of these, reducing alcohol consumption and restricting calorific intake have been shown to most effectively reduce blood pressure (Staessen et al. 1989;Beilin 1995). It is estimated that 13-31% and 41-46% of variance in systolic blood pressure are due to environmental and genetic factors, respectively (Annest et al. 1979;Annest et al. 1983;Cui et al. 2002). Evidence for a genetic component to hypertension includes results of twin studies that show a greater concordance of blood pressure between monozygotic twins than dizygotic twins (McIlhany et al. 1975;Feinleib et al. 1977;Havlik et al. 1979;Rose et al. 1979;Heiberg et al. 1981;Levine et al. 1982). Population studies show greater variation of blood pressure between families than within them (Longini, Jr. et al. 1984), and correlations in blood pressure are more significant between biological parent and child than parent and adopted child living in the same household (Biron et al. 1976;Mongeau et al. 1986). Identification of the specific genes that contribute to blood pressure regulation and how they interact in essential hypertension is a major challenge, the number of loci involved is unknown, as is the extent to which each contributes to the phenotype in given individuals, populations and environments.

1.1.3 Monogenic Forms of Hypertension

In an effort to understand the genetics of hypertension, much work has been performed to find the causes of the monogenic forms of the disease. These mutations are very rare but it is hoped identification of the genes responsible may not only provide candidates for essential hypertension, but also elucidate the mechanisms of blood pressure control and

identify novel therapeutic targets. A substantial contribution to this body of work has been made by Lifton and colleagues who have identified mutations in 10 genes responsible for hypertension and 7 causing hypotension (Lifton et al. 2001;Cowley, Jr. 2006). The known monogenic causes of hypertension are discussed in turn below. It is noteworthy that a majority of the monogenic causes of hypertension directly affect the function of the salt and water handling systems in the kidney, underlining the importance of renal involvement in blood pressure control and the likelihood that genes involved in essential hypertension may also predominantly affect salt and water homeostasis mechanisms.

1.1.3.1 Glucocorticoid-Remediable Aldosteronism (GRA)

GRA is an autosomal dominant condition characterised by early onset hypertension with normal or raised aldosterone levels and low renin activity (Sutherland et al. 1966). This is often associated with hypokalaemia and metabolic alkalosis (Rich et al. 1992). The distinguishing feature of the disease however is that glucocorticoid therapy completely reverses the hypertension. Genetically, it is caused by unequal crossover between the genes encoding steroid 11 β-hydroxylase (*CYP11B1*) and aldosterone synthase (*CYP11B2*), two closely related and closely linked genes involved in adrenal steroid biosynthesis (Lifton et al. 1992). This generates a chimeric gene whose expression is regulated at its 5' (*CYP11B1*) end by adrenocorticotropic hormone (ACTH), but whose protein product exhibits aldosterone synthase activity. Aldosterone synthase activity is therefore kept artificially high as the chimeric gene expression is stimulated in the adrenal fasciculata by ACTH rather than the normal regulating hormone, angiotensin II. This leads to expanded plasma volume due to increased Na^+ reabsorption via overactivation of ENaC by the mineralocorticoid receptor (MR). The increased plasma volume suppresses renin secretion, accounting for the low renin activity, whilst Na^+ reabsorption drives K^+ and H^+ secretion, leading to the hypokalaemia and alkalosis. Treatment with glucocorticoids (such as dexamethasone) suppresses ACTH activity, reducing the aldosterone synthase activity and restoring normotension.

1.1.3.2 Apparent Mineralocorticoid Excess (AME)

AME is an autosomal recessive disorder caused by mutations in the *11βHSD-2* (11 β-hydroxysteroid dehydrogenase) gene featuring early onset hypertension with hypokalaemia, metabolic alkalosis, suppressed renin activity and near absence of

circulating aldosterone. Despite reduced aldosterone levels, antagonists of the MR were shown to lower blood pressure in AME patients (New et al. 1977), suggesting that an unknown mineralocorticoid activates the MR. Biochemical investigations in affected patients failed to identify a novel mineralocorticoid, but did show an absence of the enzyme 11βHSD (Ulick et al. 1979), resulting in impaired conversion of cortisol to cortisone. The significance of this was not clear until the cloning of the MR (Arriza et al. 1987) and *in-vitro* studies showing that cortisol activates the MR to a similar level as aldosterone (Stewart et al. 1987;Funder et al. 1988), leading to the hypothesis that *in-vivo* (where circulating levels of cortisol are 1000-fold higher than aldosterone), 11βHSD normally 'protects' the MR from over-activation by cortisol by converting it to cortisone, which does not activate the MR. This was confirmed upon the cloning of the *11βHSD-2* gene, which was shown to be expressed in the same cells of the nephron that express ENaC (Mune et al. 1995). As with GRA, overactivation of the MR causes the hypokalaemia and alkalosis.

1.1.3.3 Liddle Syndrome

Liddle syndrome is characterised by early onset hypertension, hypokalaemic alkalosis, suppressed renin activity and low plasma aldosterone. It is caused by deletions or missense mutations of the cytoplasmic C-terminal PPPXY (proline, proline, proline, any amino acid, tyrosine) domain of the ENaC β or γ subunits. The PPPXY domains bind Nedd4-1 and Nedd4-2 proteins as a first step in the ubiquitination and clearance of ENaC via clathrin-coated pits (Staub *et al*, 1996; Kamynina *et al*, 2001). Disruption of the PPPXY domain therefore causes reduced clearance of ENaC from the tubule membrane, resulting in increased ENaC numbers and activity, leading to salt retention and hypertension (Schild et al. 1995;Shimkets et al. 1997). Directly converse to Liddle syndrome, mutations that impair ENaC function cause autosomal recessive Psuedohypoaldosternism type I, characterised by salt wasting and hypotension (Chang et al. 1996).

1.1.3.4 Pseudohypoaldosteronism type II

Pseudohypoaldosteronism type II (PHAII), also know as Gordon Syndrome, is an autosomal dominant condition caused by mutations in serine-threonine kinase genes, *WNK1* and *WNK4* (Wilson et al. 2001). WNK stands for 'with no K', the WNKs are characterised by the lack of a conserved lysine (K) found in all other serine-threonine

kinases. Along with hypertension, affected individuals also show hyperkalaemia, hyperchloraemia and metabolic acidosis. The pathogenic mutations described so far in *WNK1* are all large deletions in the first intron that cause increased *WNK1* expression, whilst all known *WNK4* mutations are missense and cluster within few amino acids distal to the kinase domain of the protein. *WNK1* and *WNK4* expression have been localised to the distal convoluted tubules and cortical collecting ducts. *WNK1* is also expressed in the medullary collecting ducts. WNK1 protein is cytoplasmic, WNK4 is present only in the intercellular junctions in the distal convoluted tubules and in the cytoplasm and intercellular junctions in the cortical collecting duct (Wilson et al 2001). Recent experimental studies have investigated the functional changes caused by *WNK4* mutations and have provided novel insights into the mechanisms of renal chloride, sodium and potassium homeostasis. *In-vitro* studies have shown that WNK4 affects the activity of a number of ion channels and transporters. It has been demonstrated that wild-type WNK4 protein inhibits the Na-Cl cotransporter (NCCT) ion channel, which mediates sodium and chloride reabsorption in the distal convoluted tubule. PHAII *WNK4* mutations abolish the activation of NCCT, contributing to salt retention (Wilson et al. 2003). These findings are consistent with pathogenesis of Gitelman's syndrome, where loss-of-function NCCT mutations cause hypotension, hypokalaemia and metabolic alkalosis (Simon et al. 1996).

As stated, WNK4 expression extends beyond the convoluted tubules to the collecting duct, raising the possibility that it regulates ion transport in distal portions of the nephron; Kahle et al (2003) demonstrated that WNK4 inhibits the ROMK potassium channel, which reabsorbs potassium throughout distal nephron, they also showed that PHAII *WNK4* mutations increase this inhibition, decreasing potassium secretion. Furthermore, WNK4 has been demonstrated to regulate paracellular chloride ion transport via gap junctions in *in-vitro* monolayer cultures of kidney epithelial cells, PHAII-mutant WNK4 increases chloride ion transport, equivalent to increased chloride reabsorption in the collecting duct *in-vivo* (Kahle et al. 2004;Yamauchi et al. 2004).

An in-vivo study has further elucidated the mechanisms by which WNK4 affects sodium chloride and potassium regulation, and shown that it has a role in regulating the mass and activity of the distal convoluted tubule. Transgenic mice were generated to homozygously express two additional copies of either the wild-type or mutant (PHAII-causing equivalent) mouse *Wnk4* gene, these mice were designated Tg($Wnk4^{WT}$) and Tg($Wnk4^{PHAII}$), respectively (Lalioti et al. 2006). The Tg($Wnk4^{WT}$) mice exhibit reduced blood pressure

with normal serum K^+ levels. Tg($Wnk4^{PHAII}$) mice have raised blood pressure and hyperkalaemia equivalent to that seen in human PHAII patients. Ultrastructural analysis of the distal convoluted tubules of the transgenic mice showed marked effects of increased mutant and wild-type *Wnk4* expression: compared to wild-type mice, Tg($Wnk4^{PHAII}$) showed increased lumen surface area and NCCT expression, whilst Tg($Wnk4^{WT}$) had reduced lumen surface area and reduced NCCT expression. These findings correlate blood pressure and electrolyte balance with distal convoluted tubule morphology and distribution of NCCT. In order to confirm this association, Tg($Wnk4^{PHAII}$) mice were cross-bred with a NCCT-knockout, generating mice with PHAII Wnk4 mutations, but no NCCT. These mice had blood pressure similar to Tg($Wnk4^{WT}$), normal serum K^+ and normal distal convoluted tubule morphology (Lalioti et al 2006).

1.1.3.5 PPARγ Mutations Causing Insulin Resistance, Diabetes Mellitus and Hypertension

Peroxisome proliferator-activated receptor gamma (PPARγ) is a nuclear receptor family transcription factor involved in adipocyte differentiation (Tontonoz et al. 1994), it also promotes insulin-induced uptake of glucose and has high affinity for the anti-diabetic medications, thiazolidinediones (TZDs), which increase its activity (Lehmann et al. 1995). A cohort of insulin resistant patients was screened for mutations in the PPARγ genes, finding novel ligand binding domain mutations in two families displaying autosomal dominant early onset insulin resistance, type II diabetes and hypertension without obesity (Barroso et al. 1999). These mutations were shown to have dominant negative effect on PPARγ activity that the authors propose causes insulin insensitivity and diabetes whilst providing sufficient residual activity to control adipocity. Barosso et al propose that PPARγ may play a role in hypertension in these patients via increased vascular tone since TZDs lower blood pressure, block calcium channel activity in smooth muscle cells (Nakamura et al. 1998) and inhibit release of the potent vasoconstrictor endothelin-I from endothelial cells (Satoh et al. 1999).

1.1.3.6 Variably Penetrant Hypertension, Hypercholesterolaemia and Hypomagnesia

Hypertension, hypercholesterolaemia and hypomagnesia are among the risk factors for metabolic syndrome, which has a genetic component. A family study was performed on a kindred of 142 relatives of a patient with hypomagnesia (Wilson et al. 2004). An increased incidence of hypertension, hypercholesterolaemia and hypomagnesia was observed among the maternal lineage related to the proband (100% of those with hypomagnesia, 87% of those with hypertension and 73% of those with hypercholesterolaemia were on the maternal lineage). This implicated mitochondrial transmission and complete sequencing of the mitochondrial genome identified a novel mutation in the gene encoding transfer RNA for isoleucine ($tRNA^{Ile}$) in the maternal lineage. Each of the three traits measured had a penetrance of approximately 50% in patients carrying the mutation, implying phenotypic modifying effects of nuclear genome and/or environmental factors (Wilson et al 2004).

1.1.3.7 Hypertension with Brachydactyly

Hypertension with brachydactyly (shortened finger bones) is an autosomal dominant condition featuring normal renin-angiotensin system function. The cause of hypertension in affected patients is not fully understood, though there is evidence from brain magnetic resonance imaging that it may be caused by neurovascular compression of the ventrolateral medulla (one of the brain structures responsible for setting basal sympathetic tone) (Naraghi et al. 1997). Autonomic nervous system function has been investigated in affected patients, they show normal sympathetic nerve activity during rest, but exaggerated blood pressure increases following sympathetic stimuli with the alpha agonist phenylephrine during baroreceptor reflex blockade (Jordan et al. 2000). This study implies that hypertension in these patients could be related to abnormal baroreceptor reflex function. Genetically, the locus responsible for hypertension with brachydactyly was mapped to chromosome 12p by a genome-wide scan, though the gene has yet to be identified (Schuster et al. 1996).

1.1.3.8 Mineralocorticoid Receptor Mutation Causing Hypertension Exacerbated in Pregnancy

The MR mutation S810L was identified in a screen of early-onset hypertensive patients, to date it has been identified in eight individuals in one pedigree (Geller et al. 2000). S810L causes dominant hypertension before the age of 20 with marked exacerbation of hypertension during pregnancy. The S810L mutant receptor shows partial activation in the absence of steroids, but a normal response to aldosterone. However MR antagonists that usually bind but do not activate the wild-type MR have an agonist effect on the S810L receptor; this includes many steroids including progesterone, levels of which increase 100-fold during pregnancy, accounting for the dramatic increase in blood pressure during pregnancy in affected individuals (Geller et al 2000). This antagonist-to-agonist response in the S810L receptor is caused by a structural change in the receptor protein. Recent work has shown that the S810L MR receptor binds with high affinity and is transactivated by cortisone and 11-dehydrocorticosterone, the main cortisol and corticosterone metabolites in the distal nephron, suggesting that these are among the endogenous steroids responsible for early onset hypertension in men and non-pregnant women carrying MR S810L (Rafestin-Oblin et al. 2003). In contrast to hypertension exacerbated in pregnancy, loss-of-function frameshift or nonsense mutations in the MR gene cause autosomal dominant psuedohypoaldosteronism type I, typified by neonatal salt wasting and hypotension (Geller et al. 1998).

1.1.3.9 Early Onset Coronary Artery Disease and Other Cardiovascular Symptoms, Including Hypertension

A large kindred with a high prevalence of early coronary artery disease (CAD), hypertension, high low-density lipoprotein (LDL) cholesterol, high triglycerides, type II diabetes and osteoporosis was identified via an index case who presented with a myocardial infarction aged 48. Obesity was absent in the pedigree, despite the frequency of other symptoms associated with metabolic syndrome. Genome-wide microarray SNP genotyping of 19 members of 2 generations identified a 750,000 bp region on chromosome 12p with strong linkage to early CAD and high LDL cholesterol (Mani et al. 2007). The exons and intron/exon boundaries of all six annotated genes in this region were sequenced in the index case and a single missense mutation was found in the *LRP6* (LDL receptor-

related protein 6) gene causing an R611C amino acid change. LRP6 is one of a family of receptor proteins that interact with frizzled proteins in Wnt receptor pathways. Mice deficient in the mouse paralogue *LRP5* develop hypercholesterolaemia and glucose intolerance when fed high fat diets (Fujino et al. 2003) and deficiency of *LRP5* (in humans and mice) or *LRP6* (in mice) causes early severe osteoporosis (Gong et al. 2001;Kokubu et al. 2004). No other mutations were found in any of the other genes in the implicated region, the remaining affected members of the kindered all carried the *LRP6* R611C mutation, while it was absent from 4000 control chromosomes; *in-vitro* studies showed the R611C version of *LRP6* is biochemically less active than the wild-type (Mani et al 2007). While the mechanism by which the mutation causes this collection of symptoms is unclear, Wnt signalling pathways have been implicated in cardiovascular disease and osteoporosis in other research (Yamagata et al. 1996;Horikawa et al. 1997;Grant et al. 2006).

1.1.3.10 Monogenic Hypertension Genes in Essential Hypertension

With the possible exception of *WNK1,* none of the genes found to cause monogenic hypertension have been conclusively implicated in essential hypertension, though several have been investigated in candidate gene linkage and association studies. Regions of the genome implicated in the continuous phenotypes such as blood pressure are known as quantitative trait loci (QTL). The *11 β-hydroxylase* gene underlies a blood pressure QTL in the rat, *WNK1* and *LRP6* are located within a region of human chromosome 12 identified as a suggestive blood pressure QTL (Rice et al. 2000), while *WNK4* lies within a blood pressure QTL on chromosome 17 (Julier et al. 1997). An association study in Japanese essential hypertensives found no association between essential hypertension and *WNK1* (Kokubo et al. 2004). However, a family-based association study of 712 severely hypertensive families in the BRitish Genetics of HyperTension study (BRIGHT study, see section 1.1.4.2) identified a promoter polymorphism 3kb upstream from the *WNK1* gene associated with hypertension (Newhouse et al. 2005), while a second study associated *WNK1* haplotypes and single nucleotide polymorphisms spanning the *WNK1* coding region with variations in blood pressure in a study of 250 white European families (Tobin et al. 2005).

Alternative methods have also been applied to studies of human essential hypertension genetics, including1 analysis of candidate genes and genome-wide linkage and association studies. These approaches are discussed below.

1.1.4 Identifying Essential Hypertension Genes

Strategies to find genes involved in complex traits broadly fall into two categories, linkage and association studies. They can further be subdivided into candidate gene analysis and genome-wide scans. In candidate gene analysis, markers in physiologically relevant genes are tested for co-inheritance with the phenotype under study, while in genome-wide scans, no such assumptions are made and markers throughout the genome are analysed. Genetic markers used in linkage and association studies have advanced in recent years. Historically, restriction-fragment-length polymorphisms and satellite repeat markers were employed for genotyping, however, advances in the cataloguing of single-nucleotide polymorphisms (SNP) throughout the genome and automation of SNP genotyping have improved high-throughput genetic screening.

In linkage analysis, family cohorts are collected and affected and unaffected family members are phenotyped and genotyped. The genetic relationship between family members is taken into account in statistical analysis to identify markers that segregate with the phenotype under study. A popular method for linkage studies analyses affected sibling pairs, the hypothesis being that since siblings have 50% genetic identity, they should share markers near loci responsible for hypertension more often than would be expected by chance. The loci responsible for hypertension may differ between families, but if a sufficient number of families are studied, the most common effect alleles may be identified. Several factors affect the statistical power of linkage analyses, including the proportion of the trait variance due to genetic factors, the family structure, the number of families, the number of markers employed and the genetic distance between them.

In contrast, association studies involve genotyping and phenotyping unrelated affected and unaffected individuals to find candidate genes, thus the power of genetic relatedness is lost, but subject recruitment is significantly easier. Though association studies have been widely employed in candidate gene analysis, historically, genome-wide association studies were not feasible for the study of complex traits due to the number of subject required and the

subsequent cost of genotyping. However, the advent of cost-effective genome-wide SNP genotyping has recently led to the first publications in this field.

1.1.4.1 Candidate Gene Analysis in Human Essential Hypertension

Numerous studies have been carried out to investigate the involvement of genes that express proteins thought to be involved in blood pressure regulation in essential hypertension. Candidates include those from the renin-angiotensin system, cell signalling pathways, autonomic nervous system, and others. Notable examples are considered below. None of the candidate genes analysed so far have consistently been shown to affect blood pressure in all studies. Typically, as many negative associations are published for a candidate as positive; the apparent effect of a gene in one population is often not replicated in others. This exemplifies the extent of heterogeneity in essential hypertension aetiology, interactions between environmental and genetic factors in different populations lead to quantitatively different influences of genetic loci. This, coupled with differences in study design, size and methods, our incomplete understanding of the physiology blood pressure control, and the likely number of loci involved, reduces the likelihood of candidate gene studies in finding major effect loci.

1.1.4.1.1 Renin-Angiotensin System

Angiotensinogen (AGT), whose conversion to angiotensin I by renin is the first step in angiotensin II production, is an obvious functional candidate for investigation in blood pressure genetics. Jeunemaitre et al (1992b) published data showing significant association of the common M235T variant with hypertension in two family studies in populations in Salt Lake City, USA and Paris, France. The M235T was associated with higher plasma concentrations of angiotensinogen in hypertensives. These results were supported by observations that transgenic mice with additional copies of the *Agt* gene have higher blood pressure than wild-type mice (Kim et al. 1995). The functional cause of increased plasma AGT with the M235T variant were explained by the observation that it is in complete linkage (i.e. is always co-inherited) with a promoter polymorphism (-6G>A) that causes increased expression of *AGT* (Inoue et al. 1997). Many further studies attempted to replicate the findings of Jeunemaitre et al, with conflicting results. Meta analyses of case-control studies were performed, they tentatively concluded that the

M235T allele is associated with hypertension, but only in Caucasians, and caveats were attached that the association found may be affected by publication bias: concerns were raised regarding selection and reporting of properly matched controls to cases in many studies (Kunz et al. 1997;Staessen et al. 1999). This example highlights the difficulties in finding minor effect alleles, it is unclear whether the difficulties in replicating initial results reflect differences between populations, diagnostic criteria, case-control ascertainment, or the small effect on phenotype.

Angiotensin-I converting enzyme (ACE) is another central renin-angiotensin system component, catalysing the conversion angiotensin I to Angiotensin II. ACE-inhibitors are effective antihypertensive medication, and early genome-wide scans for causative genes in hypertensive rat models pointed to the region on rat chromosome 10 syntenic to human chromosome 17 that harbours the ACE gene (Hilbert et al. 1991;Jacob et al. 1991). A common insertion/deletion (I/D) polymorphism in humans has been shown to dictate the serum concentration of human ACE, homozygous I/I and D/D individuals have respectively 75% and 125% ACE levels of I/D individuals (Rigat et al. 1990). Linkage analysis in humans generated conflicting results, some studies have shown limited linkage to the ACE locus (O'Donnell et al. 1998;Higaki et al. 2000), however the prevailing view is that ACE genotype does not affect essential hypertension (Jeunemaitre et al. 1992a;Kreutz et al. 1995). This is backed up experimentally by the observation that transgenic mice with additional *Ace* gene copies do not have increased blood pressure despite increased plasma ACE levels (Krege et al. 1997). It may seem paradoxical that ACE-inhibitors are effective in reducing blood pressure while increased ACE activity does not increase it, however, this is explained by the finding that conversion of angiotensinogen to angiotensin I by renin is the rate-limiting step in renin-angiotensin system activation (Sealey et al. 1990).

1.1.4.1.2 Cell Signalling

G-proteins mediate the signal transduction of many vasoactive stimuli. Immortalised lymphoblasts from hypertensive patients were found to have higher G-protein activities than those from normotensive patients (Siffert et al. 1995). Mutation screening in the α, β, and γ subunits of heteromeric G-proteins identified a C825T polymorphism in the G-protein β3 subunit gene associated with hypertension in a Caucasian population, this mutation causes alternative splicing of the gene and the loss of a highly conserved 41

amino acid region (Siffert et al. 1998). Other studies in Japanese and German cohorts failed to replicate this association (Kato et al. 1998;Beige et al. 1999).

There is decreased responsiveness of the dopamine 1 G-protein-coupled-receptor in proximal tubules in essential hypertensives (Sanada et al. 1999), potentially disrupting the regulation of sodium excretion. Speirs et al (Speirs et al. 2004) performed an association study on variants of the G-protein-coupled-receptor protein 4 (GRK4) in a Caucasian population. The V allele of the A486V GRK4 variant showed an association with elevated blood pressure. Haplotypes of two other genes analysed in the same study (3β-hydroxysteroid dehydrogenase/isomerase, involved in synthesis of steroid hormones and protein phosphotase 1, a negative regulator of insulin signalling) showed no association with hypertension.

1.1.4.1.3 Adrenergic System

Sympathetic nervous system adrenergic receptors are clear hypertension candidate genes since the adrenergic system influences many aspects of blood pressure control such as vascular tone, cardiac output, renal sodium absorption and renin release. In black populations, variants in the α2 adrenergic receptor genes *ADRA2A* and *ADRA2C* have been associated in with hypertension in a number of small studies (Lockette et al. 1995;Svetkey et al. 1996). However a large association study in 1767 blacks recently found no association of *ADRA2A* and *ADRA2C* variants with hypertension and showed that these polymorphisms are not predictors of blood pressure, heart rate cardiac output or vascular resistance (Li et al. 2006).

Three common β2 adrenergic receptor (*ADRB2*) gene polymorphisms, Arg16Gly, Glu27Gln, and Thr64Ile have been linked to variations in receptor function but association studies have shown contrasting links to hypertension in various populations. The Gly16 variant was linked to hypertension in Afro-Caribbeans (Kotanko et al. 1997), and white Americans (Hoit et al. 2000). Both the Gly16 and Gln27 alleles were associated with hypertension in Han Chinese (Ge et al. 2005), while two further studies in Chinese (Gu et al. 2006) and Japanese (Kato et al. 2001) populations showed association with Gln27, but not Gly16. However an American study reported association with Gly16 and Glu27 (Bray et al. 2000). In addition, there have been a number of negative studies in several European, black and white American and African populations. Linkage studies in a Polish cohort performed at the Glasgow laboratory confirmed a blood pressure QTL on chromosome 5 at

ADRB2, but association analysis did not support a role of the three polymorphisms individually or by haplotype (Tomaszewski et al. 2002). Subsequent analysis in the same population assessed the interaction between *ADRB2* and neuropeptide Y (*NPY*) polymorphisms on cholesterol and triglyceride levels; the β2 adrenergic receptor and neuropeptide Y are co-expressed in several tissues and are involved in several aspects of lipid metabolism. There was a consistent interaction between the *ADRB2* Arg16Gly and Glu27Gln and *NPY* Leu7Pro variants in hypertensive patients with elevated low-density lipoprotein (LDL), but not hypertensive subjects with normal LDL cholesterol (Tomaszewski et al. 2004).

1.1.4.1.4 Fibroblast Growth Factor 1

Fibroblast growth factor 1 (*FGF1*) is located on chromosome 5 under the same blood pressure QTL as *ADRB2* (Tomaszewski et al 2002) and is functionally linked to blood pressure control by its role in stimulation of endothelin-1 release (Sugo et al. 2001), expression of the endothelin receptor (Li et al. 2003) and increased plasma catecholamines and corticosteroids (Matsumoto et al. 1998). Following improved QTL analysis tightening the blood pressure QTL to the region encoding *FGF1*, haplotype analysis showed that variation in the *FGF1* haploblock was associated with hypertension in a Polish cohort and implicated a SNP in *FGF1* intron 2 (Tomaszewski et al. 2007) furthermore, western blot analysis showed increased FGF1 expression in the kidneys of hypertensive patients compared to normotensives (Tomaszewski et al 2007).

1.1.4.1.5 Other Candidate Genes

Adducin is a dimeric cytoskeletal protein composed of α and β or γ subunits encoded by *ADD1*, *ADD2* and *ADD3* genes, respectively. It has been shown to activate the sodium-potassium ATPase (NaK ATPase) ion pump, mediating tubular sodium reabsorption (Ferrandi et al. 1999). The Milan hypertensive rat strain (MHS) exhibits increased sodium reabsorption, and carries *ADD1* and *ADD2* mutations that increase adducin activity (Tripodi et al. 1996). A number of studies have analysed the effects of *ADD1* polymorphisms in human essential hypertension in several populations (Bianchi 2005), six out of a total of 14 linkage studies showed positive associations, while 19 out of 22 association studies were positive.

The endothelial nitric oxide synthase gene (eNOS) is a robust candidate for hypertension genetics given its role in defence against endothelial oxidative stress (see section 1.3). A number of studies have analysed eNOS polymorphisms and hypertension with conflicting results. A recent meta-analysis combined the results of 35 association studies and only found association of an intron 4 polymorphism with hypertension assuming a recessive model in whites, no association was found in studies of east Asian or black subjects (Zintzaras et al. 2006).

Bradykinin receptors mediate the vasoactive and metabolic actions of bradykinin, a component of the kinin-kallikrein system (see table 1.1). SNPs within coding and regulatory regions of bradykinin receptor B1 and B2 (*BDKRB1* and *2*) were associated with hypertension in association studies in African American and American Caucasian populations (Cui et al. 2005). *BDKRB2* promoter polymorphisms have also been associated with hypertension in Chinese (Wang et al. 2001) and Japanese (Mukae et al. 1999) populations.

1.1.4.2 Genome-Wide Linkage Studies

More than twenty genome-wide linkage studies have been performed to search for essential hypertension loci, resulting in over 100 hypertension QTL (table 1.2). Table 1.2 illustrates the wide spread of hypertension QTL, every chromosome is represented, however, it also shows the clustering of QTL from different studies on several chromosomes, notably 1,2,3,17 and 18. It is possible that such overlapping QTL indicate the involvement of a small number of large-effect alleles responsible for a majority of essential hypertension, however, more evidence is required for this conclusion since many of the QTLs have only 'suggestive' genome-wide significance (Cowley, Jr. 2006). In general, there has been very little replication of QTL identification between populations, and no specific genes have yet been positively identified, this likely illustrates the genetic heterogeneity between different ethnic populations, and the possibility that a large number of genetic loci have small and interacting effects on blood pressure, rather than a few genes with large effects. However there has been recent progress with analysis of the BRitish Genetics of HyperTension (BRIGHT) study (Caulfield et al. 2003). This study initially recruited 2010 affected sibling pairs from 1599 families with severe hypertension (top 5% of blood pressure distribution) and included 3599 individuals in the genome-wide scan, it is the largest homogenous linkage study in hypertension genetics. Aside from exhibiting

Study	Phenotype	No. of subjects	Chromosomes	Population
(Bell et al. 2006)	Hypertension	3863	**5**,9,11,15,**16**,19	White
(Caulfield et al 2003)	Hypertension	3599	2,5,**6**,8,9	White
(Hunt et al. 2002)	Hypertension, SBP	2959	Hypertension: 1,7,12,15 SBP: **6**	White
(Levy et al. 2000)	SBP	1585	**17**,18	White
(Shmulewitz et al. 2006)	SBP	1546	20	Micronesian
(Xu et al. 1999)	BP	1450	3,11,15,16,17	Chinese
(Rao et al. 2003)	Hypertension	1300	2	African-American
(Cooper et al. 2002)	DBP	792	2,3,5,7,10,19	Nigerian
(Hsueh et al. 2000)	DBP	694	2	White
(Rice et al 2000)	SBP	679	1,2,5,7,8,19	White
(Pankow et al. 2000)	SBP	636	6,18	White
(Harrap et al. 2002)	SBP	548	1,4,16,X	White

Table 1.2 – Continued overleaf

Study	Phenotype	No. of subjects	Chromosomes	Population
(Rice et al. 2002)	SBP	519	3,11	White
(Hamet et al. 2005)	DBP, Mean BP	500	DBP: 1,3,16. Mean BP: 16	French Canadian
(Atwood et al. 2001)	SBP	495	**2**,8,18,21	Mexican
(Kristjansson et al. 2002)	Hypertension	490	2,11,17,**18**	White
(Benjafield et al. 2005)	Hypertension	481	1,4	White
(Krushkal et al. 1999)	SBP	427	**2**,**5**,**6**,9,**15**,16,18,20,21	White
(Zhu et al. 2001)	Hypertension	393	2,3,8,15	Chinese
(Cheng et al. 2001)	SBP	390	1,2,7	White
(Pausova et al. 2005)	Hypertension	389	**1**,8,**11**,13	White
(Allayee et al. 2001)	SBP	388	4,6,8,19	White
(Thiel et al. 2003)	DBP	320	1	White
(Sharma et al. 2000)	Hypertension	288	11	White

Table 1.2 – Continued overleaf

Study	Phenotype	No. of subjects	Chromosomes	Population
(Ciullo et al. 2006)	Hypertension	173	1,4,**8**	White
(Gong et al. 2003)	Hypertension	158	**12**	Chinese
(Perola et al. 2000)	Hypertension	113	1,2,3,22,X	White
(Angius et al. 2002)	Hypertension	77	1,2,13,15,17,19	White

Table 1.2 - Genome-wide linkage studies for essential hypertension loci in humans

Numbers in bold represent chromosomes on which loci were found that surpassed genome-wide significance, otherwise, linkage is suggestive according to the criteria set by authors. Adapted from Cowley, Jr (2006) and Binder (2007).

severe hypertension, the study population were also selected on the basis of heredity, all participants were of white British ancestry at least as far as grandparents. The initial publication identified a locus on chromosome 6q that achieved genome-wide significance, and three further loci with suggestive significance on chromosomes 2q, 5q and 9q (Caulfield et al 2003). The locus at 6q was received with caution in the literature since it was located near the telomere of the chromosome, where linkage evidence can be hard to interpret (Harrap 2003). A follow-up study included additional polymorphic markers in the regions of interest, and increased the study cohort to 2142 affected sibling pairs (Munroe et al. 2006). Support for the loci at 2q, 6q and 9q were diminished in this analysis, however, there was increased support for linkage to the locus at 15q, and two further regions at 1q and 11q achieved suggestive significance. The locus at 15q was further supported by a confirmatory linkage study on a second cohort of families, or trios, comprising an affected proband and either two parents or sibling and single parent (Munroe et al 2006).

Novel statistical techniques have also been employed in analyses of the BRIGHT dataset, including a genome-wide association study specifically designed to identify pairs of interacting loci that contribute to hypertension, the first such study performed in humans (Bell et al 2006). Four pairs of loci that individually did not have effects in the single-locus scan attained suggestive or genome-wide significance in this analysis, highlighting the importance of considering gene interactions in complex disease genetics (Bell et al 2006). Wallace et al (2006) developed an analytical method to integrate blood pressure measurements and associated phenotypic data, or covariates, collected on all BRIGHT study participants (such as serum and urine metabolites and biometric measurements) to find genetic loci linked to hypertension and the covariates. Blood pressure loci associated with leaner body-mass index and renal function were identified on chromosomes 20q and 5q, respectively. Meanwhile, analysis of the data on anti-hypertensive treatments in the BRIGHT population implicate a region on chromosome 2p with non-responsiveness to antidiuretics and beta-blockers (Padmanabhan et al. 2006).

1.1.4.3 Genome-Wide Association Studies

As mentioned above, the cost of genome-wide genetic analysis at sufficient marker density in large enough study populations historically precluded genome-wide association studies for complex diseases. However, low-cost genotyping technologies have recently led to the first publications of genome-wide association studies. The largest study to date, and the

only one so far to address essential hypertension, was a collaborative effort between over 50 research groups comprising the Wellcome Trust Case Control Consortium. The study covered 7 complex diseases in the British population: bipolar disorder, coronary artery disease, Crohn's disease, hypertension, rheumatoid arthritis, type 1 and type 2 diabetes, and included approximately 2,000 affected individuals for each disease and 3,000 common controls (The Wellcome Trust Case Control Consortium 2007). Over 500,000 SNPs were genotyped per subject, using Affymetrix 500K Mapping Array chips.

The study confirmed 13 out of 15 previously reported genetic loci with strong prior evidence of linkage from previous replication studies (none for hypertension), and reported 21 loci that achieved genome-wide significance ($p<5x10^{-7}$) across 6 of the diseases, follow-up publications have replicated a number of these findings in other populations (Todd et al. 2007;Parkes et al. 2007;Zeggini et al. 2007). None were hypertension loci, though a similar number of loci achieved significance between $p=10^{-4}$ and $p=10^{-7}$ for hypertension as the other diseases. Explanations proposed include the possibility that essential hypertension may have fewer large-effect alleles than the other conditions studied, or that they may lie within regions poorly represented SNPs in the array, for example the authors reported that the *WNK1* locus is poorly tagged. Another more likely explanation is that the control population contained a number of hypertensives; the controls were not phenotyped, they constituted 1500 individuals from the 1958 British Birth Cohort and 1500 blood donors. The authors state that an incidence of the disease under consideration of 5% in the control group would have the same effect on power in the final analysis as a reduction in sample size by 10%. Given a likely prevalence of hypertension in the control group of approximately 25% or more, the effect on the power would be substantial. It is important to emphasise that this study was in many ways a very successful proof-of-principle publication, testing the effectiveness of large inter-disciplinary collaborations, novel technologies and data analysis methods. Future genome-wide association scans for essential hypertension will include appropriately phenotyped non-affected controls, so called 'hypercontrols' (The Wellcome Trust Case Control Consortium 2007).

1.2 Rat Models of Human Hypertension

The rat is an invaluable tool in physiological and genetic hypertension research, being suitable for detailed physiological study and large breeding experiments (Rapp 2000). Rats

are also experimentally advantageous given the ability to closely control factors such as diet and medication that are not be possible in experiments with humans. In addition, the draft rat genome sequence (covering an estimated 90% of the 2.8 Gb Brown Norway rat genome) has recently become available to researchers (Gibbs et al. 2004). Several inbred rat strains have been selectively bred to display particular hypertensive and normotensive phenotypes. An understanding of the genetic factors that influence blood pressure in these rats will provide insights into blood pressure regulation in humans, however it is important to note that the same genes found to impact blood pressure in inbred rats may not be factors in human essential hypertension, rather that they will inform researchers as to which physiological processes and pathways are most significant.

An inbred strain is derived by selecting for a particular trait over several generations from an outbred stock, followed by twenty generations of brother/sister mating to fix the strain, resulting in a genetically identical population. The selection procedure can include provocative dietary or environmental stimuli such as high-salt diet or stress induced by restraint. Divergent strains can also be derived simultaneously with opposing phenotypic responses to such stimuli, such as in the case of Dahl salt sensitive and Dahl salt resistant rats. Each of these strains was derived from outbred Sprague-Dawley rats fed a high salt (8% NaCl) diet; the salt sensitive rats develop high blood pressure when fed a high salt diet, while the salt resistant strain remains normotensive (Dahl et al. 1962a;Dahl et al. 1962b). The original Dahl salt sensitive and resistant rats were maintained as outbred strains, but have subsequently been fixed by two groups (Rapp et al. 1985;Iwai et al. 1986). Table 1.3 lists the common inbred hypertensive rat strains.

1.2.1 The Stroke-Prone Spontaneously Hypertensive Rat (SHRSP)

The Glasgow laboratory maintains a colony of stroke-prone spontaneously hypertensive (SHRSP) rats and a colony of inbred normotensive Wistar Kyoto (WKY) rats. The specific strains are known as $SHRSP_{Gla}$ and WKY_{Gla} but are referred to in this text as WKY and SHRSP from here. The SHRSP was derived from the spontaneously hypertensive rat (SHR), which was in turn selectively bred for hypertension from the normotensive Wistar-Kyoto (WKY) strain by phenotypic selection without dietary or environmental influences (Okamoto et al. 1963). The SHRSP was selectively bred on the basis of its increased incidence of stroke (Okamoto et al. 1974;Yamori 1994); it displays higher blood pressure than the SHR, but also has specific genetic factors that predispose it to cerebrovascular

Strains	Origin	Lines	Original Stock	Reference
Genetically hypertensive (GH)	New Zealand	H,C	Wistar derived	(Smirk et al. 1958)
Dahl salt sensitive (DSS) Dahl salt resistant (DSR)	USA	H,L	Sprague-Dawley	(Dahl et al 1962a;Dahl et al 1962b)
Spontaneously hypertensive rat (SHR)	Japan	H	Wistar derived	(Okamoto et al 1963)
DOCA salt sensitive Sabra (SBH) DOCA salt resistant Sabra (SBN)	Israel	H,L	Unknown	(Ben Ishay et al. 1972)
Lyon hypertensive (LH) Lyon Normotensive (LN) Lyon low blood pressure (LL)	France	H,C,L	Sprague-Dawley	(Dupont et al. 1973)
Stroke-prone spontaneously hypertensive rat (SHRSP)	Japan	H	Wistar derived	(Okamoto et al 1974)
Milan hypertensive strain (MHS) Milan normotensive strain (MNS)	Italy	H,C	Wistar	(Bianchi et al. 1974b)
Fawn hooded hypertensive (FHH) Fawn hooded low blood pressure (FHL)	Netherlands	H,L	German brown x white Lashley	(Kuijpers et al. 1984)
Inherited stress-induced arterial hypertensive (ISIAH)	Russia	H	Wistar derived	(Markel 1985)
Prague hypertensive (PHR) Prague normotensive (PNR)	Czech Republic	H,L	Wistar	(Heller et al. 1993)

Table 1.3 - Rat inbred models used in hypertension genetic research

Modified from Rapp (2000) H: High blood pressure. L: Low blood pressure, C: Control strain

lesions. This was demonstrated by backcrosses with SHR rats to generate populations with respectively 25%, 50% and 75% SHRSP genetic composition, incidence of stroke was positively correlated with increasing percentage of SHRSP genotype after salt challenge to result in the same blood pressures in each group (Nagaoka et al. 1976). A genome-wide scan for stroke susceptibility performed by cross-breeding SHRSP and SHR rats revealed hypertension-independent stroke susceptibility QTLs on chromosomes 1, 4 and 5 in the SHRSP, of which the chromosome 1 QTL was reported to account for 17% of phenotypic variance (Rubattu et al. 1996). Reciprocal congenic strains (see below for a discussion on congenic strains) between the SHRSP and SHR recently further confirmed the effect of the chromosome 1 stroke susceptibility QTL (Rubattu et al. 2006). A genome-wide scan performed at the Glasgow laboratory located blood a pressure-independent chromosome 5 QTL for ischaemic stroke severity following permanent occlusion of the middle cerebral artery. The locus was identified following breeding between the SHRSP and WKY and accounted for 67% of phenotypic variance (Jeffs et al. 1997). Subsequent investigations of chromosome 5 QTL candidate genes, atrial natiuretic peptide (*Anp*) and brain natiuretic peptide (*Bnp*) by sequencing, expression and functional analysis excluded them as causative genes for this phenotype (Brosnan et al. 1999).

Hypertension in the SHRSP, as in other hypertensive strains, is more pronounced in males, high blood pressure is fully established at approximately 180 mmHg in males and 150 mmHg in females by 12 weeks of age, compared to 130 mmHg in WKY rats of the same age (both sexes) (Davidson et al. 1995), the genetic influence of the Y chromosome in this sexual dimorphism was proved by the generation of reciprocal Y chromosome consomic strains (rats selectively bred to be of one genotype throughout the genome except for one chromosome, which is derived from a different strain) between the SHRSP and WKY, transferring the SHRSP Y chromosome onto the background of the WKY increased blood pressure, while the WKY Y chromosome reduced blood pressure in the SHRSP (Negrin et al. 2001). SHRSP rats are very salt sensitive, replacing drinking water with a 1% salt solution results in a blood pressure increase to approximately 240 mmHg in males and 180 mmHg in females while the blood pressure of WKY rats does not rise following the same treatment (Jeffs et al. 2000). In addition to high blood pressure and increased incidence of stroke, the SHRSP also displays many other symptoms related to human cardiovascular disease including left ventricular hypertrophy (Clark et al. 1996), and endothelial dysfunction (McIntyre et al. 1997;Kerr et al. 1999). It is also a model of the metabolic

syndrome, isolated SHRSP adipocytes display impaired glucose transport and abnormal non-esterified fatty acid (NEFA) metabolism (Collison et al. 2000). In experiments performed in Glasgow, fructose-fed SHRSP rats showed impaired glucose tolerance, increased plasma triglycerides and NEFA levels compared to fructose-fed WKY rats (Strahorn et al. 2005). In the same study, using congenic and consomic SHRSP rats harbouring WKY genes, it was demonstrated that genes on chromosome 2 and the Y chromosome act individually and interact to influence glucose metabolism (Strahorn et al 2005).

1.2.2 Identifying Quantitative Trait Loci

Genome-wide scans in segregating rat populations involve an initial cross between a hypertensive and a normotensive strain to generate heterozygotic F1 progeny. Typically, these crosses involve equal numbers of matings between hypertensive males and normotensive females and between hypertensive females and normotensive males. The F1 generation are brother-sister mated to generate F2 animals of random genetic compliments of the original parental strains. All F2 animals are genotyped with polymorphic markers spanning the genome and phenotyped for continuous traits (such as blood pressure, pulse pressure, left-ventricular mass etc.). Genotype and phenotype data is entered into computer software that calculates for each trait the probability that set genomic positions are linked to it. This probability is presented as a logarithm of odds (LOD) ratio of the likelihood that a position is linked to a trait versus the likelihood that it isn't linked, given the positions and genotypes of flanking markers and the phenotype of animals with each genotype. The significance LOD threshold for a QTL is traditionally set at >3.0 (corresponding to an odds ratio of 1/1000), however, specific thresholds can be derived for each QTL calculation based on individual experimental factors such as genome size, genetic model for inheritance of the QTL (e.g. dominant/recessive etc.) and breeding regime (Lander et al. 1995). QTL prediction provides an estimation of the percentage of variance in the quantitative trait accounted for by the QTL; blood pressure QTLs typically individually account for 5-15% of blood pressure variance, increasing marker density in the genome wide scan beyond every 10 cM does not improve QTL localisation (Darvasi et al. 1993), the greater the phenotypic effect the more likely it will be identified. Increasing the number of animals in the study also increases precision, however there are obvious cost implications, studies with 200-300 F2 rats generally locate a QTL within 20 to 35 cM

(Rapp 2000), a region likely to contain over a thousand genes. A genome-wide scan may provide a complicated picture of genomic linkage to a trait. Multiple QTL peaks may cluster in a particular region of a chromosome, overlapping to obscure the number of linked sites and their exact locations. It is important to emphasise that a QTL identified in a cross between two inbred strains may not be identified in experiments involving other strains, or in the same strains under different environmental conditions (such as diet and age of rats) since the gene(s) underlying a QTL may not be functionally polymorphic in all situations. For example there may not be sequence differences between other pairs of strains at the loci underlying the QTL, or the gene(s) may only affect blood pressure control at a certain developmental stage our dietary regime. Genome-wide scans have identified over 80 QTLs for blood pressure and associated phenotypes on almost every rat chromosome (Rapp 2000;Twigger et al. 2007).

1.2.3 Recombinant Inbred Strains

Recombinant inbred strains can be generated for QTL identification as an alternative to linkage analysis in segregating populations. The principal of the breeding program is similar: inbred hypertensive and normotensive strains are bred to produce F1 progeny which are brother-sister mated to produce an F2 generation. F2 rats are randomly segregated into breeding pairs that become founders of strains bred to homozygosity by 20 generations of brother/sister mating. Rather than a single generation of rats, a panel of recombinant inbred strains is generated each with a random genomic compliment from the hypertensive and normotensive parental strains. Each strain can be genotyped and phenotyped to identify QTLs as in segregating populations. There are advantages of recombinant inbred strains such as the ability to phenotype many animals from the same strain, potentially in different environments to assess genotype/phenotype interactions, and to examine many different animals at different stages of development to measure genetic effects at different developmental stages. The cost of developing and maintaining the strains is the main disadvantage. A panel of recombinant inbred strains for the study blood of pressure genetics were bred by Pravenec and colleagues using SHR and normotensive Brown Norway (BN) rats as progenitor strains. The 31 strains showed blood pressure continuously distributed between the BN and SHR (Pravenec et al. 1989). This panel of strains has subsequently been used in a number of studies examining multiple cardiovascular, behavioural and developmental trait traits (reviewed by Printz et al. 2003),

and was also applied in a landmark expression genetics study, discussed in section 1.2.3.4 (Hubner et al. 2005).

1.2.3.1 Congenic Strains

QTLs identified by genome wide scans are too large for gene identification by positional cloning methods, a powerful method for interrogating and narrowing QTL intervals is the generation of congenic and subcongenic strains. Congenic breeding involves selectively introgressing the genetic compliment covering the QTL from a 'donor' strain onto the background of the 'recipient' strain to produce a rat of entirely recipient genotype except at the QTL (figure 1.2). The phenotypes of the congenic rats compared to those of the original donor and recipient strains are used to confirm the effects of the genes underlying the QTL. In traditional congenic breeding once the QTL has been introgressed, the background is 'cleaned' of excess donor genotype by at least 8 backcrosses to the recipient parental strain, guaranteeing >99% recipient genotype in the final congenic strain. This strategy has been superseded in most congenics laboratories by 'speed' or marker-assisted congenic breeding, where polymorphic markers throughout the genome are genotyped at each back-cross to select the offspring with the least genetic input from the donor strain (except at the QTL) (Lander et al. 1994). With marker-assisted breeding, a congenic strain is typically produced within 4 backcrosses (Jeffs et al 2000), figure 1.2.

1.2.3.2 Subcongenics

Since a congenic strain necessarily has to encompass an entire QTL to confirm its effect, the introgressed region will contain too many genes to provide a workable number of functional candidate genes. Thus, progressively smaller genomic regions can be captured in congenic substrains (subcongenics) in order to localise the QTL to smaller genetic intervals with fewer candidate genes. Subcongenics are generated in the same manner as congenics, using the original congenic as the donor strain and relying on recombination events within the original congenic region to truncate the congenic interval in the resultant strain.

Successful application of congenic breeding is exemplified by the series of experiments that confirmed the gene encoding 11-β-hydroxylase (*Cyp11b1,* the human homologue of which is mutated monogenic GRA – see section 1.1.3.1), as responsible for a blood

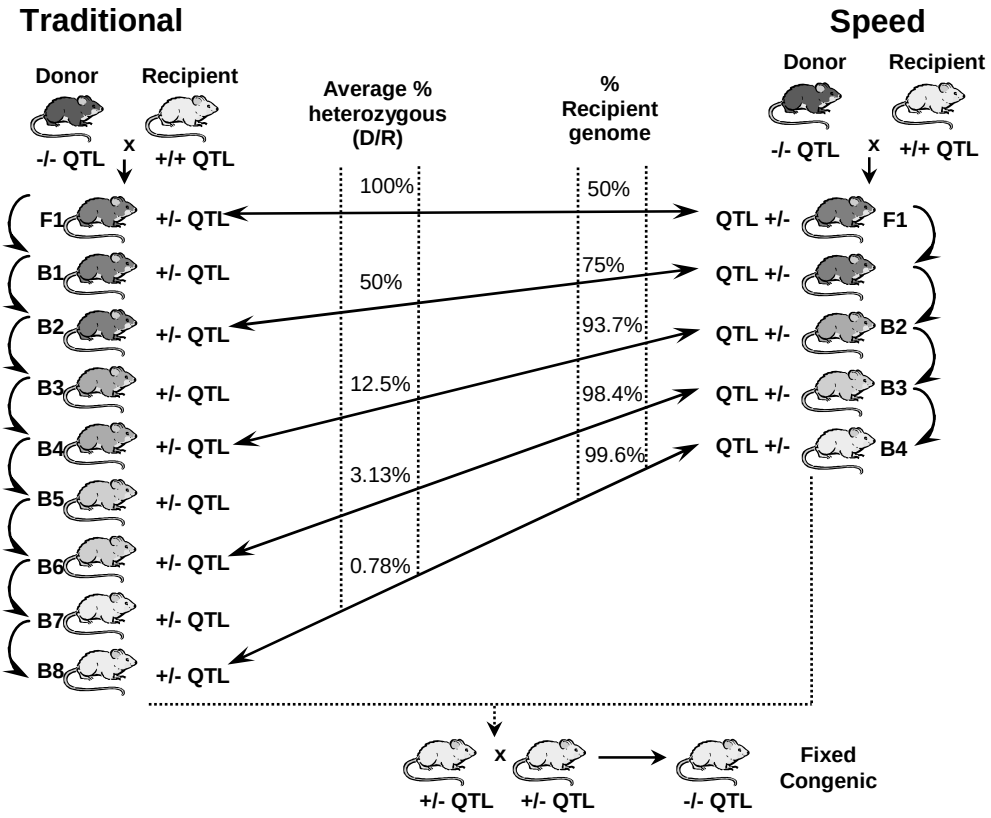

Figure 1.2 - Traditional and speed congenic breeding

Decreasing shading from grey to white represents serial dilution of the donor genome in the genetic background. D: donor strain alleles, R: recipient strain alleles, B: backcross, F1: first filial generation.

pressure QTL on chromosome 7 in the Dahl salt sensitive rat. Biochemical studies showed that the Dahl salt-sensitive rat (DSS) has higher 11-β-hydroxylase activity than the Dahl-salt resistant rat (DSR), resulting in a higher adrenal concentration of 18-hydroxy-11deoxycorticosterone (18-OH-DOC) in the DSS (Rapp et al. 1971). 18-OH-DOC has weak mineralocorticoid activity, its increased abundance was proposed to account for a degree of the salt sensitivity in the DSS (Rapp et al. 1972). Five nucleotide differences causing amino acid changes were identified between the DSR and DSS *Cyp11b1* sequences, of which those affecting amino acid residues 381 and 384 were shown to be the main determinants of 11-β-hydroxylase activity *in-vitro* (Matsukawa et al. 1993;Nonaka et al. 1998). F1 rats from crosses between DSS and DSR rats were backcrossed with DSS rats to generate an F2 population which were phenotyped and genotyped at informative markers throughout chromosome 7 (Cicila et al. 1997). Note that this differs from the

protocol for linkage analysis outlined in section 1.2.2**,** where the F1 generation is brother-sister mated. In this instance the DSS allele had a greater effect in animals with a greater proportion of DSS background genotype (Cicila et al. 1993), hence the backcross was 'weighted' to generate rats with measurable phenotypic differences to the parental strains. The linkage analysis showed suggestive linkage for blood pressure at the locus on chromosome 7 covering *Cyp11b1* and a congenic strain (S.R-Cyp11b1) was generated by introgressing a 20.2 cM region from DSR on to the DSS background. S.R-Cyp11b1 had a significantly lower blood pressure (by >20mmHg) compared to the DSS on a 4% NaCl diet (Cicila et al 1997). Subsequent studies generated subcongenic strains from S.R-Cyp11b1 to ultimately narrow the congenic interval to a 177 kb segment containing *Cyp11b1* that is responsible for approximately 15 mmHg lower blood pressure in the congenic strain compared to DSS on a 2% NaCl diet (Cicila et al. 2001;Garrett et al. 2003). Although this region also contains eight other genes, they have no known physiological role in blood pressure regulation and 177 kb remains the smallest individual congenic interval containing a QTL in mammalian genetics (Garrett et al 2003).

The Glasgow laboratory maintains a number of congenic strains harbouring blood pressure QTLs. The original blood pressure genome-wide scan involved 1 male SHRSP mating with 2 female WKYs and 1 male WKY mating with 2 female SHRSPs, 3 males and 6 females from each F1 generation were brother-sister mated to produce the F2 generation. At 16 weeks of age, blood pressure telemetry catheter/transmitters were implanted into the abdominal aorta of the rats, following 12 days post-operative rest, systolic and diastolic blood pressure, heart rate and motor activity were monitored via receivers placed under the cages and 'baseline' blood pressure was recorded for 4 days. Subsequently, animals were administered 1% NaCl in drinking water for 12 days, the last four days of which constituted 'salt loaded' haemodynamic measurement. The animals were then euthanized and body weight, heart weight, and left ventricular and septum mass were determined (Clark et al 1996). Genotyping was performed with a panel of 181 informative microsatellite markers throughout the genome. Using these markers, MAPMAKER software (Lander et al. 1987) identified two significant (LOD>3.0) blood pressure QTLs for blood pressure on chromosome 2 in males, one for baseline and salt-loaded systolic and diastolic blood pressure (for the purposes of this discussion named QTL1), and one for salt-loaded diastolic blood pressure (QTL2). Each QTL accounted for 24-31% of variance in blood pressure. A third significant QTL for baseline pulse pressure and salt-loaded

diastolic and systolic blood pressure was identified on chromosome 3 in males, each accounting for over 30% of trait variance, while a suggestive QTL for left-ventricular hypertrophy was also located on chromosome 14 in males (Clark et al 1996). The chromosome 2 blood pressure QTLs (QTL1 and QTL2) were further analysed by the creation of four congenic strains, utilising the 'speed' congenic strategy to introgress sections of WKY chromosome 2 onto the background of the SHRSP, and vice-versa (Jeffs et al 2000), figure 1.3. SP.WKYGla2a, in which both QTLs were transferred, showed an approximate 20 mmHg reduction in basal blood pressure compared to the SHRSP and a 40 mmHg reduction under salt loading. WKY.SPGla2c is the reciprocal strain, and showed a similar increase in blood pressure compared to the WKY at baseline, but no further increase under salt loading. The difference between these responses highlights an interesting and commonly observed phenomenon in congenic breeding whereby the background genotype of the recipient strain dictates the phenotypic effect observed (Rapp 2000). The SHRSP is more permissive to blood pressure changes by introduction of WKY genetic material than the reciprocal transfer; the complex deleterious phenotype is more likely to be corrected than induced by the transfer of a small chromosomal segment. Comparisons between the blood pressures of SP.WKYGla2b versus SHRSP and WKY.SPGla2d versus WKY showed no significant differences, the region transferred in the construction of SP.WKYGla2b does not cover either blood pressure QTL, while the introgressed region in WKY.SPGla2d covers QTL1 alone (Jeffs et al 2000), figure 1.3.

Other research groups have also identified blood pressure QTLs on rat chromosome 2, indeed 19 are listed with a LOD score of over 3.0 in the Rat Genome Database (Twigger et al 2007). Notably, two genome-wide scans were published concurrently involving crosses between salt-challenged (8% NaCl) Dahl salt sensitive (DSS) and Milan normotensive (MNS) rats and between DSS and WKY rats, (Deng et al. 1994). Both scans identified a blood pressure QTL on chromosome 2 that overlaps QTL2 found in the genome-wide scan between SHRSP and WKY in the Glasgow laboratory. Numerous congenic and subcongenic strains have been generated to investigate these QTLs, substitution mapping (where the limits of a QTL are inferred by analysing the blood pressures of subcongenic strains with overlapping congenic intervals) in DSS/MNS and DSS/WKY subcongenics have dissected the QTLs to at least 3 smaller interacting QTLs in each case (Dutil et al. 2001;Garrett et al. 2002;Dutil et al. 2005).

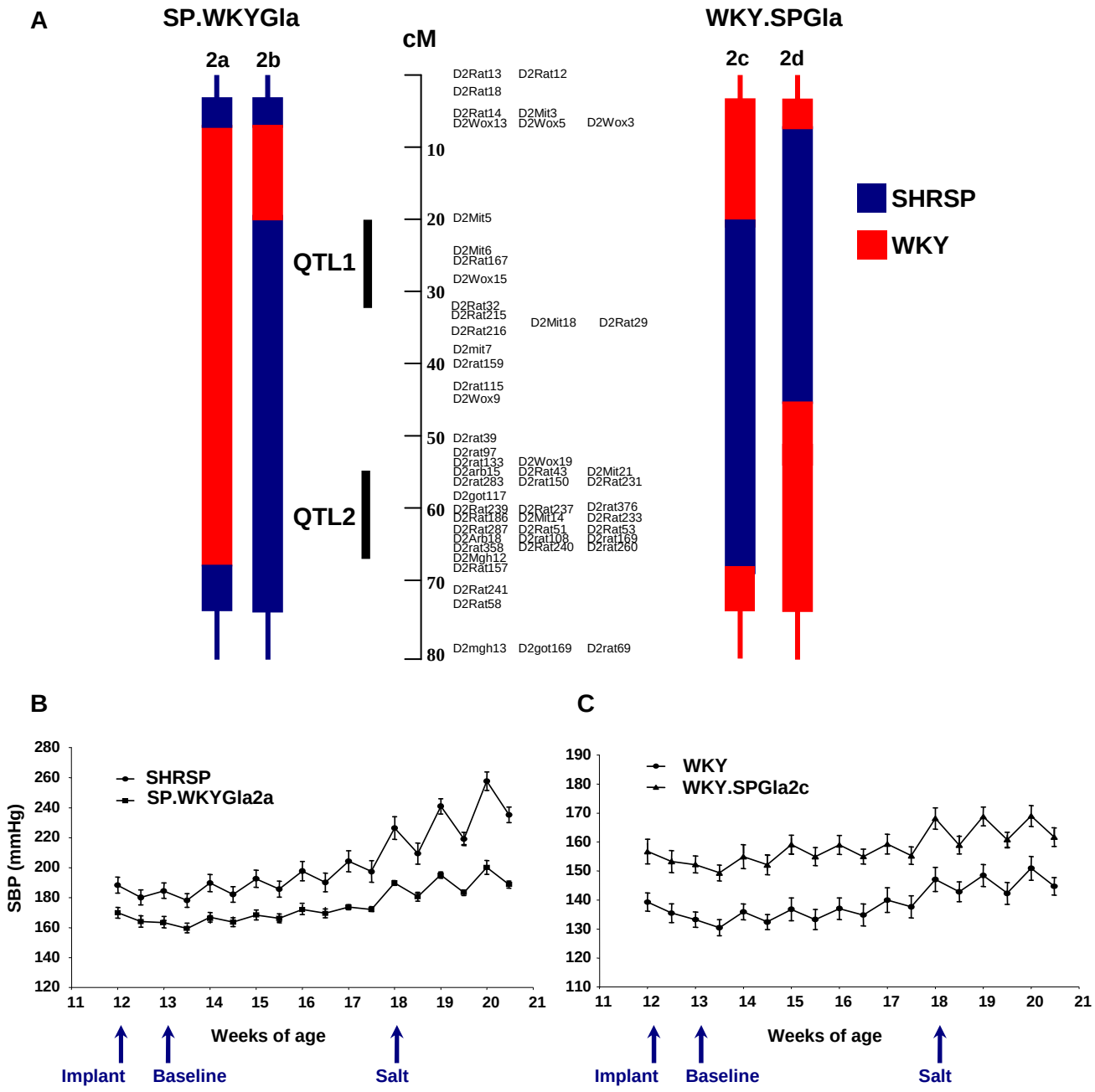

Figure 1.3 - Chromosome 2 congenic strains and blood pressures

(A) Details of chromosome 2 regions introgressed in the construction of reciprocal transgenics. SP.WKYGla2a and WKY.SPGla2c congenic intervals included QTL1 and QTL2. **(B)** and **(C)** Baseline and salt-loaded blood pressures of SP.WKYGla2a and WKY.SPGla2c. Permissiveness of genetic background is illustrated by loss of salt sensitivity in SP.WKYGla2a compared to the SHRSP, while WKY.SPGla2c was not salt sensitive. Adapted from Jeffs et al 2000.

1.2.3.3 Microarray Expression Analysis and Congenics

The advent of microarray technology has enabled the simultaneous measurement of many thousands of messenger RNAs in tissue or blood samples. They are very well suited to investigation of congenic strains for identification of candidate genes. Gene expression in parental strains can be compared to that of congenics, genes mapping to the congenic interval that are differentially expressed between the congenic and recipient parental strain but not between the congenic and donor parental strain are candidates that can be followed up in further experiments.

Research in the Glasgow laboratory employed subcongenic breeding and microarray expression analysis to follow up the work performed by Jeffs et al (2000). The SP.WKYGla2c* strain (from here referred to as 2c*) was derived from the SP.WKYGla2a (referred to as 2a) strain, the congenic interval covers QTL2 only, spanning approximately 20 cM and 2c* rats exhibit significantly reduced baseline blood pressure compared to the SHRSP, at levels comparable to the 2a strain (figure 1.4) (McBride et al. 2003). Microarrays measuring expression of 26379 probe sets were performed on cDNA derived from the kidneys of WKY, SHRSP and 2c* rats. 45 probe sets were found to be significantly differentially expressed between the WKY and SHRSP strains, of these, 12 were also differentially expressed between the SHRSP and 2c*, four of which had a known chromosomal location, with 3 of them mapping to the 2c* congenic interval. These three probe sets represented the glutathione s-transferase μ-type 1 (*Gstm1*) gene (NB – in the publication the gene is referred to as *Gstm2*, it was incorrectly annotated in the rat genome databases at the time). Quantitative reverse transcription polymerase chain reaction (PCR) was employed to measure mRNA expression levels of *Gstm1* in SHRSP, 2c* and WKY kidneys, confirming the differential expression seen in the microarrays (McBride et al 2003). *Gstm1*, an oxidative stress-defence gene, has subsequently become a focus of further investigation into hypertension genetics in the Glasgow laboratory, and is the subject for much of the research in this thesis, part of which contributed to a publication in 2005 (McBride et al. 2005). This paper demonstrated that reduced *Gstm1* expression coincided with hypertension in comparisons between a number of hypertensive and normotensive strains, and that promoter polymorphisms in the SHRSP and SHR may affect *Gstm1* expression. Furthermore, Gstm1 protein was localised to the principal cells of the collecting ducts and increased renal oxidative stress was demonstrated in the SHRSP,

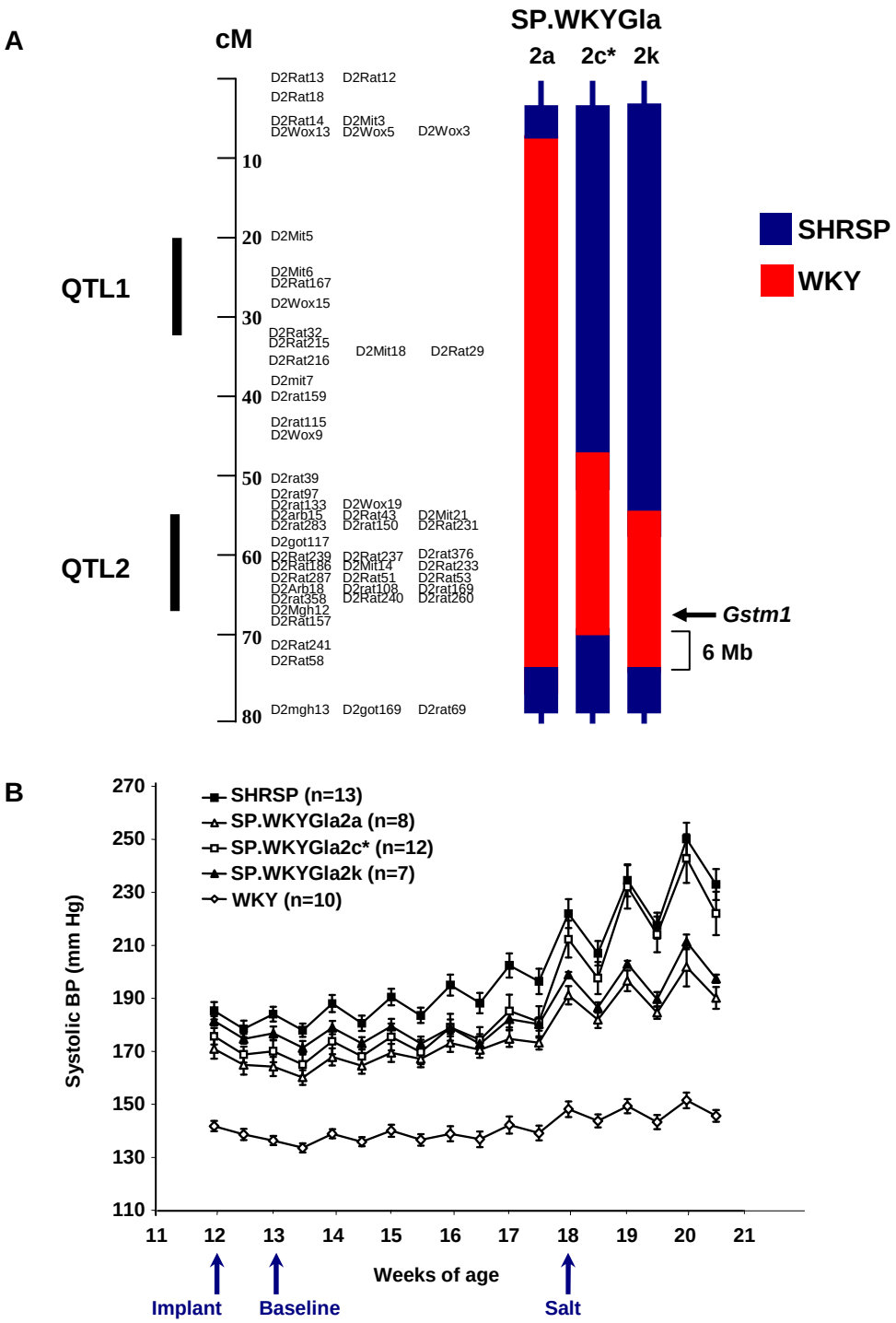

Figure 1.4 - Chromosome 2 subcongenic strains derived from SP.WKYGla2a

(A) 2c* and 2k congenic intervals cover QTL2 and *Gstm1*, the distal 6 Mb of the 2k interval may encode genes that account for the salt-resistance of the 2a and 2k strains. **(B)** Basal and salt-loaded blood pressures of SHRSP, 2a, 2c*, 2k and WKY strains. Figure adapted from Mcbride et al (2003) and Graham et al (2007).

suggesting a pathophysiological role for *Gstm1* in hypertension and oxidative stress (Mcbride et al. 2005, see also chapter 4).

A recent publication also investigated transcriptional changes in chromosome 2 genes thought to influence salt sensitivity in the SHRSP and congenic rats (Graham et al. 2007). Despite reduced baseline blood pressure compared to the SHRSP, the 2c* shows similar blood pressure to the SHRSP after 3 weeks on a high salt diet. In contrast, the 2a strain is salt resistant, showing no further increase in blood pressure on a high salt diet. This implicates genes within the 6 Mb region at the distal end of the 2a congenic interval that are not covered by the 2c* region. The subcongenic strain, SP.WKYGla2k (referred to as 2k) was generated from the 2a, capturing the 6 Mb region in a WKY congenic interval (figure 1.4) and has a similar baseline and salt loaded blood pressure profile to the 2a, both being significantly lower than the SHRSP. Microarray expression profiling was performed on kidneys from 21 week-old salt-loaded SHRSP, WKY and 2a rats, implicating two genes encoded within the 6 Mb region, endothelial differentiation gene receptor 1 (*Edg1*) and vascular cell adhesion molecule 1 (*Vcam1*), that were increased the SHRSP compared to the WKY and 2a, and subsequently also shown to be reduced in the 2k by quantitative RT-PCR (Graham et al 2007).

Another example of microarray expression profiling in congenic rats identified *Cd36* as a gene responsible for defective fatty acid and glucose metabolism in the SHR, contributing to symptoms of the metabolic syndrome. A QTL for defective catecholamine activity and reduced insulin activity in the SHR had been located on chromosome 4 in a genome wide scan involving crosses between SHR and Brown Norway (BN) rats (Aitman et al. 1997). A congenic rat strain was generated (SHR.4) whereby the region covering the QTL was replaced by the equivalent region from the normotensive Brown Norway (BN) rat. The SHR.4 rat showed a partial correction of the defects in fatty acid and glucose metabolism seen in the SHR. Differential gene expression profiling was performed on SHR, SHR.4 and BN adipose tissue using cDNA microarrays. Probes for *Cd36* consistently showed reduced expression in the SHR compared to BN and SHR.4 samples and *Cd36* was mapped to within 5cM of the peak of the QTL. Comparisons of the BN, WKY and SHR cDNA *Cd36* sequences revealed that whilst the BN and WKY have a functional copy of *Cd36* and an adjacent non-functional copy (which is thought to have arisen via an ancestral duplication event), the SHR carries a chimeric *Cd36* sequence comprising the functional sequence at the 5' end and the non-functional *Cd36* from exon 6 to the 3' UTR (thought to have arisen

by a deletion event unique to the ancestry of the SHR strain used in this series of experiments). Northern blot analysis showed that mRNA levels of *Cd36* expression in the WKY, BN and SHR were comparable, the differential expression shown in the microarrays was due to the probe sequences for *Cd36* being specific for the 3' UTR found in BN and WKY mRNA. Western analysis confirmed an absence of Cd36 protein in the adipocytes of SHR rats (Aitman et al. 1999). Ultimate experimental proof that *Cd36* deficiency contributes to insulin resistance in the SHR was provided by transgenic rescue of SHR rats expressing up to 10 copies of functional *Cd36.* The amount of Cd36 protein produced in the transgenic strains was lower than that produced by WKY controls, but was sufficient to induce improvements in glucose tolerance, insulin-stimulated conversion of glucose to glycogen and serum fatty-acid levels (Pravenec et al. 2001b).

A number of other publications have also applied microarrays in the search for hypertension loci. Moujahidine et al (Moujahidine et al. 2004) generated a double congenic strain with Dahl salt-sensitive genetic background and regions introgressed from the normotensive Lewis strain corresponding to blood pressure QTLs on chromosomes 10 and 16. Kidney microarrays were performed on the double congenic and DSS rats though no differentially probe sets genes were mapped to the congenic intervals. Yasui et al (Yasui et al. 2007) performed kidney expression microarrays to search for differentially expressed genes in a blood pressure QTL on chromosome 10. They identified small inducible cytokine A2 precursor (*Ccl2)* as a differentially expressed candidate between DSS and Lewis rats, its upregulation in the DSS under salt loading potentially contributing to salt sensitive hypertension via overactivation of inflammatory pathways. However, the absence of a congenic strain confirming a blood pressure effect of the chromosome 10 QTL compromises *Ccl2* as a candidate (Deng 2007). Yagil et al (Yagil et al. 2005) utilised DOCA salt sensitive (SBH) and salt resistant Sabra (SBN) rats in a microarray study measuring renal gene expression in the presence and absence of salt loading in each strain. The salt loading protocol involved the implantation of a 25 mg deoxycorticosterone acetate (DOCA) pellet into the back of the neck of the rats, and 1% NaCl in drinking water. The same group had previously identified 2 salt sensitivity QTLs on chromosome 1 in this model (Yagil et al. 1998) and confirmed their effect by the generation of two congenic strains (Yagil et al. 2003). In order to find genes involved in salt sensitivity, the microarray data was analysed to find genes located in the chromosome 1 QTLs and consistently differentially expressed in comparisons between salt loaded SBH rats versus all other

groups or between non-salt loaded SBH rats versus all other groups. Eight such genes were found, of which 7 were confirmed by quantitative real-time PCR (qRT-PCR) and proposed as candidates for further investigation (Yagil et al 2005).

1.2.3.4 Expression Genetics

As mentioned above, Pravenec et al (1999) derived a panel of RI strains in crosses between the BN and SHR. Thirty of these strains, plus the BN and SHR were used in a recent study that integrated microarray genome-wide expression profiling and linkage analysis (Hubner et al 2005), effectively treating gene expression as a phenotype that can be linked to loci throughout the genome in a technique known as expression genetics, or genetical genomics (Jansen et al. 2001). Such loci are known as expression QTL (eQTL) and can either act in *cis* (defined in this paper as a locus within 10 Mbp of the probe set in question), or in *trans* (affecting the expression of a probe set on a different chromosome or over 10 Mbp distant). The SHR is also a model of the metabolic syndrome, therefore linkage data on the RI panel from previous studies (Pravenec et al. 1996;Pravenec et al. 1999;Jirout et al. 2003) was combined with genome-wide microarray expression analysis of 15923 transcripts in kidney and fat tissue. Several interesting observations were made in this publication. Firstly, the proportion of eQTLs acting in *cis* or *trans* in the analysis depended on the genome-wide significance thresholds applied: at a significance level of $p<0.05$, 60-65% of the eQTLs were regulated in *trans*, while at $p\leq10^{-4}$, 85-100% of eQTL were regulated in *cis*. This was thought to reflect the larger effects of *cis* acting eQTL on gene expression levels. Secondly, of the 15% of eQTL that were detected in both fat and kidney, a high proportion (70% at $p<0.05$) had *cis*-acting effects, suggesting that the excess of *trans*-acting eQTLs found only in the kidney or fat data sets belong to tissue-specific gene expression networks. In addition, many of the *cis*-acting eQTLs showed similar gene expression levels across parental and recombinant strains when segregated by marker genotype, indicating a near-monogenic regulation of gene expression at these loci. However, a large number of transcripts showed linkage to two or more eQTLs, indicating the generally complex nature of gene expression control. In order to identify sequence variants that may be responsible for the observed effects of eQTLs, genes at the seven of the most significant *cis*-acting eQTLs were sequenced for promoter and coding SNPs in 3 inbred normotensive and 3 hypertensive strains. Genotypes at two SNPs in one of these genes, phosphatidylinositol 3-kinase (*Pik3c3*) were shared between all the hypertensive strains and distinct from all the

normotensive strains. *Pik3c3* lies on a known blood pressure QTL in the SHR, and kidney expression of *Pik3c3* (measured by real-time PCR) was significantly increased in the SHR compared to the BN, *Pik3c3* is consequently a robust candidate for blood pressure from this analysis. Another method to analyse this dataset involved comparing the locations of *cis*-eQTLs with known blood pressure and left-ventricular mass QTLs identified in previous phenotypic scans (or pQTLs); orthologous genes from the human genome were then identified to generate a list of 73 genes proposed as candidates for human essential hypertension. *Trans*-acting eQTLs that affected expression at several distant genomic loci were highlighted as strong candidates for genes involved in regulatory pathways. Two such clusters were identified on chromosomes 3 and 17 in kidney and fat tissue, respectively, though neither of these coincide with well-characterised pQTLs (Hubner et al 2005).

1.2.3.5 QTL Interactions in Complex Disease

As far as possible, laboratory conditions limit or control for environmental influences on blood pressure control. When inbred hypertensive rat strains were initially derived, optimistic predictions were forwarded that high blood pressure in the SHR was potentially controlled by 2-3 genes, and possibly only one major gene (Tanase et al. 1970;Yen et al. 1974). Analysis of blood pressure in the SHR/BN recombinant inbred strains produced by Pravenec et al suggested that more than seven loci were involved, with potentially three major effect genes and numerous minor effect genes (Pravenec et al 1989). While the exact number of loci concerned remains unknown, it is increasingly apparent that numerous genetic factors are involved, and that they interact in a complex manner to affect phenotype in hypertensive and normotensive animals; the blood pressure of a normotensive animal is such because the blood pressure raising loci it harbours are balanced by blood-pressure lowering loci, while hypertensive animals have an excess of blood-pressure raising loci. This is backed up by published reports of congenic breeding that produce counter-intuitive blood pressure effects. For instance, in order to investigate a blood pressure QTL on chromosome 2, Elipopoulos et al generated congenics by introgressing regions from the normotensive Lewis strain onto the DSS genome. Two of the congenic strains had blood pressures approximately 30 mmHg higher than the DSS under salt challenge, the boundaries of the responsible QTL were defined by overlapping congenic intervals in two other strains (that had similar blood pressures to DSS) to a 3 cM, a region encoding 19 genes (Eliopoulos et al. 2005). A similar study found an increase in

blood pressure compared to the DSS in a congenic strain carrying a region from the normotensive Lewis strain introgressed onto chromosome 3; a neighbouring QTL reduced blood pressure in congenics, while a congenic strain harbouring both QTLs had reduced blood pressure, indicating that these QTLs interacted epistatically, the blood-pressure lowering locus prevailing when both are present (Palijan et al. 2003). Other QTL interactions have also been published. For example, congenic breeding experiments were performed to investigate an interaction observed between loci on chromosomes 2 and 10 in candidate gene studies involving DSS and MNS rats (Deng et al. 1992). Congenic strains were generated to introgress the chromosome 2 and 10 regions from the WKY and MNS, respectively onto the background of the DSS, both showed blood pressure lowering effects, they were subsequently cross-bred to generate a double congenic strain carrying both transferred regions. The systolic blood pressure of the double congenic strain was 47 mmHg lower than that of the DSS; DSS genotypes at the chromosome 2 and 10 QTLs were respectively responsible for 8 mmHg and 15 mmHg alone, thus the epistatic interaction between the loci causes a 24 mmHg rise in blood pressure in the DSS (Rapp et al. 1998). Complex interactions have also been observed between blood pressure QTLs on the same chromosomes. Dutil et al (Dutil et al 2005) and Charron et al (Charron et al. 2005) showed additive and epistatic interactions between QTLs on chromosomes 2 and 10, respectively. The complexity of blood pressure regulation genetics has led to the development of increasingly sophisticated experimental models and analytical techniques. There is recognition in the scientific community that we should consider interactions between genetic elements in the search for candidate genes and focus on the study of metabolic pathways where more than one element may contribute to phenotype (Dominiczak et al. 2005). Such a technique was applied in the analysis of gene expression microarray data in chapter 3 of this project, using Ingenuity Pathway Analysis (IPA) software to identify multiple differentially expressed genes from metabolic pathways between parental and chromosome 2 congenic strains.

1.3 Oxidative Stress and Endothelial Dysfunction

One of the most widely studied molecular pathological processes linked to cardiovascular diseases is the regulation of vascular oxidative stress. Oxidative stress refers to molecular damage caused by reactive oxygen species (ROS), including free radicals such as the superoxide anion ($O_2^{-}\cdot$), hydroxyl radical ($OH\cdot$) lipid radicals, and other reactive oxygen

species such as hydrogen peroxide (H_2O_2) and peroxynitrite ($ONOO^-$). Damage caused by ROS has myriad downstream effects on cellular processes as a result of oxidative chain reactions triggered by the initial damage. Oxidised macromolecules consequently accumulate and can affect cellular function by damaging lipid membranes, enzymes and nucleic acids, with potentially cytotoxic and mutagenic effects.

The principal relationship between ROS and cardiovascular disease concerns the balance between ROS and nitric oxide (NO). The discovery of cellular NO production is regarded as one of the most important advances in vascular biology in the late 20th century. In 1980 an unknown endothelium-derived relaxing factor (EDRF) was proposed to account for vascular smooth muscle cell (VSMC) relaxation in response to acetylcholine, the release of which was dependent on the presence of endothelial cells (Furchgott et al. 1980). The endothelium is the layer of epithelial cells that lines the inner surface of the circulatory system, including blood vessels and the heart. NO was conclusively identified as EDRF by two independent groups in 1987 (Ignarro et al. 1987;Palmer et al. 1987). NO is derived from O_2 and the amino acid L-arginine (Palmer et al. 1988), its production in the endothelium is regulated by endothelial nitric oxide synthase (eNOS), it is also produced by neuronal NOS (nNOS), which is not restricted to neural cells, but was discovered in the brain, and inducible NOS (iNOS), which was identified in macrophages but is also expressed in several cell types. NO (itself an oxygen free radical) has a very short half life *in-vivo* (6-10 seconds), and acts as a local endothelial signalling molecule. NO mediates several functions of endothelial cells besides VSMC relaxation, including platelet aggregation, platelet and monocyte endothelial adhesion, low-density lipoprotein (LDL) oxidation, adhesion molecule expression, endothelin production and inhibition of smooth muscle cell proliferation. NO is very susceptible to reactions with other oxygen species, these reactions not only result in the production of a cascade of reactive oxygen species (such as $ONOO^-$ when NO combines with $O_2^{-}\cdot$), but also reduce the levels of NO itself. Reduced bioavailability of NO and vascular oxidative stress is known as endothelial dysfunction and is associated with all cardiovascular diseases, figure 1.5 illustrates endothelial dysfunction caused by oxidative stress and also includes mechanisms of oxidative stress defence, which are discussed in more detail below.

There are many lines of evidence that show increased oxidative stress can cause hypertension. For example, rats given lead in drinking water develop vascular and organ oxidative stress and hypertension that can be relieved by co-administration of the free

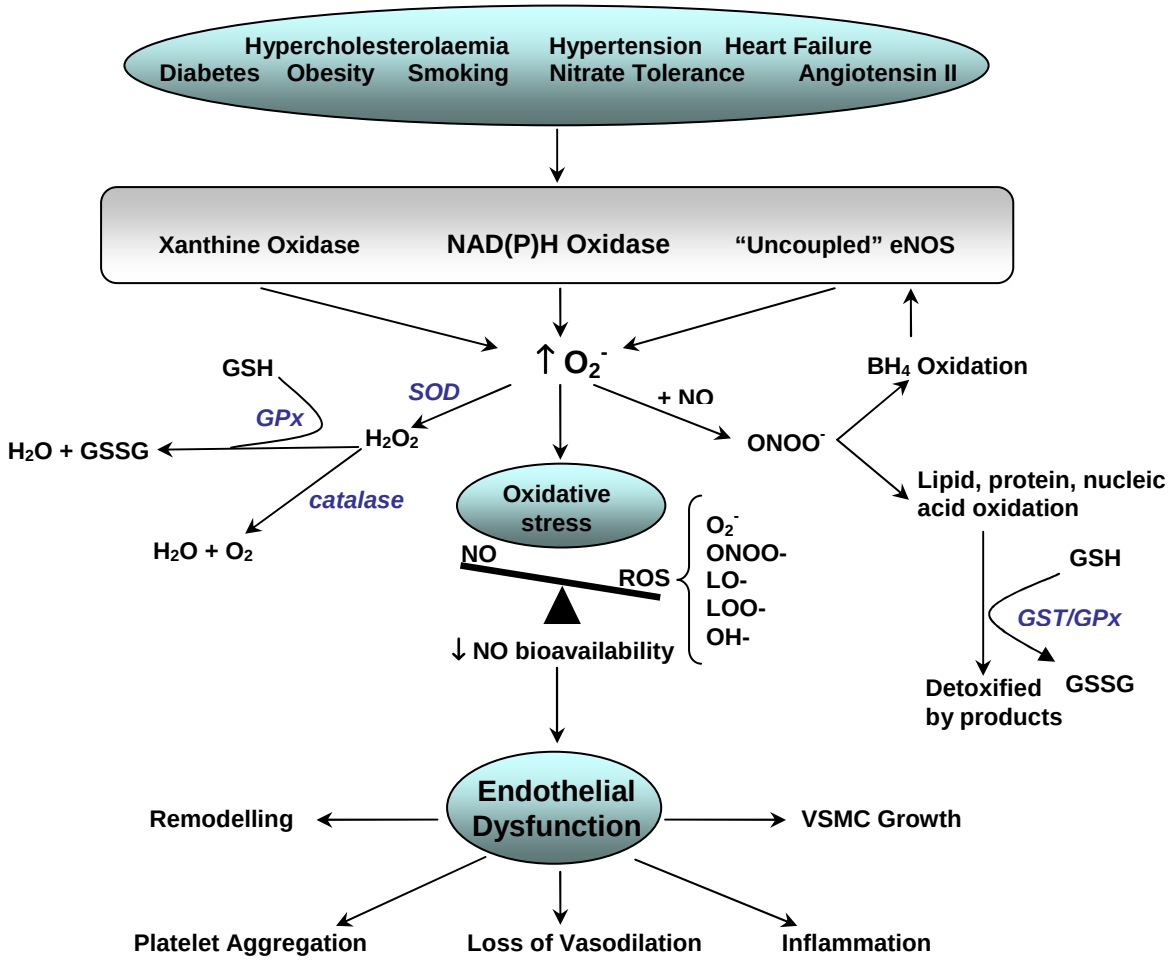

Figure 1.5 - Oxidative stress in cardiovascular disease
Environmental and physiological factors lead to the generation of O_2^- in the vasculature. O_2^- is enzymatically converted to H_2O_2 by superoxide distumtase (SOD) which is further processed by catalase, but excess O_2^- can generate a number of other reactive oxygen species and disrupt the balance of NO and ROS. Increased oxidative stress leads to decreased bioavailability of NO, contributing to endothelial dysfunction and downstream phenotypic effects. Adapted from (Cai et al. 2000). GSH: reduced glutathione, GSSG: oxidised glutathione, SOD: superoxide dismutase, O_2^-: superoxide, OH-: hydroxyl radical, LO- and LOO-: lipid radicals, GPx: glutathione peroxidase, GST: glutathione s-transferase, BH_4: tetrahydrobiopterin, VSMC: vacualr smooth muscle cell.

radical scavenger, vitamin E (Vaziri et al. 1999). Administration of the superoxide scavenger tempol to the SHR decreases blood pressure and urinary markers of oxidative stress (Schnackenberg et al. 1999). Targeted endothelial adenoviral overexpression of eNOS in the SHRSP reduced blood pressure (Miller et al. 2005), while overexpression of superoxide dismutase, one of the enzymes involved in oxidative stress defence (see below), also reduced blood pressure in the SHR (Chu et al. 2003).

ROS are generated by a number of cellular processes including respiration, arachidonic acid pathways, cytochrome p450s, xanthine oxidase and others. In the vasculature the main source of ROS is nicotinamide adenine (phosphate) dinucleotide oxidase (NAD(P)H

oxidase), a multisubunit enzyme that catalyses the formation of $O_2^{-}\cdot$ from O_2. NAD(P)H oxidase is upregulated in VSMCs by Ang II and a number of growth factors such as tumour necrosis factor alpha and platelet derived growth factor (Marumo et al. 1997;De Keulenaer et al. 1998a), its activity is also upregulated in the endothelium by shear stress caused by increased blood flow (De Keulenaer et al. 1998b). Vascular ROS are thought to act as signalling molecules, they stimulate VSMC and fibroblast growth responses (Irani et al. 1997;Zafari et al. 1998) and are intracellular second messengers is signalling cascades following ligand binding to growth, apoptotic, and stress signals (Sundaresan et al. 1995;Abe et al. 1996). Thus the equilibrium between ROS and NO in the vasculature is extremely complex, ROS have a physiological role in normal homeostasis, but their over-production or reduced NOS activity leads to an imbalance that causes endothelial dysfunction. In addition to existing cardiovascular disease, a number of behavioural and environmental factors contribute to an overabundance of ROS in endothelial dysfunction, such as smoking, excessive alcohol consumption, obesity and lack of exercise (figure 1.5). There is also a mechanism whereby eNOS itself can generate superoxide. The generation of NO by eNOS is dependent on its homodimerisation in the presence of tetrahydrobiopterin (BH_4), however BH_4 is sensitive to oxidation by $ONOO^{-}$, and in the absence of BH_4 during oxidative conditions, eNOS does not dimerise fully (it is 'uncoupled') and generates $O_2^{-}\cdot$ and H_2O_2 (Vasquez-Vivar et al. 1998), further contributing to oxidative stress.

Renal oxidative stress has been linked to hypertension in a number of models. Markers of oxidative stress such as urinary 8-isoprotane prostaglandin F2α and malondialdehyde are increased in Ang II-infused Sprague Dawley rats (Chabrashvili et al. 2003), and in the SHR (Welch et al. 2001). Increased renal nitrotyrosine levels have also been measured in the SHR (Welch et al. 2000) and in the SHRSP, see the results of anti-nitrotyrosine western blotting in section 4.4.3 and Mcbride et al. (2005). A number of specific mechanisms have been proposed that link renal oxidative stress and hypertension, for example $O_2^{-}\cdot$ has been shown to directly stimulate chloride reabsorption in the ascending limb of the loop of Henle, a response that was blunted by tempol, which also reduced chloride reabsorption alone (Ortiz et al. 2002). Renal oxidative stress is also proposed to contribute to the onset of high blood pressure via increased afferent arteriolar tone, both as a direct result of endothelial dysfunction and via indirect effects of ROS on macula densa function in tubuloglomerular feedback (TGF) responses (Wilcox 2003). Expression of nNOS is upregulated in the macula densa during tubular fluid reabsorption, reducing afferent tone and hence glomerular filtration rate (Wilcox et al. 1992); in the SHR this

mechanism is thought to be compromised as a result of increased expression of NAD(P)H oxidase subunits in the macula densa (Chabrashvili et al. 2002).

1.3.1 Oxidative Stress Defence

1.3.2 Direct ROS metabolism

A number of mechanisms exist to defend against the cytotoxic effects of oxidative stress (figure 1.5). The first line of defence act directly on ROS themselves, converting them to less reactive molecules, while the second line of defence catalyses the metabolism of oxidised molecules that have been attacked by ROS. The principal enzymes involved in metabolism of superoxide are the superoxide dismutase (SOD) enzymes, they catalyse the conversion of $O_2^{-}\cdot$ to H_2O_2 and molecular O_2. There are 3 SOD genes, *SOD1*, *SOD2* and *SOD3*. *SOD1* encodes cytosolic copper zinc (Cu/Zn)-SOD, which is thought to lower $O_2^{-}\cdot$ levels from nanomolar to picomolar concentrations. *SOD2* encodes mitochondrial manganese (Mn)-SOD and *SOD3* expresses the principal extracellular SOD isoform in the vascular wall, commonly known as extracellular SOD (ecSOD) (Zelko et al. 2002). The importance of SODs in anti-oxidant defence was demonstrated in gene transfer experiments, SOD overexpression improved endothelial function (Zanetti et al. 2001;Fennell et al. 2002) and provided protection against myocardial infarction (Li et al. 1998). Expression of *SOD* genes is regulated by mechanical, chemical or biological stimuli and is downregulated in certain pathological conditions (Fridovich 1998;Mates 2000).

The enzyme principally responsible for H_2O_2 metabolism following dismutation of $O_2^{-}\cdot$ is catalase, an intracellular anti-oxidase mainly located in peroxisomes, but also in the cytosol (Fridovich 1998). Genetic autosomal recessive catalase deficiency has been linked to a higher risk of cardiovascular disease and increased incidence of diabetes mellitus in affected families (Leopold et al. 2005) and a catalase promoter polymorphism has been associated with cardiovascular risk in a Chinese population (Jiang et al. 2001), however experimental studies have provided evidence of only moderate protection against oxidative stress by catalase (Muzykantov 2001). Protection against oxidative damage was provided by co-expression of SOD and catalase but the relative contribution of each gene was not clear (Durand et al. 2005).

1.3.3 Glutathione and Glutathione s-Transferases

Interactions between ROS and macromolecules results in the generation of reactive products that can damage lipids, proteins and nucleic acids. A number of mechanisms exist to protect the cell from these species, the primary cofactor in many of these reactions is glutathione, a tripeptide of glutamate, cysteine and glycine. Glutathione is the main non-protein thiol in the cell and has numerous functions in metabolism, synthesis, signal transduction and gene expression (Wu et al. 2004). It is mainly found in its reduced state (GSH) since the glutathione reductase enzyme that converts glutathione disulfide (GSSG) to GSH is constitutively active in cells. The liver is the main detoxification organ of the body and it is also the major source of plasma GSH, which circulates to other organs. GSH can be transported directly across cell membranes (Hagen et al. 1988;Parks et al. 1998), however the major source of intracellular GSH involves catabolism of GSH by extracellular gammglutamyltranspeptidase I (GGT1) and aminopeptidase enzymes followed by uptake of the constituent amino acids and de-novo synthesis (Lash et al. 1988). The synthesis of GSH is a two-step reaction, cysteine (the rate limiting substrate) is first conjugated to glutamate by glutamate cysteine ligase (Gcl), generating γ-glutamylcysteine, glycine is then conjugated by glutathione synthase (GSS). GCL is a dimeric enzyme consisting of a catalytic subunit (GCLC) and modulatory subunit (GCLM) that regulates GCL activity via negative feedback by GSH (Deneke et al. 1989).

GSH acts as an electron donor and can directly scavenge reactive oxygen species, it is also a cofactor in the conversion of H_2O_2 to H_2O by glutathione peroxidase (GPx). In its interaction with glutathione s-transferase (GST) enzymes, GSH is conjugated to xenobiotics such as drugs, insecticides, herbicides, carcinogens, and endogenous compounds such as oxidative by-products of cellular processes and damage. This generates more water-soluble compounds that are less reactive and amenable to further metabolism by the mercapturic acid pathway. Such a reaction is exemplified in figure 1.6, showing the conjugation of GSH to 1-chloro-2,4-dintrobenzene (CDNB).

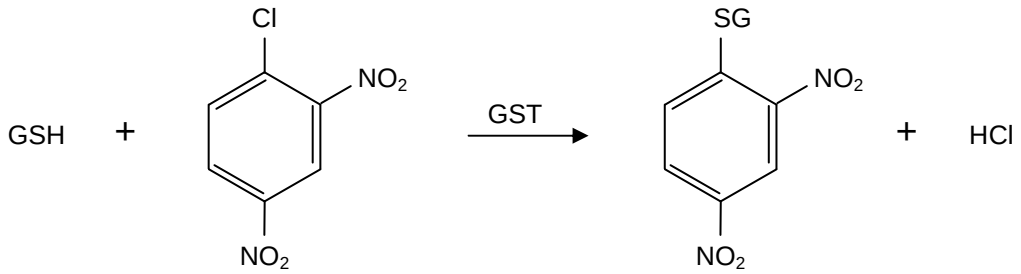

Figure 1.6 - Catalysis of glutathione conjugation to CDNB by GST enzymes
A majority of GST enzymes catalyse this reaction, it is used in biochemical assays to measure total GST activity.

There are seven classes of mammalian cytosolic, or soluble GST proteins, including Alpha, Mu, Pi, Theta, Zeta, Omega and Sigma. Cytosolic GST class nomenclature in rodents and humans is based on sequence similarity, members of the same class within a species share 40-90% identity, different classes typically share less than 25% identity (Hayes et al. 2005). There are a total of 17 human GSTs including *GSTA1-5*, *GSTM1-5*, *GSTP1*, *GSTT1-2*, *GSTZ1*, *GSTO1-2* and *GSTS1* (Mannervik et al. 2005). Each class is encoded on a different chromosome, classes with multiple members reside in closely linked gene clusters and have arisen by gene duplication events from ancestral genes. The rat *Gst*s include *Gstm1-5*, *Gstm6a* and *6b* and *Gstm7*, *Gsta1-5*, *Gstp1*, *Gstt1-2*, *Gstz1* and *Gsts1*. GST enzymes were named in the order of their identification in each species, the ortholog of a particular GST in another species cannot necessarily be identified by its name, in fact the evolution of GST gene families largely post-dates rodent and human common ancestry such that, for example, with the exception of human *GSTM3* and rat *Gstm5*, the rat *Gstm*s are more closely related to each other than any of the human *GSTM*s. In contrast, some of the rat and mouse *Gstm*s are highly orthologous, rat *Gstm1* is the ortholog of mouse *Gstm1*, they share 94% coding sequence identity and 81% genomic identity (Reinhart et al. 1993).

GSTs are primarily dimeric enzymes, they form homodimers or heterodimers of two subunits of the same class, though catalytically active heterodimers of pig *GSTP1* and rat *Gstm2* subunits have also been generated *in-vitro* (Pettigrew et al. 2001). Heterodimerisation is thought to broaden the catalytic range of GSTs by generating enzymes with different substrate affinities (Wang et al. 2000). Human GSTP1 has also been shown to act monomerically in cellular stress-defence signalling cascades (Yin et al. 2000). The GSTs catalyse a number of different reactions including conjugation, reduction, thiolysis and isomerisation, though the most widely shared catalytic activity, and the most studied, is the conjugation of reduced glutathione to electrophilic compounds. The

metabolism of oxidised membrane fatty acids by GSTs has been well studied; lipid peroxidation is toxic to cells since it can result in chain reactions generating hydroperoxides that can form secondary electrophiles such as epoxaldehydes, 2-alkenals, and ketoaldehydes, which can be genotoxic (Marnett et al. 2003). GSTs have been shown to reduce phosphatidylcholine hydroperoxide, cholesterol hydroperoxides and fatty acid hydroperoxides (Hiratsuka et al. 1997;Yang et al. 2002;Prabhu et al. 2004). Metabolising such compounds prevents the formation of downstream secondary electrophiles, though GSTs also reduce several end products of lipid peroxidation including the 2-alkenals acrolein and crotonaldehyde (Hayes et al. 1995;Hayes et al. 1999). GSTs have also experimentally been shown to catalyse the conjugation of GSH to oxidised proteins: co-incubation of peroxynitrite-pre-treated histones with GSH and GST reduced nitrotyrosine immunoreactivity compared to histones incubated without GSH (Kuo et al. 2002). In addition, catalase pre-treated with peroxynitrite showed reduced catalytic activity and increased nitrotyrosylation, which were reversible by incubation with GSH and GST (Kocis et al. 2002). GSTs also catalyse the conjugation of GSH to oxidised nucleotides such as adenine and thymine propenols and thymine hydroperoxides (Okuno et al. 1993;Berhane et al. 1994) that may otherwise cause further damage to DNA-binding proteins or chromosomal DNA.

The GSTs are widely expressed in all tissues, they are particularly abundant in the liver, the major site of detoxification in the body. Some isoforms are tissue-specific, for example, *GSTM2* is highly expressed in human striated muscle (Hussey et al. 1991) and the human *GSTM3* is selectively expressed in testes and brain (Listowsky 2005). Comprehensive tissue distribution expression profiles of the *Gst* genes have not been published for the rat, though unpublished data from our laboratory shows that *Gstm1* is the major *Gstm* isoform expressed in the WKY kidney. Expression profiling in the mouse has shown that the *Gstm1* is constitutively expressed in the mouse, but at low levels in the intestine, placenta and gonads (Knight et al. 2007).

Given the known function of GST enzymes and the proven involvement of increased oxidative stress in cardiovascular disease, the finding that *Gstm1* expression is reduced in the kidneys of the SHRSP compared to the WKY and 2c* rats (McBride et al 2003) presented *Gstm1* as a functional and positional candidate gene in hypertension. This finding formed the basis for the work performed in this project, part of which contributed to a publication showing that reduced renal *Gstm1* expression coincides with increased renal oxidative stress (McBride et al 2005). Several aspects of *Gstm1* expression and function were investigated using a variety of functional genomic techniques.

2 Materials and Methods

2.1 General Laboratory Practice

This chapter outlines general laboratory practises and laboratory methods that are common to more than one chapter. Each of the other chapters also has a specific methods section.

Laboratory equipment and reagents were of the highest commercially available grades. A laboratory coat and latex or non-latex powder-free gloves were worn during all procedures. Hazardous reagents were handled appropriately as described in the Control of Substances Hazardous to Health regulations, using laboratory spectacles or facemask and/or a fume hood where appropriate.

Laboratory glassware was cleaned in Decon 75 detergent, rinsed with distilled water and dried in a 37°C cabinet. Otherwise, sterile disposable plastic ware was used, including 0.5 ml, 1.5 ml and 2 ml microcentrifuge tubes (Greiner Bio-one) 15 ml and 50 ml Corning centrifuge tubes and 5 ml and 20 ml 'Universal' containers (Sterilin). Reagents were weighed using an Ohaus Portable Advanced balance (sensitive to 0.01 g), or a Mettler HK160 balance (sensitive to 0.0001 g). Solutions were pH'd using a Mettler Toledo digital pH meter calibrated with pH 4.0, 7.0 and 10.0 standards (Sigma). Volumes from 0.1 µl to 1,000 µl were dispensed with Gilson Medical Instruments pipettes. Volumes from 1 ml to 25 ml were measured with sterile disposable pipettes (Corning) and a Gilson battery-powered pipetting aid. Autoclaved distilled water was used to prepare aqueous solutions unless stated otherwise, a Jenway 1000 hotplate/stirrer was used to aid dissolving and mixing. Vortexing was carried out using an FSA Laboratory Supplies WhirliMixer. Centrifugation for samples up to 2 ml was performed at 4-20°C in an Eppendorf 4515 microcentrifuge, larger samples were centrifuged in a Sigma 4K15, compatible with 15 ml and 50 ml centrifuge tubes, 20 ml 'Universal' tubes and with carriers for standard reaction plates. Laboratory-ware or liquids requiring sterilisation were autoclaved in a Priorclave Tactrol 2. A Julabo TW8 water bath was used for experiments requiring incubations from 37°C to 90°C, a Grant SBB14 boiling water bath was used for temperatures up to 100°C.

Certified Nuclease-free reagents and plastic ware was used for experiments involving RNA, including Ambion RNase-free microcentrifuge tubes, RAININ nuclease-free filtered pipette tips and Ambion nuclease-free H_2O. Pipettes and benches were wiped with Ambion RNaseZap reagent before all RNA experiments.

2.2 General Techniques

2.2.1 Nucleic Acid Extraction

Specific protocols used for genomic DNA extraction from different tissues are outlined in relevant chapters. Plasmid DNA purification is described in section 2.5.3. Qiagen column and filter-based RNeasy Mini or Maxi kits were used for RNA extraction. Whole tissues or cells were homogenised in buffer RLT lysis solution, 10 µl/ml β-mercaptoethanol (350-600 µl for Mini columns, 7.5-10 ml for Maxi columns). Cultured cells were rinsed with PBS and homogenised by scraping with a pipette tip. Unless otherwise stated tissues were homogenised with a Polytron 2100 rotor homogeniser at full speed, then centrifuged at 5000 g to collect debris and lysates were transferred to fresh tubes. An equal volume of 70% ethanol was added to cell lysates before applying them to the RNeasy columns, followed by centrifugation (15 seconds at 8000 g for mini columns, 5 minutes at 5000 g for Maxi columns) to wash cellular debris through the column, binding RNA. Buffer RW1 was added to columns (700 µl for Mini columns, 15 ml for maxi columns) and washed through by centrifugation (15 seconds at 8000 g for Mini columns, 5 minutes at 5000 g for Maxi columns). Columns were transferred to new collection tubes, and 2 washes were performed with RPE buffer (70% ethanol): 500 µl for Mini columns, 10 ml for Maxi columns, centrifugation at 8000 g for 15 seconds (first wash) then 2 minutes (second wash) for Mini columns and at 5000 g for 5 minutes (first wash) then 15 minutes for Maxi columns (second wash). Columns were transferred to new collection tubes and centrifuged at full speed for 1 minute (Mini columns) or 5 minutes (Maxi columns) to completely dry membranes. RNA was eluted in 30-50 µl RNase-free H_2O (Mini columns) or 800 µl RNase-free H_2O (Maxi columns).

2.2.2 Measuring Nucleic Acid Concentration

DNA and RNA concentrations were measured using a Nanodrop ND-1000, a spectrophotometer that is sensitive from 2-37000 ng/µl double-stranded DNA. Absorbance at 260nm were used for quantification of nucleic acids, optical density of 1 corresponding to 50ng/µl DNA and 40ng/µl RNA. Absorbance ratios (260 nm/280 nm) of approximately 1.8 for DNA and 2.0 for RNA indicated that the nucleic acid preparations were sufficiently free from protein contamination for downstream experiments. Averages of duplicate or triplicate readings were taken for samples requiring very precise quantification.

2.2.3 Polymerase Chain Reaction

All thermal cycling for standard PCRs was performed on an MJ Research PTC Gradient Cycler in 96-well plates (ABgene). PCR primers were designed using the online design tool Primer3 (Rozen et al. 2000) and purchased from MWG Biotech. Oligonucleotide sequences for all PCR primers used are in table A1 in the appendix.

Two commercial 'Hotstart' Taq polymerase PCR systems were used for standard PCRs in this project, Qiagen HotStar and Roche FastStart. For amplifying from genomic DNA templates, 100 ng of genomic DNA was used, while 5-10 ng of template was used for amplifying from plasmid templates. 7.5 pmol of each primer were used in all reactions. The standard reaction mixes and temperature cycling parameters for each system were as follows:

Qiagen HotStar:

Reaction mix		**Heat Cycling**		
	Vol. (µl)			
10x PCR buffer	2.0	95°C	15 min	
dNTPs (1mM ea.)	4.0	94°C	15 sec	
Fwd primer (5pmol/µl)	1.5	58-62°C	30 sec	x35 cycles
Rvs primer (5pmol/µl)	1.5	72°C	30 sec	
DNA*	1.0-5.0	72°C	10 min	
Taq (5U/µl)	0.2			
H_2O	Up to 20ul			

Roche FastStart:

Reaction mix		**Heat Cycling**		
	Vol. (µl)			
10x PCR buffer	2.0	95°C	4 min	
dNTPs (1mM ea.)	4.0	94°C	30 sec	
Fwd primer (5pmol/µl)	1.5	58-62°C	30 sec	x35 cycles
Rvs primer (5pmol/µl)	1.5	72°C	1 min	
DNA	1.0-5.0	72°C	7 min	
Taq (5U/µl)	0.2			
H_2O	Up to 20µl			

The Taq DNA polymerases used in the above PCR systems have fast processivity, but lack a proofreading capability, they are suitable for a majority of PCR applications but incorporate incorrect nucleotides approximately every 10,000 nucleotides. For applications where absolute fidelity of DNA replication was required, for example for cloning promoter or cDNA sequences, 'Kod Hot Start' DNA polymerase (Novagen) was used. Kod DNA polymerase is derived from *Thermococcus kodakaraensis* thermophilic bacteria and

possesses 3'-5' exonuclease activity that excises mis-incorporated bases during PCR. Kod PCRs were performed according to the manufacturers instructions, reaction mixtures and temperature cycling parameters were as follows:

Reaction mix

	Vol. (µl)
10x PCR buffer	2.5
dNTPs (1mM ea.)	2.5
$MgSO_4$ (25mM)	1.0
Fwd primer (5pmol/µl)	1.5
Rvs primer (5pmol/µl)	1.5
DNA	1.0-5.0
Kod (1U/µl)	0.5
H_2O	Up to 25ul

Heat Cycling

94°C	2 min	
94°C	15 sec	←
58-62°C	30 sec	x35 cycles
68°C	2.5 min	←
68°C	10 min	

2.2.4 Agarose Gel Electrophoresis

Unless otherwise stated 1% agarose (Eurogentec) gels were used throughout, dissolved and electrophoresed in 1 X Tris-Borate EDTA (TBE) buffer (Fisher Bioreagents). Gels were electrophoresed at 6 V per cm of gel. BIO-RAD Power Pac 300 and BIO-RAD electrophoresis tanks were used, 1 ng / 100 ml ethidium bromide (Sigma) was added to molten agarose before pouring gels, unless stated otherwise. Gels were visualised by UV transillumination on a BIO-RAD Fluor-S MultiImager. Promega 1kb DNA ladder was used for sizing products. Samples were loaded with 6 X loading dye (50% glycerol, 0.05% bromophenol blue).

2.2.5 Determining Protein Concentration

Protein samples were prepared from cultured cells by rinsing with PBS and scraping with a pipette tip in PBS/0.2% Triton. Samples were freeze-thawed to -80°C and passed through a hypodermic needle 10 times before briefly centrifuging to collect debris. Tissues were homogenised in PBS buffer containing protease inhibitors, centrifuged at 5000 g for 5 minutes and supernatants were transferred to fresh tubes.

Protein concentrations were determined using a Pierce BCA (bicinchoninic acid assay) kit. The assay was performed in 96-well plates. Dilutions of an albumin protein standard (Pierce) in phosphate-buffered saline (PBS) (Gibco) from 25 ng/µl – 2 µg/µl were used to generate a standard curve for each assay. The kit consists of reagents A and B, which are mixed at a ratio of 50:1 before being added to protein samples and standards at a ratio of 8:1 (25 µl sample or standard, 200 µl BCA reagents). 96-well plates were then protected

from light by wrapping in aluminium foil and placed at 37°C for 30 minutes. Absorbance at 560 nm was ascertained in all wells using a Wallac Victor 2 plate reader. Samples and standards were measured in duplicate and averaged, the concentration of protein in the samples was interpolated from the standard curve by 'Work-Out' software (Wallac). If the concentration of protein samples fell beyond the range of the standard curve, appropriate dilutions were made in PBS and they were re-assayed, the concentration of the dilutions were multiplied by the dilution factor to ascertain the concentration of the samples.

2.3 Tissue Culture

Eukaryotic cell lines were handled under sterile conditions using class II biological safety cabinets (Holten Safe 2010). Cabinets were cleaned before and after use with distilled water and 70% ethanol. Waste plastics and fluid were decontaminated by steeping for 24hr in (10%) bleach, plastics were then incinerated, fluids were poured into domestic waste drains. Cells were maintained in 150 cm^2 tissue culture flasks with vented caps (Corning) in inCusafe 37°C, 5% carbon dioxide (CO_2) incubators. Tissue culture experiments involving genetic modification, such as recombinant adenoviruses or plasmid transfections, were performed in a dedicated tissue culture laboratory and maintained in separate incubators.

2.3.1 Cell Passage and Cryostorage

Details of specific cell lines used and media requirements are given in relevant chapters. Cell were passaged regularly to prevent overcrowding in culture flasks, experiments were performed with cells of lowest possible passage number and experiments were completed in as few passages as possible. Fresh cell culture stocks were recovered from storage in liquid nitrogen after approximately 25 passages.

Unless stated otherwise, passaging was performed by removing culture media and rinsing cells gently twice with 10ml sterile PBS (Lonza) before detaching them from the flask with 2-10 minutes incubation at 37°C with 2ml 1X TE (0.05% trypsin; 0.2% ethylenediamine tetraacetic acid (EDTA)). Cells were collected in 10 ml foetal bovine-serum (FBS)-containing medium, which inactivates the trypsin, and centrifuged at 1500 rpm for 5 minutes. Media/TE was poured off and the cell pellets were resuspended in cell media, fresh 150 cm^2 flasks with 25ml media were seeded with 1/20-1/5 of the cells from the previous passage.

For cryostorage, cells from 3 x 150 cm^2 flasks were resuspended in 10ml media/10% dimethylsulfoxide (DMSO) and aliquotted into 6 x 2 ml cryoviles. The cryoviles were placed in an isopropanol freezing container (Nalgene) in a -80°C freezer overnight, ensuring freezing no faster than 1°C per minute. The next day cells were transferred for long-term storage in liquid nitrogen. When recovering cells from liquid nitrogen they were thawed to room temperature and pipetted into 25 ml media in a fresh 150 cm^2 flask, the media was changed the next day, cells were not used for experiments until at least two passages and a week out of liquid nitrogen.

2.3.2 Cell Counting

In order to accurately seed cell culture flasks and plates with a known number of cells, cells were counted with a haemocytometer (Hausser Scientific). Approximately 10 µl of a cell suspension was pipetted under a cover slip onto the grid, the number of cells in each 1 mm square was recorded by counting the cells in each 0.25 mm squares, cell crossing the bottom or right-hand edge of any square were not counted. The average number of cells in each 1 mm square was derived, was multiplied by 10^4 to give the number of cells per ml in the suspension. Dilutions of the cell suspension were made in media to seed the correct number of cells per flask or well.

2.3.3 Plasmid Transfection of Cultured Cells

Roche FuGENE 6.0 lipofection reagent was used for all experiments involving transfection of cultured cells. FuGENE is a proprietary mix of lipids in 80% ethanol, it binds to and packages plasmid DNA into a lipid complex that allows the plasmids to cross cell membranes. Transfection protocols were optimised individually for each cell type used in experiments following suggested methods in the FuGENE product literature. This involved ascertaining the optimal ratio of FuGENE:DNA for maximal gene expression and minimal cytotoxicity. Specific optimisation procedures are described in each chapter.

Regardless of the final conditions used, the same transfection protocol was followed: Cells were seeded the day before to be at 50-70% confluence at transfection. FuGENE/DNA mixtures were made in additive-free media in 1.5 ml centrifuge tubes, FuGENE was added to the media and mixed by gently flicking the tube, plasmid DNA was added after five minutes and tubes were flicked to mix once more then left for 15 minutes to allow FuGENE/DNA complex formation. Transfection mixtures were then applied to cells, gene expression was assayed 48 hours later.

2.3.4 B-Galactosidase Expression Staining

Plasmids and viruses expressing the *LacZ* gene, which encodes β-galactosidase, were employed as controls to assess gene delivery and expression in many experiments. Regardless of the method of gene delivery, the same protocol was used to assay for β-galactosidase expression in cultures cells: Cells were fixed by removing culture media and washing cells twice with PBS, then adding sufficient 2% paraformaldehyde in 0.1M sodium phosphate ($NaPO_4$) (72mM Na_2HPO_4; 23mM NaH_2PO_4) to cover the cells and placing the cells on ice for 10 minutes. The paraformaldehyde was removed and cells were washed twice very gently with PBS to prevent dislodging the fixed cells. X-gal (5-Bromo-4-chloro-3-indolyl β-D-galactopyranoside) stain solution constituted 0.077 M Na_2HPO_4; 0.023 mM NaH_2PO_4; 0.03 M $MgCl_2$; 3 mM $K_3Fe(CN)_6$; 3 mM $K_4Fe(CN)_6$; 1 mg/ml X-gal, the X-gal stock solution was 20 mg/ml in dimethylformamide. X-gal stain was added to cover cells and plates or flasks were returned to a 37°C incubator overnight. β-gal-galactosidase cleaves X-gal to produce a dark blue precipitate, indicating cell transfection or infection.

2.4 DNA Sequencing

Unless otherwise stated, DNA sequencing was performed by purifying PCR products to remove un-incorporated dNTPs, primers and salts, followed by dideoxy sequencing reactions, and a second purification step before capillary electrophoresis to separate sequencing products by size. Each step is outlined below.

2.4.1 PCR Clean-up

PCR products were retained in PCR reaction plates and purified for sequencing using the Agencourt AMPure kit. This relies on binding of DNA products over 100bp in length to paramagnetic beads in the kit solution (i.e. they are attracted to magnets but do not exhibit magnetism themselves). 36µl of AMPure was added to each 20µl PCR reaction, the plates were briefly vortexed and centrifuged to 1000 rpm for 1 second to collect the liquid to the bottom of the wells. They were left to stand for 5 minutes and then placed onto an SPRIPlate (solid phase reversible immobilisation plate) magnetic plate holder (Agencourt) for 10 minutes. The SPRIPlate has an individual ring magnet for each well in a 96-well plate, AMPure beads are held onto the sides of the wells of the 96-well plate. Keeping the PCR plate on the SPRIPlate, the PCR reaction constituents were removed by inverting the plates and shaking forcefully upside-down. The beads were then washed with 200µl of

freshly prepared 70% ethanol for 30 seconds before shaking forcefully upside-down and centrifuging upside-down to 600rpm for 1 second to remove as much ethanol as possible. PCR Plates were removed from the SPRIPlate and left to air-dry for 20 minutes before the addition of 40µl H_2O per well. The PCR plates were vortexed to resuspend the AMPure beads, then returned to SPRIPlates plates, 10µl was carefully pipetted out per sequencing reaction. If a PCR product was to be sequenced more than 3 times, multiple 20µl PCRs were performed.

2.4.2 Dideoxy Sequencing

Applied Biosystems BigDye Terminator n3.1 Cycle Sequencing kits were used all for sequencing reactions in this project, reactions were performed in 96-well plates. Unless stated otherwise all sequencing reactions included 3.5µl 5X sequencing buffer; 0.5µl Ready Reaction; 10µl template (purified PCR product); 3.2µl primer (1pmol/µl); 2.8µl H_2O. The temperature cycling program was:

96°C 45 sec
50°C 25 sec
60°C 4 min
X25 cycles

2.4.3 Sequencing Reaction Purification

Sequencing reactions were purified to remove reaction constituents and unincorporated nucleotides and primers prior to electrophoresis using Agencourt CleanSEQ reagent. 10µl of CleanSEQ reagent was added to each sequencing reaction, followed by 62µl of freshly prepared 85% ethanol. Plates were briefly vortexed and centrifuged to 1000 rpm for 1 second to collect the liquid to the bottom of the wells, then placed on an SPRIPlate for 3 minutes. Wells were emptied by forcefully shaking the plates upside-down, the CleanSEQ beads were washed twice with 100 µl 85% ethanol for 30 seconds each, emptying the wells between washes. Wells were then emptied as much as possible by centrifugation of inverted plates to 600 rpm for one second. Plates were removed from the SPRIPlates and air dried for 20 minutes, 40 µl of H_2O was added to each well and CleanSEQ beads were resuspended by vortexing. Plates were briefly centrifuged to 1000 rpm for 1 second and returned to SPRIPlates. 20 µl of sequencing products were loaded into optically clear barcoded 96 well plates. H_2O was added to unused wells to prevent drying of capillaries and plates were covered with Applied Biosystems Septa Seals, they prevent evaporation of products but allow capillaries to enter wells.

2.4.4 Capillary Electrophoresis

Sequencing capillary electrophoresis was performed on a 48-capillary Applied Biosystems 3730 Genetic Analyser with 36 cm capillaries. Electrophoresis was preceded by filling the capillaries with fresh POP-7 polymer (Applied Biosystems) and warming the capillaries to 60°C. Sequencing products were separated by size by electrophoresis at 8500 volts for 50 minutes.

2.4.5 Sequencing Analysis

Sequencing was analysed using Applied Biosystems SeqScape software version 2. Experimental sequences were aligned with known sequences derived from bioinformatic databases such as UCSC or ENSEMBL genome browsers or product information such plasmid sequences.

2.5 DNA Cloning

Eukaryotic expression plasmids were employed in this project in promoter studies, for the generation of recombinant adenoviruses and to make expression cassettes for rat transgenesis. Specific manipulations and protocols are outlined in each chapter, a number of common techniques are outlined below.

2.5.1 Transformation of Competent Bacteria

JM109 competent *Escherichia coli* (*E.coli*) bacteria (Promega) were used as hosts for eukaryotic expression vectors throughout this project unless stated otherwise. For transformation, competent cells were thawed on ice and separated into 50µl aliquots in chilled 1.5ml centrifuge tubes. For transformation of an intact plasmid, 2ng plasmid DNA was added to the bacteria, for transformation of ligated plasmid/insert mixes 2-5µl of the ligation reaction was added to JM109s. Tubes were flicked gently to mix and returned to ice for 10 minutes, then 'heat shocked' at 42°C for 45 seconds before returning to ice for a further 2 minutes. 900 µl of chilled SOC medium (Sigma) was added to the cells and they were placed in a shaking incubator (New Brunswick Scientific Inova 44) at 37°C, 180 oscillations per minute, for one hour. Unless otherwise stated all plasmids used in this project encoded ampicillin resistance for selection of transformed cells. Transformation mixtures were spread onto 90 mm culture plates (Sterilin) of Luria agar (Sigma) containing

100 μg/ml ampicillin (Sigma). For transformations of intact plasmids 100 μl of neat, 1 in 10 and 1 in 100 dilutions in SOC media were spread, for transformations of ligation reactions, the entire transformation culture was spread onto 5 plates. Culture plates were inverted and placed in a 37°C incubator (Heraeus) overnight. Plates were checked for bacterial colonies the next morning and if necessary screened for positive clones as detailed in section 2.5.7.

2.5.2 Glycerol Stocks

Successfully transformed bacteria were preserved for long-term storage by preparing glycerol stocks. 1 ml of overnight broth cultures was mixed with 1 ml sterile 40% glycerol solution and frozen at -20°C or -80°C. Bacteria were recovered from glycerol stocks by streaking for single colonies on selective agar.

2.5.3 Plasmid DNA Purification

Plasmid DNA was extracted from bacteria using the filter column based Qiagen Plasmid Maxi kit. Bacterial cultures were streaked and grown overnight at 37°C on ampicillin Luria agar plates. Single colonies were picked and used to inoculate a 'starter' culture grown throughout the next day in 5 ml Luria broth (Sigma) containing 100 μg/ml ampicillin in a shaking incubator at 37°C. 1 ml of this culture was used to inoculate 100-500 ml 100 μg/ml ampicillin Luria broth to produce an overnight culture from which the plasmid was extracted (100 ml was sufficient for most plasmids, however when low yields were obtained, the extraction was repeated with 500 ml culture). Bacteria were harvested by centrifugation at 6,000 g for 15 minutes at 4°C in a Beckman Coulter Avanti J-26XP. Culture media was poured off and the bacteria were resuspended in 10 ml buffer P1 (50mM 2-amino-2-hydroxymethyl-1,3-propanediol, pH8; 10 mM EDTA, 100 μg/ml RNase A). 10 ml buffer P2 (200 mM NaOH; 1% sodium dodecyl sulphate (SDS)) was added and the solutions were kept on ice for exactly five minutes. 10 ml chilled buffer P3 (3 M potassium acetate at pH5.5) was added to neutralise the lysate. The precipitated lysates were centrifuged at 20000 x g at 4°C for 30 minutes, the supernatant was retained and centrifuged again at the same speed for a further 15 minutes. Columns were pre-wetted with 10ml buffer QBT (750 mM NaCl; 50 mM 3-morpholinopropanesulfonic acid pH7 (MOPS); 15% isopropanol; 0.15% Triton-X 100). The supernatant was applied and the columns were allowed to empty by gravity flow, the columns were washed twice with 30 ml buffer QC (1 M NaCl; 50 mM MOPS pH7; 15% isopropanol), and the plasmid DNA was eluted with 15 ml buffer QF (1.25 M NaCl; 50 mM Tris pH8.5; 15% isopropanol) into

polypropylene centrifuge tubes. Plasmid DNA was precipitated with 10.5 ml isopropanol and centrifuged at 15000 x g for 30 minutes at 4°C. The supernatant was carefully poured off, pellets were resuspended in 5 ml 70% ethanol and aliquoted into five 1.5 ml microfuge tubes. They were centrifuged at maximum speed for 10 minutes at 4°C. The ethanol was carefully pipetted off and the pellets were thoroughly air-dried (10-20 minutes) before resuspending the DNA in 70 µl H_2O per tube and pooling the contents of the five tubes. Total plasmid yields were typically 50-90% of the maximum yield quoted for the maxi columns (500 µg).

2.5.4 Restriction Digestion

Restriction enzymes were used in this project to enable the targeted ligation of specific DNA 'insert' sequences into plasmid backbones. Inserts and plasmids were digested with appropriate restriction endonuclease enzymes to generate compatible ends for ligation. Restriction endonucleases were purchased from Promega or New England Biolabs. Manufacturer's protocols were followed for digestions, a typical digest included 1-2 µg template DNA in a final volume of 25 µl, including 2.5 µl 10x restriction buffer, 0.25 µl bovine serum albumin (BSA) and 10-20 units of enzyme, making the reaction a '10-fold overdigest': one unit of restriction enzyme is defined as the amount required to digest 1 µg of template in one hour. Reaction mixtures were mixed gently by pipetting and briefly pulsed in a bench microcentrifuge, then incubated at 37°C for between 1 and 16 hours.

Wherever possible, cloning was performed using 'double digests', wherein the insert and backbone were digested with two restriction enzymes, resulting in different overhanging ends on each end, allowing directional cloning and minimising the likelihood of self-ligation of the plasmid backbone.

2.5.5 Agarose Gel DNA Extraction

Unless stated otherwise agarose gel extraction of PCR products or restriction-digested DNA was performed with the Qiagen QIAquick Gel Extraction kit following the manufacturer's instructions, using a bench microcentrifuge at full speed. Bands in agarose gels were visualised on a UV transiluminator (UVP) and carefully excised with a scalpel blade. The bands were weighed and 300 µl of buffer QG was added per 100 µg of agarose before heating the agarose/buffer QG mixture to 50°C for 10 minutes. After centrifugation to adsorb the DNA to the membrane, the membrane was washed with centrifugations with 500 µl of buffer QG followed by 750 µl buffer PE (which contains 70% ethanol). All traces

of ethanol were removed by a final centrifugation for 1 minute, DNA was eluted in nuclease-free water.

2.5.6 Ligation

Unless stated otherwise, digested plasmid fragments, digested PCR products or annealed oligonucleotides were ligated into digested plasmid backbones using the New England Biolabs Quick Ligation Kit. The kit includes a 2X reaction buffer (1332mM Tris pH7.6; 20mM $MgCl_2$; 2mM dithiothreitol; 2mM ATP; 15% polyethylene glycol) and 'Quick' T4 DNA ligase (supplied in 50 mM KCl, 10 mM Tris (pH7.4), 0.1 mM EDTA, 1 mM dithiothreitol, 200 μg/ml BSA and 50% glycerol). Ligation reactions constituted 10 μl 2X quick ligation buffer, 1 μl quick T4 DNA ligase, 50-100 ng backbone, insert to provide an insert:backbone molar ratio of 100:1 to 3:1 and H_2O up to 20 μl. Reactions were mixed by gentle pipetting, pulsed in a microcentrifuge and incubated at room temperature for five minutes, and then put on ice. Ligations were transformed immediately or stored at -20°C before transformation. The 100:1 insert:backbone ratio was only used for ligation of oligonucleotides, otherwise ratios of 3:1, 5:1 or 7:1 were used. The amount of insert DNA to add to the ligation reaction for a given Insert:backbone ratio and given amount of backbone DNA was calculated according to the following formula:

$$\text{ng insert DNA} = \frac{\text{(Molar ratio insert:backbone) x (ng backbone) x (insert length,bp)}}{\text{(backbone length, bp)}}$$

2.5.7 Selecting Positive Clones

Following transformation of ligation reactions, colonies were screened by PCR across the cloning site. PCR primers depended on the backbone of the recipient plasmid, but the protocol was otherwise identical: Individual colonies were picked with a sterile wooden toothpick, streaked onto a numbered 0.8 cm grid on a selective agar plate and then washed in a numbered well of a 96-well plate containing 10 μl H_2O. 10 μl of Roche FastStart or Qiagen HotStar PCR reaction master mixes were added to each well to make a 20 μl PCR reaction, where possible a positive control well was also included. Following PCR, PCR products were electrophoresed against a size marker to screen for products of the expected size. Positive PCR results were later confirmed by DNA sequencing, bacterial colonies on the grid plate were used as stocks for sequencing and future amplification of positive clones.

2.6 Western Blotting

Each step in the western blotting protocol used in this project are described below.

2.6.1 SDS-Polyacrylamide Electrophoresis

Hoefer SE600 gel tanks were used unless otherwise stated; gels were poured between 18 cm x 16 cm glass plates, 1.5 ml apart. Up to 15 samples were loaded in 6 mm wide wells. A 30% stock solution of acrylamide was used with a 19:1 acrylamide: bis-acrylamide ratio (BIO-RAD). 11 cm 12% 'resolving' gels were overlayed with 5cm 4% 'stacking' gels. The mix for each resolving gel constituted 12 ml 30% acrylamide; 7.5 ml 1.5 M Tris pH8.8; 300 µl 10% SDS; 10.2 ml H_2O; 30 µl TEMED (N,N,N',N'-tetramethylethylenediamine); 300µl 10% APS (w/v, g/ml) (ammonium persulphate). Stacking gel consisted of 2 ml 30% acrylamide; 3.75 ml 0.5M Tris pH6.8; 159 µl 10% SDS; 9.1 ml H_2O; 15 µl TEMED; 150 µl 10% APS (w/v, g/ml).

10-60µg of protein samples were prepared in a total volume of 20-60 µl, incorporating the appropriate volume of 6 X Laemmli loading dye (constituting 50% glycerol; 9% SDS; 0.375 M Tris pH6.8; 10% β-mercaptoethanol; 0.05% bromophenol blue dye). Positive protein controls were included in each blot, as were 15 µl of Amersham 'Rainbow markers' – protein molecular weight markers (low range 2.5 k Daltons (kDa) - 45 kDa or full range 10 kDa -250 kDa) linked to coloured dyes for easy identification on the blotting membrane. Samples and positive controls were heated to 95°C for 5 minutes to ensure denaturation of proteins. Empty wells were loaded with 10µl 6X Laemmli loading dye to help provide a constant resistance across the gel and avoid 'smiling' of the bands. Electrophoresis buffer consisted of 0.025 M Tris pH10.5; 0.2 M Glycine; 0.1% SDS. Electrophoresis began at 100 v for 1-1.5 hours until the dye entered the resolving gel, whereupon the voltage was increased to 200 v for 3-4 hours, separation of the rainbow markers was used a guide to ensure the target proteins were sufficiently resolved.

2.6.2 Protein Blotting

After electrophoresis the electrophoresis apparatus was dismantled, the stacking gel was removed and any lanes not including protein were cut from the resolving gel. 6 pieces of Whatman 3 mm chromatography blotting paper and a piece of Amersham Hybond-P membrane were cut to the same size of the gel. Gels and Whatman paper were equilibrated in transfer buffer for 20 minutes, membranes were pre-wet with methanol for 5 seconds,

then H_2O for 5 minutes and transfer buffer for 10 minutes. Transfer buffer consisted of 0.025 M Tris pH10.5; 0.2 M Glycine; 0.1% SDS; 20% methanol. Transfer apparatus was prepared as follows (cathode to anode): 3 x Whatman sheets, gel, membrane, 3 x Whatman sheets. Blots were transferred overnight at 88 mAmps, 7 volts overnight in a Hoefer TE 50X transfer tank.

2.6.3 Antibody Probing and Washing

Following transfer membranes were inspected for transfer of the coloured rainbow marker bands. The positions of bands were marked by snipping the edge of the membrane in the event that the coloured bands faded in subsequent washing steps. The membrane was blocked through the day in Tris-buffered saline Tween buffer (TBST) (0.025 M Tris pH7.4; 0.14 M NaCl; 0.0027 M KCl; 0.1% Tween (Sigma)), 5% (w/v, g/ml) dried skimmed milk (Marvel), on lab shaker (Luckham R100) at 50 oscillations per minute. Primary antibody exposure was performed in a total volume of 10-20 ml TBST, 5% milk. Membranes were heat-sealed into plastic bags using a Russell Hobbs heat sealer with minimal airspace to enhance contact of the antibody preparations with the membrane. The bags were taped to a lab shaker and left overnight at 4°C at 180 oscillations per minute. Primary antibody dilutions are detailed in specific methods sections.

The following morning the membranes were washed with 100ml TBST in 10 x 5 minute washes. Primary antibody preparations were recovered and stored at -20°C, each preparation was used up to four times. Horse-radish peroxidase (HRP) conjugated secondary antibodies targeting the species in which the primary antibody was raised (purchased from DAKO). Membranes were incubated with 50 ml antibody dilutions for an hour at room temperature, details of specific antibodies used and dilutions are given in relevant chapters. Membranes were then washed for 10 further 5 minute washes with 100 ml TBST.

2.6.4 Enhanced Chemiluminescence and Detection

Amersham enhanced chemiluminescence (ECL) Western blotting detection reagents were used to detect binding of the HRP-conjugated secondary antibodies. The kit includes two reagents that are mixed in equal quantities and applied to the membrane. Typically 10 ml of each reagent was used per membrane, the reagents were left in contact with the membranes for 1 minute and excess liquid was blotted off before carefully wrapping the membrane in Saran wrap, ensuring that no liquid was on the outside of the Saran.

Membranes were then taped into an 18 x 24 cm autoradiography cassette and taken to a dark room. Kodak general purpose blue medical X-ray film was used in the first instance for all blots. Films were first exposed for 1 minute, folding the top corner of the film to record its orientation. Films were developed in a Kodak X-Omat 1000. The first exposures were inspected to judge if further exposures were required, repeated exposures of 1 second to overnight were performed as necessary. Sensitive Amersham Hyperfilm was used for blots giving very faint results. Once the required image of protein bands was acquired the developed film was returned to the cassette to mark onto it the position of the edges of the membrane and of the rainbow size markers, allowing accurate sizing of protein bands.

2.6.5 Membrane Stripping and Re-Probing

Every effort was made to load exactly the same amount of protein in each well of a Western blot. However, in order to accurately measure the level of a particular protein in a sample, it was always measured relative to the level of a 'housekeeping' protein that is present at the same level in all cells, such as glyceraldehyde-3-phosphate dehydrogenase (Gapdh) or beta-actin (β-actin). Membranes were stripped to remove conjugated antibodies and re-probed with antibodies specific for the housekeeping protein. Stripping involved placing the membrane in 100ml 0.2M Glycine; 1%SDS for 30 minutes at room temperature on a shaker at 50 oscillations per minute, then rinsing the membrane twice in TBST. Membranes were then re-blocked for 4 hours in TBST, 5% milk and probed, washed and analysed for the housekeeping protein exactly as described above.

2.6.6 Densitometry

The intensities of protein bands on the photographic films were measured to compare protein levels between samples on a western blot using the BIORAD Fluor-S MultiImager and 'Quantity One' software (BIORAD). X-ray films were scanned to generate a digital image, individual bands were labelled and demarked by boxes using a drawing tool in the Quantity One software. The intensity of the bands was then measured by the software and expressed in units of optical density per mm^2 (ODU/mm^2). The intensity of the protein band of interest was divided by the intensity of the band for the housekeeping gene to find the relative level of the protein of interest in each sample.

Two methods of background subtraction were used for densitometry. A 'global' background subtraction method was used for blots with clean and constant background intensities, this involved drawing a box in an area of the image that represented the

background, the software then calculated the average intensity of all pixels in this box and subtracted it from all pixels in boxes containing bands. A 'local' background subtraction method was used for blots where the background intensity level was variable across the blot, the software calculated an average background intensity for each box by measuring the average intensity of all pixels in a one-pixel border around each box and subtracted this from each pixel in the box to find the band intensity.

2.7 Quantitative Real-Time PCR

An Applied Biosystems 7900HT Sequence Detection System (Taqman) was used for all quantitative real-time PCRs in this project. The system encompasses a heating block for thermal cycling and detectors to measure fluorescence in each well of a 96-well or 384-well optical plate. Fluorescence is measured after every amplification cycle to quantify the accumulation of PCR product; during the exponential phase of PCR cycling the rate of product accumulation is proportional to template concentration, relative template abundance can therefore be quantified by monitoring increasing fluorescence in each well during temperature cycling. This is explained in more detail below along with the specific protocols for cDNA template preparation of and reaction set up.

2.7.1 Preparation of DNA-free cDNA

cDNA preparations for quantitative real-time PCR (qRT-PCR) were made by reverse transcription from RNA templates. Unless stated otherwise stated, RNA was first treated with DNA-Free (Ambion) in order to prevent carry-over of genomic DNA that may amplify in real-time PCR reactions. If necessary the concentration of RNA preparations were adjusted down to 200 ng/µl to ensure rigorous DNase treatment as per the kit instructions. 30 µl reactions were performed including RNA template, 3 µl 10X DNAse I buffer and 0.6 µl rDNAse I (recombinant DNase I). Reactions were heated to 37°C for 30 minutes. 3 µl DNAse Inactivation Reagent was added per well and reactions were mixed by pipetting and flicking tubes. The DNase Inactivation Reagent is a dense slurry that binds and inactivates rDNase I, after incubation for 2 minutes at room temperature reactions were centrifuged for 1.5 minutes at 10000 x g, to collect the DNase Inactivation Reagent at the bottom of the tubes and the DNA-free RNA was pipetted into fresh 0.5 ml centrifuge tubes. RNA concentration was re-measured.

Clontech 'Advantage RT for PCR' and Applied Biosystems 'TaqMan Reverse Transcription Reagents' were used for cDNA synthesis using random hexamer or oligo dT primers. 1 µg

of RNA template was used unless RNA concentrations were too low; the same amount of RNA template was always used in all reactions in the same experiment, dictated by the lowest RNA concentration. Reverse transcription reactions were performed in 96-well plates to allow multichannel pipettes to be used for PCR reaction set up, the reaction constituents and temperature programs used for each kit were:

Clontech Advantage RT for PCR:

	Vol.
RNA	Up to 1μg
H_2O	Adjust to 12.5μl
Primers (20μM)	1.0μl

Heat to 70°C for 2 minutes, then straight on to ice. Add the following to each reaction from a master-mix:

	Vol.(μl)
5X Reaction Buffer	4.0
dNTPs (10mM ea.)	1.0
RNase Inhibitor (40U/μl)	0.5
MMLV RT	1.0

Heat to 40°C for 1 hour, then 94°C for 5 minutes.

Applied Biosystems TaqMan Reverse Transcription Reagents:

	Vol.
RNA	Up to 1μg
H_2O	Adjust to 7.7μl

Then add the following to each tube from a master mix:

	Vol.(μl)
10X Reaction Buffer	2.0
$MgCl_2$ (25mM)	4.4
dNTPs (2.5mM ea.)	4.0
Primers (50μM)	1.0
RNase Inhibitor (20U/μl)	0.4
MultiScribe RT (50U/μl)	0.5

Heat to 25°C for 10 minutes, 48°C for 30 minutes then 95°C for 5 minutes.

2.7.2 Real-Time PCR

Applied Biosystems Gene Expression Assays and Custom Gene Expression Assays were used for all qRT-PCRs in this project. If a pre-designed assay was not available, a custom assay was designed using Applied Biosystems software. The assays consisted of a 20 X

reaction mix containing template-specific forward and reverse primers (18 mM each) and a probe that anneals between the two primers (5 mM). The probe DNA is fluorescently tagged at its 3' end, but fluorescence from intact probes is prevented by a quencher molecule that is bound to its 5' end. During PCR amplification, the 5'-3' nucleolytic activity of the DNA polymerase cleaves the quencher from the probe, resulting in fluorescence levels proportional to the amount of PCR product present. All Gene Expression Assays and Custom Gene Expression Assays used in this project were designed to anneal across two exons in cDNA, guaranteeing that non-specific amplification did not occur from residual genomic DNA.

Every effort was made to ensure that the amount of template cDNA was the same in each reaction of an experiment, however, given the sensitivity of qRT-PCR, expression of the gene of interest was always measured relative to the β-actin housekeeping control gene. The gene of interest and β-actin were amplified in duplex PCR reactions, probes for the gene of interest were tagged to 'FAM' labelled fluorescent dyes, while β-actin probes were labelled with 'VIC' dye, they fluoresce at different wavelengths, allowing them to be measured in the same reaction without interference. Reactions were performed in 20 µl or 5 µl volumes in 96-well or 384-well plates, respectively. The reaction constituents and temperature cycling parameters were:

Reaction Mixtures:

	20µl:	***5µl:***
	Vol.(µl)	Vol.(µl)
2X PCR Master Mix	10.0	2.5
20X Gene Expression Assay	2.0	0.25
20X β-actin Expression Assay	2.0	0.25
cDNA	2.0-4.0	2.0
Nuclease-free H_2O	Up to 20µl	–

Temperature cycling:

50°C	2 min	
95°C	10 min	
95°C	15 sec	x35 cycles
60°C	1 min	

All samples were amplified in duplicate or triplicate, at least three treatment replicates were included per experiment. Fluorescence of FAM and VIC dyes was measured for all reactions during temperature cycling, data was analysed using a combination of Applied Biosystems SDS (Sequence Detection Software) and Microsoft Excel software. SDS plotted amplification curves as cycle number vs. fluorescence for both dyes in every well.

FAM and VIC fluorescence were analysed as separate data sets, a fluorescence threshold was identified for each data set where amplification curves were in their exponential phase. The 'cycle threshold value' (Ct value) for each amplification curve was interpolated by finding the precise fractional cycle number (to 5 decimal places) at which the curve crossed the fluorescence threshold. Ct values for FAM and VIC data were exported from SDS as text files and converted to Excel documents for data analysis. Relative levels of gene expression were calculated by the 'ΔΔCt method' (Livak et al. 2001). This method calculates gene expression normalised to the endogenous control relative to a calibrator from within the experiment (i.e. a sample or sample group designated to have relative gene expression level of 1.0), it is advantageous because it does not require the inclusion of a standard curve from a serial dilution of template in each experiment. The ΔΔCt method is logically derived from the equation that dictates the rate of product accumulation during PCR:

For a given PCR reaction, the amount of product (X_T) accumulated when amplification reaches the Ct threshold is:

$$X_T = X_0 \text{ x } (1 + E_X)^{Ct,X} = K_X$$

Where:
X_0 = Initial number of target molecules
E_X = Efficiency of amplification
K_X = Constant
Ct,X = Ct for target

Similarly, the equation for the endogenous reference reaction (R) is:

$$R_T = R_0 \text{ x } (1 + E_R)^{Ct,R} = K_R$$

In correcting for the level of expression of the endogenous control, the level of target amplification is divided by the level of endogenous control:

$$\frac{X_T}{R_T} = \frac{X_0 \text{ x } (1+E_x)^{Ct,X}}{R_0 \text{ x } (1+E_R)^{Ct,R}} = \frac{K_X}{K_R} = K$$

Assuming the efficiencies of the target and control amplification reactions are the same, i.e. if $E_X = E_R = E$:

$$\frac{X_0}{R_0} \times (1+E)^{Ct,X-Ct,R} = K$$

Or:

$$X_N \times (1+E)^{\Delta Ct} = K$$

Where:
$X_N = X_0/R_0$, the normalised amount of target
$\Delta Ct = Ct,X - Ct,R$, the difference in Ct values for target and control

This equation can be rearranged:

$$X_N = K \times (1+E)^{-\Delta Ct}$$

To quantify expression relative to the calibrator, divide by the X_N for the calibrator sample (X_{cb}):

$$\frac{X_N}{X_{N,cb}} = \frac{K \times (1+E)^{-\Delta Ct}}{K \times (1+E)^{-\Delta Ct,cb}} = (1+E)^{-\Delta\Delta Ct}$$

Where:
$\Delta\Delta Ct = \Delta Ct - \Delta Ct,cb$

For Gene Expression Assays designed by Applied Biosystems the efficiency is close to 1, therefore the amount of target can be calculated as:

Relative quantification (RQ) = $2^{-\Delta\Delta Ct}$

In order to use the ΔΔCt it was imperative to experimentally confirm that the amplification efficiencies of the target and control gene PCRs were the same (i.e. that $E_X = E_R$). Therefore the amplification efficiencies of each Gene Expression Assay were measured in duplex PCRs with the β-actin assay using a serial dilution of template. This process was performed for all Gene Expression Assays and Custom Gene Expression Assays for each different cDNA template (e.g. for cDNA from kidneys, carotid arteries and for each cultured cell line). A dilution series of cDNA template was prepared from neat to 1/1,000, typically including 1/5, 1/10, 1/50, 1/100, 1/500 and 1/1000 dilutions. Graphs were plotted of log(dilution) versus Ct for the target template and *β-actin*, the gradient of each line was compared, according to the Applied Biosystems guidelines they had to be within ±0.1 to be used to measure gene expression in this tissue. Each Gene Expression Assay for RNA from each tissue in this project passed this test.

2.8 Statistical Analysis

Where specialised statistical analysis techniques have been applied (for example the use of Rank Products and False Discovery Rates in microarray data analysis in Chapter 3), details and references are provided in the relevant methods or results sections. A number of experiments throughout the project applied straightforward parametric statistical tests. All statistical comparisons were performed on data collected in individual assays, eliminating error from inter-assay variability. For comparisons of a continuous variable between two experimental groups, 2 sample t-tests were applied (Bland 2000). For statistical comparisons of a continuous variable in data sets with more than two groups, analysis of variance (ANOVA) was applied, followed by the Tukey post-test for comparisons between all data sets or the Dunnett's post-test for comparison of all sample groups against a designated control (Bailer et al. 1997). The significance threshold for p-values in these analyses was set at 0.05; the specific tests applied in each experiment are detailed in figure legends.

3 Microarray Renal Gene Expression Profiling in the 5 Week-Old SHRSP

3.1 Introduction

As discussed in section 1.2.3.3, a number of studies have been performed to dissect the genetic causes of hypertension and other cardiovascular diseases by comparing microarray gene expression levels between inbred parental and congenic strains. A notable example of this approach identified *Cd36* as a causative gene underlying a QTL for fatty acid and glucose metabolism on the SHR chromosome 4 (Aitman et al 1999), and *Gstm1* was identified as a hypertension candidate gene in the SHRSP in this manner (McBride et al 2003). However, such experiments may be limited by the fact that in many of these studies gene expression is measured in adult rats where hypertension is fully established, leading to the likelihood that data could be misinterpreted: candidate genes could be differentially expressed as a secondary response to high blood pressure rather than as a primary cause of hypertension.

Blood pressure measurements in the Glasgow SHRSP and WKY colonies have demonstrated that blood pressures of SHRSP rats are higher than the WKY by 8 weeks of age, and that they rise sharply in the SHRSP between 8 and 12 weeks of age (Davidson et al 1995). It is technically very challenging to measure blood pressures accurately in young rats, though published research has demonstrated equivalent blood pressures between 6 week-old SHRSP and WKY strains (Kopf et al. 1993), and the period between 3-10 weeks after birth is thought to be important to the development of genetic hypertension in rat model strains (Zicha et al. 1999). A number of microarray studies have measured differential gene expression between normotensive, hypertensive and congenic or recombinant strains during this period (Hubner et al 2005;Garrett et al. 2005;Lee et al. 2007), and others have measured expression at more than one timepoint to assess temporal changes in gene expression during the development of hypertension. For example, gene expression was analysed during the development of hypertension in the SHR with the premise that genes consistently differentially expressed between three different substrains of the SHR and the WKY represent strong essential hypertension candidates (Hinojos et al. 2005). Renal gene expression was measured at 4, 8, 12 and 18 weeks in strains SHR-A3, SHR-B2, SHR-C and WKY, the SHR strains were all fixed at various generations of derivation during the original breeding of the SHR and SHRSP from the WKY (Okamoto et al 1974). Gene expression data reflected the relatedness of the strains: SHR-B2 and SHR-C are most closely related, sharing common ancestors at generations F_{11} an F_{14} and showed greatest concordance of gene expression, while SHR-A3 shares closest ancestors to the other strains between generations F_1-F_8 and displayed less similarity of gene

expression. The list of consistently differentially expressed genes between the WKY and all 3 SHR strains at all timepoints was refined to find candidate hypertension genes by finding those within established blood pressure QTLs in the SHR. In this manner, 14 genes and expressed sequence tags (ESTs) were identified on 11 chromosomes and proposed as potential hypertension genes, though microarray expression data was not corroborated by a second method and no specific analysis was performed on metabolic pathways known to influence blood pressure control (Hinojos et al 2005). The *Spon1* gene was identified as a hypertension candidate gene in renal microarray studies on 6 and 24 week SHR, WKY and 2 congenic strains of SHR background introgressed with overlapping regions of WKY chromosome 1 (Clemitson et al. 2007); in this study *Spon1* was the only gene from within the minimal congenic interval that was consistently differentially expressed between the congenic strains and the SHR and between the SHR and WKY at both timepoints.

Seubert et al measured renal gene expression in 3 week-old and 9 week-old SHR and WKY rats, (Seubert et al. 2005), allowing comparison of gene expression between the SHR and WKY at 3 weeks of age and at 9 weeks of age, and also between 3 week-old and 9 week-old rats of the same strain. The major findings of the paper included the observation that 20 genes were differentially expressed between the SHR and WKY at 3 weeks of age, while 104 were differentially expressed at 9 weeks of age, 7 genes were common to both timepoints. The soluble epoxide hydrolase (*sEH*) gene was upregulated in the SHR compared to the WKY at both timepoints, the authors proposed *sEH* as a candidate hypertension gene in the SHR given its role in arachidonic acid metabolism, it converts vasodilatory epoxyeicosatrienoic acids to less active diol forms. The within-strain comparisons showed that 211 genes were differentially expressed between 3 week-old and 9 week-old SHRs, while 508 genes were differentially expressed in the same comparison in the WKYs; 174 of these genes were common to both groups. The authors concluded from these analyses that there are likely to be developmental differences in renal gene expression accounting for hypertension in the SHR (Seubert et al 2005). Custom cDNA microarray chips measured the expression of just 6700 transcripts in these experiments, this, in conjunction with the lack of a congenic strain to narrow-down analysis to an established QTL, limited the power of the study. In addition, while specific analysis of arachidonic acid metabolism and blood pressure related genes was undertaken (finding no other differentially expressed genes), analysis was restricted to just these pathways. More sophisticated analysis techniques are now available, such as Ingenuity Pathway Analysis (IPA), to interrogate data from the perspective of interlinked metabolic pathways. IPA is a web-based microarray and proteomic data analysis tool that utilises published Kyoto Encyclopedia of Genes and Genomes (KEGG) pathway database; experimental data can be

linked to pathway maps to identify instances where multiple genes involved in a particular pathway are differentially expressed in comparisons between experimental groups. When applied to gene expression comparisons between congenic and parental strains this is a very powerful analysis technique, allowing the influence of the congenic interval on genome-wide expression to be functionally linked to multiple genes in a physiological pathway, identifying genes whose expression is regulated in *trans* from within the congenic interval.

The experimental work performed in this chapter assessed the changes in renal gene expression in the SHRSP and WKY and congenic 2c* strains at 5 weeks of age to assess the differential expression of *Gstm1* during the development of hypertension and to identify other hypertension candidate genes. The 5-week expression dataset was also analysed in conjunction with previously published data analysing renal gene expression in the same strains at 16 weeks of age (McBride et al 2003). This allowed the changes in gene expression over time to be measured in each strain, and between strains at each timepoint. Gene expression data was analysed with Ingenuity Pathway Analysis (IPA) software to find pathways with multiple differentially expressed genes. Secondary phenotypes related to an implicated pathway, glutathione metabolism, were measured in parental and congenic rats.

3.2 Aims

- To measure renal gene expression in the SHRSP, WKY and congenic 2c* inbred strains at 5 weeks of age.

- To assess differential expression of *Gstm1* and to identify other consistently differentially expressed genes from the congenic interval in comparisons between the SHRSP and WKY and between the SHRSP and 2c*.

- To apply Ingenuity Pathway Analysis to 5-week microarray data and 16-week renal expression data generated in the same strains in 16-week old animals (McBride et al 2003) to identify canonical metabolic pathways affected by differential expression of genes within and outwith the congenic interval.

- To compare renal glutathione and superoxide levels in all strains, and to confirm differential expression of glutathione metabolism genes in parental and congenic strains with quantitative real-time PCR.

- To sequence the coding and regulatory regions of candidate genes.

3.3 Methods

3.3.1 Renal Microarray mRNA Expression Analysis

Affymetrix GeneChip RGU34A, B and C microarray chips, with a total of 26379 gene and EST probe sets, were used to measure renal gene expression in male 5 week old WKY, SHRSP and 2c* rats. RGU34A analyses approximately 7000 full-length sequences and 1000 expressed sequence tags (ESTs), RGU34B and C analyse approximately 8000 ESTs each. Three animals from each strain were used. Microarray hybridisations were performed by Martin McBride at the microarray facility at the Sir Henry Wellcome Functional Genomics Facility, University of Glasgow.

3.3.1.1 RNA Extraction and Validation

Whole kidneys were excised from freshly killed 5 week-old rats, snap-frozen in liquid nitrogen and stored at -80°C until RNA extraction. RNA was extracted using Qiagen RNeasy Maxi columns as per section 2.5.3. RNA concentrations were quantified by Nanodrop as per section 2.2.2, and where necessary ethanol-precipitated (0.1 volume 3M NaOH pH5.5; 2.5 volumes ethanol, precipitated at -20°C for 1 hour, collected by centrifugation, removed supernatant and air dried before resuspending in a reduced volume of H_2O) to at least 2 μg/μl concentration. mRNA sample integrity was verified by electrophoresis 250 ng of RNA on an Agilent Bioanalyser 2100.

3.3.1.2 First and Second Strand cDNA Synthesis

The Invitrogen ds-cDNA synthesis kit was used for first and second strand cDNA synthesis. Ten μg of RNA was diluted with 100 pmol T7 oligo dT primer (sequence GGCCAGTGAATTGTAATACGACTCACTATAGGGAGGCGG$(T)_{24}$) in a total volume of 11 μl with RNase-free H_2O. Samples were denatured at 70°C for 10 minutes, placed on to ice and 4 μl 5 X first strand buffer, 2 μl 0.1 M DTT, 1 μl 10 mM dNTP was added to each. Reactions were heated to 42°C for 2 minutes before adding 2 μl 200 U/μl SuperScript II reverse transcriptase and heating to 42°C for 1 hour, then placing on ice to stop the reaction.

For second strand cDNA synthesis, 91 μl RNase-free H_2O, 30 μl 5 X second strand buffer, 3 μl 10 mM dNTP mix, 1 μl 10 U/μl *E.coli* DNA ligase, 4 μl 10 U/μl *E.coli* DNA polymerase I, 1 μl 2 U/μl *E.coli* RNase H was added to each tube and reactions were

incubated at 16°C for 2 hours. 2 µl of T4 DNA polymerase was added to each reaction and incubated at 16°C for a further 2 minutes; 10 µl 0.5 M EDTA was added.

3.3.1.3 Double Stranded cDNA Clean-up

ds-cDNA was purified for cRNA synthesis using the filter-based Affymetrix GeneChip Sample Cleanup Module. ds-cDNA was transferred to a 1.5 ml microfuge tube and 600 µl cDNA binding buffer was added. Samples were applied to cDNA Cleanup Spin Columns and centrifuged for 1 minute at 10000 rpm. Spin columns were transferred to new collection tubes and filters were washed by centrifugation of 750 µl cDNA wash buffer at full speed for 1 minute, discarding the flow-through. Membranes were dried by centrifugation at full speed for 5 minutes, 14 µl H_2O was added to membranes and they were incubated at room temperature for 1 minute before eluting by centrifugation at full speed for 1 minute.

3.3.1.4 Biotin-labelled cRNA Synthesis, Clean-up and Validation

Biotinylated cRNA was synthesised for each ds-cDNA using the Enzo Bioarray High Yield Transcript Labelling kit from Enzo Biochem. 5 µl cDNA, 17 µl RNase-free H_2O, 4 µl 10 x HY reaction buffer, 4 µl 10 x biotin-labelled ribonucleotides, 4 µl 10 x DTT, 4 µl RNase inhibitor mix and 2 µl T7 RNA polymerase was added per reaction, tubes were heated to 37°C for 4.5 hours.

Biotinylated cRNA was purified using the Affymetrix GeneChip Sample Cleanup Module. *In-vitro* reverse transcription reactions were transferred to 1.5 ml microfuge tubes, 60 µl RNase-free H_2O was added, followed by 350 µl cRNA binding buffer and 250 µl ethanol. Samples were mixed by pipetting and applied to IVT cRNA Cleanup Spin columns, centrifuged at full speed for 15 seconds, then the flow-through was reapplied to the columns and centrifuged at full speed for 15 seconds once more. Columns were transferred to new collection tubes and membranes were washed with 500 µl IVT cRNA wash buffer, centrifuging for 15 seconds at full speed. Flow-through was discarded and 500 µl 80 % ethanol was applied to each column, centrifuging for 15 seconds at full speed. Flow-through was discarded and membranes were thoroughly dried by centrifugation at full speed for 5 minutes. 15 µl RNase-free H_2O was added to columns, incubated for 1 minute at room temperature and eluted by centrifugation for 1 minute at full speed, an additional 15 µl elution was performed using the same protocol, collecting 30 µl cRNA in total.

One µl of each biotinylated cRNA was added to 4 µl H_2O and electrophoresed on an Agilent Bioanalyser 2100 to confirm successful cRNA amplification. Final cRNA concentration was calculated by subtracting the carried-over template genomic RNA from the total yield measured by Nanodrop.

3.3.1.5 cRNA Fragmentation

cRNA fragmentation was performed using 5 X fragmentation buffer from the Affymetrix GeneChip Sample Cleanup Module. Twenty-five µg of each cRNA sample was diluted to a total volume of 40 µl in H_2O, 8 µl 5 X fragmentation buffer was added and samples were incubated at 94°C for 35 minutes.

3.3.1.6 Microarray Hybridisation and Data Collection

Hybridisation mixes were prepared using Affymetrix microarray hybridisation reagents in a total volume of 500 µl per sample, including: 40 µl of fragmented cRNA, 8.5 µl B2 Control oligo (3 nM), 25 µl 20 X eukaryotic hybridisation controls, 5 µl herring sperm DNA (10 mg/ml), 5 µl acetylated BSA (50 mg/ml), 250 µl 2 X hybridisation buffer and 166.5 µl H_2O. Hybridisation mixes were denatured at 99°C for 5 minutes, then to 45°C for 5 minutes, and centrifuged at 14500 rpm for 5 minutes before applying to chips.

Prior to performing experimental microarrays, Affymetrix 'Test3' quality control chips were hybridised and scanned with each hybridisation mix. Test3 chips were pre-wet with 100 µl 1 X hybridisation buffer and incubating at 45°C for 10 minutes in a rotating oven at 60 rpm, after which hybridisation buffer was removed and 80 µl hybridisation mix was added, chips were returned to the 45°C oven rotating at 60 rpm for 16 hours. Hybridisation mixes were stored at -20°C until Test3 quality control checks were complete, they were then thawed, reheated to 45°C and re-centrifuged before applying to the RGU34A,B and C chips. RGU34A,B and C microarrays were hybridised using exactly the same incubation protocol as Test3 chips, but 250 µl 1 X hybridisation solution was used for pre-wetting and 200 µl hybridisation mix was used per chip. Where necessary hybridisation mixes were recovered and reused in repeat hybridisations.

Test3 and RGU34 chips were washed and stained following standard protocols in an Affymetrix Fluidics Station 400 operated by GeneChip software. Hybridisation mixtures were removed from the arrays and replaced with 250 µl non-stringent wash buffer at room temperature. Streptavidin phycoerythrin (SAPE) stain solution was prepared (600 µl 2 X

MES stain buffer, 48 µl 50 mg/ml acetylated BSA, 12 µl 1 mg/ml SAPE, 540 µl H_2O per chip), separated into 2 x 600 µl aliquots and loaded onto the fluidics station (wrapped in foil to protect from light). A 600 µl aliquot of antibody solution (300 µl 2 X MES stain buffer, 24 µl 50 mg/ml acetylated BSA, 6 µl 10 mg/ml normal goat IgG, 3.6 µl 0.5 mg/ml biotinylated antibody, 266.4 µl H_2O per chip) was prepared and loaded onto the fluidics station. Microarray washing included washes with low stringency buffer followed by high stringency buffer. Test3 and RGU34 chips were scanned using specific scanning protocols on an Affymetrix GeneChip scanner.

3.3.1.7 Microarray Data Analysis

Microarray data quality control was performed on Test3 and RGU34 chips using Affymetrix microarray suite 4 (Mas4) software. Fluorescence scaling values were compared across chips and hybridisations of control RNAs were verified. 5-week raw scanning data was combined with the raw data from 16-week renal microarrays in the same strains (McBride et al 2003), data was normalised using the robust multi-array average method (Irizarry et al. 2003) with BioConductor software. RMA applies background correction to compensate for non-specific binding and normalises probeset intensity signals across all of the chips in the experiment, allowing comparisons between arrays. Differentially expressed probesets between strains and timepoints were identified using the rank product (RP) method (Breitling et al. 2004). RP data from all microarrays was uploaded onto the IPA website (www.ingenuity.com) and analysed to identify the metabolic pathways with most genes significantly differentially expressed in pairwise comparisons between each strain at each timepoint, and in within-strain comparisons between 5 and 16 week animals.

3.3.2 Gstm1 western blotting

Gstm1 protein levels in 5 week-old SHRSP, 2c* and WKY kidneys were assessed by western blotting. Experimental protocols were follwed as per section 2.6 and 5.3.6. Forty µg of kidney protein was loaded per lane.

3.3.3 Kidney Glutathione Measurements

Tissue glutathione assays were performed by Dr Carlene Hamilton. Total GSH levels were measured in kidneys of 5 and 16 week old WKY, SHRSP and 2c* rats using the Cayman Chemical glutathione assay kit (assay no. 703002). 0.1-0.4 g of kidney tissue was

homogenised in 2 ml/g 4°C 0.2 M 2-(N-morpholino) ethanesulphonic acid; 0.05 M phosphate, 1 mM EDTA pH6 (MES buffer) using a Polytron PT 2100 homogeniser. Homogenates were centrifuged at 10000 g for 15 minutes at 4°C, supernatants were pipetted off and stored on ice. Supernatants were de-proteinated by adding an equal volume of 0.1 g/ml metaphosphoric acid, vortexing, centrifuging at 20000 g for 2 minutes and collecting the supernatant. Directly before performing GSH assays, 4 M triethanolamine was added at 50 µl/ml. Standards were prepared from 0 µM – 16 µM GSH, 50 µl of each standard and sample were measured in duplicate in a clear 96-well plate. Assay reagent was prepared with 11.25 ml MES buffer, 0.45 ml cofactor mixture ($NADP^+$ and glucose 6-phosphate), 2.1 ml enzyme mixture (glutathione reductase and glucose 6-phosphate in MES buffer), 2.3 ml H_2O, and 0.45 ml 5,5'-dithio*bis*-2-nitrobenzoic acid (DTNB) solution. 150 µl of assay reagent was added to each standard and control well and the assay plate was left for 30 minutes to allow colour development before measuring absorbance at 405 nm on a Victor Wallac2 plate reader. Standard curves were plotted (GSH concentration vs. absorbance), sample GSH concentrations levels were interpolated and converted to nM GSH per g kidney tissue.

3.3.4 Kidney Superoxide Measurements

Kidney superoxide measurements were performed by Dr Carlene Hamilton. Whole kidneys from 5 week-old SHRSP, 2c* and WKY rats (n=5 per group) were homogenised in phostphate buffered sailne, pH7.8, centrifuged at 1000 rpm for 2 minutes at 4°C and supernatants were frozen at -80°C until the assay. Protein concentrations were determined using a BCA assay as detailed in section 2.2.5. NADH-stimulated superoxide levels were measured in duplicate for each kidney using a Packard Tri-Carb 2100TR liquid scintillation counter. 2 ml assays were prepared in scintillation vials including 0.5 ml kidney homogenate, 1 µM lucigenin, and 100 µM NADH in PBS buffer. Total luminescence was measured for 3 minutes in each sample. Superoxide levels were calibrated against a standard curve generated with 70-840mM xanthine and xanthine oxidase (0.001 U/ml), superoxide measurements were expressed as n moles $O_2^{-}\cdot$ / µg total protein.

3.3.5 Quantitative RT-PCR

Taqman qRT-PCR was applied to confirm differential expression measured in microarray experiments. The same kidney mRNA from microarray experiments were used as templates for the synthesis of DNA-free cDNA as described in section 2.7.1 plus 2

additional kidney mRNAs from other animals of each strain. Duplex 5 µl RT-PCR reactions were performed using Applied Biosystems Taqman Gene Expression Assays for *Gstm1* (assay no. Rn00755117_m1), Gamma-glutamyltransferase 1 (*Ggt1*) (Rn00587709_m1), aminopeptidase N (*Anpep*) (Rn01478171_m1), solute carrier family 7, member 12-like (*Slc7a12-like*) (Rn02607204_mH) glutamate-cysteine ligase, modifier subunit (*Gclm*) (Rn00568900_m1), and thioesterase 4 (*Them4*) (Rn_01533922_m1) measuring expression relative to *β-actin* as outlined in section 2.7.

3.3.6 DNA Sequencing

2500 bp of promoter sequence and all coding exons of, *Anpep, Slc7a12-like, Gclm, Them4,* and *HistH2aa* were sequenced in WKY, and SHRSP and SHR rats according to protocols in sections 2.4.2 – 2.4.5. See section 4.4.2 for equivalent analysis for *Gstm1*. Only the coding sequence of *Ggt1* was sequenced since this gene is currently not mapped in the rat genome. Renal cDNA was used as template for coding sequences, and genomic DNA was used for promoter sequencing, two rats per strain were sequenced. Sequences were aligned to Brown Norway reference sequences from Ensembl.

3.4 Results

3.4.1 mRNA and cRNA Validation

Electrophoresis of 5 week kidney mRNA samples on the Agilent Bioanalyser 2100 confirmed RNA quality prior to cDNA synthesis, indicated by defined bands for 28S and 18S ribosomal RNA (rRNA) species and very little evidence of small RNA species smaller than the 18S band (figure 3.1).

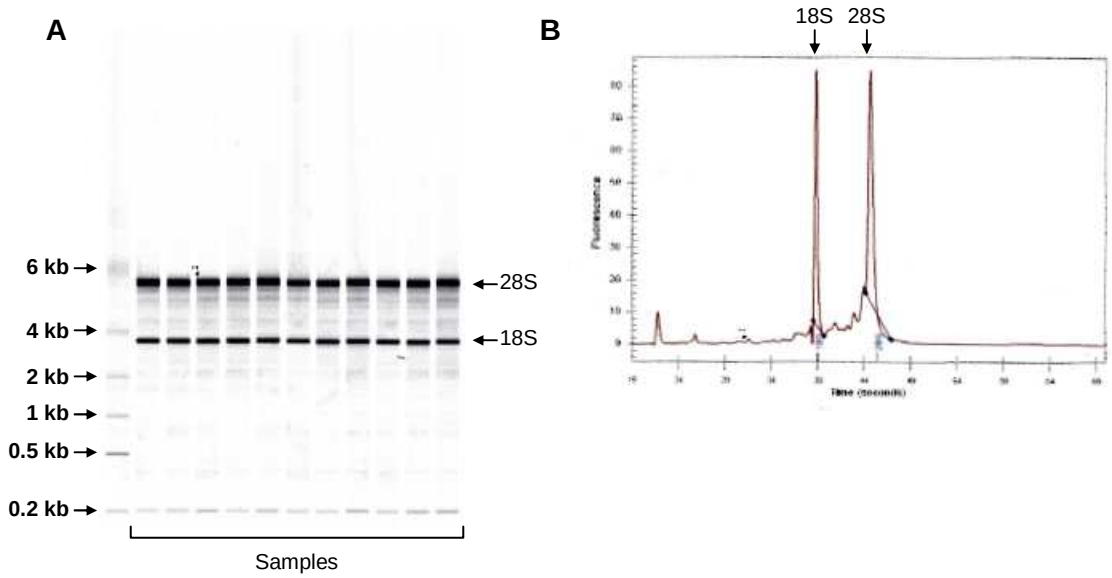

Figure 3.1 - Agilent Bioanalyser 2100 assessment of mRNA quality
(A) Electrophoresis of mRNA samples showing bands for 28S and 18S rRNA. The lower band in each lane is a 200 bp size marker to align samples and controls. **(B)** Representative individual electropherogram, with sharp peaks for 28S and 18S rRNA and no RNA species smaller than 18S rRNA.

Following *in-vitro* transcription to synthesise biotinylated cRNA, cRNA quality was assessed by electrophoresis on the Agilent Bioanalyser 2100, showing approximately normally-distributed cRNA species, all samples showed similar-shaped distributions of cRNA species and similar concentrations (figure 3.2).

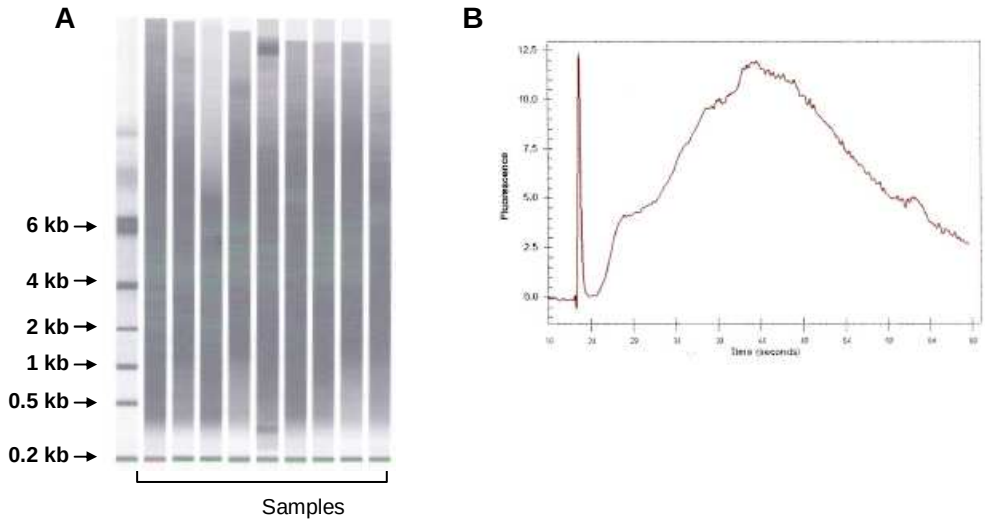

Figure 3.2 - Agilent Bioanalyser 2100 assessment of cRNA quality
(A) Electrophoresis of samples showing the distribution of cRNA species separated by size. **(B)** Representative electropherogram, showing approximately normal-distrubution of cRNAs. The sharp peak at the extreme left of the trace corresponds to the 200 bp size marker in all samples used to align samples and controls.

3.4.2 Renal Microarray mRNA Expression Profiling

3.4.2.1 Microarray Data Quality Control

Mas4 software was applied in Test3 and RGU34A quality control analysis, using quality control benchmarks stipulated by Affymetrix. Data for Test3 chips is shown in table 3.1. The scaling factors used to scale total chip fluorescence values to 100 relative units were compared between chips, a ratio of less than 3 between any scaling factors was required for the chips to pass batch analysis. All microarray chips include control probesets for *β-actin* and *Gapdh* that correspond to the 3' and 5' end of the genes. *In-vitro* transcription of cRNA has a 3'-bias since it is transcribed from DNA transcripts created by a polyT primer, therefore binding intensities are expected to be higher at 3' probsets than 5' probesets, however, a 3':5' intensity ratio of greater than 3 for *β-actin* and *Gapdh* would indicate inefficient *in-vitro* transcription and rejection of the chip in question. Hybridisation master mixtures were spiked with cRNAs for the *E.coli* genes *bioB*, *bioC*, *bioD* (from the biotin synthesis pathway), and *cre* (Cre recombinase), probeset intensities for these were required to exceed specific thresholds for a chip to pass the quality control process. An additional control RNA, the synthetic B2 oligo was also present in the hybridisation mix, correct hybridisation patterns of B2 were required to align chips for scanning. All hybridisation mixes passed the Test3 quality control tests, and RGU34 hybridisations were subject to the

same tests plus additional analysis of the number of present, marginal and absent fluorescence calls across the chips.

Hyb Mixture	Scaling Factor	3' : 5' Ratio		Pass / Fail			
		β-actin	*Gapdh*	*bioB*	*bioC*	*bioD*	*cre*
SHRSP A	0.801	1.26	1.82	Pass	Pass	Pass	Pass
SHRSP B	0.534	1.29	1.43	Pass	Pass	Pass	Pass
SHRSP C	0.729	2.46	2.52	Pass	Pass	Pass	Pass
2c* A	0.557	1.40	1.33	Pass	Pass	Pass	Pass
2c* B	0.716	1.52	1.64	Pass	Pass	Pass	Pass
2c* C	0.650	1.32	1.47	Pass	Pass	Pass	Pass
WKY A	0.528	1.36	1.40	Pass	Pass	Pass	Pass
WKY B	0.474	1.40	1.35	Pass	Pass	Pass	Pass
WKY C	0.589	1.34	1.49	Pass	Pass	Pass	Pass

Table 3.1 - Quality control data from Test3 chips.
See text for details of quality control parameters.

3.4.2.2 Rank Products Analysis

Following normalisation of gene expression data by RMA, pairwise comparisons of renal gene expression were carried out between each strain in 5 week-old rats using the rank-products (RP) method. RP performs pairwise comparisons of probeset intensities across all replicates and ranks the comparisons according to the magnitude of the intensity differences. Differentially expressed probesets are identified by computing the average rank for all of the pairwise comparisons, false-discovery rates are calculated by performing 1100 permutations of the data to generate a null distribution. RP has been demonstrated to be superior to microarray analysis software based on comparing absolute fold-changes for data sets with small sample sizes (Jeffery et al. 2006).

At a false-discovery rate (FDR) threshold of 0.05 a total of 294 probesets were differentially expressed between the SHRSP and WKY, 267 were differentially expressed between the 2c* and WKY, while 95 were differentially expressed between the SHRSP and 2c*, reflecting the genomic similarity between the SHRSP and 2c*. These data were compiled into a Venn diagram depicting the number of probesets common to multiple pairwise comparisons, highlighting the probesets common to comparisons between the WKY and SHRSP and between the 2c* and SHRSP that implicate the involvement of the

2c* congenic interval (figure 3.3A). The same comparisons were performed for the 16 week microarray data (figure 3.3B) and in comparing within-strain gene expression between 5 and 16 weeks (figure 3.3C).

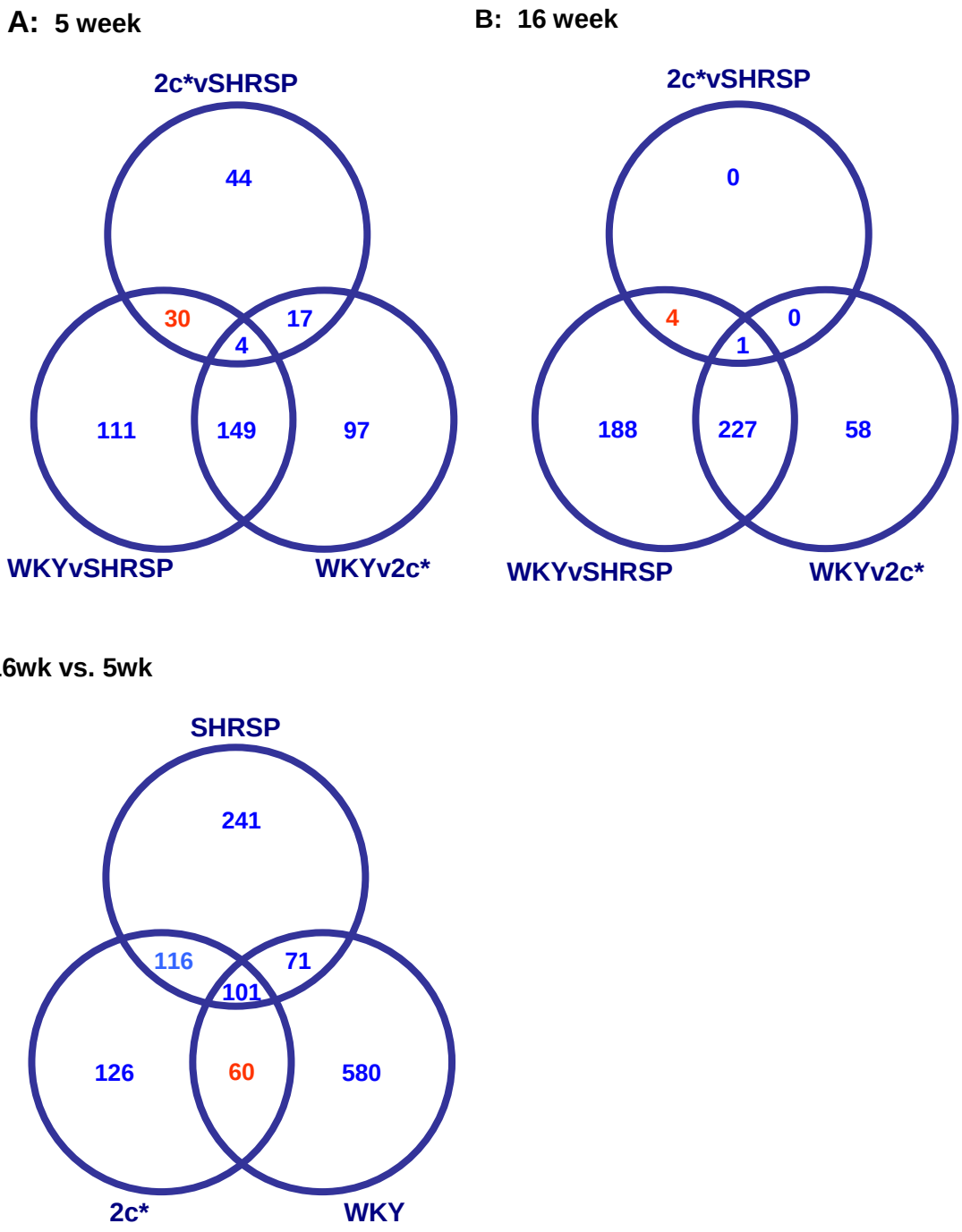

Figure 3.3 - Differential renal mRNA expression in pairwise comparisons of different strains and timepoints

Venn diagrams illustrating microarray results of renal gene expression in 5 and 16 week SHRSP, WKY and 2c* rats. The number of probesets significantly differently expressed in each pairwise comparison are shown, numbers in red represent probesets that implicate the 2c* congenic interval. **(A)** 5 week inter-strain comparisons. **(B)** 16 week inter-strain comparisons **(C)** 5 week versus 16 week comparisons.

Complete lists of the differentially expressed probesets implicating involvement of the 2c* congenic interval in the three comparisons are in tables A2-A4 in the appendix. Probeset mapping was performed by interrogating Affymetrix databases to locate all consistently differentially expressed transcripts transcribed from within the 2c* congenic interval in each of the comparisons (table 3.2). This confirmed differential expression of *Gstm1* at both timepoints, and identified further genes from the congenic interval differentially expressed between the SHRSP and both the WKY and 2c*: Solute carrier family 7, member 12-like (*Slc7a12-like*), histone 2, H2aa (*Hist2H2aa*), and thioesterase 4 (*Them4*). The differential expression of *Slc7a12-like* was significant in the light of differential *Gstm1* expression and glutathione metabolism, it encodes a protein with 98.8% amino-acid homology to the mouse *Slc7a12* amino acid transporter that is highly expressed in the kidney has high specificity for cysteine transport (Chairoungdua et al. 2001), cysteine is the rate-limiting substrate in the synthesis of GSH . In addition, 2 genes from the congenic interval were identified whose expression was significantly different between 5 and 16 weeks in the WKY and 2c* but not the SHRSP: *Claudin 11* and papillary renal cell carcinoma (*Prcc*).

3.4.2.3 *Gstm1* qRT-PCR and Western Blotting

Taqman qRT-PCR measured *Gstm1* expression relative to β-actin in each strain and timepoint. Reduced expression of *Gstm1* was demonstrated in the SHRSP compared to the WKY and 2c* at 5 and 16 weeks by 4-7 fold (figure 3.4). This indicates that reduced renal *Gstm1* expression precedes the onset of severe hypertension in the SHRSP, supporting the hypothesis that it contributes to the hypertensive phenotype, rather than being down-regulated in response to elevated blood pressure.

Differential renal Gstm1 expression was also confirmed at the protein level. Western blotting showed reduced Gstm1 protein in the SHRSP kidney compared to the WKY and 2c* (figure 3.5).

3.4.2.4 Ingenuity Pathway Analysis

RP data from 5 and 16 week microarrays was uploaded into Ingenuity Pathway Analysis (IPA) software for analysis with respect to differential expression of groups of genes involved in specific metabolic pathways (figure 3.6). Glutathione metabolism consistently featured within the top 6 most significantly affected metabolic pathways, ranked by the significance of SHRSP vs. 2c* for 5 and 16 week inter-strain comparisons and ranked by

significance of 16 week SHRSP vs. 5 week SHRSP for within-strain comparisons. Glutathione metabolism was also differentially affected at 5 weeks of age in comparisons between both the SHRSP and 2c* and between the SHRSP and WKY, implicating an effect of genes encoded from the 2c* congenic interval.

	Probeset	Gene	Location	2c* vs. SP	WKY vs. SP
5 wk	J02810mRNA_s_at	*Gstm1*	2q34	2c*(9.4)	WKY(7.5)
	X04229cds_s_at			2c*(11.2)	WKY(7.2)
	H32189_s_at			2c*(4.2)	WKY(4.1)
	rc_AI060176_at	*Slc7a12-like*	2q23	SP(3.0)	SP(2.3)
	AA801165_at	*Hist2H2aa*	2q34	SP(1.9)	SP(1.9)
	rc_AA997142_at	*Them4*	2q34	SP(2.4)	SP(2.4)
	Probeset	**Gene**	**Location**	**2c* vs. SP**	**WKY vs. SP**
16 wk	H32189_s_at	*Gstm1*	2q34	2c*(7.6)	WKY(9.5)
	J02810mRNA_s_at			2c*(4.6)	WKY(6.2)
	X04229cds_s_at			2c*(9.7)	WKY(13.8)
	Probeset	**Gene**	**Location**	**2c***	**WKY**
5 wk vs. 16 wk	rc_AA901342_at	*Claudin 11*	2q24	5 wk(2.4)	5 wk(2.2)
	rc_AA996628_at	*Prcc*	2q34	5 wk(2.9)	5 wk(3.2)

Table 3.2 - Differentially expressed probesets encoded from the 2c* congenic interval

Differentially expressed probesets located within the 2c* congenic interval common to comparisons between SHRSP and WKY and between SHRSP and 2c* at five weeks of age and 16 weeks of age. And 2c* congenic interval genes differentially expressed in *within-strain* comparisons between 5 and 16 week-old WKY rats and between 5 and 16 week-old 2c* rats, but not between 5 and 16 week-old SHRSP rats. Strain or age with highest expression is indicated, fold change in brackets. FDR<0.05.

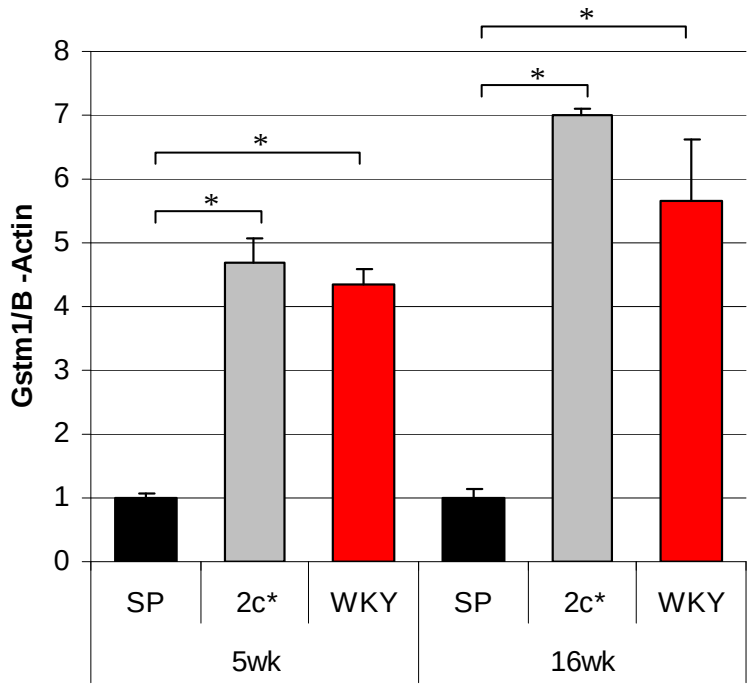

Figure 3.4 - Differential expression of *Gstm1* at 5 and 16 weeks of age confirmed by qRT-PCR

Taqman qRT-PCR confirming 4-7 fold reduced renal expression of *Gstm1* in the SHRSP at 5 and 16 weeks compared to the 2c* and WKY. n=5 per group. Mean ±SE. * p<0.01 (ANOVA and Dunnett's post-test).

Figure 3.5 - Reduced renal Gstm1 protein in the 5 week-old SHRSP

Western blotting confirmed reduced renal Gstm1 protein (26kDa) in the SHRSP compared to the WKY and 2c*. 40 µg of protein per lane, B-actin immunoreactivity observed at the expected molecular weight (42 kDa).

A: 5wk

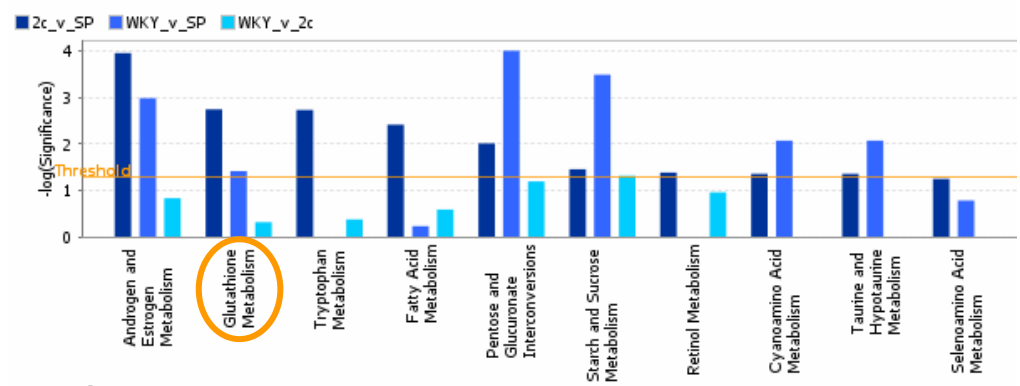

B: 16wk

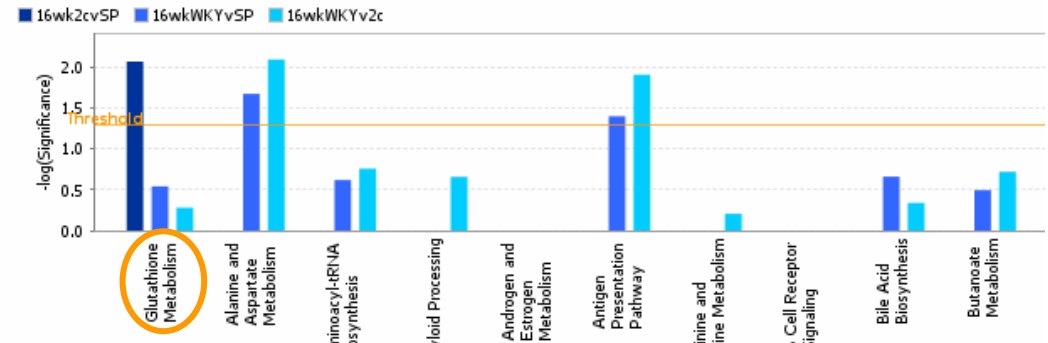

C: 5 vs. 16 wk

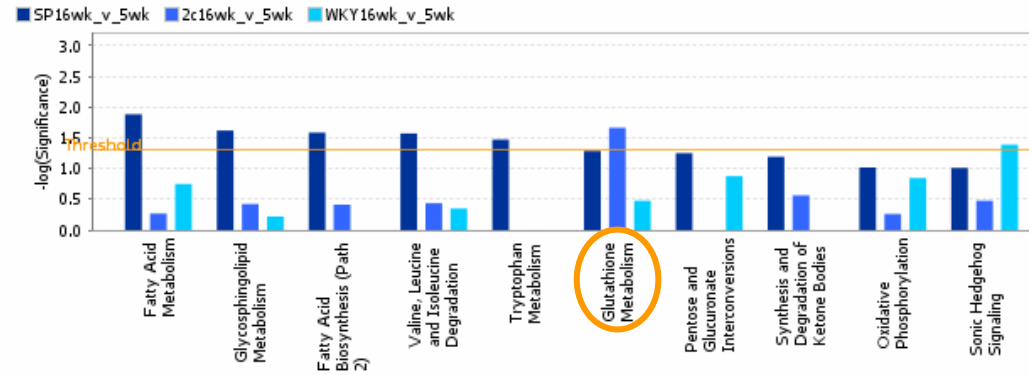

Figure 3.5 - IPA canonical pathway analysis of renal 5 and 16 week microarray data

Data output grouped by canonical metabolic pathway. Significance is based on the number of genes in the pathway that were differentially expressed, threshold line: $p<0.05$. **(A)** and **(B)**: 5 and 16 week inter-strain pairwise comparisons, respectively; pathways ranked by significance of SHRSP vs. 2c* comparison. **(C)** Within-strain comparisons between 5 and 16 week gene expression, ranked by significance of 16 week vs. 5 week SHRSP.

Examining the KEGG glutathione metabolism pathway in detail with IPA identified a number of differentially expressed genes, an example is shown in figure 3.7 for the SHRSP vs. 2c* comparison at 5 weeks of age: *Gstm1* and gamma glutamyltransferase 1 (*Ggt1*) were downregulated in the SHRSP (FDR<0.05), while aminopeptidase N (*Anpep*) also had reduced expression in the SHRSP, but with a FDR of 0.051. This analysis was repeated for the glutathione pathway in all pairwise comparisons and combined with the expression data for *Slc7a12-like* (which is not linked to glutathione metabolism by IPA), where more than one probeset for a gene was differentially expressed, only the probeset with the largest fold-change was included (table 3.3).

Anpep (encoded on chromosome 1) and *Ggt1* (not mapped) expression were both increased in the 2c* and WKY compared to the SHRSP, implying a *trans* expression effect from the 2c* congenic interval. *Anpep* expression was increased in all strains at 16 weeks compared to 5 weeks. Glutamate-cysteine ligase, modifier subunit (*Gclm*) differential expression was unique to within-strain comparisons between 5 and 16 week rats, it was upregulated in the 5 week-old SHRSP and 2c* but not the WKY, indicating differential expression dependent on SHRSP alleles. *Gclm* is situated on chromosome 2, distal of the 2c* congenic region.

3.4.3 Kidney GSH Concentrations

Following the evidence from microarray studies that GSH metabolism may be impaired in the 5 week SHRSP kidney, renal GSH levels were measured in 5 and 16 week old SHRSP, 2c* and WKY rats. Kidney GSH levels at 5 weeks in WKY rats was significantly higher than the SHRSP and 2c* by approximately 2-fold. At 16 weeks of age, despite significantly reduced GSH levels in the WKY, SHRSP GSH levels were significantly reduced compared to the WKY, but GSH levels were increased in the 2c* compared to levels at 5 weeks in the 2c* (figure 3.8). This led to the hypothesis that 2c* GSH levels were reduced at 5 weeks of age despite a WKY-like expression pattern of GSH-metabolism genes, presumably mediated by SHRSP alleles from outwith the congenic interval, but by 16 weeks of age WKY GSH levels were increased in the 2c* by chromosome 2 WKY genes.

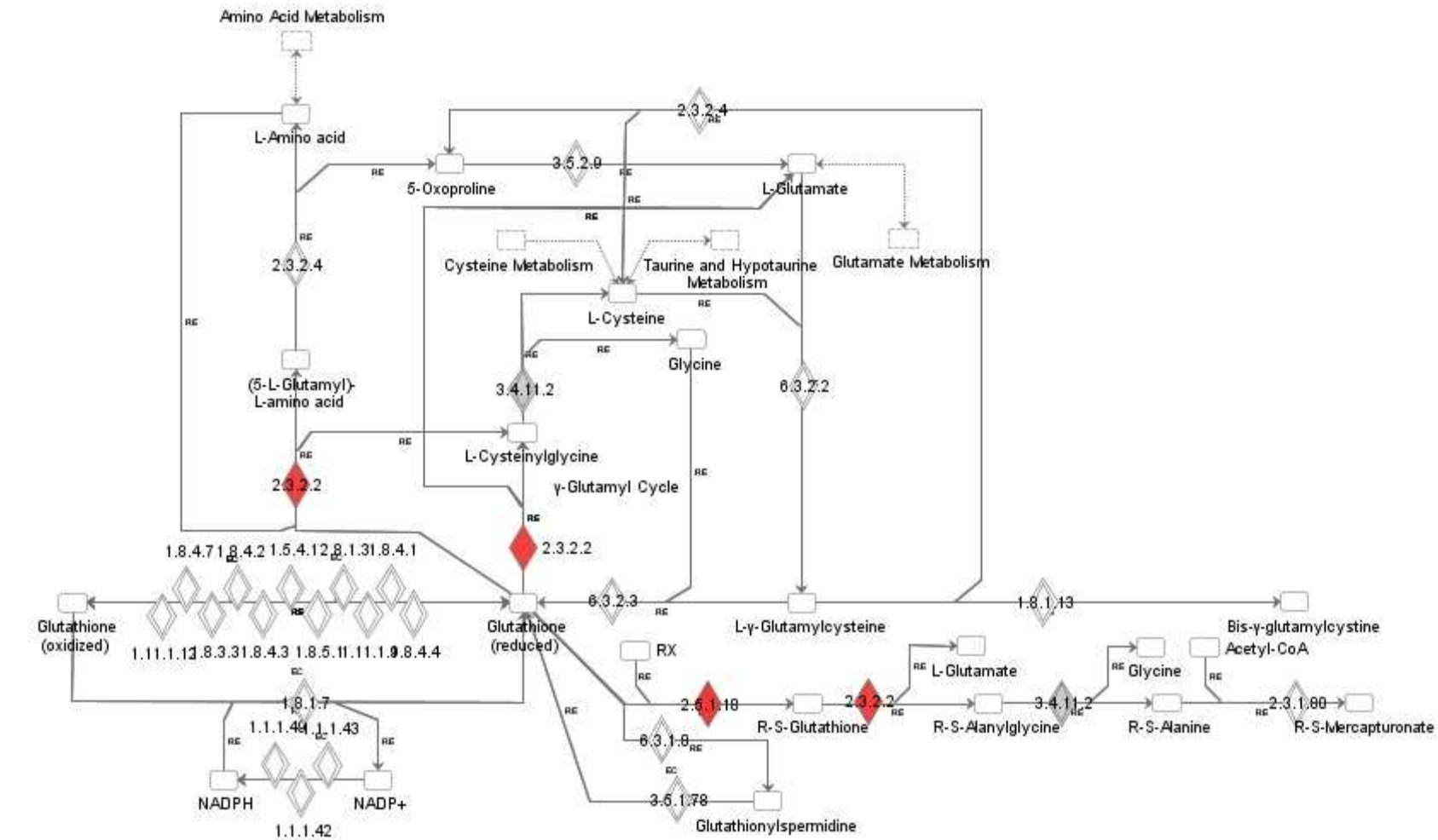

Figure 3.7 - KEGG glutathione metabolism pathway

Glutathione metabolism pathway showing differentially expressed genes between the SHRSP and 2c* at 5 weeks of age (IPA analysis). Nodes shaded red indicate genes with significantly reduced expression in the SHRSP (FDR<0.05), nodes in grey were not significantly differentially expressed in this pairwise comparison, but were in other comparisons, nodes in white were not differentially expressed in any comparisons. 2.3.2.2: *Ggt1*, 2.5.1.10: *Gstm1*, 6.3.2.2: *Gclm*. *Anpep* (3.4.11.2) expression was reduced in the SHRSP with an FDR of 0.051 in this analysis.

	Probeset	Gene	Loc.	2c* vs. SP	WKY vs. SP	WKY vs. 2c*
5 wk	AF039890mRNA_s_at	*Anpep*	1q31	2c*(2.0)#	WKY(2.9)	-
	rc_AI232192_s_at	*Ggt1*	Unk.	2c*(2.1)	WKY(2.2)	-
	H32189_s_at	*Gstm1*	2q34	2c*(9.4)	WKY(7.5)	-
	rc_AI060176_at	*Slc7a12 -like*	2q23	SP(3.0)	SP(2.3)	-
	Probeset	**Gene**	**Loc.**	**2c* vs. SP**	**WKY vs. SP**	**WKY vs. 2c***
16 wk	X04229cds_s_at	*Gstm1*	2q34	2c*(9.7)	WKY(13.8)	-
	Probeset	**Gene**	**Loc.**	**SP**	**2c***	**WKY**
5 wk vs. 16 wk	AF039890mRNA_s_at	*Anpep*	1q31	16wk (7.9)	16 wk (3.8)	16 wk (3.8)
	Rc_AC233261_i_at	*Gclm*	2q42	5 wk (5.6)	5 wk (4.6)	-

Table 3.3 - Differentially expressed glutathione metabolism genes
Differentially expressed glutathione metabolism genes in pairwise comparisons between the SHRSP, 2c* and WKY in 5 and 16 week renal microarrays. Strain or age with highest expression is indicated, fold change in brackets. FDR<0.05, except #: FDR = 0.051.

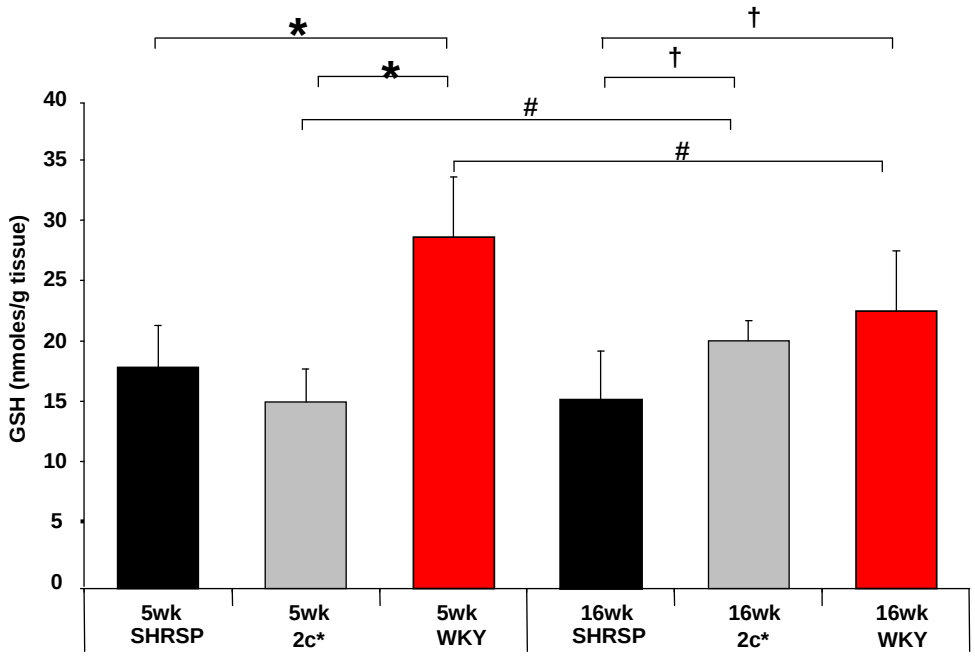

Figure 3.6 - Kidney GSH concentrations in 5 and 16 week-old SHRSP, 2c* and WKYs
Kidney GSH concentrations in 5 and 16 week-old SHRSP, 2c* and WKY rats. 5 week data, n=6 per group; 16 week data SHRSP n=11, 2c* n=7, WKY n=10. *****p<0.05, F=20.95; † p<0.05, F=9.04 (ANOVA and Tukey post-test); # p<0.05 (2 sample t test).

3.4.4 Kidney Superoxide Measurements

Kidney superoxide levels in 5 week old SHRSP rats were significantly higher than in the WKY and 2c* (figure 3.9), indicating that oxidative stress defence mechanisms are compromised in the SHRSP prior to the onset of hypertension. Equivalent superoxide levels in the WKY and 2c* at this timepoint suggest that differential expression of one or more genes in the 2c* congenic interval may have a protective effect, enhancing oxidative stress defence.

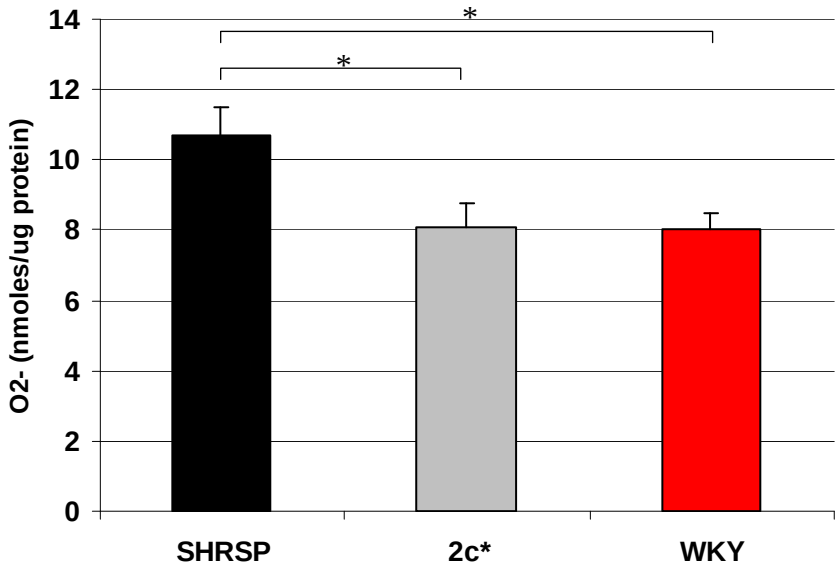

Figure 3.7 – Kidney superoxide levels in 5 week old SHRSP, 2c* and WKY rats
NADH-stimulated superoxide levels were measured in triplicate kidney homogenates. SHRSP superoxide levels were higher compared to both other strains. Mean ± SE *p<0.05 (ANOVA and Tukey post-test).

3.4.5 qRT-PCR of Other Candidate Genes

Differential expression of genes identified in microarray studies was assessed by Taqman qRT-PCR. Relative expression of genes was measured between strains at the 5 and 16 week timepoints, comparing expression to the SHRSP in each case (figure 3.10). Differential expression of *Them4* was shown at both 5 and 16 weeks, SHRSP expression was 3-5 fold higher than in the WKY and 2c*. The only other gene for which differential expression was observed by qRT-PCR was *Slc7a12-like*, confirming the 5-week microarray results, SHRSP expression was approximately 2.5-fold higher than the WKY and 2c*.

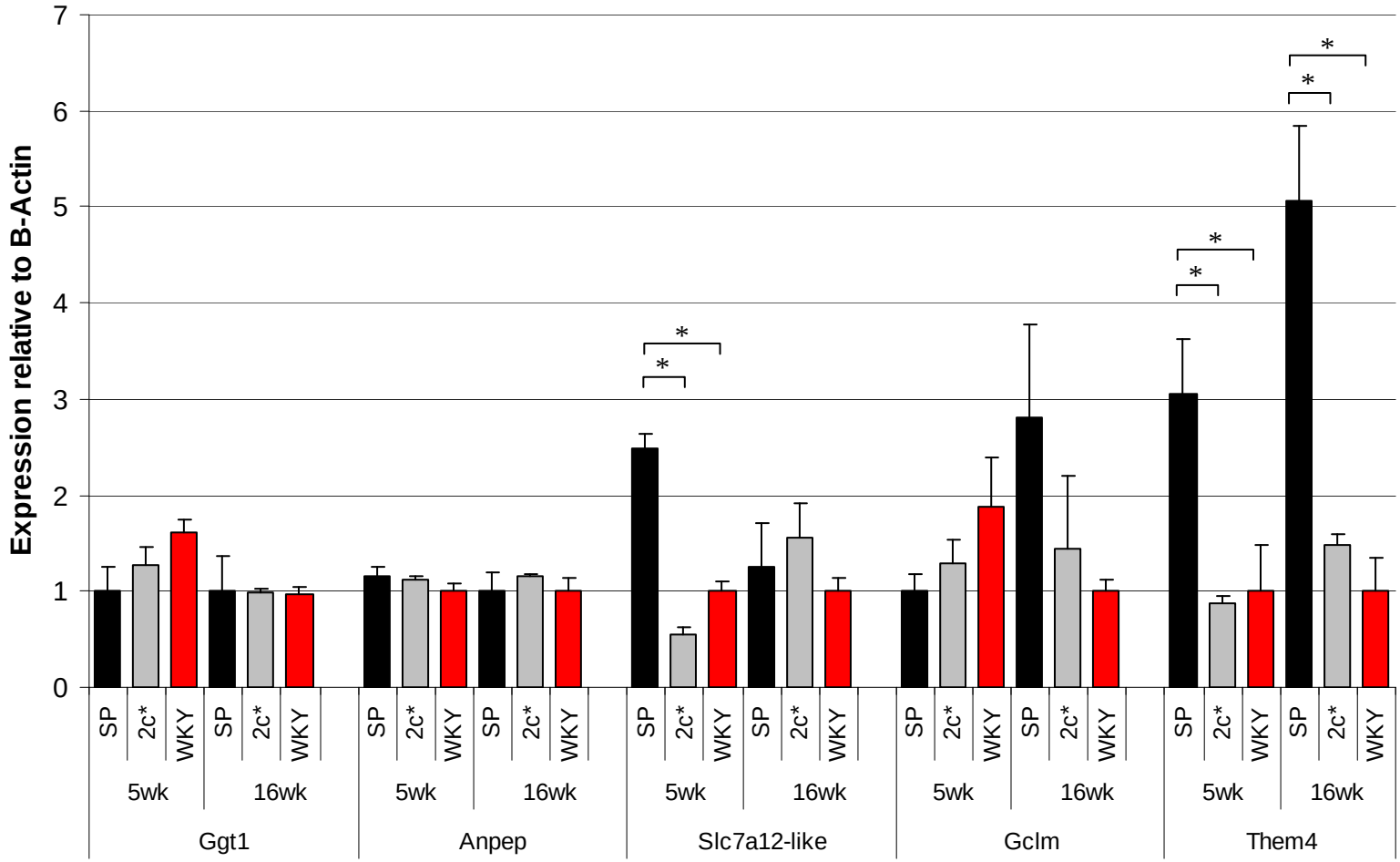

Figure 3.8 - Taqman qRT-PCR of genes differentially expressed in microarrays

Expression of each gene was quantified relative to β-actin and calibrated to the lowest WKY or SHRSP expression levels at each time point. n=5 per group. *p<0.01 (ANOVA and Dunnett's post-test).

3.4.6 Promoter and Coding DNA Sequencing

DNA sequencing was carried out to identify coding and promoter polymorphisms in differentially expressed genes from microarray data. Equivalent data for *Gstm1* is presented in section 4.4.2. Representative images from PCR and sequencing are presented (figure 3.11). Polymorphisms were identified in *Ggt1*, *Them4* and *Hist2H2aa* (table 3.4). Sequencing of *Slc7a12-like* coding sequences was unsuccessful, generating mixed sequence, this is likely to be due to the existence of several closely-related members of the *slc7a* gene family in the rat genome. The single polymorphism identified in *Ggt1* was a conserved G at base 137 in the SHRSP, SHR and WKY, differing from the BN reference sequence, which encodes T at this position, this results in an amino acid change at residue 46, encoding a serine in the BN and an alanine in the other strains. Two polymorphisms were identified in the *Them4* 3'UTR, the polymorphism at position +465 was unique to the BN, the polymorphism at base +833 was unique to the WKY; a promoter variant unique to the WKY was also identified at base -105 in *Them4*. A single promoter polymorphism was identified in *HistH2aa* with a C in the SHRSP and SHR, an A in the WKY and BN. No polymorphisms were observed in *Anpep* or *Gclm* coding or promoter sequences.

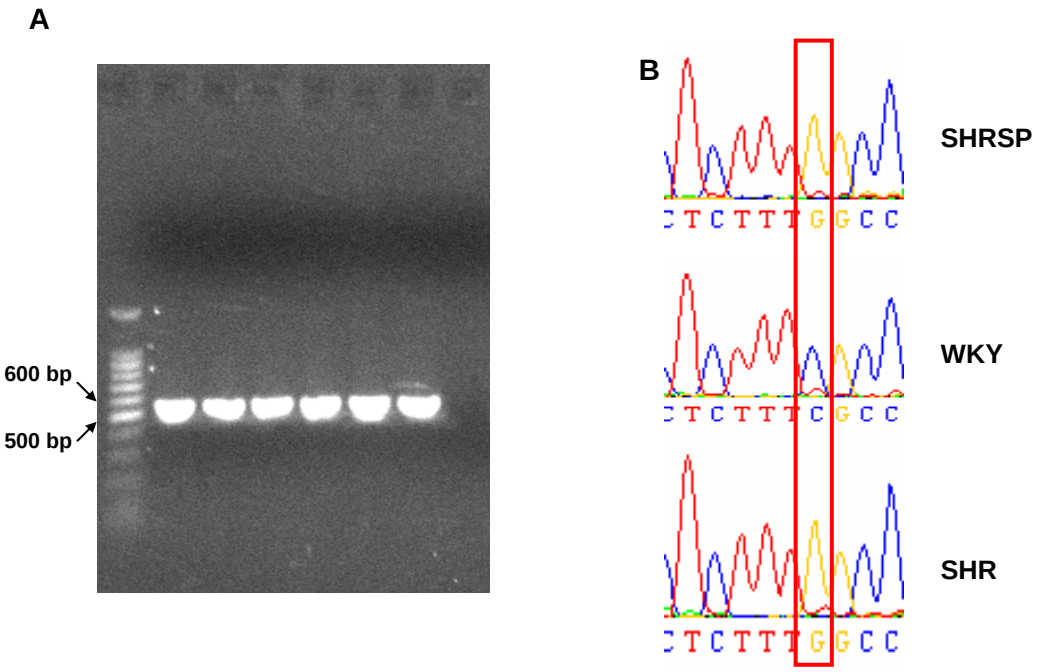

Figure 3.9 – PCR and sequencing candidate gene coding and regulatory regions
Them4 3'UTR sequences. **(A)** PCR amplification from duplicate SHRSP, WKY and SHR genomic DNAs with THEM4upAF+R primer pair, expected product size: 532 bp. **(B)** DNA sequencing electropherogram showing 3'UTR SNP in the WKY Them4 3'UTR at base +465.

Gene	Position	SHRSP	SHR	WKY	BN
Ggt1	137	G	G	G	T
Them4	+465	G	G	C	G
	+833	C	C	C	T
	-105	G	G	A	G
Hist2H2aa	-2293	C	C	A	A

Table 3.4 - Candidate gene coding and regulatory sequence variants

Polymorphisms identified by DNA sequencing of coding and regulatory regions of *Ggt1*, *Them4* and *Hist2H2aa, Slc7a12-like, Anpep* and *Gclm*. Sequence variants were only identified in *Ggt1*, *Them4* and *Hist2H2aa*, patterns of conservation of SNPs varied between the SNPs.

3.5 Discussion

The experiments presented in this chapter examined differential gene expression in the SHRSP, WKY and the 2c* congenic strain, which is of SHRSP genotype except for a 20 cM region covering a blood pressure QTL on chromosome 2, which is derived from the WKY (McBride et al 2003). Expression levels of over 26000 mRNA transcripts were measured using Affymetrix GeneChip RGU34A, B and C microarrays in kidneys from five week old animals, a timepoint prior to the onset of severe hypertension in the SHRSP. Reduced expression of *Gstm1* mRNA was measured in the SHRSP and validated by qRT-PCR, this is a significant finding that strengthens the case for *Gstm1* as a hypertension candidate gene. Impaired renal oxidative stress defence is likely to contribute to the onset of hypertension through cytotoxic effects leading to disrupted regulation of salt and water homeostasis (McBride et al 2003;McBride et al 2005). The 5-week gene expression data was also combined with an equivalent microarray dataset from 16 week-old rats (McBride et al 2003); pairwise comparisons between each strain at 5 and 16 weeks of age and IPA data analysis identified several genes involved in glutathione metabolism in addition to *Gstm1* that were differentially expressed in microarray analysis, of which *Slc7a12-like* is also encoded from within the 2c* congenic interval. Analysis of secondary phenotypes related to hypertension included renal superoxide and GSH levels, showing that the SHRSP has increased renal oxidative stress during the onset of hypertension, and that the SHRSP and 2c* have reduced glutathione levels at 5 weeks of age compared to the WKY. At 16 weeks of age renal superoxide levels are significantly higher in the SHRSP than the WKY and the 2c* is intermediate (McBride et al. 2005), data presented here showed that at 16 weeks renal GSH levels are reduced in the SHRSP compared to the WKY, while levels in the 2c* were significantly increased compared to 5 week levels, indicating that changes in expression of chromosome 2 WKY alleles may affect GSH cycling and renal oxidative stress in the 2c* by 16 weeks of age. The hypothesis that impaired renal GSH metabolism and reduced renal GSH contributes to hypertension in the SHRSP is consistent with published observations that glutathione depletion by two week administration of buthionine sulphoxide (BSO), an inhibitor of GSH synthase, to Sprague Dawley rats causes renal oxidative stress and severe hypertension (Vaziri et al. 2000).

IPA allows the expression of several genes involved in numerous metabolic pathways to be inspected automatically in multiple comparisons of large datasets. Analysis of the canonical glutathione metabolism pathway with IPA identified probesets for gammaglutamyltransferase 1 (*Ggt1*) and aminopeptidase N (*Anpep*) that were

downregulated in microarray data in the SHRSP compared to the WKY and 2c* at 5 weeks of age. These results, in conjunction with the differential expression of *Gstm1* and *Slc7a12-like* from RP data analysis suggested that renal glutathione metabolism in the 5-week SHRSP is impaired (figure 3.12).

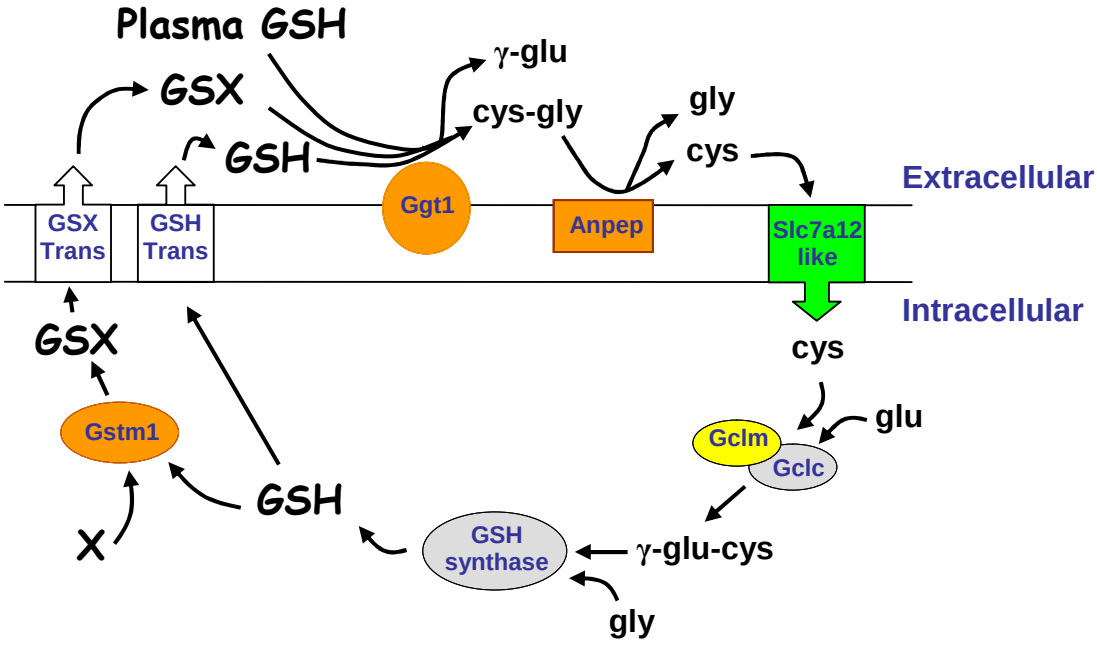

Figure 3.10 - Renal glutathione metabolism

Genes differentially expressed in renal 5 week microarrays between the SHRSP and WKY and between the SHRSP and 2c* are highlighted in orange (downregulated in the SHRSP) or green (upregulated in the SHRSP). Genes not found to be differentially regulated in the microarrays are coloured grey, *Gclm* (yellow) was upregulated in the SHRSP and 2c* at 5 weeks compared to 16 weeks. Following conjugation of GSH with oxidative or xenobiotic molecules (X) by Gstm1 (or other GST enzymes), the GSX conjugate is exported from the cell by the GSX transporter (GSX Trans). GSH is also exported to the extracellular space by the GSH transporter (GSH Trans) and the kidney is also a major site of plasma GSH uptake. Both GSX and GSH are metabolised by Ggt1 to generate cysteinylglycine (cys-gly) dipeptide, which is further metabolised by Anpep dipeptidase. Cysteine (cys), the limiting substrate for GSH synthesis, is recycled into the cell by amino-acid transporters such as Slc7a12-like. The first step in de-novo GSH synthesis is catalysed by glutamate cysteine ligase, a heterodimeric enzyme consisting of the catalytic subunit (Gclc) and the rate-limiting modulatory subunit (Gclm), generating γ-glu-cys. GSH synthase catalyses the final enzymatic addition of glycine (gly). Figure adapted from (Zhang et al. 2005)

One of the major functions of plasma GSH circulation is to supply cysteine for de-novo intracellular GSH synthesis (Lash et al 1988); in aqueous conditions at physiological pH cysteine oxidises to insoluble cystine (cysteine dipeptide). The liver is the major source of plasma GSH, and while there is evidence that GSH can be absorbed directly by kidney

proximal tubular membranes (Hagen et al 1988;Parks et al 1998), the GSH cycling pathway is the principal source of renal GSH. Ggt1 is central to GSH metabolism, it is the only known peptidase able to hydrolyse γ-glutamyl peptide bonds, catalysing the cleavage of GSH to liberate cysteinylglycine, and, following the export of GSH-conjugated oxidative or xenobiotic molecules, also catalyses the first step in their detoxification, also generating cysteinylglycine. Ggt1 is expressed in several cell types in the body including in the small intestine, choroid plexus, retinal pigment epithelium and lung, though its expression and activity in are highest in the proximal tubular epithelium (Hinchman et al. 1990). Further evidence that renal GSH levels are maintained by glutathione cycling comes from the observation that the *Ggt1*-null mouse (Lieberman et al. 1996) has reduced GSH and cysteine levels and increased levels of DNA oxidative damage in the kidney, liver and lung (Rojas et al. 2000). The *Ggt1*-null phenotype is significantly ameliorated by n-acetylcysteine supplementation, which increases cysteine and GSH levels (Lieberman et al 1996;Barrios et al. 2001). Increased serum GGT1 in humans has long been recognized as a marker of alcohol abuse and/or liver damage (Teschke et al. 1977) however there is also recent epidemiological evidence that serum GGT1 levels are also an independent risk factor for hypertension, diabetes and cardiovascular disease (Lee et al. 2003;Lee et al. 2006), these associations are thought to relate to persistent increased oxidative stress in at-risk individuals, resulting in increased GGT1 expression. Conversely, accumulation of GGT1 has also been associated with increased oxidative stress in atherosclerotic plaques, contributing to the likelihood of plaque rupture, though this mechanism is unique to the atherosclerotic milieu and relates to reduction of Fe^{3+} ions by γ-glutamylcysteine generated by GGT1 catalysis (Paolicchi et al. 1999).

Anpep is a membrane bound dipeptidase that has been demonstrated to cleave cysteinylglycine to cysteine and glycine, providing amino acids for recirculation into the cell in GSH cycling (Tate 1985). Renal *Anpep* expression has also been implicated in other experimental rat models of hypertension; it is located on a chromosome 1 QTL between the DSS and DSR rats and while DSR and Lewis respond to high salt diet by increased renal *Anpep* expression, the same response was not observed in the DSS (Farjah et al. 2004). In this model, *Anpep* is hypothesized to regulate renal salt reabsorption by catalysing conversion of AngIII – AngIV, which suppresses Na/K ATPase, leading to increased sodium excretion. In the DSS, decreased *Anpep* expression under salt loading was therefore proposed to contribute to salt retention and increased blood pressure (Kotlo et al. 2007b). Alternative dipeptidase enzymes may also be responsible for catabolism of cysteinylglycine in the kidney, indeed, dehydropeptidase I has been suggested to play a

greater role than Anpep in cysteinylglycine metabolism (Kozak et al. 1982;Hirota et al. 1987).

It is hypothesised that upregulation of the cysteine transporter *Slc7a12-like* in the SHRSP at 5 weeks of age in the SHRSP is a response to reduced intracellular GSH, cysteine supply is the rate-limiting substrate for GSH synthesis. However it is likely that *Slc7a12-like* is not the only membrane amino acid transporter involved in cysteine transport and glutathione cycling in the kidney, the human isoforms of other solute carrier family proteins show specificity for cysteine transport, such as SLC1A4 (Arriza et al. 1993) and SLC1A5 (Kekuda et al. 1996), and *Slc1a5* expression has been specifically detected in rabbit kidney proximal tubules (Avissar et al. 2001). In addition, though principally a neuronal amino acid transporter, pharmacological inhibition of SLC1A1 in human embryonic kidney cells has been shown to reduce cellular GSH levels *in-vitro* (Watabe et al. 2007). Therefore differential expression or activity of alternative amino acid transporters may account for the fact that *Slc7a12-like* was not differentially expressed at 16 weeks of age in SHRSP, despite reduced glutathione. Furthermore, a mechanism exists in the kidney to directly import γ-glutamylcysteine into cells for glutathione synthesis (Anderson et al. 1983), bypassing the conjugation of cysteine and glycine catalysed by glutamate cysteine ligase, though this mechanism is thought to be an adjunct to de-novo GSH synthesis (Lash 2005). The difficulties in sequencing the *Slc7a12-like* transcripts in kidney cDNA are likely to be due to multiple closely-related solute-carrier genes in the transcriptome; Ensembl lists 11 paralogues with 24-92% identity to *Slc7a12-like*. However this observation does not compromise the qRT-PCR results for *Slc7a12-like*, Gene Expression Assays from Applied Biosystems for genes that are part of closely related families are validated to amplify the intended sequence with 1000-3000 fold higher sensitivity than the closest-related family member. *Slc7a12-like* exonic sequencing could be accomplished in future studies by designing PCR primers that anneal in the introns of the gene.

qRT-PCR did not verify differential expression of *Ggt1* and *Anpep* from the 5 week microarray data and the hypothesis to explain reduced GSH levels in the SHRSP by reduced expression of *Ggt1* and *Anpep* was not supported. There are several possible explanations for the disparity between the microarray and Taqman results. First, one would expect a certain rate of false-positive calls in any data set, and the false discovery rate threshold was set at 5% for the RP analysis. Other published studies have reported non-validation of microarray data by qRT-PCR, for example, Yagil et al. 2005 reported 9 out of 16 candidates not showing strong concordance between microarray and Taqman analysis,

with one probe showing discordant results, i.e. increased expression in a strain in Taqman results where the microarray had shown decreased expression (Yagil et al 2005). Alternate splicing of *Ggt1* and *Anpep* mRNA could also explain the discordant results, microarray probesets and Taqman probes may target different isoforms that differ in transcript abundance. Only one transcript is listed for *Anpep* in the Ensembl database, and while 7 different transcripts for *Ggt1* are known to exist in the rat, they differ in the 5'UTR only (Chikhi et al. 1999).

Despite the Taqman results for *Ggt1* and *Anpep*, these data nevertheless provide evidence of a genetic effect of the 2c* congenic interval on GSH metabolism and oxidative stress: Renal GSH levels at 5 weeks in the 2c* were similar to the SHRSP, but at 16 weeks of age were similar to the WKY, meanwhile kidney superoxide levels at 5 weeks of age in the 2c* were similar to the WKY, but at sixteen weeks are intermediate between the SHRSP and WKY (McBride et al 2005). Thus WKY alleles in the 2c* congenic interval are proposed to have a protective effect on kidney oxidative stress at 5 weeks despite decreased GSH, but by 16 weeks of age the preponderance of SHRSP genotype in the 2c* increases kidney oxidative stress despite increased GSH. The identity of the genes responsible for the phenotypic differences between the SHRSP, 2c* and WKY could be identified in future experiments using microarrays with improved coverage, for example, Affymetrix now produce a microarray chip that surveys expression of all known exons, enabling analysis of gene expression and alternative splicing of genes.

An intriguing hypothesis regarding *Gclm* expression was also raised by the microarray data that showed increased expression in the SHRSP and 2c* strains, but not the WKY, at 5 weeks of age compared to 16 weeks of age. This implied an SHRSP allele-specific expression pattern for *Glcm* that may contribute to the development of hypertension over time in the SHRSP and 2c*, however, Taqman mRNA measurements did not confirm the microarray results and no promoter polymorphisms were identified in the SHRSP *Gclm* promoter.

The renal differential expression of *Hist2H2aa* and *Them4* at 5 weeks of age, both expressed from within the 2c* congenic interval provide novel candidates for genes involved in the development of hypertension in the SHRSP. *Them4* differential expression was confirmed by qRT-PCR, and also a showed similar differential expression pattern at 16 weeks of age, being upregualted in the SHRSP compared to both other strains at both timepoints. No functional data is published for rat *Them4*, though the human ortholog, *THEM4*, also known as carboxy-terminal modulator protein (*CTMP*) has been shown to

regulate phosphorylation and thus activity of protein kinase B alpha (PKBα) (Maira et al. 2001;Ono et al. 2007). PKBα, also known as AKT1, is a well described target of downstream receptor tyrosine kinases that signal via phosphatidylinositol 3-kinase (PI 3-kinase), mediating mitogenic responses to a range of growth factors such as platelet-derived growth factor, insulin and insulin-like growth factor-1 (IGF-1) (Galetic et al. 1999). Among many cellular effects, activation of PKBα has been associated with the inactivation of glycogen synthesis (Cross et al. 1995), suppression of apoptotic signals (Ahmed et al. 1997) and increasing cellular glucose uptake (Kohn et al. 1996). There are conflicting reports of the regulatory effects of CTMP on PKBα activity, a study has shown that CTMP negatively regulates PKBα phosphorylation and reverses oncogenic phenotype of cells expressing the PKBα-related oncogene v-Akt (Maira et al 2001), while a recent study showed that upregulation of CTMP leads to increased PKBα phosphorylation and enhanced antiapoptotic and glucose metabolic processes (Ono et al 2007). *Hist2H2aa* encodes one of the core histone proteins that are the structural subunits of nucleosomes, a Taqman probe is not available for *Hist2aa*, hence confirmation of its differential expression would depend on designing a custom probe.

Claudin11 and *Prcc* genes were differentially expressed between 5 and 16 week 2c* and WKY rats, both are encoded within the chromosome 2 congenic interval and their reduced expression at 16 weeks may therefore be related to a blood-pressure lowering effect. Claudin 11 is one of a large family of tight junction transmembrane proteins that mediate cell-cell associations and can ion channels. The *Claudin 11*-null mouse shows neurological defects and male sterility due to reduced parallel tight-junction strands in central nervous system myelin and between sertoli cells (Gow et al. 1999). Interestingly, WNK4 protein has been shown to mediate phosphorlyation of claudin protiens (though only claudins 1-4 were examined) in *in-vitro* canine kidney cells, leading to increased chloride permeability (Yamauchi et al 2004). Psuedohypoaldosteronism type II-mutant WNK4 upregulated chloride permeability to a greater extent than wild-type WNK4, leading to the postulation that the phenotypic effects of WNK4 mutations may be related in part to regulation of claudins (Yamauchi et al 2004). Claudin 11 expression has been co-localisesd to the thick ascending limb of the loop of Henle in the mouse (Kiuchi-Saishin et al. 2002), the region of the nephron largely responsible for active sodium and chloride reabsorption. The human ortholog of *Prcc* was first identified in a subset of renal carcinoma patients with a translocation between Xp11 and 1q21 that generated a novel fusion protein between the *TF3* transcription factor gene and the gene that subsequently became known as *PRCC* (Weterman et al. 1996). Further investigation has identified a dominant-negative

interaction between the TF3/PRCC fusion protein and the mitotic checkpoint control protein MAD2B which is thought to account for tumourigenesis (Weterman et al. 2001), though the role of PRCC remains unknown.

DNA sequencing identified single nucleotide polymorphisms in the promoter region of *Them4* and *Hist2H2aa*, a missense mutation in *Ggt1* and 2 3'UTR variants in *Them4*. The patterns of conservation of these mutations differed, with most being unique to the BN or WKY strains, hence they were not implicated in hypertension in the SHRSP. Only the *Hist2H2aa* -2293 C>A polymorphism was found uniquely in hypertensive strains (both the SHRSP and SHR) and hence may be a functional candidate for increased expression in the SHRSP once differential expression of *Hist2H2aa* is confirmed. See chapter 4 for experiments performed to investigate the polymorphisms identified in the *Gstm1* promoter.

The major finding in this chapter was reduced renal *Gstm1* expression in the 5 week old SHRSP compared to the WKY and 2c*; the following chapters outline the work that was subsequently performed to investigate the control of *Gstm1* expression and the functional effects of modulating *Gstm1* expression *in-vitro* and *in-vivo*. The transcriptomic and pathway analysis techniques applied in this chapter represent a significant advance on traditional microarray data analysis. The ability to automatically consider differential expression of multiple genes affecting specific physiological pathways in pairwise comparisons with parental and congenic strains is an extremely efficient technique for very large data sets. Even given that differential expression of candidate genes was not confirmed in follow-up analysis, the hypothesis that GSH metabolism may be controlled by the influence of genes within the congenic interval is supported by analysis of renal GSH levels and warrants additional study.

4 Gstm1 Expression and Promoter Analysis

4.1 Introduction

Following the discovery of reduced *Gstm1* mRNA expression in the 16-week old SHRSP kidney compared to the WKY (McBride et al 2003), and the results presented in chapter 3 that showed similarly reduced renal *Gstm1* expression in the prehypertesnive SHRSP, one of the focuses of this project was to investigate the molecular mechanisms of differential *Gstm1* expression and its relation to renal oxidative stress. As discussed in section 1.3, reactive oxygen species inflict damage on macromolecules including lipids, nucleic acids and proteins, such damage impairs cellular function and may lead to apoptotic or carcinogenic effects. It is hypothesised that reduced *Gstm1* expression contributes to hypertension in the SHRSP by compromising renal oxidative stress defence, leading to cytotoxicity and impaired salt and water homeostasis (McBride et al 2005).

The large number of closely related GST isoforms and their widely overlapping substrate specificities present a particular challenge to researchers investigating individual GST enzymes. A vast majority of this research has focussed on investigations of the roles of specific GSTs in drug metabolism, and particularly in resistance to chemotherapeutic agents (Hayes JD et al. 1995). Considerable research has also been performed in humans to assess whether polymorphisms in *GST* genes confer increased risks to disease. For example, there are common deletion polymorphisms of human *GSTM1* and *GSTT1* that have been the focus of much study. The deletions arise through unequal crossover between repeat sequences either side of the genes and result in individuals with 0, 1 or 2 copies of the genes. *GSTM1* and *GSTT1* deletions occur on 50% and 13% of chromosomes in Caucasians, respectively (Garte et al. 2001). Many studies have linked *GSTM1* and *GSTT1* deletions to susceptibility to a number of cancers, including colorectal, lung, skin, bladder and breast cancers, however there have been many conflicting publications (Hayes et al 2005). Other studies correlating an increased incidence of lung and bladder cancer with smoking and *GSTM1* deletions have shown to be much more reproducible (Norppa 2003).

There is also evidence that human *GST* polymorphisms may influence cardiovascular diseases. For example, a case-control study in a Chinese population found a significant increase in type 2 diabetes risk among *GSTT1*-null individuals compared to those with at least one copy (Wang et al. 2006a). In addition, *GSTM1*-null and *GSTT1*-null genotypes have been associated with an increased risk of coronary heart disease in smokers in American populations (Li et al. 2000). Faster progression of atherosclerotic lesions has also been demonstrated among *GSTM1*-null smokers (de Waart et al. 2001). Paradoxically however, non-deletion *GSTT1* smokers have been shown to have relative protection against

lower extremity arterial disease compared to *GSTT1*-null smokers (Li et al. 2001), while the *GSTM1*-null genotype has also been shown to be associated with a decreased risk of acute myocardial infarction in smokers (Wilson et al. 2000).

A majority of the experimental work relating to the control of *GST* gene expression relates to the antioxidant response element (ARE), a transcription factor (TF) binding motif first characterised in the rat *Gsta2* gene where it was demonstrated to mediate basal and stimulated expression of *Gsta2* in response to xenobiotic phenolic antioxidants, hydrogen peroxide and di- and trihydroxybenzene ROS generators (Rushmore et al. 1991). A number of publications have characterised the minimum functional ARE consensus sequence, there is widespread agreement that the core sequence is: TGACnnnGCA (Wasserman et al. 1997;Yang et al 2002). The transcription factor Nuclear-factor-erythroid 2-related factor 2 (Nrf2) was first identified as the activating ligand for the ARE in the rat *Nqo1* gene (Venugopal et al. 1996), and was firmly identified as a crucial factor in mediating antitoxic and oxidative stress defence mechanisms in Nrf2-knockout ($Nrf2^{-/-}$) mice that showed reduced expression of a number of detoxifying enzymes (Itoh et al. 1997). Further studies in the $Nrf2^{-/-}$ mice showed reduced liver constitutive and inducible expression of *Gsta1*, *Gsta2*, *Gstm1*, *Gstm2*, *Gstm3* and *Gstm4* (Chanas et al. 2002), though functional ARE sequences have not been published for all of these genes. The ARE has subsequently been found in the regulatory regions of many genes encoding proteins involved in detoxification and oxidative stress defence, including other *GST*s, *NADP(H):quinone reductase* (*NQO1*), *Glutamate cysteine ligase*, *UDP-glucuronyl transferase* and *Metallothionein-1* (Lee et al. 2004). Other transcription factors that have been experimentally linked to control of rat, mouse and human GST expression are listed in table 4.1. Very little is known about the control of rat *Gstm1* expression though it has been shown to be up-regulated by induction of MAPK signalling pathways in response to geniposide, an extract of gardenia fruit (Kuo et al. 2005).

The work performed in this chapter investigated the differential expression of renal *Gstm1* in a panel of hypertensive and normotensive rat strains and correlated reduced *Gstm1* expression with hypertension and renal oxidative stress, measured by nitrotyrosine western blotting. Luciferase promoter constructs and *in-silico* sequence analysis examined the *Gstm1* promoter in the SHRSP and WKY, identifying polymorphisms at several potential transcription factor binding sites that may affect *Gstm1* expression in the SHRSP.

Gene	Species	TF binding site	Evidence	Primary Reference
Gsta1	Rat	Nrf2	Mutation and deletion analysis	(Rushmore et al 1991)
Gsta1	Rat	C/EBPα	Competition assay, antibody immunodepletion	(Pimental et al. 1993)
Gsta1	Rat	AR	Site-directed mutagenesis and glucocorticoid receptor overexpression	(Falkner et al. 1998)
Gsta1	Mouse	HNF1, HNF4	5' deletion, EMSA, competition assay	(Paulson et al. 1990)
Gsta2	Rat	Nrf2, C/EBPβ, PPARγ	EMSA, competition assays, deletion analysis	(Park et al. 2004)
Gsta3	Mouse	Nrf2	Site-directed mutagenesis, Nrf2 overexpression, EMSA	(Jowsey et al. 2003)
Gstm1	Mouse	c-Myb	c-Myb and mutant c-Myb overexpression, EMSA	(Bartley et al. 2003)
Gstm2	Mouse	SP1, MYB	Deletion analysis, Overexpression of MYB	(Kumar et al. 2001)
Gstp1	Rat	c-Jun	EMSA, competition assay	(Kawamoto et al. 2000)
Gstp1	Rat	Nrf2, AR	EMSA	(Ikeda et al. 2002)
GSTP1	Human	Nrf2	Deletion analysis, EMSA	(Montano et al. 2004)
GSTP1	Human	NFκB	Site-directed mutagenesis and NFκB overexpression	(Morceau et al. 2004)
GSTP1	Human	SP1	Site-directed mutagenesis, EMSA	(Moffat et al. 1996)
GSTP1	Human	AP1, NFκB	Site-directed mutagenesis, NFκB overexpression	(Xia et al. 1996)

Table 4.1 - Transcription factors implicated in regulation of expression of human, mouse and rat GST genes
Instances where experimental evidence has shown binding of transcription factors to a promoter sequence are included, indicating the techniques used. EMSA: Electrophoretic mobility shift assay, AP1: Activator protein 1/2 , NFκB: Nuclear factor kappa B, AR: Androgen Receptor, HNF1/4: Hepatic nuclear factor 1/4, C/EBPα/ β: CCAAT enhancer-binding protein alpha/beta, PPARγ: Peroxisome proliferator-activated receptor gamma, SP1: Specificity protein 1, c-Myb: Myoblastosis oncogene. Modified from: (Pool-Zobel et al. 2005)

4.2 Aims

- To compare the renal mRNA expression levels of *Gstm1* in 16 week old SHRSP, WKY, BN and SHR rats using Taqman qRT-PCR.

- To assess renal oxidative stress in SHRSP, 2c* and WKY strains with anti-nitrotyrosine western blotting.

- To sequence the coding and regulatory regions of *Gstm1* in the SHRSP and WKY and to investigate the transcriptional effects of promoter polymorphisms with luciferase expression constructs.

- To use the 'Transfac' transcription factor database to identify candidate transcription factor binding sites that affect *Gstm1* transcription.

4.3 Methods

4.3.1 Renal *Gstm1* Quantitative Real-time PCR

Gstm1 expression levels were measured in mRNA extracts from 16 week old SHRSP, WKY, BN and SHR rats (BN and SHR rats were purchased from Harlan UK), three rats from each strain. Liquid nitrogen snap-frozen kidneys were homogenised in Qiagen QLT buffer and homogenised using a Polytron PT2100 rotor homogeniser and RNA extraction was performed as per section 2.5.3 using Qiagen RNeasy Maxi columns. RNA was treated with DNA-free and cDNA was synthesised using the Clontech Advantage RT for PCR kit as described in section 2.7.1. Applied Biosystems Gene Expression Assay probe for rat *Gstm1* (assay number Rn00755117_m1) and rat *β-actin* endogenous control probe (part number 4352340E) were multiplexed 20µl reactions in 96-well plates. Probe amplification efficiencies were confirmed and relative gene expression was calculated as described in section 2.7.2.

4.3.2 *Gstm1* Promoter and Exon Sequencing

Gstm1 promoters encompassing 2.5kb upstream of the *Gstm1* translation initiation site were sequenced in WKY, SHRSP, BN and SHR rats using 8 overlapping primer pairs (Gstm10R +11F, 12R+13F, 14R+15F, 16R+17F, 18R+19F, 20F+21R, 22F+23R, 24F+25R). Coding exons were sequenced from kidney cDNA templates with primers Gstm1F+2R and Gstm3F+4R. Sequencing protocols were followed as per section 2.4.

4.3.3 Renal Anti-Nitrotyrosine Western Blotting

Kidney proteins from 16 week old SHRSP, 2c* and WKY rats were prepared and concentrations were ascertained as described in section 2.2.5 Protein from three animals per strain was analysed using the standard western blotting protocol, section 2.6. Eighty µg of protein in reducing buffer was loaded per lane and full-range Rainbow marker was used as a size standard. Mouse anti-nitrotyrosine primary antibody (Abcam ab53232) was used at a dilution of 1/750, followed by HRP-conjugated goat anti-mouse secondary antibody (Upstate 12-349) at 1/5000 dilution. After ECL detection and membrane stripping, immunoreactive Gapdh levels were assayed using mouse anti-Gapdh primary antibody (Chemicon MAB374) diluted 1/100, followed by HRP conjugated rabbit anti-mouse

antibody (DAKO P0260) diluted 1/2000. Densitometry was performed as per section 2.6.6 using 'local' background correction.

4.3.4 Promoter Sequence Alignment

2.5kb rat and mouse *Gstm1* promoter sequences were aligned using 'zPicture' (Ovcharenko et al. 2004), an online sequence alignment and visualisation tool that uses a local alignment algorithm to compare input sequences and generate graphical and textual alignments. Display settings for graphical output of alignments were set to shade areas of over 70% homology in a 100bp sliding window. Textual alignments at the sites of individual rat *Gstm1* promoter polymorphisms and a putative ARE site were copied and pasted from the zPicture browser.

4.3.5 Promoter Sequence PCR

SHRSP and WKY promoter sequences were cloned into the Promega pGL3 Basic luciferase plasmid for promoter activity analysis. pGL3 Basic is a promoterless eukaryotic expression plasmid encoding modified firefly luciferase. A multiple cloning site (MCS) immediately 5' of the luciferase coding sequence allows promoter sequences to be cloned in, transcriptional efficiencies of different promoter sequences can be compared by measuring luciferase activities in transfected cells.

Four promoter regions were amplified for cloning, ranging in size from 0.9 kb-2.5 kb. Each promoter sequence was amplified with the same reverse primer, Gstm1-1R, which anneals immediately 5' of the rat *Gstm1* translational start site. Forward primers incorporated a *MluI* restriction site preceded by 3xC residues, Gstm1-1R incorporated an *XhoI* restriction site preceded by 3xC residues. Forward primers were named Gstm1-0.9F, Gstm1-1.6F, Gstm1-2.2F and Gstm1-2.5F. Promoter sequences were amplified for cloning using genomic template DNA from SHRSP and WKY rats. Novagen HotStart polymerase was used as detailed in section 2.2.3 with annealing temperatures of 62°C.

4.3.6 Promoter Sequence Cloning

PCR products were 'blunt cloned' into Stratagene PCR-Script Amp SK(+) (PCR-Script) plasmid following the manufacturer's instructions in the PCR-Script Amp Cloning kit. The PCR-Script plasmid is supplied linearised by digestion with *SrfI* restriction enzyme. This cloning platform also allowed blue/white selection based on *lacZ* gene disruption; IPTG

(isopropyl-beta-D-thiogalactopyranoside) (20 mM) and X-gal (8 μg/ml) were added to ampicilin (100 μg/ml) selective LB agar, white colonies were screened for the insert. All cloning in this chapter utilised plasmids expressing the ampicillin resistance gene, selective Luria agar and broth were used with 100 μg/ml ampicilin (Sigma).

Promoter sequence PCR reactions were electrophoresed as described in section 2.2.4, bands were excised from the agarose and pooled prior to gel purification as per section 2.5.5. DNA was eluted in 40 μl H_2O; 10 μl of this was 'polished' using Stratagene Pfu (*Pyrococcus furiosus*) polymerase enzyme that catalyses 5'-3' proofreading polymerisation. Reaction conditions were: 10 μl PCR product; 1 μl 10mM dNTP; 1.3 μl 10x Polishing buffer; 1 μl *Pfu* DNA polymerase (0.5 U/μl); heat to 72°C for 30 minutes. 5 μl of the polished PCR products were used in ligation reactions with 10 ng PCR-Script plasmid, the precise molar ratio of plasmid:insert was not calculated but the insert was vastly in excess, as is necessary in PCR-cloning. The ligation reactions constituted: 1 μl PCR-Script vector (10 ng/μl), 1 μl 10X PCR-Script reaction buffer; 0.5 μl 10 mM rATP; 5 μl polished PCR product; 1 μl 5 U/μl SrfI; 1 μl T4 DNA ligase; 0.5 μl H_2O. Ligation reactions were incubated at room temperature for an hour, then de-activated by heating to 65°C for 5 minutes.

Forty μl of XL-10 Gold cells were thawed on ice and 1.6 μl β-mercaptoethanol was added. Cells were incubated on ice for 10 minutes, 4 μl of ligation reaction was added and cells were incubated on ice for 30 minutes, then heat-shocked at 42°C for 30 seconds before returning to ice for 2 minutes. Four hundred and fifty μl of 42°C SOC media was added and transformation cultures were incubated in a shaking incubator at 37°C for an hour. Transformation cultures were spread over IPTG/X-Gal/ampicillin agar plates. The following morning, white colonies were selected for PCR screening as detailed in section 2.5.7. PCR-Script-specific T7F and T3R PCR primers that span the cloning site were used. Successful clones were further confirmed by sequencing: T7F/T3R PCR products were sequenced with T7F and T3R and *Gstm1* promoter primers.

PCR-Script clones containing SHRSP and WKY promoter sequences were amplified and purified using Qiagen plasmid purification Maxi columns as described in section 2.5.3. Promoter sequences were digested with *MluI* and *XhoI* restriction enzymes prior to subcloning into similarly double-digested pGL3 Basic plasmid; digestion was performed as per section 2.5.4. Digested PCR-Script plasmids and pGL3 Basic vectors were electrophoresed and gel purified. Ligation was performed using 50 ng linearised pGL3 Basic plasmid and a 3:1 insert:vector ratio. Transformation was performed as per section

2.5.1, colonies were PCR-screened screened as per section 2.5.7 using RV3F and GL2R primers that anneal either side of the pGL3 Basic MCS. Positive clones were definitively confirmed by DNA sequencing and Maxi-preps were prepared for each pGL3 Basic plasmid. The eight pGL3 Basic plasmids were named according to the promoter sequences they encoded: pWKY0.9, pSP0.9, pWKY1.6, pSP1.6, pWKY2.2, pSP2.2, pWKY2.5 and pSP2.5.

4.3.7 Promoter Activity Analysis

Transfection is a variable procedure as transfection efficiency can differ from well to well due to differences in cell number and distribution and variable DNA/FuGENE complex density in transfection mixtures. Consequently, the pGL3 Basic plasmids were co-transfected with pMV10 at a ratio of 3:1. pMV10 expresses *lacZ* driven by a CMV promoter. β-galactosidase activity was measured in lysates to correct for variations in transfection efficiencies between wells. Total protein concentration per well, measured by BCA assay as described in section 2.2.5, was also used to correct for variations in cell number between wells. Promoter activities were calculated as: luciferase activity (relative light units) / β-galactosidase activity (relative light units) / protein concentration (ng/μl).

Each pGL3 Basic plasmid was transfected into triplicate wells of NRK52E cells at approximately 50-60% confluence. The experiment was repeated 3 times. Triplicate untransfected control wells were included in each experiment and triplicate control wells were also transfected with 200 ng pGL3 Control (identical to pGL3 Basic except that luciferase expression is driven by an SV40 promoter), 200 ng pMV10 or co-transfected with 150 ng pGL3 Control and 50 ng pMV10. Luciferase and β-galactosidase activities and BCA protein levels were measured in all cell lysates except those transfected with 200ng pMV10, which were fixed and stained for β-galactosidase activity as per section 2.3.4. Specific experimental protocols are outlined below.

4.3.7.1 Optimising Transfection of NRK52E Cells

NRK52E cells were obtained from the European Collection of Cell Culture (ECACC) and maintained in Dulbecco's Modified Eagle Medium containing 4.5g/L D-glucose; 10% foetal calf serum (FCS); 2mM GlutaMAX; 1mM sodium pyruvate; 100 U/ml penicillin; 0.1mg/ml streptomycin. Transfections were optimised and performed in 24-well culture plates. All transfections followed the protocol outlined in section 2.3.3, cell culture media was exchanged for serum-free media immediately prior to transfections.

Promega pGL3 Control plasmid was used for the initial experiments to optimise NRK52E transfection, performed according to the manufacturer's instructions. Ratios of 3:1, 3:2 and 6:1 FuGENE:DNA (µl:µg) were used, with a total amount of DNA per well of 200 ng, 500 ng and 1 µg. Pilot dual transfections were also performed with a 150 ng pGL3 Control and 50ng pMV10 plasmids to ensure that measurable β-galactosidase activities could be achieved.

4.3.7.2 Luciferase Activity Assay

Transfected NRK52E cells were lysed using Promega Reporter Lysis Buffer (RLB), 200 µl 1 X RLB was added per well, complete cell lysis was ensured by a cycle of freeze/thawing to -20°C. Lysates were collected and centrifuged to collect cellular debris, then stored on ice. The luciferase assay reaction was performed in white 96-well flat-bottomed plates. The total reaction volume was 200 µl, comprising 60 µl 1 X RLB, 40 µl lysate and 100 µl Promega luciferase assay reagent (LAR). Each well was read by measuring total luminescence in a 10-second period on a Wallac Victor 2 plate reader. Standards were measured in duplicate, samples were measured in triplicate. A standard curve using recombinant luciferase (0.3 ng/µl to 5 µg/µl) was used to confirm that all experimental readings were within the linear range of the assay. Background luminescence from control wells with no cell lysate or recombinant luciferase were subtracted from all readings.

4.3.7.3 β-Galactosidase Activity Assay

The Tropix Galacto-Light Plus β-galactosidase activity assay kit (Applied Biosystems) was used for β-galactosidase activity assays. Prior to β-galactosidase activity measurements all cell lysates were pretreated by adding dithiothreitol (DTT) to a final concentration of 0.5 mM and heating to 48°C for 50 minutes. A dilution series of β-galactosidase standards from 0.25 ng/µl to 1 µg/µl was assayed in each experiment to confirm that all experimental readings were within the linear range of the assay. A total volume of 20 µl of NRK52E cells lysates or diluted standards were aliquoted into white 96-well assay plates. Standards were assayed in duplicate, samples were assayed singly. Galacton Plus substrate mix was diluted 1:100 in β-galactosidase assay diluent (100 mM $NaPO_4$; 1 mM $MgCl_2$, pH 8) and 70 µl was added to each well. Samples were left at room temperature for an hour. 100 µl Light-Emission Accelerator II was added to each well. Full-spectrum luminescence was measured on a Wallac Victor 2 plate reader. Background luminescence from control wells with no β-galactosidase standard or cell lysates were subtracted from all values.

4.3.7.4 pGL3 Basic Subcloning

The plasmid sequences of pSP1.6 and pWKY1.6 were analysed for restriction sites that occurred in the interval between SNPs 1-7 and SNPs 8-12. A *BsrGI* restriction site was identified within this region and a second *BsrGI* site was also identified in the pGL3 Basic backbone (within the luciferase coding region), figure 4.1.

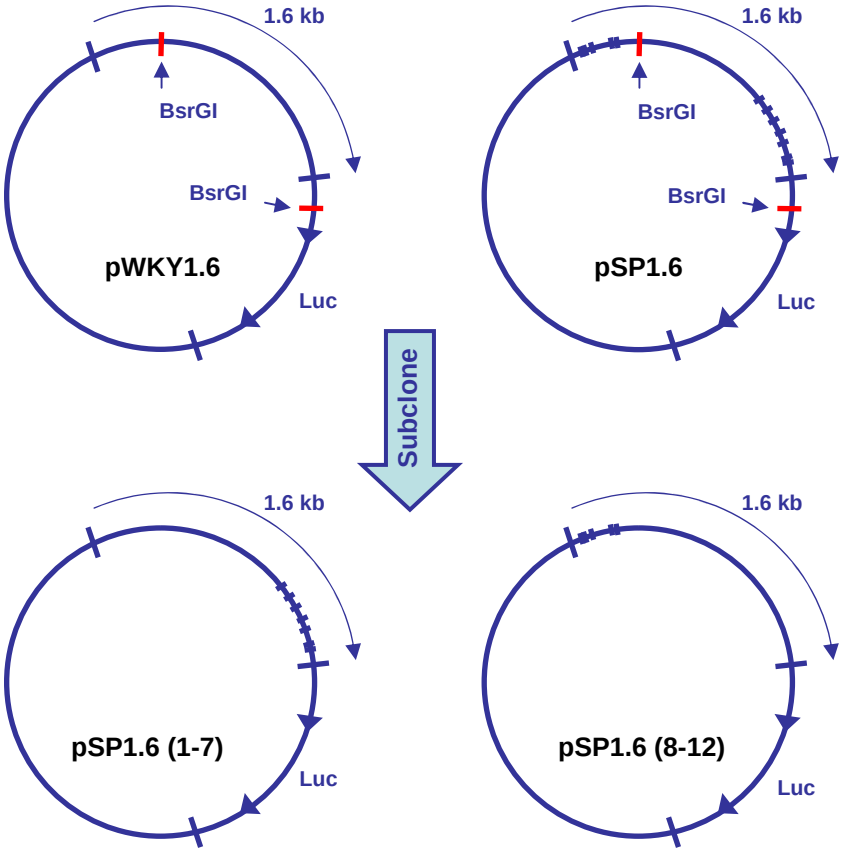

Figure 4.1 - Subcloning to generate novel 1.6 kb promoter constructs
Promoter sequences and the positions of the SNPs in pSP1.6 are indicated. pSP1.6 and pWKY1.6 were digested with *BsrGI*, generating 1.4 kb and 5 kb fragments from each. The 1.4 kb fragment of pSP1.6 was ligated to the 5 kb fragment of pWKY1.6 to generate pSP1.6(1-7), and the reciprocal ligation generated pSP1.6(8-12). Luc: luciferase gene.

pSP1.6 and pWKY1.6 plasmids were digested with *BsrGI*, generating 1433 bp and 4987 bp fragments. All restriction digests products were gel purified. 2.5 µg of the 4987 bp fragments were dephosphorylated with Roche shrimp alkaline phosphatase (SAP) using the following protocol: 5 µl 10X buffer, 5 µl SAP (1 U/µl), and H_2O in a total volume of 50 ul; heated to 37°C for 15 minutes followed by 65°C for 15 minutes.

50 ng of 4987bp digest product from pSP1.6 was ligated with the 1433 bp digest product from pWKY1.6, and vice-versa. Ligations were performed with 1433 bp:4937 bp fragment

ratios of 3:1 as per section 2.5.6 and transformed into JM109 cells. Colonies were PCR screened with RV3F and GL2R primers and sequenced for definitive confirmation of successful subcloning. The resultant plasmids all encoded 1.6 kb *Gstm1* promoters, pSP1.6(1-7) carried only SHRSP SNPs 1-7 with WKY sequence at SNPs 8-12, while pSP1.6(8-12) carried only SHRSP SNPs 8-12 with WKY sequence at SNPs 1-7 (figure 4.1). The promoter activities of the novel promoter sequences were assessed alongside pSP1.6 and pWKY1.6. Transfections, luciferase activity, β-galactosidase activity and BCA assays were performed as described above.

4.3.7.5 Site-Directed Mutagenesis

Site directed mutagenesis was performed by 'PCR sewing', illustrated in figure 4.2. This strategy utilises PCR primers to introduce mutations, the mutagenic primers do not anneal 100% to the template, they have mismatches near the middle of their sequence; in order to ensure annealing they are longer than standard PCR primers, 30-33bp in this project. Novagen KOD Hotstart was used throughout with a 60°C annealing temperature. Site-directed mutagenesis primers were named SNP8F, SNP8R, SNP9F, SNP9R, SNP10+11F, SNP10+11R, SNP12F, and SNP12R, they were used with Gstm1-1R and Gstm1-1.6F primers (represented by primers 1 and 3 in figure 4.2).

One μg of PCR product from the final PCR reaction was double-digested with *MluI* and *XhoI*. Digests were gel purified and ligated into *MluI* and *XhoI*- digested pGL3 Basic with an insert:vector molar ratio of 3:1. Colonies were PCR-screened with RV3F and GL2R primers and presence of the correct combination of promoter mutations was verified by DNA sequencing. Maxi-preps of the novel plasmids were prepared using Qiagen Plasmid Maxi columns. The novel plasmids were named pSP1.6 (1-7+8), pSP1.6 (1-7+9), pSP1.6 (1-7+10+11) and pSP1.6 (1-7+12). The promoter activities of the mutated plasmids was assayed in NRK52E cells alongside pSP1.6, and pWKY1.6 using exactly the same protocols as above.

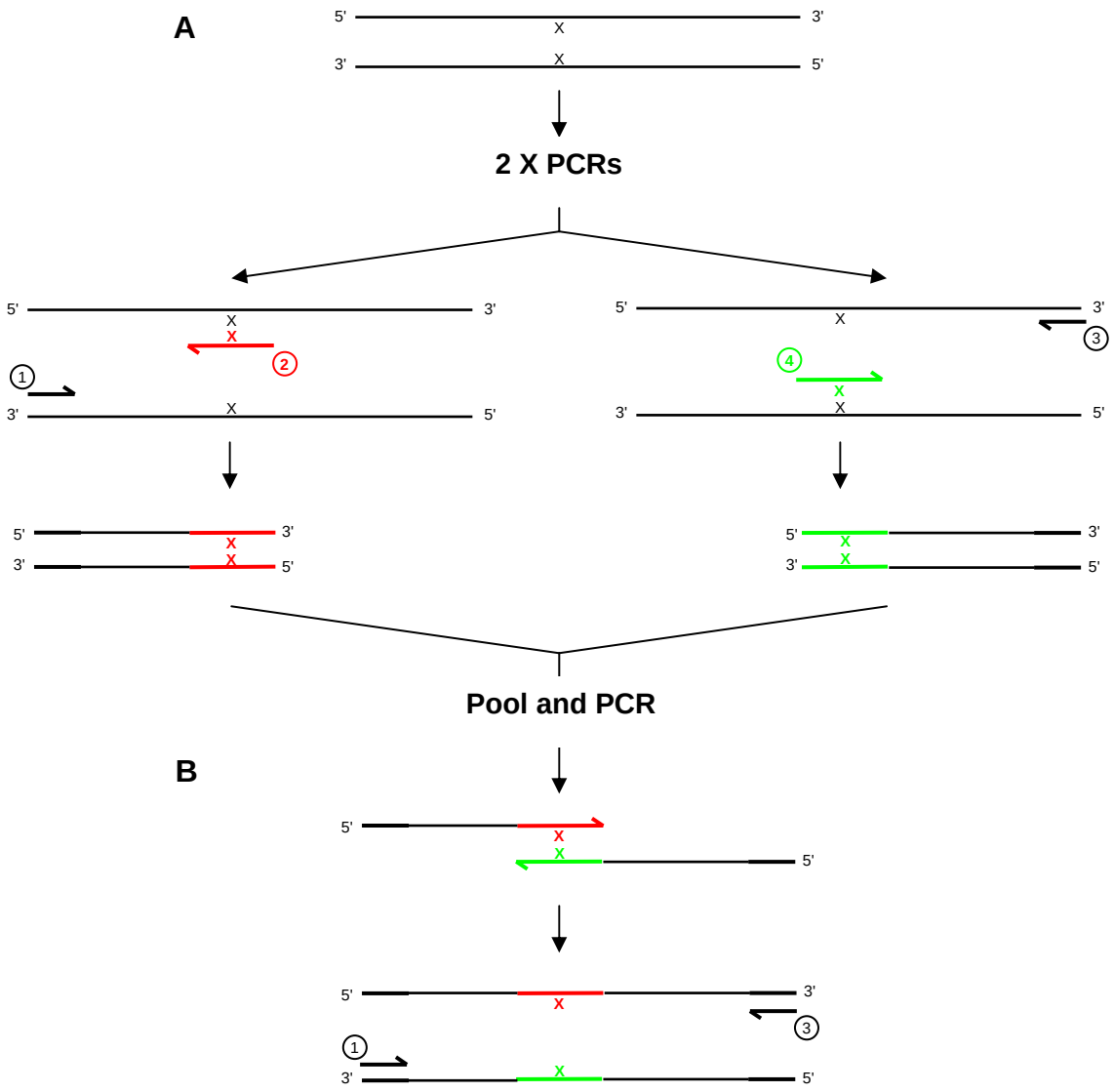

Figure 4.2 – PCR sewing for site-directed mutagenesis

(A) To introduce a specific mutation at site 'X' in a double-stranded DNA molecule, four PCR primers were used in 2 PCRs, primers 2 and 4 incorporated mismatches at site X. **(B)** The two PCRs were purified, pooled and used in a second PCR with primers 1 and 3. In the initial rounds of the second PCR products from the first PCR prime each other to generate templates for primers 1 and 3. The final full-length PCR product incorporated the mutation encoded by primers 2 and 4.

4.3.8 Transfac Professional Promoter Sequence Analysis

Transfac Professional is a commercial transcription factor database curated by the bioinformatics company Biobase, it includes information on over 8,000 TFs and over 18,000 TF binding sequences found in vertebrate, bacteria, fungi, insect, nematode and plant genomic sequences. Transfac Professional requires a subscription for access, it is distinct from the publicly available Transfac databases in that it includes the most up-to date releases of the database and allows specialised searches to be performed. The work

presented here was performed using release 10.1 of Transfac professional, from 31/03/2006. From herein, 'Transfac' is used to denote 'Transfac Professional' in this text.

Biobase use experimental and bioinformatic evidence of TF binding to construct nucleotide positional weight matrices that can provide the user with a measure of the relative likelihood that a TF binds to particular input sequences. Matrices are constructed by aligning multiple known TF binding sequences and recording the frequency that each nucleotide occurs at each position. This is collated into a consensus sequence for the matrix, typically 7-25 bases long. The five most highly conserved consecutive bases are designated the 'core' binding sequence. Many matrices are constructed using the evidence of a single experimental study in a particular species, for example where libraries of random or mutated sequences were tested for TF binding. Thus a particular TF will have multiple matrices, relating to evidence from different studies and species. Other matrices are constructed by collating the evidence of several publications, often across several species.

4.3.8.1 Generating Transcription Factor Matrix Tables

Transfac includes a module called Match (Kel et al. 2003) that accepts input nucleotide sequences to be searched for alignment with transcription factor matrices. Fifty base pair sequences either side of SNPs 1-13 (SNPs 1+2, and SNPs 10+11 were analysed together due to their close proximity) from the SHRSP and WKY were input to Match to generate a table of TF binding sites for each. The tables (SHRSP and WKY) generated for each SNP site were then compared to find TF binding sites lost or created by the SNPs in the SHRSP. Thus this analysis searched for binding sites for activating TFs for which binding is disrupted by the SNPs in the SHRSP, or sites for inhibitory TFs for which novel binding sites are created. The following parameters were applied for Match searches:

Groups of Matrices: Only matrices relating to vertebrate TFs were considered

Matrix Quality: Only 'high quality' matrices were considered, defined as matrices that generate less than 10 hits per 1000 nucleotides in test alignments with promoter sequences by Biobase. This discounts about 5% of the matrices in the Transfac database that would generate a high number of false-positive hits

Similarity Scores: Transfac searches for motifs within query sequences that pass a threshold of similarity with the 'core' and 'matrix' consensus sequences. A score is assigned

to each base in a motif based on the frequency of that particular nucleotide (A, T, C, or G) occurring in the core or matrix consensus sequence. The maximum core or matrix score is 1.0. Similarity thresholds were set at the default values of 0.75 for core sequences and 0.7 for matrix sequences. Transfac scores the core sequence first, if it passes the threshold it then inspects the matrix sequence, if this also passes this threshold, the matrix is included in the output.

Match outputs were converted to Microsoft Excel files, outputs from WKY and SHRSP searches were combined for each SNP or pair of SNPs analysed. All TF binding sites that were shared by SHRSP and WKY sequences and sites where the core or matrix scores differed by less than 0.1 between SHRSP and WKY sequences were deleted. This analysis technique has been applied in published research investigating functional effects of promoter polymorphisms (Moreno et al. 2007). This generated spreadsheets for each SNP (or combined SNPs for SNPs 1+2 and 10+11) of putative TF binding sites that were unique in the SHRSP or WKY sequence, or where the presence of the SNP alters affinity of the TF to the sequence. Each of these spreadsheets was combined into a single Microsoft Excel spreadsheet that was used for detailed searches.

4.3.8.2 Transcription Factor Binding Site Analysis

The matrix table generated by Match analysis was interrogated in a number of ways to find candidate TF binding sites affected by the polymorphic bases between the WKY and SHRSP *Gstm1* promoter. Searches were first performed for potential binding sites for transcription factors Bach1, Maf and Nrf2, looking for a site affected by a SNP in cluster 1-7 and a second affected by a SNP in cluster 8-12. Secondly, the table was sorted by matrix identifier and carefully inspected to find instances where two binding sites for the same TF were lost or created in the SHRSP, one in SNP cluster 1-7, one in SNP cluster 1-8. The matrix table also was inspected for binding sites of TFs with core match scores of over 0.9 and for TFs previously shown to influence GST expression (from table 4.1). Candidate TFs were investigated by literature analysis to assess the likelihood that they are involved in transcriptional regulation of *Gstm1* based on published information such as their actual consensus binding sequences (as opposed to Transfac consensus sequences), tissue and developmental expression profile, or functional role in cellular and physiological systems.

4.4 Results

4.4.1 Renal *Gstm1* Quantitative Real-Time PCR

Gstm1 mRNA expression, measured by Taqman qRT-PCR relative to β-actin in 16-week-old rat kidneys, showed approximate 4.5-fold higher expression in the WKY and BN relative to the SHRSP and SHR (figure 4.3). These results further confirmed differential expression seen in renal microarray and RT-PCR experiments between the WKY and SHRSP (McBride et al 2003;McBride et al 2005) and demonstrated a correlation between reduced *Gstm1* expression and increased blood pressure in multiple rat strains. These results were also presented in McBride et al (2005).

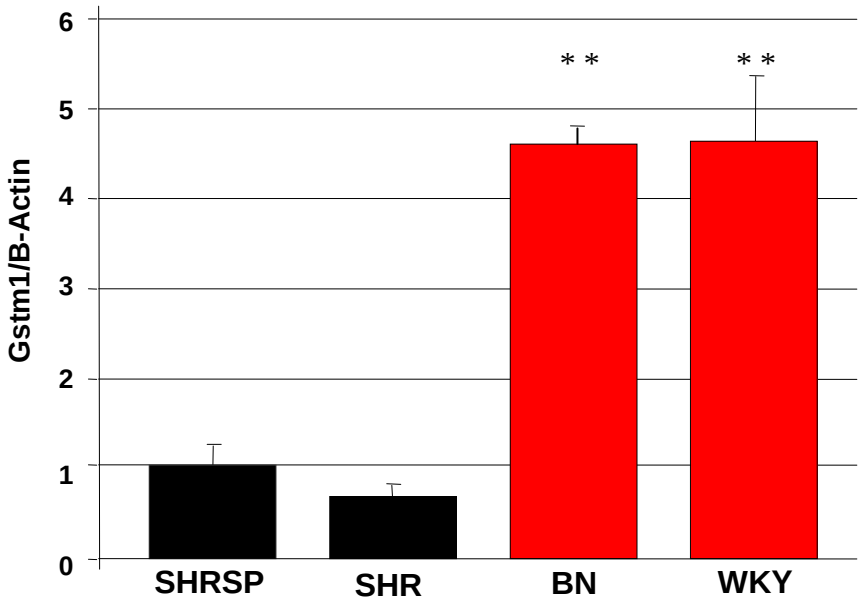

Figure 4.3 - Renal *Gstm1* mRNA expression in the SHRSP, SHR, BN and WKY
qRT-PCR measured by Taqman in 16 week old rats relative to β-actin and calibrated to expression in the SHRSP. n=3, Mean ± SE. F=119.9 ** p<0.01 vs. SHRSP (ANOVA and Dunnett's post-test).

4.4.2 *Gstm1* Sequencing

Sequencing the promoter and coding regions of *Gstm1* in the SHRSP, SHR, WKY strains and comparisons with the BN reference sequence revealed 13 promoter polymorphisms within 2.4 kb upstream of the translational start site in the SHRSP and SHR, the promoter polymorphisms were numbered sequentially (SNP1–SNP13) from the SNP closest to the translational start site in a 3'-5' direction. The promoter mutations included 11 substitutions, an insertion and a deletion. A nonsynonymous mutation in the coding region

(exon 8, nucleotide 605, H202R) was identified, and a 3'UTR polymorphism at base +29 (Table 4.2). All *Gstm1* polymorphisms were conserved between the two hypertensive strains. These results were also presented in McBride et al (2005).

SNP no.	Position	SHRSP	SHR	WKY	BN
-	+29	A	A	G	G
-	605	G	G	A	A
SNP1	-101	G	G	A	A
SNP2	-103	delT	delT	T	T
SNP3	-178	T	T	C	C
SNP4	-255	T	T	C	C
SNP5	-280	G	G	A	A
SNP6	-380	C	C	G	G
SNP7	-483	C	C	A	A
SNP8	-1048	G	G	A	A
SNP9	-1140	C	C	T	T
SNP10	-1211	insC	insC	-	-
SNP11	-1212	C	C	A	A
SNP12	-1238	C	C	T	T
SNP13	-2390	C	C	A	A

Table 4.2 - *Gstm1* coding and promoter SNPs in the SHRSP, SHR, WKY and BN
A 3'UTR polymorphism was identified 29 bases downstream of the STOP codon, and a base change at position 605 codes for a histidine at amino acid 202 in the SHR and SHRSP and an arginine in the WKY and BN. 13 promoter polymorphisms were identified within 2.4 kb. All polymorphisms were conserved between the SHRSP and the SHR

4.4.3 Renal Anti-Nitrotyrosine Western Blotting

Renal anti-nitrotyrosine western blotting revealed multiple bands in each sample, consistent with nitrotyrosinylated groups on multiple proteins in the cell; expected Gapdh bands were observed at 36 KDa (figure 4.4A). Densitometry revealed the highest level of nitrotyrosine relative to Gapdh in SHRSP kidneys (figure 4.4B). These results were also presented in McBride et al (2005) and are consistent with other data in this publication showing increased superoxide in kidneys and aortas of the SHRSP.

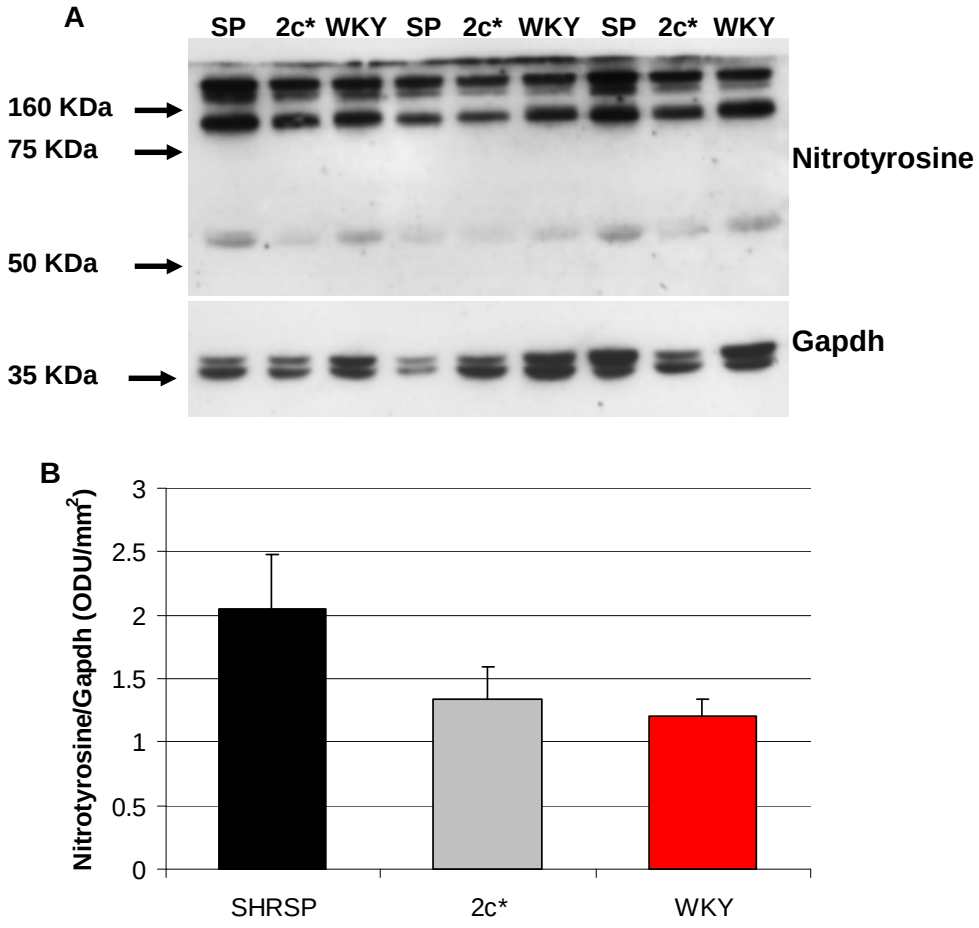

Figure 4.4 – Anti-nitrotyrosine western blot in 16 week SHRSP, 2c* and WKY kidneys
(A) A range of bands were observed for nitrotyrosine, Gapdh loading control bands were observed at the correct size (36-40 kDa). **(B)** Densitometry correcting for Gapdh in each sample showed highest nitrotyrosine levels in the SHRSP

4.4.4 Rat and Mouse *Gstm1* Promoter Sequence Alignments

Given the large number of polymorphisms in the SHRSP promoter and their clustered distribution, it would have been impractical to clone promoter sequences isolating each polymorphism individually. Therefore it was decided to analyse the transcriptional effects of multiple SNPs in the first instance. Cross-species promoter analysis and putative ARE sequence searching was also carried out to aid the process of deciding where to place upstream primers for promoter sequence amplification. SNPs 1-12 occur in regions of high homology between the rat and mouse *Gstm1* promoter sequences, while the sequence surrounding SNP13 is not conserved (figure 4.5). A core ARE sequence was identified 1,887bp upstream of the rat *Gstm1* translational initiation site. On the basis of this analysis,

four promoter regions were amplified for cloning, ranging in size from 0.9kb-2.5kb. The smallest promoter fragment was 0.9 kb in length and covered SNPs 1-7 in the SHRSP. The second fragment (1.6 kb) encompassed SNPs 8-12 additional to the 7 covered by the 0.9 kb fragment. The third fragment (2.2 kb) also encompassed the putative ARE, while the fourth (2.5 kb) also included SNP13 (figure 4.5).

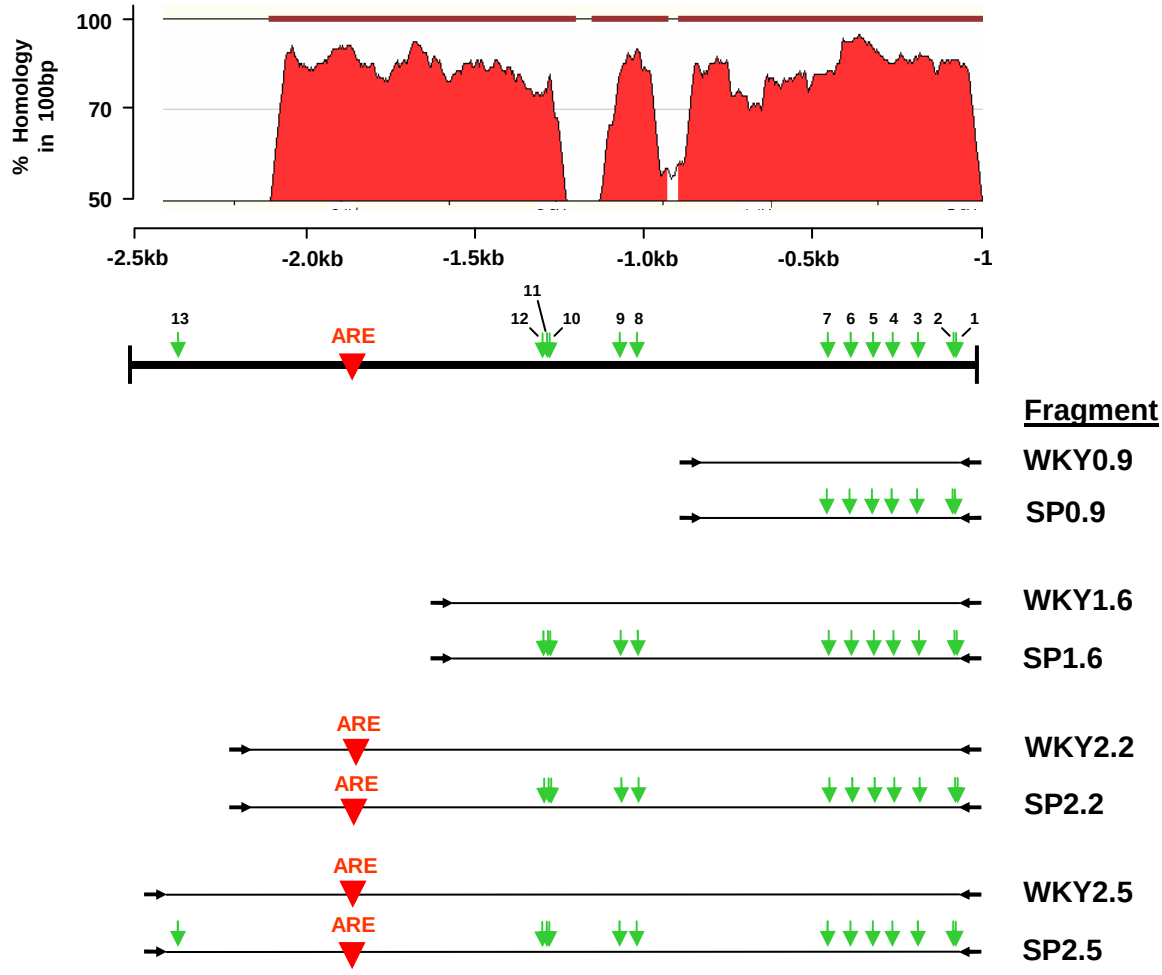

Figure 4.5 - zPicture alignment of rat and mouse *Gstm1* promoters
Percentage homology between the rat and mouse Gstm1 promoters in a 100 base-pair sliding window. The positions of the 13 SHRSP promoter polymorphisms and a putative ARE site are indicated. The alignment was used to aid primer placement for promoter cloning, the promoter sequences cloned from the WKY and SHRSP are illustrated in the alignment

The precise sequences at the sites of the promoter polymorphisms and the putative ARE sequence in the SHRSP and WKY *Gstm1* promoter were compared with the corresponding sequences in the mouse *Gstm1* promoter (figure 4.6). The alignments between the rat and mouse sequences was close to 100% in most cases, the mouse sequence at the site of the polymorphisms was conserved with the SHRSP sequence at some SNPs and with the WKY sequence in others. The exceptional homology at the sites of the putative ARE sequences in rat and mouse lends weight to this being a functional element.

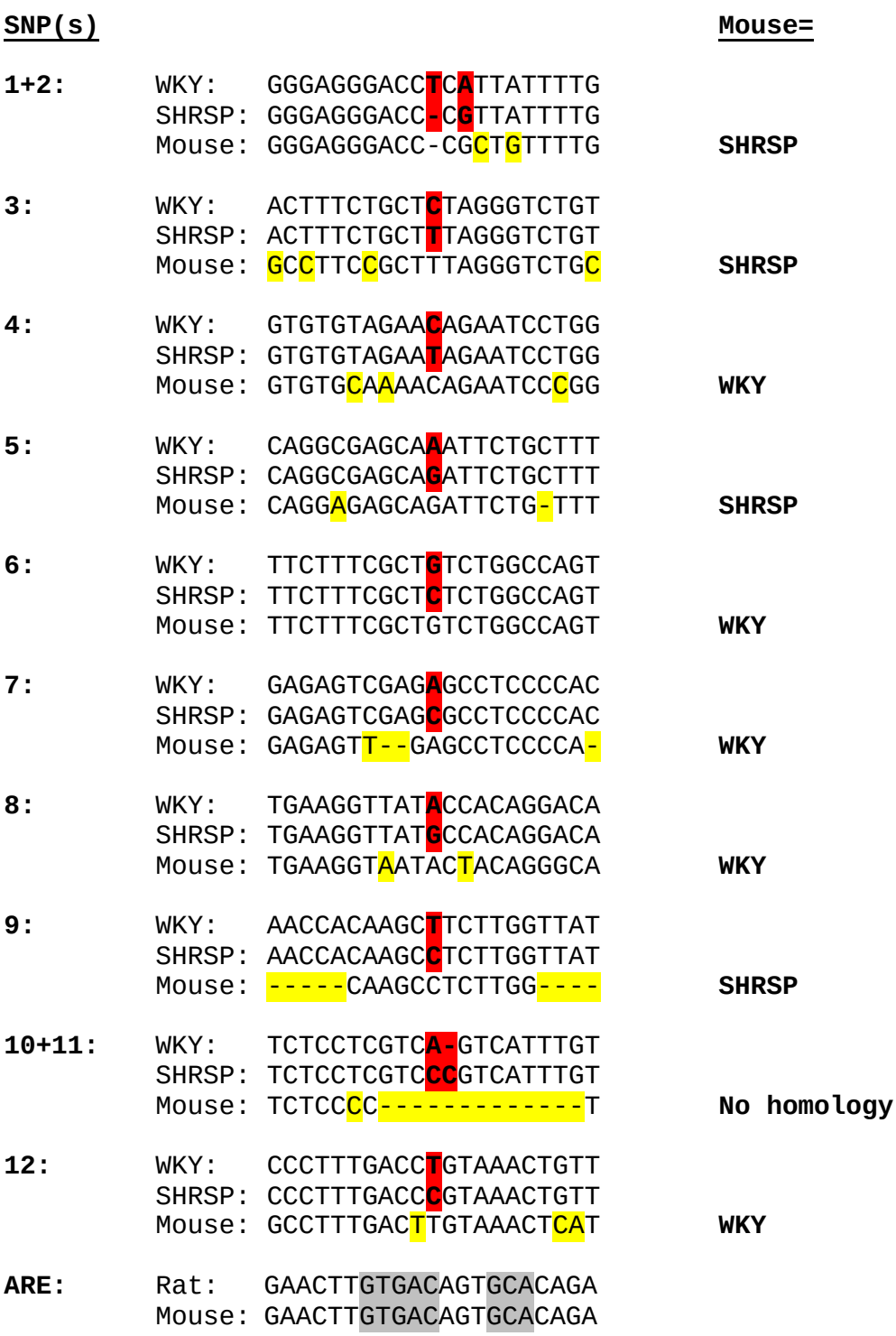

Figure 4.6 - Individual alignments of rat *Gstm1* promoter polymorphisms with mouse *Gstm1* promoter sequences
Rat polymorphisms are shaded in red, bases in the mouse promoter that do not align with the rat sequence are shade in yellow. Conservation of the mouse sequence with either the WKY or SHRSP sequence at each individual SNP is indicated (Mouse=). The putative ARE in the rat *Gstm1* promoter is also aligned with the equivalent sequence in the mouse, showing 100% homology, ARE consensus is shaded in grey.

4.4.5 Promoter Sequence Cloning

PCR Script and pGL3 Basic promoter plasmids were successfully cloned, representative gel and sequencing images are illustrated in figure 4.7.

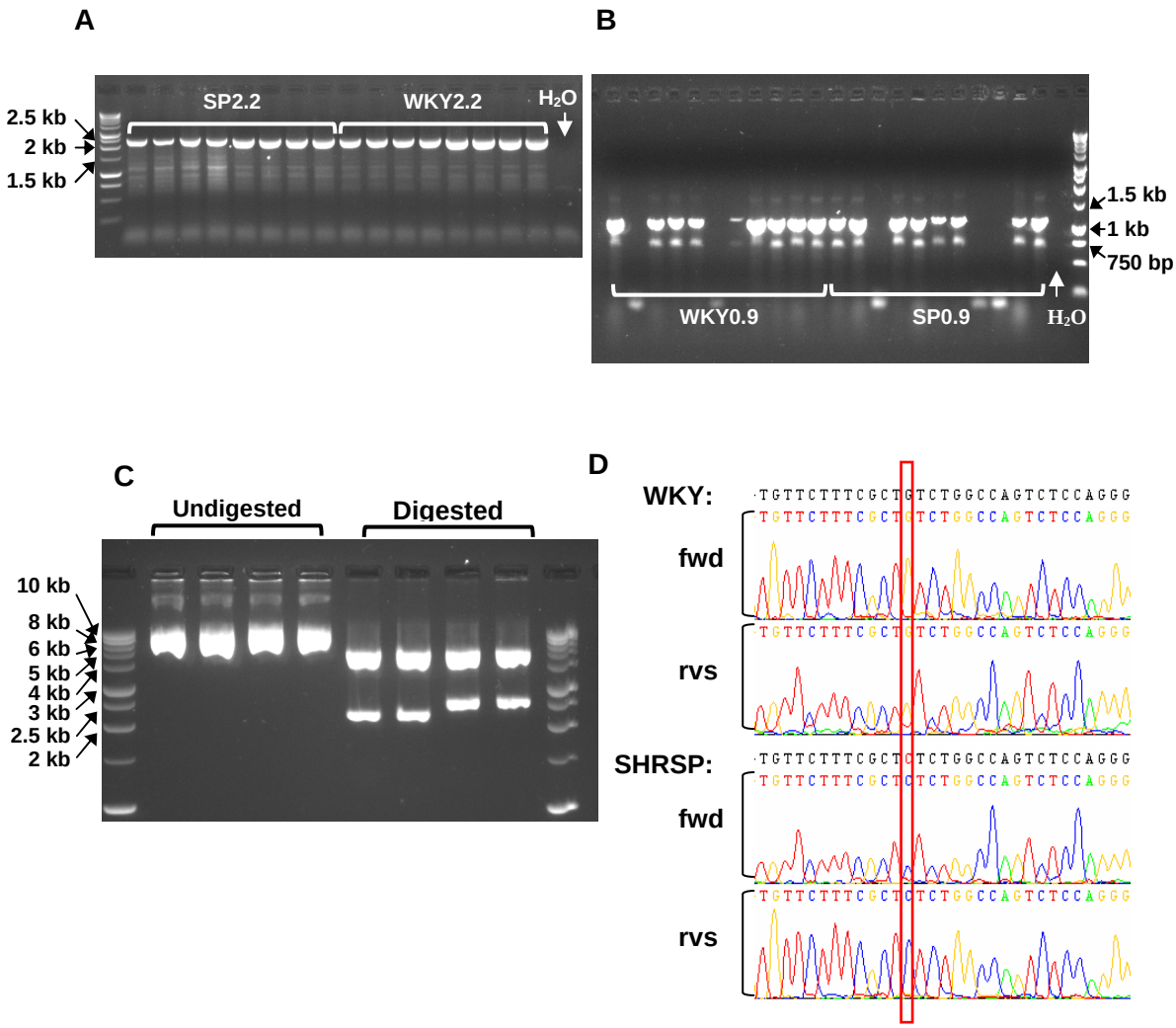

Figure 4.7 - Agarose gel and sequencing images from *Gstm1* promoter cloning

(A) Amplification of 2.2 kb promoter sequences from SHRSP and WKY (expected size 2192 bp), bands were gel purified for cloning into PCR-Script. **(B)** PCR-screening of colonies after cloning 0.9 kb promoter sequences into PCR-Script (expected size 1105 bp) **(C)** Undigested and double-digested (*MluI* and *XhoI*) pGL3 Basic plasmids, 2.5 kb and 2.2 kb promoter fragments of the expected sizes were observed following restriction-digestion. 1 µg plasmid DNA per lane. (**D**) Sequencing confirmed presence of promoter SNPs in plasmids. Sequencing from SNP 6 is shown, encoding G in the WKY and C in the SHRSP.

4.4.5.1 Optimising NRK52E Transfections

Transfection of NRK52E cells in 24-well plates with over 200 ng DNA per well was toxic to the cells, transfection with 200 ng pGL3 Control at DNA:FuGENE ratios of 3:1, 3:2 and 6:1 (µl:µg) resulted in high luciferase activities in cell lysates after 48 hours (figure 4.8 A), 200ng DNA at a ratio of 3:1 was used for further transfections since it showed highest transfection efficiency with the least DNA. Pilot co-transfections with pGL3 Control and pMV10 assesd levels of β-galactosidase expression (figure 4.8 B), and β-galactosidase activity staining further confirmed NRK52E transfection (figure 4.8 C).

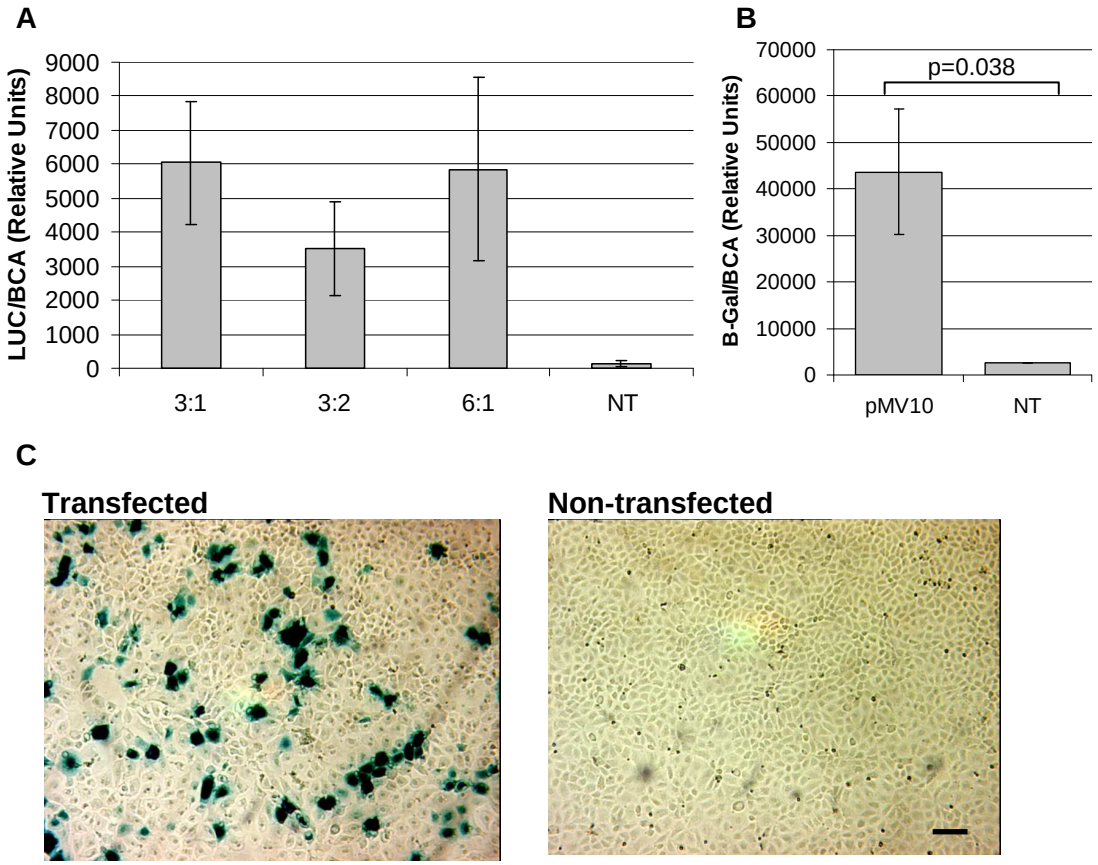

Figure 4.8 - Optimisating transfection of NRK52E cells

(A) Transfection of 200 ng pGL3 Control DNA at DNA:FuGENE ratios of 3:1, 3:2 and 6:1 resulted in luciferase expression, 3:1 ratio was used for experimental transfections. Mean ± SE, n=3 **(B)** Co-transfection with 50 ng pMV10 and 150 ng pGL3 Control resulted in significant β-galactosidase activity in NRK52E cell lysates compared to non-transfected cells (NT). Mean ± SE, n=3 (2 sample t test) (**C**) β-galactosidase activity staining following transfection with 200 ng pGL3 Control showed 5-10% transfection of NRK52E cells. Scale bar =100 µm

4.4.5.2 Comparing SHRSP and WKY Promoter Activities

The relative promoter activities of pSP0.9, pWKY0.9, pSP1.6, pWKY1.6, pSP2.2, pWKY2.2, pSP2.5 and pWKY2.5 were measured in NRK52E cells (figure 4.9). pSP1.6 had a consistent 2.2-2.6-fold lower luciferase promoter activity than pWKY1.6 across repeated experiments, otherwise no significant differences in promoter activities were observed between the promoters. This data indicated that one or more of SNPs 8-12 may be responsible for reduced expression of pSP1.6 compared to pWKY1.6, that the putative ARE sequence may have an upregulatory effect on Gstm1 expression and that SNP13 does not affect Gstm1 expression.

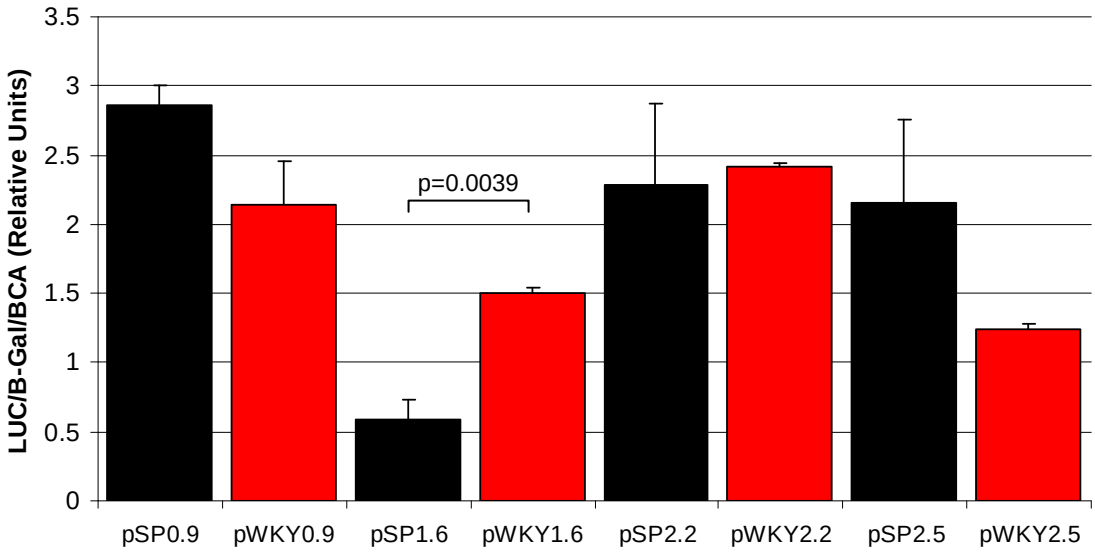

Figure 4.9 - Luciferase activities of 0.9 kb -2.5 kb *Gstm1* promoter sequences
In comparisons between SHRSP and WKY sequences of the same length, significantly reduced promoter activity was observed pSP1.6 compared to pWKY 1.6 kb. No other significant differences in promoter activities were observed. Mean ± SE, n=3 (2 sample t test).

4.4.5.3 Luciferase Activities of Novel Subcloned SP1.6 plasmids

Plasmids pSP1.6(1-7) and pSP1.6(8-12) were generated to test the hypothesis that one or more SNPs in cluster 8-12 may be responsible for reduced expression from pSP1.6. Promoter activities of pSP1.6(1-7) and pSP1.6(8-12) were comparable to pWKY1.6 (figure 4.10). This indicated that an interaction between one or more SNPs in cluster 1-7 and one or more SNPs in cluster 8-12 is responsible for reduced expression from pSP1.6, this was tested by site-directed mutagenesis.

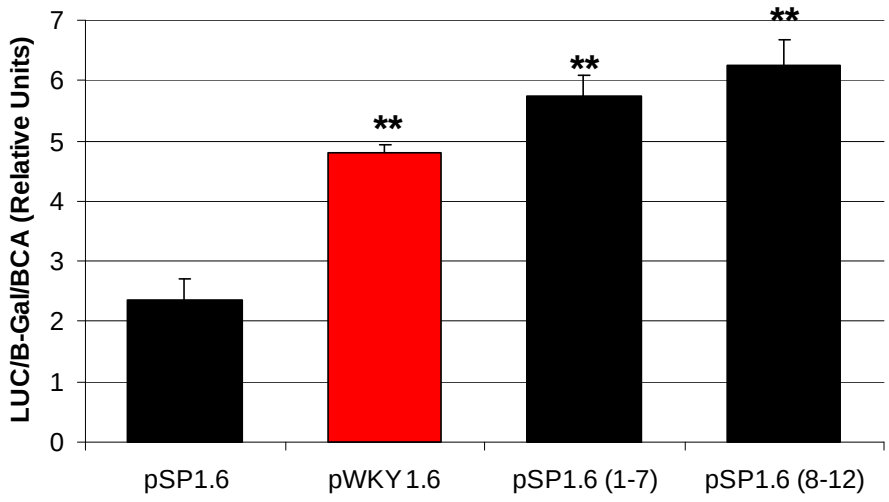

Figure 4.10 – Luciferase activities of subcloned 1.6 kb promoter plasmids
pSP1.6(1-7) and pSP1.6(8-12) promoter activities were significantly higher then pSP1.6 and equivalent to that of pWKY1.6, implicating an interaction between SNPs in cluster 1-7 and 8-12 in reduced expression from pSP1.6. Mean ± SE, n=3, F=26.9 **p<0.01 vs. pSP1.6 (ANOVA and Dunnett's post-test).

4.4.5.4 Luciferase Activities of Novel SP1.6 Site-Directed Mutagenesis Plasmids

SNPs 8, 9, 10+11 and 12 were introduced into pSP1.6(1-7) by site-directed mutagenesis, creating four further novel plasmids. Luciferase promoter activities of pSP1.6, pWKY1.6, pSP1.6(1.7+8), pSP1.6(1-7+9), pSP1.6(1-7+10+11) and pSP1.6(1-7+12) were compared by transfection into NRK52E cells, relative promoter luciferase activities were measured 48 hours after transfection (figure 4.11). These assays failed to identify a SNP from cluster 8-12 that interacts with SNPs 1-7, the presented data implies that SNP 8 or 9 may interact with SNPs 1-7, but this was not shown consistently in repeat experiments.

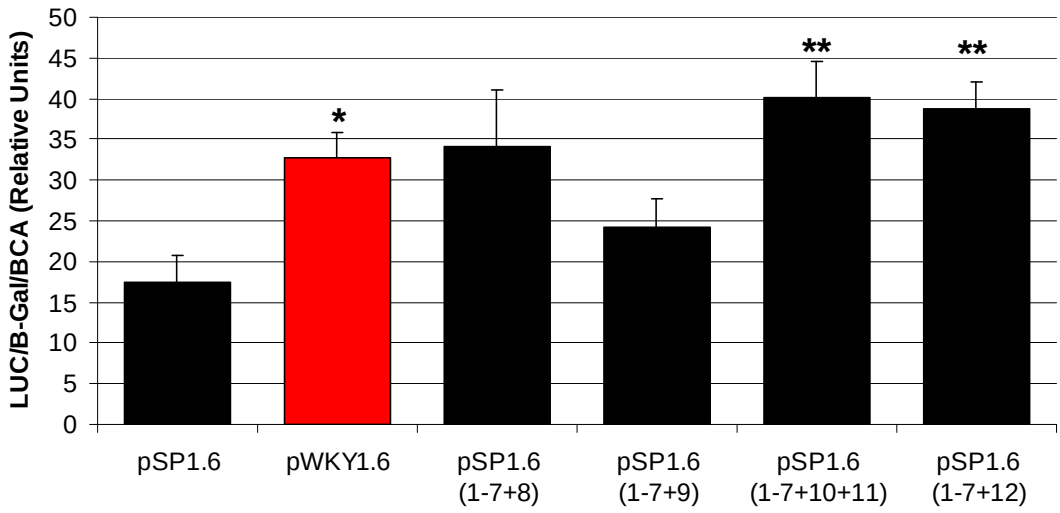

Figure 4.11 - Luciferase activities of novel site-directed mutagenesis plasmids
Compared to pWKY1.6 and pSP1.6, luciferase activities of pSP1.6(1-7+10+11) and pSP1.6(1-7+12) were significantly higher than pSP1.6 and equivalent to pWKY1.6, while activities of pSP1.6(1-7+8) and pSP1.6(1-7+9) were not significantly different to pSP1.6. However this pattern was not replicated in repeat experiments. Mean ± SE, n=3, **p<0.01 vs. pSP1.6, F=4.77, *p<0.05 vs. pSp1.6 (ANOVA and Dunnett's post-test).

4.4.6 Transfac Professional Matrix Table

Transfac analysis identified 435 TF matrices that align to sequences surrounding each SNP at either SHRSP or WKY sequences with a core alignment and matrix alignment score over 0.75 and 0.7, respectively (table A5), these cut-offs are default settings in the Match module. All matrices that that uniquely bind to SHRSP or WKY sequences are included, and matrices for which the core alignment or matrix scores differ by more than 0.1 between the WKY and SHRSP. The data is grouped by SNP with each row showing the alignment at a particular SNP site in the SHRSP or WKY with a Transfac matrix. The sequence shown in the 'Aligned sequence' column shows the sequence in the SHRSP or WKY that aligns with the matrix sequence in question, note that the +ve strand sequence is always shown, but the matrix may align with the –ve strand (i.e. the reverse-complement of the sequence shown in the 'Aligned sequence' column), in these cases, a (-) is shown in the 'Strand' column. Five bases in the 'Aligned sequences' are always in upper case, these are the bases that align with the matrix core sequence, the lower case bases align with the rest of the matrix. Alignment scores for core and matrix sequences are given. The 'Position' column refers to the base number in the inputted sequence where the matrix alignment starts, these are synchronous between the SHRSP and WKY inputs for most SNPs but where base numbering is affected by an insertion or deletion (SNPs 2 and 10), alignments

may not begin at the same base number. Many transcription factors are represented by more than one matrix, a consequence of the fact that different evidence (gene, species etc.) was used to compile different matrices. The same conventions apply to the data presented in tables 4.3 and 4.4.

As would be expected the largest number of matrices are listed for SNPs 1+2 and SNPs 10+11 (93 and 101 respectively) since these affect two bases, while the fewest are listed for SNP 13 (8 matrices). Table A5 includes a large proportion of false-positive alignments for TFs unlikely to be involved in renal *Gstm1* expression control, either because the TFs concerned are involved in other cellular processes, are not expressed in the kidney, or simply do not actually bind to the sequence in question, despite the alignment scores. A curtailed list could have been generated by increasing the cut-off values for matrix alignment, however it was decided to use table A5 in the first instance as an exhaustive list to be interrogated using the results of the experimental studies to inform specific searches. Table A5 could be sorted according to strain, SNP, TF, matrix identifier, or any of the other column headings, a number of approaches were taken to analyse the data, as discussed below.

4.4.7 Transcription Factor Binding Site Analysis

The first line of analysis of Transfac data involved searching the PubMed database for instances where TFs have been shown to physically associate with multiple TF sites in a single promoter over at least 1.1kb (SNPs 1-12 span 1,138bp). Such a precedent exists for a basic leucine zipper (bZIP) cap'n'collar (CNC) TF called Bach1 that can mediate interactions between DNA binding sites up to 4.1 kb apart (Yoshida et al. 1999). Bach1 protein has bZIP and CNC motifs at the carboxyl terminus, and a BTB/POZ (broad complex-tramtrack-bric-a-brac/Pox virus and Zinc finger) domain at the amino terminus; the BTB/POZ domain mediates protein/protein interactions between Bach1 molecules bound at distant DNA binding sites. Similar to Nrf2, Bach1 dimerises with Maf TFs via the bZIP domain prior to DNA binding and intriguingly, Bach1 has also been demonstrated as a transcriptional repressor of several genes involved in oxidative-stress defence, binding to some of the same sites where Nrf2 upregulates expression.

Given the ability of Bach1/Maf dimers to bind to multiple distant sites over several kb and the fact that Bach1/Maf binds to many of the same sequences as Nrf2/Maf dimers, table A5 was inspected for multiple Nrf2, Bach1 and Maf TF binding sites, specifically for one or more sites affected by SNPs 1-7 and one or more affected by SNPs 8-12. No such pairs of

sites were found, but SNP10+11 does appear to affect the binding of Nrf2/Maf/Bach1 at a non-ARE consensus site at SNP10+11 (table 4.3). SNPs 10+11 reduce the core and matrix alignment scores for the Nrf2 matrix V$NRF2_Q4, while the core and matrix scores for alignments with Maf matrices V$TCF11MAFG_01, V$VMAF_01 and V$BACH1_01 were only high enough for the WKY sequence to pass the criteria for inclusion in the TF binding site table. Note that the alignment for V$TCF11MAFG_01 and V$VMAF_01 are on the reverse strand. In order to assess the likelihood that Nrf2/Maf or Bach1/Maf actually bind to this site, the alignments were considered in more detail. V$TCF11MAFG_01 was constructed by assessing TCF11/MafG heterodimer binding to a random sequence library (Johnsen et al. 1998), while V$VMAF_01 was derived from a publication assessing vMaf, an avian retrovirus Maf TF (Kataoka et al. 1994), as they do not relate to Nrf2 or Bach1 heterodimers, they were not considered further. WKY and SP sequences at SNP10+11 are shown below aligned with the binding sequences for Nrf2 and Bach1 from V$NRF2_Q4 and V$BACH1_01, respectively. The V$NRF2_Q4 consensus sequence is a non-ARE sequence, it was constructed by aligning Nrf2 binding sequences from multiple rat, mouse and human genes, each of these sequences is included on the alignment. V$BACH1_01 was constructed using a random sequence library to find recognition sequences for human Bach1 (Kanezaki et al. 2001), the single consensus sequence is shown. In each case the most conserved bases are in upper case, alignments with the WKY sequence are highlighted by shading in yellow, while the sites off SNPs 10+11 are shaded in red in the WKY and SHRSP sequences. A '-' has been inserted into the alignments in order to accommodate the insertion in the SHRSP sequence. Where Nrf2 binds to the reverse strand of the promoter, the reverse complement (RC) sequence is shown:

V$NRF2_Q4:

	Species and gene
gcTGA-GTCAtgaTGAGTCAtgctg	Human *β-globin* LCR
tctgttttCGCTGA-GTCATggttcccgttg	Mouse *Ho-1*
tacagagAT-GTCATAacagaa (RC)	Mouse *Gstp1*
ctccAGA-TTCAgtaaat (RC)	Mouse *Gstp1*
gtgtTGA-GTCAGcatcc	Mouse *Gstp1*
taaagtTGCTGA-TTCATtg	Rat *Tbxas1*
aactggcGCCACA-GTCAgccggt	Mouse *Nrf2*
ctccaTGA-CAAAgcattt	Mouse *Ferritin H*
agaaTGCTGA-GTCACggtg	Mouse *Ferritin H*

TGTTTTTAGTCTCCTCGTCA-GTCATTTGTTTTTCATCTG **WKY**
TGTTTTTAGTCTCCTCGTCCCGTCATTTGTTTTTCATCTG **SHRSP**

SNP	Strain	Matrix Identifier	Position	Strand	Core match	Matrix match	Aligned sequence (+ strand)	Factor name
SNP11+10	**WKY**	V$NRF2_Q4	80	(+)	1	0.845	ctcgtcAGTCAtt	Nrf2
SNP11+10	**SHRSP**	V$NRF2_Q4	81	(+)	0.873	0.742	tcgtccCGTCAtt	Nrf2
SNP11+10	**WKY**	V$TCF11MAFG_01	75	(-)	1	0.747	gtctcctcgtcaGTCATttgtt	TCF11:MafG
SNP11+10	**WKY**	V$VMAF_01	74	(-)	0.778	0.713	agtctcctcgTCAGTcatt	v-Maf
SNP11+10	**WKY**	V$BACH1_01	80	(+)	0.8	0.821	ctcgTCAGTcatttg	Bach1

Table 4.3 - Transfac alignment data of Nrf2, Maf and Bach1 matrices with SNP11+10

Transfac matrix alignments with WKY and SHRSP sequences at SNP11+10. V$NRF2_Q4 aligned with both SHRSP and WKY sequences, but the core match score differed by more than 0.1. Alignments of the other matrices in the table with the SHRSP sequence did not pass core and/or matrix alignment score thresholds (>0.75 core match, >0.7 matrix match), thus only WKY alignments are shown.

V$BACH1_01:

```
              acgATGA-GTCATgct
TGTTTTTAGTCTCCTCGTCA-GTCATTTGTTTTTCATCTG WKY
TGTTTTTAGTCTCCTCGTCCCGTCATTTGTTTTTCATCTG SHRSP
```

A second strategy to explain the interaction between SNPs 1-7 and 8-12 was employed by searching the matrix table for pairs of binding sites for the same TF, one in each cluster. A large number of TFs were considered in this analysis, though most were discounted on the basis of their known function and tissue expression profiles. The remaining matrices are listed in table 4.4. The first matrices in table 4.4 relate to the bZIP transcription factor, cyclic AMP response element-binding protein (CREB). CREB binds to the palindromic binding sequence: TGACGTCA. Table 4.4 lists a number of CREB matrix alignments that are affected by SNPs 1+2 and 10+11, the large number of matrices is related to the fact that CREB is a well studied transcription factor, that it has a palindromic binding site and thus aligns in both orientations, and, as seen below, it aligns twice at SNPs 10+11 in the SHRSP. The alignment of the canonical CREB family binding sequence with the SHRSP and WKY sequences at SNPs 1+2 and SNPs 10+11 is shown below, once again, SNPs are highlighted in red, and alignment with the WKY sequence is highlighted in yellow, alignment with the SHRSP sequence at SNPs 10+11 is highlighted in blue:

SNPs 1+2:

```
                  TGACGTCA
TGCAGGGCTGGGAGGGACCTCATTATTTTGTCCGGCCCACG WKY
TGCAGGGCTGGGAGGGACC-CGTTATTTTGTCCGGCCCACG SHRSP
```

SNPs 10+11:

```
              TGACGTCA
TGTTTTTAGTCTCCTCGTCA-GTCATTTGTTTTTCATCTG WKY
TGTTTTTAGTCTCCTCGTCCCGTCATTTGTTTTTCATCTG SHRSP
                    TGACGTCA
```

The remaining TF in table 4.4, COUP (chicken ovalbumin upstream promoter) is a member of the nuclear receptor (NR) superfamily of TFs. The NRs are subdivided into classes depending on their DNA binding specificities. COUP is a member of a subset of class III that also includes peroxisome proliferator-activated receptors (PPARs), retinoic acid receptors (RARs) and retinoid X receptor (RXR), they bind to the following consensus sequence, known as direct repeat 1 (DR1) as heterodimers with RXR: AGGTCAnAGGTCA.

SNP	Strain	Matrix Identifier	Position	Strand	Core match	Matrix match	Aligned sequence (+ strand)	Factor name
SNP1+2	WKY	V$CREB_01	55	(-)	0.788	0.805	ggaCCTCA	CREB
SNP1+2	WKY	V$CREB_02	55	(-)	0.832	0.794	ggaCCTCAttat	CREB
SNP1+2	SHRSP	V$CREB_02	57	(-)	0.82	0.721	accCGTTAtttt	CREB
SNP1+2	WKY	V$CREB_Q4_01	55	(-)	0.901	0.881	ggaCCTCAtta	CREB
SNP1+2	SHRSP	V$CREB_Q4_01	57	(-)	0.789	0.715	accCGTTAttt	CREB
SNP1+2	WKY	V$CREB_Q2	53	(-)	0.79	0.721	agggaCCTCAtt	CREB
SNP1+2	WKY	V$CREB_Q2_01	53	(+)	0.888	0.855	agggaCCTCAttat	CREB
SNP1+2	SHRSP	V$CREB_Q2_01	55	(+)	0.796	0.723	ggaccCGTTAtttt	CREB
SNP1+2	WKY	V$CREB_Q4	53	(-)	0.792	0.745	agggaCCTCAtt	CREB
SNP10+11	WKY	V$CREB_Q2	77	(-)	1	0.863	ctcctCGTCAgt	CREB
SNP10+11	SHRSP	V$CREB_Q2	77	(-)	0.79	0.703	ctcctCGTCCcg	CREB
SNP10+11	WKY	V$CREB_Q4	77	(-)	1	0.871	ctcctCGTCAgt	CREB
SNP10+11	SHRSP	V$CREB_Q4	77	(-)	0.792	0.708	ctcctCGTCCcg	CREB
SNP10+11	WKY	V$CREB_Q2_01	77	(+)	1	0.896	ctcctCGTCAgtca	CREB
SNP10+11	SHRSP	V$CREB_Q2_01	77	(+)	0.804	0.736	ctcctCGTCCcgtc	CREB
SNP10+11	WKY	V$CREB_Q4_01	79	(-)	1	0.906	cctCGTCAgtc	CREB
SNP10+11	SHRSP	V$CREB_Q4_01	79	(-)	0.764	0.703	cctCGTCCcgt	CREB
SNP10+11	WKY	V$CREB_Q4	81	(-)	0.831	0.727	tcgtcAGTCAtt	CREB
SNP10+11	SHRSP	V$CREB_Q4	82	(-)	1	0.886	cgtccCGTCAtt	CREB
SNP10+11	SHRSP	V$CREB_Q2	82	(-)	1	0.853	cgtccCGTCAtt	CREB
SNP10+11	SHRSP	V$CREB_Q2_01	82	(+)	1	0.921	cgtccCGTCAtttg	CREB
SNP10+11	WKY	V$CREB_Q4_01	83	(-)	0.789	0.723	gtcAGTCAttt	CREB
SNP10+11	SHRSP	V$CREB_Q4_01	84	(-)	1	0.918	tccCGTCAttt	CREB
SNP3	WKY	V$COUP_DR1_Q6	56	(-)	0.917	0.702	tgctctaGGGTCt	COUP
SNP3	WKY	V$COUPTF_Q6	51	(+)	0.848	0.726	ctttcTGCTCtagggtctgtagc	COUP
SNP3	WKY	V$COUPTF_Q6	51	(-)	0.814	0.726	ctttctgctctagGGTCTgtagc	COUP
SNP3	SHRSP	V$COUPTF_Q6	51	(-)	0.814	0.708	ctttctgctttagGGTCTgtagc	COUP
SNP4	WKY	V$COUPTF_Q6	69	(-)	0.827	0.734	ttcagggtgtgtaGAACAgaatc	COUP
SNP12	WKY	V$COUP_DR1_Q6	55	(+)	1	0.739	tGACCTgtaaact	COUP

Table 4.4 - TF matrices that aligned with SNPs in cluster 1-7 and cluster 8-12

Matrices aligning with one or more SNP in cluster 1-7 and one or more SNP in cluster 8-12. CREB: cyclic AMP response element-binding protein, COUP: chicken ovalbumin upstream promoter

The alignments of the sequences surrounding SNPs 3,4 and 12 in the WKY and SHRSP with DR1 is below. Since the sequence aligns with SNPs 4 and 12 on the reverse strand, the reverse complement sequence is shown:

SNP3:

```
             AGGTCAnAGGTCA
CCCTCTACTTTCTGCTCTAGGGTCTGTAGCTCT      WKY
CCCTCTACTTTCTGCTTTAGGGTCTGTAGCTCT      SHRSP
```

SNP4:

```
             TGACCTnTGACCT   (RC)
TTCAGGGTGTGTAGAACAGAATCCTGGGGCAGA      WKY
TTCAGGGTGTGTAGAATAGAATCCTGGGGCAGA      SHRSP
```

SNP12:

```
    TGACCTnTGACCT            (RC)
GCATTGCCCTTTGACCTGTAAACTGTTTTTAGT      WKY
GCATTGCCCTTTGACCCGTAAACTGTTTTTAGT      SHRSP
```

Note the exceptionally high homology between the consensus sequence and the WKY sequence at SNP12, with just one mismatch. The homology is lower for SNPs 3 and 4, but in each case the SNP occurs at a conserved base between the consensus and WKY. The fact that this search only highlighted COUP and not other class III NRs is due to the low homology with SNP 3 and 4 sequences; PPAR and RAR matrices also aligned with SNP12, but not with SNPs 3 and 4, the matrix alignment of the COUP matrices at SNPs 3 and 4 was close to the 0.7 threshold, between 0.702 and 0.734. Thus all class III TFs could be considered as potential regulators at SNP12 and possibly for SNPs 3 and 4 to provide an explanation of the interaction between SNPs in clusters 1-7 and 8-12.

Inspections of table A5 were also performed without consideration of the *in-vitro* evidence for TF binding site interactions. The table was inspected for binding sites for TFs previously experimentally shown to affect GST expression (from table 4.1), and foreshortened by filtering out core matrix alignments of less than 0.9. These analyses also included SNP13. As before, literature analysis was carried out to assess the likelihood that candidate TFs affect *Gstm1* expression, significant findings are presented.

A nuclear factor kappa β (NFκB) binding site has been identified in the human *GSTP1* promoter (Morceau et al 2004), and NFκB is a well established redox sensitive mediator of expression of inflammatory and antioxidant genes. A potential site was identified by Transfac binding to the WKY sequence at SNPs 1+2, though a closer comparison with the NFκB consensus sequence (GGGRNWYYCC; R = A or G; W = A or T; Y = C or T)

revealed a poor alignment with both WKY and SHRSP sequences. Alignment on the reverse strand at SNP 7 however indicates that NFκB binding could be affected by the SNP in the SHRSP. The alignment of the NFκB reverse-complemented consensus sequence with the WKY and SHRSP sequences is shown below, the SNP is highlighted in red, alignment with the WKY sequence is highlighted in yellow:

SNP7:

```
                    GGRRWNYCCC      (RC)
CTTTAAGCTGAGAGTCGAGAGCCTCCCCACCCCCCGCTGACAGATT WKY
CTTTAAGCTGAGAGTCGAGCGCCTCCCCACCCCCCGCTGACAGATT SHRSP
```

Finally, Transfac analysis revealed that SNP4 may affect an NF consensus sequence that binds the 'steroid receptors': androgen receptor (AR), glucocorticoid receptor (GR), mineralocorticoid receptor (MR) and progesterone receptor (PR). Rat *Gsta2* and *Gstp1* expression have been shown to be regulated by androgen (Falkner et al 1998;Falkner et al. 2001;Ikeda et al 2002). The consensus sequence for the steroid receptors consists of two 'half sites' separated by three unconserved bases: AGAACAnnnTGTACC, though AR has also been shown to bind to sequences related to AGAACAnnnAGAACA (Claessens et al. 2004). The WKY and SHRSP alignments with these two sequences is shown below:

SNP4:

```
                    AGAACANNNAGAACA
                    AGAACANNNTGTACC
GCTTTCAGGGTGTGTAGAACAGAATCCTGGGGCAGAGGC WKY
GCTTTCAGGGTGTGTAGAATAGAATCCTGGGGCAGAGGC SHRSP
```

4.5 Discussion

The experiments outlined in this chapter investigated the molecular mechanisms behind differential expression of *Gstm1* between the WKY and SHRSP. The data presented figure 4.3, 4.4 and table 4.2 was published in Mcbride et al 2005; qRT-PCR *Gstm1* mRNA expression analysis confirmed renal differential gene expression previously seen in microarrays between SHRSP and WKY (McBride et al 2003), and demonstrated reduced *Gstm1* expression in a second hypertensive strain, the SHR, compared to a second normotensive strain, the BN. Increased renal levels of nitrotyrosine in the SHRSP correlated with other data on renal and vascular oxidative stress that was published alongside the nitrotyrosine data in the same paper; superoxide levels measured by lucigenin-enhanced chemiluminescence in renal cortex and medulla and thoracic aortas of SHRSP were significantly higher than in WKY rats (McBride et al, 2005).

Taken together, these data show that reduced renal *Gstm1* expression coincides with increased renal oxidative stress, hypertension and the presence of 13 polymorphisms in the SHRSP *Gstm1* promoter. These observations led to the hypothesis that one or more of the promoter polymorphisms are responsible for reduced renal *Gstm1* expression in the SHRSP and that this contributes to hypertension in the SHRSP. The high number of polymorphisms found in the SHRSP *Gstm1* promoter was initially surprising, however this agrees with published observations (Zimdahl et al. 2004) wherein genome-wide SNP analysis in the BN, WKY and SHRSP revealed an average polymorphism rate between the BN and the other strains as approximately 1 every 1100 base pairs, however the SNP distribution was non-random, with an excess of loci with no or multiple SNPs. This was attributed to effects of artificial selection in derivation of these closely related laboratory rat strains; some loci have very recent common ancestors, and hence low frequency of SNPs, while other loci have distant common ancestors and thus higher SNP frequency (Zimdahl et al 2004). The functional relevance of the H202R variant was considered in McBride et al, 2005. Two lines of analysis were undertaken, first, the amino acid sequences of 19 GSTM enzymes from rat, mouse and human were aligned, amino acid 202 occurs in a highly conserved region; in 15 of the 19 sequences, including the consensus rat genome sequence, an arginine (R) residue is encoded; the histidine (H) residue is only present in the BN and WKY sequences indicating that Gstm1 activity is unlikely to be compromised by this mutation in the SHRSP and SHR. Secondly, the crystal structure of the rat Gstm1 protein was inspected; amino acid 202 is located on the surface of the protein and thus not likely to affect Gstm1 activity (Ji et al. 1992;McBride et al 2005).

Experiments were designed to compare the catalytic activities of WKY and SHRSP Gstm1 protein in chapter 5, where adenoviruses were constructed to express each sequence; the likelihood that the 3'UTR polymorphism identified at base +29 affects *Gstm1* expression was also addressed in this study, see sections 5.4.5 and 5.5.

The initial experiments to compare the activities of the WKY and SHRSP promoter sequences indicated that SNPs 8-12 may be responsible for reduced expression in pSP1.6, the lack of a significant difference in promoter activities between the pSP2.2 and pWKY2.2 plasmids suggested that the putative ARE sequence increased promoter activity in pSP2.2 to a level equivalent to that of pWKY2.2 despite the effects of SNPs 8-12. The lack of a significant difference in activities between pSP2.5 and pWKY2.5 indicated that SNP13 does not affect *Gstm1* promoter activity.

The hypothesis that SNPs 8-12 may reduce expression of SP1.6 was tested by sublconing between pSP1.6 and pWKY1.6 to generate plasmids pSP1.6(1-7) and pSP1.6(8-12). Equivalent promoter activities of pSP1.6(1-7) pSP(8-12) and pWKY1.6 indicated that an interaction between one or more SNPs in cluster 1-7 with one or more SNPs in cluster 8-12 was required for reduced expression from pSP1.6. In order to test this hypothesis, plasmids pSP1.6(1-7+8), pSP1.6(1-7+9), pSP1.6(1-7+10+11) and pSP1.6(1-7+12) were generated by site-directed mutagenesis of pSP1.6(1-7) and their promoter activities were assayed. These experiments did not conclusively identify a SNP from cluster 8-12 that individually interacts with SNPs in cluster 1-7 to reduce expression from the pSP1.6 promoter, SNPs 8 and 9 were implicated in one experiment, but this result was not observed in repeat experiments. These results can be explained by the limitatons of luciferase activity measurements despite corrections for transfection efficiency and total protein, combined with the small difference in promoter activity observed in the original experiments (2.2-2.6-fold difference in expression between pSP1.6 and pWKY1.6). In addition, it is possible that more than one of SNPs 8-12 are required for the interaction to reduce SP1.6 expression. It was not practical to test this due to lack of time, it would have required the generation by site-directed mutagenesis of a further ten plasmids to analyse every possible combination of SNP from cluster 8-12. If continuing these experiments, transfection protocols could be redesigned to ensure less variability within experimental groups. Renilla luciferase is derived from the sea pansy (*Renilla reniformis*) and fluoresces at a different wavelength to the beetle luciferase encoded by the pGL3 plasmids used in this project; co-transfection with renilla luciferase plasmids rather than pMV10 would allow fluorescence measurement of both luciferases in the same aliquot of lysate, significantly simplifying the experimental protocol and enabling sample replicate numbers to be increased.

A combination of cross-species sequence comparison, literature searching and Transfac promoter sequence analysis was performed on SNPs 1-12 to identify the most likely SNPs involved in reduced expression from SP1.6. The rat and mouse *Gstm1* promoter sequences show very high sequence homology, each of the SNPs 1-12 lie within regions of 70-90% identity with the mouse promoter, with no alignment at SNP13. Given the hypothesis that *Gstm1* expression is reduced in the SHRSP due to one or more of SNPs 1-12 and accepting that the homology between the rat and mouse *Gstm1* promoters is indicative of similar promoter elements controlling expression in each species, one is led to conclude that the SNPs where the mouse promoter has homology with the SHRSP are less likely to be involved in reduced *Gstm1* expression (SNPs 1+2, SNP3, SNP5 and SNP9). One may also conclude in this analysis that the sequence surrounding SNPs 10+11 is less likely to regulate rat *Gstm1* expression given that this is not conserved between the mouse and rat at all. However, these assumptions may not be correct, *Gstm1* may have acquired specific renal function in the rat that it does not have in the mouse, its expression in this instance may be controlled by different elements, that being the case there may be a stronger case for the sequence surrounding SNPs 10+11 having specific function in the rat.

A table of Transfac matrices was generated to list potential TF binding sites lost, created or affected by the polymorphisms in the SHRSP promoter. The Transfac analysis protocol used here has been successfully applied in published research, in the demonstration that the 'A' variant of the -675A/T polymorphism in the human *CYBA* gene (encoding p22phox) reduces promoter activity compared to the 'T' variant by disrupting binding of the hypoxia inducible factor 1 alpha transcription factor (Moreno et al 2007). A number of approaches were taken to interrogate the matrix table to find candidate transcription factor binding sites to explain the reduced promoter activity of pSP1.6.

The identification of a disrupted potential binding site for the structural TF Bach1 at SNP10+11, despite the fact that a similar site was not found for any of the SNPs in cluster 1-7, was an interesting finding. Bach1, Nrf2 and Maf TFs have been shown to bind to the ARE and a range of promoter sequences distinct from the ARE to regulate expression of a number of genes involved in oxidative stress defence. For example, Bach1/Maf heterodimers repress human *NQO-1* expression by binding to the *NQO-1* ARE, this repression is reversed by overexpression of Nrf2 and by administration of the pro-oxidant, heme (Dhakshinamoorthy et al. 2005). In addition, Bach1 has also been shown to compete with Nrf2 at non-ARE binding sites in the promoter of the mouse *heme oxygenase 1 (Ho-1)* gene, again, Bach1 represses *Ho-1* expression, while Nrf2 activates expression and heme alleviates Bach1 binding to the *Ho-1* promoter (Sun et al. 2002). Given that pSP(1-

7+10+11) did not show significantly reduced luciferase activity, it may not be responsible for reduced expression of pSP1.6, but it may be involved in reduced *Gstm1* expression *in-vivo*. As mentioned above, Bach1 is a heme-sensitive repressor of *Ho-1* and *NQO-1* expression, and while it is yet to be shown to regulate expression of any GST genes, it has also shown to respond to oxidative stress induced by the sulfhydyl oxidising agent diamide by dissociating from the human *HO-1* promoter, suggesting that it may respond to a range of pro-oxidant stimuli (Ishikawa et al. 2005). The evidence for a potential role of the non-ARE Nrf2 binding sequence in the rat *Gstm1* promoter is enhanced by the observation that such sequences have been described in the mouse *Gstp1* promoter (Ikeda et al 2002). Interstingly, Nrf2 transcription factor has also been implicated in a rat model of hypertension, where it has been shown to be downregulated in DSS rats relative to chromosome 1 congenic rats harbouring Lewis rat Nrf2 alleles (Joe et al. 2005).

CREB related TFs are among the most studied transcriptional regulators, they have been shown to affect the expression of genes involved in cellular proliferation, development and adaptive responses (Shaywitz et al. 1999). Transcriptional activation by CREB-related TFs is dependent on their phosphorylation in signalling cascades such as the MAPK pathway which has been shown to be involved rat *Gstm1* upregulation by geniposide (Kuo et al 2005), thus the finding of differential binding of CREB-like TFs to the WKY and SHRSP promoters at SNPs 1+2 and SNPs 10+11 was of interest. However, detailed analysis showed that while SNPs 1+2 and 10+11 do affect a potential CREB binding site in the WKY, SNPs 10+11 *create* a binding site in the SHRSP, thus disruption of interacting CREB family transcription factor binding sites are unlikely to affect expression in pSP1.6.

The identification of potential disrupted binding sites for class III NR TFs COUP, RAR, PPAR and RXR (with which the other members of the family dimerise in DNA binding) at SNPs 3,4 and 12 presents the best hypothesis to explain the reduced promoter activity of pSP1.6. The NRs are an exceptionally diverse family of TFs with roles in development, reproduction, metabolism and homeostasis, they include 48 distinct members in humans and over 200 in *C.elegans*. NRs generally bind to lipophilic molecules such as steroid hormones, fatty acids, vitamins and prostaglandins. Structurally, the NR family are well conserved, with a modular structure including a C-terminal ligand-binding domain (LBD), a DNA binding domain (DBD) and N-terminal domain (NTD). The NTD is the most variable region and is responsible for the specific transactivation properties of NRs (McEwan 2004). Although Transfac analysis identified COUP as the binding factor at SNPs 3,4 and 12, each of the class III NRs could be considered candidates since they bind to the same recognition sequence. COUP transcription factors were initially described

through their role in regulation of ovalbumin expression in chickens (Sagami et al. 1986), and have subsequently been shown to have diverse roles in development, though their post-developmental role is less well understood (Cooney et al. 2001). RAR TFs include a number of members with roles in development and as tumour suppressors (Altucci et al. 2007). A precedent for PPAR-mediated regulation of GST expression has been demonstrated for the mouse *Gsta2* gene, where three DR1-like sequences were shown to be required for induced hepatic expression of *Gsta2* by PPARγ/RXR heterodimers in response to the RXR and PPAR activating ligands retinoic acid (RA) and 15-deoxy-δ (12,14)-prostaglandin J_2 (PGJ_2), (Park et al 2004). In a similar manner to the pattern of sites seen in the rat *Gstm1* promoter, one of the PPARγ sites in the mouse *Gsta* promoter is highly homologous with the DR1 consensus, while the other two are poorly conserved, and one of the sites is in the reverse orientation. Park et al suggested that the three sites form a co-operative PPAR responsive enhancer module (PPARM) since deletion of any one of them disrupts RA and PGJ_2 induced *Gsta2* expression. In this model, multiple TFs bind to the DR1 sites and other local TF binding sites, including an Nrf2-binding ARE, in induced *Gsta2* expression. A similar model could be proposed for the rat *Gstm1* promoter, though the TF binding sites are distributed over 1.0 - 1.7kb (depending on the inclusion of the putative ARE sequence) rather than 0.5kb as in mouse *Gsta2*; also note that the experiments presented here also differ to the model used by Park et al in that no transcriptional activating agents were used to stimulate expression.

PPARγ is predominantly expressed in adipose tissue, though it is expressed in the kidney and its expression in the rat nephron has been localised to the outer-medullary collecting duct, (Yang et al. 1999). Immunohistochemical studies in our laboratory have localised Gstm1 to the collecting duct by co-localisation with aquaporin 2 (McBride et al 2005) thus Gstm1 and PPARγ expression are co-localised in the rat kidney. As discussed in section 1.1.3.5, dominant negative PPARγ mutations can cause hypertension associated with type 2 diabetes without obesity in a mechanism thought to relate to changes in vascular tone (Barroso et al 1999). PPARγ agonist medications such as the thiazolinendiones (TZDs) have a blood pressure lowering effect, though this has predominantly been related to improved insulin sensitivity (Sarafidis et al. 2006). The precise role of PPARγ in the kidney is not well understood, though TZDs can influence renal sodium handling, occasionally leading to oedema via a mechanisms thought to involve upregulation of ENaC. This relationship has been studied in an experimental model; TZD treatment causes oedema in mice, but fluid retention and ENaC activation are prevented in transgenic mice selectively lacking PPARγ expression in the collecting ducts (Guan et al. 2005). In

addition, PPARγ modulates renal oxidative stress by inhibiting expression of NAD(P)H oxidase subunits (Hwang et al. 2005) and may also upregulate renal NO synthesis, though this is disputed (Dobrian 2006). PPARy upregualtion by the TZD rosiglitazone has also been shown to enhance recovery of tubular epithelial cells after oxidative damage by H_2O_2.

The Transfac data analysis discussed above presents hypotheses to explain the results of the *in-vitro* luciferase studies. These studies indicated that an interaction between SNPs in clusters 1-7 and 8-12 reduces expression in the SHRSP promoter and that this can be overcome by the putative ARE sequence in the 2.2kb fragment. It is interesting to consider how these results relate to the full promoter sequences in the SHRSP and WKY; in the genomic context the ARE sequence is present in the SHRSP and WKY, yet *Gstm1* expression is constitutively reduced in the SHRSP. This is a reflection of the limitations of *in-vitro* promoter analysis. Though no agents were used to stimulate promoter activity in these studies, the data does not necessarily represent basal promoter activity *in-vivo*, regulatory factors may be present in the rat kidney that affect constitutive expression via the elements proposed to interact at SNPs 1-7 and 8-12, while the ARE sequence may only upregulate expression in certain conditions *in-vivo*.

Final analysis of the Transfac matrix table involved searching for transcription factors with the highest alignment scores at the SNPs, and for TFs previously shown to affect GST expression, without consideration of the *in-vitro* experimental results. This identified potential a potential binding site at SNP7 for NFκB at SNP 7 and a steroid receptor binding site at SNP4. NFκB is a well characterised mediator of inflammatory and immune responses, and is regulated by oxidative stress conditions (Schreck et al. 1991;Schulze-Osthoff et al. 1993), and NFκB has been demonstrated to mediate human *GSTP1* expression in a leukemic cell line, where it is proposed to play a role in chemoresistance by upregulating xenobiotic metabolism (Morceau et al 2004). In addition, NFκB has been shown to upregulate other genes involved in oxidative stress defence such as glutamate cysteine ligase catalytic subunit gene, one of the mediators of glutathione synthesis (Morales et al. 1997). The WKY sequence at SNP4 aligns 100% with the first half of the steroid receptor consensus sequence, and SNP4 disrupts the alignment in the SHRSP. The second half of the binding sequence does not have high homology with the promoters. Like most NRs the steroid receptors bind to their recognition sequences as dimers, experimental evidence has demonstrated that the first unit in the dimer binds to the 5' conserved five bases of the recognition sequence, leading to conformational change of the TF that leads to recruitment of the second moiety (Luisi et al. 1991). It has long been recognised that the second half site tends to have much less homology to the consensus sequence (Evans

1988), thus the poor alignment with the second half site does not necessarily preclude steroid receptor binding to the sequence above. However, it is difficult to speculate which of the steroid receptors may bind to this site to regulate *Gstm1* expression. Several factors have been shown to dictate which steroid receptor binds to a particular promoter element including the availability of the receptor and its ligand in the cell, the availability of cell-specific co-regulators that participate in transcriptional complexes, the local binding of other TFs that can potentiate binding of one steroid receptor over another, the incidence of other steroid receptor binding sites in the promoter, and finally, specific binding sequence preferences (Nelson et al. 1999). The rat *Gsta2* promoter contains steroid receptor binding sequence that regulates *Gsta2* expression in cultured liver cells in a biphasic manner. Low concentrations of the synthetic corticosteroid dexamethasone (10-100 nM) repress expression, while at high concentrations (>1μM), expression is induced (Falkner et al 1998;Falkner et al 2001). Unpublished data from our laboratory shows that renal *Gstm1* expression is approximately 1.8-fold higher in males than females, perhaps suggesting a role for androgen-stimulated expression via the AR. Androgen has been implicated in increased expression of *Gstp1* in the livers of male rats, in this case several AR response elements were located to the 5th intron of the gene (Ikeda et al 2002).

Transfac is the gold standard transcriptional regulation database, it is well curated and regularly updated with new additions to the database, however it is not without its limitations. For example, it restricts each matrix to a five-base core alignment sequence that is used as the first threshold in sequence alignment, this does not necessarily reflect the structure of the actual TF binding sequences. The ARE is a case in point, as seen above, the ARE consensus sequence is spread over at least 10 bases with two highly conserved sequences of 4 and 3 bases separated by non-conserved bases. Other TF binding sites consist of variable repeated elements spread over 20-30 bases or more with non-conserved bases between them. Thus good matrix alignments did not guarantee TF binding at that site, the original literature used to compile to matrices, and other published evidence, was also considered. These limitations highlight the challenges of *in-silico* promoter sequence analysis, understanding gene expression is probably the greatest challenge in molecular biology, databases must make certain assumptions in order to categorise data for searching, and compromises are made.

A number of potential transcription factor binding sites affected by the SNPs in the SHRSP have been identified, some of which may account for the observed reduction in expression from the pSP1.6 promoter construct, and a putative ARE has been identified between SNPs 12 and 13 that may account for increased expression of SP2.2. Proof that a particular TF is

involved in *Gstm1* regulation would require further laboratory investigation. A number of techniques are available that could be applied to SHRSP and WKY sequences to compare TF activity. Cells could be co-transfected with plasmids expressing a TF to compare luciferase activities from the promoter constructs; similarly agents could be applied to cells to activate the TFs in question, such as rosiglitazone or another TZD to activate PPARγ, or phenolic antioxidants to stimulate Nrf2. Site-directed mutagenesis could be used to disrupt the ARE sequence in pSP2.2 to assess its activity. Specific techniques to assess TF binding to WKY and SHRSP *Gstm1* promoter sequences are also available such as DNaseI footprinting and electrophoretic mobility shift assays, which have been applied to a number of studies investigating the promoters of several GST genes (Kawamoto et al 2000;Ikeda et al 2002;Bartley et al 2003).

The above techniques can all be applied to cells transfected with promoter constructs, it would also be informative to study cell lines derived from the SHRSP and WKY. The most faithful replication of the *in-vivo* renal expression of *Gstm1* would be from primary collecting duct cells. Techniques have been described to isolate inner medullary collecting duct cells from the rat kidney involving careful dissection followed by collagenase treatment and selection with high salt and urea (Maric et al. 1998) or hypotonic conditions (Laplace et al. 1992). Other protocols have applied immunoselective surfaces coated with antibodies specifically targeting collecting duct cell surface antigens in human and mouse (Sweeney, Jr. et al. 1998) and rabbit (Fejes-Toth et al. 1992). The *Gstm1* promoter could be analysed in isolated SHRSP and WKY collecting duct cells using chromatin immunoprecipitation (ChIP), a technique that provides a precise view of the DNA sequences that bind to a particular TF in the cell.

Despite the evidence that the polymorphisms differentiating the WKY and SHRSP *Gstm1* promoter may affect expression, it is important to recognise that other elements may be responsible for reduced SHRSP expression. For example, control elements have been described within the introns of genes, such as the AR sequences in intron 5 of rat *Gstp1* mentioned above (Ikeda et al 2002), and it is well documented that enhancer elements can also operate from several kilobases upstream or downstream of a gene. Furthermore, negative regulation of gene expression by microRNAs (miRNAs) has recently attracted much attention. The possibility that this mechanism may affect *Gstm1* expression is considered in chapter 5.

5 Adenovirus-Mediated Modulation of *Gstm1* Expression *in-vitro* and *in-vivo*

5.1 Introduction

To further assess the role of *Gstm1* and its contribution to renal oxidative stress, *in-vitro* and *in-vivo* gene transfer approaches were taken. Recombinant adenovirus serotype 5 (RAd5) vectors were generated to overexpress *Gstm1* and to express short-hairpin RNA sequences designed to knock down expression of several members of the *Gstm* family. Recombinant vectors used for gene delivery were replication deficient, lacking genes (*E1a* and *E1b*) that mediate viral replication through transactivation of viral gene expression and deregulation of the host cell cycle. Adenovirus vectors are an extremely efficient means of gene delivery, they are popular platforms for short-term transgene expression studies for several reasons (Nicklin et al. 2003), for example, large DNA constructs can be cloned into the viral genome, up to 8 kb (though the largest fragment cloned in this experiment was 0.74kb) and efficient cloning and amplification techniques have been perfected by many laboratories, high titre stocks can be generated with relative ease. In addition adenoviruses infect a very wide range of dividing and non-dividing cell types. They are disadvantageous for long-term studies since they only mediate transient gene expression. Research from the Glasgow laboratory has demonstrated that local adenoviral overexpression of human endothelial nitric oxide synthase or extracellular superoxide dismutase improves NO bioavailability in SHRSP carotid arteries (Alexander et al. 2000;Fennell et al 2002), many of the techniques developed in these studies were applied in this project. Local delivery of adenoviruses has also been applied in other studies examining cardiovascular phenotypes, for example, administration of eNOs and iNOS overexpressing adenoviruses to isolated rabbit carotid arteries following endothelial denudation was demonstrated to ameliorate intimal hyperplasia compared to uninfused vessels, while eNOS overexpression, but not iNOS overexpression, also promoted the regeneration of the endothelium (Cooney et al. 2007). A similar therapeutic effect was observed by adenoviral overexpression of copper-zinc superoxide dismutase in denuded rabbit carotid arteries, intimal hyperplasia was reduced compared to uninfused arteries (Kuo et al. 2004). Local delivery of adenoviruses overexpressing eNOS to the brain stem following experimentally-induced myocardial infarction in mice has been demonstrated to lessen the increase in sympathetic drive that accompanies the onset of heart failure, as measured by urinary noradrenalin (Sakai et al. 2005). Tail-vein delivery of adenoviruses overexpressing human kallikrein to severely hypertensive uninephrectomised DOCA-salt rats reduced systolic blood pressure by up to 32 mmHg. Blood pressure reduction lasted for at least 23 days and morphological examination showed that kallikrein overexpression prevented DOCA-salt mediated kidney damage such as glomerular sclerosis and proximal tubular dilation (Dobrzynski et al.

1999). Systemic injection of an adenovirus overexpressing another vasodilatory peptide, adrenomedullin, has also been shown to reduce blood pressure and attenuate left-ventricular hypertrophy in DSS rats fed a 4% NaCl diet (Zhang et al. 2000).

RNA interference (RNAi) is an endogenous mechanism of transcriptional regulation that has been demonstrated in mammals, plants, nematodes, Drosophila and protozoa. First observed in plants where overexpression of a pigment gene suppressed flower colour development in petunias (Napoli et al. 1990), the RNAi mechanism is thought to be an adaptation of defence mechanisms that target dsRNA viruses and transposons (mobile genetic elements that propagate via an RNA intermediary). A crucial breakthrough in the understanding of RNAi occurred with the demonstration that sense and anti-sense RNA (i.e. dsRNA) is required for RNAi (Fire et al. 1998). In the RNAi pathway, depicted in figure 5.1, dsRNAs are processed by the RNase III enzyme Dicer to double stranded short interfering RNAs (siRNAs) 21-25 base-pairs in length with a dinucleotide 3' overhang. siRNAs associate with the RNA-induced silencing complex (RISC) and target mRNA that encodes the same sequence as the siRNA. In association with siRNAs, the RISC complex catalyses cleavage of the target mRNA, preventing transcription, mRNA fragments are further processed by exonuclease enzymes. This pathway is exploited by biologists wishing to investigate gene function by targeted knockdown. siRNAs can be delivered to cells via several pathways to mediate transcriptional repression: Long dsRNAs can be transfected into cells for processing by Dicer to siRNAs, however dsRNAs over 30 nucleotides in length stimulate anti-viral interferon responses in most mammalian cell lines leading to non-sequence specific degradation of dsRNA, therefore the preferred technique, particularly for *in-vitro* studies, is to transfect chemically synthesised siRNAs, bypassing the Dicer complex to interact with RISC directly (Elbashir et al. 2001a). Alternatively, plasmids or adenoviruses encoding shRNA sequences can be utilised, shRNA sequences consist of the inverted repeats of the siRNA sequence separated by a 6-9 base pair loop sequence. Vector-expressed shRNAs were first described by Sui et al as a tool for synthesis of siRNAs from a plasmid template (Sui et al. 2002) and have been extended to expression from a viral platform (Xia et al. 2002;Davidson et al. 2005). After transcription the shRNA folds back to self anneal, and is processed by Dicer to generate functional siRNAs (figure 5.1). Adenoviral expression of shRNAs has been applied to investigate the function of a number of cardiovascular and glutathione metabolism genes. For example an *in-vivo* study infected primary rat myocytes with adenoviruses expressing a shRNA directed against protein kinase c alpha (PKCα), resulting in increased contractility of myocytes compared to uninfected cells and confirming the role of PKCα in cardiac

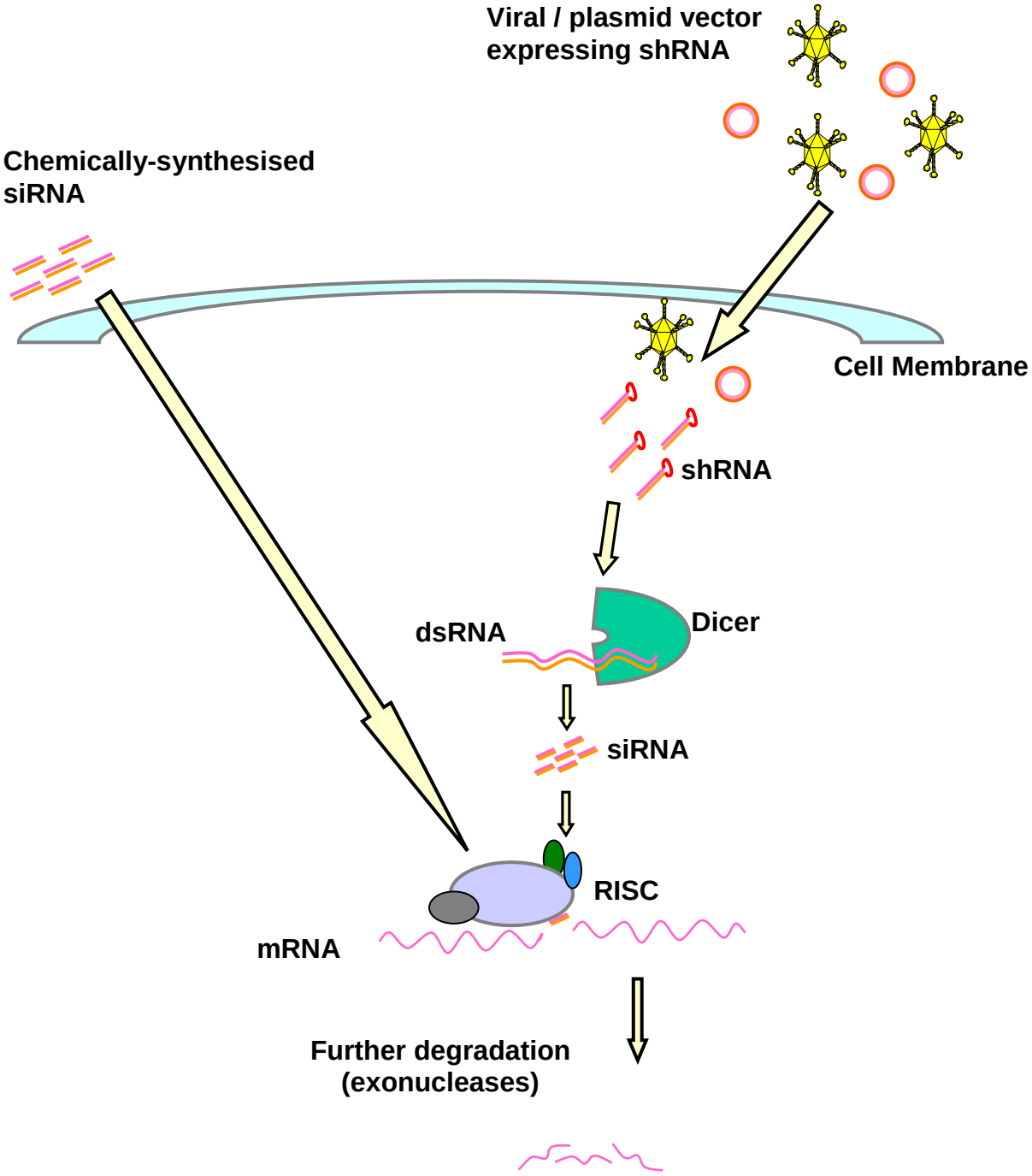

Figure 5.1 - Exploitation of the endogenous RNA interference pathway in experimental biology
RNAi sequences can be introduced via transfection of chemically synthesised siRNA, plasmids expressing shRNAs, or infection of viruses expressing shRNAs.

contractility (El Armouche et al. 2007). Direct injection of adenoviruses expressing a shRNA targeted against AngII 1a receptors to the intracerebroventricular region of the brain increased water intake in mice but had no effect on blood pressure, while injection into the brain stem nucleus tractus solitarius reduced blood pressure but not drinking

activity (Chen et al. 2006). Systemic injection to rats of adenoviruses expressing anti-glutathione synthase catalytic subunit (alternatively known as gamma glutamylcysteine synthase heavy chain) resulted in an 80% reduction in liver GSH levels, but not other organs since systemically-injected adenoviruses are delivered predominantly to the liver (Huard et al. 1995). GSH depletion continued for 2 weeks and hepatic acetaminophen toxicity was significantly potentiated in infused rats compared to controls (Akai et al. 2007).

The RNAi pathway overlaps with many functional elements of the microRNA (miRNA) transcriptional regulation pathway. miRNAs are single-stranded short (typically 21-24 bp long) RNA negative regulators of gene expression, they are increasingly acknowledged as major regulators of development and cellular homeostasis. miRNAs are encoded in the genome and expressed initially as pri-miRNAs, RNA templates that can encode single miRNAs or several tandemly aligned miRNAs. pri-miRNAs are processed by the enzyme complex Drosha to generate pre-miRNAs, hairpin structures that that resemble shRNA sequences and are processed by Dicer, producing short dsRNA molecule, similar to siRNAs, with a 1-4 base 3' overhang. The RISC complex mediates separation of the dsRNA into a single stranded molecule (this is the mature miRNA) and the association with the target mRNA. Unlike siRNAs, miRNAs bind exclusively to the 3'UTR of genes and mediate downregulation of expression by two routes: perfectly aligned miRNAs lead to gene silencing via the degradation of mRNAs, while imperfectly aligned miRNAs reduce expression by repressing translation. The overlap between the RNAi and miRNA pathways, and the importance of miRNAs in regulating post-developmental gene expression, was highlighted in research showing that systemic administration of adeno-associated virus (AAV) vectors mediating long-term overexpression of shRNAs to mice caused fatality due to oversaturation of the endogenous miRNA pathways (Grimm et al. 2006).

Given the wide substrate specificity of the GST genes and the possibility that reducing *Gstm1* expression alone may be compensated by upregulation of other members of the family, a single siRNA sequence designed to knock down expression of several Gstm genes is an appropriate tool. Previous experiments performed in the Glasgow laboratory by Dr William Miller identified the Gstmf sequence (AAGCCAGTGGCTGAATGAGAA) that aligns within a highly conserved region in the *Gstm* genes *Gstm1*,*2*,*3*,*5* and *7* and effectively knocked down expression of Gstm1 protein in NRK52E cells when transfected as a naked chemically synthesised siRNA.

5.2 Aims

- To analyse the *in-vitro* and *in-vivo* functional effects of modulating *Gstm1* and *Gstm* family expression. Adenoviruses were constructed to express a shRNA sequence designed to reduce expression of multiple members of the rat *Gstm* family, and to overexpress WKY and SHRSP *Gstm1* cDNA sequences.

- To assess knockdown of multiple *Gstm* genes by the shRNA sequence at the mRNA and protein level *in-vitro* and to compare the *Gstm1* expression and catalytic activity of the two overexpression viruses. The functional effects of modulating Gstm expression were assessed *in-vitro* by measuring changes in total GST activity and cytotoxicity mediated by an oxidising agent, tert-butyl hydrogen peroxide (TBHP).

- To test the hypothesis that overexpression of *Gstm1* in the carotid artery of the SHRSP improves endothelial NO bioavailability, measured by wire myography.

5.3 Methods

5.3.1 Generating viruses by homologous recombination in HEK293 cells

The overexpression and shRNAi viruses used in this project were generated in the same manner, (Anderson et al. 2000), relying upon homologous recombination between linearised plasmid shuttle and genome vectors in HEK293 cells stably transformed to express *E1a* and *E1b* genes (Graham et al. 1977) (figure 5.2).

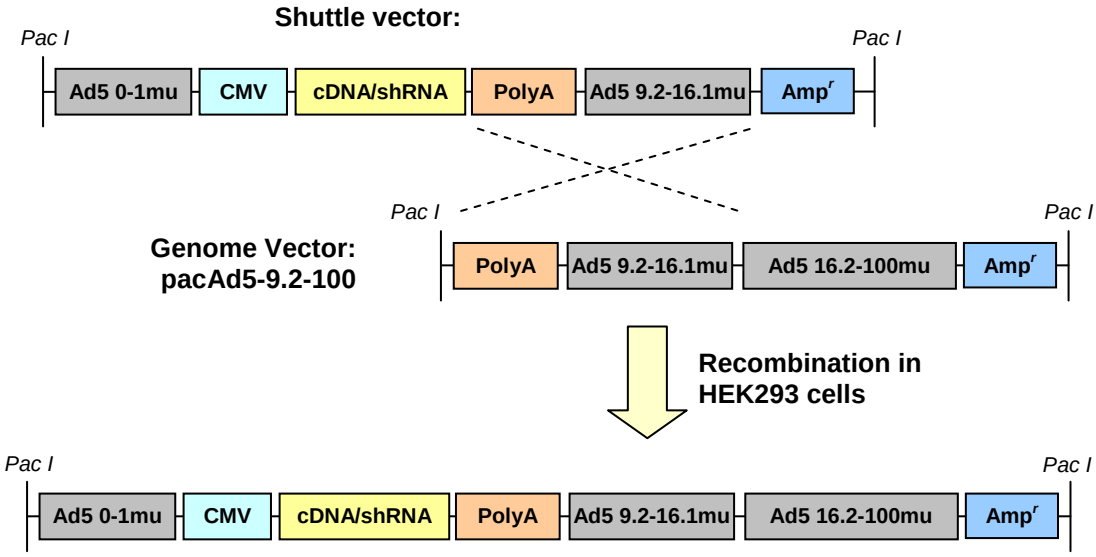

Figure 5.2 - Generation of recombinant adenoviruses by recombination in HEK293 cells
Plasmid shuttle and genome vectors encoded homologous polyA and viral genome sequences; cDNA or shRNA sequences were cloned into the shuttle vectors. Shuttle and genome vectors were linearised by digestion with *PacI* restriction endonuclease. Co-transfection into HEK293 cells followed by homologous recombination resulted in a linear recombinant adenoviral genome and assembly of replication deficient adenoviruses.

5.3.1.1 Anti-*Gstm* family shRNA sequence cloning

shRNA sequences were cloned into the Ambion *pSilencer* adeno 1.0-CMV (abbreviated to p1.0-CMV) shuttle vector, which was supplied double digested at its multiple cloning site between a CMV promoter and minimal polyA sequence with *XhoI* and *SpeI* restriction enzymes. The Gstmf siRNA target sequence (AAGCCAGTGGCTGAATGAGAA) was converted to a double stranded short-hairpin sequence with overhanging ends suitable for cloning into the *XhoI*/*SpeI*-digested shuttle vector using and online sequence design tool on the Ambion website; unmodified oligonucleotides were ordered from MWG biotech. The

oligonucleotides were diluted to 1 μg/μl in 10mM Tris HCl, 0.5mM EDTA, pH 9.0. 2 μl of each was mixed with 46 μl Ambion 1 X DNA annealing solution and heated to 90°C for 3 minutes, followed by 1 hour at 37°C. Annealed oligonucleotides were ligated into p1.0-CMV as per section 2.5.6 using 100 ng p1.0-CMV with an insert:vector molar ratio of 100:1. Positive clones were confirmed by sequencing with pSilencer CMV1.0F and pSilencer CMV1.0R primers. The plasmid, named p1.0-CMV Gstmf shRNA, was amplified and purified as per section 2.5.3. A scrambled shRNA control plasmid, p1.0-CMV Scr shRNA (Ambion) was transformed into JM109 cells as per section 2.5.1 and similarly purified.

5.3.1.2 Cloning *Gstm1* cDNA and Verifying Gstm1 Expression

WKY and SHRSP cDNA sequences were cloned into the shuttle vector pacAd5 CMV K-NpA (abbreviated to pK-NpA); the pK-NpA multiple cloning site resides between a CMV promoter and SV40 polyA sequence. *Gstm1* sequences were amplified from WKY and SHRSP kidney cDNA by PCR using primers annealing in the 5'UTR and 3'UTR. Forward and reverse primers incorporated *HindIII* and *XbaI* restriction sites, respectively, preceded by 3 X 'C' residues, primers were named Gstm1HindIIIF and Gstm4aXbaIR. KOD proofreading polymerase was used as per section 2.2.3 with an annealing temperature of 60°C. PCR product and pK-NpA were double digested with *HindIII* and *XbaI* and digests were electrophoresed and gel purified. Standard ligation and transformation protocols were performed as per section 2.5.6 with an insert:vector molar ratio of 3:1. Colonies were PCR screened with Gstm1HindIIIF and Gstm4aXbaIR primers, successful clones were further confirmed by sequencing. Plasmids, named pK-NpA WKY Gstm1 and pK-NpA SHRSP Gstm1 were amplified and purified .

HeLa cells in 6-well plates were transfected at 70% confluence with 1 μg of pK-NpA WKY Gstm1 or pK-NpA SHRSP Gstm1 in triplicate wells of 6-well plates using a FuGene:DNA ratio of 3:1 and 1 μg DNA per well following the transfection protocol in section 2.3.3. A control well was transfected with pMV10 expressing β-galactosidase. Two days after transfection, HeLa cell protein was collected for Gstm1 western blotting and total GST activity assays (see below).

5.3.1.3 Co-Transfection into HEK293 Cells

HEK293 cells were maintained in Eagle's modified media with 10% FCS; 2mM L-glutamine; 1mM sodium pyruvate; 100U/ml penicillin; 0.1mg/ml streptomycin. HEK293

cells were passaged using citric saline (0.13M KCl; 0.017M sodium citrate in PBS) in place of trypsin. Citric saline was applied to cells for 5 minutes at room temperature, dislodging them from the growth surface, they were then resuspended in PBS and passaged as per the protocol in section 2.3.1.

The same genome vector, pacAd5 9.2-100, was used for all viruses. Genome and shuttle vectors were digested with *PacI* enzyme as per section 2.5.4. Digests were purified by phenol/chloroform purification and ethanol precipitation using the following method: A volume of 25:24:1 phenol:chloroform:iosamyl alcohol saturated with 10mM Tris pH8, 10mM EDTA (Sigma) equal to the volume of the digestion reaction was added. Mixtures were vortexed for 30 seconds and centrifuged at 13000 rpm for 2 minutes. The upper aqueous layer was transferred to a fresh microcentrifuge tube and an equal volume of chloroform was added, vortexed for 30 seconds and centrifuged at 13000 rpm for 2 minutes, the aqueous layer was removed once again. A $1/10^{th}$ volume of 3M sodium acetate pH5.2 and 2 volumes 100% ethanol was added, the mixtures were gently mixed by inverting the tubes and incubated at -70°C for 30 minutes to precipitate the DNA, then centrifuged at 13000 rpm at 4°C for 10 minutes. The supernatant was removed and the pellet was washed with 100 µl 70% ethanol and centrifuged at 13000 rpm at 4°C for 2 minutes. The supernatant was removed and the pellets were air dried for 20 minutes at room temperature before resuspending in H_2O.

Dual transfection of HEK293 cells was carried out in $25cm^2$ flasks with the cells at 70% confluence using a differential pH method. This required the preparation of two specialised media: Media A consisted of DMEM with 1000mg/L glucose and no phenol red, with 10% FCS and 25mM HEPES pH 7.9. Media B consisted of DMEM with 1000mg/L glucose and no phenol red, and 25mM HEPES pH 7.1. Both Media A and Media B were freshly pH'd and filter sterilised before each use. Culture media was removed from the HEK293 cells and cells were washed once with PBS, 1.5ml media A was added to the flask. In a 1.5ml microcentrifuge tube, 320 µl Media B was mixed with 16 µl sterile 1M $CaCl_2$, to which 14 µg of linearised genome vector and 7 µg shuttle vector was added. The Media B/vector mix was added dropwise to the flask and it was incubated overnight. The next morning the media was exchanged for regular culture media.

Triplicate 25 cm^2 flasks were transfected for each virus. Formation of viruses was evidenced by the appearance of 'plaques', or areas of clearing in the HEK293 monolayer. When inspected under the microscope, cells were elongated and 'spider-web' like, over the days following their first appearance, plaques became more evident as 'comet-like' trails of

lysed cells in the monolayer. Upon the first plaques appearing the media was not replaced in the flasks, but 2 ml fresh media was added. 3-4 days after the plaques appeared, all the cells in the flask were detached, media containing cell debris was collected and centrifuged for 5 minutes at 2000rpm. Supernatant was poured off, resuspended in 500 µl PBS, and crude virus stocks were made following the Arklone-P method below. Crude stocks were divided into 50 µl aliquots and stored at -70°C. Recombinant adenoviruses were named:

RAd WKY Gstm1
RAd SP Gstm1
RAd Gstmf shRNA
RAd Scr shRNA

5.3.2 Arklone P virus extraction

Arklone-P (trichlorotrifluoroethane) is an industrial solvent used for virus preparations, it releases virus particles from unlysed cells. After centrifugation, cell pellets were resuspended in PBS, an equal volume of Arklone-P was added and the mixture was shaken following a strict protocol: 20 seconds of vigorous shaking followed by 20 seconds of slow shaking, repeated 3 times. The PBS/Arklone-P mixture was then centrifuged at 8,000 rpm for 15 minutes and the top (aqueous) layer containing the virus particles was carefully pipetted off, separated into 50 µl or 100 µl aliquots and stored at -70°C.

5.3.3 Pure virus stock preparation

Crude virus stocks were used to make 'seed' stocks by infecting a 150 cm^2 flask of 90% confluent HEK293 cells with one 50 µl aliquot of crude stock. 5 ml media containing cell debris was added to the flask the next day. Within 3 days all cells were detached, media was removed, centrifuged at 2000 rpm for 10 minutes and resuspended in 2 ml PBS. The seed stocks were prepared by a second Arklone-P extraction, 100 µl seed stock aliquots were stored at -70°C.

To prepare pure viral stocks, 50 µl of seed stock was added to a fresh 500 ml bottle of HEK293 media, this was exchanged for media on 20 X 150 cm^2 flasks of 90% confluent HEK293 cells. Two days after infection, 10 ml fresh media was added to each flask, within four to five days after infection all the cells were detached. Media containing cell debris was removed from each of the 20 flasks and centrifuged at 2000 rpm for 10 minutes. Cell debris was pooled into 8 ml PBS and viruses were extracted by Arklone-P. This extract was subjected to caesium chloride (CsCl) density-gradient centrifugation to prepare the

final pure stock. 1.45 and 1.32 d g/cm^3 CsCl solutions were prepared in 0.05 M Tris pH7.9. Plastic ultracentrifuge tubes were sterilised by rinsing with 70% ethanol followed by sterile H_2O; 2 ml 1.45 d g/cm^3 CsCl was added to the tubes followed by slow dropwise addition of 3 ml 1.32 d g/cm^3 CsCl, 2 ml 40% glycerol, and then the Arklone-P virus extract. Tubes were topped up with PBS, and centrifuged for 1.5 hours at 25000 X g at 4°C. After centrifugation the virus was present in a discrete white layer between the two CsCl layers, it was removed with 1 ml syringe and hypodermic needle, puncturing the centrifuge tube.

10000 KDa membrane molecular weight dialysis cassettes (Pierce) were pre-soaked in 0.01M TE pH8 for 30 minutes before injecting the virus using a hypodermic needle. Excess air was removed from the cassettes and they were dialysed for 1.5 hrs in 0.01M TE pH8 twice, then overnight in 0.01M TE pH8, 10% glycerol. Virus stocks were separated into 50 µl aliquots and stored at -70°C.

5.3.4 Calculating Virus Titres

Particle and plaque-forming unit titres were determined for all viruses. Particle titres were calculated with a Micro BCA Assay (Pierce). 1 µl, 3 µl and 5 µl of virus preparations were diluted in duplicate wells of a 96-well plate to a total volume of 150 µl with PBS. 150 µl of 0.5 µg/ml – 200 µg/ml albumin standards and PBS 'blanks' were also assayed in duplicate. 150 µl of 'working reagent' (25 parts Solution A, 24 parts Solution B, 1 part Solution C) was added to each well, and plate was incubated at 37°C for two hours protected from light. Absorbance at 560 nm (Abs 560nm) was measured for each standard and sample, duplicates were averaged and blank readings were subtracted. The Abs 560nm values of the standards were inspected to find the value closest to the absorbance value for each sample, this was used in the following formula for each volume of virus preparation assayed (1 µl, 3 µl or 5 µl):

$$\left(\frac{\left(\frac{\text{Conc. of standard (µg/µl)}}{\text{Abs 560nm of standard}} \text{ X Abs 560nm of sample} \right)}{\text{no. of µl of virus prep in sample}} \right) \text{ X } 1000 = \text{Protein conc. of sample (µg/ml)}$$

The 1 µl, 3 µl and 5 µl measurements were averaged to derive the protein concentration of the virus preparation and multiplied by $4x10^9$ to calculate the particle titre of the virus preparation in particles/ml.

Plaque forming unit (pfu) titres were calculated using a published protocol (Nicklin SA 1999). HEK293 cells were seeded on day one to result in 60% confluence the next day in 8 rows of 10 wells in a 96 well plate; remaining wells (columns 1 and 12) were filled with 200 µl PBS to prevent evaporation of media. On day two, media was removed from the cells and replaced with 100 µl per well of dilutions in media of virus preparations from 10^{-4} to 10^{-11}: Media in all wells in row A was replaced with the 10^{-4} dilution, row B with 10^{-5} and so on until row G (10^{-11}), media in row H was replaced with virus-free media. On day three, media was replaced on each well, media was changed every 48 hours on all wells thereafter. On day 9, all wells were inspected for plaques in the monolayer, the number of plaque-positive wells per row was recorded. Two adjacent rows were identified, one with >50% of plaque-positive wells, one with <50% plaque-positive wells. The % of plaque-positive wells per row and dilution factor of the virus dilutions added to these rows was entered into the following formulae to calculate the 'tissue culture infectivity $dose_{50}$' ($TCID_{50}$) for the prep, an index of the dilution required to produce plaques in 50% of wells infected:

$$\text{Proportional distance (PD)} = \frac{\%\text{ positive} > 50\% - 50\%}{\%\text{ positive} > 50\% - \%\text{ positive} < 50\%}$$

$$\text{Log } ID_{50} = \log(\text{dilution} > 50\%) + (\text{PD} \times \text{dilution factor})$$

$$TCID_{50} = 1 / ID_{50}$$

This was the $TCID_{50}$ for the 100 µl of the original dilutions added to the cells, it was multiplied by 10 to derive the $TCID_{50}$ per ml. 1 $TCID_{50}$ is approximately equal to 0.7 pfu, therefore pfu/ml = 0.7 X $TCID_{50}$/ml.

Genome viral titres were also calculated for Gstm1 over-expressing viruses. Serial 1/10-fold dilutions of RAd WKY Gstm1 and RAd SP Gstm1 were made from 10^{-3} to 10^{-6}. A serial 1/10-fold dilution of K-NpA WKY Gstm1 cDNA was made from 5 ng/µl to 0.05 pg/µl to generate a standard curve. Triplicate 20 µl simplex Taqman RT-PCR was performed using the Applied Biosystems Taqman probe for rat *Gstm1* (part no. Rn00755117_m1) as per section 2.7 with 2µl of template per reaction. Ct values of triplicates were averaged, the standard curve was plotted as log (concentration plasmid (ng/µl)) vs. Ct and the equation of the line was derived. Ct values of virus dilutions were used to interpolate the equivalent concentration of template in each, giving a virus genome titre in units of: ng of plasmid DNA.

5.3.5 *In-vitro* Virus Infections

Standard *in-vitro* virus infections followed a similar protocol for all cell types. Cells were infected at 90% confluence. Prior to infection the precise number of cells per well was calculated in a control well by trypsinisation and counting with a haemocytomoter as per section 2.3.2. Appropriate dilutions of virus stocks were made in PBS and added to cell culture. The next day, media was replaced. Three different cell culture strains were used in *in-vitro* experiments: HeLa, NRK52E and RGE (rat glomerular endothelial) cells. Optimisation of infection was performed in 6-well plates using RAd35, a recombinant adenovirus encoding *LacZ* with a CMV promoter at various multiplicities of infection (MOI). 48 hours after infection, cells were stained and fixed for β-galactosidase activity as per section 2.3.4.

NRK52E infection was further optimised using a modified protocol incorporating $CaCl_2$ to enhance viral infection (Fasbender et al. 1998). RAd35 dilutions were made in culture media plus 0.025 M $CaCl_2$. Media was exchanged and 24 hours after infection and 48 hours post infection, cells were fixed and stained for β-galactosidase activity. The $CaCl_2$ protocol was used for all NRK52E infections thereafter.

5.3.6 Gstm1 Western Blotting

Standard western blots were performed for Gstm1 in cell lysates as detailed in section 2.6, The primary polyclonal anti *Gstm1* antibody, named, 'Alexis' was obtained from the laboratory of Professor John Hayes, Dundee University and used at 1/2000 dilution in TBS tween 5% milk. The secondary antibody, DAKO 3099 swine anti-rabbit HRP-conjugated, was also diluted 1/2000 in TBS Tween 5% milk. Following development of Gstm1 bands the blot was stripped as per section 2.6.5 and re-probed with anti β-actin primary antibody (Abcam 8226) at 1/1000 dilution in TBS Tween 5% milk, secondary antibody (DAKO P0260 rabbit anti-mouse HRP-conjugated) was used at 1/2000 dilution.

5.3.7 GST Activity Assays

Sigma total GST Assay Kit was used to measure total GST activity in cultured cell lysates. Assays were performed in 96-well plates. 1 µl or 2 µl of PBS/0.2% Triton lysates were diluted in a total volume of 20 µl sample buffer in duplicate wells. A standard curve was generated by assaying duplicate wells of a serial dilution of GST standard from 5 µg/ml to 0.31 µg/ml. substrate solution was made fresh for each assay, consisting of 19.6 ml PBS,

200 µl 200 mM GSH, 100mM CDNB. Substrate solution was added to all wells to a total volume of 200 µl. Absorbance at 340 nm (Abs 340nm) was measured in each well once a minute for 10 minutes to measure the accumulation of GS-DNB conjugate. Duplicates were averaged. Abs 340nm per minute was plotted for each sample and the linear portion of the curve ($R^2 \geq 0.95$ over at least three points) was used to derive the GST activity. GST concentrations of samples were interpolated from the standard curve and corrected for concentration of protein in the original sample to give GST a reading of µg GST protein/ µg total protein.

5.3.8 Taqman RT-PCR of *Gstm* Isoforms

Taqman RT-PCR was performed on the following Gstm isoforms using Applied Biosystems Taqman Gene Expression Assays: *Gstm1* (part no. Rn00755117_m1) *Gstm2* (Rn00598597_m1) *Gstm3* (Rn00579867_m1), and *Gstm5* (Rn00597012_m1). A Gene Expression Assay was not available for rat *Gstm7*, a custom Applied Biosystems assay was designed by a colleague, Dr Caline Tan, to anneal to unique sequences spanning exons 6 and 7 to ensure gene and cDNA-specific amplification. The expression levels of Gstm isoforms was measured relative to β-actin by multiplex PCR in all samples as per section 2.7, equivalent amplification efficiencies of Gstm and β-actin probes in all sample types were verified. 5 µl reactions were performed in 384-well reaction plates using 2 µl template per reaction.

5.3.9 Sequencing of RNAi Target Sequences

The Gstmf target sequence in *Gstm1*, *Gstm2*, *Gstm3*, *Gstm5* and *Gstm7* was sequenced in DNA extracted from NRK52E cells. DNA was extracted using a Qiagen QIAmp DNA Mini Kit. $5x10^6$ cells were collected by trypsinisation and centrifugation and resuspended in 200 µl PBS. 200 µl buffer AL was added, the mixture was vortexed for 15 seconds and incubated at 56°C for 10 minutes. 200 µl 100% ethanol was added, the mixture was vortexed, applied to a QIAmp spin column and washed through the membrane by centrifugation at 6000 x g for 1 minute. 500µl AW1 buffer was applied to the column and it was centrifuged at 6000 x g for 1 minute. This was repeated with buffer AW2, centrifuging for 3 minutes. The column was dried completely by a further centrifugation at full speed for 1 minute and DNA was eluted in 200 µl H_2O.

Forward and reverse primers binding to unique sequences of exon 3 in *Gstm1, 2,3,5* and *7* were used in standard Roche FastStart PCR reactions as per section 2.2.3 with an annealing

temperature of 60°C (primers were named Gstm1 Ex3F+R, Gstm2 Ex3F+R, Gstm3 Ex3F+R, Gstm5 Ex3F+R, Gstm7 Ex3F+R). PCR clean-up, sequencing reaction, sequencing clean-up and electrophoresis were performed as per section 2.4.

5.3.10 Cytotoxicity Assays

Cytotoxicity of tert-butyl hydrogen peroxide (TBHP) to RGE cells was measured with the Promega CytoTox 96 Non-Radioactive Cytotoxicity Assay kit, which measures lactate dehydrogenase activity released from cells. For assays involving infected cells, RGE cells were infected 48 hours prior to cytotoxicity assays. TBHP was applied 24 hours prior to cytotoxicity assays in all experiments. Media was removed from experimental wells, Triton was added to three control 'max cytotoxicity' wells to a final concentration of 0.1% and they were freeze-thawed to -20°C to lyse cells. Media from experimental and control wells was centrifuged at full speed at 4°C for 5 minutes. 50µl of supernatant was aliquoted into duplicate wells of a clear 96-well assay plate, cell-free media was aliquoted into three control wells. 50µl of substrate mix was added to each well and the plate was incubated at room temperature for 30 minutes, protected from light. 50µl Stop solution was added to wells and absorbance at 490nm (Abs 490nm) was measured. Absorbance levels from triplicates were averaged, background absorbance from cell-free media was subtracted from all other wells. Abs 490nm of experimental wells were expressed as a percentage of the Abs 490nm of the max cytotoxicity wells.

5.3.11 Local Delivery of RAd WKY Gstm1 to SHRSP Carotid Arteries

5.3.11.1 Surgical Procedure and Viral Delivery

Surgical procedures were performed by Elizabeth Beattie. Rats were anaesthetised with halothane and the skin covering the left side of the neck was incised. The left common carotid artery was exposed by blunt dissection at the base of the neck and surgical thread was looped under the artery. The upper section of the common carotid was then exposed at the level of the bifurcation into the internal and external carotid. An artery clip was applied to the internal carotid and the external carotid was tied off approximately 0.5 cm anterior to the bifurcation. A hole was punctured in the external carotid posterior to the tie using a hypodermic needle. A teased 0.28 mm bore catheter connected to a 0.5 ml syringe containing virus dilution in PBS was introduced to the hole and the end of the catheter was

inserted as far as the bifurcation. The section of the external carotid containing the catheter was tied to prevent backflow and $2.4x10^8$ or $6x10^8$ pfu of virus in 30 µl PBS was injected into the vessel. Immediately after the injection, the lower loop of surgical thread below the common carotid was lifted to close off the artery and an artery clip was applied. The section of the common carotid containing the virus was kept isolated for twenty minutes, after which the catheter was removed and both ties on the external carotid secured, artery clips were removed and the rat was sutured. Rats were administered 0.05 ml veturgesic after surgery. Twenty-four or 48 hours after surgery, rats were euthanized under anaesthetic, left and right carotid arteries were removed and placed in physiological saline, RNA-later or β-galactosidase activity assay fixative. In the finalised experimental protocol $6x10^8$ pfu virus was infused and animals were sacrificed 48 hours later.

5.3.11.2 Carotid Artery Wire Myography

Wire myography protocols were performed by Angela Spiers according to published protocols (Spiers et al. 2005). Excised carotid arteries were placed in physiological saline solution (PSS) (118.4 mM NaCl, 4.7 mM KCl, 1.2 mM $MgSO_4H_2O$, 24.9 mM $NaHCO_3$, 2.5 mM $CaCl_2$, 11.1 mM glucose, 0.023 mM EDTA) and dissected into 2 mm rings under a dissection microscope. Two rings were cut per vessel. Rings were mounted on two 40 µm stainless steel wires on the stage of a four channel small vessel myograph (Danish MyoTechnologies 610M), one wire was attached to a force transducer and the other to a micrometer. Vessels were maintained at 37°C in PSS, pH7.4, gassed with 95% O_2, 5% CO_2 for the duration of experiments. After mounting, vessels were equilibrated under 1 g tension for 30 minutes, then a 'wake-up' protocol was followed to ensure contractility: Vessel rings were maximally contracted twice by depolarisation with 125 mM potassium physiological saline solution (KPSS), washing with PSS and relaxing to baseline after contractions. To check endothelial integrity, rings were contracted with $1x10^{-5}$M PE then relaxed with $3x10^{-6}$M carbechol, rings that did not respond to these protocols were discarded from the study. Vessel rings were re-equilibrated for 30 minutes before recording a cumulative concentration response curve to phenylephrine (PE) from $1x10^{-9}$M to $3x10^{-5}$M. 10^{-4}M N-Nitro-L-Arginine Methyl Ester (L-NAME) was applied to the vessel rings for 40 minutes and a second contractile response curve to $1x10^{-9}$M – $3x10^{-5}$M PE was recorded. Contraction to PE in the presence of L-NAME was expressed as a percentage of the maximal contraction in the first PE response curve as a measure of NO bioavailability in infused and contra-lateral uninfused vessels.

5.3.11.3 RNA Extraction from Carotid Arteries and cDNA Sequencing

RAd WKY Gstm1-infused and uninfused carotid arteries were dissected from freshly euthanized SHRSP rats and placed directly into RNA-Later stabilisation solution (Ambion). Carotids were also obtained from 2c* and WKY rats. Vessels were dissected under RNA-Later using a dissection microscope, removing nervous and connective tissue. RNA extraction was performed using a modified protocol for Qiagen RNEasy Mini columns for fibrous tissue. Vessels were homogenised with a 13 mm ball bearing in 400 µl RLT buffer (10 µl/ml β-mercaptoethanol) using a Qiagen Tissuelyser set at 25 Hz for 4 minutes. The homogenate was diluted with 786 µl H_2O, 13 µl proteinase K (600 mU/ml) was added and tubes were incubated at 55°C for 10 minutes. Lysates were centrifuged for 3 minutes at 10000 x g, supernatant was removed to a fresh tube, 0.5 volume of 100% ethanol was added and mixed by pipetting. Samples were applied to RNeasy Mini columns and centrifuged for 15s at 8000 x g. 350 µl RW1 buffer was applied and columns were centrifuged for 15s at 8000 x g. 10 µl Qiagen DNAse I (3 U/µl) was diluted in 70µl RDD buffer and applied to each column for 15 minutes at room temperature. Columns were washed with 350 µl RW1, followed by two washes with 500 µl RPE buffer, centrifuging for 15s at 8000 x g after each addition, then dried by centrifugation for 1 minute at full speed. DNase-free RNA was eluted in 40 µl RNase-free H_2O. cDNA was generated using Applied Biosystems TaqMan Reverse Transcription Reagents as per section 2.7.1, the lowest RNA concentration among the samples dictated 210.2 ng RNA template per reverse transcription.

Carotid artery cDNAs were PCRd using Roche FastStart taq with an annealing temperature of 61°C using Gstm1HindIII and Gstm4aXbaI primers as per section 2.2.3. PCR products were electrophoresed (2% agarose) and gel purified as per section 2.5.5, eluting in 40 µl H_2O. 10 µl of gel purified PCR product of the expected size (759 bp) was amplified in sequencing reactions as per section 2.4.2 and standard sequencing clean-up and electrophoresis protocols were performed as per sections 2.4.3-4.

5.3.11.4 Carotid Artery Gstm1 Immunohistochemistry

RAd WKY Gstm1-infused and uninfused carotid arteries were dissected in PSS under a dissection microscope to remove blood, connective and nervous tissue. Tissues were fixed in 10% formalin for 1 hour and stored in PBS. Fixed samples were embedded into paraffin

blocks by Andrew Carswell. 6 μm sections were cut onto silanised microscope using a Shandon Finesse 3 microtome and baked overnight at 60°C. Immunohistochemistry was performed by Andrew Carswell. Tissue sections were de-paraffinised and hydrated by washing twice in Histoclear for 7 minutes, 100% ethanol for 7 minutes, 70% ethanol for 7 minutes, and H_2O for 7 minutes. Endogenous peroxidase activity was quenched by incubation in 0.3% H_2O_2 in methanol for 30 minutes, followed by two washes in H_2O for 10 minutes. Sections were blocked with 0.01% horse serum for 1 hour. 'Alexis' rabbit anti-Gstm1 antibody was applied at a 1/6000 dilution in blocking solution; negative control sections were treated with rabbit serum at the same total protein concentration as the positive slides. Slides were left in humidified trays at room temperature overnight then washed three times in PBS for five minutes. Vectastain Elite ABC Universal kit was used for secondary antibody application; horse anti-rabbit secondary antibody was diluted in blocking reagent and applied to the slides for 30 minutes, slides were washed three times in PBS for five minutes. Vectastain ABC reagent was prepared and pre-incubated for 30 minutes, then applied to the slides for 30 minutes, slides were washed three times in PBS. Vector Lab DAB (3,3'-diaminobenzidine) substrate kit was used for colour development; DAB substrate reagent was added, incubated for 5 minutes and washed in H_2O for five minutes. Nuclei were counterstained with Harris's modified haematoxylin for 2 minutes, then rinsed in running water for 5 minutes. Finally, sections were dehydrated by 10 minute washes in 70% ethanol, 95% ethanol, 100% ethanol and two washes in Histoclear. Cover slips were applied with Histomount.

5.4 Results

5.4.1 Recombinant Virus Construction and Titring

The Gstmf shRNA oligonucleotides were annealed and cloned into the *pSilencer* adeno 1.0-CMV backbone. Co-transfection of *PacI*-linearised 1.0-CMV Gstmf shRNA or 1.0-CMV Scrambled shRNA with *PacI*-linearised pacAd5 9.2-100 into HEK293 cells resulted in the generation of recombinant adenoviruses, confirmed by sequencing.

PCR primers Gstm1F and Gstm4R that anneal within the Gstm1 5'UTR and 3'UTR, respectively, and had already been applied for Gstm1 cDNA sequencing (See section 4.3.2) were to be used for cloning, however, while planning the cDNA PCR procedure it was noticed that there is an ambiguous base in the 3'UTR (position +35) between different *Gstm1* reference sequences: NM_017014 and X04229 sequences code for a 'G' at this residue, while Ensembl reference sequence ENSRNOT00000041192 denotes an 'A'. This residue lies within 3 bases of the 5' end of the primer binding site for primer Gstm4R, therefore the primer was redesigned to anneal 4 bases upstream, avoiding the ambiguous base, the new primer (synthesised to also encode a *HindIII* restriction site) was designated Gstm4aXbaIR. Cloning of digested PCR products from amplification of *Gstm1* cDNAs in WKY and SHRSP kidney cDNA into the K-NpA backbone was confirmed by PCR (figure 5.3). Sequencing confirmed correct insertion of the WKY and SHRSP cDNA sequences into K-NpA and the presence of the known coding variant at base 605 (WKY = A; SHRSP = G), it also identified the previously noted 3'UTR SNP at base +29, and the sequence at base +35 also differed between the two strains: WKY = A, SHRSP = G. Particle and pfu titres were ascertained for all recombinant viruses, genome titres were also ascertained for RAd WKY Gstm1 and RAd SP Gstm1 (table 5.1).

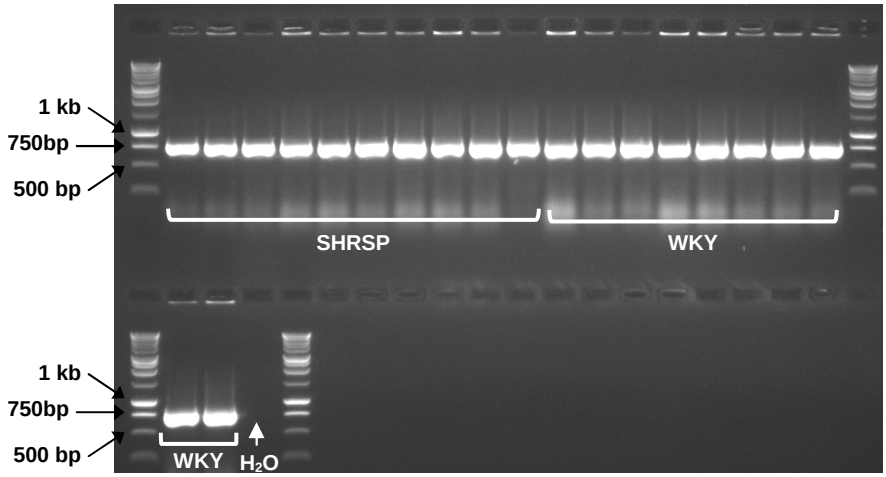

Figure 5.3 - PCR screen following *Gstm1* cDNA cloning
SHRSP and WKY *Gstm1* cDNA sequences were ligated into pK-NpA, colonies were screened with Gstm1HindIIIF and Gstm4aXbaIR primers. All clones screened were positive. Expected product size = 759 bp.

Virus	Particle titre (particles/ml)	pfu titre (pfu/ml)	Genome titre (ng plasmid DNA)
RAd WKY Gstm1	$3.25x10^{11}$	$6.90x10^{12}$	0.082
RAd SP Gstm1	$2.21x10^{11}$	$5.22x10^{12}$	0.063
RAd Gstmf shRNA	$2.21x10^{11}$	$3.29x10^{12}$	ND
RAd Scr shRNA	$4.417x10^{11}$	$4.30x10^{12}$	ND

Table 5.1 - Recombinant adenovirus particle, pfu and genome titres
ND: not determined

5.4.2 K-NpA Gstm1 Plasmid Transfections in HeLa cells

HeLa cells were transfected with pK-NpA WKY Gstm1 cDNA and pK-NpA SHRSP Gstm1 cDNA to confirm *Gstm1* expression from the shuttle vectors prior to adenovirus construction. Control transfection with pMV10 verified transfection of HeLa cells (figure 5.4 A). Gstm1 protein levels were equivalent in HeLa cells transfected with pK-NpA WKY Gstm1 cDNA and pK-NpA SHRSP Gstm1, measured by densitometry relative to β-actin protein (figure 5.4 B and C). There was no significant difference between total GST activities in the same cell lysates (figure 5.4 D).

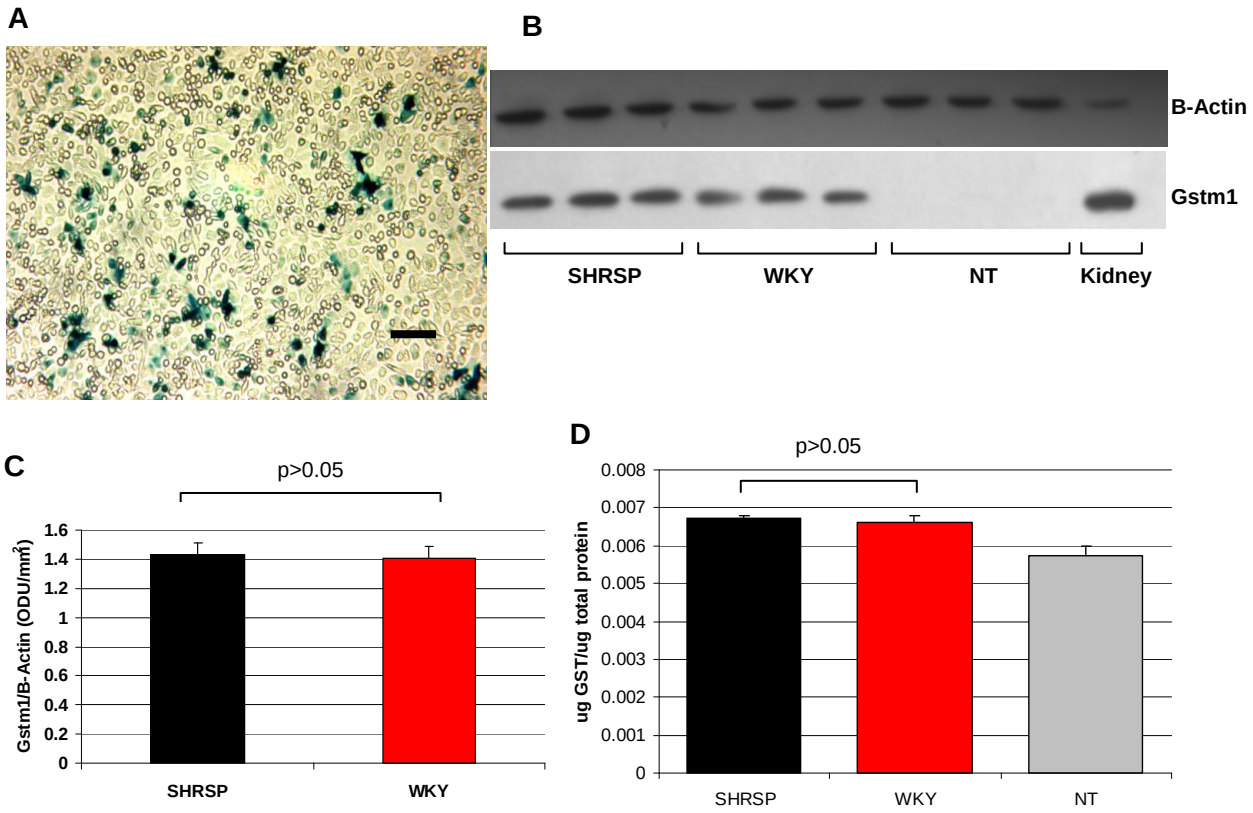

Figure 5.4 - Transfection of K-NpA Gstm1 cDNA plasmids into HeLa cells
(A) Control well transfected with pMV10 expressing β-galactosidase demonstrated efficient transfection of HeLa cells. **(B)** Western blotting confirmed expression of Gstm1 protein (26 KDa) in transfected wells. β-actin expression (42 KDa) was verified in all wells. 20 µg protein loaded in all wells except kidney control, 30 µg loaded. **(C)** Gstm1 densitometry, corrected for β-actin, showed equivalent levels of Gstm1 expression from each plasmid. Mean ± SE **(D)** Total GST activity measurements were not significantly different between cells transfected with K-NpA WKY and SHRSP Gstm1 cDNA plasmids. Mean ± SE. Scale bar = 100 µm. NT = non-transfected (2 sample t test).

5.4.3 Optimising *In-vitro* Viral Infections

In experiments to optimise viral infection protocols, low transduction levels were observed in NRK52E cells following infection with RAd35 from 10-300 pfu/cell and infection with MOIs above 300 was toxic to the cells. The $CaCl_2$-enhanced infection method (25-100 pfu/cell) was not toxic, increasing transduction was observed with increasing MOI, 100 pfu/cell resulted in the highest level of viral transduction (figure 5.5A). 48 hours following infection of HeLa cells with RAd35 from 10-100 pfu/cell, increasing transduction levels were observed with increasing MOI (figure 5.5B). Very efficient transgene expression was observed in RGE cells at low MOIs (figure 5.5**C**).

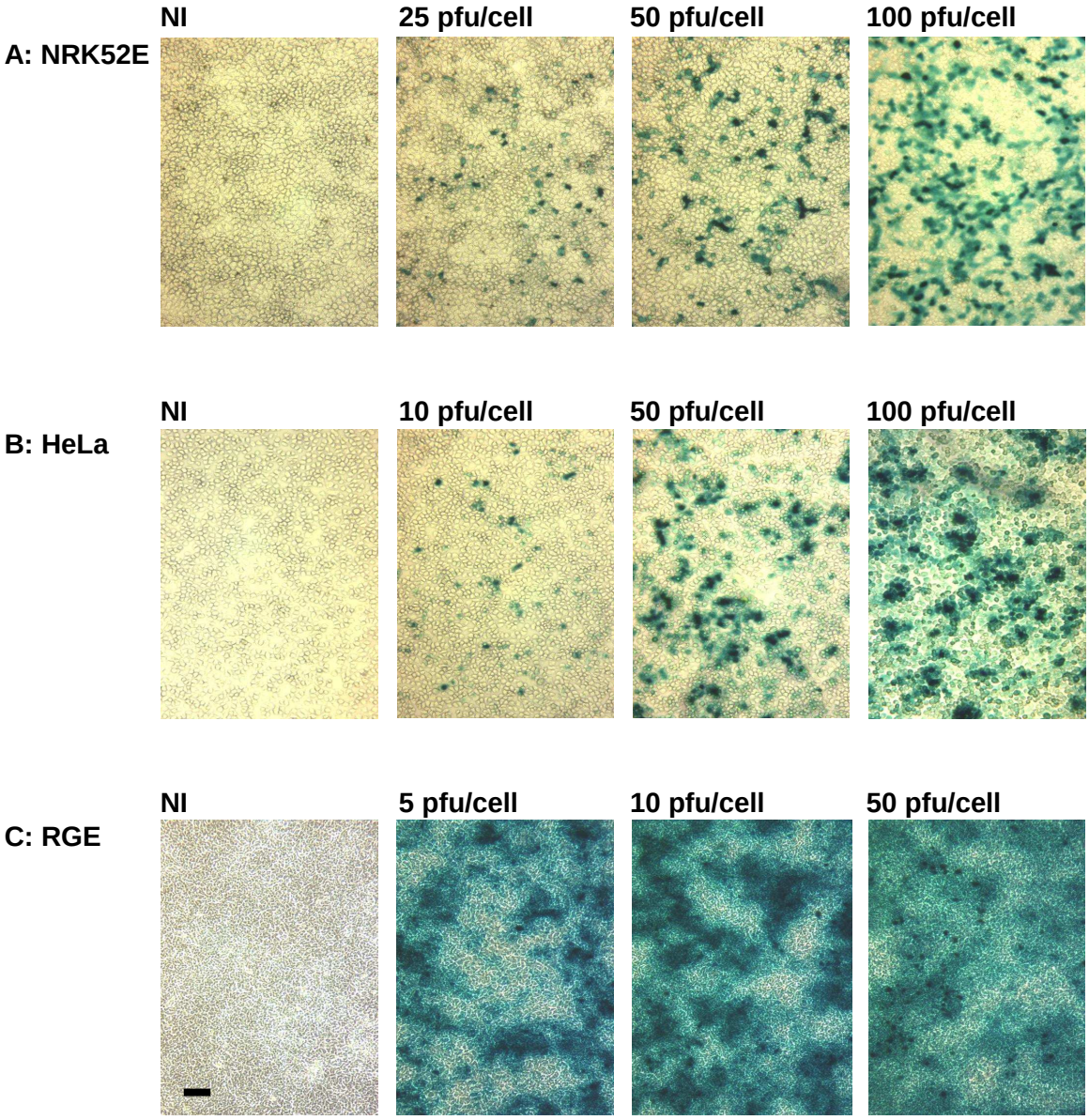

Figure 5.5 - Optimisation of *in-vitro* virus infections with RAd35
β-galactosidase staining 48 hours post infection at indicated MOIs. **(A)** NRK52E infections with modified $CaCl_2$ protocol. **(B)** HeLa infections. **(C)** RGE infections. Scale bar = 100 μm. NI: non-infected.

5.4.4 Gstm Knockdown by RAd Gstmf shRNA in NRK52E Cells

NRK52E cells were infected at 25, 50 and 100 pfu/cell with RAd Gstmf shRNA and control viruses. qRT-PCR for Gstm isoforms was performed to measure knockdown of *Gstm1,2,3,5* and *7*. Expression of *Gstm3* was significantly reduced compared to all controls at 50 and 100 pfu/cell, while *Gstm1* and *2* expression were reduced compared to all controls at 100 pfu/cell. Expression of *Gstm5* and *Gstm7* was not significantly reduced (figure 5.6).

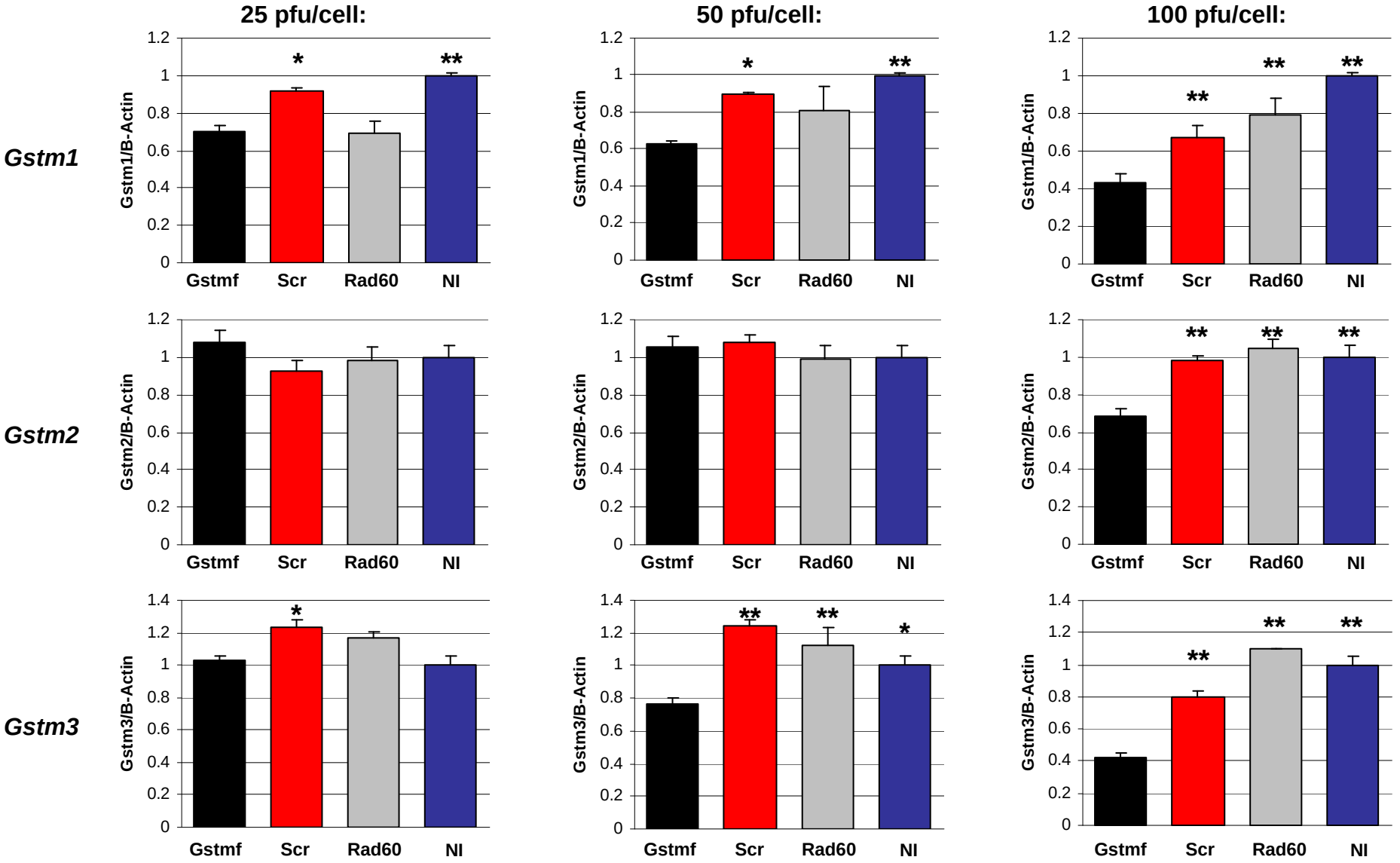

Figure 5.6 – Continued overleaf

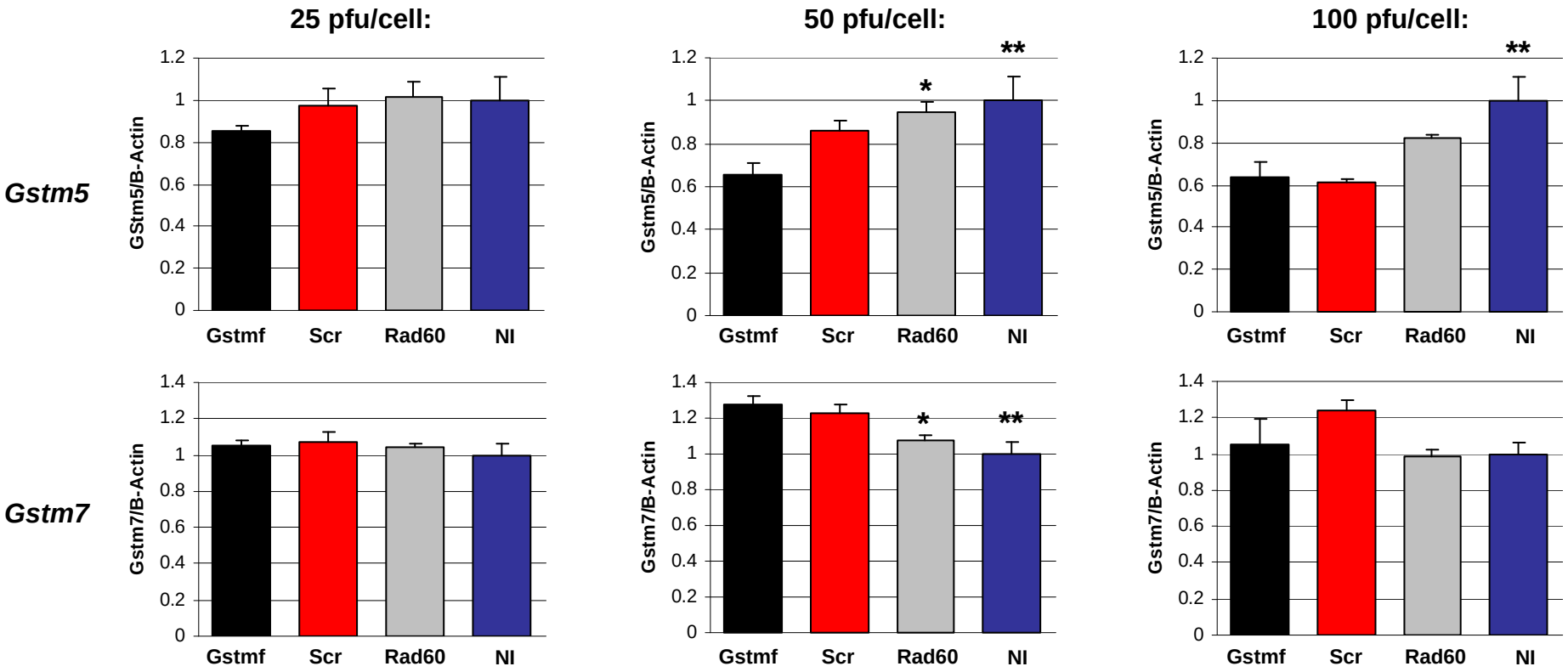

Figure 5.6 - Anti-Gstm family shRNA-mediated mRNA knockdown of *Gstm* isoforms

NRK52E cells were infected in triplicate wells at 25, 50 and 100 pfu/cell with RAd Gstmf shRNA, RAd Scr shRNA and RAd60 using a modified $CaCl_2$ protocol. RNA was extracted 48-hours post infection for gene expression measurements of *Gstm1*, *Gstm2*, *Gstm3*, *Gstm5* and *Gstm7* by Taqman RT-PCR. Gene expression is expressed relative to β-actin in each case and normalised to non-infected wells (NI). n=3, mean ± SE * $p<0.05$ vs. Gstmf, ** $p<0.01$ vs. Gstmf (ANOVA and Dunnett's post-test).

RAd Gstmf shRNA was infected into NRK52E cells at an MOI of 100 pfu/cell and western blotting confirmed Gstm1 knockdown compared to RAd Scr shRNA and NI controls (figure 5.7 A and B). GST activities were assayed on the same lysates, reduction in *Gstm* expression mediated by Gstmf did not reduce total GST activity (figure 5.7 C).

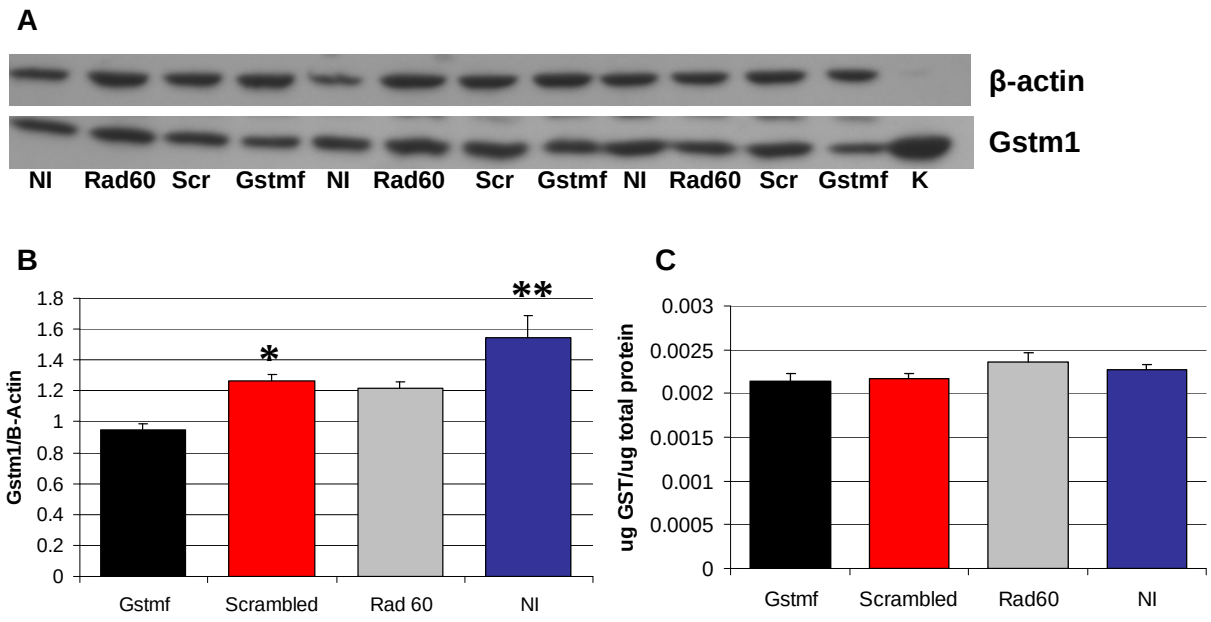

Figure 5.7 - Anti-Gstm family shRNA-mediated knockdown of Gstm1 protein
NRK52E cells were infected in triplicate wells at 100 pfu/cell with RAd Gstmf shRNA, RAd Scr shRNA and RAd60 using a modified $CaCl_2$ protocol. Protein was extracted 48-hours post infection for Gstm1 Western blotting and total GST activity assays **(A)** Immunoreactive Gstm1 protein (26 kDa) and β-actin (42 kDa) was observed in all wells. 40 µg NRK protein per lane, 30 µg kidney protein. **(B)** Densitometry measuring Gstm1 protein relative to β-actin in infected cells showed reduced Gstm1 protein in RAd Gstmf shRNA-infected cells relative to RAd Scr shRNA infected and non-infected cells (NI). F = 10.2 * $p<0.05$ vs. Gstmf, ** $p<0.01$ vs. Gstmf (ANOVA and Dunnett's post-test). **(C)** No differences in total GST activity in cells lysates was measured.

5.4.5 Gstmf Target Site Sequencing in *Gstm1,2,3,5* and *7*

Given the variable capacity for RAd Gstmf shRNA to mediate knockdown of *Gstm* genes at the mRNA level in NRK52E cells (figure 5.6), the target sites for Gstmf in *Gstm1,2,3,5* and *7* were sequenced from NRK52E genomic DNA. During this process it was observed that the published reference sequences for these genes have changed since Gstmf was originally designed (in 2004), Gstmf does not align 100% with all of the sequences. Exon 3 sequences surrounding the Gstmf target were sequenced in each gene and aligned with Gstmf, homology between the genes and Gstmf is shaded:

```
Gstmf:        AAGCCAGTGGCTGAATGAGAA
Gstm1: TGACAGAAGCCAGTGGCTGAATGAGAAGTTCAA
Gstm2: TGACAGAAGCCAGTGGCTGAGTGAGAAGTTCAA
Gstm3: TGACAGAAGCCAGTGGCTGAATGAGAAGTTCAA
Gstm5: TGATAGAAGCCAATGGCTGGACGTGAAATTCAA
Gstm7: TGACAGAAGCCAGTGGCTGAGTGAGAAGTTCAA
```

The sequences above agree with the current consensus sequences for the *Gstm*s from Ensembl. The homology of Gstmf with *Gstm1* and *Gstm3* is 100%, while there are mismatches between Gstmf and *Gstm2,5* and *7* sequences.

5.4.6 Gstm1 Expression from Crude Viral Stocks

Serial dilutions of crude stocks of RAd WKY Gstm1 and RAd SP Gstm1 were used to infect HeLa cells. No viral plaques were seen in any wells confirming the absence of wild-type virus was present in the preparations. 8 days following infection, cells were recovered and Gstm1 protein levels were assessed by western blot. Increasing dose of virus resulted in increasing Gstm1 staining in cell lysates, confirming viral transgene expression (figure 5.8).

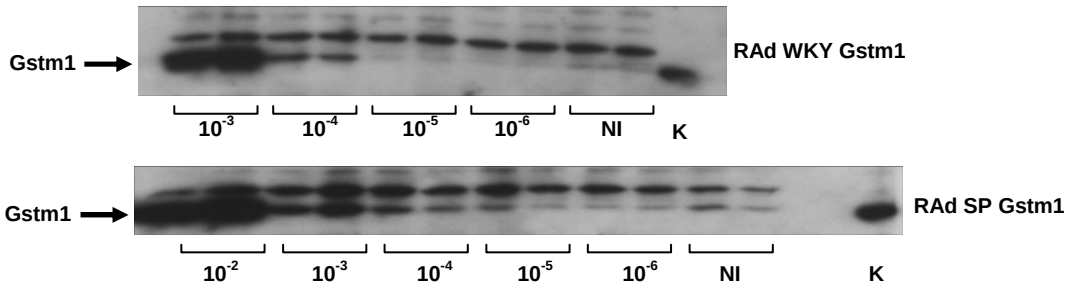

Figure 5.8 - Verification of Gstm1 overexpression viruses
Crude stocks of RAd WKY Gstm1 and RAd SHRSP Gstm1 were serially diluted from 10^{-3} to 10^{-6} and 10^{-2} to 10^{-6}, respectively and used to infect HeLa cells in duplicate wells. Gstm1 western blotting was performed directly on cell debris with 10 µg rat kidney control protein. Gstm1 protein (26 kDa) was present at highest concentrations after infection with lowest dilutions of crude extracts. NI: non-infected, K: kidney.

5.4.7 Comparing WKY and SHRSP Gstm1 Overexpression Viruses

RAd WKY Gstm1 and RAd SP Gstm1 were infected into HeLa cells at MOIs of 10, 50 and 100 pfu/cell in experiments designed to compare the transcriptional and catalytic activities of the WKY and SHRSP Gstm1 sequences, control wells were infected with RAd60 or were uninfected. After 48 hours cells were lysed and a western blotting was performed to compare Gstm1 expression; rat Gstm1 immunoreactivity was observed in cells infected with Gstm1 overexpression viruses at all MOIs but not RAd60 or non-infected cells (figure 5.9 A). Densitometry showed higher Gstm1 expression level in cells infected with RAd SP Gstm1 compared to RAd WKY Gstm1 at 10, 50 and 100pfu/cell (figure 5.9 B). GST activity assays on cell lysates showed increased total GST activity in cell lysates infected with RAd SP Gstm1 compared to RAd WKY Gstm1 at each MOI, no increase in GST activity was seen in RAd60-infected cells compared to non-infected cells (figure 5.9 C).

5.4.8 miRNA Alignments in the WKY and SHRSP Gstm1 3'UTR

The Wellcome Trust Sanger Institute in Cambridge, UK, maintains an online database of verified functional miRNAs, called miRBase (http://microrna.sanger.ac.uk); release 10.0 (August 2007) was interrogated to find miRNAs that bind to the SNPs between the 3'UTR of WKY and SHRSP *Gstm1*. One miRNA was identified, rno-miR-10b, that aligns at its extreme 3' end with the SNP at base +35, base-paring is indicated by a vertical line:

```
rno-miR-10b:        3' UGUGUUUAAGCCAAGAUGUCCC 5'
                        |  || ||| | | || ||||
WKY:          5' GGACCTATCCACATTGGATCCTGCAGGCCACCCT 3'
SHRSP:        5' GGACCTGTCCACATTGGATCCTGCAGGCCACCCT 3'
```

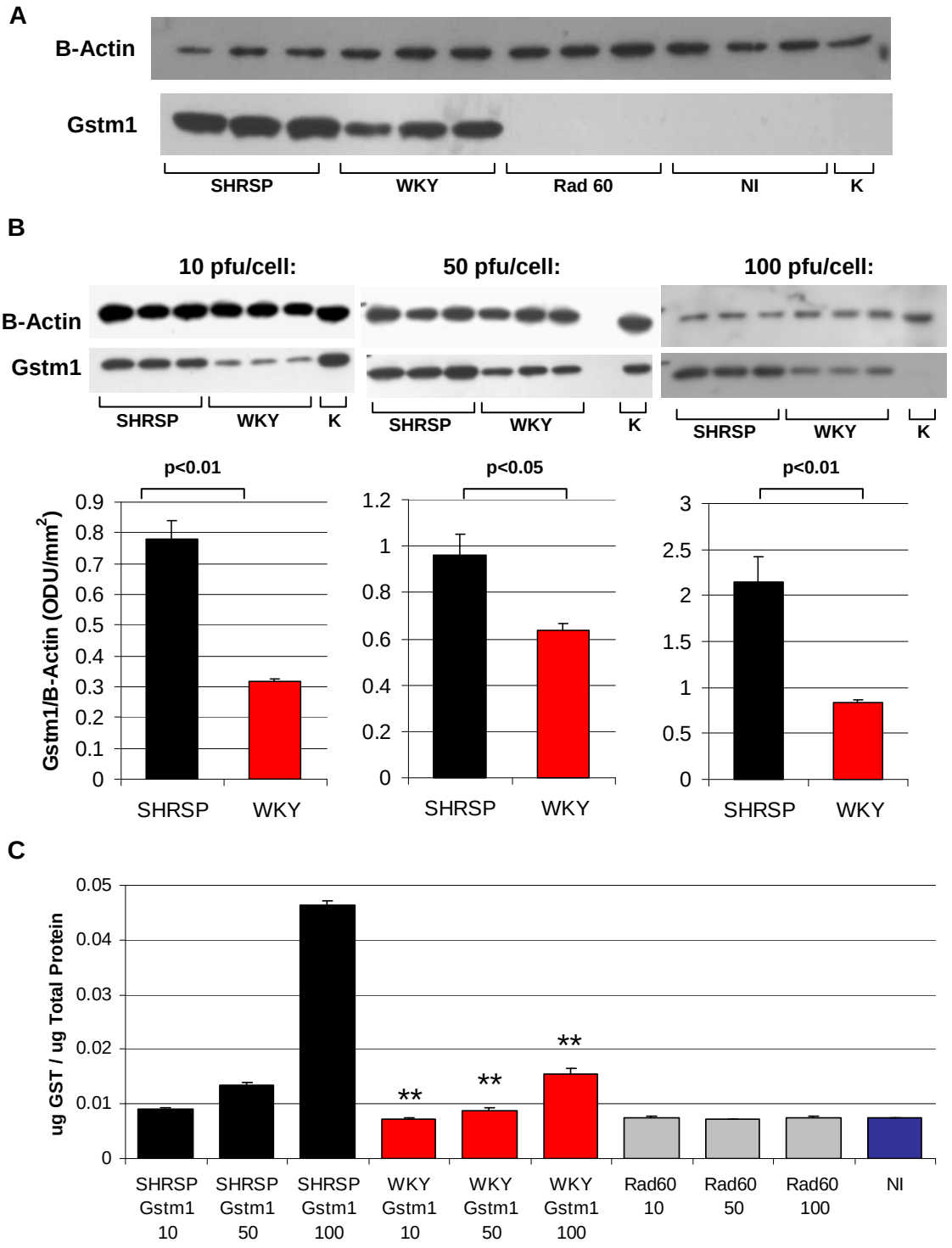

Figure 5.9 - Adenovirus-mediated WKY and SHRSP Gstm1 expression in HeLa cells
HeLa cells were infected with RAd WKY Gstm1, RAd SP Gstm1 and RAd60 at 10, 50 and 100 pfu/cell in triplicate wells. 48 hours post infection, protein was harvested. **(A)** Gstm1 expression (26kDa) in cells infected at 100 pfu/cell, no Gstm1 expression in RAd60-infected or non-infected (NI) cells. β-actin (42kDa) immunoreactivity in all wells. **(B)** Western blotting and densitometry relative to β-actin showing higher Gstm1 expression from RAd SP Gstm1 than RAd WKY Gstm1 at all titres. **(C)** Total GST activity was higher in cells infected with RAd SP GStm1 than RAd WKY Gstm1. 10 μg NRK52E protein per lane, 30 μg kidney (K) protein. ** p<0.01 vs. SHRSP at equivalent pfu (2 sample t test).

5.4.9 Gstm1 expression in RGE Cells and Cytotoxicity Assays

Experiments performed in 96-well plates showed increasing cytotoxicity of 0-0.1mM TBHP to RGE cells (figure 5.10 A). Concentrations of 0.07 mM, 0.08 mM and 0.09 mM TBHP were used in an experiment to assess the protective effects of *Gstm1* expression from TBHP cytotoxicity in RGE cells. Infection of RGE cells with RAd WKY Gstm1 at 10 pfu/cell resulted in *Gstm1* expression (figure 5.10 B) but did not protect against cytotoxicity mediated by TBHP (figure 5.10 C).

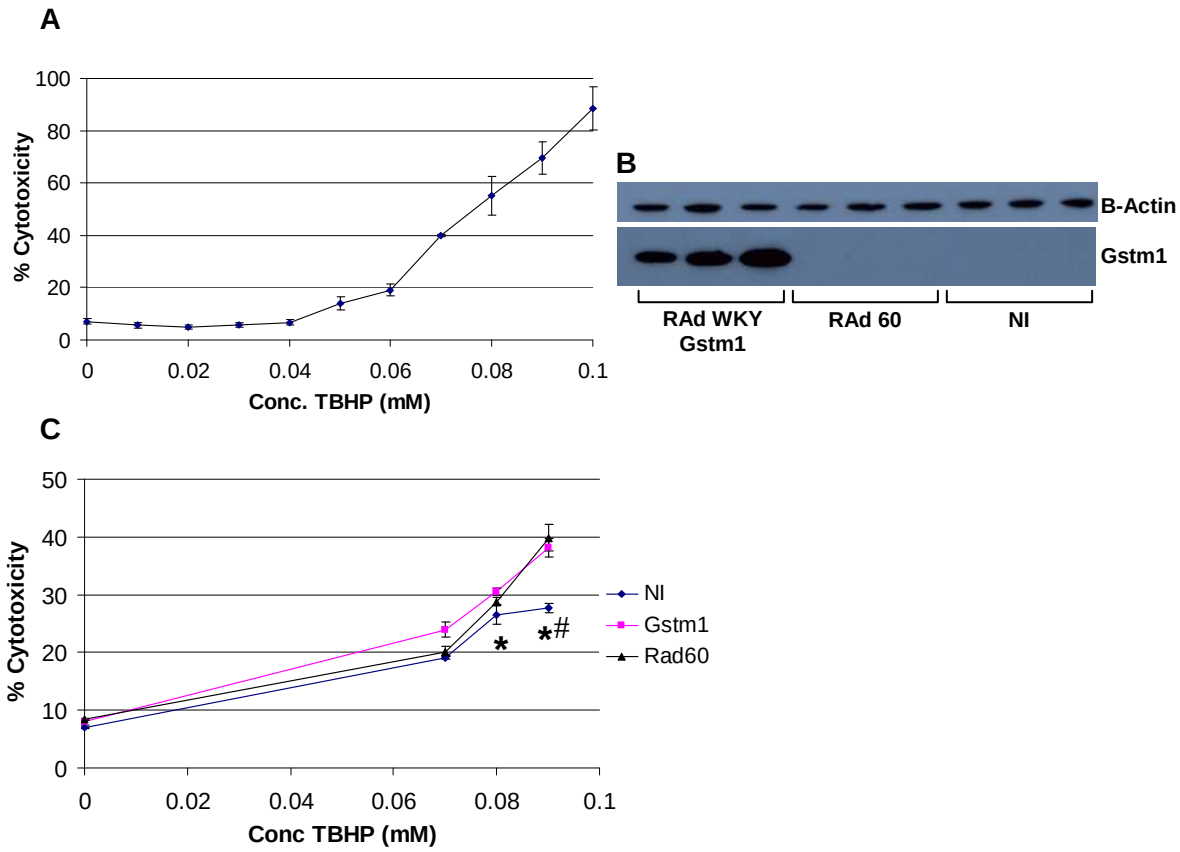

Figure 5.10 - Cytotoxicity assays in RGE cells treated with TBHP

(A) Treatment of RGE cells with 0-0.1mM TBHP in 96-well paltes mediated increasing cytotoxicity after 24 hours. **(B)** Gstm1 Western blot in RGE cells 48 hours post-infection with 10 pfu/cell RAd WKY Gstm1 and RAd60. Gstm1 protein observes at 26 kDa, β-actin at 42 kDa. **(C)** RGE cells were infected with RAd WKY Gstm1 or RAd60 24 hours prior to treatment with 0.07, 0.08 and 0.09 mM TBHP in 6-well plates. Overexpression of Gstm1 did not protect cells against TBHP cytotoxicty. NI: non-infected, n=3, mean ± SE * $p<0.05$ NI vs. Gstm1, # $p<0.01$ NI vs. Rad60 (ANOVA and Tukey post-test).

5.4.10 Local Delivery of RAd WKY Gstm1 to SHRSP Carotid Arteries

5.4.10.1 Optimising Viral Dose and Expression Time

SHRSP carotids were infused with $2.4x10^8$ or $6x10^8$ pfu of RAd WKY Gstm1 and sacrificed after 24 or 48 hours. Left and right carotid arteries were fixed and stained for β-galactosidase activity. Only vessels infused with $6x10^8$ virus for 48 hours showed significant levels of β-galactosidase staining, β-galactosidase activity was evident in the endothelium and interstitial tissue (figure 5.11); consequently this protocol was used for experimental infusions with RAd WKY Gstm1.

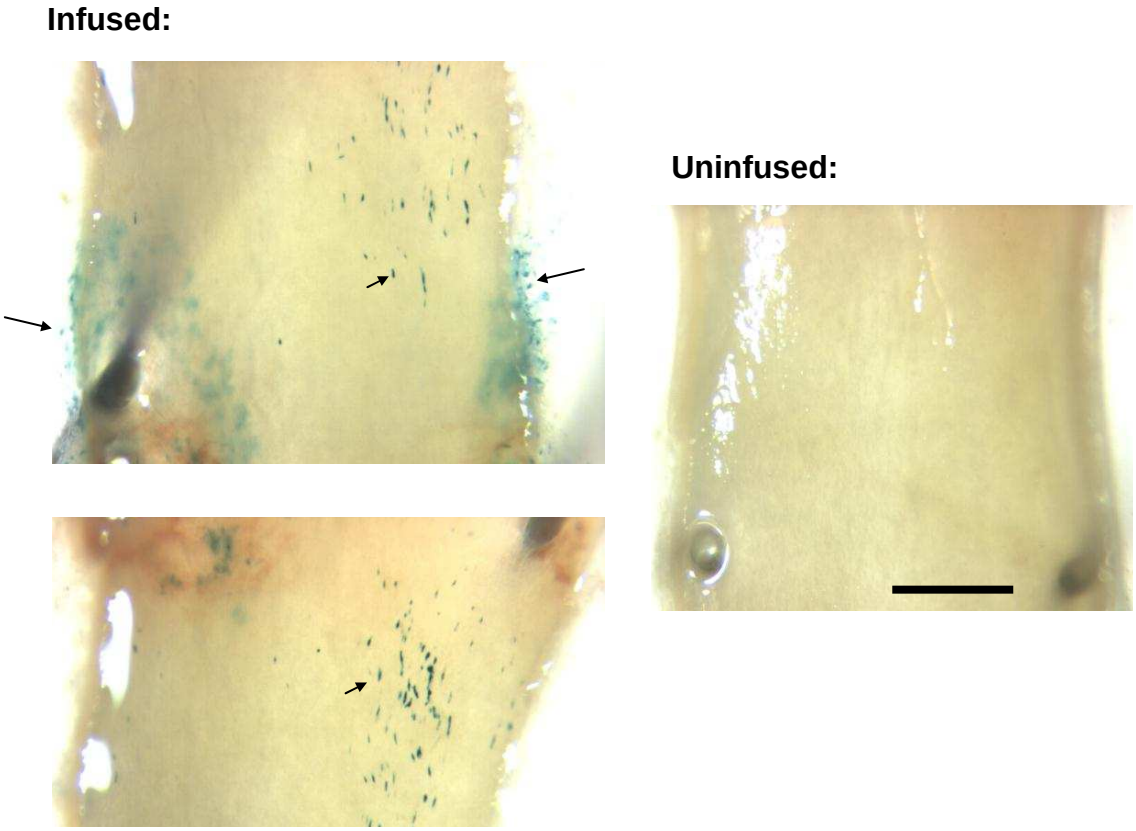

Figure 5.11 - β-galactosidase expression in RAd35-infected SHRSP carotid arteries
48 hours after infection with $6x10^8$ pfu of RAd35, carotids were fixed and stained for b-galctosidase activity. Transgene expression was observed in endothelial (short arrows) and adventitial (long arrows) tissue layers. Scale bar = 100 μm.

5.4.10.2 Gstm1 Expression in Carotid Arteries

Expression of *Gstm1* mRNA was significantly lower, by approximately 2-fold, in the carotid arteries of SHRSP rats compared to 2c* and WKY (figure 5.12A). Infusion of RAd WKY Gstm1 into SHRSP carotid arteries increased *Gstm1* expression by 1.1-3.6 fold compared to contra-lateral controls (figure 5.12B). PCR of *Gstm1* cDNA from infused and uninfused SHRSP carotid arteries produced two PCR products, of approximately 690 bp and 640 bp, in addition to the expected 759 bp product (figure 5.12C), indicating either amplification of non-specific templates or the expression of alternatively spliced *Gstm1* isoforms in the rat carotid artery. Sequencing of the 759 bp product revealed clear heterozygosity at the polymorphic bases between the WKY and SHRSP *Gstm1* cDNA sequences (figure 5.12D), indicating expression of WKY *Gstm1* sequence in infused vessels. Immunohistochemistry for Gstm1 protein demonstrated Gstm1 expression in infused and uninfused vessels, Gstm1 protein levels were higher in infused vessels in endothelial, smooth muscle and adventitial layers (figure 5.13).

5.4.10.3 Wire Myography to Assess NO Bioavailability

Wire myography was performed on vessel rings from infused and uninfused carotid arteries to assess changes in NO bioavailability following overexpression of Gstm1. There was no increase in NO bioavailability in infused vessels compared to uninfused vessels (figure 5.14).

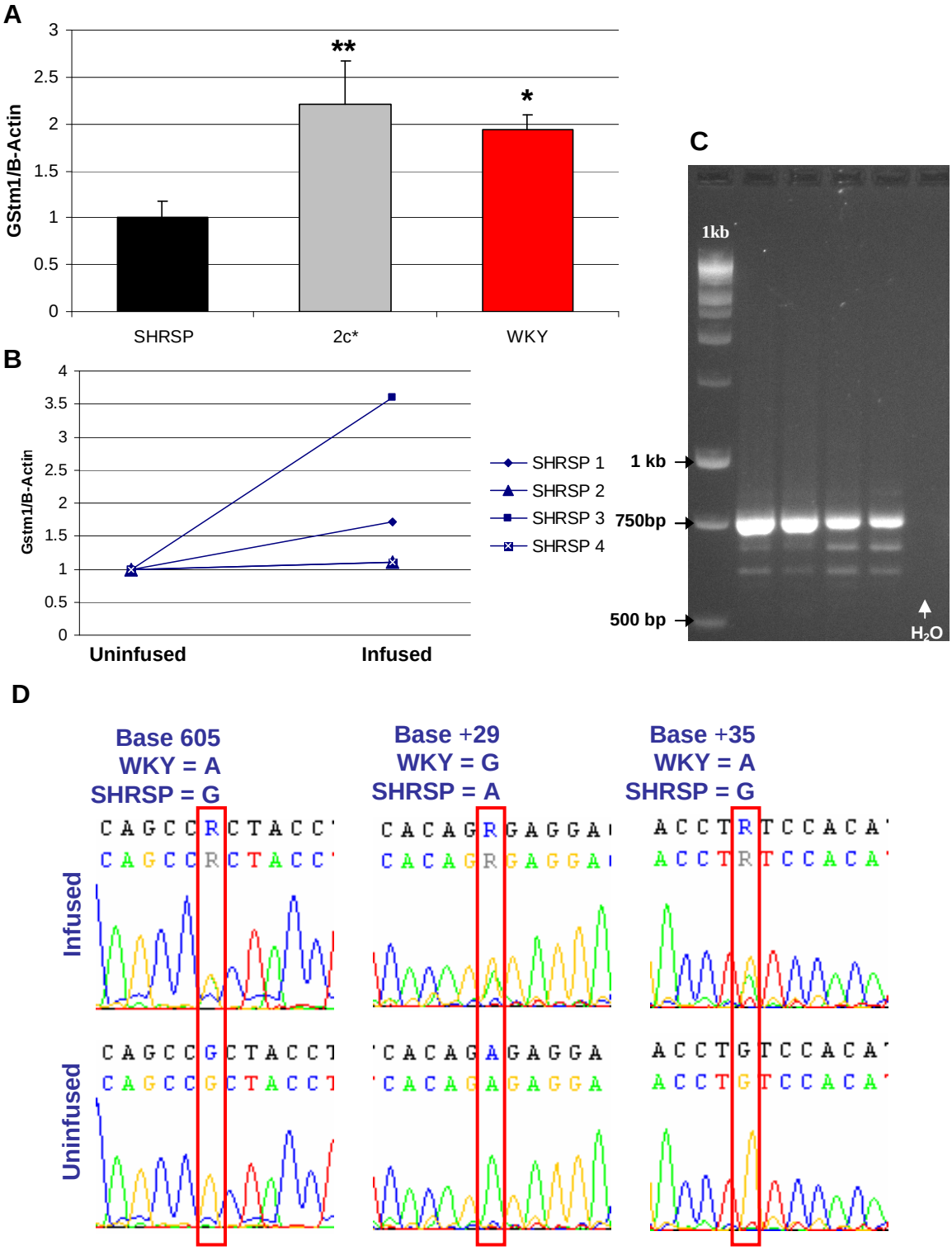

Figure 5.12 - *Gstm1* expression in infused and uninfused carotid arteries

(A) *Gstm1* mRNA expression in uninfused WKY and 2c* carotid arteries measured by Taqman qRT-PCR was approximately 2-fold higher than in the SHRSP. n=4, mean ± SE, F=7.7 * p<0.05, ** p<0.01 vs. SHRSP (ANOVA and Dunnett's post-test). **(B)** Infusion with RAd WKY Gstm1 increased SHRSP carotid artery *Gstm1* expression 1.1-3.6 fold compared to contra-lateral control vessels. **(C)** Gstm1 PCR from carotid cDNA resulted in multiple bands in infused and uninfused arteries, the expected 759 bp band was gel-purified for cDNA sequencing, **(D)** which revealed heterozygous base-calls at sites of coding and 3'UTR polymorphisms between the SHRSP and WKY bases in SHRSP vessels infused with RAd WKY *Gstm1*, confirming transgene expression.

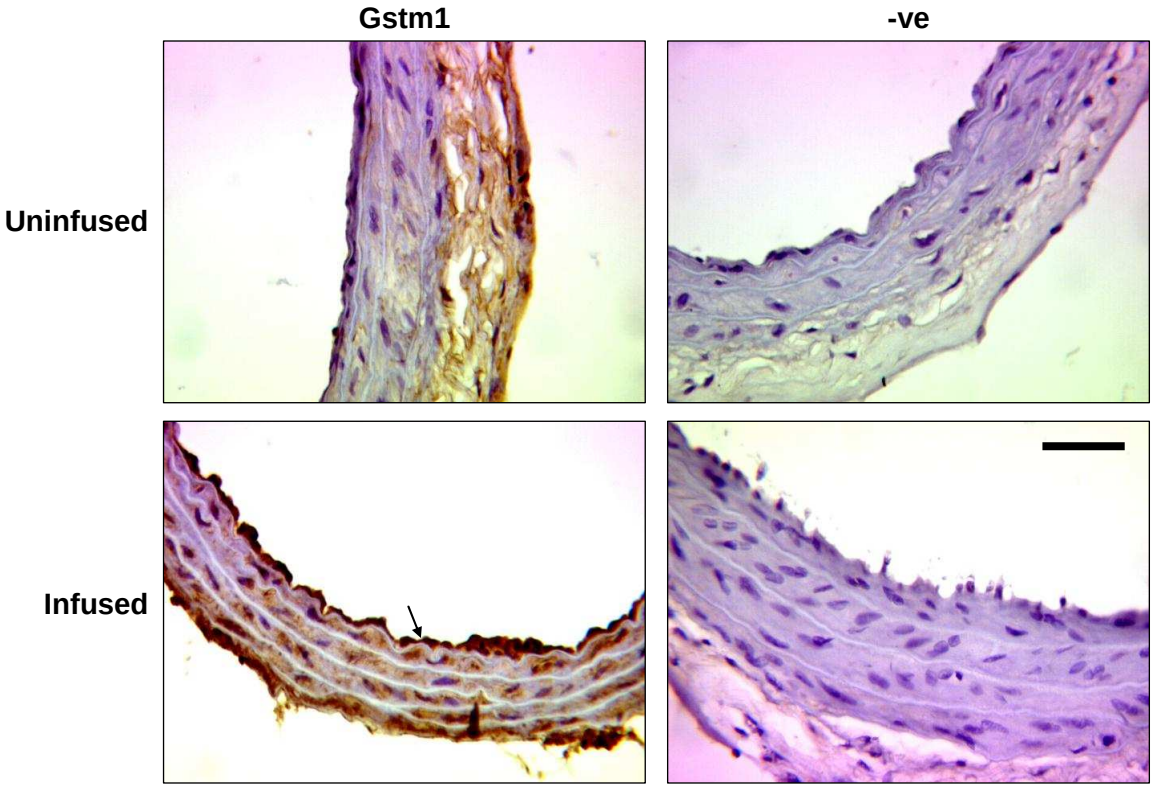

Figure 5.13 - Gstm1 immunohistochemistry in SHRSP carotid arteries
Gstm1 staining in smooth-muscle and adventitial carotid artery tissues was increased following infusion with RAd WKY Gstm1, adenoviruses also mediated endothelial Gstm1 expression (arrow). Gstm1 staining was absent in negative control sections of the same vessels. Scale bar = 50 μm.

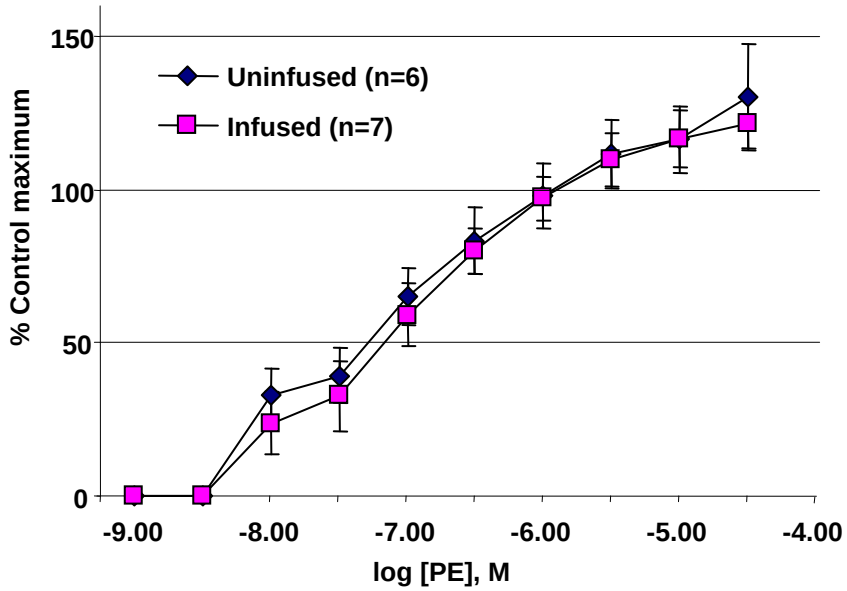

Figure 5.14 - NO bioavailability in SHRSP carotid arteries

PE concentration response curves of SHRSP carotid artery rings, uninfused vs. infused with RAd WKY Gstm1. Contraction following incubation of vessels with 10^{-4}M L-NAME is expressed as a percentage of maximal contraction to $3x10^{-5}$M PE in the absence of L-NAME. No significant difference between infused and uninfused groups comparing area under curves.

5.5 Discussion

Recombinant adenoviruses have been applied to assess the functional effects of modulating expression of *Gstm* genes *in-vitro* and *in-vivo*. RAd Gstmf shRNA mediated consistent *in-vitro* knockdown of *Gstm1,2* and *3* mRNA in NRK52E cells. mRNA expression measurements for *Gstm5* and *7* were more variable and no consistent knockdown was observed. This led to the sequencing of the Gstmf target sequence in each of the genes. Four mismatches were identified between the Gstmf sequence and the target sequence in *Gstm5*, this is likely to explain the lack of significant knockdown of *Gstm5* observed in these experiments and is consistent with published research that any more than 3 mismatches in a target alignment is not compatible with knockdown (Saxena et al. 2003).

A single base mismatch was identified at the same base in the target sequences of *Gstm2* and *7*, knockdown of *Gstm2* but not *Gstm7* may be explained by low absolute levels of *Gstm7* expression in NRK52E cells, the lower the expression level the more sensitive the technique required to measure changes in expression. Unpublished results from our laboratory show that *Gstm7* is expressed to a low level in the rat kidney, and the raw data from these experiments corroborated this, Ct values for *Gstm7* were the highest among all the genes analysed, indicating low template abundance. The mis-matched base in the *Gstm2* target sequence is likely to be responsible for the lower knockdown of *Gstm2* (32% at 100 pfu/cell) compared to that of *Gstm1* and *3* (56% and 58%, respectively), this is consistent with published studies that have shown reduced knockdown from single base mismatches between siRNAs and target sites. For example, Du et al (2005) analysed the effect of systematically mutating every base in the target site of a well-characterised siRNA of the human *CD46* gene, covering every possible permutation of base pair mismatches. They found that the siRNA reduced expression of the wild-type *CD46* by 92% and that the position and base composition of a mismatch influenced the effect on RNAi efficacy. Mismatches were well tolerated at either of the two 5'-most or 3'-most bases of the alignments, having little or no effect on silencing, mismatches in bases 7-11 had the greatest effect on silencing, while mismatches at bases 12-17 (corresponding to the mismatch between Gstmf and *Gstm2* and *7*) had variable effects, knockdown varied for these targets from 55%-92% (Du et al. 2005). Du et al showed that alignment of the central region of an RNAi sequence is the most critical for effective knockdown, this has been confirmed by other publications (Yuan et al. 2005;Dykxhoorn et al. 2006). Furthermore, they confirmed other reports that the specific mismatch between Gstmf and *Gstm2* and *7* (U on the siRNA antisense strand pairing with G in the target sequence) was well tolerated

(Saxena et al 2003;Holen et al. 2005), consistent with the preserved knock-down of *Gstm2* in this study.

Given the 100% homology between Gstmf and *Gstm1* and *3* target sequences, greater knockdown of *Gstm1* and *3* may have been expected, shRNA-expressing adenoviruses have been shown to mediate 90% mRNA and 50% protein knockdown *in-vitro* (El Armouche et al 2007), and Ambion currently guarantee that at least a third of their chemically-synthesised siRNAs mediate at least 70% knockdown *in-vitro*. That this level of gene silencing was not achieved in these experiments could be related to many factors. First, NRK52E cells have low transduction efficiency, even with $CaCl_2$-enhanced infection they showed the lowest infectivity at 100 pfu/cell of all the cells used in this study, and infection with MOIs above 100 pfu/cell were toxic. Secondly, the choice of the Gstmf sequence, in 2004, was limited not only by finding homologous sequences in all 5 *Gstm*s, but also the accepted conventions applied to RNAi design at that time. These conventions included a recommendation from a published protocol to locate the siRNA target sequence at an AA dinucleotide at its 5' end (Elbashir et al. 2001b), and to ensure <50% GC content in the 21-base sequence, as recommended by Ambion and other published work e.g. (Holen et al. 2002). These criteria have subsequently been superseded by more sophisticated algorithms to design siRNA sequences that are based on extensive experimental evidence, Ambion now use a proprietary algorithm, and there are numerous published algorithms publicly available via the internet. These algorithms are not limited to AA dinucleotide 5' anchor sites, they consider sequence-dependent factors that dictate, for example, the entry of the RNAi sequence into the RISC complex, the likelihood of secondary structure formation in mRNA targets and other less well understood factors whereby specific bases at specific positions influence RNAi (Matveeva et al. 2007). If this study were to be extended, other cell types would be infected and additional RNAi sequences would be screened for RNAi efficacy against the Gstm family using newer algorithms. It may be necessary to consider using more than one shRNA sequence, though this may not necessarily require more than one recombinant adenovirus to be made, several publications have described expression cassettes that express multiple shRNA sequences simultaneously, for example, a bispecific lentiviral vector has been engineered to express two shRNAs targeted against cellular receptors for HIV (Anderson et al. 2005), and retroviral vectors have been developed to express 3 shRNAs (Wang et al. 2006b).

The relatively modest knockdown of Gstm genes in NRK cells partially explains the lack of reduced GST activity in RAd Gstmf shRNA-infected cell lysates, though the non-specificity of the assay and the abundance of other GST enzymes expressed in the cells are

contributory factors. Given the demonstrated relative specificity of mouse Gstm1 as a metaboliser of the alternative substrate, DCNB (Fujimoto et al. 2006), future experiments could assess reduced DCNB metabolism as a functional measure of Gstm1 knockdown.

RAd WKY Gstm1 and RAd SP Gstm1 both expressed functional Gstm1 protein that dose-dependently increased total GST activity in HeLa cells. However, despite titring the overexpression viruses as accurately as possible by three methods (particle, pfu and genome titring), RAd SP Gstm1 consistently expressed more protein and increased total GST activity in to a greater degree than RAd WKY Gstm1. This, coupled with the intrinsic insensitivity of western blot densitometry and the fact that the enzymatic activity assay measured *total* GST activity prevented an accurate comparisons of catalytic activities of the adenovirally-expressed WKY and SHRSP Gstm1 proteins. In order to compare the catalytic activity of the two enzymes they should be purified by a method such as high-pressure liquid chromatography, which has been applied for the purification of GST enzymes in the past, for example, see Rouimi et al (1996).

The higher expression from RAd SP Gstm1 was surprising given the lower expression of Gstm1 in the SHRSP *in-vivo* and in the light of equal protein expression and GST activity after transfection of HeLa cells with pK-NpA WKY Gstm1 and pK-NpA SHRSP Gstm1, though no corrections for transfection efficiency were made in this experiment. Possible explanations could include a virus preparation-specific effect not related to the viral titres, or a spontaneous mutation in the promoter sequence of either virus: upregulating SHRSP *Gstm1* cDNA expression or downregulating WKY *Gstm1* cDNA expression. In order to test these hypotheses further viral preparations could be made and the existing preparations could be sequenced. An alternative explanation is a cell-specific sequence dependent effect in HeLa cells whereby one of the polymorphisms between the WKY and SHRSP Gstm1 cDNA sequences affects transcriptional or translational efficiency in HeLa cells. For example, the 3'UTR SNP at base +35 potentially affects binding of rno-miR-10b, base-pairing with the WKY 3'UTR but not the SHRSP 3'UTR. That the miRNA aligns to the polymorphic base at its very 3' end may reduce the likelihood that the polymorphism would direct differential knockdown of *Gstm1*, it has been shown that miRNA target binding is mediated primarily at the 5' end of the miRNA, high complementarity from bases 2-8 (5'-3' in the miRNA) are required for miRNA binding, with less stringency required at the 3' end of the miRNA; if there is low complementarity at the 5' end then the 3' end becomes critical (Brennecke et al. 2005), however this is not the case in this alignment. Furthermore there are conflicts between the published mature miRNA sequence for miR-10b: none have been published for the rat, though its genomic sequence is

identical to that of the mouse and human, while published mouse and human sequences differ. Some cloned sequences encompass the 3' base that aligns with the *Gstm1* 3'UTR SNP (Lagos-Quintana et al. 2003;Kajimoto et al. 2006), while in other publications the miRNA sequence is shifted by 2 bases 5' at its 5' end and by one or two bases at its 3' end, so that it no longer aligns with the polymorphism (Landgraf et al. 2007;Ma et al. 2007), as illustrated below:

```
                    3'   UGUUUAAGCCAAGAUGUCCCAU 5'
                    3'  GUGUUUAAGCCAAGAUGUCCCAU 5'
                    3' UGUGUUUAAGCCAAGAUGUCCC   5'
                       |  || ||| | | || ||||
WKY:        5' GGACCTATCCACATTGGATCCTGCAGGCCACCCT 3'
SHRSP:      5' GGACCTGTCCACATTGGATCCTGCAGGCCACCCT 3'
```

Thus the involvement of miR-10b in RAd WKY Gstm1 expression would depend on the exact sequence expressed in the HeLa cells. Given that HeLa cells are cancerous in origin it is interesting to note that miR-10b has recently been demonstrated to have a role in tumourigenesis, being highly expressed in breast cancer cells (Ma et al 2007). A precedent for a single SNP affecting gene expression via disruption of miRNA-binding was recently published, showing that the +1166A/C polymorphism in the human AngII type 1 receptor gene (AT_1R) 3'UTR dictates the binding of miR-155, the 'A' allele pairs with the miRNA, while the C allele does not, leading to increased AT_1R expression (Martin et al. 2007), in this instance the mismatch was 5 bases from the 5' end of the miRNA.

Increasing concentration of TBHP mediated increasing cytotoxicity in RGE cells cultured in 96-well plates, however lower cytotoxicity was observed for the same concentrations of TBHP when the experiments were performed in 6-well plates. This was attributed to greater evaporation from 96-well plates, effectively increasing the concentration of TBHP in each well. Infection of RGE cells with RAd Gstm1 viruses did not protect them from TBHP-mediated cell death, indeed lower toxicity was observed in the non-infected cells. This result is likely to be due to variability of LDH assay rather than virus-mediated toxicity, only 10 pfu/cell was used in these experiments, the cytotoxicity plateaued in the non-infected cells between 0.08M TBHP and 0.09M TBHP, which was not observed in preliminary experiments in 96 well plates. The lack of a cytoprotective effect of *Gstm1* overexpression in these experiments has a number of possible explanations. For example, the administration of TBHP over 24 hours represents acute oxidative attack, which *Gstm1* does not defend against directly. Cytotoxicity over 24 hours is an end-point far removed from the specific cellular role of *Gstm1*, which operates as part of a large battery of cellular defences to metabolise oxidised macromolecules. In future studies a more appropriate

assay may be to measure the effect of *Gstm1* overexpression or knockdown on an intermediate marker of cellular oxidative stress, such as lipid peroxidation, since it is well documented that GST enzymes directly metabolise lipid peroxides (Hiratsuka et al 1997;Hayes et al 1999). Other studies have shown increases in lipid peroxides in renal cells following short-term treatment with TBHP at higher doses (0.25mM – 2mM) for much shorter time periods (30 minutes to 4 hours) (Schnellmann 1988;Martin et al. 2001). Such protocols could be applied to cells previously infected with viruses overexpressing *Gstm1*.

The distribution of transgene expression from RAd35 and RAd WKY Gstm1 in infused carotids showed predominantly endothelial and adventitial expression and increased medial expression, consistent with previous studies using this protocol of adenoviral delivery to carotid arteries in rats (Alexander et al 2000;Fennell et al 2002) and rabbits (Cooney et al 2007). Gstm1 cDNA sequencing of RAd WKY Gstm1 infused and uninfused vessels confirmed transgene expression and also highlighted the possibility that alternative transcripts of Gstm1 may be expressed in the rat carotid artery; the additional bands in the carotid artery cDNA PCR were not observed when amplifying from rat kidney cDNA during the construction of the virus shuttle vector. An alternative explanation is non-specific PCR amplification from other transcripts unique to the carotid artery transcriptome. There are no published rat *Gstm1* splice variants, though exon-skipping has been observed in a human testes-specific transcript of human *GSTM1* (Ross et al. 1993). The additional bands could be analysed by DNA sequencing in future analysis.

Overexpression of WKY *Gstm1* cDNA did not improve NO bioavailability in isolated SHRSP carotid arteries, there are a number of possible explanations for this. For example, inconsistent increases in *Gstm1* mRNA expression were observed in infused arteries, increasing the number of vessels used in each group in the study may have revealed differences in NO bioavailability not apparent in the small study presented here. In addition, published studies from the Glasgow laboratory using the same local delivery protocol showed that overexpression of eNOS (Alexander et al. 1999;Alexander et al 2000) and extracellular superoxide dismutase (ecSOD) (Fennell et al 2002) improved NO bioavailability, while copper/zinc superoxide dismutase (Cu/Zn SOD) (Alexander et al 2000) and mitochondrial manganese SOD (MnSOD) (Fennell et al 2002) overexpression did not have an effect in this model. This was explained by the physical range of effects of the specific candidates in the endothelium (Fennell et al 2002); eNOS generates NO that is able to diffuse freely from the cell, while ecSOD is membrane-bound on either the intracellular or extracellular face, thus they are able to exert their effect on ROS balance to

beyond the cell they are expressed from. Meanwhile, Cu/Zn SOD and MnSOD are intracellular, as is *Gstm1*, which furthermore is not involved directly in ROS metabolism itself, but metabolises the by-products of oxidative damage. Overexpression of *Gstm1* may have a positive effect if extended over a longer period of time than 48 hours, increased capacity to metabolise reactive lipids, proteins and nucleic acids would reduce the total oxidative load on the cell, over time this may improve vascular oxidative balance. The 2-fold constitutively increased *in-vivo* expression levels of *Gstm1* in the WKY, coupled with lower vascular $O_2^{-}\cdot$ levels than in the SHRSP (Alexander et al 2000;McBride et al 2005), support this analysis. Had the *in-vivo* studies demonstrated that overexpression of *Gstm1* improved endothelial NO bioavailability in the SHRSP carotid artery, similar studies would have been performed with the anti-Gstmf shRNA virus in the WKY. However, given that the anti-Gstmf sequence did not knock down all the *Gstm*s tested and did not reduce total GST activity in cultured cells, these experiments were not justified. Note also that any extended *in-vivo* study would have included further control groups of rats infused with Rad60 and mock-infused with PBS.

The experiments presented in this chapter applied recombinant adenoviruses designed to assess the functional consequences of modulating Gstm1 expression *in-vitro* and *in-vivo*. Recombinant adenoviruses have been generated that express catalytically active Gstm1, and successfully knock down the expression of several Gstm family members. They have also identified a novel 3'UTR polymorphism that potentially affects WKY *Gstm1* expression *in-vitro*, and found that several *Gstm1* transcripts may be expressed in the rat carotid artery. Overexpression of Gstm1 in the SHRSP carotid artery did not improve endothelial NO bioavailability, however, this does not rule out a role for Gstm1 in vascular oxidative stress defence, future studies with transgenic SHRSP rats expressing multiple copies of WKY *Gstm1* will provide a better model of long-term Gstm1 expression. Chapter 6 outlines the work performed towards generating a transgenic *Gstm1* rat. The adenoviral studies will be taken forward using recombinant targeted viruses. When administered intravenously, Ad5 gene delivery is restricted almost exclusively to the liver (Huard et al 1995), while the Ad19p virus, an Ad5 serotype subgroup virus expressing a different fibre protein, shows markedly reduced liver tropism in the rat (Denby et al. 2004). Research in the Glasgow laboratory has developed recombinant Ad19p vectors expressing adenoviral fibre peptides that specifically target gene delivery to kidney tubules (Denby et al. 2007), sequences encoding *Gstm1* cDNA and anti-*Gstm* shRNAs will be cloned into this platform to assess the functional consequences of modulating *Gstm1* expression at the site of its renal expression *in-vivo*.

6 Production of a *Gstm1* Transgenic Rat

6.1 Introduction

Our understanding of hypertension genetics has been advanced by QTL analysis and congenic breeding strategies in the rat, identifying numerous candidate genes. However, establishing definitive proof that a gene affects blood pressure control requires evidence that changing the expression of the candidate in isolation alters blood pressure from a knockout or transgenic strain. It is not currently possible to generate gene-targetted knockout rats, this technique depends on genetic modification of embryonic stem cell lines, which can only be generated for the mouse at present. One of the first transgenic rat lines developed overexpressed the mouse renin (*Ren-2*) gene and displayed severe hypertension that was remediable by the ACE inhibitor captopril (Mullins et al. 1990). Over 100 transgenic rat lines have subsequently been generated including some that express antisense sequences to reduce expression of target genes (Tesson et al. 2005), a number of these transgenic strains have been designed for cardiovascular disease research (table 6.1).

The experiments that led to the derivation of the *Cd36* transgenic rat, discussed in section 1.2.3.3, exemplify the progression from identification of a QTL, construction of congenic strains and an identification of a positional and functional candidate gene to confirmation of its functional effect (Aitman et al 1997;Aitman et al 1999;Pravenec et al 2001b). Similar experiments were recently performed to investigate the functional effects of reduced expression of sterol regulatory element binding transcription factor 1 (*Sreb1f*) in the SHR (Pravenec et al. 2008). A chromosome 10 QTL for hepatic steatosis in the BN after feeding with a high cholesterol diet was identified in a panel of recombinant inbred strains between the BN-*Lx*/Cub and SHR/Ola (Bottger et al. 1998), and a unique coding mutation was subsequently identified in the SHR *Srebf1* gene that underlies the QTL (Pravenec et al. 2001a). Congenic and subcongenic strains were generated by substituting the BN chromosome 10 QTL onto the SHR, the BN allele corresponded to approximately 2.5-fold higher *SrebfI* expression, and 2-fold increased liver cholesterol levels (Pravenec et al 2008). An SHR transgenic rat was generated to overexpress *SrebfI*, which showed equivalent liver cholesterol levels to the SHR congenic rat harbouring the BN *SrebfI* allele, further verifying the functional role of *SrebfI*, despite the counter-intuitive incidence of the allele conferring hepatic steatosis in the BN (Pravenec et al 2008).

Transgene	Construct	Phenotype	Reference
Mouse *renin*	17.6 kb linear genomic construct, including promoter	Severe hypertension	(Mullins et al 1990)
Human *renin* and *angiotensinogen* (double transgenic)	17.6 and 16.3 kb linear genomic constructs, including promoters	Moderately severe hypertension, death by renal and cardiac damage by week 7.	(Ganten et al. 1992)
Rat *prorenin*	3.5 kb linear, liver specific promoter	Normotensive, severe renal and cardiac damage in males	(Veniant et al. 1996)
Rat *vasopressin*	12 kb linear hypothalamus-specific promoter.	Exaggerated responses to osmotic challenge	(Waller et al. 1996)
Human *endothelin 2*	9.4 kb linear genomic construct, including promoter	Normotensive	(Liefeldt et al. 1999)
Angiotensinogen antisense	3 kb linear, brain specific promoter	Reduced BP in normotensive rats	(Schinke et al. 1999)
Rat *Cd36*	4.8 kb linear construct, human EF1-alpha promoter	Amelioration of metabolic syndrome phenotype in SHR	(Pravenec et al 2001b)
Human *Arginine vasopressin*	3 kb linear, CNS-specific promoter	Hyponatraemia	(Nagasaki et al. 2002)
Ang-(1-7) fusion protein	Linear construct, CMV promoter	Improved cardiac contractility, protection from cardiac hypertrophy	(Santos et al. 2004)
Rat *Srebfl*	4 kb linear construct, *Pepck* promoter	Increased liver cholesterol in transgenic SHR	(Pravenec et al 2008)

Table 6.1 - Transgenic rat strains for the study of cardiovascular diseases

Unless otherwise stated, recipient strains were normotensive. *Srebf1*: sterol regulatory element binding transcription factor 1. *Pepck*: phospoenolpyruvate carboxykinase.

Traditional techniques to generate transgenic rats are fundamentally the same as those used for mice, involving the microinjection of the transgenic construct into the pronucleus of single-cell embryos, followed by implantation into recipient females. Resultant pups are screened for insertion of the transgene by PCR or southern blot and used as founders for homozygous transgenic lines. These techniques are more successful in mice, typically generating 3%-5% transgene-positive offspring per injected embryo (Brinster et al. 1985), compared to 0.2%-2% in rats (Charreau et al. 1996;Popova et al. 2002). The lower success in rats is in part due to the physical characteristics of the embryo pronucleus, which tend to be harder to microinject; the cytoplasmic membrane of the rat is more resistant to injection and the pronucleus is very sticky; up to 10-50% of embryos may be lost during microinjection (Popova et al. 2005).

Different DNA constructs can be used for microinjection, common techniques include small linear (up to 40 kb) constructs artificially constructed to overexpress the transgene from a constitutive or tissue-specific promoter, or large circular or linearised plasmids can be used such as bacterial, bacteriophage P1 or yeast artificial chromosomes (BAC, PAC or YAC) accommodating up to 300 kb, 100 kb and 2 Mb genomic DNA sequences including the gene of interest (Giraldo et al. 2001). Insertion into the genome is a random process and may occur more than once in a single embryo, every transgenic line is unique and may have different transgene expression patterns and levels to others. Insertion into a non-transcriptionally active region of the genome may silence expression of the transgene, while insertion adjacent to tissue specific enhancers may influence expression patterns, this is known as the 'position-effect' (Wilson et al. 1990;al Shawi et al. 1990). Integration of the transgene into a coding sequence will usually ablate endogenous gene expression, with potentially lethal consequences for the embryo (Mullins et al. 2006). BAC, PAC and YAC transgenic lines are less susceptible to transcriptional effects from the genome since the gene is insulated by large flanking sequences; in addition, large genomic clones are likely to include short-range and long-range control elements, increasing the likelihood of physiologically faithful gene expression patterns in the transgenic (Giraldo et al 2001). Large inserts can also encode multiple genes in addition to the gene of interest, which may also be expressed in the transgenic animal (Nistala et al. 2004). Short expression constructs in contrast are easier to amplify and prepare, express only the gene of interest and are less likely to shear or recombine before microinjection (Giraldo et al 2001).

Given the low efficiency of microinjection protocols, successful transgenesis depends on a large supply of recipient embryos. This is achieved by administering hormones to stimulate superovulation of female recipient rats. Following mating, embryos are harvested,

microinjected and implanted into recipient females. Recipient females are made psuedopregnant by mating with vasectomised males on the day prior to implantation. This chapter outlines experimental work performed to prepare BAC and linear expression constructs for the generation of transgenic SHRSP rats overexpressing *Gstm1*.

6.2 Aims

- To amplify and purify a bacterial artificial chromosome encoding *Gstm1* in preparation for direct micronuclear injection.

- To verify the integrity and purity of BAC preparations by restriction digestion, linear and pulse-field gel electrophoresis and direct BAC sequencing.

- To clone the WKY Gstm1 cDNA sequence into an expression vector to generate a linear expression construct for *Gstm1* transgenesis and to prepare linear fragment microinjection solutions.

- Following microinjection and birth of pups, to screen prospective transgenics for integration of BAC and linear transgenic constructs.

6.3 Methods

6.3.1 BAC Microinjection Construct Preparation

6.3.1.1 BAC Selection and Purification

The CHORI-230 BAC library was in initially constructed as part of the rat genome project; it contains approximately 200000 clones of 200 kb average size on the pTARBAC2.1 plasmid backbone, which encodes chloramphenicol resistance for clone selection (Osoegawa et al. 2004). Clones encompassing *Gstm1* were identified by mapping BAC alignments in the University of California Santa Clara (UCSC) Genome Browser. The *Gstm* gene family is aligned in a cluster on chromosome 2, at the time of selecting the BAC for the transgenic study (2004), the rat genome annotation was less complete and *Gstm1* was the most distal of the *Gstm* genes aligned in the assembly. The 234 kb clone, CH230-90M3 was selected since it encompassed *Gstm1* but no other *Gstm* genes, the gene encoding guanine nucleotide binding protein (*Gnai3*) was annotated at that time. Since 2004 more genes have been mapped to this region of the genome and CH230-90M3 is now known to cover 9 transcripts, including *Gstm1*, *Gstm7*, and 7 other transcripts, including 4 predicted genes (figure 6.1).

CH230-90M3-containing bacterial cultures was purchased from the BACPAC Resource Centre, Children's Hospital Oakland Research Institute, Oakland, California. Cultures were streaked for single colonies overnight on LB agar (12.5 μg/ml chloramphenicol). The BAC purification was performed using modifications of a published protocol (Gama et al. 2002). A single colony was picked into 10 ml LB culture media (30 μg/ml chloramphenicol) and incubated at 30°C in a shaking incubator (180 oscillations per minute) overnight. One litre of LB culture media (30 μg/ml chloramphenicol) was inoculated with 2 ml overnight starter culture was incubated at 30°C in for approximately 11.5 hours, following bacterial growth until culture optical density at 600 nm (OD_{600}) reached 1.0. Cultures were grown at 30°C rather than 37°C because large DNA constructs can adopt sequence-dependent secondary structures at 37°C that can lead to deletion of insert sequences (Gama Sosa et al. 1988). Optical density was measured using a Pharmacia Biotech Ultraspec 2000 spectrophotometer in a quartz cuvette with a sterile culture media blank. The culture was centrifuged for 5 minutes at 5000 g, culture media was poured off and pellets were stored at -20°C. Column-based Nucleobond BAC Maxi kits were used for BAC purification following the manufacturer's instructions. The 1 litre culture was split over 2 columns,

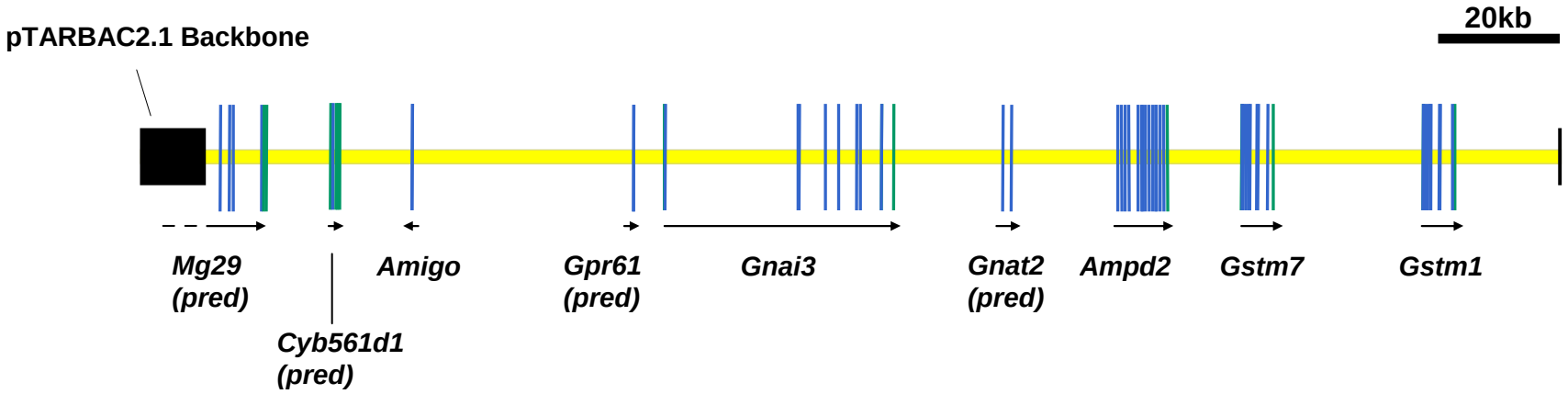

Figure 6.1 - Linear depiction of transcripts encoded by the circular CH230-90M3 BAC

Exons are shaded blue, UTR sequences are shaded green, the direction of transcription is indicated under each transcript. Only the 3'-most exons of the *Mg29* transcript is covered by the BAC. pred: predicted, *Mg29*: mitsugumin 29, *Cyb561d1*: cytochrome b-561 domain containing 1, *Amigo*: amphoretin-induced gene and open-reading frame, *Gpr61*: G-protein coupled receptor 61, *Gnat2*: guanine nucleotide binding protein alpha 2, *Ampd2*: adenosine monophosphate deaminase 2

producing 2 preparations, 90M3A and 90M3B. Pellets from each 500 ml was resuspended in 24 ml Buffer S1 + RNase A and 24 ml buffer S2 was added, mixed and left for 3 minutes at room temperature. 24 ml Buffer S3 was added, mixed and left for 5 minutes on ice. Precipitates were filtered through a Nucleobond Folded Filter paper, flow through was collected and applied to pre-wet (buffer N2) BAC Maxi columns. Flow-through was re-loaded to ensure maximum DNA binding. Columns were washed with 2 x 18 ml buffer N3 and eluted with 15 ml buffer N5, preheated to 50°C. 11 ml isopropanol was added to precipitate BAC DNA and samples were centrifuged at 15000 g for 30 minutes at 4°C. Supernatant was replaced with 5 ml ice-cold 70% ethanol, samples were centrifuged at 15000 g for 10 minutes at 4°C, ethanol was removed, pellets were air-dried and DNA was resuspended in 320 µl RNase-free H_2O using wide-bore pipette tips to minimise shearing of BAC DNA.

For microinjection, prep 90M3B was diluted to 3 ng/µl in 0.2µlm sterile-filtered BAC microinjection buffer: 10 mM Tris; 0.1 mM EDTA; 0.1 M NaCl, 7 mM Spermidine; 3 mM Spermine. The inclusion of polyamine spermine and spermidine in BAC microinjection buffer helps to stabilise BAC DNA and protect it from shearing during microinjection (Schedl et al. 1993;Montoliu et al. 1995). BAC microinjection buffer was made with fresh sterile solutions and filter-sterilised, microinjection solutions were made fresh on the day of injection.

6.3.1.2 BAC Restriction Digestion and Electrophoresis

BAC sample integrity and purity were assessed by restriction digestion followed by standard or pulse-field gel electrophoresis. Three µg of 90M3A and 90M3B DNA preparations were digested with *HindIII* or *NotI* restriction enzymes following the protocol in section 2.5.4. *HindIII* digests were electrophoresed for 8 hours at 90 V through a 25 cm 0.8% agarose gel in 1 x TAE at 4°C. 1 µg of uncut BAC preparations were also electrophoresed. After electrophoresis the gel was stained with 0.5 µg/ml ethidium bromide for 30 minutes and destained in 1 mM $MgSO_4$ for 25 minutes before visualisation under UV light.

Pulse-field gel electrophoresis (PFGE) was performed on *NotI* digested BAC DNA at the laboratory of Professor John Mullins at the Centre for Cardiovascular Science, University of Edinburgh. Digested DNA was electrophoresed alongside 1 µg undigested BAC preparations, λ *HindIII* DNA size markers and New England Biolabs Mid Range I and Mid Range II PFGE DNA size markers. BAC digests and uncut DNA were loaded for

electrophoresis by mixing with molten low-melting point agarose and pipetting into wells. Electrophoresis was performed at 10°C through 0.8% agarose gel in 0.5 x TAE using BioRad Chef DR2 apparatus. DNA was electrophoresed for 24 hours at 6 V/cm with current orientation switching every 1-20 seconds. After electrophoresis gels were stained with ethidium bromide, destained and visualised exactly as linear gels.

6.3.1.3 Direct BAC Sequencing

BAC preparation purity was assessed by direct sequencing. 1 μg BAC DNA template was used in modified sequencing reactions with 30 pmol primer and temperature cycling as suggested by Applied Biosystems:

Sequencing reaction		***Heat cycling:***
BAC DNA (200 ng/μl)	5 μl	95°C
5 X Sequencing buffer	4 μl	95°C ←
Ready Reaction	8 μl	50°C ⌐ x 100 cycles
Primer (15pmol/μl)	2 μl	60°C ⌙
H_2O	1 μl	

Primers pBACSp6F and Gstm13F were used for sequencing. Sequencing reaction clean up and analysis protocols were otherwise followed exactly as described in section 2.4.

6.3.2 Linear Microinjection Fragment Preparation

A 2.7 kb linear microinjection construct was cloned for *Gstm1* transgenesis using the same expression platform and microinjection fragment purification protocol employed in *Cd36* rat transgenesis (Pravenec et al 2001b). The WKY *Gstm1* cDNA sequence was cloned into pEF1/*Myc*-HisA (Invitrogen), an expression construct including the constitutive human elongation factor 1 α subunit (EF1α) promoter and bovine growth hormone (BGH) polyadenylation signal separated by a multiple cloning site. A linear expression construct was subsequently cleaved from the plasmid by restriction digestion and purified for microinjection.

6.3.2.1 pEF1 WKY Gstm1 Cloning

pEF1/*Myc*-HisA plasmid was double-digested with *KpnI* and *XbaI* restriction enzymes following the protocol in section 2.5.4. WKY *Gstm1* cDNA sequence was similarly double-digested from pK-NpA WKY Gstm1 plasmid (previously used in construction of

Gstm1 overexpression virus – see section 5.3.1.2) and cloning protocols from section 2.5 were followed, confirming insert ligation in positive clones by sequencing with pEF1 T7F and BGH PolyAR primers. The resultant expression plasmid, named pEF1 WKY Gstm1, was amplified and purified using the Qiagen Maxi kit as outlined in section 2.5.3.

6.3.2.2 Restriction Digestion of pEF1 WKY Gstm1 to Generate Linear Fragment

The linear microinjection fragment was produced by sequential digestion of pEF1 WKY Gstm1 with *PvuII* and *AatII* enzymes (figure 6.2). A total of 20 μg plasmid was digested with *PvuII* in 10 x 20 μl digests following the protocol in section 2.5.4. Restriction digests were pooled and electrophoresed on 1% agarose gel for 3 hours. The 4705 bp fragment was gel purified using the Qiagen QIAquick protocol in section 2.5.5. The DNA was concentrated by ethanol precipitation: A 1/10 volume of 3 M sodium acetate (pH 5.2) and 2 volumes of 100% ethanol were added, the mixture was vortexed and placed at -80°C for an hour before centrifuging at 13000 rpm for 2 minutes. Supernatant was removed and the pellet air-dried before resuspending in H_2O to give a final concentration of approximately 200 ng/μl. The DNA was digested with *AatII* following the standard protocol and electrophoresed on 1% agarose for 3 hours. The 2725 bp fragment was purified for microinjection using the Qiagen QIAEX II kit. The band was excised from the gel and 300 μl of QX1 buffer was added per 100 mg of gel; QIAEXII beads were resuspend by vortexing and 10 μl was added before incubating the mix for 10 minutes at 50°C, vortexing every 2 minutes to dissolve the gel. The mixture was centrifuged for 30 seconds at 13000 rpm and supernatant was removed, the pellet was washed by resuspending in 500 μl buffer QX1 and centrifuged for 30 seconds at 13000 rpm. The pellet was washed twice more with 500 μl buffer RPE and supernatant was removed. The pellet was air-dried for 15 minutes before resuspending in 0.2μlm sterile-filtered linear fragment microinjection buffer (10mM Tris pH 7.4, 0.1 mM EDTA), vortexing, centrifuging at 13000 rpm for 1 minute and transferring the DNA solution to a fresh tube. For microinjection DNA solutions, linear fragment DNA was diluted to 10 ng/μl in linear fragment microinjection buffer.

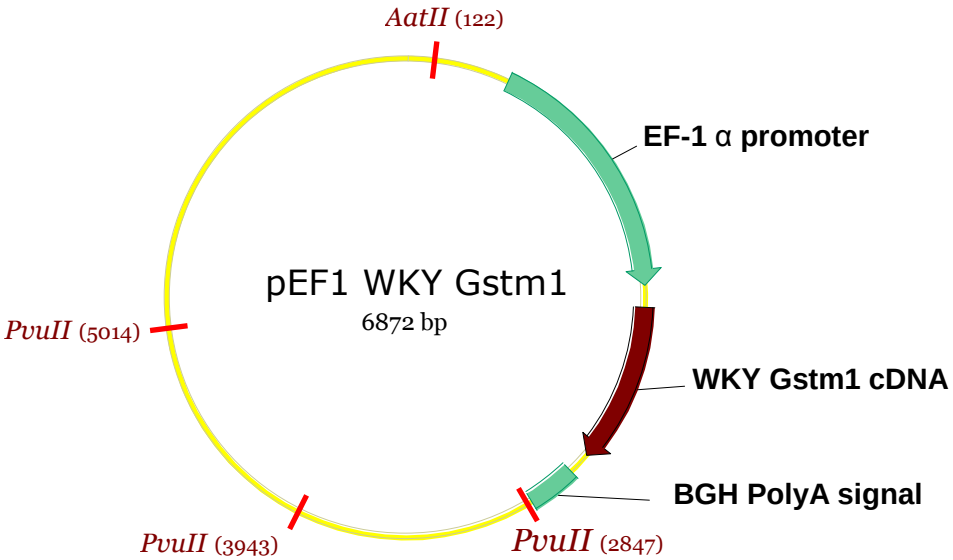

Figure 6.2 - pEF1 WKY Gstm1 plasmid
The restriction sites for *PvuII* and *AatII* enzymes are indicated in red, coordinates in brackets. Digestion with *PvuII* resulted in the generation of 4705 bp, 1096 bp and 1071 bp fragments, the 4705 bp fragment was gel-purified and digested with *AatII* to produce a 1980 bp fragment and the 2725 bp microinjection fragment encompassing the EF-1α promter, Gstm1 cDNA and BGH polyadenylation sequences.

6.3.2.3 Gstm1 Expression from pEF1 WKY Gstm1

Gstm1 protein expression from pEF1 WKY Gstm1 was confirmed by transfection into HeLa cells and western blotting. HeLa cells were transfected in 6 well plates with 1 μg DNA per well at 3:1 FuGene:DNA ratio (μg:μl), control wells were untransfected or transfected with pMV10. After 48 hours HeLa cells were harvested in PBS/0.2% Triton and 20 μg protein was used for Gstm1 and β-actin western blotting following the protocol in section 5.3.6, 30 μg control rat kidney protein was also loaded.

6.3.3 Superovulation, Microinjection and Implantation

Initial microinjections of CH230-90M3 BAC DNA were performed by technical staff at the University of Glasgow Central Research Facility. Subsequently, BAC and linear fragment microinjection solutions and SHRSP male and female rats were sent to the laboratory of Dr Michal Pravenec, Institute of Physiology, Academy of Sciences of the Czech Republic, Prague. Animal procedures are briefly outlined below.

Superovulation in six-week old SHRSP females was initiated by intraperitoneal (IP) injection of 15 U of pregnant mare's serum gonadotrophin (PMSG), followed 48 hour later by IP injection with 20 U human chorionic gonadotrophin (HCG). Immediately after HCG

injection females were placed with mature male stud SHRSPs for fertilisation. The next morning, females with cervical plugs (an indication that they have mated) were sacrificed and fertilised embryos were harvested for microinjection. Four days prior to microinjection, oestrus was synchronised in recipient SHR (Glasgow laboratory) or Sprague Dawley (Prague laboratory) rats with donor SHRSPs by injection with 20 U leutenising hormone releasing hormone (LHRH). On the day prior to microinjection recipient rats were placed with vasectomised male rats to induce pseudopregnancy.

Microinjections were performed on single cell embryos immobilised by gentle suction with a holding pipette. The microinjection needle, with an internal tip diameter of less than 1 μm, was filled with microinjection solution and manipulated to inject the egg. In order to ensure pronuclear injection, the needle tip was injected though both membranes of one of the pronuclei and then drawn back in to the pronucleus before injecting; successful injection was observed by swelling of the pronucleus. Embryos were incubated overnight and pseudopregnant females were surgically implanted with viable one or two cell embryos on the following day, surgery involved making an incision in the back of the anaesthetised rat just below the ribs, locating the oviducts and making a small incision to inject the embryos. An average of 12 microinjected embryos were implanted into each recipient female.

6.3.4 Transgenic Screening

Genomic DNA from potential transgenic rats was extracted from tail tips and screened for transgene sequences by PCR. Potential BAC transgenics were screened with 5 PCRs, amplifying the regions across each 'BAC-end' with 2 primer pairs (pBACSp6F + 90M3-1R and pBACT7R + 90M3-3F), amplifying two regions of the pTARBAC2.1 backbone (pBAC1F + pBAC2R and pBAC3F + pBAC4R) and with one primer pair that amplified a region of the *Gstm1* promoter (Gstm10F and Gstm13R). Gstm10R/Gstm13F PCR products were also sequenced in all animals, incorporation of WKY sequence would have been revealed by heterozygosity at several SNPs in the *Gstm1* promoter. Potential linear-fragment transgenics were screened with three PCRs, amplifying across the EF1α promoter sequence (primers pEF1F + pEF1R), and with two primer pairs that spanned EF1α promoter and Gstm1 cDNA sequence (pEF2F + pEF2R and pEF3F + pEF3R). All PCRs were performed following protocols as described in section 2.2.3 using an annealing temperature of 58°C. Positive control plasmid DNA (20 ng CH230-90M3 or 5 ng pEF1 WKY Gstm1) and negative control WKY DNA were included in all PCRs.

6.4 Results

6.4.1 BAC Restriction Digestion and Electrophoresis

HindIII digestion of 90M3A and 90M3B BAC preparations resulted in multiple well-resolved bands upon electrophoresis, digested and uncut lanes were clean, indicating undamaged DNA (figure 6.3 A). The expected banding pattern for *HindIII* digestion of CH230-90M3 was retrieved from Internet Contig Explorer (iCE) database, an internet-based library of 'fingerprint maps' for BAC digests that was designed to aid in sequence alignments for the rat genome sequencing project (Fjell et al. 2003); alignment of the iCE *HindIII* digest of CH230-90M3 showed an identical band pattern to the digests performed in these experiments, confirming the identity and integrity of the BAC preps (figure 6. 3 B).

NotI digests of 90M3A and 90M3B were electrophoresed by PFGE, generating the expected band pattern and uncut DNA resolved to approximately 234kb (figure 6.4). 90M3B was chosen for microinjections because when uncut it resolved better than 90M3A in both gels with slightly less smearing of at the top of the lanes, though 90M3A integrity was also confirmed and could be used in future microinjections.

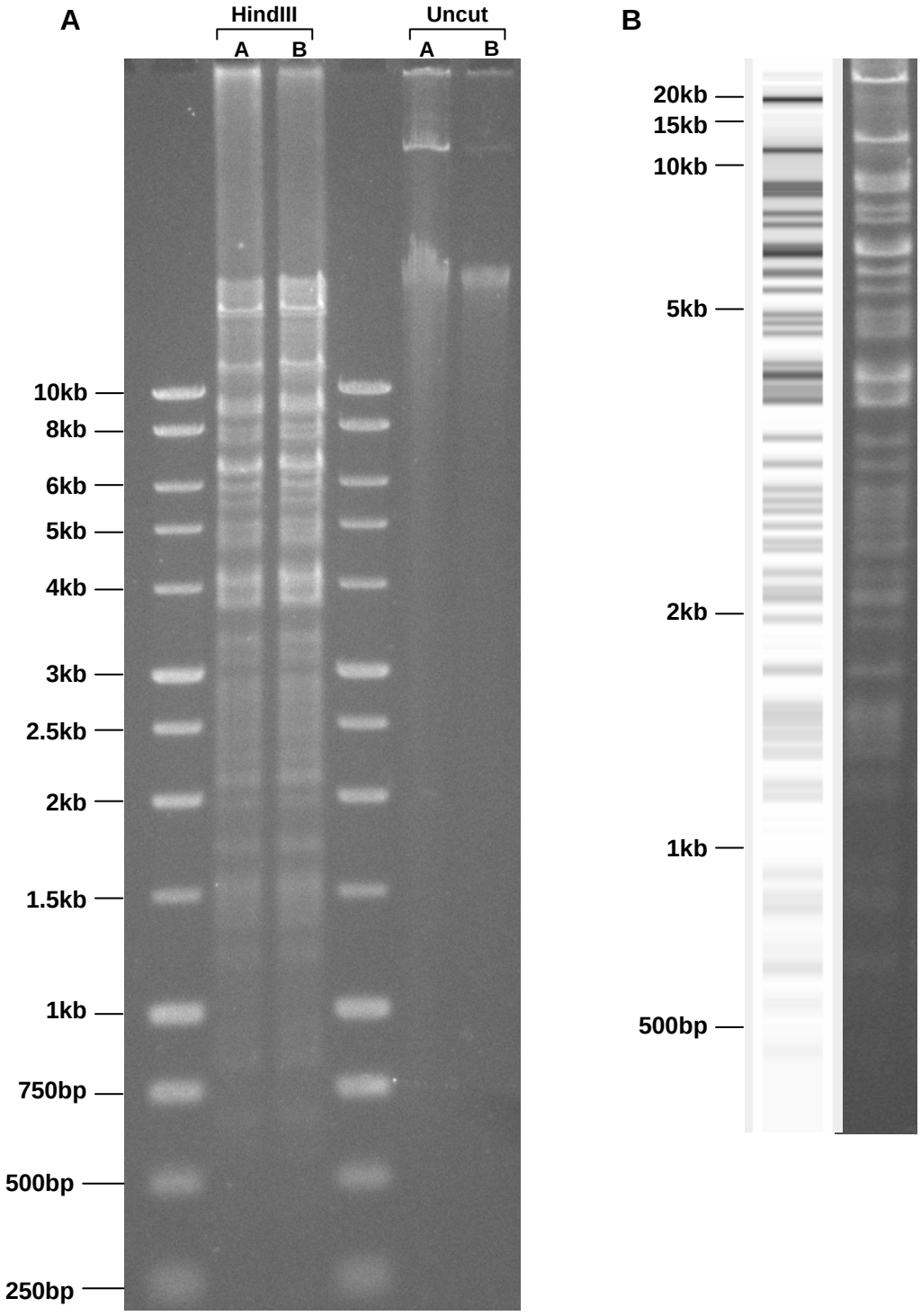

Figure 6.3 - Agarose electrophoresis of *HindIII*-digested CH230-90M3 BAC
(A) *HindIII*-digested and undigested BAC preparations 90M3A and 90M3B resolved to produce consistent banding pattern with little evidence of smearing in uncut lanes. **(B)** Alignment of *HindIII*-digested BAC DNA with expected band pattern from Internet Contig Explorer revealed the expected band pattern, confirming intact BAC DNA.

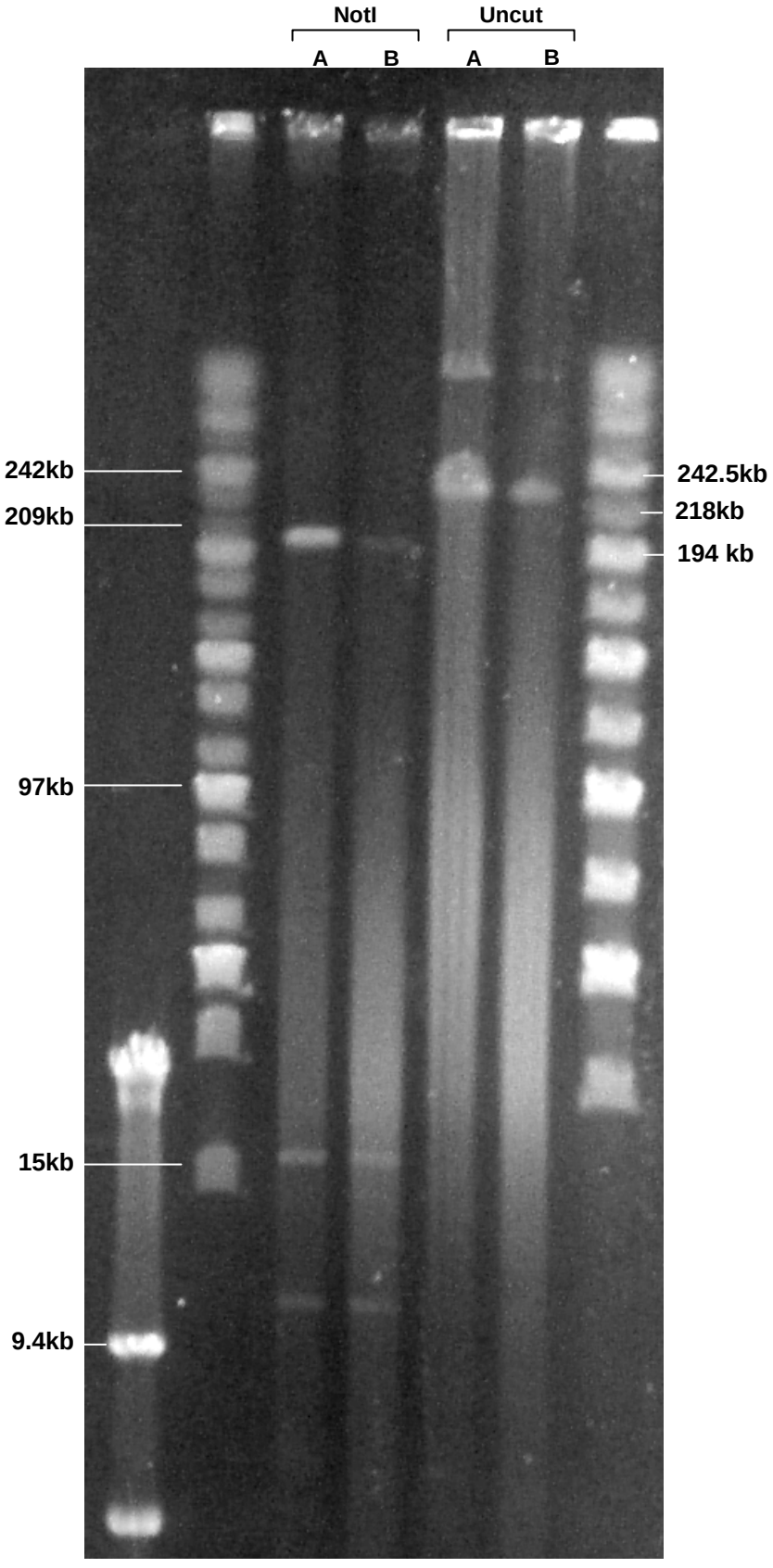

Figure 6.4 - PFGE of *NotI*-digested CH230-90M3 BAC
NotI digestion produced fragments at the expected sizes of 204 kb, 18.4 kb and 10.6 kb. The major band in uncut lanes corresponded to the intact 234kb plasmid. There was minimal smearing in digested or undigested lanes indicating intact BAC preparations.

6.4.2 Direct BAC Sequencing

Direct sequencing from CH230-90M3 BAC template was performed with pBAC SP6F and Gstm10F primers. Sequencing read lengths of 400-550 bp were achieved with clean backgrounds, confirming BAC preparation purity and confirming BAC expected sequences (figure 6.5).

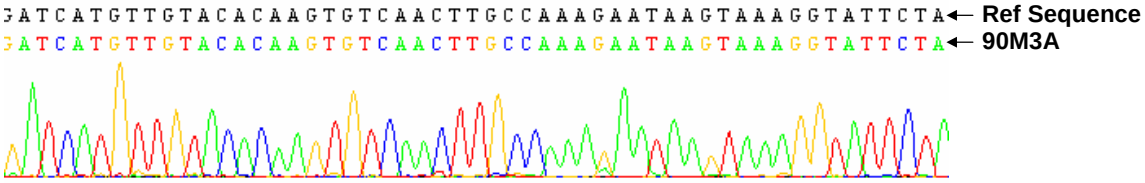

Figure 6.5 - Electropherogram from direct sequencing of 90M3
Sequencing of 90M3 with pBACSp6F was of high quality, traces showed low background and aligned 100% with expected (Ref) sequences.

6.4.3 Gstm1 Expression from pEF1 WKY Gstm1

Transfection of HeLa cells with pEF1 WKY Gstm1 resulted in expression of immunoreactive Gstm1 protein in cell lysates 48 hour later, indicating effective Gstm1 expression from the plasmid construct (figure 6.6).

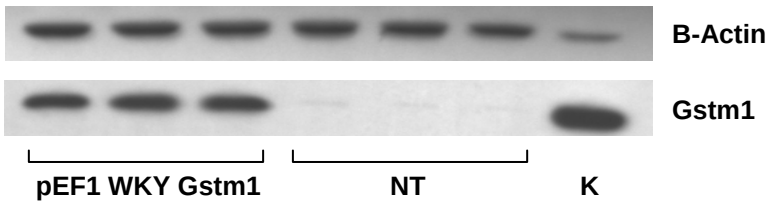

Figure 6.6 - Gstm1 protein expression from pEF1 WKY Gstm1
HeLa cells were lysed 48 hours post-transfection. 20 µg protein was loaded in each lane. Expected 26 kDa Gstm1 protein bands were observed transfected wells, but not in non-transfected (NT) cells. β-actin immunoreactivity (42 kDa) was observed in all cells. K = control rat kidney protein (30 µg).

6.4.4 Transgenic Screening

Five BAC construct implantations were carried out in Glasgow, generating a total of 18 potential transgenic pups, though 2 from one litter were consumed by the mother within 48 hours of being born. Six recipient females were implanted on each occasion (table 6.2). This represents a live birth rate per implantation of 5%; none of the pups were positive in

BAC-specific PCR screens (figure 6.7A). Microinjection and implantation was performed three times in Prague, once with the BAC construct only and twice with both constructs; a total of 35 potential BAC transgenic and 25 potential linear fragment transgenic pups were born (table 6.3), a live birth rate per implantation of 9.7% and 14.8 %, respectively. PCR screening was negative in all cases (figure 6.7B). Data supplied by the Prague laboratory showed that approximately 65% of microinjected embryos were viable the following day.

Microinjection	No. of Recipients	No. of Pups
1	6	0
2	6	7
3	6	2*
4	6	9
5	6	0

Table 6.2 - Microinjected embryos implanted at Glasgow University
Implantations of microinjected embryos performed with the BAC transgenic construct at the Central Research Facility, University of Glasgow. An average of 12 microinjected embryos was implanted on each occasion, a total of 18 pups were born, 2 (*) were cannibalised.

Microinjection	BAC Recipients	BAC Pups	Linear Fragment Recipients	Linear Fragment Pups
1	10	13	-	-
2	12	5	6	6
3	8	17	8	19

Table 6.3 - Microinjected embryos implanted at Academy of Sciences of the Czech Republic
Implantations of microinjected embryos performed with BAC and linear fragment transgenic constructs at the Institute of Physiology, Academy of Sciences of the Czech Republic, Prague. An average of 12 microinjected embryos were implanted on each occasion, generating a total of 60 potential transgenic rats.

A

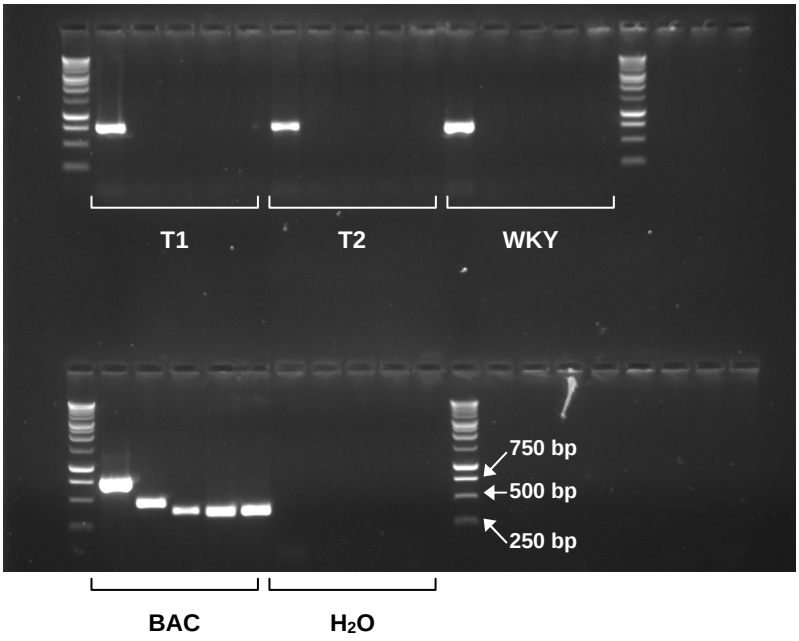

B

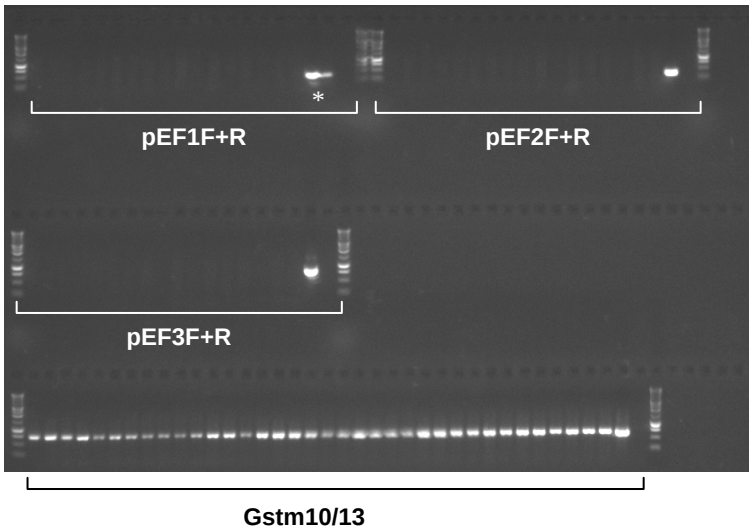

Figure 6.7 - PCR Screening for BAC and linear fragment transgenic rats
PCR Screening for BAC and linear fragment transgenic rats. **(A)** BAC Transgenic screening in two potential transgenics (T1 ans T2). Control WKY and CH230-90M3 BAC DNA also PCRd. Loading order and expected band size: Gstm10+Gstm13 (738 bp), pBACSp6F + 90M3-1R (442 bp), pBACT7R + 90M3-3F (380 bp), pBAC1F + pBAC2R,(371 bp) and pBAC3F + pBAC4R (387 bp). **(B)** Linear fragment transgenic screening in 17 potential transgenic rats. Loading order in pEF1F+R, pEF2F+R, pEF3F+R PCRs: Potential transgenics 1-17, pEF1 WKY Gstm1 +ve control, H_2O. Gstm10+Gstm13 positive control PCRs also performed on all rats, 19 potential BAC transgenics were included in the same PCR. Expected product sizes: pEF1F+R: 381 bp, pEF2F+R: 380, pEF3F+R: 838 bp. * double band in +ve control lane for pEF1 F+R due to split well.

6.5 Discussion

This chapter has outlined the work performed to date in the ongoing project to develop a transgenic SHRSP rat overexpressing *Gstm1*. A genomic BAC clone encompassing *Gstm1* and a linear construct encoding *Gstm1* have been cloned and purified using published protocols and several techniques have been applied to verify the purity, integrity and transcriptional activity of the constructs. To date approximately 720 microinjected embryos have been implanted but no transgenic pups have been born, despite 78 live births.

The lack of transgenic rats produced so far could have many possible explanations. For example, scientists at Glasgow University have no experience in rat transgenesis, all previous microinjections having been performed on mouse embryos; as noted above, microinjection is the limiting factor in rat transgenics due to the physical properties of the rat embryo and pronucleus. The Prague laboratory however have extensive practical experience in rat transgenesis (Pravenec et al 2001b;Pravenec et al. 2003;Pravenec et al 2008), and it is expected that collaboration with this laboratory will result in a transgenic *Gstm1* rat presently. The lack of a transgenic rats from microinjections performed to date in Prague may simply be due to chance and further microinjections are ongoing. It is also possible that either of the transgenic constructs have integrated on several occasions but in each case have disrupted the expression of vital genes. There is also the possibility that overexpression of transgenes in the constructs was lethal to the developing embryo; this is more likely for the BAC transgenics since CH230-90M3 encodes a number of transcripts in addition to *Gstm1* (figure 6.1), though there is no published evidence that any of these genes may be toxic if overexpressed. There are several published reports of transgenic overexpression causing embryonic lethality in mice, including the membrane protein *neurophilin* that is involved in cell-cell interactions (Kitsukawa et al. 1995), the cardiac developmental transcription factor *Nkx2.5* (Wakimoto et al. 2003) and the vascular endothelial growth factor (*Vegf-A*) gene (Miquerol et al. 2000), note however that these are all genes with established roles in development or transcriptional control, which does not apply to *Gstm1*.

BAC-mediated transgenesis has been attempted in this study in an effort to ensure a physiological *Gstm1* expression pattern, however there are drawbacks to this procedure, for example, it has recently been learnt that CH230-90M3 encodes *Gstm7* in addition to *Gstm1*, and though circular BAC microinjection has been used to successfully derive transgenic animals in numerous studies (Antoch et al. 1997;Kaufman et al. 1999;Duff et al.

2000), BAC growth and purification are challenging procedures and other researchers have used linearised BAC molecules that have undergone more rigorous purification protocols such as caesium chloride gradient centrifugation or dialysis (Antoch et al 1997;Probst et al. 1998). Given these factors, future microinjections will concentrate on the linear expression construct. However it must be recognised that kidney *Gstm1* expression will not be guaranteed in all transgenic rats; tissue-specific expression pattern and consequent phenotype of transgenics is dependent on the 'position effect' of random insertion into the genome (Wilson et al 1990;al Shawi et al 1990). The *Cd36* transgenesis experiments, which used exactly the same expression construct as employed in these experiments, exemplify this phenomenon: Two transgenic lines were generated, SHR-TG10, which carried 6-8 transgenic copies of *Cd36* but did not show kidney transgene expression, and SHR-TG19, which carried a single transgene which was expressed at low levels in the kidney (Pravenec et al 2001b). Thus more than one *Gstm1* transgenic rat line may need to be generated before renal transgene expression is shown.

Alternative strategies to DNA pronuclear microinjection are also being considered for *Gstm1* transgenesis, a particularly promising technique is lentiviral vector transgenesis. Lentivirus vectors are engineered replication-deficient virus particles designed to deliver transgenes to replicating cells or embryos. They are well suited to transgenesis due to their ability cross cell and nuclear membranes and to integrate sequences into the host genome, they have been employed for transgenesis in several species including mice, rats, chickens, pigs, quail and cows (Park 2007). A particular advantage with respect to rat transgenesis is that lentiviruses are not injected into the embryo itself, rather they are introduced under the zona pelucida and mediate their own passage across the cell membrane and to the pronucleus, thus avoiding the problems associated with rat pronuclear injection. An alternative to microinjection in lentiviral transgenesis has also been employed whereby mice embryos were denuded of the zona pelucida and incubated in medium containing lentiviruses (Pfeifer et al. 2002). Transgenesis with lentiviral vectors has been demonstrated to be far more efficient than by DNA microinjection, in a recent study to generate transgenic rats expressing green fluorescent protein (GFP), 49.6% of microinjected embryos generated live births, of which 22% born to Sprague Dawley mothers and 14% born to Dahl S rats were transgenic (Michalkiewicz et al. 2007). The main disadvantages of lentiviral vectors are the size of transgenic insert that can be packaged by the virus, which is limited to approximately 10 kb, and the laboratory expertise required to grow and purify the vectors, though the Glasgow laboratory has extensive experience of these protocols. In initial studies with lentiviral vectors there were

also concerns that the efficiency of transgene insertion may slow the creation of fixed transgenic lines; multiple insertions throughout the genome resulted in variable copy numbers being transmitted to subsequent generations (Lois et al. 2002). However it has been shown that viral titres used for injections correlate with the number of genomic insertions in transgenic pups, reducing viral titres reduces the number of insertions (Michalkiewicz et al 2007).

Given the proposed kidney-specific effects of reduced *Gstm1* expression on hypertension in the SHRSP, it is worth considering a renal-specific promoter in *Gstm1* transgenesis. Gstm1 protein has been specifically located to the principal cells of the collecting duct by immunohistochemical colocalisation with aquaporin-2 (Aqp2) (McBride et al 2005), a 9.5 kb *Aqp2* promoter sequence has been used in mouse transgenesis to specifically direct GFP expression to principal cells of the collecting ducts in the cortex, outer and inner medulla (Zharkikh et al. 2002). In this study, GFP expression was upregulated by dehydration of the mice and no expression was observed in the adjacent intercalated cells in the collecting duct. An alternative kidney tubule-specific promoter has also been described, constituting 3.3 kb of the kidney-specific cadherin gene (*Ksp-cadherin*) upstream regulatory region. Transgenic mice expressing *LacZ* driven by the *Ksp-cadherin* promoter showed β-galactosidase expression exclusively in the kidney, specifically in the tubular epithelium of the inner medulla, the renal papilla and pelvis, and weakly in the cortex and outer medulla (Yang et al. 2006).

Once *Gstm1* transgenic SHRSP rats have been derived and confirmed by PCR, they will be subject to a number of experiments. Blood pressure will be measured by radiotelemetry and kidney GSH levels will be measured. The tissue-specific expression pattern of the transgene will be established by qRT-PCR or northern blotting and germline transmission of the transgene will be confirmed in future generations. Genomic copy number of the transgene will be assessed by southern blotting. Primary cell lines could also be derived from transgenic rats to assess *Gstm1* catalytic activity by total GST activity assays and with the proposed Gstm1-specific substrate 1,2-dichloro-4-nitrobenzene (DCNB) (Fujimoto et al 2006). Changes in renal and vascular oxidative stress levels will also be measured. Generation of a transgenic animal with altered expression of a candidate gene for a complex physiological trait is a critical test of its contribution to a disease phenotype; increased expression of *Gstm1* alone may not affect blood pressure in the SHRSP to a great extent, however as detailed above, numerous secondary phenotypes can also be measured.

7 General Discussion

The experiments performed in this project applied a wide range of functional genomic techniques in the investigation of hypertension in the SHRSP. The hypertension candidate gene *Gstm1* has been extensively examined with genome-wide expression profiling (which also implicated other GSH metabolism-related genes), promoter sequence analysis, and adenoviral *in-vitro* and *in-vivo* overexpression and knock-down experiments. Functional studies examined the effects of modulating *Gstm1* expression on *in-vitro* enzyme activities and *in-vivo* oxidative stress and NO bioavailability. Significant steps have also been taken towards the production of a transgenic SHRSP rat overexpressing *Gstm1*. Together, the strategies developed in these experiments represent a thorough approach to the assessment of a hypertension candidate gene.

Blood pressure QTL analysis by congenic breeding in rats has been established for many years (Rapp 2000), however, the success of this strategy alone for positive identification of blood pressure genes is probably limited to confirmation that *Cyp11b1* accounts for increased blood pressure in the DSS compared to the DSR under salt loading (Cicila et al 2001;Garrett et al 2003). This approach has otherwise been hampered by difficulties including the large numbers of genes under QTL peaks, epistatic interactions between QTLs and loss of phenotype in small congenic intervals (Rapp 2000;Saad et al. 2001;Dutil et al 2005). Combining congenic breeding with microarray expression profiling in the manner that led to the identification of *Gstm1* was therefore an important advance, and this approach was further extended by the data analysis techniques applied in this project. The finding presented here, that *Gstm1* expression is reduced in the SHRSP prior to the development of severe hypertension, was significant in determining that the reduced expression observed at 16 weeks of age (McBride et al 2003) was not secondary to high blood pressure and likely to be a causative factor in increased blood pressure. This observation is also corroborated by published data comparing gene expression between 3 week old SHR and WKY rats that showed reduced *Gstm1* expression in the SHR at this earlier timepoint (Seubert et al 2005). Though the differentially expressed GSH metabolism genes identified in microarray mRNA expression data were not confirmed by qRT-PCR, the finding that GSH levels may be affected by genetic elements from the 2c* congenic interval was also significant and demonstrates the value of metabolic pathway analysis by IPA. It is predicted that this type of analysis, where candidate genes are not necessarily considered in isolation, but as part of interacting pathways will become increasingly important in complex genetic research (Dominiczak et al 2005). Indeed, IPA software has been applied in published hypertension research in rat inbred models. For example, research in the Glasgow laboratory has implicated differential expression of *Edg1*

and *Vcam1* in salt-sensitive hypertension in the SHRSP, and IPA software provided a functional transcriptional network that implicated activation of *Edg1* in the expression of *Vcam1* via numerous cell signalling molecules and transcription factors (Graham et al 2007). The pathways, including elements such as platelet-derived growth factor-β (PDGFRB), protein kinase B (Akt1), PI3 kinase regulatory subunit 1 (PIK3R1), mitogen-activated protein kinase kinase kinase 8 (MAP3K8) and transcription factors such as NFκB1, MYC and CCAAT/enhancer binding protein-β (CEBPB) will be the subject of further research and are hoped to lead to the identification of novel biomarkers for salt sensitive hypertension (Graham et al 2007). In addition, IPA has also been applied in conjunction with Transfac promoter sequence analysis in the identification of functional networks of genes whose expression may be affected by the differential expression of transcription factors from hypertension QTLs (Joe et al 2005;Lee et al 2007).

Having established *Gstm1* as a robust hypertension candidate gene, the subsequent experiments were designed to analyse the molecular mechanisms behind its reduced expression in the SHRSP and its relation to oxidative stress. The co-incidence of reduced renal *Gstm1* expression and increased renal oxidative stress was an important result that, along with the identification of a coding mutation and 13 promoter polymorphisms in the SHRSP and SHR *Gstm1* promoter, contributed to a recent publication (McBride et al 2005). Significantly, reduced *Gstm1* expression was also demonstrated in SHRSP carotid arteries, which is also consistent with increased vascular oxidative stress in the SHRSP (McBride et al 2005).

Transfac promoter analysis was an invaluable tool in the identification of candidate transcription factors that may influence *Gstm1* expression. Of the potential transcription factors who's binding may be affected by SHRSP *Gstm1* promoter polymorphisms, PPARγ represents the strongest candidate since binding sites in both implicated clusters may be affected, and a precedent for PPARγ-mediated GST expression exists (Park et al 2004). If confirmed, this finding would increase the many roles for PPARγ in transcription regulation already proposed, including those in adipocyte differentiation (Tontonoz et al 1994), lipid metabolism (Motojima et al. 1998;Tordjman et al. 2003), renal sodium homeostasis (Guan et al 2005) and reduced renal NADPH oxidase activity (Hwang et al 2005). That PPARγ has a proven role in oxidative stress defence is significant in the light of the results presented here and is also corroborated by recent studies demonstrating that increased PPARγ expression facilitates recovery of cultured renal tubular epithelial cells after H_2O_2-induced injury (Sommer et al. 2007), and inhibits AngII synthesis in mesangial cells from SHR rats fed a high sodium diet (Efrati et al. 2007). However, the picture is

complicated by the recent publication that PPARγ upregulates renin expression via binding to a novel response element in the renin promoter (Todorov et al. 2007). Overall, the analysis of the *Gstm1* promoter warrants further study, it would be particularly informative to confirm the role of the putative ARE sequence, especially given that a functional ARE has not been described for the rat or mouse *Gstm1* promoter, despite the fact that the *Nrf2*-null mouse exhibits reduced *Gstm1* expression (Chanas et al 2002). It may be interesting to consider an electrophoretic mobility shift assay (EMSA)-led approach to promoter analysis in future studies. Such a methodology was applied in the investigation of reduced expression of *Anpep* in the kidneys of the DSS rat compared to the DSR (Farjah et al 2004), leading to the identification of a disrupted CEBPB motif in the DSR *Anpep* promoter (Kotlo et al. 2007a).

The adenoviral overexpression platform applied in this project proved extremely flexible for the cloning and construction of several viruses to modulate *Gstm* expression. The anti-*Gstm* family shRNA sequence was effective in the knockdown of genes against which it was fully aligned, the finding that target sequences differed from published gene sequences should be borne in mind in any future RNAi experiments. The hypothesis that reduced expression from the WKY Gstm1 virus in HeLa cells is due to differential binding of miR-10b is interesting but does not relate to the *in-vivo* differential expression of *Gstm1*, unless it is hypothesised that miR-10b is overexpressed in the SHRSP and that the 3'UTR SNP at +35 has no effect, in this case, any other miRNA that putatively aligns with the *Gstm1* 3'UTR is equally a candidate. The lack of increased NO bioavailability following *Gstm1* overexpression in the SHRSP carotid artery does not exclude a role for it in oxidative-stress defence or hypertension and further experiments to develop targeting gene expression vectors are underway.

The functional studies discussed above evaluated the effects of modulating *Gstm1* expression on *in-vitro* or intermediate phenotypes, these experiments could lend weight to the association of reduced *Gstm1* expression to hypertension. In contrast, the blood pressure of a transgenic SHRSP overexpressing *Gstm1* in the kidney would provide clearer evidence of the direct role played by this gene in hypertension. As discussed in chapter 6, these efforts are ongoing and may be extended to include lentiviral transgenesis.

Collectively, these expression, functional and transgenic approaches were applied to the investigation of a candidate gene identified via a QTL, congenic and mRNA expression profiling strategy. While this approach has yielded successes in the identification of genes that may contribute to complex disease states (Aitman et al 1999;Pravenec et al

2001b;Yagil et al 2005), several other studies have identified differentially expressed genes that on further analysis do not locate to minimal congenic intervals (Frantz et al. 2001;Moujahidine et al 2004;Garrett et al 2005). Hence there is considerable interest in a number of other high-throughput functional genomic techniques that are likely to play an important role in the continued search for genes, proteins and pathways affecting complex polygenic traits (Dominiczak et al 2005;McBride et al. 2006).

Our increasing understanding of the complexities of gene expression control and the improved cost-effectiveness of genetic and expression analysis has led to the advent of techniques such as genetical genomics, or expression genetics, where mRNA expression is treated as a phenotype in linkage analysis to locate eQTLs. As discussed in section 1.2.3.4, this technique has been applied in a panel of recombinant inbred strains to study a rat model of metabolic syndrome, identifying several *cis*- and *trans*- acting eQTLs and potential candidate genes (Hubner et al 2005). While *cis*-acting eQTLs are intrinsically easier to investigate since the elements that control their expression are likely to be within the gene itself or in nearby regulatory regions, *trans*-acting eQTLs often cluster to the same genetic location and point to potential major effect loci with central roles in metabolic pathways (Petretto et al. 2006). Thus this technique is potentially tremendously powerful provided experiments are appropriately designed and data is analysed correctly; the expression genetics field is in its early stages and tools for statistical data analysis and for translating findings into testable hypotheses in implicated pathways are still under development (Drake et al. 2006). Many of the concepts and approaches developed for linkage of gene expression to quantitative trait loci also applicable to analysis of the genetics of proteomic and metabolomic traits, as discussed below.

Proteomics, which involves the identification of polymorphic protein expression and isoforms between samples, is being increasingly applied in complex disease genetics research. Proteomic strategies are particularly useful because they allow researchers to assess the distribution and relative concentrations of proteins, which are the functional units of the organism that have the greatest direct effect on phenotype. A common strategy in proteomic experiments is to locate polymorphic protein spots following separation of proteins electrophoretically in 2 dimensions (by size and by isoelectric point) and to identify the proteins concerned by mass spectrometry and mass fingerprint analysis. One of the limitations of proteomic strategies in the past has been the reproducibility of techniques used to separate protein samples (McBride et al 2006), however advances such as 2 dimensional difference in gel electrophoresis (2D-DIGE), where samples to be compared are differentially labelled and separated on the same gel, help resolve this limitation. Such

a technique has examined the specific proteins expressed within inner-medullary collecting duct (IMCD) cells compared to inner-medullary non-collecting duct cells (Hoffert et al. 2004), and was also used to examine the regulation of proteins in IMCD cells following long-term administration of vasopressin (van Balkom et al. 2004). Proteomic strategies have also been combined with linkage analysis in some models, for example, Klose et al (2002) performed genetic analysis of the mouse brain proteome by comparing protein composition and genetic linkage data on a panel of mice from a backcross between two genetically divergent mouse species, *Mus musculus* and *Mus spretus.* They found that polymorphic proteins showed a high degree of allele-specific transmission, which was particularly evident in heterozygotes, and that variations in protein quantities and isoforms often mapped distant to their genomic coding location, an illustration of the many post-transcriptional and post-translational events that occur to a protein that are mediated by proteins encoded elsewhere in the genome (Klose et al. 2002).

Proteomic approaches have also been applied by colleagues in Glasgow examining human cardiovascular disease; urinary protein biomarkers were assayed in healthy individuals and patients with coronary artery disease (CAD) to distinguish a signature polypeptide pattern specific to CAD patients (Zimmerli et al. 2007). In this instance capillary electrophoresis and mass-spectrometry was applied to search for metabolomic markers of disease with potential clinical application, rather than to assay for genetically mediated differences in protein expression. However, metabolomic analysis has also been combined with genetic analysis to map the genetic determinants of different metabolite profiles in disease states. For example, proton nuclear magnetic resonance (^{1}H NMR) was recently applied in a study to compare the metabolite profile of an inbred rat model of diabetes, the Goto-Kakizaki (GK) rat, with the normoglycaemic BN (Dumas et al. 2007). Genotyping data was available on F_2 rats from a GKxBN cross (Gauguier et al. 1996); ^{1}H NMR spectra were obtained for plasma samples of a subset of these animals and linked to their genotype data to examine the genetic influence of metabolite levels. Metabotypic QTLs for proline and tyrosine on Chromosome1 and glucose on chromosomes 5 were validated by the examination of the plasma metabolite profiles of congenic strains harbouring the appropriate alleles at each locus. The metabotypic QTL with the highest LOD score (13.7) was examined in greater detail, revealing that increased plasma benzoate concentration was associated with GK alleles at a locus encoding several uridine diphosphate-glucuronosyl-transferase (UGT) enzymes, the expression of one of which (*Ugt2b*) was found to be reduced 78-fold in the GK compared to the BN. Benzoate is a gut microbial degradation product that is metabolised via conjugation reactions catalysed by UGT enzymes, thus

while the significance of this finding to diabetes is unclear (indeed, the same allele at this locus in the GK rat is shared by the WKY). This emphasizes the utility of genetic analysis of metabolomic data by uncovering a genetic polymorphism affecting a mammalian/bacterial symbiotic relationship (Dumas et al 2007).

Traditional QTL mapping typically identifies large genomic regions encompassing several potential candidate genes, and strategies such as congenic and subcongenic breeding followed by substitution mapping can reduce the implicated region but are laborious. Increasing marker density for genetic mapping only moderately improves QTL resolution (Rapp 2000), the main limitation being the limited opportunity for recombination by the F_2 generation, when most genome-wide scans are performed. This experimental design is typically necessitated by the cost of breeding and housing large numbers of animals (particularly for rats), and the expense and poor coverage of traditional genotyping methods; this subsequently leads to the situation where only large-effect QTLs reach statistical significance. A recent landmark study addressed these issues by breeding a population of 'heterogeneous stock' mice in 50 generations from 8 inbred progenitor strains (Valdar et al. 2006). Over 2000 mice were genotyped at 13549 SNPs and phenotyped for 101 phenotypes varying from body weight, immunological marker antibody staining, glucose tolerance testing, blood count to behavioural traits such as startle response, anxiety measurements and activity. Using bespoke statistical analysis techniques they identified 843 QTL peaks that exceeded the significance threshold for 97 of the phenotypes, only 1% of which individually accounted for more than 5% of phenotypic trait variance. Thus each of the traits examined appear to be under the influence of a large number of small effect QTLs, and the analysis accounted for an average of 73% QTL-based additive variance in phenotype for all traits (as a percentage of the pedigree-based variance), leaving considerable scope for epistatic and environmental factors to affect phenotype. Of 40 previously described QTLs from traditional QTL mapping in the parental strains, between a third and half mapped to the same location in this study. The challenge of gene identification at the QTLs identified remains, there were an average of 27 genes within the 95% confidence interval of the QTLs identified (Valdar et al 2006), however this study is particularly significant for the possible implications on the analysis of human complex genetic diseases. As with any novel analytical technique, the robustness of the statistical methods applied by Valdar et al remains to be proven (Darvasi 2006), however it is important to reemphasize that the population used in this study was derived from 8 founder inbred strains, thus in human populations that are on the whole considerably more outbred,

QTLs may exhibit even smaller effects on complex traits, requiring extremely large experimental groups to identify all but the largest effect alleles.

The last year has seen the publication of risk loci for a number of human complex diseases following genome wide association studies in large populations. Risk loci have been identified for six of the 7 diseases studied by the Wellcome Trust Case Control Consortium (WTCCC), including bipolar disorder, coronary artery disease, Crohn's disease, rheumatoid arthritis and type 1 and 2 diabetes (The Wellcome Trust Case Control Consortium 2007), and further loci have been identified for obesity (Frayling et al. 2007), prostate cancer (Gudmundsson et al. 2007) and others. However, the odds ratios associated with the risk alleles at these loci are modest, (between 1.2 and 1.7). While disease risk odds ratios and trait variance are not directly comparable, the low odds ratios associated with the disease risk loci mirror the low phenotypic variance explained by a majority of the QTLs identified by Valdar et al, leading to the conclusion that in animals and humans any given continuous trait is likely to be governed by allelic variants at very few (if any) large effect loci, some with intermediate effect, and many with small effects.

An example of a complex trait for which large-effect alleles have been identified is high-density lipoprotein cholesterol (HDL-C) levels in humans; candidate gene investigations have demonstrated that small number of rare SNPs contribute to low HDL-C levels and multiple mildy-penetrant alleles are concluded to account for a remainder of the phenotype (Cohen et al. 2004). Hypertension was the only condition for which a risk locus was not identified above the significance threshold in the WTCCC study. As discussed in section 1.1.4.3 there are a number of plausible explanations for this, not least the likely incidence of hypertension in the unphenotyped control population (The Wellcome Trust Case Control Consortium 2007). With this in mind, the discussion above points to the possibility that essential hypertension too is caused by the cumulative effects of many small-effect loci in most cases. This is not to detract from the importance of genetic studies in models of complex disease, identification of robust candidate genes and pathways will shed light on the physiological pathways of blood pressure control that are applicable to humans.

In addition to the recent methodological advances that have contributed to our understanding of complex genetic traits, a number of important findings regarding the fundamental mechanisms of genomic organisation, gene expression and inheritance are also likely to have an impact on genetic hypertension research in the near future. Data from phase I of the HapMap project (The International HapMap consortium 2005) has already proved invaluable for the design and interpretation of genome-wide scans through the

information it provides on the haplotypes associated with alleles at tagging SNPs. The recent release of phase II of HapMap, with a SNP density of approximately one per kilobase, allows for improved haplotype tagging and has also revealed insights into genome-wide recombination rates. For example, the locations of several recombination hotspots have been confirmed and it is estimated that they account for approximately 60% of all recombination, despite covering just 6% of the genome. Furthermore, recombination rates were shown to be lower in transcribed regions overall, while rates varied by gene class, with defence and immunity genes showing the highest recombination rates (The International HapMap consortium 2007). Another international collaborative project has recently provided fascinating insights into the regulation and extent of transcription in humans. The pilot phase of the encyclopaedia of DNA elements (ENCODE) project analysed 1% of the human genome, assessing transcription and chromatin structure and applying comparative sequence analysis to gauge the extent to which transcriptionally functional sequences are conserved across evolution (Birney et al. 2007). Unexpectedly, they showed that 80% of the analysed sequence is transcribed, despite the fact that only 2% encodes protein. Even after accounting for known functional non-coding RNAs such as siRNAs and miRNAs, vastly more of the genome appears to be transcribed than previously thought. It is possible that RNA polymerase 'reads through' the template during transcription, but the ENCODE investigators also showed that many of the unexpected transcripts are derived from regions of the genome previously thought to be transcriptionally silent. In another surprising finding, they showed that approximately 50% of functional sequences (i.e. those directing transcription) were not well conserved in comparisons with 20 other mammalian species, while approximately 40% of well conserved sequences did not appear to be functional in humans. The latter observation may be explained by the limited cell types used in the ENCODE study, expression analysis in different cell types may yield many more functional sequences. But the non-conservation of functional sequence is intriguing; ENCODE authors and commentators have speculated that the a more detailed examination of such divergent sequences may be necessary to locate the critical, well conserved bases that are presumably central to transcription factor binding at these locations (Birney et al 2007;Greally 2007;Henikoff 2007).

The preliminary results of the ENCODE project therefore confirm the complexity of genomic organisation and highlight our incomplete understanding of the mechanisms that underlie expression and phenotypic variance. A number of other studies have also recently shed light on mechanisms affecting gene expression and expression of complex traits, including copy number variation, miRNAs, heritable epigenetic influences on gene

expression, and the influence of the mitochondrial genome. Duplications and deletions arising commonly through unequal crossover during cell replication give rise to copy number variations (CNVs) in genes and genomic regions. Though the focus of genetic research has concentrated on SNP variation, there is increasing recognition that CNV also affects phenotype. Genome-wide studies have demonstrated that up to 12% of the human genome is affected by copy-number variation in genetic segments down to 1 kb in size (Redon et al. 2006), while larger rearrangements (from 40 kb) affect approximately 3% of the genome (Wong et al. 2007), several hundred genes and disease loci are therefore potentially affected by CNV. Variation in gene copy number may affect phenotype by causing a direct relative change in protein levels, or by affecting regulatory regions. Despite widespread deletion and duplication, it is interesting to note that single-nucleotide variations have been shown to account for over 80% of variation in gene expression, with CNVs accounting for less than 20% (Stranger et al. 2007). Nevertheless, CNV has been shown to affect disease phenotype in numerous monogenic diseases (reviewed by Inoue et al. 2002), and low copy number polymorphisms in the constant fragment (Fc) receptor γR3-related sequence (*Fcgr3-rs*) in rats and the orthologous *FCGR3B* gene in humans have been shown to cause predisposition to macrophage-dependent autoimmune glomerulonephritis (Aitman et al. 2006).

The role of miRNA in the regulation of gene expression has attracted considerable research interest, revealing insights into developmental processes (Zhao et al. 2007), tumour classification in cancer research (Lu et al. 2005), and stem cell division (Hatfield et al. 2005). The ability of miRNAs to affect the expression of complex traits is considered all the more likely since they are known to target multiple mRNAs (Lim et al. 2005), indeed genome-wide expression profiling of miRNAs in patients with heart disease (ischaemic cardiomyopathy, dilated cardiomyopathy and aortic stenosis) revealed disease-specific miRNA expression patterns particular to each condition compared to healthy controls (Ikeda et al. 2007). The impact of non-coding RNAs on gene expression has also been demonstrated in epigenetic research. Epigenetics is the study of chromatin modifications that affect gene expression. Classically, the inheritance of epigenetic modifications was thought to be restricted to somatic cell divisions, though transgenerational epigenetic modifications are known to occur in plants (Chandler et al. 2000), a recent study showed that RNA-mediated epigenetic changes can also be transmitted to offspring in mice (Rassoulzadegan et al. 2006), thus adding to the list of functions ascribed to non-coding RNAs.

Several studies have examined the relative paternal or maternal contributions to the heritability of blood pressure, some showing a bias towards paternal transmission (Uehara et al. 1998) while others suggests a maternal bias that could implicate variants in the mitochondrial genome (Destefano et al. 2001;Sun et al. 2003;Yang et al. 2007). However, it is acknowledged that exclusive maternal influences also include the *in-utero* environment which has been shown to affect other complex traits such as diabetes (Fetita et al. 2006) and lipoprotein levels (Bansal et al. 2005), making the direct influence of the mitochondrial genome difficult to quantify. Examples of rare mitochondrial mutations that cause hypertension (Wilson et al 2004) and diabetes (Maassen et al. 2005) have provided indirect evidence of a role for the mitochondrial genome in complex diseases, but variations in copy number and tissue distribution of mitochondrial mutations make experimental investigations extremely challenging. Thus the recent development of conplastic rat strains that are of identical nuclear genotype but carry mitochondria from different strains (Pravenec et al. 2007), is extremely valuable. Pravenec et al developed rat strains carrying the SHR nuclear genome and mitochondria derived either from the SHR or BN and showed significant differences between the two strains in glucose tolerance, muscle glycogen levels and muscle ATP levels. Sequence differences between the two mitochondrial genomes were also detected in several genes, providing candidates for further investigation (Pravenec et al 2007).

This discussion has outlined many recent methodological developments and advances in our understanding of gene expression and inheritance that are likely to impact the search for causative loci (genes *and* expressed non-coding sequences) in complex diseases such as essential hypertension. The utility of advanced strategies such as IPA and shRNA-expressing adenoviruses has been demonstrated by work performed in this project which has used a range of techniques to examine a robust hypertension candidate gene. While the role of reduced *Gstm1* expression in hypertension in the SHRSP is still to be fully elucidated, significant progress has been made in the development of many tools to study its function. These approaches can also be applied in the analysis of other candidate genes in the future. The advances discussed above can be applied in conjunction with inbred models of disease such as the SHRSP and congenic strains; candidate genes and pathways identified by such studies can be investigated using many of the techniques applied in this work; in this manner we are very likely to make considerable strides in our understanding of conditions such as hypertension that will aid in the development of new therapies and preventative strategies in the near future.

Appendix

Primer Name	Sequence
***Anpep* coding sequence primers**	
Anpep1F	CTCCCTGCCCACCAGCATCA
Anpep2R	CCATTGATGAGGGCCATGGT
Anpep3F	GACCCTTCAGGAAGATCCTT
Anpep4R	TTGAGATACGGAATGGGCAC
Anpep5F	AGTGAGCACCATCATGGACC
Anpep6R	TCACCACAGTTGCTTTCCGG
Anpep7F	AGTGGTCTCGAAGAGTGTAG
Anpep8R	GATAGTCATAGGCGTCACGC
ANPEPcDNA1F	GTTAGGTGTGGCAGCCGTAT
ANPEPcDNA1R	GATGTTAGGTGCCGGAGTGT
ANPEPcDNA2F	TACCCGACTCCTACCAGGTG
ANPEPcDNA2R	CTCATCAAGCAAGGAAAGG
ANPEPcDNA3F	ACACTCCGGCACCTAACATC
ANPEPcDNA3R	CTTGCAGAGCGTAATCACCA
***Anpep* promoter sequence primers**	
ANPEPup1F	CAGGGTGACAGGAACCCTAA
ANPEPup1R	GTTCCCCAGCCTTTATCTCC
ANPEPup2F	GAAGAATCAGATGGGCTGGA
ANPEPup2R	TTGCCCTCTGCTCTCTATCC
ANPEPup3F	CCCGAGTTCTATGGAGCAAA
ANPEPup3R	GCACGGGATAGATGACTGCT
ANPEPup4F	GGTGGAGCCAGTGTGCTTAT
ANPEPup4R	CACCTGGTAGGAGTCGGGTA
ANPEPup5F	CATCAGCCCAGACCTGATAG
ANPEPup5R	GTCGGGATGGACTGGACATA
ANPEPup6F	TTCTCAAAGGCCCAGAGGTA
ANPEPup6R	CAGGACCTTTTCCTCTCACG
ANPEPup7F	GGCTCATGTGTTTCCCCTTA
ANPEPup7R	GCACGGGATAGATGACTGCT
***Gclm* Coding sequence primers**	
GCLM1F	CAGCGGTCTTCCCGCCTGCC
GCLM2R	ACATTCACGCCTCAGTGACG
GCLMcDNA3F	AAAGTGTCCGTCCACGCACA
GCLMcDNA3R	CTGTTTAGCAAATGCAGTCA
GCLMcDNA4F	TTGCTATAGGCACCTCGGAT
GCLMcDNA4R	ATTCACGCCTCAGTGACGCT
GCLMcDNA5F	CACTGTGGCTGCTGAGGTAC
GCLMcDNA5R	CTCTTCCAGTATGTCTTAAC
***Gclm* Promoter sequence primers**	
GCLMup1F	CGGCCAAGTGAGAGGAATAG
GCLMup1R	GAGGCCACAGGACATGAGAT
GCLMup2F	TTTGAGGGCTGGAGATGTTC
GCLMup2R	AGGTATGTCGGAGCCAGATG
GCLMup3F	CTTCTGGGAAACCTTTGCTC
GCLMup3R	CAAAAGGACAGCCAGAGGTC
GCLMup4F	AAGCAAAGCAAAGCAAAGGA
GCLMup4R	CGTGGACGGACACTTTTTC
GCLMup5F	GCATTCCTGATAGGAGTTTG
GCLMup5R	CATTTGGGAGGCAGAGCTGT
GCLMup6F	CACCACTGCCTGGAGGCTAAACT
GCLMup6R	AAAGGCCTAAGCCCATGAAT
GCLMup7F	GGGCTGTGCACAACAAATAC

Table A1 – Continued overleaf

Primer Name	Sequence
GCLMup7R	CGCTTGCCTGCTTCTATTTC
GCLMup8F	GAAATCAACACGCTGGGAGA
GCLMup8R	GTCGCTGCGGTTTTTGAGGC
GCLMup9F	AGGCCTTTCTCTCGAAGGAT
GCLMup9R	ACCCGAGAAAGTGCTTCGTA
GCLMup10F	CGCCGTCAGCTCTTACCAG
GCLMup10R	AGCTCACCGCGGTATCTCTA
GCLMup11F	CGGGAACCTGCTCAACTG
GCLMup11R	TTGTCCCGAATCCAATTCA
***Ggt1* coding sequence primers**	
GGT1AF	CAGCCTAGCTGGACCTCTTG
GGT1AR	ACGTGGGCATTAATGAGTCC
GGT1BF	AAGCGTTGCTCAGAGATTGG
GGT1BR	GGCCAACTTCGGCATAGTTA
GGT1CF	GCAAGAGCCTTGGACAAAAA
GGT1CR	TTGGGTGAGTGGTTTCATCA
GGT1DF	TCCGCAACATGAGTTCTGAG
GGT1DR	GTATGGTGGTGCCGAGTCTT
***Them4* coding sequence primers**	
THEM4cDNA1F	TGGTTGAGAGGACATTGCAG
THEM4cDNA1R	GTGATGTCGATGATGGTTGC
THEM4cDNA2F	AGGCTTTGAGTACGCGATGT
THEM4cDNA2R	TCAGCAGCTGTGACAGGAGT
THEM4cDNA3F	GGTGAGTTCCACACCGTTCT
THEM4cDNA3R	GCAATGAGCTGTGTTCCTGA
THEM4cDNA4F	TCCACAGAGCGTTGAGTGAC
THEM4cDNA4R	GAAAGCTGGATGCTTCCTTG
***Them4* promoter sequence primers**	
THEM4upAF	GCCTCCAACGAAAGAGAAAA
THEM4upAR	TCAGGGCTTCAGGGATATTG
THEM4upBF	CAATATCCCTGAAGCCCTGA
THEM4upBR	GTACATGGGTTCGTGTGTGG
THEM4upCF	TGTCTCCTAGTCCCCAATGC
THEM4upCR	TCTCTAGGCTGGCATGGTCT
THEM4upDF	TGGAACTGGAATTGCAAACA
THEM4upDR	TAAAGGGAGCCTGTTTCACG
THEM4upEF	GTGCACCCTTCGACAGAAAT
THEM4upER	CTGCAATGTCCTCTCAACCA
THEM4upFF	TGATGATGTCTTGACTGCTCCT
THEM4upFR	CTGCAGAAGGCCAGAGTTTT
THEM4upGF	TGCCATGGAAAAGGGAGTTA
THEM4upGR	GTACATGGGTTCGTGTGTGG
THEM4upHF	TGTCTCCTAGTCCCCAATGC
THEM4upHR	GCTGGAGAGATGGTTCACAAG
THEM4upIF	TGGAACTGGAATTGCAAACA
THEM4upIR	TCTCTAGGCTGGCATGGTCT
***Slc7a12* coding sequence primers**	
Slc7a12AF	ACACAAATTGACAGAGAAGC
Slc7a12BR	AGGAAAGACTCTGTTCATCC
Slc7a12CF	GAAATAAAAAGGCCAGCTGA
Slc7a12DR	TGTAGGACCAACGGCTTCCC
Slc_1F	CACCATTGGTACAGGGATTT
Slc_1R	AAAAAGGAGAACGTGTCCAG
Slc_2F	CTAACTGGAATTGTGGTGC
Slc_2R	CAGTAGTAGCTGACTTACAGGC
Slc_3F	AGTAGTAGCTGACTTACAGGCT
Slc_3R	CGTTGGTCCTACAAAGGT

Table A1 – Continued overleaf

Primer Name	Sequence
***Slc7a12* promoter sequence primers**	
slc7a12_UP_1F	CAGTTGAAATGCATGGCTGA
slc7a12_UP_1R	GCATCTCATCTTGATGTCCTGA
slc7a12_UP_2F	TTTGGCAGAAGCCAGAACAT
slc7a12_UP_2R	TGCTGGGCAATACATGTCAG
slc7a12_UP_3F	GCGTGTGTGTGTGTGTGTGT
slc7a12_UP_3R	TTCTCCCTCCCTTTTTCACC
slc7a12_UP_4F	GGCTCTTCTGCTCTGCTTGT
slc7a12_UP_4R	TTGGAGCCTCCCATAAAATG
slc7a12_UP_5F	AGTGGGGAGAGGGAACTTGT
slc7a12_UP_5R	TCTGCTGGCTCTTGTCTTCA
slc7a12_UP_6F	TCTTGGACACTGAACCACCA
slc7a12_UP_6R	TGCATGGTTATGCCTTTTTG
***Gstm1* promoter sequence primers**	
Gstm10R	CCGCGGACGTTCCAGTATCC
Gstm11F	AGTCTCCAGGGAAAGTGCTAG
Gstm12R	CTGTTCTACACACCCTGAAAGC
Gstm13F	ACAGAAGGACTGAGTTCCCAA
Gstm14R	CAGGAACAGTTGGCGACATGG
Gstm15F	CCCAGGATAACCTGAATTTGAG
Gstm16R	AGGACACAAGGAGCCCAAAGC
Gstm17F	GGTGACACACTGGCTTCATAC
Gstm18R	CAAATGACTGACGAGGAGACT
Gstm19F	CTCTGGCTCCCTTCCAGGCCC
Gstm20R	CGCATCAGCACATTTTCATGC
Gstm21F	GATTATTCCTGCACAGTGTCC
Gstm22R	TGTCCTGGAGAATTCAATCCC
Gstm23F	GGTTCAGCACAACACAACACG
Gstm24R	CTCTGCCCCATTGAGGCTCTC
Gstm25F	CCTTCTCCTTCCCCTTTATCC
***Gstm1* coding sequence primers**	
Gstm1F	CAAATTGAGAAGACCACAGC
Gstm2R	AAGAGGGAGTATCGAACTCAG
Gstm3F	TTTGAGCCCAAGTGCCTGGA
Gstm4R	GCAGGATCCAATGTGGATAG
***Gstm1* promoter sequence cloning primers**	
Gstm1-1R	CCCCTCGAGGGTTCTGGCGCTGTGGTC
Gstm1-0.9F	CCCACGCGTTTGTGTCCTGTGCAGAGTGTT
Gstm1-1.6F	CCCACGCGTCTCTGAGCCCTTTGTTCTGG
Gstm1-2.2F	CCCACGCGTGGAAGGTTGGAAACCACTGA
Gstm1-2.5F	CCCACGCGTGTGAGCTGGCCACGTCTTAG
RV3F	CTAGCAAAATAGGCTGTCCC
GL2R	CTTTATGTTTTTGGCGTCTTCC
T7F	GTAATACGACTCACTATAGGGC
T3R	AATTAACCCTCACTAAAGGG
Site directed mutagenesis primers	
SNP8F	CCTTGTGAAGGTTATGCCACAGGACATATATCC
SNP8R	GGATATATGTCCTGTGGCATAACCTTCACAAG G
SNP9F	CAATTAACCACAAGCCTCTTGGTTATGGAAG
SNP9R	CTTCCATAACCAAGAGGCTTGTGGTTAATTG
SNP10+11F	TTTAGTCTCCTCGTCCCGTCATTTGTTTTTCA
SNP10+11R	TGAAAAACAAATGACGGGACGAGGAGACTAAA
SNP12F	TGCCCTTTGACCCGTAAACTGTTTTTAGTC
SNP12R	GACTAAAAACAGTTTACGGGTCAAAGGGCA
Adenoviral shuttle plasmid cloning and sequencing primers	
Gstm1HindIIIF	CCCAAGCTTCAAATTGAGAAGACCACAGC

Table A1 – Continued overleaf

Primer Name	Sequence
Gstm4aXbaI	CCCTCTAGACCTGCAGGATCCAATGTGG
mCMVpF	GTGGGAGGTCTATATAAGCAGAGCTCG
polyAR	TTAAAAAACCTCCCACACCTCCCCC
pSilencer CMV1.0F	GGATTTCCAAGTCTCCAC
pSilencer CMV1.0R	AGCACCTTCCAGATCTGC
shRNA target sequence primers	
Gstm1 Ex3F	TGCTGGTCTCCCTCTAGCTG
Gstm1 Ex3R	ACAGCCCATCACAGAAACAC
Gstm2 Ex3F	TTGAATTTTGGAGGGCTGAC
Gstm2 Ex3R	CTGGGTGAGGATAGACATGG
Gstm3 Ex3F	AACCCTTGATGGTGTGGTGT
Gstm3 Ex3R	AGCCCATCACAGAAAGATGG
Gstm5 Ex3F	TCTCCAGTCAGCTGGGAACT
Gstm5 Ex3R	TCAGAGACCTGGCTAGCAACT
Gstm7 Ex3F	GGTCCCCTTCCTGTTGAAAT
Gstm7 Ex3R	CATTCATCGTGGCTAGCATG
pEF1/*Myc*-HisA sequencing primers	
pEF1 T7F	TAATACGACTCACTATAGGG
BGH PolyAR	TAGAAGGCACAGTCGAGG
BAC transgenic screening primers	
pBACT7R	CGCTAATACGACTCACTATA
90M3-3F	TTACCATTAGCATGATACAAG
pBACSp6F	GACATTTAGGTGACACTATA
90M3-1R	GCCTTGAGTTGCGTCATTAAG
pBAC-1R	CCGCTGCTTCACCTATTCTC
pBAC-2F	TTCTTCTTTGCTTCCTCGCC
pBAC-3R	CCAACCAGAACACGATAATCAC
pBAC-4F	ACATACGCTCAATACTCAACC
Gstm10	CCGCGGACGTTCCAGTATCC
Gstm1	ACAGAAGGACTGAGTTCCCAA
Linear fragment transgenic screening primers	
pEF1_Gstm1cDNA_1F	GCCAGATATACGCGTTGACA
pEF1_Gstm1cDNA_1R	ACCACACACGGCACTTACCT
pEF1_Gstm1cDNA_2F	TTTGCCCTTTTTGAGTTTGG
pEF1_Gstm1cDNA_2R	GGCCCAGTTTGAACTTCTCA
pEF1_Gstm1cDNA_3F	GACCCAAGCTGGCTAGGTAA
pEF1_Gstm1cDNA_3R	TGAGATGAGTTTTTGTTCGAAGG

Table A1 – Primer sequences

Probe Set ID	GeneChip Array	Gene Title	Location
L07281_at	U34A	carboxypeptidase E	16p13
rc_AA799448_g_at	U34A	Transcribed locus, strongly similar to NP_084275.3 limb-bud and heart [Mus musculus]	---
rc_AI014135_g_at	U34A	Mss4 protein	13q13
rc_AI232192_s_at	U34C	gamma-glutamyltransferase 1	---
rc_AI232402_at	U34C	---	---
rc_AI233164_i_at	U34C	---	---
rc_AI180260_at	U34C	synaptic vesicle glycoprotein 2b	1q31
rc_AA875269_at	U34A	stearoyl-Coenzyme A desaturase 2	1q54
rc_AI043990_at	U34B	Transcribed locus	---
rc_AI236231_at	U34C	NAD(P)H:quinone oxidoreductase type 3, polypeptide A2 (predicted)	13q13
rc_AI044292_s_at	U34B	---	---
rc_AI233127_at	U34C	Similar to CDNA sequence BC036333 (predicted)	16q12.4
rc_AI071578_g_at	U34C	Neuronal regeneration related protein	18p12
L46791_at	U34A	carboxylesterase 3	19p11
rc_AI111561_at	U34C	Transcribed locus	---
rc_AA997142_at	U34B	Them4	2q34
J02810mRNA_s_at	U34A	glutathione S-transferase, mu 1	2q34
X04229cds_s_at	U34A	glutathione S-transferase, mu 1	2q34
H32189_s_at	U34A	glutathione S-transferase, mu 1	2q34
AA801165_at	U34C	histone 2, H2aa (predicted)	2q34
rc_AI060176_at	U34B	Similar to solute carrier family 7 (cationic amino acid transporter, y+ system), member 12	2q23
rc_AA924865_at	U34B	similar to RIKEN cDNA 2900010J23	3p11
AF007758_g_at	U34A	synuclein, alpha	4q24
rc_AI009183_s_at	U34B	alkaline phosphatase, tissue-nonspecific	5q36
rc_AI073168_at	U34C	---	---

Table A2 – Continued overleaf

Probe Set ID	GeneChip Array	Gene Title	Location
rc_AI070350_at	U34C	deleted in polyposis 1-like 1 (predicted)	7q11
rc_AI235320_at	U34C	aconitase 2, mitochondrial	1q13 or 20q11
rc_AA893148_at	U34A	solute carrier family 22 (organic cation transporter), member 13 (predicted)	8q32
S56937_s_at	U34A	UDP glycosyltransferase 1 family, polypeptide A1, A6, A7, A8, A2, A4, A11, A5	9q35-q36 /// 9q35
D38065exon_s_at	U34A	UDP glycosyltransferase 1 family, polypeptide A1	9q35-q36

Table A2 – Differentially expressed probesets implicating the 2c* congenic interval at 5 weeks of age
Probesests consistently differentially expressed in renal gene expression microarrays in comparisons between the WKY and SHRSP and between the 2c* and SHRSP at five weeks of age.

Probe Set ID	GeneChip Array	Gene Title	Location
H32189_s_at	U34A	glutathione S-transferase, mu 1	2q34
J02810mRNA_s_at	U34A	glutathione S-transferase, mu 1	2q34
rc_AA894148_s_at	U34A	---	---
X04229cds_s_at	U34A	glutathione S-transferase, mu 1	2q34

Table A3 – Differentially expressed probesets implicating the 2c* congenic interval at 16 weeks of age
Probesests consistently differentially expressed in renal gene expression microarrays in comparisons between the WKY and SHRSP and between the 2c* and SHRSP at five weeks of age.

Probe Set ID	GeneChip Array	Gene Title	Location
AF004017_at	U34A	solute carrier family 4, member 4	14p22
D28557_s_at	U34A	cold shock domain protein A	4q42
J02585_at	U34A	stearoyl-Coenzyme A desaturase 1	1q54
J04035_at	U34A	elastin	12q12
L19998_at	U34A	sulfotransferase family 1A, phenol-preferring, member 1	---
rc_AA892750_at	U34A	regulator of G-protein signaling 1	13q21
rc_AA945611_at	U34A	ribosomal protein L10	Xq37
rc_AI029920_s_at	U34A	insulin-like growth factor binding protein 5	9q33
rc_AI231472_s_at	U34A	collagen, type 1, alpha 1	10q31
S60054_s_at	U34A	renin 1	13q13
S77528cds_s_at	U34A	CCAAT/enhancer binding protein (C/EBP), beta	3q42
X05834_at	U34A	fibronectin 1	9q33
X55183_at	U34A	amphiregulin	14p22
X56325mRNA_s_at	U34A	hemoglobin alpha, adult chain 1 /// hemoglobin alpha 2	10q12
X76489cds_g_at	U34A	CD9 antigen	4q42
X81449cds_g_at	U34A	keratin complex 1, acidic, gene 19	10q32.1
AFFX-BioDn-5_at	U34B	dethiobiotin synthetase	---
rc_AA849965_at	U34B	calcium binding protein 39 (predicted)	9q35
rc_AA850038_at	U34B	Nuclear receptor subfamily 2, group F, member 2	1q31
rc_AA851497_f_at	U34B	hemoglobin alpha, adult chain 1 /// hemoglobin alpha 2 chain	10q12
rc_AA899197_at	U34B	poly(A) binding protein, cytoplasmic 1	7q22
rc_AA899590_at	U34B	ribonucleotide reductase M2	6q16
rc_AA901342_at	U34B	claudin 11	2q24
rc_AA925340_at	U34B	ubiquitin-conjugating enzyme E2N	4q12
rc_AA925364_i_at	U34B	---	---
rc_AA943281_at	U34B	Transcribed locus	---

Table A4 – Continued overleaf

Probe Set ID	GeneChip Array	Gene Title	Location
rc_AA944180_at	U34B	similar to Cyclin-dependent kinases regulatory subunit 2 (CKS-2)	17p14
rc_AA955914_i_at	U34B	fibrillarin (predicted)	1q21
rc_AA957296_at	U34B	CTD (carboxy-terminal domain, RNA polymerase II, polypeptide A) small phosphatase-like (predicted)	8q32
rc_AA996628_at	U34B	papillary renal cell carcinoma (translocation-associated) (predicted)	2q34
rc_AA996710_at	U34B	zinc finger, BED domain containing 3 (predicted)	2q12
rc_AA997684_at	U34B	Procollagen, type VIII, alpha 2 (predicted)	5q36
rc_AI013050_at	U34B	SRY-box containing gene 4 (predicted)	17p12
rc_AI044100_at	U34B	---	---
AFFX-BioDn-5_at	U34C	dethiobiotin synthetase	---
rc_AA818949_at	U34C	similar to DnaJ (Hsp40) homolog, subfamily B, member 12	20q11
rc_AA859323_at	U34C	similar to spinster-like protein (predicted)	10q24
rc_AI071738_at	U34C	Transcribed locus	---
rc_AI071887_at	U34C	Transcribed locus	---
rc_AI072107_at	U34C	---	---
rc_AI072144_at	U34C	A kinase (PRKA) anchor protein 2 (predicted)	5q24
rc_AI073081_at	U34C	low density lipoprotein receptor-related protein 6 (predicted)	4q43
rc_AI104996_at	U34C	LOC499304	---
rc_AI176294_at	U34C	small nuclear ribonucleoprotein D2 (predicted)	1q21
rc_AI177902_s_at	U34C	polymerase (DNA-directed), delta interacting protein 2	10q25
rc_AI178901_at	U34C	Transcribed locus	---
rc_AI178966_at	U34C	delta sleep inducing peptide, immunoreactor	Xq35
rc_AI180353_at	U34C	lysyl oxidase-like 2 (predicted)	15p11
rc_AI180373_at	U34C	mitogen activated protein kinase kinase kinase 1	2q14
rc_AI227643_at	U34C	similar to olfactomedin-like 1 /// olfactomedin-like 1 (predicted)	1q33

Table A4 – Continued overleaf

Probe Set ID	GeneChip Array	Gene Title	Location
rc_AI228159_at	U34C	similar to HECT domain containing 1	6q22
rc_AI229785_at	U34C	keratin complex 1, acidic, gene 19	10q32.1
rc_AI231339_at	U34C	6-phosphogluconolactonase (predicted)	16p14
rc_AI231350_at	U34C	Dual specificity phosphatase 6	7q13
rc_AI233200_at	U34C	Synaptonemal complex protein 3	7q13
rc_AI235186_i_at	U34C	---	---
rc_AI235284_at	U34C	CD99	---
rc_AI235749_at	U34C	similar to tensin	9q33
rc_AI236668_at	U34C	ectonucleoside triphosphate diphosphohydrolase 5	6q31
rc_AI237606_at	U34C	B-cell leukemia/lymphoma 6 (predicted)	11q23

Table A4 – Differentially expressed probesets implicating the 2c* congenic interval between 5 and 16 weeks of age
Probesests consistently differentially expressed in renal gene expression microarrays in comparisons between 5 week old and 16 week old 2c* rats and between 5 week old and 16 week old WKY rats

SNP	Strain	Matrix Identifier	Position	Strand	Matrix match	Core match	Matrix sequence (+ strand)	Factor name
SNP1+2	WKY	V$HOX13_01	49	(+)	1	0.9	tgggagggacctCATTAttttgtccggccc	Hox-1.3
SNP1+2	SHRSP	V$HTF_01	49	(+)	0.849	0.804	tgggagggaCCCGTtattttgtcc	HTF
SNP1+2	SHRSP	V$NFKB_C	50	(-)	0.76	0.714	gggaggGACCCg	NF-kappaB
SNP1+2	WKY	V$T3R_01	50	(-)	0.8	0.839	gggagGGACCtcatta	v-ErbA
SNP1+2	SHRSP	V$CMYB_01	51	(+)	0.895	0.817	ggagggacccGTTATttt	c-Myb
SNP1+2	SHRSP	V$GFI1_01	51	(-)	0.765	0.761	ggagggacccgTTATTttgtccgg	Gfi-1
SNP1+2	SHRSP	V$NFKAPPAB_01	51	(-)	0.877	0.795	ggaggGACCC	NF-kappaB
SNP1+2	WKY	V$VJUN_01	51	(-)	0.8	0.72	ggagggaCCTCAttat	v-Jun
SNP1+2	WKY	V$ATF_B	52	(-)	0.8	0.785	gagggaCCTCAt	ATF
SNP1+2	WKY	V$ATF3_Q6	52	(-)	0.877	0.79	gagggaCCTCAtta	ATF3
SNP1+2	WKY	V$GFI1_01	52	(-)	0.765	0.701	gagggacctcaTTATTttgtccgg	Gfi-1
SNP1+2	WKY	V$MINI20_B	52	(+)	0.968	0.711	gagggaCCTCAttattttgtc	Muscle
SNP1+2	SHRSP	V$XBP1_01	52	(-)	0.779	0.744	gagggaCCCGTtatttt	XBP-1
SNP1+2	WKY	V$AML_Q6	53	(-)	0.874	0.817	agggaCCTCAttatt	AML
SNP1+2	WKY	V$AREB6_02	53	(+)	0.8	0.77	aggGACCTcatt	AREB6
SNP1+2	SHRSP	V$ARNT_01	53	(-)	0.792	0.737	agggaCCCGTatttt	Arnt
SNP1+2	WKY	V$CREB_Q2	53	(-)	0.79	0.721	agggaCCTCAtt	CREB
SNP1+2	WKY	V$CREB_Q2_01	53	(+)	0.888	0.855	agggaCCTCAttat	CREB
SNP1+2	WKY	V$CREB_Q4	53	(-)	0.792	0.745	agggaCCTCAtt	CREB
SNP1+2	WKY	V$CREBP1_Q2	53	(-)	0.8	0.762	agggaCCTCAtt	CRE-BP1
SNP1+2	WKY	V$PEBP_Q6	53	(+)	0.881	0.803	agggACCTCattatt	PEBP
SNP1+2	SHRSP	V$WHN_B	53	(+)	0.761	0.759	aggGACCCgtt	Whn
SNP1+2	WKY	V$AP1_Q2	54	(-)	0.773	0.738	gggaCCTCAtt	AP-1
SNP1+2	WKY	V$E4F1_Q6	54	(+)	0.8	0.713	gggaCCTCAt	E4F1
SNP1+2	WKY	V$NFKAPPAB_01	54	(+)	0.986	0.71	GGGACctcat	NF-kappaB
SNP1+2	WKY	V$PADS_C	54	(-)	0.772	0.721	gggACCTCa	Poly
SNP1+2	SHRSP	V$RORA1_01	54	(-)	0.8	0.717	gGGACCcgttatt	RORalpha1
SNP1+2	WKY	V$RORA1_01	54	(-)	0.8	0.808	gGGACCtcattat	RORalpha1
SNP1+2	WKY	V$RORA2_01	54	(-)	0.8	0.749	gGGACCtcattat	RORalpha2
SNP1+2	WKY	V$S8_01	54	(+)	0.865	0.861	gggacctCATTAtttt	S8
SNP1+2	WKY	V$CHX10_01	55	(-)	0.784	0.773	ggacctCATTAttt	CHX10
SNP1+2	WKY	V$COREBINDINGFACTOR_Q6	55	(-)	0.846	0.809	ggaCCTCA	core-binding

Table A5 – Continued overleaf

SNP	Strain	Matrix Identifier	Position	Strand	Matrix match	Core match	Matrix sequence (+ strand)	Factor name
SNP1+2	WKY	V$CREB_01	55	(-)	0.788	0.805	ggaCCTCA	CREB
SNP1+2	WKY	V$CREB_02	55	(-)	0.832	0.794	ggaCCTCAttat	CREB
SNP1+2	SHRSP	V$CREB_Q2_01	55	(+)	0.796	0.723	ggaccCGTTAtttt	CREB
SNP1+2	WKY	V$CREB_Q4_01	55	(-)	0.901	0.881	ggaCCTCAtta	CREB
SNP1+2	WKY	V$CREBATF_Q6	55	(-)	0.873	0.867	ggaCCTCAt	CREBATF
SNP1+2	WKY	V$CREBP1CJUN_01	55	(+)	0.844	0.746	gGACCTca	CRE-BP1
SNP1+2	WKY	V$CREBP1CJUN_01	55	(-)	0.78	0.73	ggACCTCa	CRE-BP
SNP1+2	WKY	V$FOXJ2_02	56	(-)	1	0.701	gacctcATTATttt	FOXJ2
SNP1+2	WKY	V$FREAC7_01	56	(-)	0.766	0.739	gacctcATTATtttgt	Freac-7
SNP1+2	WKY	V$GATA1_03	56	(+)	0.766	0.73	gacctCATTAtttt	GATA-1
SNP1+2	SHRSP	V$GATA4_Q3	56	(-)	0.907	0.756	gacccgtTATTT	GATA-4
SNP1+2	WKY	V$IPF1_Q4_01	56	(+)	1	0.933	gacctCATTAttttg	IPF1
SNP1+2	WKY	V$S8_01	56	(-)	0.785	0.783	gaccTCATTattttgt	S8
SNP1+2	WKY	V$XFD2_01	56	(-)	0.781	0.713	gacctcATTATttt	XFD-2
SNP1+2	SHRSP	V$CREB_02	57	(-)	0.82	0.721	accCGTTAtttt	CREB
SNP1+2	SHRSP	V$CREB_Q4_01	57	(-)	0.789	0.715	accCGTTAttt	CREB
SNP1+2	SHRSP	V$CREBATF_Q6	57	(-)	0.773	0.725	accCGTTAt	CREBATF
SNP1+2	SHRSP	V$GFI1B_01	57	(-)	0.792	0.753	acccgTTATTtt	GFI1B
SNP1+2	SHRSP	V$VMYB_01	57	(-)	1	0.985	acCCGTTatt	v-Myb
SNP1+2	SHRSP	V$FOXJ2_01	58	(-)	0.96	0.754	cccgtTATTTtgtccggc	FOXJ2
SNP1+2	SHRSP	V$FOXJ2_02	58	(-)	0.897	0.709	cccgttATTTTgtc	FOXJ2
SNP1+2	SHRSP	V$GATA1_02	58	(-)	0.754	0.737	cccgtTATTTtgtc	GATA-1
SNP1+2	SHRSP	V$HNF3B_01	58	(+)	1	0.821	cccgtTATTTtgtcc	HNF-3beta
SNP1+2	WKY	V$IPF1_Q4	58	(-)	1	0.898	cctCATTAtttt	IPF1
SNP1+2	WKY	V$NKX25_02	58	(+)	0.778	0.74	ccTCATTa	Nkx2-5
SNP1+2	SHRSP	V$PTF1BETA_Q6	58	(-)	0.795	0.827	cccgttattTTGTC	PTF1-beta
SNP1+2	SHRSP	V$S8_01	58	(-)	0.785	0.741	cccgTTATTttgtccg	S8
SNP1+2	WKY	V$SOX9_B1	58	(-)	0.758	0.757	cctcATTATtttgt	SOX-9
SNP1+2	SHRSP	V$VMYB_02	58	(-)	1	0.973	cCCGTTatt	v-Myb
SNP1+2	WKY	V$FOXJ2_01	59	(-)	0.96	0.76	ctcatTATTTtgtccggc	FOXJ2
SNP1+2	WKY	V$FOXJ2_02	59	(-)	0.897	0.775	ctcattATTTTgtc	FOXJ2
SNP1+2	WKY	V$GATA1_02	59	(-)	0.754	0.739	ctcatTATTTtgtc	GATA-1

Table A5 – Continued overleaf

SNP	Strain	Matrix Identifier	Position	Strand	Matrix match	Core match	Matrix sequence (+ strand)	Factor name
SNP1+2	WKY	V$HNF3B_01	59	(+)	1	0.863	ctcatTATTTtgtcc	HNF-3beta
SNP1+2	WKY	V$LHX3_01	59	(-)	0.85	0.783	ctcATTATtt	Lhx3
SNP1+2	SHRSP	V$LMO2COM_02	59	(+)	0.751	0.709	cCGTTAttt	Lmo2
SNP1+2	SHRSP	V$S8_01	59	(-)	0.785	0.748	ccgtTATTTtgtccgg	S8
SNP1+2	WKY	V$S8_01	59	(-)	0.785	0.743	ctcaTTATTttgtccg	S8
SNP1+2	SHRSP	V$GATA1_05	60	(-)	0.8	0.781	cgTTATTttg	GATA-1
SNP1+2	SHRSP	V$GATA1_06	60	(-)	0.79	0.789	cgTTATTttg	GATA-1
SNP1+2	SHRSP	V$GATA2_02	60	(-)	0.785	0.772	cgTTATTttg	GATA-2
SNP1+2	SHRSP	V$HFH3_01	60	(+)	0.981	0.769	cgtTATTTtgtcc	HFH-3
SNP1+2	SHRSP	V$HNF4_01_B	60	(-)	0.8	0.706	cgttaTTTTGtccgg	HNF-4alpha1
SNP1+2	SHRSP	V$LMO2COM_02	60	(-)	0.757	0.762	cgtTATTTt	Lmo2
SNP1+2	SHRSP	V$MEF2_Q6_01	60	(+)	1	0.766	cgtTATTTtgtc	MEF-2
SNP1+2	WKY	V$NKX25_02	60	(-)	0.887	0.773	tCATTAtt	Nkx2-5
SNP1+2	SHRSP	V$NKX25_02	60	(+)	0.778	0.729	cgTTATTt	Nkx2-5
SNP1+2	WKY	V$S8_01	60	(-)	0.785	0.746	tcatTATTTtgtccgg	S8
SNP1+2	WKY	V$SOX5_01	60	(-)	0.823	0.842	tcATTATttt	Sox-5
SNP1+2	WKY	V$FOX_Q2	61	(+)	0.934	0.733	catTATTTtgtcc	FOX
SNP1+2	WKY	V$GATA1_05	61	(-)	0.8	0.747	caTTATTttg	GATA-1
SNP1+2	WKY	V$GATA1_06	61	(-)	0.79	0.784	caTTATTttg	GATA-1
SNP1+2	WKY	V$GATA2_02	61	(-)	0.785	0.76	caTTATTttg	GATA-2
SNP1+2	WKY	V$HFH3_01	61	(+)	0.981	0.767	catTATTTtgtcc	HFH-3
SNP1+2	WKY	V$HNF4_01_B	61	(-)	0.8	0.706	cattaTTTTGtccgg	HNF-4alpha1
SNP1+2	WKY	V$LHX3_01	61	(+)	0.782	0.701	caTTATTttg	Lhx3
SNP1+2	WKY	V$LMO2COM_02	61	(-)	0.757	0.751	catTATTTt	Lmo2
SNP1+2	WKY	V$NKX25_02	61	(+)	0.778	0.766	caTTATTt	Nkx2-5
SNP3	WKY	V$AR_02	41	(+)	0.8	0.74	tggccctctactttcTGCTCtagggtc	AR
SNP3	WKY	V$AR_03	41	(+)	0.8	0.756	tggccctctactttcTGCTCtagggtc	AR
SNP3	WKY	V$GR_01	41	(+)	0.8	0.806	tggccctctactttcTGCTCtagggtc	GR
SNP3	WKY	V$PR_01	41	(+)	0.8	0.782	tggccctctactttcTGCTCtagggtc	PR
SNP3	WKY	V$PR_02	41	(+)	0.8	0.81	tggccctctactttcTGCTCtagggtc	PR
SNP3	WKY	V$DR3_Q4	45	(+)	0.804	0.76	cctctactttcTGCTCtaggg	VDR,
SNP3	SHRSP	V$GFI1_01	45	(-)	0.765	0.719	cctctactttcTGCTTtagggtct	Gfi-1

Table A5 – Continued overleaf

SNP	Strain	Matrix Identifier	Position	Strand	Matrix match	Core match	Matrix sequence (+ strand)	Factor name
SNP3	SHRSP	V$PLZF_02	46	(-)	1	0.714	ctctactttctgCTTTAgggtctgtagct	PLZF
SNP3	WKY	V$GRE_C	47	(+)	0.762	0.716	tctactttctGCTCTa	GR
SNP3	SHRSP	V$HNF1_Q6	49	(+)	0.809	0.732	tacTTTCTgctttagggt	HNF-1
SNP3	SHRSP	V$BARBIE_01	51	(-)	1	0.904	ctttctGCTTTaggg	Barbie Box
SNP3	WKY	V$BARBIE_01	51	(-)	0.759	0.715	ctttctGCTCTaggg	Barbie Box
SNP3	WKY	V$COUPTF_Q6	51	(+)	0.848	0.726	ctttcTGCTCtagggtctgtagc	COUPTF
SNP3	SHRSP	V$COUPTF_Q6	51	(-)	0.814	0.708	ctttctgctttagGGTCTgtagc	COUPTF
SNP3	WKY	V$COUPTF_Q6	51	(-)	0.814	0.726	ctttctgctctagGGTCTgtagc	COUPTF
SNP3	SHRSP	V$GFI1B_01	51	(-)	0.792	0.718	ctttcTGCTTta	GFI1B
SNP3	SHRSP	V$MTATA_B	51	(-)	0.901	0.767	ctttctgcTTTAGggtc	Muscle
SNP3	SHRSP	V$LDSPOLYA_B	52	(+)	0.886	0.774	tttcTGCTTtagggtc	Poly A
SNP3	SHRSP	V$MMEF2_Q6	52	(-)	0.9	0.737	tttctgCTTTAgggtc	MEF-2
SNP3	WKY	V$MTF1_Q4	54	(+)	0.9	0.733	tcTGCTCtagggtc	MTF-1
SNP3	SHRSP	V$PIT1_Q6	54	(+)	0.837	0.736	tcTGCTTtagggtctgta	Pit-1
SNP3	WKY	V$COUP_01	55	(-)	0.825	0.72	ctgctctagGGTCT	COUP-TF,
SNP3	SHRSP	V$POU1F1_Q6	55	(+)	0.868	0.712	cTGCTTtagg	POU1F1
SNP3	SHRSP	V$TITF1_Q3	55	(-)	0.857	0.738	ctgCTTTAgg	TTF1
SNP3	WKY	V$ZID_01	55	(+)	0.888	0.842	cTGCTCtagggtc	ZID
SNP3	WKY	V$COUP_DR1_Q6	56	(-)	0.917	0.702	tgctctaGGGTCt	COUP
SNP3	WKY	V$GATA4_Q3	57	(-)	0.752	0.701	gctctagGGTCT	GATA-4
SNP3	WKY	V$HNF4ALPHA_Q6	57	(-)	0.79	0.776	gctCTAGGgtctg	HNF-4alpha
SNP3	SHRSP	V$LEF1TCF1_Q4	57	(+)	0.822	0.712	gCTTTAgggtc	LEF1TCF1
SNP3	SHRSP	V$RORA1_01	57	(+)	0.8	0.73	gctttagGGTCTg	RORalpha1
SNP3	SHRSP	V$TATA_C	57	(-)	0.79	0.715	gCTTTAgggt	TATA
SNP3	WKY	V$MINI20_B	58	(-)	0.929	0.712	ctctagggtcTGTAGctctgg	Muscle
SNP3	SHRSP	V$E2F_Q4	59	(+)	0.773	0.798	tTTAGGgt	E2F
SNP4	WKY	V$COUPTF_Q6	69	(-)	0.827	0.734	ttcagggtgtgtaGAACAgaatc	COUPTF
SNP4	SHRSP	V$BRN2_01	74	(+)	0.917	0.721	ggtgtgtAGAATagaa	Brn-2
SNP4	WKY	V$AR_02	75	(-)	1	0.713	gtgtgtaGAACAgaatcctggggcaga	AR
SNP4	WKY	V$AR_03	75	(-)	1	0.757	gtgtgtaGAACAgaatcctggggcaga	AR
SNP4	WKY	V$GR_01	75	(-)	1	0.917	gtgtgtaGAACAgaatcctggggcaga	GR
SNP4	SHRSP	V$GR_01	75	(-)	0.8	0.768	gtgtgtaGAATAgaatcctggggcaga	GR

Table A5 – Continued overleaf

SNP	Strain	Matrix Identifier	Position	Strand	Matrix match	Core match	Matrix sequence (+ strand)	Factor name
SNP4	SHRSP	V$OCT1_06	75	(+)	0.829	0.726	gtgtgTAGAAtaga	Oct-01
SNP4	WKY	V$PR_01	75	(-)	1	0.897	gtgtgtaGAACAgaatcctggggcaga	PR
SNP4	SHRSP	V$PR_01	75	(-)	0.8	0.753	gtgtgtaGAATAgaatcctggggcaga	PR
SNP4	WKY	V$PR_02	75	(-)	1	0.843	gtgtgtaGAACAgaatcctggggcaga	PR
SNP4	SHRSP	V$PR_02	75	(-)	0.8	0.705	gtgtgtaGAATAgaatcctggggcaga	PR
SNP4	SHRSP	V$SOX9_B1	76	(+)	0.758	0.724	tgtgtAGAATagaa	SOX-9
SNP4	SHRSP	V$GATA1_03	77	(+)	0.766	0.756	gtgtaGAATAgaat	GATA-1
SNP4	SHRSP	V$MRF2_01	77	(+)	0.914	0.814	gtgtagAATAGaat	MRF-2
SNP4	WKY	V$MRF2_01	77	(+)	0.773	0.704	gtgtagAACAGaat	MRF-2
SNP4	SHRSP	V$OCT1_02	77	(-)	0.992	0.766	gtgtaGAATAgaatc	Oct-01
SNP4	WKY	V$CMYB_01	78	(-)	0.869	0.797	tgtAGAACagaatcctgg	c-Myb
SNP4	SHRSP	V$PITX2_Q2	78	(-)	0.834	0.705	tgtaGAATAga	PITX2
SNP4	SHRSP	V$SOX5_01	78	(+)	0.815	0.715	tgtAGAATag	Sox-5
SNP4	WKY	V$GRE_C	80	(-)	1	0.713	tAGAACagaatcctgg	GR
SNP4	WKY	V$HAND1E47_01	80	(-)	0.859	0.794	tagaACAGAatcctgg	Hand1:E47
SNP4	SHRSP	V$MTATA_B	80	(+)	0.846	0.706	tagaATAGAatcctggg	Muscle
SNP4	SHRSP	V$OCT1_06	80	(+)	0.829	0.825	tagaaTAGAAtcct	Oct-01
SNP4	WKY	V$VMYB_01	80	(+)	0.904	0.861	tagAACAGaa	v-Myb
SNP4	WKY	V$VMYB_02	80	(+)	0.889	0.831	tagAACAGa	v-Myb
SNP4	WKY	V$AR_Q2	81	(-)	1	0.744	AGAACagaatcctgg	AR
SNP4	SHRSP	V$OCT1_06	81	(-)	0.893	0.868	agaaTAGAAtcctg	Oct-01
SNP4	SHRSP	V$TATA_C	81	(+)	0.841	0.758	agaaTAGAAt	TATA
SNP4	SHRSP	V$HNF6_Q6	82	(-)	0.843	0.752	gaATAGAatcct	HNF-6
SNP4	SHRSP	V$LPOLYA_B	82	(+)	0.8	0.778	gAATAGaa	Lentiviral
SNP4	WKY	V$FOXJ2_02	83	(+)	0.897	0.718	aacAGAATcctggg	FOXJ2
SNP4	SHRSP	V$GATA2_03	85	(-)	0.802	0.783	taGAATCctg	GATA-2
SNP5	WKY	V$AIRE_01	37	(+)	0.891	0.703	gtgttttgGGGAGcaggcgagcaaat	AIRE
SNP5	SHRSP	V$GFI1_01	48	(-)	0.96	0.847	agcaggcgagcAGATTctgctttc	Gfi-1
SNP5	WKY	V$E2F_01	50	(+)	0.8	0.753	caggcgaGCAAAttc	E2F
SNP5	WKY	V$CEBPDELTA_Q6	51	(-)	0.846	0.772	aggcgaGCAAAt	C/EBPdelta
SNP5	WKY	V$ELF1_Q6	51	(+)	0.784	0.76	aggcgAGCAAat	ELF-1
SNP5	WKY	V$E2F_Q3_01	52	(-)	0.788	0.751	gGCGAGcaa	E2F

Table A5 – Continued overleaf

SNP	Strain	Matrix Identifier	Position	Strand	Matrix match	Core match	Matrix sequence (+ strand)	Factor name
SNP5	SHRSP	V$HSF_Q6	52	(+)	0.928	0.714	ggcgagcaGATTC	HSF
SNP5	WKY	V$NFY_Q6_01	52	(+)	0.814	0.773	ggcgagCAAATtc	NF-Y
SNP5	SHRSP	V$HAND1E47_01	53	(-)	0.871	0.803	gcgaGCAGAttctgct	Hand1:E47
SNP5	WKY	V$LEF1TCF1_Q4	53	(-)	0.81	0.763	gcgagCAAATt	LEF1TCF1
SNP5	WKY	V$NFY_01	53	(+)	0.812	0.753	gcgagCAAATtctgct	NF-Y
SNP5	WKY	V$S8_01	53	(+)	0.785	0.751	gcgagcaAATTCtgct	S8
SNP5	SHRSP	V$TAL1ALPHAE47_01	53	(+)	1	0.778	gcgagCAGATtctgct	Tal-1alpha
SNP5	SHRSP	V$TAL1BETAE47_01	53	(+)	1	0.781	gcgagCAGATtctgct	Tal-1beta:E47
SNP5	SHRSP	V$TAL1BETAITF2_01	53	(+)	1	0.777	gcgagCAGATtctgct	Tal-1beta
SNP5	WKY	V$CHX10_01	54	(-)	0.824	0.767	cgagcaAATTCtgc	CHX10
SNP5	SHRSP	V$E47_01	54	(+)	0.934	0.737	cgagCAGATtctgct	E47
SNP5	WKY	V$ETS1_B	54	(+)	0.773	0.715	cgAGCAAattctgct	c-Ets-1
SNP5	WKY	V$HNF3B_01	54	(-)	0.767	0.728	cgagcAAATTctgct	HNF-3beta
SNP5	SHRSP	V$AREB6_01	55	(-)	0.8	0.71	gagCAGATtctgc	AREB6
SNP5	WKY	V$E2F_Q3	55	(-)	0.917	0.728	gaGCAAAt	E2F
SNP5	SHRSP	V$GATA1_02	55	(+)	0.754	0.738	gagcAGATTctgct	GATA-1
SNP5	SHRSP	V$GATA1_03	55	(+)	0.945	0.909	gagcaGATTCtgct	GATA-1
SNP5	SHRSP	V$MYOD_01	55	(+)	0.873	0.719	gagCAGATtctg	MyoD
SNP5	WKY	V$NFY_Q6	55	(+)	0.779	0.734	gagCAAATtct	NF-Y
SNP5	WKY	V$S8_01	55	(-)	0.785	0.742	gagcAAATTctgcttt	S8
SNP5	SHRSP	V$E12_Q6	56	(+)	0.943	0.772	agCAGATtctg	E12
SNP5	SHRSP	V$IRF_Q6	56	(+)	0.781	0.705	agcagATTCTgcttt	IRF
SNP5	SHRSP	V$ICSBP_Q6	58	(-)	0.783	0.757	caGATTCtgctt	ICSBP
SNP5	SHRSP	V$ISRE_01	58	(+)	0.8	0.759	caGATTCtgctttca	ISRE
SNP5	SHRSP	V$LMO2COM_02	58	(+)	0.757	0.755	cAGATTctg	Lmo2
SNP5	WKY	V$NKX25_02	59	(-)	0.778	0.766	aAATTCtg	Nkx2-5
SNP5	WKY	V$GFI1B_01	60	(-)	0.792	0.7	aattcTGCTTtc	GFI1B
SNP6	WKY	V$AP4_01	48	(-)	0.915	0.712	tgttctttCGCTGtctgg	AP-4
SNP6	SHRSP	V$PBX_Q3	49	(-)	0.8	0.792	gttctttCGCTC	PBX
SNP6	SHRSP	V$CEBPDELTA_Q6	51	(+)	0.807	0.718	tCTTTCgctctc	C/EBPdelta
SNP6	SHRSP	V$DR3_Q4	52	(+)	0.881	0.706	ctttcgctctcTGGCCagtct	VDR,
SNP6	WKY	V$MINI20_B	53	(-)	0.813	0.722	tttcgctgtcTGGCCagtctc	Muscle

Table A5 – Continued overleaf

SNP	Strain	Matrix Identifier	Position	Strand	Matrix match	Core match	Matrix sequence (+ strand)	Factor name
SNP6	SHRSP	V$AP2ALPHA_02	55	(-)	0.898	0.737	tcgctctcTGGCCag	AP-2alphaA
SNP6	SHRSP	V$HNF4_01_B	55	(-)	0.8	0.774	tcgctCTCTGgccag	HNF-4alpha1
SNP6	SHRSP	V$HNF4_Q6_01	55	(-)	0.888	0.803	tcgctCTCTGgcca	HNF4
SNP6	WKY	V$LDSPOLYA_B	55	(+)	0.966	0.846	tcgcTGTCTggccagt	Poly A
SNP6	WKY	V$MEIS1_01	55	(-)	0.833	0.845	tcgcTGTCTggc	MEIS1
SNP6	WKY	V$SRF_C	55	(+)	0.836	0.7	tcgctgTCTGGccag	SRF
SNP6	SHRSP	V$ZID_01	55	(+)	0.908	0.768	tCGCTCtctggcc	ZID
SNP6	SHRSP	V$HNF4_DR1_Q3	56	(+)	0.846	0.748	cgctCTCTGgcca	HNF-4
SNP6	SHRSP	V$MAZ_Q6	56	(-)	0.819	0.785	cgCTCTCt	MAZ
SNP6	WKY	V$SMAD4_Q6	56	(-)	0.99	0.83	cgcTGTCTggccagt	SMAD-4
SNP6	WKY	V$TGIF_01	56	(+)	0.85	0.786	cgcTGTCTggc	TGIF
SNP6	WKY	V$SMAD4_Q6	57	(+)	0.878	0.736	gctgtctGGCCAgtc	SMAD-4
SNP6	WKY	V$SMAD3_Q6	59	(+)	1	0.912	tGTCTGgcc	SMAD-3
SNP6	SHRSP	V$SMAD3_Q6	59	(+)	0.825	0.794	tCTCTGgcc	SMAD-3
SNP6	WKY	V$SMAD4_Q6	60	(-)	0.878	0.717	gtcTGGCCagtctcc	SMAD-4
SNP7	SHRSP	V$E2F1_Q3_01	50	(-)	0.936	0.726	gagagtcgAGCGCctc	E2F-1
SNP7	WKY	V$GATA4_Q3	51	(+)	0.752	0.708	AGAGTcgagagc	GATA-4
SNP7	WKY	V$ZID_01	52	(-)	1	0.785	gagtcgaGAGCCt	ZID
SNP7	WKY	V$SMAD4_Q6	53	(+)	0.876	0.7	agtcgagAGCCTccc	SMAD-4
SNP7	SHRSP	V$E2F1_Q6_01	54	(+)	0.88	0.735	gtcgAGCGCc	E2F-1
SNP7	SHRSP	V$E2F_Q3_01	55	(+)	0.903	0.701	tcgAGCGCc	E2F
SNP7	WKY	V$LMO2COM_02	55	(+)	0.751	0.733	tCGAGAgcc	Lmo2
SNP7	WKY	V$PPARA_02	56	(-)	0.81	0.718	cgagagcctccCCACCccc	PPARalpha
SNP7	SHRSP	V$WHN_B	56	(-)	0.761	0.74	cgaGCGCCtcc	Whn
SNP7	SHRSP	V$AREB6_02	57	(+)	0.8	0.763	gagCGCCTcccc	AREB6
SNP7	WKY	V$NFKB_C	57	(-)	0.96	0.714	gagagcCTCCCc	NF-kappaB
SNP7	SHRSP	V$E2F_Q3_01	58	(-)	1	0.707	aGCGCCtcc	E2F
SNP7	SHRSP	V$E2F1_Q6_01	58	(-)	0.935	0.702	aGCGCCtccc	E2F-1
SNP7	SHRSP	V$GABP_B	58	(-)	0.8	0.74	agcgCCTCCcca	GABP
SNP7	WKY	V$NFKAPPAB_01	58	(-)	0.965	0.717	agagcCTCCC	NF-kappaB
SNP7	SHRSP	V$EGR1_01	59	(-)	0.83	0.749	gcgCCTCCccac	Egr-1
SNP7	SHRSP	V$NGFIC_01	59	(-)	0.773	0.716	gcgCCTCCccac	NGFI-C

Table A5 – Continued overleaf

SNP	Strain	Matrix Identifier	Position	Strand	Matrix match	Core match	Matrix sequence (+ strand)	Factor name
SNP7	SHRSP	V$UF1H3BETA_Q6	59	(-)	0.8	0.784	gcgcctCCCCAccc	UF1H3BETA
SNP7	SHRSP	V$KROX_Q6	60	(+)	0.75	0.709	cgccTCCCCacccc	KROX
SNP8	WKY	V$MTATA_B	47	(-)	0.819	0.75	ttgtgaagGTTATacca	Muscle
SNP8	SHRSP	V$HNF4ALPHA_Q6	48	(-)	0.816	0.703	tgtGAAGGttatg	HNF-4alpha
SNP8	SHRSP	V$RFX1_02	49	(+)	0.804	0.706	gtgaaggttatGCCACag	RFX1
SNP8	SHRSP	V$CDX2_Q5	50	(+)	0.854	0.703	tgaagGTTATgcca	Cdx-2
SNP8	SHRSP	V$IPF1_Q4_01	51	(-)	0.802	0.778	gaaggTTATGccaca	IPF1
SNP8	SHRSP	V$IPF1_Q4	52	(+)	0.783	0.708	aaggTTATGcca	IPF1
SNP8	SHRSP	V$OCT1_01	52	(+)	1	0.717	aaggtTATGCcacaggaca	Oct-01
SNP8	SHRSP	V$OCT1_02	52	(+)	1	0.809	aaggtTATGCcacag	Oct-01
SNP8	WKY	V$OCT1_02	52	(+)	0.94	0.763	aaggtTATACcacag	Oct-01
SNP8	WKY	V$TBX5_01	54	(-)	0.781	0.701	ggttATACCaca	TBX5
SNP8	SHRSP	V$CEBPGAMMA_Q6	55	(+)	0.752	0.762	gttATGCCacagg	C/EBPgamma
SNP8	SHRSP	V$MEIS1_01	55	(-)	0.868	0.792	gttaTGCCAcag	MEIS1
SNP8	SHRSP	V$AML_Q6	56	(-)	1	0.843	ttatgCCACAggaca	AML
SNP8	WKY	V$AML_Q6	56	(-)	1	0.945	ttataCCACAggaca	AML
SNP8	SHRSP	V$MEIS1_01	56	(+)	0.863	0.797	ttaTGCCAcagg	MEIS1
SNP8	WKY	V$PEBP_Q6	56	(+)	1	0.91	ttatACCACaggaca	PEBP
SNP8	SHRSP	V$PEBP_Q6	56	(+)	0.82	0.772	ttatGCCACaggaca	PEBP
SNP8	SHRSP	V$TGIF_01	56	(-)	0.79	0.704	ttaTGCCAcag	TGIF
SNP8	SHRSP	V$AP2ALPHA_02	57	(+)	0.911	0.884	taTGCCAcaggacat	AP-2alphaA
SNP8	SHRSP	V$AP2ALPHA_03	57	(+)	0.855	0.755	taTGCCAcaggacat	AP-2alphaA
SNP8	SHRSP	V$E2F1DP1_01	57	(+)	0.771	0.715	taTGCCAc	E2F-1:DP-1
SNP8	SHRSP	V$HNF4_01_B	57	(+)	0.8	0.736	tatgcCACAGgacat	HNF-4alpha1
SNP8	WKY	V$LEF1TCF1_Q4	57	(-)	0.763	0.715	tatacCACAGg	LEF1TCF1
SNP8	WKY	V$PADS_C	57	(-)	1	0.903	tatACCACa	Poly
SNP8	SHRSP	V$PADS_C	57	(-)	0.772	0.728	tatGCCACa	Poly
SNP8	SHRSP	V$COREBINDINGFACTOR_Q6	58	(-)	1	0.876	atgCCACA	core-binding
SNP8	WKY	V$COREBINDINGFACTOR_Q6	58	(-)	1	0.983	ataCCACA	core-binding
SNP9	SHRSP	V$MINI20_B	46	(+)	0.937	0.706	aattaaCCACAagcctcttgg	Muscle
SNP9	WKY	V$RORA1_01	48	(-)	0.8	0.701	tTAACCacaagct	RORalpha1
SNP9	WKY	V$NERF_Q2	51	(-)	0.8	0.808	accacaagctTCTTGgtt	NERF1a

Table A5 – Continued overleaf

SNP	Strain	Matrix Identifier	Position	Strand	Matrix match	Core match	Matrix sequence (+ strand)	Factor name
SNP9	WKY	V$BARBIE_01	52	(-)	0.759	0.727	ccacaaGCTTCttgg	Barbie Box
SNP9	WKY	V$ETS1_B	52	(-)	0.773	0.762	ccacaagcTTCTTgg	c-Ets-1
SNP9	WKY	V$ETS2_B	54	(-)	0.785	0.768	acaagcTTCTTggt	c-Ets-2
SNP9	WKY	V$EVI1_06	54	(+)	1	0.739	ACAAGcttc	Evi-1
SNP9	SHRSP	V$AP2ALPHA_02	55	(+)	0.989	0.811	caAGCCTcttggtta	AP-2alphaA
SNP9	WKY	V$SF1_Q6	55	(-)	0.8	0.734	CAAGCttc	SF-1
SNP9	WKY	V$HNF1_Q6	57	(+)	0.787	0.722	agcTTCTTggttatggaa	HNF-1
SNP9	SHRSP	V$NKX25_Q5	57	(+)	0.8	0.766	agcCTCTTgg	NKX25
SNP9	WKY	V$NRF2_01	57	(-)	0.8	0.703	agCTTCTtgg	NRF-2
SNP9	WKY	V$PEBP_Q6	57	(-)	0.766	0.707	agcttcTTGGTtatg	PEBP
SNP9	WKY	V$ELF1_Q6	58	(-)	0.784	0.722	gcTTCTTggtta	ELF-1
SNP9	WKY	V$PIT1_Q6	58	(+)	0.932	0.857	gcTTCTTggttatggaag	Pit-1
SNP9	SHRSP	V$PIT1_Q6	58	(-)	0.886	0.727	gcctcttggttATGGAag	Pit-1
SNP9	WKY	V$PIT1_Q6	58	(-)	0.886	0.737	gcttcttggttATGGAag	Pit-1
SNP9	WKY	V$ALPHACP1_01	59	(-)	0.8	0.763	cttCTTGGtta	alpha-CP1
SNP9	SHRSP	V$NKX25_01	60	(-)	0.783	0.749	CTCTTgg	Nkx2-5
SNP11+10	WKY	V$COMP1_01	72	(-)	0.786	0.78	ttagtctcctcgtCAGTCatttgt	COMP1
SNP11+10	WKY	V$VMAF_01	74	(-)	0.778	0.713	agtctcctcgTCAGTcatt	v-Maf
SNP11+10	WKY	V$RORA1_01	75	(+)	0.8	0.706	gtctcctCGTCAg	RORalpha1
SNP11+10	WKY	V$TCF11MAFG_01	75	(-)	1	0.747	gtctcctcgtcaGTCATttgtt	TCF11:MafG
SNP11+10	WKY	V$ATF_01	76	(-)	1	0.917	tctcctCGTCAgtc	ATF
SNP11+10	SHRSP	V$ATF_01	76	(-)	0.8	0.744	tctcctCGTCCcgt	ATF
SNP11+10	WKY	V$ATF_B	76	(-)	1	0.793	tctcctCGTCAg	ATF
SNP11+10	SHRSP	V$HTF_01	76	(+)	0.849	0.8	tctcctcgtCCCGTcatttgtttt	HTF
SNP11+10	WKY	V$MINI20_B	76	(+)	0.96	0.741	tctcctCGTCAgtcatttgtt	Muscle
SNP11+10	SHRSP	V$PAX3_B	76	(+)	0.818	0.721	tctcctcgTCCCGtcatttgt	Pax-3
SNP11+10	WKY	V$ATF4_Q2	77	(-)	1	0.765	ctcctCGTCAgt	ATF4
SNP11+10	SHRSP	V$CETS1P54_03	77	(-)	0.812	0.8	ctcctcGTCCCgtcat	c-Ets-1
SNP11+10	WKY	V$CREB_Q2	77	(-)	1	0.863	ctcctCGTCAgt	CREB
SNP11+10	SHRSP	V$CREB_Q2	77	(-)	0.79	0.703	ctcctCGTCCcg	CREB
SNP11+10	WKY	V$CREB_Q2_01	77	(+)	1	0.896	ctcctCGTCAgtca	CREB
SNP11+10	SHRSP	V$CREB_Q2_01	77	(+)	0.804	0.736	ctcctCGTCCcgtc	CREB

Table A5 – Continued overleaf

SNP	Strain	Matrix Identifier	Position	Strand	Matrix match	Core match	Matrix sequence (+ strand)	Factor name
SNP11+10	WKY	V$CREB_Q4	77	(-)	1	0.871	ctcctCGTCAgt	CREB
SNP11+10	SHRSP	V$CREB_Q4	77	(-)	0.792	0.708	ctcctCGTCCcg	CREB
SNP11+10	WKY	V$CREBP1_Q2	77	(-)	1	0.788	ctcctCGTCAgt	CRE-BP1
SNP11+10	SHRSP	V$ELK1_01	77	(-)	0.9	0.728	ctcctCGTCCcgtcat	Elk-1
SNP11+10	WKY	V$AP1_Q2	78	(-)	0.967	0.932	tcctCGTCAgt	AP-1
SNP11+10	WKY	V$E4F1_Q6	78	(+)	1	0.771	tcctCGTCAg	E4F1
SNP11+10	SHRSP	V$E4F1_Q6	78	(+)	0.8	0.701	tcctCGTCCc	E4F1
SNP11+10	SHRSP	V$GABP_B	78	(-)	0.8	0.791	tcctCGTCCcgt	GABP
SNP11+10	SHRSP	V$HOX13_01	78	(+)	0.767	0.749	tcctcgtcccgtCATTTgtttttcatctga	Hox-1.3
SNP11+10	WKY	V$MEIS1_01	78	(-)	0.77	0.702	tcctCGTCAgtc	MEIS1
SNP11+10	WKY	V$PBX_Q3	78	(-)	0.887	0.814	tcctcgtCAGTC	PBX
SNP11+10	WKY	V$TAXCREB_01	78	(-)	1	0.755	tcctCGTCAgtcatt	Tax/CREB
SNP11+10	WKY	V$ATF6_01	79	(-)	1	0.864	cctCGTCA	ATF6
SNP11+10	SHRSP	V$ATF6_01	79	(-)	0.8	0.729	cctCGTCC	ATF6
SNP11+10	WKY	V$CREB_01	79	(-)	1	0.819	cctCGTCA	CREB
SNP11+10	WKY	V$CREB_02	79	(-)	1	0.883	cctCGTCAgtca	CREB
SNP11+10	WKY	V$CREB_Q4_01	79	(-)	1	0.906	cctCGTCAgtc	CREB
SNP11+10	SHRSP	V$CREB_Q4_01	79	(-)	0.764	0.703	cctCGTCCcgt	CREB
SNP11+10	WKY	V$CREBATF_Q6	79	(-)	1	0.937	cctCGTCAg	CREBATF
SNP11+10	SHRSP	V$CREBATF_Q6	79	(-)	0.794	0.749	cctCGTCCc	CREBATF
SNP11+10	SHRSP	V$ELK1_02	79	(-)	0.767	0.765	cctcGTCCCgtcat	Elk-1
SNP11+10	WKY	V$ER_Q6	79	(-)	0.846	0.768	cctCGTCAgtcatttgttt	ER
SNP11+10	SHRSP	V$IK1_01	79	(-)	0.837	0.755	cctcGTCCCgtca	Ik-1
SNP11+10	WKY	V$LDSPOLYA_B	79	(-)	0.896	0.748	cctcgtcAGTCAtttg	Poly A
SNP11+10	WKY	V$SMAD4_Q6	79	(+)	0.959	0.777	cctcgtcAGTCAttt	SMAD-4
SNP11+10	SHRSP	V$ARNT_01	80	(-)	0.792	0.709	ctcgtCCCGTcatttg	Arnt
SNP11+10	WKY	V$ATF_01	80	(-)	0.8	0.724	ctcgtcAGTCAttt	ATF
SNP11+10	WKY	V$BACH1_01	80	(+)	0.8	0.821	ctcgTCAGTcatttg	Bach1
SNP11+10	SHRSP	V$HIF1_Q3	80	(-)	0.793	0.719	ctcgtCCCGTcatt	HIF-1
SNP11+10	SHRSP	V$MYC_Q2	80	(+)	0.814	0.709	CTCGTcc	Myc
SNP11+10	SHRSP	V$NRF2_01	80	(-)	0.8	0.75	ctCGTCCcgt	NRF-2
SNP11+10	WKY	V$NRF2_Q4	80	(+)	1	0.845	ctcgtcAGTCAtt	Nrf2

Table A5 – Continued overleaf

SNP	Strain	Matrix Identifier	Position	Strand	Matrix match	Core match	Matrix sequence (+ strand)	Factor name
SNP11+10	WKY	V$PBX1_02	80	(+)	0.789	0.722	ctcgtCAGTCatttg	Pbx1b
SNP11+10	SHRSP	V$SMAD4_Q6	80	(+)	0.837	0.775	ctcgtccCGTCAttt	SMAD-4
SNP11+10	SHRSP	V$ATF_01	81	(-)	1	0.907	tcgtccCGTCAttt	ATF
SNP11+10	SHRSP	V$ATF_B	81	(-)	1	0.832	tcgtccCGTCAt	ATF
SNP11+10	WKY	V$ATF4_Q2	81	(-)	0.933	0.732	tcgtcAGTCAtt	ATF4
SNP11+10	WKY	V$BEL1_B	81	(-)	0.782	0.733	tcgtcagtcatttgttttTCATCtgata	Bel-1
SNP11+10	WKY	V$CREB_Q2	81	(-)	0.839	0.756	tcgtcAGTCAtt	CREB
SNP11+10	WKY	V$CREB_Q4	81	(-)	0.831	0.727	tcgtcAGTCAtt	CREB
SNP11+10	SHRSP	V$E2F1_Q6_01	81	(+)	0.815	0.73	tcgtCCCGTc	E2F-1
SNP11+10	SHRSP	V$HIF1_Q5	81	(-)	0.788	0.73	tcgtCCCGTcat	HIF-1
SNP11+10	WKY	V$HNF1_Q6	81	(+)	0.802	0.806	tcgTCAGTcatttgtttt	HNF-1
SNP11+10	SHRSP	V$NRF2_Q4	81	(+)	0.873	0.742	tcgtccCGTCAtt	Nrf2
SNP11+10	SHRSP	V$STRA13_01	81	(+)	0.793	0.703	tcgtCCCGTcattt	Stra13
SNP11+10	WKY	V$AP1_Q2	82	(-)	1	0.953	cgtcAGTCAtt	AP-1
SNP11+10	SHRSP	V$ATF4_Q2	82	(-)	1	0.818	cgtccCGTCAtt	ATF4
SNP11+10	SHRSP	V$CEBPDELTA_Q6	82	(-)	0.772	0.742	cgtcccGTCATt	C/EBPdelta
SNP11+10	SHRSP	V$CREB_Q2	82	(-)	1	0.853	cgtccCGTCAtt	CREB
SNP11+10	SHRSP	V$CREB_Q2_01	82	(+)	1	0.921	cgtccCGTCAtttg	CREB
SNP11+10	SHRSP	V$CREB_Q4	82	(-)	1	0.886	cgtccCGTCAtt	CREB
SNP11+10	SHRSP	V$CREBP1_Q2	82	(-)	1	0.831	cgtccCGTCAtt	CRE-BP1
SNP11+10	SHRSP	V$E2F1DP1_01	82	(+)	1	0.729	cgTCCCGt	E2F-1:DP-1
SNP11+10	SHRSP	V$GCM_Q2	82	(+)	0.783	0.833	cgtcCCGTCatt	GCM
SNP11+10	WKY	V$MEIS1_01	82	(-)	0.77	0.789	cgtcAGTCAttt	MEIS1
SNP11+10	WKY	V$POU1F1_Q6	82	(-)	0.848	0.753	cgtcAGTCAt	POU1F1
SNP11+10	WKY	V$SMAD3_Q6	82	(-)	0.874	0.828	cgtCAGTCa	SMAD-3
SNP11+10	WKY	V$SMAD3_Q6	82	(+)	0.825	0.791	cGTCAGtca	SMAD-3
SNP11+10	WKY	V$AP1_C	83	(+)	1	0.885	gtcAGTCAt	AP-1
SNP11+10	WKY	V$AP1_C	83	(-)	0.808	0.853	gTCAGTcat	AP-1
SNP11+10	SHRSP	V$AP1_Q2	83	(-)	0.967	0.896	gtccCGTCAtt	AP-1
SNP11+10	WKY	V$CREB_02	83	(-)	0.832	0.736	gtcAGTCAtttg	CREB
SNP11+10	WKY	V$CREB_Q4_01	83	(-)	0.789	0.723	gtcAGTCAttt	CREB
SNP11+10	WKY	V$CREBATF_Q6	83	(-)	0.773	0.726	gtcAGTCAt	CREBATF

Table A5 – Continued overleaf

SNP	Strain	Matrix Identifier	Position	Strand	Matrix match	Core match	Matrix sequence (+ strand)	Factor name
SNP11+10	SHRSP	V$E4F1_Q6	83	(+)	1	0.816	gtccCGTCAt	E4F1
SNP11+10	WKY	V$ER_Q6	83	(-)	0.837	0.769	gtcAGTCAtttgtttttca	ER
SNP11+10	SHRSP	V$GATA4_Q3	83	(-)	0.791	0.706	gtcccgtCATTT	GATA-4
SNP11+10	WKY	V$HNF6_Q6	83	(+)	0.789	0.726	gtcagTCATTtg	HNF-6
SNP11+10	SHRSP	V$MEIS1_01	83	(-)	0.77	0.79	gtccCGTCAttt	MEIS1
SNP11+10	WKY	V$NFE2_01	83	(-)	0.777	0.726	gtcagTCATTt	NF-E2
SNP11+10	WKY	V$NKX22_01	83	(+)	0.762	0.744	gTCAGTcatt	Nkx2-2
SNP11+10	SHRSP	V$WHN_B	83	(-)	0.761	0.755	gtcCCGTCatt	Whn
SNP11+10	SHRSP	V$ATF6_01	84	(-)	1	0.781	tccCGTCA	ATF6
SNP11+10	SHRSP	V$CREB_01	84	(-)	1	0.842	tccCGTCA	CREB
SNP11+10	SHRSP	V$CREB_02	84	(-)	1	0.878	tccCGTCAtttg	CREB
SNP11+10	SHRSP	V$CREB_Q4_01	84	(-)	1	0.918	tccCGTCAttt	CREB
SNP11+10	SHRSP	V$CREBATF_Q6	84	(-)	1	0.946	tccCGTCAt	CREBATF
SNP11+10	SHRSP	V$CREBP1_01	84	(-)	0.897	0.704	tccCGTCA	CRE-BP1
SNP11+10	SHRSP	V$ER_Q6	84	(-)	0.846	0.78	tccCGTCAtttgtttttca	ER
SNP11+10	SHRSP	V$VMYB_01	84	(-)	0.763	0.781	tcCCGTCatt	v-Myb
SNP11+10	WKY	V$HNF1_Q6	85	(+)	0.809	0.786	cagTCATTtgtttttcat	HNF-1
SNP11+10	SHRSP	V$SP3_Q3	85	(-)	0.925	0.786	cCCGTCatttgttt	Sp3
SNP11+10	SHRSP	V$VMYB_02	85	(-)	0.778	0.77	cCCGTCatt	v-Myb
SNP11+10	SHRSP	V$HNF1_Q6	86	(+)	0.809	0.776	ccgTCATTtgtttttcat	HNF-1
SNP11+10	SHRSP	V$NKX25_02	87	(+)	0.778	0.729	cgTCATTt	Nkx2-5
SNP12	SHRSP	V$AIRE_01	44	(-)	0.886	0.854	gcattgccctttgACCCGtaaactgt	AIRE
SNP12	WKY	V$HTF_01	47	(-)	0.756	0.72	ttgccctttgACCTGtaaactgtt	HTF
SNP12	SHRSP	V$HTF_01	49	(+)	0.849	0.788	gcccttgaCCCGTaaactgtttt	HTF
SNP12	SHRSP	V$PAX6_01	49	(-)	0.96	0.8	gcccttgaccCGTAAactgt	Pax-6
SNP12	WKY	V$CEBPGAMMA_Q6	51	(-)	0.752	0.724	cctttGACCTgta	C/EBPgamma
SNP12	WKY	V$E47_02	51	(-)	1	0.752	cctttgACCTGtaaac	E47
SNP12	WKY	V$XBP1_01	51	(+)	0.779	0.737	cctttgACCTGtaaact	XBP-1
SNP12	WKY	V$AREB6_01	52	(+)	1	0.926	ctttgACCTGtaa	AREB6
SNP12	SHRSP	V$AREB6_01	52	(+)	0.8	0.753	ctttgACCCGtaa	AREB6
SNP12	WKY	V$DEC_Q1	52	(-)	0.973	0.716	ctttgACCTGtaa	DEC
SNP12	WKY	V$MTATA_B	52	(-)	0.797	0.749	ctttgaccTGTAAactg	Muscle

Table A5 – Continued overleaf

SNP	Strain	Matrix Identifier	Position	Strand	Matrix match	Core match	Matrix sequence (+ strand)	Factor name
SNP12	SHRSP	V$XBP1_01	52	(-)	0.779	0.767	ctttgaCCCGTaaactg	XBP-1
SNP12	SHRSP	V$ARNT_01	53	(-)	0.792	0.701	tttgaCCCGTaaactg	Arnt
SNP12	WKY	V$CREBP1_Q2	53	(+)	0.8	0.713	ttTGACCtgtaa	CRE-BP1
SNP12	WKY	V$E12_Q6	53	(-)	1	0.778	tttgACCTGta	E12
SNP12	SHRSP	V$E2F_02	53	(+)	0.852	0.761	TTTGAccc	E2F
SNP12	SHRSP	V$E2F_Q4	53	(+)	0.813	0.741	tTTGACcc	E2F
SNP12	SHRSP	V$HIF1_Q3	53	(-)	0.793	0.725	tttgaCCCGTaaac	HIF-1
SNP12	WKY	V$MYOD_01	53	(-)	1	0.713	tttgACCTGtaa	MyoD
SNP12	SHRSP	V$NRF2_Q4	53	(-)	0.873	0.702	ttTGACCcgtaaa	Nrf2
SNP12	SHRSP	V$WHN_B	53	(+)	0.761	0.732	tttGACCCgta	Whn
SNP12	SHRSP	V$ATF_01	54	(-)	0.8	0.726	ttgaccCGTAAact	ATF
SNP12	WKY	V$ATF_B	54	(+)	0.8	0.771	tTGACCtgtaaa	ATF
SNP12	SHRSP	V$E2F_01	54	(+)	0.8	0.734	ttgacccGTAAActg	E2F
SNP12	WKY	V$PAX6_Q2	54	(+)	0.821	0.753	ttgaccTGTAAact	PAX6
SNP12	WKY	V$RORA2_01	54	(-)	1	0.728	tTGACCtgtaaac	RORalpha2
SNP12	WKY	V$ATF6_01	55	(+)	0.8	0.771	TGACCtgt	ATF6
SNP12	SHRSP	V$CEBPDELTA_Q6	55	(-)	0.823	0.702	tgacccGTAAAc	C/EBPdelta
SNP12	WKY	V$COUP_DR1_Q6	55	(+)	1	0.739	tGACCTgtaaact	COUP
SNP12	WKY	V$CREB_01	55	(+)	0.824	0.806	TGACCtgt	CREB
SNP12	SHRSP	V$CREB_Q2_01	55	(+)	0.796	0.716	tgaccCGTAAactg	CREB
SNP12	WKY	V$CREBP1CJUN_01	55	(+)	0.844	0.756	tGACCTgt	CRE-BP1
SNP12	WKY	V$PPARG_03	55	(-)	0.9	0.802	tgaCCTGTaaactgttt	PPAR
SNP12	WKY	V$TFE_Q6	55	(-)	0.932	0.742	tgACCTGt	TFE
SNP12	WKY	V$MEIS1_01	56	(-)	0.77	0.788	gaccTGTAAact	MEIS1
SNP12	SHRSP	V$TAXCREB_01	56	(-)	0.906	0.72	gaccCGTAAactgtt	Tax/CREB
SNP12	SHRSP	V$CREB_02	57	(-)	0.832	0.787	accCGTAAactg	CREB
SNP12	SHRSP	V$CREB_Q4_01	57	(-)	0.789	0.709	accCGTAAact	CREB
SNP12	SHRSP	V$CREBATF_Q6	57	(-)	0.773	0.722	accCGTAAa	CREBATF
SNP12	SHRSP	V$E2F_Q4_01	57	(+)	0.75	0.736	accCGTAAact	E2F
SNP12	WKY	V$TGIF_01	57	(+)	0.79	0.786	accTGTAAact	TGIF
SNP12	SHRSP	V$VMYB_01	57	(-)	0.773	0.741	acCCGTAaac	v-Myb
SNP12	SHRSP	V$E2F1_Q4_01	58	(-)	0.75	0.745	ccCGTAAac	E2F-1

Table A5 – Continued overleaf

SNP	Strain	Matrix Identifier	Position	Strand	Matrix match	Core match	Matrix sequence (+ strand)	Factor name
SNP12	SHRSP	V$VMYB_02	58	(-)	0.778	0.77	cCCGTAaac	v-Myb
SNP12	WKY	V$XFD2_01	58	(+)	0.901	0.749	cctGTAAActgttt	XFD-2
SNP12	SHRSP	V$E2F1_Q4	59	(-)	0.785	0.845	ccGTAAAc	E2F-1
SNP12	SHRSP	V$E2F1DP1_01	59	(-)	0.802	0.743	cCGTAAac	E2F-1:DP-1
SNP12	SHRSP	V$E2F4DP2_01	59	(-)	0.821	0.737	cCGTAAac	E2F-4:DP-2
SNP12	WKY	V$HP1SITEFACTOR_Q6	59	(-)	0.941	0.831	CTGTAaactgtt	HP1
SNP12	SHRSP	V$MYOD_01	60	(-)	0.873	0.707	cgtaAACTGttt	MyoD
SNP13	SHRSP	V$E2_Q6_01	22	(+)	0.917	0.705	ccTACCTtctcctatt	E2
SNP13	SHRSP	V$ETS1_B	22	(-)	0.907	0.771	cctaccttCTCCTat	c-Ets-1
SNP13	WKY	V$AIRE_01	24	(-)	0.987	0.701	taccttctactatTACCActtctacc	AIRE
SNP13	SHRSP	V$CETS1P54_03	24	(-)	0.855	0.774	taccttCTCCTattac	c-Ets-1
SNP13	SHRSP	V$ETS2_B	24	(-)	0.861	0.708	taccttCTCCTatt	c-Ets-2
SNP13	SHRSP	V$CETS1P54_02	26	(-)	0.907	0.872	ccttCTCCTatta	c-Ets-1(p54)
SNP13	SHRSP	V$CETS1P54_01	27	(-)	0.782	0.706	cttcTCCTAt	c-Ets-1(p54)
SNP13	SHRSP	V$WT1_Q6	28	(+)	0.972	0.824	tTCTCCtat	WT1

Table A5 – Transfac Match output for all Gstm1 promoter SNP

All Transfac matrices aligning with either SHRSP or WKY sequences with core and matrix alignment scores over 0.75 and 0.7, respectively. And matrices where core or matrix alignment scores at an individual SNP differ by more than 0.1 between the SHRSP and WKY.

Publications, Awards and Presentations

Publications:

Graham D *, McBride MW*, Gaasenbeek M, Gilday K, Beattie E, **Polke JM**, Miller WH, McClure JD, He Y, Touyz RM, Dominiczak AF. 2005 "Candidate genes that determine response to salt in the stroke prone spontaneously hypertensive rat: Congenic analysis" *Hypertension*. [Epub ahead of print]

McBride MW, Brosnan MJ, Mathers J, McLellan LI, Miller WH, Graham D, Hanlon N, Hamilton CA, **Polke JM**, Lee WK, Dominiczak AF. 2005 "Reduction of Gstm1 expression in the stroke-prone spontaneously hypertension rat contributes to increased oxidative stress" *Hypertension*, vol. 45 no. 4, pp 786-92.

Awards:

Jack Ledingham Young Investigators poster prize, British Society of Hypertension Conference, Cambridge, 2007.

Jack Ledingham Young Investigators poster prize, British Society of Hypertension Conference, Cambridge, 2006.

Presentations:

British Society of Hypertension Conference. Cambridge University, UK 24th-26th September 2007. Poster: RNA-Interference and Adenovirus Mediated Selective Modulation of Cardiovascular Candidate Genes. **JM Polke**, L Graham, WH Miller, SA Nicklin, MW McBride, AH Baker, AF Dominiczak**..**

European Society of Hypertension Conference. Milan, Italy June 15th-19th 2007. Oral presentation: RNA-Interference for Selective Modulation of Cardiovascular Candidate Genes **JM Polke**, L Graham, WH Miller, SA Nicklin, MW McBride, AH Baker, AF Dominiczak. Abstract published in the Journal of Hypertension, Volume 25, Supplement 2, June 2007

International Society of Hypertension Conference (and Satellite SHR Genetics Symposium). Fukuoka and Kyoto, Japan 15^{th}-20^{th} October 2006 Poster: Interactions Between Multiple Promoter Polymorphisms are Required for Reduced Expression of Gstm1 in the SHRSP. **JM Polke**, MW McBride, SA Nicklin, AH Baker, D Graham, AF Dominiczak

European Society of Hypertension Conference. Madrid, Spain June 12^{th}-15^{th} 2006. Oral presentation: Promoter polymorphisms implicated in reduced expression of Gstm1 in the SHRSP. **JM Polke**, MW McBride, SA Nicklin, AH Baker, D Graham, AF Dominiczak.

British Society of Hypertension Conference. Cambridge University, UK 18^{th}-20^{th} September 2006. Poster: Interactions Between Multiple Promoter Polymorphisms are Required for Reduced Expression of Gstm1 in the SHRSP. **JM Polke**, MW McBride, SA Nicklin, AH Baker, D Graham, AF Dominiczak.

Scottish Cardiovascular Forum. University of Strathclyde, UK February 4^{th} 2006. Oral presentation: Promoter polymorphisms implicated in reduced expression of Gstm1 in the SHRSP. **JM Polke**, MW McBride, SA Nicklin, AH Baker, D Graham, AF Dominiczak

Scottish Society of Experimental Medicine. Glasgow University, UK November 25th 2005. Oral presentation: Promoter studies identify potential functional single nucleotide polymorphisms in the Gstm1 regulatory region. **JM Polke**, MW McBride, SA Nicklin, AH Baker, D Graham, AF Dominiczak.

Other abstracts, presenter underlined:

American Heart Association Annual High Blood Pressure Research Conference**.** Westin La Paloma - Tucson, AZ. Sep 26-29, 2007 Oral presentation: Candidate Genes for Salt Sensitive Hypertension in the SHRSP. MW McBride, JD McClure, **JM Polke**, D Graham, AF Dominiczak

Cold Spring Harbour Laboratories Rat Genomics and Models Conference. December 6 - 9, 2007. Oral presentation: GSH levels are significantly reduced in the SHRSP during the development of hypertension. MW McBride, JD McClure, **JM Polke**, CA Hamilton, D Graham, AF Dominiczak

International Society of Hypertension Conference (and Satellite SHR Genetics Symposium). Fukuoka and Kyoto, Japan 15th-20th October 2006. Oral presentation: Gene expression profiling identifies genes and pathways contributing to the development of hypertension. MW McBride, JD McClure, **JM Polke**, D Graham, AF Dominiczak.

Rat Genomics & Models Meeting. Cold Spring Harbour Laboratories, USA (2005) Oral presentation: Proteome and gene profiling identify perturbed pathways in the SHRSP and congenic strains. MW McBride, D Graham, **JM Polke**, R Burchmore, A Pitt, AF Dominiczak

American Heart Association Council for High Blood Pressure Research Meeting Washington USA (2005). Oral presentation: Combined Genomic and Proteomic Approaches to Identify Pathophysiological Pathways in Rodent Models of Hypertension. MW McBride, D Graham, L Zimmerli, **JM Polke**, CA Hamilton, R Burchmore, A Pitt, AF Dominiczak

References

Abe, J., Kusuhara, M., Ulevitch, R. J., Berk, B. C., & Lee, J. D. 1996, "Big mitogen-activated protein kinase 1 (BMK1) is a redox-sensitive kinase", *J.Biol.Chem.*, vol. 271, no. 28, pp. 16586-16590.

Ahmed, N. N., Grimes, H. L., Bellacosa, A., Chan, T. O., & Tsichlis, P. N. 1997, "Transduction of interleukin-2 antiapoptotic and proliferative signals via Akt protein kinase", *Proc.Natl.Acad.Sci.U.S.A*, vol. 94, no. 8, pp. 3627-3632.

Aitman, T. J., Dong, R., Vyse, T. J., Norsworthy, P. J., Johnson, M. D., Smith, J., Mangion, J., Roberton-Lowe, C., Marshall, A. J., Petretto, E., Hodges, M. D., Bhangal, G., Patel, S. G., Sheehan-Rooney, K., Duda, M., Cook, P. R., Evans, D. J., Domin, J., Flint, J., Boyle, J. J., Pusey, C. D., & Cook, H. T. 2006, "Copy number polymorphism in Fcgr3 predisposes to glomerulonephritis in rats and humans", *Nature*, vol. 439, no. 7078, pp. 851-855.

Aitman, T. J., Glazier, A. M., Wallace, C. A., Cooper, L. D., Norsworthy, P. J., Wahid, F. N., Al-Majali, K. M., Trembling, P. M., Mann, C. J., Shoulders, C. C., Graf, D., St Lezin, E., Kurtz, T. W., Kren, V., Pravenec, M., Ibrahimi, A., Abumrad, N. A., Stanton, L. W., & Scott, J. 1999, "Identification of Cd36 (Fat) as an insulin-resistance gene causing defective fatty acid and glucose metabolism in hypertensive rats", *Nat Genet*, vol. 21, no. 1, pp. 76-83.

Aitman, T. J., Gotoda, T., Evans, A. L., Imrie, H., Heath, K. E., Trembling, P. M., Truman, H., Wallace, C. A., Rahman, A., Dore, C., Flint, J., Kren, V., Zidek, V., Kurtz, T. W., Pravenec, M., & Scott, J. 1997, "Quantitative trait loci for cellular defects in glucose and fatty acid metabolism in hypertensive rats", *Nat.Genet.*, vol. 16, no. 2, pp. 197-201.

Akai, S., Hosomi, H., Minami, K., Tsuneyama, K., Katoh, M., Nakajima, M., & Yokoi, T. 2007, "Knock down of gamma-glutamylcysteine synthetase in rat causes acetaminophen-induced hepatotoxicity", *J.Biol.Chem.*, vol. 282, no. 33, pp. 23996-24003.

al Shawi, R., Kinnaird, J., Burke, J., & Bishop, J. O. 1990, "Expression of a foreign gene in a line of transgenic mice is modulated by a chromosomal position effect", *Mol.Cell Biol.*, vol. 10, no. 3, pp. 1192-1198.

Alexander, M. Y., Brosnan, M. J., Hamilton, C. A., Downie, P., Devlin, A. M., Dowell, F., Martin, W., Prentice, H. M., O'Brien, T., & Dominiczak, A. F. 1999, "Gene transfer of endothelial nitric oxide synthase improves nitric oxide-dependent endothelial function in a hypertensive rat model", *Cardiovasc.Res*, vol. 43, no. 3, pp. 798-807.

Alexander, M. Y., Brosnan, M. J., Hamilton, C. A., Fennell, J. P., Beattie, E. C., Jardine, E., Heistad, D. D., & Dominiczak, A. F. 2000, "Gene transfer of endothelial nitric oxide synthase but not Cu/Zn superoxide dismutase restores nitric oxide availability in the SHRSP", *Cardiovasc.Res*, vol. 47, no. 3, pp. 609-617.

Allayee, H., de Bruin, T. W., Michelle, D. K., Cheng, L. S., Ipp, E., Cantor, R. M., Krass, K. L., Keulen, E. T., Aouizerat, B. E., Lusis, A. J., & Rotter, J. I. 2001, "Genome scan for blood pressure in Dutch dyslipidemic families reveals linkage to a locus on chromosome 4p", *Hypertension*, vol. 38, no. 4, pp. 773-778.

Altucci, L., Leibowitz, M. D., Ogilvie, K. M., de Lera, A. R., & Gronemeyer, H. 2007, "RAR and RXR modulation in cancer and metabolic disease", *Nat.Rev.Drug Discov.*, vol. 6, no. 10, pp. 793-810.

Anderson, J. & Akkina, R. 2005, "CXCR4 and CCR5 shRNA transgenic CD34+ cell derived macrophages are functionally normal and resist HIV-1 infection", *Retrovirology.*, vol. 2, p. 53.

Anderson, M. E. & Meister, A. 1983, "Transport and direct utilization of gamma-glutamylcyst(e)ine for glutathione synthesis", *Proc.Natl.Acad.Sci.U.S.A*, vol. 80, no. 3, pp. 707-711.

Anderson, R. D., Haskell, R. E., Xia, H., Roessler, B. J., & Davidson, B. L. 2000, "A simple method for the rapid generation of recombinant adenovirus vectors", *Gene Ther.*, vol. 7, no. 12, pp. 1034-1038.

Angius, A., Petretto, E., Maestrale, G. B., Forabosco, P., Casu, G., Piras, D., Fanciulli, M., Falchi, M., Melis, P. M., Palermo, M., & Pirastu, M. 2002, "A new essential hypertension susceptibility locus on chromosome 2p24-p25, detected by genomewide search", *Am.J.Hum.Genet.*, vol. 71, no. 4, pp. 893-905.

Annest, J. L., Sing, C. F., Biron, P., & Mongeau, J. G. 1979, "Familial aggregation of blood pressure and weight in adoptive families. II. Estimation of the relative contributions of genetic and common environmental factors to blood pressure correlations between family members", *Am.J.Epidemiol.*, vol. 110, no. 4, pp. 492-503.

Annest, J. L., Sing, C. F., Biron, P., & Mongeau, J. G. 1983, "Familial aggregation of blood pressure and weight in adoptive families. III. Analysis of the role of shared genes and shared household environment in explaining family resemblance for height, weight and selected weight/height indices", *Am.J.Epidemiol.*, vol. 117, no. 4, pp. 492-506.

Antoch, M. P., Song, E. J., Chang, A. M., Vitaterna, M. H., Zhao, Y., Wilsbacher, L. D., Sangoram, A. M., King, D. P., Pinto, L. H., & Takahashi, J. S. 1997, "Functional identification of the mouse circadian Clock gene by transgenic BAC rescue", *Cell*, vol. 89, no. 4, pp. 655-667.

Arriza, J. L., Kavanaugh, M. P., Fairman, W. A., Wu, Y. N., Murdoch, G. H., North, R. A., & Amara, S. G. 1993, "Cloning and expression of a human neutral amino acid transporter with structural similarity to the glutamate transporter gene family", *J.Biol.Chem.*, vol. 268, no. 21, pp. 15329-15332.

Arriza, J. L., Weinberger, C., Cerelli, G., Glaser, T. M., Handelin, B. L., Housman, D. E., & Evans, R. M. 1987, "Cloning of human mineralocorticoid receptor complementary DNA: structural and functional kinship with the glucocorticoid receptor", *Science*, vol. 237, no. 4812, pp. 268-275.

Atwood, L. D., Samollow, P. B., Hixson, J. E., Stern, M. P., & MacCluer, J. W. 2001, "Genome-wide linkage analysis of blood pressure in Mexican Americans", *Genet.Epidemiol.*, vol. 20, no. 3, pp. 373-382.

Avissar, N. E., Ryan, C. K., Ganapathy, V., & Sax, H. C. 2001, "Na(+)-dependent neutral amino acid transporter ATB(0) is a rabbit epithelial cell brush-border protein", *Am.J.Physiol Cell Physiol*, vol. 281, no. 3, p. C963-C971.

Bailer, A. & Piegorsch, W. 1997, *Statistics for Environmental Biology and Toxicology* CRC Press, London.

Bansal, N., Cruickshank, J. K., McElduff, P., & Durrington, P. N. 2005, "Cord blood lipoproteins and prenatal influences", *Curr.Opin.Lipidol.*, vol. 16, no. 4, pp. 400-408.

Barrios, R., Shi, Z. Z., Kala, S. V., Wiseman, A. L., Welty, S. E., Kala, G., Bahler, A. A., Ou, C. N., & Lieberman, M. W. 2001, "Oxygen-induced pulmonary injury in gamma-glutamyl transpeptidase-deficient mice", *Lung*, vol. 179, no. 5, pp. 319-330.

Barroso, I., Gurnell, M., Crowley, V. E., Agostini, M., Schwabe, J. W., Soos, M. A., Maslen, G. L., Williams, T. D., Lewis, H., Schafer, A. J., Chatterjee, V. K., & O'Rahilly, S. 1999, "Dominant negative mutations in human PPARgamma associated with severe insulin resistance, diabetes mellitus and hypertension", *Nature*, vol. 402, no. 6764, pp. 880-883.

Bartley, P. A., Keough, R. A., Lutwyche, J. K., & Gonda, T. J. 2003, "Regulation of the gene encoding glutathione S-transferase M1 (GSTM1) by the Myb oncoprotein", *Oncogene*, vol. 22, no. 48, pp. 7570-5.

Beige, J., Hohenbleicher, H., Distler, A., & Sharma, A. M. 1999, "G-Protein beta3 subunit C825T variant and ambulatory blood pressure in essential hypertension", *Hypertension*, vol. 33, no. 4, pp. 1049-1051.

Beilin, L. J. 1995, "Alcohol, hypertension and cardiovascular disease", *J.Hypertens.*, vol. 13, no. 9, pp. 939-942.

Bell, J. T., Wallace, C., Dobson, R., Wiltshire, S., Mein, C., Pembroke, J., Brown, M., Clayton, D., Samani, N., Dominiczak, A., Webster, J., Lathrop, G. M., Connell, J., Munroe, P., Caulfield, M., & Farrall, M. 2006, "Two-dimensional genome-scan identifies novel epistatic loci for essential hypertension", *Hum.Mol.Genet.*, vol. 15, no. 8, pp. 1365-1374.

Ben Ishay, D., Saliternik, R., & Welner, A. 1972, "Separation of two strains of rats with inbred dissimilar sensitivity to Doca-salt hypertension", *Experientia*, vol. 28, no. 11, pp. 1321-1322.

Benjafield, A. V., Wang, W. Y., Speirs, H. J., & Morris, B. J. 2005, "Genome-wide scan for hypertension in Sydney Sibships: the GENIHUSS study", *Am.J.Hypertens.*, vol. 18, no. 6, pp. 828-832.

Berhane, K., Widersten, M., Engstrom, A., Kozarich, J. W., & Mannervik, B. 1994, "Detoxication of base propenals and other alpha, beta-unsaturated aldehyde products of radical reactions and lipid peroxidation by human glutathione transferases", *Proc.Natl.Acad.Sci.U.S.A*, vol. 91, no. 4, pp. 1480-1484.

Bianchi, G. 2005, "Genetic variations of tubular sodium reabsorption leading to "primary" hypertension: from gene polymorphism to clinical symptoms", *Am.J.Physiol Regul.Integr.Comp Physiol*, vol. 289, no. 6, p. R1536-R1549.

Bianchi, G., Fox, U., Di Francesco, G. F., Giovanetti, A. M., & Pagetti, D. 1974a, "Blood pressure changes produced by kidney cross-transplantation between spontaneously hypertensive rats and normotensive rats", *Clin.Sci.Mol.Med.*, vol. 47, no. 5, pp. 435-448.

Bianchi, G., Fox, U., & Imbasciati, E. 1974b, "The development of a new strain of spontaneously hypertensive rats", *Life Sci.*, vol. 14, no. 2, pp. 339-347.

Binder, A. 2007, "A review of the genetics of essential hypertension", *Curr.Opin.Cardiol.*, vol. 22, no. 3, pp. 176-184.

Birney, E., Stamatoyannopoulos, J. A., Dutta, A., Guigo, R., Gingeras, T. R., Margulies, E. H., Weng, Z., Snyder, M., Dermitzakis, E. T., Thurman, R. E., Kuehn, M. S., Taylor, C. M., Neph, S., Koch, C. M., Asthana, S., Malhotra, A., Adzhubei, I., Greenbaum, J. A., Andrews, R. M., Flicek, P., Boyle, P. J., Cao, H., Carter, N. P., Clelland, G. K., Davis, S., Day, N., Dhami, P., Dillon, S. C., Dorschner, M. O., Fiegler, H., Giresi, P. G., Goldy, J., Hawrylycz, M., Haydock, A., Humbert, R., James, K. D., Johnson, B. E., Johnson, E. M., Frum, T. T., Rosenzweig, E. R., Karnani, N., Lee, K., Lefebvre, G. C., Navas, P. A., Neri, F., Parker, S. C., Sabo, P. J., Sandstrom, R., Shafer, A., Vetrie, D., Weaver, M., Wilcox, S., Yu, M., Collins, F. S., Dekker, J., Lieb, J. D., Tullius, T. D., Crawford, G. E., Sunyaev, S., Noble, W. S., Dunham, I., Denoeud, F., Reymond, A., Kapranov, P., Rozowsky, J., Zheng, D., Castelo, R., Frankish, A., Harrow, J., Ghosh, S., Sandelin, A., Hofacker, I. L., Baertsch, R., Keefe, D., Dike, S., Cheng, J., Hirsch, H. A., Sekinger, E. A., Lagarde, J., Abril, J. F., Shahab, A., Flamm, C., Fried, C., Hackermuller, J., Hertel, J., Lindemeyer, M., Missal, K., Tanzer, A., Washietl, S., Korbel, J., Emanuelsson, O., Pedersen, J. S., Holroyd, N., Taylor, R., Swarbreck, D., Matthews, N., Dickson, M. C., Thomas, D. J., Weirauch, M. T., Gilbert, J., Drenkow, J., Bell, I., Zhao, X., Srinivasan, K. G., Sung, W. K., Ooi, H. S., Chiu, K. P., Foissac, S., Alioto, T., Brent, M., Pachter, L., Tress, M. L., Valencia, A., Choo, S. W., Choo, C. Y., Ucla, C., Manzano, C., Wyss, C., Cheung, E., Clark, T. G., Brown, J. B., Ganesh, M., Patel, S., Tammana, H., Chrast, J., Henrichsen, C. N., Kai, C., Kawai, J., Nagalakshmi, U., Wu, J., Lian, Z., Lian, J., Newburger, P., Zhang, X., Bickel, P., Mattick, J. S., Carninci, P., Hayashizaki, Y., Weissman, S., Hubbard, T., Myers, R. M., Rogers, J., Stadler, P. F., Lowe, T. M., Wei, C. L., Ruan, Y., Struhl, K., Gerstein, M., Antonarakis, S. E., Fu, Y., Green, E. D., Karaoz, U., Siepel, A., Taylor, J., Liefer, L. A., Wetterstrand, K. A., Good, P. J., Feingold, E. A., Guyer, M. S., Cooper, G. M., Asimenos, G., Dewey, C. N., Hou, M., Nikolaev, S., Montoya-Burgos, J. I., Loytynoja, A., Whelan, S., Pardi, F., Massingham, T., Huang, H., Zhang, N. R., Holmes, I., Mullikin, J. C., Ureta-Vidal, A., Paten, B., Seringhaus, M., Church, D., Rosenbloom, K., Kent, W. J., Stone, E. A., Batzoglou, S., Goldman, N., Hardison, R. C., Haussler, D., Miller, W., Sidow, A., Trinklein, N. D., Zhang, Z. D., Barrera, L., Stuart, R., King, D. C., Ameur, A., Enroth, S., Bieda, M. C., Kim, J., Bhinge, A. A., Jiang, N., Liu, J., Yao, F., Vega, V. B., Lee, C. W., Ng, P., Shahab, A., Yang, A., Moqtaderi, Z., Zhu, Z., Xu, X., Squazzo, S., Oberley, M. J., Inman, D., Singer, M. A., Richmond, T. A., Munn, K. J., Rada-Iglesias, A., Wallerman, O., Komorowski, J., Fowler, J. C., Couttet, P., Bruce, A. W., Dovey, O. M., Ellis, P. D., Langford, C. F., Nix, D. A., Euskirchen, G., Hartman, S., Urban, A. E., Kraus, P., Van Calcar, S., Heintzman, N., Kim, T. H., Wang, K., Qu, C., Hon, G., Luna, R., Glass, C. K., Rosenfeld, M. G., Aldred, S. F., Cooper, S. J., Halees, A., Lin, J. M., Shulha, H. P., Zhang, X., Xu, M., Haidar, J. N., Yu, Y., Ruan, Y., Iyer, V. R., Green, R. D., Wadelius, C., Farnham, P. J., Ren, B., Harte, R. A., Hinrichs, A. S., Trumbower, H., & Clawson, H. 2007, "Identification and analysis of functional elements in 1% of the human genome by the ENCODE pilot project", *Nature*, vol. 447, no. 7146, pp. 799-816.

Biron, P., Mongeau, J. G., & Bertrand, D. 1976, "Familial aggregation of blood pressure in 558 adopted children", *Can.Med.Assoc.J.*, vol. 115, no. 8, pp. 773-774.

Bland, M. 2000, *An Introduction to Medical Statistics*, 3rd edn, Oxford University Press, Oxford.

Bottger, A., Lankhorst, E., van Lith, H. A., van Zutphen, L. F., Zidek, V., Musilova, A., Simakova, M., Poledne, R., Bila, V., Koen, V., & Pravenec, M. 1998, "A genetic and correlation analysis of liver cholesterol concentration in rat recombinant inbred strains fed a high cholesterol diet", *Biochem.Biophys.Res Commun.*, vol. 246, no. 1, pp. 272-275.

Bray, M. S., Krushkal, J., Li, L., Ferrell, R., Kardia, S., Sing, C. F., Turner, S. T., & Boerwinkle, E. 2000, "Positional genomic analysis identifies the beta(2)-adrenergic

receptor gene as a susceptibility locus for human hypertension", *Circulation*, vol. 101, no. 25, pp. 2877-2882.

Breitling, R., Armengaud, P., Amtmann, A., & Herzyk, P. 2004, "Rank products: a simple, yet powerful, new method to detect differentially regulated genes in replicated microarray experiments", *FEBS Lett.*, vol. 573, no. 1-3, pp. 83-92.

Brennecke, J., Stark, A., Russell, R. B., & Cohen, S. M. 2005, "Principles of microRNA-target recognition", *PLoS.Biol.*, vol. 3, no. 3, p. e85.

Brinster, R. L., Chen, H. Y., Trumbauer, M. E., Yagle, M. K., & Palmiter, R. D. 1985, "Factors affecting the efficiency of introducing foreign DNA into mice by microinjecting eggs", *Proc.Natl.Acad.Sci.U.S.A*, vol. 82, no. 13, pp. 4438-4442.

Brosnan, M. J., Clark, J. S., Jeffs, B., Negrin, C. D., Van Vooren, P., Arribas, S. M., Carswell, H., Aitman, T. J., Szpirer, C., Macrae, I. M., & Dominiczak, A. F. 1999, "Genes encoding atrial and brain natriuretic peptides as candidates for sensitivity to brain ischemia in stroke-prone hypertensive rats", *Hypertension*, vol. 33, no. 1 Pt 2, pp. 290-297.

Cai, H. & Harrison, D. G. 2000, "Endothelial dysfunction in cardiovascular diseases: the role of oxidant stress", *Circ Res*, vol. 87, no. 10, pp. 840-4.

Caulfield, M., Munroe, P., Pembroke, J., Samani, N., Dominiczak, A., Brown, M., Benjamin, N., Webster, J., Ratcliffe, P., O'Shea, S., Papp, J., Taylor, E., Dobson, R., Knight, J., Newhouse, S., Hooper, J., Lee, W., Brain, N., Clayton, D., Lathrop, G. M., Farrall, M., & Connell, J. 2003, "Genome-wide mapping of human loci for essential hypertension", *Lancet*, vol. 361, no. 9375, pp. 2118-2123.

Chabrashvili, T., Kitiyakara, C., Blau, J., Karber, A., Aslam, S., Welch, W. J., & Wilcox, C. S. 2003, "Effects of ANG II type 1 and 2 receptors on oxidative stress, renal NADPH oxidase, and SOD expression", *Am.J.Physiol Regul.Integr.Comp Physiol*, vol. 285, no. 1, p. R117-R124.

Chabrashvili, T., Tojo, A., Onozato, M. L., Kitiyakara, C., Quinn, M. T., Fujita, T., Welch, W. J., & Wilcox, C. S. 2002, "Expression and cellular localization of classic NADPH oxidase subunits in the spontaneously hypertensive rat kidney", *Hypertension*, vol. 39, no. 2, pp. 269-274.

Chairoungdua, A., Kanai, Y., Matsuo, H., Inatomi, J., Kim, D. K., & Endou, H. 2001, "Identification and characterization of a novel member of the heterodimeric amino acid transporter family presumed to be associated with an unknown heavy chain", *J.Biol.Chem.*, vol. 276, no. 52, pp. 49390-49399.

Chanas, S. A., Jiang, Q., McMahon, M., McWalter, G. K., McLellan, L. I., Elcombe, C. R., Henderson, C. J., Wolf, C. R., Moffat, G. J., Itoh, K., Yamamoto, M., & Hayes, J. D. 2002, "Loss of the Nrf2 transcription factor causes a marked reduction in constitutive and inducible expression of the glutathione S-transferase Gsta1, Gsta2, Gstm1, Gstm2, Gstm3 and Gstm4 genes in the livers of male and female mice", *Biochem.J.*, vol. 365, no. Pt 2, pp. 405-416.

Chandler, V. L., Eggleston, W. B., & Dorweiler, J. E. 2000, "Paramutation in maize", *Plant Mol.Biol.*, vol. 43, no. 2-3, pp. 121-145.

Chang, S. S., Grunder, S., Hanukoglu, A., Rosler, A., Mathew, P. M., Hanukoglu, I., Schild, L., Lu, Y., Shimkets, R. A., Nelson-Williams, C., Rossier, B. C., & Lifton, R. P. 1996, "Mutations in subunits of the epithelial sodium channel cause salt wasting with

hyperkalaemic acidosis, pseudohypoaldosteronism type 1", *Nat.Genet.*, vol. 12, no. 3, pp. 248-253.

Charreau, B., Tesson, L., Soulillou, J. P., Pourcel, C., & Anegon, I. 1996, "Transgenesis in rats: technical aspects and models", *Transgenic Res*, vol. 5, no. 4, pp. 223-234.

Charron, S., Duong, C., Menard, A., Roy, J., Eliopoulos, V., Lambert, R., & Deng, A. Y. 2005, "Epistasis, not numbers, regulates functions of clustered Dahl rat quantitative trait loci applicable to human hypertension", *Hypertension*, vol. 46, no. 6, pp. 1300-1308.

Chen, Y., Chen, H., Hoffmann, A., Cool, D. R., Diz, D. I., Chappell, M. C., Chen, A. F., & Morris, M. 2006, "Adenovirus-mediated small-interference RNA for in vivo silencing of angiotensin AT1a receptors in mouse brain", *Hypertension*, vol. 47, no. 2, pp. 230-237.

Cheng, L. S., Davis, R. C., Raffel, L. J., Xiang, A. H., Wang, N., Quinones, M., Wen, P. Z., Toscano, E., Diaz, J., Pressman, S., Henderson, P. C., Azen, S. P., Hsueh, W. A., Buchanan, T. A., & Rotter, J. I. 2001, "Coincident linkage of fasting plasma insulin and blood pressure to chromosome 7q in hypertensive hispanic families", *Circulation*, vol. 104, no. 11, pp. 1255-1260.

Chikhi, N., Holic, N., Guellaen, G., & Laperche, Y. 1999, "Gamma-glutamyl transpeptidase gene organization and expression: a comparative analysis in rat, mouse, pig and human species", *Comp Biochem.Physiol B Biochem.Mol.Biol.*, vol. 122, no. 4, pp. 367-380.

Chu, Y., Iida, S., Lund, D. D., Weiss, R. M., DiBona, G. F., Watanabe, Y., Faraci, F. M., & Heistad, D. D. 2003, "Gene transfer of extracellular superoxide dismutase reduces arterial pressure in spontaneously hypertensive rats: role of heparin-binding domain", *Circ Res*, vol. 92, no. 4, pp. 461-468.

Cicila, G. T., Dukhanina, O. I., Kurtz, T. W., Walder, R., Garrett, M. R., Dene, H., & Rapp, J. P. 1997, "Blood pressure and survival of a chromosome 7 congenic strain bred from Dahl rats", *Mamm.Genome*, vol. 8, no. 12, pp. 896-902.

Cicila, G. T., Garrett, M. R., Lee, S. J., Liu, J., Dene, H., & Rapp, J. P. 2001, "High-resolution mapping of the blood pressure QTL on chromosome 7 using Dahl rat congenic strains", *Genomics*, vol. 72, no. 1, pp. 51-60.

Cicila, G. T., Rapp, J. P., Wang, J. M., St Lezin, E., Ng, S. C., & Kurtz, T. W. 1993, "Linkage of 11 beta-hydroxylase mutations with altered steroid biosynthesis and blood pressure in the Dahl rat", *Nat.Genet.*, vol. 3, no. 4, pp. 346-353.

Ciullo, M., Bellenguez, C., Colonna, V., Nutile, T., Calabria, A., Pacente, R., Iovino, G., Trimarco, B., Bourgain, C., & Persico, M. G. 2006, "New susceptibility locus for hypertension on chromosome 8q by efficient pedigree-breaking in an Italian isolate", *Hum.Mol.Genet.*, vol. 15, no. 10, pp. 1735-1743.

Claessens, F. & Gewirth, D. T. 2004, "DNA recognition by nuclear receptors", *Essays Biochem.*, vol. 40, pp. 59-72.

Clark, J. S., Jeffs, B., Davidson, A. O., Lee, W. K., Anderson, N. H., Bihoreau, M. T., Brosnan, M. J., Devlin, A. M., Kelman, A. W., Lindpaintner, K., & Dominiczak, A. F. 1996, "Quantitative trait loci in genetically hypertensive rats. Possible sex specificity", *Hypertension*, vol. 28, no. 5, pp. 898-906.

Clemitson, J. R., Dixon, R. J., Haines, S., Bingham, A. J., Patel, B. R., Hall, L., Lo, M., Sassard, J., Charchar, F. J., & Samani, N. J. 2007, "Genetic dissection of a blood pressure quantitative trait locus on rat chromosome 1 and gene expression analysis identifies SPON1 as a novel candidate hypertension gene", *Circ Res*, vol. 100, no. 7, pp. 992-999.

Cohen, J. C., Kiss, R. S., Pertsemlidis, A., Marcel, Y. L., McPherson, R., & Hobbs, H. H. 2004, "Multiple rare alleles contribute to low plasma levels of HDL cholesterol", *Science*, vol. 305, no. 5685, pp. 869-872.

Collison, M., Glazier, A. M., Graham, D., Morton, J. J., Dominiczak, M. H., Aitman, T. J., Connell, J. M., Gould, G. W., & Dominiczak, A. F. 2000, "Cd36 and molecular mechanisms of insulin resistance in the stroke-prone spontaneously hypertensive rat", *Diabetes*, vol. 49, no. 12, pp. 2222-2226.

Cooney, A. J., Lee, C. T., Lin, S. C., Tsai, S. Y., & Tsai, M. J. 2001, "Physiological function of the orphans GCNF and COUP-TF", *Trends Endocrinol.Metab*, vol. 12, no. 6, pp. 247-251.

Cooney, R., Hynes, S. O., Sharif, F., Howard, L., & O'Brien, T. 2007, "Effect of gene delivery of NOS isoforms on intimal hyperplasia and endothelial regeneration after balloon injury", *Gene Ther.*, vol. 14, no. 5, pp. 396-404.

Cooper, R. S., Luke, A., Zhu, X., Kan, D., Adeyemo, A., Rotimi, C., Bouzekri, N., & Ward, R. 2002, "Genome scan among Nigerians linking blood pressure to chromosomes 2, 3, and 19", *Hypertension*, vol. 40, no. 5, pp. 629-633.

Cowley, A. W., Jr. 2006, "The genetic dissection of essential hypertension", *Nat.Rev.Genet.*, vol. 7, no. 11, pp. 829-840.

Cross, D. A., Alessi, D. R., Cohen, P., Andjelkovich, M., & Hemmings, B. A. 1995, "Inhibition of glycogen synthase kinase-3 by insulin mediated by protein kinase B", *Nature*, vol. 378, no. 6559, pp. 785-789.

Cui, J., Hopper, J. L., & Harrap, S. B. 2002, "Genes and family environment explain correlations between blood pressure and body mass index", *Hypertension*, vol. 40, no. 1, pp. 7-12.

Cui, J., Melista, E., Chazaro, I., Zhang, Y., Zhou, X., Manolis, A. J., Baldwin, C. T., Destefano, A. L., & Gavras, H. 2005, "Sequence variation of bradykinin receptors B1 and B2 and association with hypertension", *J.Hypertens.*, vol. 23, no. 1, pp. 55-62.

Dahl, L., Heine, M. M., & Tassinari, L. L. 1962a, "Effects of chronia excess salt ingestion. Evidence that genetic factors play an important role in susceptibility to experimental hypertension", *J.Exp.Med.*, vol. 115, pp. 1173-1190.

Dahl, L., Heine, M. M., & Tassinari, L. L. 1962b, "Role of genetic factors in susceptibility to experimental hypertension due to chronic excess salt ingestion", *Nature*, vol. 194, pp. 480-482.

Darvasi, A. 2006, "Closing in on complex traits", *Nat.Genet.*, vol. 38, no. 8, pp. 861-862.

Darvasi, A., Weinreb, A., Minke, V., Weller, J. I., & Soller, M. 1993, "Detecting marker-QTL linkage and estimating QTL gene effect and map location using a saturated genetic map", *Genetics*, vol. 134, no. 3, pp. 943-951.

Davidson, A. O., Schork, N., Jaques, B. C., Kelman, A. W., Sutcliffe, R. G., Reid, J. L., & Dominiczak, A. F. 1995, "Blood pressure in genetically hypertensive rats. Influence of the Y chromosome", *Hypertension*, vol. 26, no. 3, pp. 452-459.

Davidson, B. L. & Harper, S. Q. 2005, "Viral delivery of recombinant short hairpin RNAs", *Methods Enzymol.*, vol. 392, pp. 145-173.

De Keulenaer, G. W., Alexander, R. W., Ushio-Fukai, M., Ishizaka, N., & Griendling, K. K. 1998a, "Tumour necrosis factor alpha activates a p22phox-based NADH oxidase in vascular smooth muscle", *Biochem.J.*, vol. 329 (Pt 3), pp. 653-657.

De Keulenaer, G. W., Chappell, D. C., Ishizaka, N., Nerem, R. M., Alexander, R. W., & Griendling, K. K. 1998b, "Oscillatory and steady laminar shear stress differentially affect human endothelial redox state: role of a superoxide-producing NADH oxidase", *Circ Res*, vol. 82, no. 10, pp. 1094-1101.

de Waart, F. G., Kok, F. J., Smilde, T. J., Hijmans, A., Wollersheim, H., & Stalenhoef, A. F. 2001, "Effect of glutathione S-transferase M1 genotype on progression of atherosclerosis in lifelong male smokers", *Atherosclerosis*, vol. 158, no. 1, pp. 227-231.

DelliPizzi, A. M., Hilchey, S. D., & Bell-Quilley, C. P. 1994, "Natriuretic action of angiotensin(1-7)", *Br.J.Pharmacol.*, vol. 111, no. 1, pp. 1-3.

Denby, L., Work, L. M., Graham, D., Hsu, C., von Seggern, D. J., Nicklin, S. A., & Baker, A. H. 2004, "Adenoviral serotype 5 vectors pseudotyped with fibers from subgroup D show modified tropism in vitro and in vivo", *Hum.Gene Ther.*, vol. 15, no. 11, pp. 1054-1064.

Denby, L., Work, L. M., Seggern, D. J., Wu, E., McVey, J. H., Nicklin, S. A., & Baker, A. H. 2007, "Development of renal-targeted vectors through combined in vivo phage display and capsid engineering of adenoviral fibers from serotype 19p", *Mol.Ther.*, vol. 15, no. 9, pp. 1647-1654.

Deneke, S. M. & Fanburg, B. L. 1989, "Regulation of cellular glutathione", *Am.J.Physiol*, vol. 257, no. 4 Pt 1, p. L163-L173.

Deng, A. Y. 2007, "Positional cloning of quantitative trait Loci for blood pressure: how close are we?: a critical perspective", *Hypertension*, vol. 49, no. 4, pp. 740-747.

Deng, A. Y., Dene, H., & Rapp, J. P. 1994, "Mapping of a quantitative trait locus for blood pressure on rat chromosome 2", *J.Clin.Invest*, vol. 94, no. 1, pp. 431-436.

Deng, Y. & Rapp, J. P. 1992, "Cosegregation of blood pressure with angiotensin converting enzyme and atrial natriuretic peptide receptor genes using Dahl salt-sensitive rats", *Nat.Genet.*, vol. 1, no. 4, pp. 267-272.

Destefano, A. L., Gavras, H., Heard-Costa, N., Bursztyn, M., Manolis, A., Farrer, L. A., Baldwin, C. T., Gavras, I., & Schwartz, F. 2001, "Maternal component in the familial aggregation of hypertension", *Clin.Genet.*, vol. 60, no. 1, pp. 13-21.

Dhakshinamoorthy, S., Jain, A. K., Bloom, D. A., & Jaiswal, A. K. 2005, "Bach1 competes with Nrf2 leading to negative regulation of the antioxidant response element (ARE)-mediated NAD(P)H:quinone oxidoreductase 1 gene expression and induction in response to antioxidants", *J.Biol.Chem.*, vol. 280, no. 17, pp. 16891-16900.

Dobrian, A. D. 2006, "The complex role of PPARgamma in renal dysfunction in obesity: managing a Janus-faced receptor", *Vascul.Pharmacol.*, vol. 45, no. 1, pp. 36-45.

Dobrzynski, E., Yoshida, H., Chao, J., & Chao, L. 1999, "Adenovirus-mediated kallikrein gene delivery attenuates hypertension and protects against renal injury in deoxycorticosterone-salt rats", *Immunopharmacology*, vol. 44, no. 1-2, pp. 57-65.

Dominiczak, A. F., Graham, D., McBride, M. W., Brain, N. J., Lee, W. K., Charchar, F. J., Tomaszewski, M., Delles, C., & Hamilton, C. A. 2005, "Corcoran Lecture. Cardiovascular genomics and oxidative stress", *Hypertension*, vol. 45, no. 4, pp. 636-42.

Donoghue, M., Hsieh, F., Baronas, E., Godbout, K., Gosselin, M., Stagliano, N., Donovan, M., Woolf, B., Robison, K., Jeyaseelan, R., Breitbart, R. E., & Acton, S. 2000, "A novel angiotensin-converting enzyme-related carboxypeptidase (ACE2) converts angiotensin I to angiotensin 1-9", *Circ Res*, vol. 87, no. 5, p. E1-E9.

Drake, T. A., Schadt, E. E., & Lusis, A. J. 2006, "Integrating genetic and gene expression data: application to cardiovascular and metabolic traits in mice", *Mamm.Genome*, vol. 17, no. 6, pp. 466-479.

Du, Q., Thonberg, H., Wang, J., Wahlestedt, C., & Liang, Z. 2005, "A systematic analysis of the silencing effects of an active siRNA at all single-nucleotide mismatched target sites", *Nucleic Acids Res*, vol. 33, no. 5, pp. 1671-1677.

Duff, K., Knight, H., Refolo, L. M., Sanders, S., Yu, X., Picciano, M., Malester, B., Hutton, M., Adamson, J., Goedert, M., Burki, K., & Davies, P. 2000, "Characterization of pathology in transgenic mice over-expressing human genomic and cDNA tau transgenes", *Neurobiol.Dis.*, vol. 7, no. 2, pp. 87-98.

Dumas, M. E., Wilder, S. P., Bihoreau, M. T., Barton, R. H., Fearnside, J. F., Argoud, K., D'Amato, L., Wallis, R. H., Blancher, C., Keun, H. C., Baunsgaard, D., Scott, J., Sidelmann, U. G., Nicholson, J. K., & Gauguier, D. 2007, "Direct quantitative trait locus mapping of mammalian metabolic phenotypes in diabetic and normoglycemic rat models", *Nat.Genet.*, vol. 39, no. 5, pp. 666-672.

Dupont, J., Dupont, J. C., Froment, A., Milon, H., & Vincent, M. 1973, "Selection of three strains of rats with spontaneously different levels of blood pressure", *Biomedicine.*, vol. 19, no. 1, pp. 36-41.

Durand, E., Al Haj, Z. A., Addad, F., Brasselet, C., Caligiuri, G., Vinchon, F., Lemarchand, P., Desnos, M., Bruneval, P., & Lafont, A. 2005, "Adenovirus-mediated gene transfer of superoxide dismutase and catalase decreases restenosis after balloon angioplasty", *J.Vasc.Res*, vol. 42, no. 3, pp. 255-265.

Dutil, J. & Deng, A. Y. 2001, "Further chromosomal mapping of a blood pressure QTL in Dahl rats on chromosome 2 using congenic strains", *Physiol Genomics*, vol. 6, no. 1, pp. 3-9.

Dutil, J., Eliopoulos, V., Tremblay, J., Hamet, P., Charron, S., & Deng, A. Y. 2005, "Multiple quantitative trait loci for blood pressure interacting epistatically and additively on dahl rat chromosome 2", *Hypertension*, vol. 45, no. 4, pp. 557-64.

Dykxhoorn, D. M., Schlehuber, L. D., London, I. M., & Lieberman, J. 2006, "Determinants of specific RNA interference-mediated silencing of human beta-globin alleles differing by a single nucleotide polymorphism", *Proc.Natl.Acad.Sci.U.S.A*, vol. 103, no. 15, pp. 5953-5958.

Efrati, S., Berman, S., Ilgiyeav, E., Averbukh, Z., & Weissgarten, J. 2007, "PPAR-gamma activation inhibits angiotensin II synthesis, apoptosis, and proliferation of mesangial cells from spontaneously hypertensive rats", *Nephron Exp.Nephrol.*, vol. 106, no. 4, p. e107-e112.

El Armouche, A., Singh, J., Naito, H., Wittkopper, K., Didie, M., Laatsch, A., Zimmermann, W. H., & Eschenhagen, T. 2007, "Adenovirus-delivered short hairpin RNA targeting PKCalpha improves contractile function in reconstituted heart tissue", *J.Mol.Cell Cardiol.*, vol. 43, no. 3, pp. 371-376.

Elbashir, S. M., Harborth, J., Lendeckel, W., Yalcin, A., Weber, K., & Tuschl, T. 2001a, "Duplexes of 21-nucleotide RNAs mediate RNA interference in cultured mammalian cells", *Nature*, vol. 411, no. 6836, pp. 494-498.

Elbashir, S. M., Martinez, J., Patkaniowska, A., Lendeckel, W., & Tuschl, T. 2001b, "Functional anatomy of siRNAs for mediating efficient RNAi in Drosophila melanogaster embryo lysate", *EMBO J.*, vol. 20, no. 23, pp. 6877-6888.

Eliopoulos, V., Dutil, J., Deng, Y., Grondin, M., & Deng, A. Y. 2005, "Severe hypertension caused by alleles from normotensive Lewis for a quantitative trait locus on chromosome 2", *Physiol Genomics*, vol. 22, no. 1, pp. 70-75.

Evans, R. M. 1988, "The steroid and thyroid hormone receptor superfamily", *Science*, vol. 240, no. 4854, pp. 889-895.

Falkner, K. C., Pinaire, J. A., Xiao, G. H., Geoghegan, T. E., & Prough, R. A. 2001, "Regulation of the rat glutathione S-transferase A2 gene by glucocorticoids: involvement of both the glucocorticoid and pregnane X receptors", *Mol.Pharmacol.*, vol. 60, no. 3, pp. 611-619.

Falkner, K. C., Rushmore, T. H., Linder, M. W., & Prough, R. A. 1998, "Negative regulation of the rat glutathione S-transferase A2 gene by glucocorticoids involves a canonical glucocorticoid consensus sequence", *Mol.Pharmacol.*, vol. 53, no. 6, pp. 1016-1026.

Farjah, M., Washington, T. L., Roxas, B. P., Geenen, D. L., & Danziger, R. S. 2004, "Dietary NaCl regulates renal aminopeptidase N: relevance to hypertension in the Dahl rat", *Hypertension*, vol. 43, no. 2, pp. 282-285.

Fasbender, A., Lee, J. H., Walters, R. W., Moninger, T. O., Zabner, J., & Welsh, M. J. 1998, "Incorporation of adenovirus in calcium phosphate precipitates enhances gene transfer to airway epithelia in vitro and in vivo", *J.Clin.Invest*, vol. 102, no. 1, pp. 184-193.

Feinleib, M., Garrison, R. J., Fabsitz, R., Christian, J. C., Hrubec, Z., Borhani, N. O., Kannel, W. B., Rosenman, R., Schwartz, J. T., & Wagner, J. O. 1977, "The NHLBI twin study of cardiovascular disease risk factors: methodology and summary of results", *Am.J.Epidemiol.*, vol. 106, no. 4, pp. 284-285.

Fejes-Toth, G. & Naray-Fejes-Toth, A. 1992, "Differentiation of renal beta-intercalated cells to alpha-intercalated and principal cells in culture", *Proc.Natl.Acad.Sci.U.S.A*, vol. 89, no. 12, pp. 5487-5491.

Fennell, J. P., Brosnan, M. J., Frater, A. J., Hamilton, C. A., Alexander, M. Y., Nicklin, S. A., Heistad, D. D., Baker, A. H., & Dominiczak, A. F. 2002, "Adenovirus-mediated overexpression of extracellular superoxide dismutase improves endothelial dysfunction in a rat model of hypertension", *Gene Ther.*, vol. 9, no. 2, pp. 110-117.

Ferrandi, M., Salardi, S., Tripodi, G., Barassi, P., Rivera, R., Manunta, P., Goldshleger, R., Ferrari, P., Bianchi, G., & Karlish, S. J. 1999, "Evidence for an interaction between adducin and Na(+)-K(+)-ATPase: relation to genetic hypertension", *Am.J.Physiol*, vol. 277, no. 4 Pt 2, p. H1338-H1349.

Fetita, L. S., Sobngwi, E., Serradas, P., Calvo, F., & Gautier, J. F. 2006, "Consequences of fetal exposure to maternal diabetes in offspring", *J.Clin.Endocrinol.Metab*, vol. 91, no. 10, pp. 3718-3724.

Fire, A., Xu, S., Montgomery, M. K., Kostas, S. A., Driver, S. E., & Mello, C. C. 1998, "Potent and specific genetic interference by double-stranded RNA in Caenorhabditis elegans", *Nature*, vol. 391, no. 6669, pp. 806-811.

Fjell, C. D., Bosdet, I., Schein, J. E., Jones, S. J., & Marra, M. A. 2003, "Internet Contig Explorer (iCE)--a tool for visualizing clone fingerprint maps", *Genome Res*, vol. 13, no. 6A, pp. 1244-1249.

Frantz, S., Clemitson, J. R., Bihoreau, M. T., Gauguier, D., & Samani, N. J. 2001, "Genetic dissection of region around the Sa gene on rat chromosome 1: evidence for multiple loci affecting blood pressure", *Hypertension*, vol. 38, no. 2, pp. 216-221.

Frayling, T. M., Timpson, N. J., Weedon, M. N., Zeggini, E., Freathy, R. M., Lindgren, C. M., Perry, J. R., Elliott, K. S., Lango, H., Rayner, N. W., Shields, B., Harries, L. W., Barrett, J. C., Ellard, S., Groves, C. J., Knight, B., Patch, A. M., Ness, A. R., Ebrahim, S., Lawlor, D. A., Ring, S. M., Ben Shlomo, Y., Jarvelin, M. R., Sovio, U., Bennett, A. J., Melzer, D., Ferrucci, L., Loos, R. J., Barroso, I., Wareham, N. J., Karpe, F., Owen, K. R., Cardon, L. R., Walker, M., Hitman, G. A., Palmer, C. N., Doney, A. S., Morris, A. D., Smith, G. D., Hattersley, A. T., & McCarthy, M. I. 2007, "A common variant in the FTO gene is associated with body mass index and predisposes to childhood and adult obesity", *Science*, vol. 316, no. 5826, pp. 889-894.

Fridovich, I. 1998, "Oxygen toxicity: a radical explanation", *J.Exp.Biol.*, vol. 201, no. Pt 8, pp. 1203-1209.

Fujimoto, K., Arakawa, S., Shibaya, Y., Miida, H., Ando, Y., Yasumo, H., Hara, A., Uchiyama, M., Iwabuchi, H., Takasaki, W., Manabe, S., & Yamoto, T. 2006, "Characterization of phenotypes in Gstm1-null mice by cytosolic and in vivo metabolic studies using 1,2-dichloro-4-nitrobenzene", *Drug Metab Dispos.*, vol. 34, no. 9, pp. 1495-1501.

Fujino, T., Asaba, H., Kang, M. J., Ikeda, Y., Sone, H., Takada, S., Kim, D. H., Ioka, R. X., Ono, M., Tomoyori, H., Okubo, M., Murase, T., Kamataki, A., Yamamoto, J., Magoori, K., Takahashi, S., Miyamoto, Y., Oishi, H., Nose, M., Okazaki, M., Usui, S., Imaizumi, K., Yanagisawa, M., Sakai, J., & Yamamoto, T. T. 2003, "Low-density lipoprotein receptor-related protein 5 (LRP5) is essential for normal cholesterol metabolism and glucose-induced insulin secretion", *Proc.Natl.Acad.Sci.U.S.A*, vol. 100, no. 1, pp. 229-234.

Funder, J. W., Pearce, P. T., Smith, R., & Smith, A. I. 1988, "Mineralocorticoid action: target tissue specificity is enzyme, not receptor, mediated", *Science*, vol. 242, no. 4878, pp. 583-585.

Furchgott, R. F. & Zawadzki, J. V. 1980, "The obligatory role of endothelial cells in the relaxation of arterial smooth muscle by acetylcholine", *Nature*, vol. 288, no. 5789, pp. 373-376.

Galetic, I., Andjelkovic, M., Meier, R., Brodbeck, D., Park, J., & Hemmings, B. A. 1999, "Mechanism of protein kinase B activation by insulin/insulin-like growth factor-1 revealed by specific inhibitors of phosphoinositide 3-kinase--significance for diabetes and cancer", *Pharmacol.Ther.*, vol. 82, no. 2-3, pp. 409-425.

Gama Sosa, M. A., Hall, J. C., & Ruprecht, R. M. 1988, "Slipped DNA structures within the enhancer region of the Moloney murine leukemia virus", *Biochem.Biophys.Res Commun.*, vol. 156, no. 1, pp. 417-423.

Gama, S. M., De Gasperi, R., Wen, P. H., Gonzalez, E. A., Kelley, K., Lazzarini, R. A., & Elder, G. A. 2002, "BAC and PAC DNA for the generation of transgenic animals", *Biotechniques*, vol. 33, no. 1, pp. 51-53.

Ganten, D., Wagner, J., Zeh, K., Bader, M., Michel, J. B., Paul, M., Zimmermann, F., Ruf, P., Hilgenfeldt, U., Ganten, U., & . 1992, "Species specificity of renin kinetics in transgenic rats harboring the human renin and angiotensinogen genes", *Proc.Natl.Acad.Sci.U.S.A*, vol. 89, no. 16, pp. 7806-7810.

Garrett, M. R., Meng, H., Rapp, J. P., & Joe, B. 2005, "Locating a blood pressure quantitative trait locus within 117 kb on the rat genome: substitution mapping and renal expression analysis", *Hypertension*, vol. 45, no. 3, pp. 451-9.

Garrett, M. R. & Rapp, J. P. 2002, "Multiple blood pressure QTL on rat Chromosome 2 defined by congenic Dahl rats", *Mamm Genome*, vol. 13, no. 1, pp. 41-4.

Garrett, M. R. & Rapp, J. P. 2003, "Defining the blood pressure QTL on chromosome 7 in Dahl rats by a 177-kb congenic segment containing Cyp11b1", *Mamm.Genome*, vol. 14, no. 4, pp. 268-273.

Garte, S., Gaspari, L., Alexandrie, A. K., Ambrosone, C., Autrup, H., Autrup, J. L., Baranova, H., Bathum, L., Benhamou, S., Boffetta, P., Bouchardy, C., Breskvar, K., Brockmoller, J., Cascorbi, I., Clapper, M. L., Coutelle, C., Daly, A., Dell'Omo, M., Dolzan, V., Dresler, C. M., Fryer, A., Haugen, A., Hein, D. W., Hildesheim, A., Hirvonen, A., Hsieh, L. L., Ingelman-Sundberg, M., Kalina, I., Kang, D., Kihara, M., Kiyohara, C., Kremers, P., Lazarus, P., Le Marchand, L., Lechner, M. C., van Lieshout, E. M., London, S., Manni, J. J., Maugard, C. M., Morita, S., Nazar-Stewart, V., Noda, K., Oda, Y., Parl, F. F., Pastorelli, R., Persson, I., Peters, W. H., Rannug, A., Rebbeck, T., Risch, A., Roelandt, L., Romkes, M., Ryberg, D., Salagovic, J., Schoket, B., Seidegard, J., Shields, P. G., Sim, E., Sinnet, D., Strange, R. C., Stucker, I., Sugimura, H., To-Figueras, J., Vineis, P., Yu, M. C., & Taioli, E. 2001, "Metabolic gene polymorphism frequencies in control populations", *Cancer Epidemiol.Biomarkers Prev.*, vol. 10, no. 12, pp. 1239-1248.

Gauguier, D., Froguel, P., Parent, V., Bernard, C., Bihoreau, M. T., Portha, B., James, M. R., Penicaud, L., Lathrop, M., & Ktorza, A. 1996, "Chromosomal mapping of genetic loci associated with non-insulin dependent diabetes in the GK rat", *Nat.Genet.*, vol. 12, no. 1, pp. 38-43.

Ge, D., Huang, J., He, J., Li, B., Duan, X., Chen, R., & Gu, D. 2005, "beta2-Adrenergic receptor gene variations associated with stage-2 hypertension in northern Han Chinese", *Ann.Hum.Genet.*, vol. 69, no. Pt 1, pp. 36-44.

Geller, D. S., Farhi, A., Pinkerton, N., Fradley, M., Moritz, M., Spitzer, A., Meinke, G., Tsai, F. T., Sigler, P. B., & Lifton, R. P. 2000, "Activating mineralocorticoid receptor mutation in hypertension exacerbated by pregnancy", *Science*, vol. 289, no. 5476, pp. 119-123.

Geller, D. S., Rodriguez-Soriano, J., Vallo, B. A., Schifter, S., Bayer, M., Chang, S. S., & Lifton, R. P. 1998, "Mutations in the mineralocorticoid receptor gene cause autosomal dominant pseudohypoaldosteronism type I", *Nat.Genet.*, vol. 19, no. 3, pp. 279-281.

Gibbs, R. A., Weinstock, G. M., Metzker, M. L., Muzny, D. M., Sodergren, E. J., Scherer, S., Scott, G., Steffen, D., Worley, K. C., Burch, P. E., Okwuonu, G., Hines, S., Lewis, L., DeRamo, C., Delgado, O., Dugan-Rocha, S., Miner, G., Morgan, M., Hawes, A., Gill, R., Celera, Holt, R. A., Adams, M. D., Amanatides, P. G., Baden-Tillson, H., Barnstead, M., Chin, S., Evans, C. A., Ferriera, S., Fosler, C., Glodek, A., Gu, Z., Jennings, D., Kraft, C. L., Nguyen, T., Pfannkoch, C. M., Sitter, C., Sutton, G. G., Venter, J. C., Woodage, T., Smith, D., Lee, H. M., Gustafson, E., Cahill, P., Kana, A., Doucette-Stamm, L., Weinstock, K., Fechtel, K., Weiss, R. B., Dunn, D. M., Green, E. D., Blakesley, R. W., Bouffard, G. G., De Jong, P. J., Osoegawa, K., Zhu, B., Marra, M., Schein, J., Bosdet, I., Fjell, C., Jones, S., Krzywinski, M., Mathewson, C., Siddiqui, A., Wye, N., McPherson, J., Zhao, S., Fraser, C. M., Shetty, J., Shatsman, S., Geer, K., Chen, Y., Abramzon, S., Nierman, W. C., Havlak, P. H., Chen, R., Durbin, K. J., Egan, A., Ren, Y., Song, X. Z., Li, B., Liu, Y., Qin, X., Cawley, S., Cooney, A. J., D'Souza, L. M., Martin, K., Wu, J. Q., Gonzalez-Garay, M. L., Jackson, A. R., Kalafus, K. J., McLeod, M. P., Milosavljevic, A., Virk, D., Volkov, A., Wheeler, D. A., Zhang, Z., Bailey, J. A., Eichler, E. E., Tuzun, E., Birney, E., Mongin, E., Ureta-Vidal, A., Woodwark, C., Zdobnov, E., Bork, P., Suyama, M., Torrents, D., Alexandersson, M., Trask, B. J., Young, J. M., Huang, H., Wang, H., Xing, H., Daniels, S., Gietzen, D., Schmidt, J., Stevens, K., Vitt, U., Wingrove, J., Camara, F., Mar Alba, M., Abril, J. F., Guigo, R., Smit, A., Dubchak, I., Rubin, E. M., Couronne, O., Poliakov, A., Hubner, N., Ganten, D., Goesele, C., Hummel, O., Kreitler, T., Lee, Y. A., Monti, J., Schulz, H., Zimdahl, H., Himmelbauer, H., Lehrach, H., Jacob, H. J., Bromberg, S., Gullings-Handley, J., Jensen-Seaman, M. I., Kwitek, A. E., Lazar, J., Pasko, D., Tonellato, P. J., Twigger, S., Ponting, C. P., Duarte, J. M., Rice, S., Goodstadt, L., Beatson, S. A., Emes, R. D., Winter, E. E., Webber, C., Brandt, P., Nyakatura, G., Adetobi, M., Chiaromonte, F., Elnitski, L., Eswara, P., Hardison, R. C., Hou, M., Kolbe, D., Makova, K., Miller, W., Nekrutenko, A., Riemer, C., Schwartz, S., Taylor, J., Yang, S., Zhang, Y., Lindpaintner, K., Andrews, T. D., Caccamo, M., Clamp, M., Clarke, L., Curwen, V., Durbin, R., Eyras, E., Searle, S. M., Cooper, G. M., Batzoglou, S., Brudno, M., Sidow, A., Stone, E. A., Payseur, B. A., Bourque, G., Lopez-Otin, C., Puente, X. S., Chakrabarti, K., Chatterji, S., Dewey, C., Pachter, L., Bray, N., Yap, V. B., Caspi, A., Tesler, G., Pevzner, P. A., Haussler, D., Roskin, K. M., Baertsch, R., Clawson, H., Furey, T. S., Hinrichs, A. S., Karolchik, D., Kent, W. J., Rosenbloom, K. R., Trumbower, H., Weirauch, M., Cooper, D. N., Stenson, P. D., Ma, B., Brent, M., Arumugam, M., Shteynberg, D., Copley, R. R., Taylor, M. S., Riethman, H., Mudunuri, U., Peterson, J., Guyer, M., Felsenfeld, A., Old, S., Mockrin, S., & Collins, F. 2004, "Genome sequence of the Brown Norway rat yields insights into mammalian evolution", *Nature*, vol. 428, no. 6982, pp. 493-521.

Giraldo, P. & Montoliu, L. 2001, "Size matters: use of YACs, BACs and PACs in transgenic animals", *Transgenic Res*, vol. 10, no. 2, pp. 83-103.

Gong, M., Zhang, H., Schulz, H., Lee, Y. A., Sun, K., Bahring, S., Luft, F. C., Nurnberg, P., Reis, A., Rohde, K., Ganten, D., Hui, R., & Hubner, N. 2003, "Genome-wide linkage reveals a locus for human essential (primary) hypertension on chromosome 12p", *Hum.Mol.Genet.*, vol. 12, no. 11, pp. 1273-1277.

Gong, Y., Slee, R. B., Fukai, N., Rawadi, G., Roman-Roman, S., Reginato, A. M., Wang, H., Cundy, T., Glorieux, F. H., Lev, D., Zacharin, M., Oexle, K., Marcelino, J., Suwairi, W., Heeger, S., Sabatakos, G., Apte, S., Adkins, W. N., Allgrove, J., Arslan-Kirchner, M., Batch, J. A., Beighton, P., Black, G. C., Boles, R. G., Boon, L. M., Borrone, C., Brunner, H. G., Carle, G. F., Dallapiccola, B., De Paepe, A., Floege, B., Halfhide, M. L., Hall, B.,

Hennekam, R. C., Hirose, T., Jans, A., Juppner, H., Kim, C. A., Keppler-Noreuil, K., Kohlschuetter, A., LaCombe, D., Lambert, M., Lemyre, E., Letteboer, T., Peltonen, L., Ramesar, R. S., Romanengo, M., Somer, H., Steichen-Gersdorf, E., Steinmann, B., Sullivan, B., Superti-Furga, A., Swoboda, W., van den Boogaard, M. J., Van Hul, W., Vikkula, M., Votruba, M., Zabel, B., Garcia, T., Baron, R., Olsen, B. R., & Warman, M. L. 2001, "LDL receptor-related protein 5 (LRP5) affects bone accrual and eye development", *Cell*, vol. 107, no. 4, pp. 513-523.

Gow, A., Southwood, C. M., Li, J. S., Pariali, M., Riordan, G. P., Brodie, S. E., Danias, J., Bronstein, J. M., Kachar, B., & Lazzarini, R. A. 1999, "CNS myelin and sertoli cell tight junction strands are absent in Osp/claudin-11 null mice", *Cell*, vol. 99, no. 6, pp. 649-659.

Graham, D., McBride, M. W., Gaasenbeek, M., Gilday, K., Beattie, E., Miller, W. H., McClure, J. D., Polke, J. M., Montezano, A., Touyz, R. M., & Dominiczak, A. F. 2007, "Candidate genes that determine response to salt in the stroke-prone spontaneously hypertensive rat: congenic analysis", *Hypertension*, vol. 50, no. 6, pp. 1134-1141.

Graham, F. L., Smiley, J., Russell, W. C., & Nairn, R. 1977, "Characteristics of a human cell line transformed by DNA from human adenovirus type 5", *J.Gen.Virol.*, vol. 36, no. 1, pp. 59-74.

Grant, S. F., Thorleifsson, G., Reynisdottir, I., Benediktsson, R., Manolescu, A., Sainz, J., Helgason, A., Stefansson, H., Emilsson, V., Helgadottir, A., Styrkarsdottir, U., Magnusson, K. P., Walters, G. B., Palsdottir, E., Jonsdottir, T., Gudmundsdottir, T., Gylfason, A., Saemundsdottir, J., Wilensky, R. L., Reilly, M. P., Rader, D. J., Bagger, Y., Christiansen, C., Gudnason, V., Sigurdsson, G., Thorsteinsdottir, U., Gulcher, J. R., Kong, A., & Stefansson, K. 2006, "Variant of transcription factor 7-like 2 (TCF7L2) gene confers risk of type 2 diabetes", *Nat.Genet.*, vol. 38, no. 3, pp. 320-323.

Greally, J. M. 2007, "Genomics: Encyclopaedia of humble DNA", *Nature*, vol. 447, no. 7146, pp. 782-783.

Grimm, D., Streetz, K. L., Jopling, C. L., Storm, T. A., Pandey, K., Davis, C. R., Marion, P., Salazar, F., & Kay, M. A. 2006, "Fatality in mice due to oversaturation of cellular microRNA/short hairpin RNA pathways", *Nature*, vol. 441, no. 7092, pp. 537-541.

Grobe, J. L., Mecca, A. P., Mao, H., & Katovich, M. J. 2006, "Chronic angiotensin-(1-7) prevents cardiac fibrosis in DOCA-salt model of hypertension", *Am.J.Physiol Heart Circ Physiol*, vol. 290, no. 6, p. H2417-H2423.

Gu, D., Su, S., Ge, D., Chen, S., Huang, J., Li, B., Chen, R., & Qiang, B. 2006, "Association study with 33 single-nucleotide polymorphisms in 11 candidate genes for hypertension in Chinese", *Hypertension*, vol. 47, no. 6, pp. 1147-1154.

Guan, Y., Hao, C., Cha, D. R., Rao, R., Lu, W., Kohan, D. E., Magnuson, M. A., Redha, R., Zhang, Y., & Breyer, M. D. 2005, "Thiazolidinediones expand body fluid volume through PPARgamma stimulation of ENaC-mediated renal salt absorption", *Nat.Med.*, vol. 11, no. 8, pp. 861-866.

Gudmundsson, J., Sulem, P., Steinthorsdottir, V., Bergthorsson, J. T., Thorleifsson, G., Manolescu, A., Rafnar, T., Gudbjartsson, D., Agnarsson, B. A., Baker, A., Sigurdsson, A., Benediktsdottir, K. R., Jakobsdottir, M., Blondal, T., Stacey, S. N., Helgason, A., Gunnarsdottir, S., Olafsdottir, A., Kristinsson, K. T., Birgisdottir, B., Ghosh, S., Thorlacius, S., Magnusdottir, D., Stefansdottir, G., Kristjansson, K., Bagger, Y., Wilensky, R. L., Reilly, M. P., Morris, A. D., Kimber, C. H., Adeyemo, A., Chen, Y., Zhou, J., So, W. Y., Tong, P. C., Ng, M. C., Hansen, T., Andersen, G., Borch-Johnsen, K., Jorgensen,

T., Tres, A., Fuertes, F., Ruiz-Echarri, M., Asin, L., Saez, B., van Boven, E., Klaver, S., Swinkels, D. W., Aben, K. K., Graif, T., Cashy, J., Suarez, B. K., van Vierssen, T. O., Frigge, M. L., Ober, C., Hofker, M. H., Wijmenga, C., Christiansen, C., Rader, D. J., Palmer, C. N., Rotimi, C., Chan, J. C., Pedersen, O., Sigurdsson, G., Benediktsson, R., Jonsson, E., Einarsson, G. V., Mayordomo, J. I., Catalona, W. J., Kiemeney, L. A., Barkardottir, R. B., Gulcher, J. R., Thorsteinsdottir, U., Kong, A., & Stefansson, K. 2007, "Two variants on chromosome 17 confer prostate cancer risk, and the one in TCF2 protects against type 2 diabetes", *Nat.Genet.*, vol. 39, no. 8, pp. 977-983.

Guidelines Subcommittee WHO-ISH 1999, "1999 World Health Organization-International Society of Hypertension Guidelines for the Management of Hypertension. Guidelines Subcommittee", *J.Hypertens.*, vol. 17, no. 2, pp. 151-183.

Hagen, T. M., Aw, T. Y., & Jones, D. P. 1988, "Glutathione uptake and protection against oxidative injury in isolated kidney cells", *Kidney Int.*, vol. 34, no. 1, pp. 74-81.

Hamet, P., Merlo, E., Seda, O., Broeckel, U., Tremblay, J., Kaldunski, M., Gaudet, D., Bouchard, G., Deslauriers, B., Gagnon, F., Antoniol, G., Pausova, Z., Labuda, M., Jomphe, M., Gossard, F., Tremblay, G., Kirova, R., Tonellato, P., Orlov, S. N., Pintos, J., Platko, J., Hudson, T. J., Rioux, J. D., Kotchen, T. A., & Cowley, A. W., Jr. 2005, "Quantitative founder-effect analysis of French Canadian families identifies specific loci contributing to metabolic phenotypes of hypertension", *Am.J.Hum.Genet.*, vol. 76, no. 5, pp. 815-832.

Harrap, S. B. 2003, "Where are all the blood-pressure genes?", *Lancet*, vol. 361, no. 9375, pp. 2149-2151.

Harrap, S. B., Wong, Z. Y., Stebbing, M., Lamantia, A., & Bahlo, M. 2002, "Blood pressure QTLs identified by genome-wide linkage analysis and dependence on associated phenotypes", *Physiol Genomics*, vol. 8, no. 2, pp. 99-105.

Hatfield, S. D., Shcherbata, H. R., Fischer, K. A., Nakahara, K., Carthew, R. W., & Ruohola-Baker, H. 2005, "Stem cell division is regulated by the microRNA pathway", *Nature*, vol. 435, no. 7044, pp. 974-978.

Havlik, R. J., Garrison, R. J., Feinleib, M., Kannel, W. B., Castelli, W. P., & McNamara, P. M. 1979, "Blood pressure aggregation in families", *Am.J.Epidemiol.*, vol. 110, no. 3, pp. 304-312.

Hayes JD & Pulford, D. J. 1995, "The glutathione S-transferase supergene family: regulation of GST and the contribution of the isoenzymes to cancer chemoprotection and drug resistance.", *Critical Reviews in Biochemistry and Molecular Biology*, vol. 30, no. 6, pp. 445-600.

Hayes, J. D., Flanagan, J. U., & Jowsey, I. R. 2005, "Glutathione transferases", *Annu Rev Pharmacol Toxicol*, vol. 45, pp. 51-88.

Hayes, J. D. & McLellan, L. I. 1999, "Glutathione and glutathione-dependent enzymes represent a co-ordinately regulated defence against oxidative stress", *Free Radic.Res*, vol. 31, no. 4, pp. 273-300.

Hayes, J. D. & Pulford, D. J. 1995, "The glutathione S-transferase supergene family: regulation of GST and the contribution of the isoenzymes to cancer chemoprotection and drug resistance", *Crit Rev.Biochem.Mol.Biol.*, vol. 30, no. 6, pp. 445-600.

Heiberg, A., Magnus, P., Berg, K., & Nance, W. E. 1981, "Blood pressure in Norwegian twins", *Prog.Clin.Biol.Res.*, vol. 69 Pt C, pp. 163-168.

Heller, J., Hellerova, S., Dobesova, Z., Kunes, J., & Zicha, J. 1993, "The Prague Hypertensive Rat: a new model of genetic hypertension", *Clin.Exp.Hypertens.*, vol. 15, no. 5, pp. 807-818.

Henikoff, S. 2007, "ENCODE and our very busy genome", *Nat.Genet.*, vol. 39, no. 7, pp. 817-818.

Higaki, J., Baba, S., Katsuya, T., Sato, N., Ishikawa, K., Mannami, T., Ogata, J., & Ogihara, T. 2000, "Deletion allele of angiotensin-converting enzyme gene increases risk of essential hypertension in Japanese men : the Suita Study", *Circulation*, vol. 101, no. 17, pp. 2060-2065.

Hilbert, P., Lindpaintner, K., Beckmann, J. S., Serikawa, T., Soubrier, F., Dubay, C., Cartwright, P., De Gouyon, B., Julier, C., Takahasi, S., & . 1991, "Chromosomal mapping of two genetic loci associated with blood-pressure regulation in hereditary hypertensive rats", *Nature*, vol. 353, no. 6344, pp. 521-529.

Hinchman, C. A. & Ballatori, N. 1990, "Glutathione-degrading capacities of liver and kidney in different species", *Biochem.Pharmacol.*, vol. 40, no. 5, pp. 1131-1135.

Hinojos, C. A., Boerwinkle, E., Fornage, M., & Doris, P. A. 2005, "Combined genealogical, mapping, and expression approaches to identify spontaneously hypertensive rat hypertension candidate genes", *Hypertension*, vol. 45, no. 4, pp. 698-704.

Hiratsuka, A., Yamane, H., Yamazaki, S., Ozawa, N., & Watabe, T. 1997, "Subunit Ya-specific glutathione peroxidase activity toward cholesterol 7-hydroperoxides of glutathione S-transferases in cytosols from rat liver and skin", *J.Biol.Chem.*, vol. 272, no. 8, pp. 4763-4769.

Hirota, T., Nishikawa, Y., Komai, T., Igarashi, T., & Kitagawa, H. 1987, "Role of dehydropeptidase-I in the metabolism of glutathione and its conjugates in the rat kidney", *Res Commun.Chem.Pathol.Pharmacol.*, vol. 56, no. 2, pp. 235-242.

Hoffert, J. D., van Balkom, B. W., Chou, C. L., & Knepper, M. A. 2004, "Application of difference gel electrophoresis to the identification of inner medullary collecting duct proteins", *Am.J.Physiol Renal Physiol*, vol. 286, no. 1, p. F170-F179.

Hoit, B. D., Suresh, D. P., Craft, L., Walsh, R. A., & Liggett, S. B. 2000, "beta2-adrenergic receptor polymorphisms at amino acid 16 differentially influence agonist-stimulated blood pressure and peripheral blood flow in normal individuals", *Am.Heart J.*, vol. 139, no. 3, pp. 537-542.

Holen, T., Amarzguioui, M., Wiiger, M. T., Babaie, E., & Prydz, H. 2002, "Positional effects of short interfering RNAs targeting the human coagulation trigger Tissue Factor", *Nucleic Acids Res*, vol. 30, no. 8, pp. 1757-1766.

Holen, T., Moe, S. E., Sorbo, J. G., Meza, T. J., Ottersen, O. P., & Klungland, A. 2005, "Tolerated wobble mutations in siRNAs decrease specificity, but can enhance activity in vivo", *Nucleic Acids Res*, vol. 33, no. 15, pp. 4704-4710.

Horikawa, Y., Iwasaki, N., Hara, M., Furuta, H., Hinokio, Y., Cockburn, B. N., Lindner, T., Yamagata, K., Ogata, M., Tomonaga, O., Kuroki, H., Kasahara, T., Iwamoto, Y., & Bell, G. I. 1997, "Mutation in hepatocyte nuclear factor-1 beta gene (TCF2) associated with MODY", *Nat.Genet.*, vol. 17, no. 4, pp. 384-385.

Hsueh, W. C., Mitchell, B. D., Schneider, J. L., Wagner, M. J., Bell, C. J., Nanthakumar, E., & Shuldiner, A. R. 2000, "QTL influencing blood pressure maps to the region of PPH1 on chromosome 2q31-34 in Old Order Amish", *Circulation*, vol. 101, no. 24, pp. 2810-2816.

Huard, J., Lochmuller, H., Acsadi, G., Jani, A., Massie, B., & Karpati, G. 1995, "The route of administration is a major determinant of the transduction efficiency of rat tissues by adenoviral recombinants", *Gene Ther.*, vol. 2, no. 2, pp. 107-115.

Hubner, N., Wallace, C. A., Zimdahl, H., Petretto, E., Schulz, H., Maciver, F., Mueller, M., Hummel, O., Monti, J., Zidek, V., Musilova, A., Kren, V., Causton, H., Game, L., Born, G., Schmidt, S., Muller, A., Cook, S. A., Kurtz, T. W., Whittaker, J., Pravenec, M., & Aitman, T. J. 2005, "Integrated transcriptional profiling and linkage analysis for identification of genes underlying disease", *Nat Genet*, vol. 37, no. 3, pp. 243-53.

Hunt, S. C., Ellison, R. C., Atwood, L. D., Pankow, J. S., Province, M. A., & Leppert, M. F. 2002, "Genome scans for blood pressure and hypertension: the National Heart, Lung, and Blood Institute Family Heart Study", *Hypertension*, vol. 40, no. 1, pp. 1-6.

Hussey, A. J., Kerr, L. A., Cronshaw, A. D., Harrison, D. J., & Hayes, J. D. 1991, "Variation in the expression of Mu-class glutathione S-transferase isoenzymes from human skeletal muscle. Evidence for the existence of heterodimers", *Biochem.J.*, vol. 273(Pt 2), pp. 323-332.

Hwang, J., Kleinhenz, D. J., Lassegue, B., Griendling, K. K., Dikalov, S., & Hart, C. M. 2005, "Peroxisome proliferator-activated receptor-gamma ligands regulate endothelial membrane superoxide production", *Am.J.Physiol Cell Physiol*, vol. 288, no. 4, p. C899-C905.

Ignarro, L. J., Buga, G. M., Wood, K. S., Byrns, R. E., & Chaudhuri, G. 1987, "Endothelium-derived relaxing factor produced and released from artery and vein is nitric oxide", *Proc.Natl.Acad.Sci.U.S.A*, vol. 84, no. 24, pp. 9265-9269.

Ikeda, H., Serria, M. S., Kakizaki, I., Hatayama, I., Satoh, K., Tsuchida, S., Muramatsu, M., Nishi, S., & Sakai, M. 2002, "Activation of mouse Pi-class glutathione S-transferase gene by Nrf2(NF-E2-related factor 2) and androgen", *Biochem.J.*, vol. 364, no. Pt 2, pp. 563-570.

Ikeda, S., Kong, S. W., Lu, J., Bisping, E., Zhang, H., Allen, P. D., Golub, T. R., Pieske, B., & Pu, W. T. 2007, "Altered microRNA expression in human heart disease", *Physiol Genomics*, vol. 31, no. 3, pp. 367-373.

Inoue, I., Nakajima, T., Williams, C. S., Quackenbush, J., Puryear, R., Powers, M., Cheng, T., Ludwig, E. H., Sharma, A. M., Hata, A., Jeunemaitre, X., & Lalouel, J. M. 1997, "A nucleotide substitution in the promoter of human angiotensinogen is associated with essential hypertension and affects basal transcription in vitro", *J.Clin.Invest*, vol. 99, no. 7, pp. 1786-1797.

Inoue, K. & Lupski, J. R. 2002, "Molecular mechanisms for genomic disorders", *Annu.Rev.Genomics Hum.Genet.*, vol. 3, pp. 199-242.

Irani, K., Xia, Y., Zweier, J. L., Sollott, S. J., Der, C. J., Fearon, E. R., Sundaresan, M., Finkel, T., & Goldschmidt-Clermont, P. J. 1997, "Mitogenic signaling mediated by oxidants in Ras-transformed fibroblasts", *Science*, vol. 275, no. 5306, pp. 1649-1652.

Irizarry, R. A., Hobbs, B., Collin, F., Beazer-Barclay, Y. D., Antonellis, K. J., Scherf, U., & Speed, T. P. 2003, "Exploration, normalization, and summaries of high density oligonucleotide array probe level data", *Biostatistics.*, vol. 4, no. 2, pp. 249-264.

Ishikawa, M., Numazawa, S., & Yoshida, T. 2005, "Redox regulation of the transcriptional repressor Bach1", *Free Radic.Biol.Med.*, vol. 38, no. 10, pp. 1344-1352.

Itoh, K., Chiba, T., Takahashi, S., Ishii, T., Igarashi, K., Katoh, Y., Oyake, T., Hayashi, N., Satoh, K., Hatayama, I., Yamamoto, M., & Nabeshima, Y. 1997, "An Nrf2/small Maf heterodimer mediates the induction of phase II detoxifying enzyme genes through antioxidant response elements", *Biochem.Biophys.Res Commun.*, vol. 236, no. 2, pp. 313-322.

Iwai, J. & Heine, M. M. 1986, "Dahl salt-sensitive rats and human essential hypertension", *J.Hypertens.Suppl*, vol. 4, no. 3, p. S29-S31.

Jacob, H. J., Lindpaintner, K., Lincoln, S. E., Kusumi, K., Bunker, R. K., Mao, Y. P., Ganten, D., Dzau, V. J., & Lander, E. S. 1991, "Genetic mapping of a gene causing hypertension in the stroke-prone spontaneously hypertensive rat", *Cell*, vol. 67, no. 1, pp. 213-224.

Jansen, R. C. & Nap, J. P. 2001, "Genetical genomics: the added value from segregation", *Trends Genet.*, vol. 17, no. 7, pp. 388-391.

Jeffery, I. B., Higgins, D. G., & Culhane, A. C. 2006, "Comparison and evaluation of methods for generating differentially expressed gene lists from microarray data", *BMC.Bioinformatics.*, vol. 7, p. 359.

Jeffs, B., Clark, J. S., Anderson, N. H., Gratton, J., Brosnan, M. J., Gauguier, D., Reid, J. L., Macrae, I. M., & Dominiczak, A. F. 1997, "Sensitivity to cerebral ischaemic insult in a rat model of stroke is determined by a single genetic locus", *Nat.Genet.*, vol. 16, no. 4, pp. 364-367.

Jeffs, B., Negrin, C. D., Graham, D., Clark, J. S., Anderson, N. H., Gauguier, D., & Dominiczak, A. F. 2000, "Applicability of a "speed" congenic strategy to dissect blood pressure quantitative trait loci on rat chromosome 2", *Hypertension*, vol. 35, no. 1 Pt 2, pp. 179-87.

Jeunemaitre, X., Lifton, R. P., Hunt, S. C., Williams, R. R., & Lalouel, J. M. 1992a, "Absence of linkage between the angiotensin converting enzyme locus and human essential hypertension", *Nat.Genet.*, vol. 1, no. 1, pp. 72-75.

Jeunemaitre, X., Soubrier, F., Kotelevtsev, Y. V., Lifton, R. P., Williams, C. S., Charru, A., Hunt, S. C., Hopkins, P. N., Williams, R. R., Lalouel, J. M., & . 1992b, "Molecular basis of human hypertension: role of angiotensinogen", *Cell*, vol. 71, no. 1, pp. 169-180.

Ji, X., Zhang, P., Armstrong, R. N., & Gilliland, G. L. 1992, "The three-dimensional structure of a glutathione S-transferase from the mu gene class. Structural analysis of the binary complex of isoenzyme 3-3 and glutathione at 2.2-A resolution", *Biochemistry*, vol. 31, no. 42, pp. 10169-10184.

Jiang, Z., Akey, J. M., Shi, J., Xiong, M., Wang, Y., Shen, Y., Xu, X., Chen, H., Wu, H., Xiao, J., Lu, D., Huang, W., & Jin, L. 2001, "A polymorphism in the promoter region of catalase is associated with blood pressure levels", *Hum.Genet.*, vol. 109, no. 1, pp. 95-98.

Jirout, M., Krenova, D., Kren, V., Breen, L., Pravenec, M., Schork, N. J., & Printz, M. P. 2003, "A new framework marker-based linkage map and SDPs for the rat HXB/BXH strain set", *Mamm.Genome*, vol. 14, no. 8, pp. 537-546.

Joe, B., Letwin, N. E., Garrett, M. R., Dhindaw, S., Frank, B., Sultana, R., Verratti, K., Rapp, J. P., & Lee, N. H. 2005, "Transcriptional profiling with a blood pressure QTL interval-specific oligonucleotide array", *Physiol Genomics*, vol. 23, no. 3, pp. 318-326.

Johnsen, O., Murphy, P., Prydz, H., & Kolsto, A. B. 1998, "Interaction of the CNC-bZIP factor TCF11/LCR-F1/Nrf1 with MafG: binding-site selection and regulation of transcription", *Nucleic Acids Res*, vol. 26, no. 2, pp. 512-520.

Jordan, J., Toka, H. R., Heusser, K., Toka, O., Shannon, J. R., Tank, J., Diedrich, A., Stabroth, C., Stoffels, M., Naraghi, R., Oelkers, W., Schuster, H., Schobel, H. P., Haller, H., & Luft, F. C. 2000, "Severely impaired baroreflex-buffering in patients with monogenic hypertension and neurovascular contact", *Circulation*, vol. 102, no. 21, pp. 2611-2618.

Jowsey, I. R., Jiang, Q., Itoh, K., Yamamoto, M., & Hayes, J. D. 2003, "Expression of the aflatoxin B1-8,9-epoxide-metabolizing murine glutathione S-transferase A3 subunit is regulated by the Nrf2 transcription factor through an antioxidant response element", *Mol.Pharmacol.*, vol. 64, no. 5, pp. 1018-1028.

Julier, C., Delepine, M., Keavney, B., Terwilliger, J., Davis, S., Weeks, D. E., Bui, T., Jeunemaitre, X., Velho, G., Froguel, P., Ratcliffe, P., Corvol, P., Soubrier, F., & Lathrop, G. M. 1997, "Genetic susceptibility for human familial essential hypertension in a region of homology with blood pressure linkage on rat chromosome 10", *Hum.Mol.Genet.*, vol. 6, no. 12, pp. 2077-2085.

Kahle, K. T., MacGregor, G. G., Wilson, F. H., Van Hoek, A. N., Brown, D., Ardito, T., Kashgarian, M., Giebisch, G., Hebert, S. C., Boulpaep, E. L., & Lifton, R. P. 2004, "Paracellular Cl- permeability is regulated by WNK4 kinase: insight into normal physiology and hypertension", *Proc.Natl.Acad.Sci.U.S.A*, vol. 101, no. 41, pp. 14877-14882.

Kahle, K. T., Wilson, F. H., Leng, Q., Lalioti, M. D., O'Connell, A. D., Dong, K., Rapson, A. K., MacGregor, G. G., Giebisch, G., Hebert, S. C., & Lifton, R. P. 2003, "WNK4 regulates the balance between renal NaCl reabsorption and K+ secretion", *Nat.Genet.*, vol. 35, no. 4, pp. 372-376.

Kajimoto, K., Naraba, H., & Iwai, N. 2006, "MicroRNA and 3T3-L1 pre-adipocyte differentiation", *RNA.*, vol. 12, no. 9, pp. 1626-1632.

Kanezaki, R., Toki, T., Yokoyama, M., Yomogida, K., Sugiyama, K., Yamamoto, M., Igarashi, K., & Ito, E. 2001, "Transcription factor BACH1 is recruited to the nucleus by its novel alternative spliced isoform", *J.Biol.Chem.*, vol. 276, no. 10, pp. 7278-7284.

Kataoka, K., Noda, M., & Nishizawa, M. 1994, "Maf nuclear oncoprotein recognizes sequences related to an AP-1 site and forms heterodimers with both Fos and Jun", *Mol.Cell Biol.*, vol. 14, no. 1, pp. 700-712.

Kato, N., Sugiyama, T., Morita, H., Kurihara, H., Sato, T., Yamori, Y., & Yazaki, Y. 2001, "Association analysis of beta(2)-adrenergic receptor polymorphisms with hypertension in Japanese", *Hypertension*, vol. 37, no. 2, pp. 286-292.

Kato, N., Sugiyama, T., Morita, H., Kurihara, H., Yamori, Y., & Yazaki, Y. 1998, "G protein beta3 subunit variant and essential hypertension in Japanese", *Hypertension*, vol. 32, no. 5, pp. 935-938.

Kaufman, R. M., Pham, C. T., & Ley, T. J. 1999, "Transgenic analysis of a 100-kb human beta-globin cluster-containing DNA fragment propagated as a bacterial artificial chromosome", *Blood*, vol. 94, no. 9, pp. 3178-3184.

Kawamoto, Y., Nakamura, Y., Naito, Y., Torii, Y., Kumagai, T., Osawa, T., Ohigashi, H., Satoh, K., Imagawa, M., & Uchida, K. 2000, "Cyclopentenone prostaglandins as potential inducers of phase II detoxification enzymes. 15-deoxy-delta(12,14)-prostaglandin j2-induced expression of glutathione S-transferases", *J.Biol.Chem.*, vol. 275, no. 15, pp. 11291-11299.

Kearney, P. M., Whelton, M., Reynolds, K., Muntner, P., Whelton, P. K., & He, J. 2005, "Global burden of hypertension: analysis of worldwide data", *Lancet*, vol. 365, no. 9455, pp. 217-223.

Kekuda, R., Prasad, P. D., Fei, Y. J., Torres-Zamorano, V., Sinha, S., Yang-Feng, T. L., Leibach, F. H., & Ganapathy, V. 1996, "Cloning of the sodium-dependent, broad-scope, neutral amino acid transporter Bo from a human placental choriocarcinoma cell line", *J.Biol.Chem.*, vol. 271, no. 31, pp. 18657-18661.

Kel, A. E., Gossling, E., Reuter, I., Cheremushkin, E., Kel-Margoulis, O. V., & Wingender, E. 2003, "MATCH: A tool for searching transcription factor binding sites in DNA sequences", *Nucleic Acids Res*, vol. 31, no. 13, pp. 3576-3579.

Kerr, S., Brosnan, M. J., McIntyre, M., Reid, J. L., Dominiczak, A. F., & Hamilton, C. A. 1999, "Superoxide anion production is increased in a model of genetic hypertension: role of the endothelium", *Hypertension*, vol. 33, no. 6, pp. 1353-1358.

Kim, H. S., Krege, J. H., Kluckman, K. D., Hagaman, J. R., Hodgin, J. B., Best, C. F., Jennette, J. C., Coffman, T. M., Maeda, N., & Smithies, O. 1995, "Genetic control of blood pressure and the angiotensinogen locus", *Proc.Natl.Acad.Sci.U.S.A*, vol. 92, no. 7, pp. 2735-2739.

Kitsukawa, T., Shimono, A., Kawakami, A., Kondoh, H., & Fujisawa, H. 1995, "Overexpression of a membrane protein, neuropilin, in chimeric mice causes anomalies in the cardiovascular system, nervous system and limbs", *Development*, vol. 121, no. 12, pp. 4309-4318.

Kiuchi-Saishin, Y., Gotoh, S., Furuse, M., Takasuga, A., Tano, Y., & Tsukita, S. 2002, "Differential expression patterns of claudins, tight junction membrane proteins, in mouse nephron segments", *J.Am.Soc.Nephrol.*, vol. 13, no. 4, pp. 875-886.

Klose, J., Nock, C., Herrmann, M., Stuhler, K., Marcus, K., Bluggel, M., Krause, E., Schalkwyk, L. C., Rastan, S., Brown, S. D., Bussow, K., Himmelbauer, H., & Lehrach, H. 2002, "Genetic analysis of the mouse brain proteome", *Nat.Genet.*, vol. 30, no. 4, pp. 385-393.

Knight, T. R., Choudhuri, S., & Klaassen, C. D. 2007, "Constitutive mRNA Expression of Various Glutathione S-Transferase Isoforms in Different Tissues of Mice", *Toxicol.Sci.*

Kocis, J. M., Kuo, W. N., Liu, Y., Guruvadoo, L. K., & Langat, J. L. 2002, "Regulation of catalase: inhibition by peroxynitrite and reactivation by reduced glutathione and glutathione S-transferase", *Front Biosci.*, vol. 7, p. a175-a180.

Kohn, A. D., Summers, S. A., Birnbaum, M. J., & Roth, R. A. 1996, "Expression of a constitutively active Akt Ser/Thr kinase in 3T3-L1 adipocytes stimulates glucose uptake and glucose transporter 4 translocation", *J.Biol.Chem.*, vol. 271, no. 49, pp. 31372-31378.

Kokubo, Y., Kamide, K., Inamoto, N., Tanaka, C., Banno, M., Takiuchi, S., Kawano, Y., Tomoike, H., & Miyata, T. 2004, "Identification of 108 SNPs in TSC, WNK1, and WNK4 and their association with hypertension in a Japanese general population", *J.Hum.Genet.*, vol. 49, no. 9, pp. 507-515.

Kokubu, C., Heinzmann, U., Kokubu, T., Sakai, N., Kubota, T., Kawai, M., Wahl, M. B., Galceran, J., Grosschedl, R., Ozono, K., & Imai, K. 2004, "Skeletal defects in ringelschwanz mutant mice reveal that Lrp6 is required for proper somitogenesis and osteogenesis", *Development*, vol. 131, no. 21, pp. 5469-5480.

Kopf, D., Waldherr, R., & Rettig, R. 1993, "Source of kidney determines blood pressure in young renal transplanted rats", *Am.J.Physiol*, vol. 265, no. 1 Pt 2, p. F104-F111.

Kotanko, P., Binder, A., Tasker, J., DeFreitas, P., Kamdar, S., Clark, A. J., Skrabal, F., & Caulfield, M. 1997, "Essential hypertension in African Caribbeans associates with a variant of the beta2-adrenoceptor", *Hypertension*, vol. 30, no. 4, pp. 773-776.

Kotlo, K., Hughes, D. E., Herrera, V. L., Ruiz-Opazo, N., Costa, R. H., Robey, R. B., & Danziger, R. S. 2007a, "Functional polymorphism of the Anpep gene increases promoter activity in the Dahl salt-resistant rat", *Hypertension*, vol. 49, no. 3, pp. 467-472.

Kotlo, K., Shukla, S., Tawar, U., Skidgel, R. A., & Danziger, R. S. 2007b, "Aminopeptidase N reduces basolateral Na+ -K+ -ATPase in proximal tubule cells", *Am.J.Physiol Renal Physiol*, vol. 293, no. 4, p. F1047-F1053.

Kozak, E. M. & Tate, S. S. 1982, "Glutathione-degrading enzymes of microvillus membranes", *J.Biol.Chem.*, vol. 257, no. 11, pp. 6322-6327.

Krege, J. H., Kim, H. S., Moyer, J. S., Jennette, J. C., Peng, L., Hiller, S. K., & Smithies, O. 1997, "Angiotensin-converting enzyme gene mutations, blood pressures, and cardiovascular homeostasis", *Hypertension*, vol. 29, no. 1 Pt 2, pp. 150-157.

Kreutz, R., Hubner, N., Ganten, D., & Lindpaintner, K. 1995, "Genetic linkage of the ACE gene to plasma angiotensin-converting enzyme activity but not to blood pressure. A quantitative trait locus confers identical complex phenotypes in human and rat hypertension", *Circulation*, vol. 92, no. 9, pp. 2381-2384.

Kristjansson, K., Manolescu, A., Kristinsson, A., Hardarson, T., Knudsen, H., Ingason, S., Thorleifsson, G., Frigge, M. L., Kong, A., Gulcher, J. R., & Stefansson, K. 2002, "Linkage of essential hypertension to chromosome 18q", *Hypertension*, vol. 39, no. 6, pp. 1044-1049.

Krushkal, J., Ferrell, R., Mockrin, S. C., Turner, S. T., Sing, C. F., & Boerwinkle, E. 1999, "Genome-wide linkage analyses of systolic blood pressure using highly discordant siblings", *Circulation*, vol. 99, no. 11, pp. 1407-1410.

Kuijpers, M. H. & Gruys, E. 1984, "Spontaneous hypertension and hypertensive renal disease in the fawn-hooded rat", *Br.J.Exp.Pathol.*, vol. 65, no. 2, pp. 181-190.

Kumar, A. & Reddy, E. P. 2001, "Genomic organization and characterization of the promoter region of murine GSTM2 gene", *Gene*, vol. 270, no. 1-2, pp. 221-229.

Kunz, R., Kreutz, R., Beige, J., Distler, A., & Sharma, A. M. 1997, "Association between the angiotensinogen 235T-variant and essential hypertension in whites: a systematic review and methodological appraisal", *Hypertension*, vol. 30, no. 6, pp. 1331-1337.

Kuo, M. D., Bright, I. J., Wang, D. S., Ghafouri, P., Yuksel, E., Hilfiker, P. R., Miniati, D. N., & Dake, M. D. 2004, "Local resistance to oxidative stress by overexpression of copper-zinc superoxide dismutase limits neointimal formation after angioplasty", *J.Endovasc.Ther.*, vol. 11, no. 6, pp. 585-594.

Kuo, W. H., Chou, F. P., Young, S. C., Chang, Y. C., & Wang, C. J. 2005, "Geniposide activates GSH S-transferase by the induction of GST M1 and GST M2 subunits involving the transcription and phosphorylation of MEK-1 signaling in rat hepatocytes", *Toxicol.Appl.Pharmacol.*, vol. 208, no. 2, pp. 155-162.

Kuo, W. N., Kocis, J. M., & Mewar, M. 2002, "Protein denitration/modification by glutathione-S-transferase and glutathione peroxidase", *J.Biochem.Mol.Biol.Biophys.*, vol. 6, no. 2, pp. 143-146.

Lagos-Quintana, M., Rauhut, R., Meyer, J., Borkhardt, A., & Tuschl, T. 2003, "New microRNAs from mouse and human", *RNA.*, vol. 9, no. 2, pp. 175-179.

Lalioti, M. D., Zhang, J., Volkman, H. M., Kahle, K. T., Hoffmann, K. E., Toka, H. R., Nelson-Williams, C., Ellison, D. H., Flavell, R., Booth, C. J., Lu, Y., Geller, D. S., & Lifton, R. P. 2006, "Wnk4 controls blood pressure and potassium homeostasis via regulation of mass and activity of the distal convoluted tubule", *Nat.Genet.*, vol. 38, no. 10, pp. 1124-1132.

Lander, E. & Kruglyak, L. 1995, "Genetic dissection of complex traits: guidelines for interpreting and reporting linkage results", *Nat.Genet.*, vol. 11, no. 3, pp. 241-247.

Lander, E. S., Green, P., Abrahamson, J., Barlow, A., Daly, M. J., Lincoln, S. E., & Newburg, L. 1987, "MAPMAKER: an interactive computer package for constructing primary genetic linkage maps of experimental and natural populations", *Genomics*, vol. 1, no. 2, pp. 174-181.

Lander, E. S. & Schork, N. J. 1994, "Genetic dissection of complex traits", *Science*, vol. 265, no. 5181, pp. 2037-2048.

Landgraf, P., Rusu, M., Sheridan, R., Sewer, A., Iovino, N., Aravin, A., Pfeffer, S., Rice, A., Kamphorst, A. O., Landthaler, M., Lin, C., Socci, N. D., Hermida, L., Fulci, V., Chiaretti, S., Foa, R., Schliwka, J., Fuchs, U., Novosel, A., Muller, R. U., Schermer, B., Bissels, U., Inman, J., Phan, Q., Chien, M., Weir, D. B., Choksi, R., De Vita, G., Frezzetti, D., Trompeter, H. I., Hornung, V., Teng, G., Hartmann, G., Palkovits, M., Di Lauro, R., Wernet, P., Macino, G., Rogler, C. E., Nagle, J. W., Ju, J., Papavasiliou, F. N., Benzing, T., Lichter, P., Tam, W., Brownstein, M. J., Bosio, A., Borkhardt, A., Russo, J. J., Sander, C., Zavolan, M., & Tuschl, T. 2007, "A mammalian microRNA expression atlas based on small RNA library sequencing", *Cell*, vol. 129, no. 7, pp. 1401-1414.

Laplace, J. R., Husted, R. F., & Stokes, J. B. 1992, "Cellular responses to steroids in the enhancement of Na+ transport by rat collecting duct cells in culture. Differences between glucocorticoid and mineralocorticoid hormones", *J.Clin.Invest*, vol. 90, no. 4, pp. 1370-1378.

Lash, L. H. 2005, "Role of glutathione transport processes in kidney function", *Toxicol.Appl.Pharmacol.*, vol. 204, no. 3, pp. 329-342.

Lash, L. H., Jones, D. P., & Anders, M. W. 1988, "Glutathione homeostasis and glutathione S-conjugate toxicity in the kidney.," E. Hodgson, J. R. Bend, & R. M. Philpot, eds., Elsevier, pp. 29-67.

Lee, D. H., Jacobs, D. R., Jr., Gross, M., Kiefe, C. I., Roseman, J., Lewis, C. E., & Steffes, M. 2003, "Gamma-glutamyltransferase is a predictor of incident diabetes and hypertension: the Coronary Artery Risk Development in Young Adults (CARDIA) Study", *Clin.Chem.*, vol. 49, no. 8, pp. 1358-1366.

Lee, D. H., Silventoinen, K., Hu, G., Jacobs, D. R., Jr., Jousilahti, P., Sundvall, J., & Tuomilehto, J. 2006, "Serum gamma-glutamyltransferase predicts non-fatal myocardial infarction and fatal coronary heart disease among 28,838 middle-aged men and women", *Eur.Heart J.*, vol. 27, no. 18, pp. 2170-2176.

Lee, J. M. & Johnson, J. A. 2004, "An important role of Nrf2-ARE pathway in the cellular defense mechanism", *J.Biochem.Mol.Biol.*, vol. 37, no. 2, pp. 139-143.

Lee, N. H., Haas, B. J., Letwin, N. E., Frank, B. C., Luu, T. V., Sun, Q., House, C. D., Yerga-Woolwine, S., Farms, P., Manickavasagam, E., & Joe, B. 2007, "Cross-talk of expression quantitative trait loci within 2 interacting blood pressure quantitative trait loci", *Hypertension*, vol. 50, no. 6, pp. 1126-1133.

Lehmann, J. M., Moore, L. B., Smith-Oliver, T. A., Wilkison, W. O., Willson, T. M., & Kliewer, S. A. 1995, "An antidiabetic thiazolidinedione is a high affinity ligand for peroxisome proliferator-activated receptor gamma (PPAR gamma)", *J.Biol.Chem.*, vol. 270, no. 22, pp. 12953-12956.

Leopold, J. A. & Loscalzo, J. 2005, "Oxidative enzymopathies and vascular disease", *Arterioscler.Thromb.Vasc.Biol.*, vol. 25, no. 7, pp. 1332-1340.

Levine, R. S., Hennekens, C. H., Perry, A., Cassady, J., Gelband, H., & Jesse, M. J. 1982, "Genetic variance of blood pressure levels in infant twins", *Am.J.Epidemiol.*, vol. 116, no. 5, pp. 759-764.

Levy, D., Destefano, A. L., Larson, M. G., O'Donnell, C. J., Lifton, R. P., Gavras, H., Cupples, L. A., & Myers, R. H. 2000, "Evidence for a gene influencing blood pressure on chromosome 17. Genome scan linkage results for longitudinal blood pressure phenotypes in subjects from the framingham heart study", *Hypertension*, vol. 36, no. 4, pp. 477-483.

Li, J. L., Canham, R. M., Vongpatanasin, W., Leonard, D., Auchus, R. J., & Victor, R. G. 2006, "Do allelic variants in alpha2A and alpha2C adrenergic receptors predispose to hypertension in blacks?", *Hypertension*, vol. 47, no. 6, pp. 1140-1146.

Li, P., Oparil, S., Sun, J. Z., Thompson, J. A., & Chen, Y. F. 2003, "Fibroblast growth factor mediates hypoxia-induced endothelin-- a receptor expression in lung artery smooth muscle cells", *J.Appl.Physiol*, vol. 95, no. 2, pp. 643-651.

Li, Q., Bolli, R., Qiu, Y., Tang, X. L., Murphree, S. S., & French, B. A. 1998, "Gene therapy with extracellular superoxide dismutase attenuates myocardial stunning in conscious rabbits", *Circulation*, vol. 98, no. 14, pp. 1438-1448.

Li, R., Boerwinkle, E., Olshan, A. F., Chambless, L. E., Pankow, J. S., Tyroler, H. A., Bray, M., Pittman, G. S., Bell, D. A., & Heiss, G. 2000, "Glutathione S-transferase genotype as a susceptibility factor in smoking-related coronary heart disease", *Atherosclerosis*, vol. 149, no. 2, pp. 451-462.

Li, R., Folsom, A. R., Sharrett, A. R., Couper, D., Bray, M., & Tyroler, H. A. 2001, "Interaction of the glutathione S-transferase genes and cigarette smoking on risk of lower extremity arterial disease: the Atherosclerosis Risk in Communities (ARIC) study", *Atherosclerosis*, vol. 154, no. 3, pp. 729-738.

Lieberman, M. W., Wiseman, A. L., Shi, Z. Z., Carter, B. Z., Barrios, R., Ou, C. N., Chevez-Barrios, P., Wang, Y., Habib, G. M., Goodman, J. C., Huang, S. L., Lebovitz, R. M., & Matzuk, M. M. 1996, "Growth retardation and cysteine deficiency in gamma-glutamyl transpeptidase-deficient mice", *Proc.Natl.Acad.Sci.U.S.A*, vol. 93, no. 15, pp. 7923-7926.

Liefeldt, L., Schonfelder, G., Bocker, W., Hocher, B., Talsness, C. E., Rettig, R., & Paul, M. 1999, "Transgenic rats expressing the human ET-2 gene: a model for the study of endothelin actions in vivo", *J.Mol.Med.*, vol. 77, no. 7, pp. 565-574.

Lifton, R. P., Dluhy, R. G., Powers, M., Rich, G. M., Cook, S., Ulick, S., & Lalouel, J. M. 1992, "A chimaeric 11 beta-hydroxylase/aldosterone synthase gene causes glucocorticoid-remediable aldosteronism and human hypertension", *Nature*, vol. 355, no. 6357, pp. 262-265.

Lifton, R. P., Gharavi, A. G., & Geller, D. S. 2001, "Molecular mechanisms of human hypertension", *Cell*, vol. 104, no. 4, pp. 545-556.

Lim, L. P., Lau, N. C., Garrett-Engele, P., Grimson, A., Schelter, J. M., Castle, J., Bartel, D. P., Linsley, P. S., & Johnson, J. M. 2005, "Microarray analysis shows that some microRNAs downregulate large numbers of target mRNAs", *Nature*, vol. 433, no. 7027, pp. 769-773.

Listowsky, I. 2005, "A subclass of mu glutathione S-transferases selectively expressed in testis and brain", *Methods Enzymol.*, vol. 401, pp. 278-287.

Livak, K. J. & Schmittgen, T. D. 2001, "Analysis of relative gene expression data using real-time quantitative PCR and the 2(-Delta Delta C(T)) Method", *Methods*, vol. 25, no. 4, pp. 402-8.

Lockette, W., Ghosh, S., Farrow, S., MacKenzie, S., Baker, S., Miles, P., Schork, A., & Cadaret, L. 1995, "Alpha 2-adrenergic receptor gene polymorphism and hypertension in blacks", *Am.J.Hypertens.*, vol. 8, no. 4 Pt 1, pp. 390-394.

Lois, C., Hong, E. J., Pease, S., Brown, E. J., & Baltimore, D. 2002, "Germline transmission and tissue-specific expression of transgenes delivered by lentiviral vectors", *Science*, vol. 295, no. 5556, pp. 868-872.

Longini, I. M., Jr., Higgins, M. W., Hinton, P. C., Moll, P. P., & Keller, J. B. 1984, "Environmental and genetic sources of familial aggregation of blood pressure in Tecumseh, Michigan", *Am.J.Epidemiol.*, vol. 120, no. 1, pp. 131-144.

Lu, J., Getz, G., Miska, E. A., Alvarez-Saavedra, E., Lamb, J., Peck, D., Sweet-Cordero, A., Ebert, B. L., Mak, R. H., Ferrando, A. A., Downing, J. R., Jacks, T., Horvitz, H. R., & Golub, T. R. 2005, "MicroRNA expression profiles classify human cancers", *Nature*, vol. 435, no. 7043, pp. 834-838.

Luisi, B. F., Xu, W. X., Otwinowski, Z., Freedman, L. P., Yamamoto, K. R., & Sigler, P. B. 1991, "Crystallographic analysis of the interaction of the glucocorticoid receptor with DNA", *Nature*, vol. 352, no. 6335, pp. 497-505.

Ma, L., Teruya-Feldstein, J., & Weinberg, R. A. 2007, "Tumour invasion and metastasis initiated by microRNA-10b in breast cancer", *Nature*, vol. 449, no. 7163, pp. 682-688.

Maassen, J. A., Janssen, G. M., & 't Hart, L. M. 2005, "Molecular mechanisms of mitochondrial diabetes (MIDD)", *Ann.Med.*, vol. 37, no. 3, pp. 213-221.

Maira, S. M., Galetic, I., Brazil, D. P., Kaech, S., Ingley, E., Thelen, M., & Hemmings, B. A. 2001, "Carboxyl-terminal modulator protein (CTMP), a negative regulator of PKB/Akt and v-Akt at the plasma membrane", *Science*, vol. 294, no. 5541, pp. 374-380.

Mancia, G., De Backer, G., Dominiczak, A., Cifkova, R., Fagard, R., Germano, G., Grassi, G., Heagerty, A. M., Kjeldsen, S. E., Laurent, S., Narkiewicz, K., Ruilope, L., Rynkiewicz, A., Schmieder, R. E., Boudier, H. A., & Zanchetti, A. 2007, "2007 ESH-ESC Practice Guidelines for the Management of Arterial Hypertension: ESH-ESC Task Force on the Management of Arterial Hypertension", *J.Hypertens.*, vol. 25, no. 9, pp. 1751-1762.

Mani, A., Radhakrishnan, J., Wang, H., Mani, A., Mani, M. A., Nelson-Williams, C., Carew, K. S., Mane, S., Najmabadi, H., Wu, D., & Lifton, R. P. 2007, "LRP6 mutation in a family with early coronary disease and metabolic risk factors", *Science*, vol. 315, no. 5816, pp. 1278-1282.

Mannervik, B., Board, P. G., Hayes, J. D., Listowsky, I., & Pearson, W. R. 2005, "Nomenclature for mammalian soluble glutathione transferases", *Methods Enzymol.*, vol. 401, pp. 1-8.

Maric, K., Oksche, A., & Rosenthal, W. 1998, "Aquaporin-2 expression in primary cultured rat inner medullary collecting duct cells", *Am J Physiol*, vol. 275, no. 5 Pt 2, pp. 796-801.

Markel, A. L. 1985, "[Genetic model of stress-induced arterial hypertension]", *Izv.Akad.Nauk SSSR Biol.* no. 3, pp. 466-469.

Marnett, L. J., Riggins, J. N., & West, J. D. 2003, "Endogenous generation of reactive oxidants and electrophiles and their reactions with DNA and protein", *J.Clin.Invest*, vol. 111, no. 5, pp. 583-593.

Martin, C., Martinez, R., Navarro, R., Ruiz-Sanz, J. I., Lacort, M., & Ruiz-Larrea, M. B. 2001, "tert-Butyl hydroperoxide-induced lipid signaling in hepatocytes: involvement of glutathione and free radicals", *Biochem.Pharmacol.*, vol. 62, no. 6, pp. 705-712.

Martin, M. M., Buckenberger, J. A., Jiang, J., Malana, G. E., Nuovo, G. J., Chotani, M., Feldman, D. S., Schmittgen, T. D., & Elton, T. S. 2007, "The human angiotensin II type 1 receptor +1166 A/C polymorphism attenuates microrna-155 binding", *J.Biol.Chem.*, vol. 282, no. 33, pp. 24262-24269.

Marumo, T., Schini-Kerth, V. B., Fisslthaler, B., & Busse, R. 1997, "Platelet-derived growth factor-stimulated superoxide anion production modulates activation of transcription factor NF-kappaB and expression of monocyte chemoattractant protein 1 in human aortic smooth muscle cells", *Circulation*, vol. 96, no. 7, pp. 2361-2367.

Mates, J. M. 2000, "Effects of antioxidant enzymes in the molecular control of reactive oxygen species toxicology", *Toxicology*, vol. 153, no. 1-3, pp. 83-104.

Matsukawa, N., Nonaka, Y., Higaki, J., Nagano, M., Mikami, H., Ogihara, T., & Okamoto, M. 1993, "Dahl's salt-resistant normotensive rat has mutations in cytochrome P450(11

beta), but the salt-sensitive hypertensive rat does not", *J.Biol.Chem.*, vol. 268, no. 12, pp. 9117-9121.

Matsumoto, I., Niijima, A., Oomura, Y., Sasaki, K., Tsuchiya, K., & Aikawa, T. 1998, "Acidic fibroblast growth factor activates adrenomedullary secretion and sympathetic outflow in rats", *Am.J.Physiol*, vol. 275, no. 4 Pt 2, p. R1003-R1012.

Matveeva, O., Nechipurenko, Y., Rossi, L., Moore, B., Saetrom, P., Ogurtsov, A. Y., Atkins, J. F., & Shabalina, S. A. 2007, "Comparison of approaches for rational siRNA design leading to a new efficient and transparent method", *Nucleic Acids Res*, vol. 35, no. 8, p. e63.

McBride, M. W., Brosnan, M. J., Mathers, J., McLellan, L. I., Miller, W. H., Graham, D., Hanlon, N., Hamilton, C. A., Polke, J. M., Lee, W. K., & Dominiczak, A. F. 2005, "Reduction of Gstm1 expression in the stroke-prone spontaneously hypertension rat contributes to increased oxidative stress", *Hypertension*, vol. 45, no. 4, pp. 786-92.

McBride, M. W., Carr, F. J., Graham, D., Anderson, N. H., Clark, J. S., Lee, W. K., Charchar, F. J., Brosnan, M. J., & Dominiczak, A. F. 2003, "Microarray analysis of rat chromosome 2 congenic strains", *Hypertension*, vol. 41, no. 3 Pt 2, pp. 847-53.

McBride, M. W., Graham, D., Delles, C., & Dominiczak, A. F. 2006, "Functional genomics in hypertension", *Curr.Opin.Nephrol.Hypertens.*, vol. 15, no. 2, pp. 145-151.

McEwan, I. J. 2004, "Sex, drugs and gene expression: signalling by members of the nuclear receptor superfamily", *Essays Biochem.*, vol. 40, pp. 1-10.

McIlhany, M. L., Shaffer, J. W., & Hines, E. A., Jr. 1975, "The heritability of blood pressure: an investigation of 200 pairs of twins using the cold pressor test", *Johns.Hopkins.Med.J.*, vol. 136, no. 2, pp. 57-64.

McIntyre, M., Hamilton, C. A., Rees, D. D., Reid, J. L., & Dominiczak, A. F. 1997, "Sex differences in the abundance of endothelial nitric oxide in a model of genetic hypertension", *Hypertension*, vol. 30, no. 6, pp. 1517-1524.

Mendes, A. C., Ferreira, A. J., Pinheiro, S. V., & Santos, R. A. 2005, "Chronic infusion of angiotensin-(1-7) reduces heart angiotensin II levels in rats", *Regul.Pept.*, vol. 125, no. 1-3, pp. 29-34.

Michalkiewicz, M., Michalkiewicz, T., Geurts, A. M., Roman, R. J., Slocum, G. R., Singer, O., Weihrauch, D., Greene, A. S., Kaldunski, M., Verma, I. M., Jacob, H. J., & Cowley, A. W., Jr. 2007, "Efficient transgenic rat production by a lentiviral vector", *Am.J.Physiol Heart Circ Physiol*, vol. 293, no. 1, p. H881-H894.

Miller, W. H., Brosnan, M. J., Graham, D., Nicol, C. G., Morecroft, I., Channon, K. M., Danilov, S. M., Reynolds, P. N., Baker, A. H., & Dominiczak, A. F. 2005, "Targeting endothelial cells with adenovirus expressing nitric oxide synthase prevents elevation of blood pressure in stroke-prone spontaneously hypertensive rats", *Mol.Ther.*, vol. 12, no. 2, pp. 321-327.

Miquerol, L., Langille, B. L., & Nagy, A. 2000, "Embryonic development is disrupted by modest increases in vascular endothelial growth factor gene expression", *Development*, vol. 127, no. 18, pp. 3941-3946.

Moffat, G. J., McLaren, A. W., & Wolf, C. R. 1996, "Sp1-mediated transcriptional activation of the human Pi class glutathione S-transferase promoter", *J.Biol.Chem.*, vol. 271, no. 2, pp. 1054-1060.

Mongeau, J. G., Biron, P., & Sing, C. F. 1986, "The influence of genetics and household environment upon the variability of normal blood pressure: the Montreal Adoption Survey", *Clin.Exp.Hypertens.A*, vol. 8, no. 4-5, pp. 653-660.

Montano, M. M., Deng, H., Liu, M., Sun, X., & Singal, R. 2004, "Transcriptional regulation by the estrogen receptor of antioxidative stress enzymes and its functional implications", *Oncogene*, vol. 23, no. 14, pp. 2442-2453.

Montoliu, L., Bock, C. T., Schutz, G., & Zentgraf, H. 1995, "Visualization of large DNA molecules by electron microscopy with polyamines: application to the analysis of yeast endogenous and artificial chromosomes", *J.Mol.Biol.*, vol. 246, no. 4, pp. 486-492.

Morales, A., Garcia-Ruiz, C., Miranda, M., Mari, M., Colell, A., Ardite, E., & Fernandez-Checa, J. C. 1997, "Tumor necrosis factor increases hepatocellular glutathione by transcriptional regulation of the heavy subunit chain of gamma-glutamylcysteine synthetase", *J.Biol.Chem.*, vol. 272, no. 48, pp. 30371-30379.

Morceau, F., Duvoix, A., Delhalle, S., Schnekenburger, M., Dicato, M., & Diederich, M. 2004, "Regulation of glutathione S-transferase P1-1 gene expression by NF-kappaB in tumor necrosis factor alpha-treated K562 leukemia cells", *Biochem.Pharmacol.*, vol. 67, no. 7, pp. 1227-1238.

Moreno, M. U., San Jose, G., Fortuno, A., Beloqui, O., Redon, J., Chaves, F. J., Corella, D., Diez, J., & Zalba, G. 2007, "A novel CYBA variant, the -675A/T polymorphism, is associated with essential hypertension", *J.Hypertens.*, vol. 25, no. 8, pp. 1620-1626.

Motojima, K., Passilly, P., Peters, J. M., Gonzalez, F. J., & Latruffe, N. 1998, "Expression of putative fatty acid transporter genes are regulated by peroxisome proliferator-activated receptor alpha and gamma activators in a tissue- and inducer-specific manner", *J.Biol.Chem.*, vol. 273, no. 27, pp. 16710-16714.

Moujahidine, M., Lambert, R., Dutil, J., Palijan, A., Sivo, Z., Ariyarajah, A., & Deng, A. Y. 2004, "Combining congenic coverage with gene profiling in search of candidates for blood pressure quantitative trait loci in Dahl rats", *Hypertens.Res*, vol. 27, no. 3, pp. 203-212.

Mukae, S., Aoki, S., Itoh, S., Nishio, K., Iwata, T., Ueda, H., Geshi, E., Fuzimaki, T., & Katagiri, T. 1999, "Promoter polymorphism of the beta2 bradykinin receptor gene is associated with essential hypertension", *Jpn.Circ J.*, vol. 63, no. 10, pp. 759-762.

Mullins, J. J., Peters, J., & Ganten, D. 1990, "Fulminant hypertension in transgenic rats harbouring the mouse Ren-2 gene", *Nature*, vol. 344, no. 6266, pp. 541-544.

Mullins, L. J., Bailey, M. A., & Mullins, J. J. 2006, "Hypertension, kidney, and transgenics: a fresh perspective", *Physiol Rev.*, vol. 86, no. 2, pp. 709-746.

Mune, T., Rogerson, F. M., Nikkila, H., Agarwal, A. K., & White, P. C. 1995, "Human hypertension caused by mutations in the kidney isozyme of 11 beta-hydroxysteroid dehydrogenase", *Nat.Genet.*, vol. 10, no. 4, pp. 394-399.

Munroe, P. B., Wallace, C., Xue, M. Z., Marcano, A. C., Dobson, R. J., Onipinla, A. K., Burke, B., Gungadoo, J., Newhouse, S. J., Pembroke, J., Brown, M., Dominiczak, A. F.,

Samani, N. J., Lathrop, M., Connell, J., Webster, J., Clayton, D., Farrall, M., Mein, C. A., & Caulfield, M. 2006, "Increased support for linkage of a novel locus on chromosome 5q13 for essential hypertension in the British Genetics of Hypertension Study", *Hypertension*, vol. 48, no. 1, pp. 105-111.

Muzykantov, V. R. 2001, "Targeting of superoxide dismutase and catalase to vascular endothelium", *J.Control Release*, vol. 71, no. 1, pp. 1-21.

Nagaoka, A., Iwatsuka, H., Suzuoki, Z., & Okamoto, K. 1976, "Genetic predisposition to stroke in spontaneously hypertensive rats", *Am.J.Physiol*, vol. 230, no. 5, pp. 1354-1359.

Nagasaki, H., Yokoi, H., Arima, H., Hirabayashi, M., Ishizaki, S., Tachikawa, K., Murase, T., Miura, Y., & Oiso, Y. 2002, "Overexpression of vasopressin in the rat transgenic for the metallothionein-vasopressin fusion gene", *J.Endocrinol.*, vol. 173, no. 1, pp. 35-44.

Napoli, C., Lemieux, C., & Jorgensen, R. 1990, "Introduction of a Chimeric Chalcone Synthase Gene into Petunia Results in Reversible Co-Suppression of Homologous Genes in trans", *Plant Cell*, vol. 2, no. 4, pp. 279-289.

Naraghi, R., Schuster, H., Toka, H. R., Bahring, S., Toka, O., Oztekin, O., Bilginturan, N., Knoblauch, H., Wienker, T. F., Busjahn, A., Haller, H., Fahlbusch, R., & Luft, F. C. 1997, "Neurovascular compression at the ventrolateral medulla in autosomal dominant hypertension and brachydactyly", *Stroke*, vol. 28, no. 9, pp. 1749-1754.

Negrin, C. D., McBride, M. W., Carswell, H. V., Graham, D., Carr, F. J., Clark, J. S., Jeffs, B., Anderson, N. H., Macrae, I. M., & Dominiczak, A. F. 2001, "Reciprocal consomic strains to evaluate y chromosome effects", *Hypertension*, vol. 37, no. 2 Part 2, pp. 391-397.

Nelson, C. C., Hendy, S. C., Shukin, R. J., Cheng, H., Bruchovsky, N., Koop, B. F., & Rennie, P. S. 1999, "Determinants of DNA sequence specificity of the androgen, progesterone, and glucocorticoid receptors: evidence for differential steroid receptor response elements", *Mol.Endocrinol.*, vol. 13, no. 12, pp. 2090-2107.

New, M. I., Levine, L. S., Biglieri, E. G., Pareira, J., & Ulick, S. 1977, "Evidence for an unidentified steroid in a child with apparent mineralocorticoid hypertension", *J.Clin.Endocrinol.Metab*, vol. 44, no. 5, pp. 924-933.

Newhouse, S. J., Wallace, C., Dobson, R., Mein, C., Pembroke, J., Farrall, M., Clayton, D., Brown, M., Samani, N., Dominiczak, A., Connell, J. M., Webster, J., Lathrop, G. M., Caulfield, M., & Munroe, P. B. 2005, "Haplotypes of the WNK1 gene associate with blood pressure variation in a severely hypertensive population from the British Genetics of Hypertension study", *Hum.Mol.Genet.*, vol. 14, no. 13, pp. 1805-1814.

Nicklin SA, B. A. 1999, "Simple methods for preparing recombinant adenoviruses for high efficiency transduction of vascular cells," in *Vascular Disease: Molecular Biology and Gene Therapy Protocols*, A. H. Baker, ed., Humana Press, New York, pp. 271-283.

Nicklin, S. A. & Baker, A. H. 2003, "Development of targeted viral vectors for cardiovascular gene therapy", *Genet.Eng (N.Y.)*, vol. 25, pp. 15-49.

Nistala, R., Zhang, X., & Sigmund, C. D. 2004, "Differential expression of the closely linked KISS1, REN, and FLJ10761 genes in transgenic mice", *Physiol Genomics*, vol. 17, no. 1, pp. 4-10.

Nonaka, Y., Fujii, T., Kagawa, N., Waterman, M. R., Takemori, H., & Okamoto, M. 1998, "Structure/function relationship of CYP11B1 associated with Dahl's salt-resistant rats--

expression of rat CYP11B1 and CYP11B2 in Escherichia coli", *Eur.J.Biochem.*, vol. 258, no. 2, pp. 869-878.

Norppa, H. 2003, "Genetic susceptibility, biomarker respones, and cancer", *Mutat.Res*, vol. 544, no. 2-3, pp. 339-348.

O'Donnell, C. J., Lindpaintner, K., Larson, M. G., Rao, V. S., Ordovas, J. M., Schaefer, E. J., Myers, R. H., & Levy, D. 1998, "Evidence for association and genetic linkage of the angiotensin-converting enzyme locus with hypertension and blood pressure in men but not women in the Framingham Heart Study", *Circulation*, vol. 97, no. 18, pp. 1766-1772.

Okamoto, K., Yamori, Y., & Nagaoka, A. 1974, "Establishment of the stroke-prone spontaneously hypertensive rat (SHR).", *Circ Res*, vol. 34, Supplement I, p. I-143-I-153.

Okamoto, K. & Aoki, K. K. 1963, "Development of a strain of spontaneously hypertensive rats", *Jpn.Circ.J.*, vol. 27, pp. 282-293.

Okuno, H., Akahori, A., Sato, H., Xanthoudakis, S., Curran, T., & Iba, H. 1993, "Escape from redox regulation enhances the transforming activity of Fos", *Oncogene*, vol. 8, no. 3, pp. 695-701.

Ono, H., Sakoda, H., Fujishiro, M., Anai, M., Kushiyama, A., Fukushima, Y., Katagiri, H., Ogihara, T., Oka, Y., Kamata, H., Horike, N., Uchijima, Y., Kurihara, H., & Asano, T. 2007, "Carboxy-terminal modulator protein induces Akt phosphorylation and activation, thereby enhancing antiapoptotic, glycogen synthetic, and glucose uptake pathways", *Am.J.Physiol Cell Physiol*, vol. 293, no. 5, p. C1576-C1585.

Ortiz, P. A. & Garvin, J. L. 2002, "Superoxide stimulates NaCl absorption by the thick ascending limb", *Am.J.Physiol Renal Physiol*, vol. 283, no. 5, p. F957-F962.

Osoegawa, K., Zhu, B., Shu, C. L., Ren, T., Cao, Q., Vessere, G. M., Lutz, M. M., Jensen-Seaman, M. I., Zhao, S., & De Jong, P. J. 2004, "BAC resources for the rat genome project", *Genome Res*, vol. 14, no. 4, pp. 780-785.

Ovcharenko, I., Loots, G. G., Hardison, R. C., Miller, W., & Stubbs, L. 2004, "zPicture: dynamic alignment and visualization tool for analyzing conservation profiles", *Genome Res*, vol. 14, no. 3, pp. 472-477.

Padmanabhan, S., Wallace, C., Munroe, P. B., Dobson, R., Brown, M., Samani, N., Clayton, D., Farrall, M., Webster, J., Lathrop, M., Caulfield, M., Dominiczak, A. F., & Connell, J. M. 2006, "Chromosome 2p shows significant linkage to antihypertensive response in the British Genetics of Hypertension Study", *Hypertension*, vol. 47, no. 3, pp. 603-608.

Palijan, A., Dutil, J., & Deng, A. Y. 2003, "Quantitative trait loci with opposing blood pressure effects demonstrating epistasis on Dahl rat chromosome 3", *Physiol Genomics*, vol. 15, no. 1, pp. 1-8.

Palmer, R. M., Ashton, D. S., & Moncada, S. 1988, "Vascular endothelial cells synthesize nitric oxide from L-arginine", *Nature*, vol. 333, no. 6174, pp. 664-666.

Palmer, R. M., Ferrige, A. G., & Moncada, S. 1987, "Nitric oxide release accounts for the biological activity of endothelium-derived relaxing factor", *Nature*, vol. 327, no. 6122, pp. 524-526.

Pankow, J. S., Rose, K. M., Oberman, A., Hunt, S. C., Atwood, L. D., Djousse, L., Province, M. A., & Rao, D. C. 2000, "Possible locus on chromosome 18q influencing postural systolic blood pressure changes", *Hypertension*, vol. 36, no. 4, pp. 471-476.

Paolicchi, A., Minotti, G., Tonarelli, P., Tongiani, R., De Cesare, D., Mezzetti, A., Dominici, S., Comporti, M., & Pompella, A. 1999, "Gamma-glutamyl transpeptidase-dependent iron reduction and LDL oxidation--a potential mechanism in atherosclerosis", *J.Investig.Med.*, vol. 47, no. 3, pp. 151-160.

Park, E. Y., Cho, I. J., & Kim, S. G. 2004, "Transactivation of the PPAR-responsive enhancer module in chemopreventive glutathione S-transferase gene by the peroxisome proliferator-activated receptor-gamma and retinoid X receptor heterodimer", *Cancer Res*, vol. 64, no. 10, pp. 3701-3713.

Park, F. 2007, "Lentiviral vectors: are they the future of animal transgenesis?", *Physiol Genomics*, vol. 31, no. 2, pp. 159-173.

Parkes, M., Barrett, J. C., Prescott, N. J., Tremelling, M., Anderson, C. A., Fisher, S. A., Roberts, R. G., Nimmo, E. R., Cummings, F. R., Soars, D., Drummond, H., Lees, C. W., Khawaja, S. A., Bagnall, R., Burke, D. A., Todhunter, C. E., Ahmad, T., Onnie, C. M., McArdle, W., Strachan, D., Bethel, G., Bryan, C., Lewis, C. M., Deloukas, P., Forbes, A., Sanderson, J., Jewell, D. P., Satsangi, J., Mansfield, J. C., Cardon, L., & Mathew, C. G. 2007, "Sequence variants in the autophagy gene IRGM and multiple other replicating loci contribute to Crohn's disease susceptibility", *Nat.Genet.*, vol. 39, no. 7, pp. 830-832.

Parks, L. D., Zalups, R. K., & Barfuss, D. W. 1998, "Heterogeneity of glutathione synthesis and secretion in the proximal tubule of the rabbit", *Am.J.Physiol*, vol. 274, no. 5 Pt 2, p. F924-F931.

Paulson, K. E., Darnell, J. E., Jr., Rushmore, T., & Pickett, C. B. 1990, "Analysis of the upstream elements of the xenobiotic compound-inducible and positionally regulated glutathione S-transferase Ya gene", *Mol.Cell Biol.*, vol. 10, no. 5, pp. 1841-1852.

Pausova, Z., Gaudet, D., Gossard, F., Bernard, M., Kaldunski, M. L., Jomphe, M., Tremblay, J., Hudson, T. J., Bouchard, G., Kotchen, T. A., Cowley, A. W., & Hamet, P. 2005, "Genome-wide scan for linkage to obesity-associated hypertension in French Canadians", *Hypertension*, vol. 46, no. 6, pp. 1280-1285.

Perola, M., Kainulainen, K., Pajukanta, P., Terwilliger, J. D., Hiekkalinna, T., Ellonen, P., Kaprio, J., Koskenvuo, M., Kontula, K., & Peltonen, L. 2000, "Genome-wide scan of predisposing loci for increased diastolic blood pressure in Finnish siblings", *J.Hypertens.*, vol. 18, no. 11, pp. 1579-1585.

Petretto, E., Mangion, J., Pravanec, M., Hubner, N., & Aitman, T. J. 2006, "Integrated gene expression profiling and linkage analysis in the rat", *Mamm.Genome*, vol. 17, no. 6, pp. 480-489.

Pettigrew, N. E. & Colman, R. F. 2001, "Heterodimers of glutathione S-transferase can form between isoenzyme classes pi and mu", *Arch.Biochem.Biophys.*, vol. 396, no. 2, pp. 225-230.

Pfeifer, A., Ikawa, M., Dayn, Y., & Verma, I. M. 2002, "Transgenesis by lentiviral vectors: lack of gene silencing in mammalian embryonic stem cells and preimplantation embryos", *Proc.Natl.Acad.Sci.U.S.A*, vol. 99, no. 4, pp. 2140-2145.

Pimental, R. A., Liang, B., Yee, G. K., Wilhelmsson, A., Poellinger, L., & Paulson, K. E. 1993, "Dioxin receptor and C/EBP regulate the function of the glutathione S-transferase Ya gene xenobiotic response element", *Mol.Cell Biol.*, vol. 13, no. 7, pp. 4365-4373.

Pool-Zobel, B., Veeriah, S., & Bohmer, F. D. 2005, "Modulation of xenobiotic metabolising enzymes by anticarcinogens -- focus on glutathione S-transferases and their role as targets of dietary chemoprevention in colorectal carcinogenesis", *Mutat.Res*, vol. 591, no. 1-2, pp. 74-92.

Popova, E., Bader, M., & Krivokharchenko, A. 2005, "Production of transgenic models in hypertension", *Methods Mol.Med.*, vol. 108, pp. 33-50.

Popova, E., Krivokharchenko, A., Ganten, D., & Bader, M. 2002, "Comparison between PMSG and FSH induced superovulation for the generation of transgenic rats", *Mol.Reprod.Dev.*, vol. 63, no. 2, pp. 177-182.

Prabhu, K. S., Reddy, P. V., Jones, E. C., Liken, A. D., & Reddy, C. C. 2004, "Characterization of a class alpha glutathione-S-transferase with glutathione peroxidase activity in human liver microsomes", *Arch.Biochem.Biophys.*, vol. 424, no. 1, pp. 72-80.

Pravenec, M., Gauguier, D., Schott, J. J., Buard, J., Kren, V., Bila, V., Szpirer, C., Szpirer, J., Wang, J. M., Huang, H., St Lezin, E., Spence, M. A., Flodman, P., Printz, M., Lathrop, G. M., Vergnaud, G., & Kurtz, T. W. 1996, "A genetic linkage map of the rat derived from recombinant inbred strains", *Mamm.Genome*, vol. 7, no. 2, pp. 117-127.

Pravenec, M., Hyakukoku, M., Houstek, J., Zidek, V., Landa, V., Mlejnek, P., Miksik, I., Dudova-Mothejzikova, K., Pecina, P., Vrbacky, M., Drahota, Z., Vojtiskova, A., Mracek, T., Kazdova, L., Oliyarnyk, O., Wang, J., Ho, C., Qi, N., Sugimoto, K., & Kurtz, T. 2007, "Direct linkage of mitochondrial genome variation to risk factors for type 2 diabetes in conplastic strains", *Genome Res.*, vol. 17, no. 9, pp. 1319-1326.

Pravenec, M., Jansa, P., Kostka, V., Zidek, V., Kren, V., Forejt, J., & Kurtz, T. W. 2001a, "Identification of a mutation in ADD1/SREBP-1 in the spontaneously hypertensive rat", *Mamm.Genome*, vol. 12, no. 4, pp. 295-298.

Pravenec, M., Kazdova, L., Landa, V., Zidek, V., Mlejnek, P., Jansa, P., Wang, J., Qi, N., & Kurtz, T. W. 2003, "Transgenic and recombinant resistin impair skeletal muscle glucose metabolism in the spontaneously hypertensive rat", *J.Biol.Chem.*, vol. 278, no. 46, pp. 45209-45215.

Pravenec, M., Kazdova, L., Landa, V., Zidek, V., Mlejnek, P., Simakova, M., Jansa, P., Forejt, J., Kren, V., Krenova, D., Qi, N., Wang, J. M., Chan, D., Aitman, T. J., & Kurtz, T. W. 2008, "Identification of mutated Srebf1 as a QTL influencing risk for hepatic steatosis in the spontaneously hypertensive rat", *Hypertension*, vol. 51, no. 1, pp. 148-153.

Pravenec, M., Klir, P., Kren, V., Zicha, J., & Kunes, J. 1989, "An analysis of spontaneous hypertension in spontaneously hypertensive rats by means of new recombinant inbred strains", *J.Hypertens.*, vol. 7, no. 3, pp. 217-221.

Pravenec, M., Kren, V., Krenova, D., Bila, V., Zidek, V., Simakova, M., Musilova, A., van Lith, H. A., & van Zutphen, L. F. 1999, "HXB/Ipcv and BXH/Cub recombinant inbred strains of the rat: strain distribution patterns of 632 alleles", *Folia Biol.(Praha)*, vol. 45, no. 5, pp. 203-215.

Pravenec, M., Landa, V., Zidek, V., Musilova, A., Kren, V., Kazdova, L., Aitman, T. J., Glazier, A. M., Ibrahimi, A., Abumrad, N. A., Qi, N., Wang, J. M., St Lezin, E. M., &

Kurtz, T. W. 2001b, "Transgenic rescue of defective Cd36 ameliorates insulin resistance in spontaneously hypertensive rats", *Nat Genet*, vol. 27, no. 2, pp. 156-8.

Printz, M. P., Jirout, M., Jaworski, R., Alemayehu, A., & Kren, V. 2003, "Genetic Models in Applied Physiology. HXB/BXH rat recombinant inbred strain platform: a newly enhanced tool for cardiovascular, behavioral, and developmental genetics and genomics", *J.Appl.Physiol*, vol. 94, no. 6, pp. 2510-2522.

Probst, F. J., Fridell, R. A., Raphael, Y., Saunders, T. L., Wang, A., Liang, Y., Morell, R. J., Touchman, J. W., Lyons, R. H., Noben-Trauth, K., Friedman, T. B., & Camper, S. A. 1998, "Correction of deafness in shaker-2 mice by an unconventional myosin in a BAC transgene", *Science*, vol. 280, no. 5368, pp. 1444-1447.

Rafestin-Oblin, M. E., Souque, A., Bocchi, B., Pinon, G., Fagart, J., & Vandewalle, A. 2003, "The severe form of hypertension caused by the activating S810L mutation in the mineralocorticoid receptor is cortisone related", *Endocrinology*, vol. 144, no. 2, pp. 528-533.

Rao, D. C., Province, M. A., Leppert, M. F., Oberman, A., Heiss, G., Ellison, R. C., Arnett, D. K., Eckfeldt, J. H., Schwander, K., Mockrin, S. C., & Hunt, S. C. 2003, "A genome-wide affected sibpair linkage analysis of hypertension: the HyperGEN network", *Am.J.Hypertens.*, vol. 16, no. 2, pp. 148-150.

Rapp, J. P. 2000, "Genetic analysis of inherited hypertension in the rat", *Physiol Rev*, vol. 80, no. 1, pp. 135-72.

Rapp, J. P. & Dahl, L. 1971, "Adrenal steroidogenesis in rats bred for susceptibility and resistance to the hypertensive effect of salt", *Endocrinology*, vol. 88, no. 1, pp. 52-65.

Rapp, J. P. & Dahl, L. 1972, "Possible role of 18-hydroxy-deoxycorticosterone in hypertension", *Nature*, vol. 237, no. 5354, pp. 338-339.

Rapp, J. P. & Dene, H. 1985, "Development and characteristics of inbred strains of Dahl salt-sensitive and salt-resistant rats", *Hypertension*, vol. 7, no. 3 Pt 1, pp. 340-349.

Rapp, J. P., Garrett, M. R., & Deng, A. Y. 1998, "Construction of a double congenic strain to prove an epistatic interaction on blood pressure between rat chromosomes 2 and 10", *J.Clin.Invest*, vol. 101, no. 8, pp. 1591-1595.

Rassoulzadegan, M., Grandjean, V., Gounon, P., Vincent, S., Gillot, I., & Cuzin, F. 2006, "RNA-mediated non-mendelian inheritance of an epigenetic change in the mouse", *Nature*, vol. 441, no. 7092, pp. 469-474.

Redon, R., Ishikawa, S., Fitch, K. R., Feuk, L., Perry, G. H., Andrews, T. D., Fiegler, H., Shapero, M. H., Carson, A. R., Chen, W., Cho, E. K., Dallaire, S., Freeman, J. L., Gonzalez, J. R., Gratacos, M., Huang, J., Kalaitzopoulos, D., Komura, D., MacDonald, J. R., Marshall, C. R., Mei, R., Montgomery, L., Nishimura, K., Okamura, K., Shen, F., Somerville, M. J., Tchinda, J., Valsesia, A., Woodwark, C., Yang, F., Zhang, J., Zerjal, T., Zhang, J., Armengol, L., Conrad, D. F., Estivill, X., Tyler-Smith, C., Carter, N. P., Aburatani, H., Lee, C., Jones, K. W., Scherer, S. W., & Hurles, M. E. 2006, "Global variation in copy number in the human genome", *Nature*, vol. 444, no. 7118, pp. 444-454.

Reinhart, J. & Pearson, W. R. 1993, "The structure of two murine class-mu glutathione transferase genes coordinately induced by butylated hydroxyanisole", *Arch.Biochem.Biophys.*, vol. 303, no. 2, pp. 383-393.

Rice, T., Rankinen, T., Chagnon, Y. C., Province, M. A., Perusse, L., Leon, A. S., Skinner, J. S., Wilmore, J. H., Bouchard, C., & Rao, D. C. 2002, "Genomewide linkage scan of resting blood pressure: HERITAGE Family Study. Health, Risk Factors, Exercise Training, and Genetics", *Hypertension*, vol. 39, no. 6, pp. 1037-1043.

Rice, T., Rankinen, T., Province, M. A., Chagnon, Y. C., Perusse, L., Borecki, I. B., Bouchard, C., & Rao, D. C. 2000, "Genome-wide linkage analysis of systolic and diastolic blood pressure: the Quebec Family Study", *Circulation*, vol. 102, no. 16, pp. 1956-1963.

Rich, G. M., Ulick, S., Cook, S., Wang, J. Z., Lifton, R. P., & Dluhy, R. G. 1992, "Glucocorticoid-remediable aldosteronism in a large kindred: clinical spectrum and diagnosis using a characteristic biochemical phenotype", *Ann.Intern.Med.*, vol. 116, no. 10, pp. 813-820.

Rigat, B., Hubert, C., Alhenc-Gelas, F., Cambien, F., Corvol, P., & Soubrier, F. 1990, "An insertion/deletion polymorphism in the angiotensin I-converting enzyme gene accounting for half the variance of serum enzyme levels", *J.Clin.Invest*, vol. 86, no. 4, pp. 1343-1346.

Rojas, E., Valverde, M., Kala, S. V., Kala, G., & Lieberman, M. W. 2000, "Accumulation of DNA damage in the organs of mice deficient in gamma-glutamyltranspeptidase", *Mutat.Res*, vol. 447, no. 2, pp. 305-316.

Rose, R. J., Miller, J. Z., Grim, C. E., & Christian, J. C. 1979, "Aggregation of blood pressure in the families of identical twins", *Am.J.Epidemiol.*, vol. 109, no. 5, pp. 503-511.

Ross, V. L. & Board, P. G. 1993, "Molecular cloning and heterologous expression of an alternatively spliced human Mu class glutathione S-transferase transcript", *Biochem.J.*, vol. 294 (Pt 2), pp. 373-380.

Rouimi, P., Anglade, P., Debrauwer, L., & Tulliez, J. 1996, "Characterization of pig liver glutathione S-transferases using HPLC-electrospray-ionization mass spectrometry", *Biochem.J.*, vol. 317 (Pt 3), pp. 879-884.

Rozen, S. & Skaletsky, H. 2000, "Primer3 on the WWW for general users and for biologist programmers", *Methods Mol.Biol.*, vol. 132, pp. 365-386.

Rubattu, S., Hubner, N., Ganten, U., Evangelista, A., Stanzione, R., Di Angelantonio, E., Plehm, R., Langanki, R., Gianazza, E., Sironi, L., D'Amati, G., & Volpe, M. 2006, "Reciprocal congenic lines for a major stroke QTL on rat chromosome 1", *Physiol Genomics*, vol. 27, no. 2, pp. 108-113.

Rubattu, S., Volpe, M., Kreutz, R., Ganten, U., Ganten, D., & Lindpaintner, K. 1996, "Chromosomal mapping of quantitative trait loci contributing to stroke in a rat model of complex human disease", *Nat.Genet.*, vol. 13, no. 4, pp. 429-434.

Rushmore, T. H., Morton, M. R., & Pickett, C. B. 1991, "The antioxidant responsive element. Activation by oxidative stress and identification of the DNA consensus sequence required for functional activity", *J.Biol.Chem.*, vol. 266, no. 18, pp. 11632-11639.

Saad, Y., Garrett, M. R., & Rapp, J. P. 2001, "Multiple blood pressure QTL on rat chromosome 1 defined by Dahl rat congenic strains", *Physiol Genomics*, vol. 4, no. 3, pp. 201-214.

Sagami, I., Tsai, S. Y., Wang, H., Tsai, M. J., & O'Malley, B. W. 1986, "Identification of two factors required for transcription of the ovalbumin gene", *Mol.Cell Biol.*, vol. 6, no. 12, pp. 4259-4267.

Sakai, K., Hirooka, Y., Shigematsu, H., Kishi, T., Ito, K., Shimokawa, H., Takeshita, A., & Sunagawa, K. 2005, "Overexpression of eNOS in brain stem reduces enhanced sympathetic drive in mice with myocardial infarction", *Am.J.Physiol Heart Circ Physiol*, vol. 289, no. 5, p. H2159-H2166.

Sampaio, W. O., Souza dos Santos, R. A., Faria-Silva, R., Mata Machado, L. T., Schiffrin, E. L., & Touyz, R. M. 2007, "Angiotensin-(1-7) through receptor Mas mediates endothelial nitric oxide synthase activation via Akt-dependent pathways", *Hypertension*, vol. 49, no. 1, pp. 185-192.

Sanada, H., Jose, P. A., Hazen-Martin, D., Yu, P. Y., Xu, J., Bruns, D. E., Phipps, J., Carey, R. M., & Felder, R. A. 1999, "Dopamine-1 receptor coupling defect in renal proximal tubule cells in hypertension", *Hypertension*, vol. 33, no. 4, pp. 1036-1042.

Santos, R. A., Ferreira, A. J., Nadu, A. P., Braga, A. N., de Almeida, A. P., Campagnole-Santos, M. J., Baltatu, O., Iliescu, R., Reudelhuber, T. L., & Bader, M. 2004, "Expression of an angiotensin-(1-7)-producing fusion protein produces cardioprotective effects in rats", *Physiol Genomics*, vol. 17, no. 3, pp. 292-299.

Santos, R. A., Simoes e Silva AC, Magaldi, A. J., Khosla, M. C., Cesar, K. R., Passaglio, K. T., & Baracho, N. C. 1996, "Evidence for a physiological role of angiotensin-(1-7) in the control of hydroelectrolyte balance", *Hypertension*, vol. 27, no. 4, pp. 875-884.

Sarafidis, P. A. & Lasaridis, A. N. 2006, "Actions of peroxisome proliferator-activated receptors-gamma agonists explaining a possible blood pressure-lowering effect", *Am.J.Hypertens.*, vol. 19, no. 6, pp. 646-653.

Satoh, H., Tsukamoto, K., Hashimoto, Y., Hashimoto, N., Togo, M., Hara, M., Maekawa, H., Isoo, N., Kimura, S., & Watanabe, T. 1999, "Thiazolidinediones suppress endothelin-1 secretion from bovine vascular endothelial cells: a new possible role of PPARgamma on vascular endothelial function", *Biochem.Biophys.Res.Commun.*, vol. 254, no. 3, pp. 757-763.

Saxena, S., Jonsson, Z. O., & Dutta, A. 2003, "Small RNAs with imperfect match to endogenous mRNA repress translation. Implications for off-target activity of small inhibitory RNA in mammalian cells", *J.Biol.Chem.*, vol. 278, no. 45, pp. 44312-44319.

Schedl, A., Larin, Z., Montoliu, L., Thies, E., Kelsey, G., Lehrach, H., & Schutz, G. 1993, "A method for the generation of YAC transgenic mice by pronuclear microinjection", *Nucleic Acids Res*, vol. 21, no. 20, pp. 4783-4787.

Schiavone, M. T., Santos, R. A., Brosnihan, K. B., Khosla, M. C., & Ferrario, C. M. 1988, "Release of vasopressin from the rat hypothalamo-neurohypophysial system by angiotensin-(1-7) heptapeptide", *Proc.Natl.Acad.Sci.U.S.A*, vol. 85, no. 11, pp. 4095-4098.

Schild, L., Canessa, C. M., Shimkets, R. A., Gautschi, I., Lifton, R. P., & Rossier, B. C. 1995, "A mutation in the epithelial sodium channel causing Liddle disease increases channel activity in the Xenopus laevis oocyte expression system", *Proc.Natl.Acad.Sci.U.S.A*, vol. 92, no. 12, pp. 5699-5703.

Schinke, M., Baltatu, O., Bohm, M., Peters, J., Rascher, W., Bricca, G., Lippoldt, A., Ganten, D., & Bader, M. 1999, "Blood pressure reduction and diabetes insipidus in transgenic rats deficient in brain angiotensinogen", *Proc.Natl.Acad.Sci.U.S.A*, vol. 96, no. 7, pp. 3975-3980.

Schnackenberg, C. G. & Wilcox, C. S. 1999, "Two-week administration of tempol attenuates both hypertension and renal excretion of 8-Iso prostaglandin f2alpha", *Hypertension*, vol. 33, no. 1 Pt 2, pp. 424-428.

Schnellmann, R. G. 1988, "Mechanisms of t-butyl hydroperoxide-induced toxicity to rabbit renal proximal tubules", *Am.J.Physiol*, vol. 255, no. 1 Pt 1, p. C28-C33.

Schreck, R., Rieber, P., & Baeuerle, P. A. 1991, "Reactive oxygen intermediates as apparently widely used messengers in the activation of the NF-kappa B transcription factor and HIV-1", *EMBO J.*, vol. 10, no. 8, pp. 2247-2258.

Schulze-Osthoff, K., Beyaert, R., Vandevoorde, V., Haegeman, G., & Fiers, W. 1993, "Depletion of the mitochondrial electron transport abrogates the cytotoxic and gene-inductive effects of TNF", *EMBO J.*, vol. 12, no. 8, pp. 3095-3104.

Schuster, H., Wienker, T. E., Bahring, S., Bilginturan, N., Toka, H. R., Neitzel, H., Jeschke, E., Toka, O., Gilbert, D., Lowe, A., Ott, J., Haller, H., & Luft, F. C. 1996, "Severe autosomal dominant hypertension and brachydactyly in a unique Turkish kindred maps to human chromosome 12", *Nat.Genet.*, vol. 13, no. 1, pp. 98-100.

Sealey, J. E. & Laragh, J. H. 1990, "The Renin-angiotensin-aldosterone system for normal regulation of blood presure and sodium and potassium homeostasis," in *Hypertension: Pathophysiology, Diagnosis and Management*, J. H. Laragh & B. M. Brenner, eds., Raven Press, New York, pp. 1287-1317.

Seubert, J. M., Xu, F., Graves, J. P., Collins, J. B., Sieber, S. O., Paules, R. S., Kroetz, D. L., & Zeldin, D. C. 2005, "Differential renal gene expression in prehypertensive and hypertensive spontaneously hypertensive rats", *Am.J.Physiol Renal Physiol*, vol. 289, no. 3, p. F552-F561.

Sharma, P., Fatibene, J., Ferraro, F., Jia, H., Monteith, S., Brown, C., Clayton, D., O'Shaughnessy, K., & Brown, M. J. 2000, "A genome-wide search for susceptibility loci to human essential hypertension", *Hypertension*, vol. 35, no. 6, pp. 1291-1296.

Shaywitz, A. J. & Greenberg, M. E. 1999, "CREB: a stimulus-induced transcription factor activated by a diverse array of extracellular signals", *Annu.Rev.Biochem.*, vol. 68, pp. 821-861.

Shimkets, R. A., Lifton, R. P., & Canessa, C. M. 1997, "The activity of the epithelial sodium channel is regulated by clathrin-mediated endocytosis", *J.Biol.Chem.*, vol. 272, no. 41, pp. 25537-25541.

Shmulewitz, D., Heath, S. C., Blundell, M. L., Han, Z., Sharma, R., Salit, J., Auerbach, S. B., Signorini, S., Breslow, J. L., Stoffel, M., & Friedman, J. M. 2006, "Linkage analysis of quantitative traits for obesity, diabetes, hypertension, and dyslipidemia on the island of Kosrae, Federated States of Micronesia", *Proc.Natl.Acad.Sci.U.S.A*, vol. 103, no. 10, pp. 3502-3509.

Siffert, W., Rosskopf, D., Moritz, A., Wieland, T., Kaldenberg-Stasch, S., Kettler, N., Hartung, K., Beckmann, S., & Jakobs, K. H. 1995, "Enhanced G protein activation in immortalized lymphoblasts from patients with essential hypertension", *J.Clin.Invest*, vol. 96, no. 2, pp. 759-766.

Siffert, W., Rosskopf, D., Siffert, G., Busch, S., Moritz, A., Erbel, R., Sharma, A. M., Ritz, E., Wichmann, H. E., Jakobs, K. H., & Horsthemke, B. 1998, "Association of a human G-protein beta3 subunit variant with hypertension", *Nat.Genet.*, vol. 18, no. 1, pp. 45-48.

Simon, D. B., Nelson-Williams, C., Bia, M. J., Ellison, D., Karet, F. E., Molina, A. M., Vaara, I., Iwata, F., Cushner, H. M., Koolen, M., Gainza, F. J., Gitleman, H. J., & Lifton, R. P. 1996, "Gitelman's variant of Bartter's syndrome, inherited hypokalaemic alkalosis, is caused by mutations in the thiazide-sensitive Na-Cl cotransporter", *Nat.Genet.*, vol. 12, no. 1, pp. 24-30.

Smirk, F. & Hall, W. 1958, "Inherited hypertension in rats", *Nature*, vol. 182, no. 4637, pp. 727-728.

Sommer, M. & Wolf, G. 2007, "Rosiglitazone increases PPARgamma in renal tubular epithelial cells and protects against damage by hydrogen peroxide", *Am.J.Nephrol.*, vol. 27, no. 4, pp. 425-434.

Speirs, H. J., Katyk, K., Kumar, N. N., Benjafield, A. V., Wang, W. Y., & Morris, B. J. 2004, "Association of G-protein-coupled receptor kinase 4 haplotypes, but not HSD3B1 or PTP1B polymorphisms, with essential hypertension", *J.Hypertens.*, vol. 22, no. 5, pp. 931-936.

Spiers, A. & Padmanabhan, N. 2005, "A guide to wire myography", *Methods Mol.Med.*, vol. 108, pp. 91-104.

Staessen, J., Fagard, R., Lijnen, P., & Amery, A. 1989, "Body weight, sodium intake and blood pressure", *J.Hypertens.Suppl*, vol. 7, no. 1, p. S19-S23.

Staessen, J. A., Kuznetsova, T., Wang, J. G., Emelianov, D., Vlietinck, R., & Fagard, R. 1999, "M235T angiotensinogen gene polymorphism and cardiovascular renal risk", *J.Hypertens.*, vol. 17, no. 1, pp. 9-17.

Stewart, P. M., Wallace, A. M., Valentino, R., Burt, D., Shackleton, C. H., & Edwards, C. R. 1987, "Mineralocorticoid activity of liquorice: 11-beta-hydroxysteroid dehydrogenase deficiency comes of age", *Lancet*, vol. 2, no. 8563, pp. 821-824.

Strahorn, P., Graham, D., Charchar, F. J., Sattar, N., McBride, M. W., & Dominiczak, A. F. 2005, "Genetic determinants of metabolic syndrome components in the stroke-prone spontaneously hypertensive rat", *J.Hypertens.*, vol. 23, no. 12, pp. 2179-2186.

Stranger, B. E., Forrest, M. S., Dunning, M., Ingle, C. E., Beazley, C., Thorne, N., Redon, R., Bird, C. P., de Grassi, A., Lee, C., Tyler-Smith, C., Carter, N., Scherer, S. W., Tavare, S., Deloukas, P., Hurles, M. E., & Dermitzakis, E. T. 2007, "Relative impact of nucleotide and copy number variation on gene expression phenotypes", *Science*, vol. 315, no. 5813, pp. 848-853.

Sugo, S., Minamino, N., Shoji, H., Isumi, Y., Nakao, K., Kangawa, K., & Matsuo, H. 2001, "Regulation of endothelin-1 production in cultured rat vascular smooth muscle cells", *J.Cardiovasc.Pharmacol.*, vol. 37, no. 1, pp. 25-40.

Sui, G., Soohoo, C., Affar, e. B., Gay, F., Shi, Y., Forrester, W. C., & Shi, Y. 2002, "A DNA vector-based RNAi technology to suppress gene expression in mammalian cells", *Proc.Natl.Acad.Sci.U.S.A*, vol. 99, no. 8, pp. 5515-5520.

Sun, F., Cui, J., Gavras, H., & Schwartz, F. 2003, "A novel class of tests for the detection of mitochondrial DNA-mutation involvement in diseases", *Am.J.Hum.Genet.*, vol. 72, no. 6, pp. 1515-1526.

Sun, J., Hoshino, H., Takaku, K., Nakajima, O., Muto, A., Suzuki, H., Tashiro, S., Takahashi, S., Shibahara, S., Alam, J., Taketo, M. M., Yamamoto, M., & Igarashi, K.

2002, "Hemoprotein Bach1 regulates enhancer availability of heme oxygenase-1 gene", *EMBO J.*, vol. 21, no. 19, pp. 5216-5224.

Sundaresan, M., Yu, Z. X., Ferrans, V. J., Irani, K., & Finkel, T. 1995, "Requirement for generation of H2O2 for platelet-derived growth factor signal transduction", *Science*, vol. 270, no. 5234, pp. 296-299.

Sutherland, D. J., Ruse, J. L., & Laidlaw, J. C. 1966, "Hypertension, increased aldosterone secretion and low plasma renin activity relieved by dexamethasone", *Can.Med.Assoc.J.*, vol. 95, no. 22, pp. 1109-1119.

Svetkey, L. P., Timmons, P. Z., Emovon, O., Anderson, N. B., Preis, L., & Chen, Y. T. 1996, "Association of hypertension with beta2- and alpha2c10-adrenergic receptor genotype", *Hypertension*, vol. 27, no. 6, pp. 1210-1215.

Sweeney, W. E., Jr. & Avner, E. D. 1998, "Functional activity of epidermal growth factor receptors in autosomal recessive polycystic kidney disease", *Am.J.Physiol*, vol. 275, no. 3 Pt 2, p. F387-F394.

Tallant, E. A., Ferrario, C. M., & Gallagher, P. E. 2005, "Angiotensin-(1-7) inhibits growth of cardiac myocytes through activation of the mas receptor", *Am.J.Physiol Heart Circ Physiol*, vol. 289, no. 4, p. H1560-H1566.

Tanase, H., Suzuki, Y., Ooshima, A., Yamori, Y., & Okamoto, K. 1970, "Genetic analysis of blood pressure in spontaneously hypertensive rats", *Jpn.Circ J.*, vol. 34, no. 12, pp. 1197-1212.

Tate, S. S. 1985, "Microvillus membrane peptidases that catalyze hydrolysis of cysteinylglycine and its derivatives", *Methods Enzymol.*, vol. 113, pp. 471-484.

Teschke, R., Brand, A., & Strohmeyer, G. 1977, "Induction of hepatic microsomal gamma-glutamyltransferase activity following chronic alcohol consumption", *Biochem.Biophys.Res Commun.*, vol. 75, no. 3, pp. 718-724.

Tesson, L., Cozzi, J., Menoret, S., Remy, S., Usal, C., Fraichard, A., & Anegon, I. 2005, "Transgenic modifications of the rat genome", *Transgenic Res*, vol. 14, no. 5, pp. 531-546.

The International HapMap consortium 2005, "A haplotype map of the human genome", *Nature*, vol. 437, no. 7063, pp. 1299-1320.

The International HapMap consortium 2007, "A second generation human haplotype map of over 3.1 million SNPs", *Nature*, vol. 449, no. 7164, pp. 851-861.

The Wellcome Trust Case Control Consortium 2007, "Genome-wide association study of 14,000 cases of seven common diseases and 3,000 shared controls", *Nature*, vol. 447, no. 7145, pp. 661-678.

Thiel, B. A., Chakravarti, A., Cooper, R. S., Luke, A., Lewis, S., Lynn, A., Tiwari, H., Schork, N. J., & Weder, A. B. 2003, "A genome-wide linkage analysis investigating the determinants of blood pressure in whites and African Americans", *Am.J.Hypertens.*, vol. 16, no. 2, pp. 151-153.

Tipnis, S. R., Hooper, N. M., Hyde, R., Karran, E., Christie, G., & Turner, A. J. 2000, "A human homolog of angiotensin-converting enzyme. Cloning and functional expression as a captopril-insensitive carboxypeptidase", *J.Biol.Chem.*, vol. 275, no. 43, pp. 33238-33243.

Tobin, M. D., Raleigh, S. M., Newhouse, S., Braund, P., Bodycote, C., Ogleby, J., Cross, D., Gracey, J., Hayes, S., Smith, T., Ridge, C., Caulfield, M., Sheehan, N. A., Munroe, P. B., Burton, P. R., & Samani, N. J. 2005, "Association of WNK1 gene polymorphisms and haplotypes with ambulatory blood pressure in the general population", *Circulation*, vol. 112, no. 22, pp. 3423-3429.

Todd, J. A., Walker, N. M., Cooper, J. D., Smyth, D. J., Downes, K., Plagnol, V., Bailey, R., Nejentsev, S., Field, S. F., Payne, F., Lowe, C. E., Szeszko, J. S., Hafler, J. P., Zeitels, L., Yang, J. H., Vella, A., Nutland, S., Stevens, H. E., Schuilenburg, H., Coleman, G., Maisuria, M., Meadows, W., Smink, L. J., Healy, B., Burren, O. S., Lam, A. A., Ovington, N. R., Allen, J., Adlem, E., Leung, H. T., Wallace, C., Howson, J. M., Guja, C., Ionescu-Tirgoviste, C., Simmonds, M. J., Heward, J. M., Gough, S. C., Dunger, D. B., Wicker, L. S., & Clayton, D. G. 2007, "Robust associations of four new chromosome regions from genome-wide analyses of type 1 diabetes", *Nat.Genet.*, vol. 39, no. 7, pp. 857-864.

Todorov, V. T., Desch, M., Schmitt-Nilson, N., Todorova, A., & Kurtz, A. 2007, "Peroxisome proliferator-activated receptor-gamma is involved in the control of renin gene expression", *Hypertension*, vol. 50, no. 5, pp. 939-944.

Tomaszewski, M., Brain, N. J., Charchar, F. J., Wang, W. Y., Lacka, B., Padmanabahn, S., Clark, J. S., Anderson, N. H., Edwards, H. V., Zukowska-Szczechowska, E., Grzeszczak, W., & Dominiczak, A. F. 2002, "Essential hypertension and beta2-adrenergic receptor gene: linkage and association analysis", *Hypertension*, vol. 40, no. 3, pp. 286-291.

Tomaszewski, M., Charchar, F. J., Lacka, B., Pesonen, U., Wang, W. Y., Zukowska-Szczechowska, E., Grzeszczak, W., & Dominiczak, A. F. 2004, "Epistatic interaction between beta2-adrenergic receptor and neuropeptide Y genes influences LDL-cholesterol in hypertension", *Hypertension*, vol. 44, no. 5, pp. 689-694.

Tomaszewski, M., Charchar, F. J., Lynch, M. D., Padmanabhan, S., Wang, W. Y., Miller, W. H., Grzeszczak, W., Maric, C., Zukowska-Szczechowska, E., & Dominiczak, A. F. 2007, "Fibroblast growth factor 1 gene and hypertension: from the quantitative trait locus to positional analysis", *Circulation*, vol. 116, no. 17, pp. 1915-1924.

Tontonoz, P., Hu, E., & Spiegelman, B. M. 1994, "Stimulation of adipogenesis in fibroblasts by PPAR gamma 2, a lipid-activated transcription factor", *Cell*, vol. 79, no. 7, pp. 1147-1156.

Tordjman, J., Chauvet, G., Quette, J., Beale, E. G., Forest, C., & Antoine, B. 2003, "Thiazolidinediones block fatty acid release by inducing glyceroneogenesis in fat cells", *J.Biol.Chem.*, vol. 278, no. 21, pp. 18785-18790.

Tripodi, G., Valtorta, F., Torielli, L., Chieregatti, E., Salardi, S., Trusolino, L., Menegon, A., Ferrari, P., Marchisio, P. C., & Bianchi, G. 1996, "Hypertension-associated point mutations in the adducin alpha and beta subunits affect actin cytoskeleton and ion transport", *J.Clin.Invest*, vol. 97, no. 12, pp. 2815-2822.

Twigger, S. N., Shimoyama, M., Bromberg, S., Kwitek, A. E., & Jacob, H. J. 2007, "The Rat Genome Database, update 2007--easing the path from disease to data and back again", *Nucleic Acids Res*, vol. 35, no. Database issue, p. D658-D662.

Uehara, Y., Shin, W. S., Watanabe, T., Osanai, T., Miyazaki, M., Kanase, H., Taguchi, R., Sugano, K., & Toyo-Oka, T. 1998, "A hypertensive father, but not hypertensive mother, determines blood pressure in normotensive male offspring through body mass index", *J.Hum.Hypertens.*, vol. 12, no. 7, pp. 441-445.

Ulick, S., Levine, L. S., Gunczler, P., Zanconato, G., Ramirez, L. C., Rauh, W., Rosler, A., Bradlow, H. L., & New, M. I. 1979, "A syndrome of apparent mineralocorticoid excess associated with defects in the peripheral metabolism of cortisol", *J.Clin.Endocrinol.Metab*, vol. 49, no. 5, pp. 757-764.

Valdar, W., Solberg, L. C., Gauguier, D., Burnett, S., Klenerman, P., Cookson, W. O., Taylor, M. S., Rawlins, J. N., Mott, R., & Flint, J. 2006, "Genome-wide genetic association of complex traits in heterogeneous stock mice", *Nat.Genet.*, vol. 38, no. 8, pp. 879-887.

Vallon, V., Richter, K., Heyne, N., & Osswald, H. 1997, "Effect of intratubular application of angiotensin 1-7 on nephron function", *Kidney Blood Press Res*, vol. 20, no. 4, pp. 233-239.

van Balkom, B. W., Hoffert, J. D., Chou, C. L., & Knepper, M. A. 2004, "Proteomic analysis of long-term vasopressin action in the inner medullary collecting duct of the Brattleboro rat", *Am.J.Physiol Renal Physiol*, vol. 286, no. 2, p. F216-F224.

Vasquez-Vivar, J., Kalyanaraman, B., Martasek, P., Hogg, N., Masters, B. S., Karoui, H., Tordo, P., & Pritchard, K. A., Jr. 1998, "Superoxide generation by endothelial nitric oxide synthase: the influence of cofactors", *Proc.Natl.Acad.Sci.U.S.A*, vol. 95, no. 16, pp. 9220-9225.

Vaziri, N. D., Liang, K., & Ding, Y. 1999, "Increased nitric oxide inactivation by reactive oxygen species in lead-induced hypertension", *Kidney Int.*, vol. 56, no. 4, pp. 1492-1498.

Vaziri, N. D., Wang, X. Q., Oveisi, F., & Rad, B. 2000, "Induction of oxidative stress by glutathione depletion causes severe hypertension in normal rats", *Hypertension*, vol. 36, no. 1, pp. 142-146.

Veniant, M., Menard, J., Bruneval, P., Morley, S., Gonzales, M. F., & Mullins, J. 1996, "Vascular damage without hypertension in transgenic rats expressing prorenin exclusively in the liver", *J.Clin.Invest*, vol. 98, no. 9, pp. 1966-1970.

Venugopal, R. & Jaiswal, A. K. 1996, "Nrf1 and Nrf2 positively and c-Fos and Fra1 negatively regulate the human antioxidant response element-mediated expression of NAD(P)H:quinone oxidoreductase1 gene", *Proc.Natl.Acad.Sci.U.S.A*, vol. 93, no. 25, pp. 14960-14965.

Wakimoto, H., Kasahara, H., Maguire, C. T., Moskowitz, I. P., Izumo, S., & Berul, C. I. 2003, "Cardiac electrophysiological phenotypes in postnatal expression of Nkx2.5 transgenic mice", *Genesis.*, vol. 37, no. 3, pp. 144-150.

Wallace, C., Xue, M. Z., Newhouse, S. J., Marcano, A. C., Onipinla, A. K., Burke, B., Gungadoo, J., Dobson, R. J., Brown, M., Connell, J. M., Dominiczak, A., Lathrop, G. M., Webster, J., Farrall, M., Mein, C., Samani, N. J., Caulfield, M. J., Clayton, D. G., & Munroe, P. B. 2006, "Linkage analysis using co-phenotypes in the BRIGHT study reveals novel potential susceptibility loci for hypertension", *Am.J.Hum.Genet.*, vol. 79, no. 2, pp. 323-331.

Waller, S., Fairhall, K. M., Xu, J., Robinson, I. C., & Murphy, D. 1996, "Neurohypophyseal and fluid homeostasis in transgenic rats expressing a tagged rat vasopressin prepropeptide in hypothalamic neurons", *Endocrinology*, vol. 137, no. 11, pp. 5068-5077.

Wang, B., Dang, A., & Liu, G. 2001, "Genetic variation in the promoter region of the beta2 bradykinin receptor gene is associated with essential hypertension in a Chinese Han population", *Hypertens.Res*, vol. 24, no. 3, pp. 299-302.

Wang, G., Zhang, L., & Li, Q. 2006a, "Genetic polymorphisms of GSTT1, GSTM1, and NQO1 genes and diabetes mellitus risk in Chinese population", *Biochem.Biophys.Res Commun.*, vol. 341, no. 2, pp. 310-313.

Wang, J., Bauman, S., & Colman, R. F. 2000, "Probing subunit interactions in alpha class rat liver glutathione S-transferase with the photoaffinity label glutathionyl S-[4-(succinimidyl)benzophenone]", *J.Biol.Chem.*, vol. 275, no. 8, pp. 5493-5503.

Wang, S., Shi, Z., Liu, W., Jules, J., & Feng, X. 2006b, "Development and validation of vectors containing multiple siRNA expression cassettes for maximizing the efficiency of gene silencing", *BMC.Biotechnol.*, vol. 6, p. 50.

Wasserman, W. W. & Fahl, W. E. 1997, "Functional antioxidant responsive elements", *Proc Natl Acad Sci U S A*, vol. 94, no. 10, pp. 5361-6.

Watabe, M., Aoyama, K., & Nakaki, T. 2007, "Regulation of glutathione synthesis via interaction between glutamate transport-associated protein 3-18 (GTRAP3-18) and excitatory amino acid carrier-1 (EAAC1) at plasma membrane", *Mol.Pharmacol.*, vol. 72, no. 5, pp. 1103-1110.

Welch, W. J., Tojo, A., & Wilcox, C. S. 2000, "Roles of NO and oxygen radicals in tubuloglomerular feedback in SHR", *Am J Physiol Renal Physiol*, vol. 278, no. 5, pp. 769-76.

Welch, W. J. & Wilcox, C. S. 2001, "AT1 receptor antagonist combats oxidative stress and restores nitric oxide signaling in the SHR", *Kidney Int.*, vol. 59, no. 4, pp. 1257-1263.

Weterman, M. A., van Groningen, J. J., Tertoolen, L., & van Kessel, A. G. 2001, "Impairment of MAD2B-PRCC interaction in mitotic checkpoint defective t(X;1)-positive renal cell carcinomas", *Proc.Natl.Acad.Sci.U.S.A*, vol. 98, no. 24, pp. 13808-13813.

Weterman, M. A., Wilbrink, M., Janssen, I., Janssen, H. A., van den, B. E., Fisher, S. E., Craig, I., & Geurts, v. K. 1996, "Molecular cloning of the papillary renal cell carcinoma-associated translocation (X;1)(p11;q21) breakpoint", *Cytogenet.Cell Genet.*, vol. 75, no. 1, pp. 2-6.

Wilcox, C. S. 2003, "Redox regulation of the afferent arteriole and tubuloglomerular feedback", *Acta Physiol Scand.*, vol. 179, no. 3, pp. 217-223.

Wilcox, C. S., Welch, W. J., Murad, F., Gross, S. S., Taylor, G., Levi, R., & Schmidt, H. H. 1992, "Nitric oxide synthase in macula densa regulates glomerular capillary pressure", *Proc.Natl.Acad.Sci.U.S.A*, vol. 89, no. 24, pp. 11993-11997.

Wilson, C., Bellen, H. J., & Gehring, W. J. 1990, "Position effects on eukaryotic gene expression", *Annu.Rev.Cell Biol.*, vol. 6, pp. 679-714.

Wilson, F. H., Disse-Nicodeme, S., Choate, K. A., Ishikawa, K., Nelson-Williams, C., Desitter, I., Gunel, M., Milford, D. V., Lipkin, G. W., Achard, J. M., Feely, M. P., Dussol, B., Berland, Y., Unwin, R. J., Mayan, H., Simon, D. B., Farfel, Z., Jeunemaitre, X., & Lifton, R. P. 2001, "Human hypertension caused by mutations in WNK kinases", *Science*, vol. 293, no. 5532, pp. 1107-1112.

Wilson, F. H., Hariri, A., Farhi, A., Zhao, H., Petersen, K. F., Toka, H. R., Nelson-Williams, C., Raja, K. M., Kashgarian, M., Shulman, G. I., Scheinman, S. J., & Lifton, R. P. 2004, "A cluster of metabolic defects caused by mutation in a mitochondrial tRNA", *Science*, vol. 306, no. 5699, pp. 1190-1194.

Wilson, F. H., Kahle, K. T., Sabath, E., Lalioti, M. D., Rapson, A. K., Hoover, R. S., Hebert, S. C., Gamba, G., & Lifton, R. P. 2003, "Molecular pathogenesis of inherited hypertension with hyperkalemia: the Na-Cl cotransporter is inhibited by wild-type but not mutant WNK4", *Proc.Natl.Acad.Sci.U.S.A*, vol. 100, no. 2, pp. 680-684.

Wilson, M. H., Grant, P. J., Hardie, L. J., & Wild, C. P. 2000, "Glutathione S-transferase M1 null genotype is associated with a decreased risk of myocardial infarction", *FASEB J.*, vol. 14, no. 5, pp. 791-796.

Wong, K. K., deLeeuw, R. J., Dosanjh, N. S., Kimm, L. R., Cheng, Z., Horsman, D. E., MacAulay, C., Ng, R. T., Brown, C. J., Eichler, E. E., & Lam, W. L. 2007, "A comprehensive analysis of common copy-number variations in the human genome", *Am.J.Hum.Genet.*, vol. 80, no. 1, pp. 91-104.

Wu, G., Fang, Y. Z., Yang, S., Lupton, J. R., & Turner, N. D. 2004, "Glutathione metabolism and its implications for health", *J.Nutr.*, vol. 134, no. 3, pp. 489-492.

Xia, C., Hu, J., Ketterer, B., & Taylor, J. B. 1996, "The organization of the human GSTP1-1 gene promoter and its response to retinoic acid and cellular redox status", *Biochem.J.*, vol. 313 (Pt 1), pp. 155-161.

Xia, H., Mao, Q., Paulson, H. L., & Davidson, B. L. 2002, "siRNA-mediated gene silencing in vitro and in vivo", *Nat.Biotechnol.*, vol. 20, no. 10, pp. 1006-1010.

Xu, X., Rogus, J. J., Terwedow, H. A., Yang, J., Wang, Z., Chen, C., Niu, T., Wang, B., Xu, H., Weiss, S., Schork, N. J., & Fang, Z. 1999, "An extreme-sib-pair genome scan for genes regulating blood pressure", *Am.J.Hum.Genet.*, vol. 64, no. 6, pp. 1694-1701.

Yagil, C., Hubner, N., Kreutz, R., Ganten, D., & Yagil, Y. 2003, "Congenic strains confirm the presence of salt-sensitivity QTLs on chromosome 1 in the Sabra rat model of hypertension", *Physiol Genomics*, vol. 12, no. 2, pp. 85-95.

Yagil, C., Hubner, N., Monti, J., Schulz, H., Sapojnikov, M., Luft, F. C., Ganten, D., & Yagil, Y. 2005, "Identification of hypertension-related genes through an integrated genomic-transcriptomic approach", *Circ Res*, vol. 96, no. 6, pp. 617-25.

Yagil, C., Sapojnikov, M., Kreutz, R., Katni, G., Lindpaintner, K., Ganten, D., & Yagil, Y. 1998, "Salt susceptibility maps to chromosomes 1 and 17 with sex specificity in the Sabra rat model of hypertension", *Hypertension*, vol. 31, no. 1, pp. 119-124.

Yamagata, K., Furuta, H., Oda, N., Kaisaki, P. J., Menzel, S., Cox, N. J., Fajans, S. S., Signorini, S., Stoffel, M., & Bell, G. I. 1996, "Mutations in the hepatocyte nuclear factor-4alpha gene in maturity-onset diabetes of the young (MODY1)", *Nature*, vol. 384, no. 6608, pp. 458-460.

Yamauchi, K., Rai, T., Kobayashi, K., Sohara, E., Suzuki, T., Itoh, T., Suda, S., Hayama, A., Sasaki, S., & Uchida, S. 2004, "Disease-causing mutant WNK4 increases paracellular chloride permeability and phosphorylates claudins", *Proc.Natl.Acad.Sci.U.S.A*, vol. 101, no. 13, pp. 4690-4694.

Yamori, Y. 1994, "Development of the spontaneously hypertensive rat (SHR), the stroke-prone SHR (SHRSP) and their various substrain models for hypertension -related cardiovascular diseases.," in *Handbook of Hypertension. Experimental and Genetic Models of Hypertension*, vol. 16 D. Ganten & W. de Jong, eds., Elsevier, New York, pp. 346-364.

Yang, J. Y., Tam, W. Y., Tam, S., Guo, H., Wu, X., Li, G., Chau, J. F., Klein, J. D., Chung, S. K., Sands, J. M., & Chung, S. S. 2006, "Genetic restoration of aldose reductase to the collecting tubules restores maturation of the urine concentrating mechanism", *Am.J.Physiol Renal Physiol*, vol. 291, no. 1, p. F186-F195.

Yang, Q., Kim, S. K., Sun, F., Cui, J., Larson, M. G., Vasan, R. S., Levy, D., & Schwartz, F. 2007, "Maternal influence on blood pressure suggests involvement of mitochondrial DNA in the pathogenesis of hypertension: the Framingham Heart Study", *J.Hypertens.*, vol. 25, no. 10, pp. 2067-2073.

Yang, T., Michele, D. E., Park, J., Smart, A. M., Lin, Z., Brosius, F. C., III, Schnermann, J. B., & Briggs, J. P. 1999, "Expression of peroxisomal proliferator-activated receptors and retinoid X receptors in the kidney", *Am.J.Physiol*, vol. 277, no. 6 Pt 2, p. F966-F973.

Yang, Y., Sharma, R., Zimniak, P., & Awasthi, Y. C. 2002, "Role of alpha class glutathione S-transferases as antioxidant enzymes in rodent tissues", *Toxicol.Appl.Pharmacol.*, vol. 182, no. 2, pp. 105-115.

Yasui, N., Kajimoto, K., Sumiya, T., Okuda, T., & Iwai, N. 2007, "The monocyte chemotactic protein-1 gene may contribute to hypertension in Dahl salt-sensitive rats", *Hypertens.Res*, vol. 30, no. 2, pp. 185-193.

Yen, T. T., Yu, P. L., Roeder, H., & Willard, P. W. 1974, "A genetic study of hypertension in Okamoto-Aoki spontaneously hypertensive rats", *Heredity*, vol. 33, no. 3, pp. 309-316.

Yin, Z., Ivanov, V. N., Habelhah, H., Tew, K., & Ronai, Z. 2000, "Glutathione S-transferase p elicits protection against H2O2-induced cell death via coordinated regulation of stress kinases", *Cancer Res*, vol. 60, no. 15, pp. 4053-4057.

Yoshida, C., Tokumasu, F., Hohmura, K. I., Bungert, J., Hayashi, N., Nagasawa, T., Engel, J. D., Yamamoto, M., Takeyasu, K., & Igarashi, K. 1999, "Long range interaction of cis-DNA elements mediated by architectural transcription factor Bach1", *Genes Cells*, vol. 4, no. 11, pp. 643-655.

Yuan, J., Cheung, P. K., Zhang, H. M., Chau, D., & Yang, D. 2005, "Inhibition of coxsackievirus B3 replication by small interfering RNAs requires perfect sequence match in the central region of the viral positive strand", *J.Virol.*, vol. 79, no. 4, pp. 2151-2159.

Zafari, A. M., Ushio-Fukai, M., Akers, M., Yin, Q., Shah, A., Harrison, D. G., Taylor, W. R., & Griendling, K. K. 1998, "Role of NADH/NADPH oxidase-derived H2O2 in angiotensin II-induced vascular hypertrophy", *Hypertension*, vol. 32, no. 3, pp. 488-495.

Zanetti, M., Sato, J., Katusic, Z. S., & O'Brien, T. 2001, "Gene transfer of superoxide dismutase isoforms reverses endothelial dysfunction in diabetic rabbit aorta", *Am.J.Physiol Heart Circ Physiol*, vol. 280, no. 6, p. H2516-H2523.

Zeggini, E., Weedon, M. N., Lindgren, C. M., Frayling, T. M., Elliott, K. S., Lango, H., Timpson, N. J., Perry, J. R., Rayner, N. W., Freathy, R. M., Barrett, J. C., Shields, B., Morris, A. P., Ellard, S., Groves, C. J., Harries, L. W., Marchini, J. L., Owen, K. R., Knight, B., Cardon, L. R., Walker, M., Hitman, G. A., Morris, A. D., Doney, A. S., McCarthy, M. I., & Hattersley, A. T. 2007, "Replication of genome-wide association

signals in UK samples reveals risk loci for type 2 diabetes", *Science*, vol. 316, no. 5829, pp. 1336-1341.

Zelko, I. N., Mariani, T. J., & Folz, R. J. 2002, "Superoxide dismutase multigene family: a comparison of the CuZn-SOD (SOD1), Mn-SOD (SOD2), and EC-SOD (SOD3) gene structures, evolution, and expression", *Free Radic.Biol.Med.*, vol. 33, no. 3, pp. 337-349.

Zhang, H., Forman, H. J., & Choi, J. 2005, "Gamma-glutamyl transpeptidase in glutathione biosynthesis", *Methods Enzymol.*, vol. 401, pp. 468-483.

Zhang, J. J., Yoshida, H., Chao, L., & Chao, J. 2000, "Human adrenomedullin gene delivery protects against cardiac hypertrophy, fibrosis, and renal damage in hypertensive dahl salt-sensitive rats", *Hum.Gene Ther.*, vol. 11, no. 13, pp. 1817-1827.

Zhao, Y., Ransom, J. F., Li, A., Vedantham, V., von Drehle, M., Muth, A. N., Tsuchihashi, T., McManus, M. T., Schwartz, R. J., & Srivastava, D. 2007, "Dysregulation of cardiogenesis, cardiac conduction, and cell cycle in mice lacking miRNA-1-2", *Cell*, vol. 129, no. 2, pp. 303-317.

Zharkikh, L., Zhu, X., Stricklett, P. K., Kohan, D. E., Chipman, G., Breton, S., Brown, D., & Nelson, R. D. 2002, "Renal principal cell-specific expression of green fluorescent protein in transgenic mice", *Am.J.Physiol Renal Physiol*, vol. 283, no. 6, p. F1351-F1364.

Zhu, D. L., Wang, H. Y., Xiong, M. M., He, X., Chu, S. L., Jin, L., Wang, G. L., Yuan, W. T., Zhao, G. S., Boerwinkle, E., & Huang, W. 2001, "Linkage of hypertension to chromosome 2q14-q23 in Chinese families", *J.Hypertens.*, vol. 19, no. 1, pp. 55-61.

Zicha, J. & Kunes, J. 1999, "Ontogenetic aspects of hypertension development: analysis in the rat", *Physiol Rev.*, vol. 79, no. 4, pp. 1227-1282.

Zimdahl, H., Nyakatura, G., Brandt, P., Schulz, H., Hummel, O., Fartmann, B., Brett, D., Droege, M., Monti, J., Lee, Y. A., Sun, Y., Zhao, S., Winter, E. E., Ponting, C. P., Chen, Y., Kasprzyk, A., Birney, E., Ganten, D., & Hubner, N. 2004, "A SNP map of the rat genome generated from cDNA sequences", *Science*, vol. 303, no. 5659, p. 807.

Zimmerli, L. U., Schiffer, E., Zurbig, P., Good, D. M., Kellmann, M., Mouls, L., Pitt, A. R., Coon, J. J., Schmieder, R. E., Peter, K., Mischak, H., Kolch, W., Delles, C., & Dominiczak, A. F. 2007, "Urinary proteomic biomarkers in coronary artery disease", *Mol.Cell Proteomics.*

Zintzaras, E., Kitsios, G., & Stefanidis, I. 2006, "Endothelial NO synthase gene polymorphisms and hypertension: a meta-analysis", *Hypertension*, vol. 48, no. 4, pp. 700-710.